New Methods and Reagents for Carbon–Fluorine Bond Formation

Lukas Pfeifer

A thesis submitted to the board of the faculty of Physical Sciences in partial fulfilment of the requirements for the degree of Doctor of Philosophy at the University of Oxford.

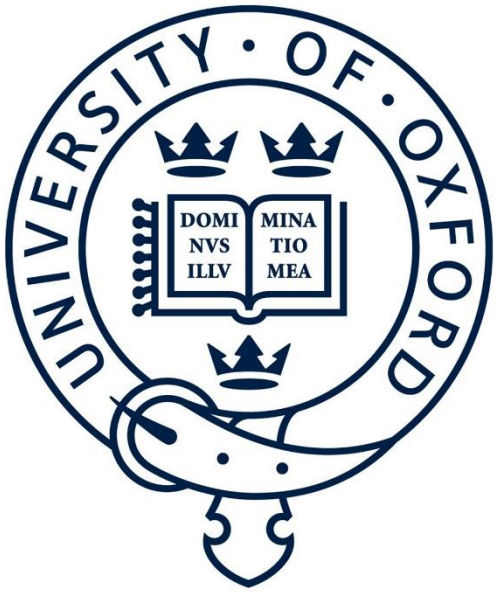

Wadham College

Hilary Term 2017

Author's Declaration

The work presented in this thesis was conducted at the Chemistry Research Laboratory at the University of Oxford under the supervision of Prof. Véronique Gouverneur. All the work is my own, except where otherwise stated, and has not been submitted for any other degree at this or any other university.

Lukas Pfeifer

November 2016

Abstract

After a general introduction about the properties and preparation of organofluorine compounds (Chapter 1), this thesis is divided into two parts focussing on the development of new methods for C–F bond formation (Part A) as well as studies towards the development of novel fluorinating reagents (Part B).

Part A: New Methods for Carbon–Fluorine Bond Formation

Part A consists of two chapters outlining the development of a Pd-catalysed hydrofluorination of alkenylarenes (Chapter 2) as well as a halofluorination of alkynes (Chapter 3).

Chapter 2

This chapter describes the development of a novel, regioselective, *syn*-specific hydrofluorination of alkenylarenes under Pd-catalysis leading to the formation of benzylic fluorides. An extensive substrate scope is presented together with a model of the catalytic cycle, based on observations during the development of this reaction, deuterium labelling experiments as well as mechanistic control experiments starting from isolated palladacycles.

Chapter 3

In this chapter the development of a novel iodo- as well as bromofluorination of internal and terminal alkynes, leading to the formation of (*E*)-halofluoroalkenes, is presented. For the former substrate class, the effects of steric as well as electronic bias on

regioselectivity are discussed. For the latter substrate class, this methodology could be extended to the corresponding double iodofluorination, and for both transformations it was found to exclusively lead to the fluorination of the internal carbon. An extensive substrate scope as well as different iodofluorination-cross-coupling sequences including Suzuki, Sonogashira and Ullmann couplings, are illustrated. A representative reaction was successfully carried out on gram-scale and an iodofluorination-Suzuki-coupling sequence was used to prepare a fluorinated tamoxifen derivative.

Part B: Hydrogen-Bonded Fluoride Complexes as Novel Reagents for Carbon–Fluorine Bond Formation

Part B consists of two chapters describing structural as well as reactivity studies of fluoride–alcohol (Chapter 4) and fluoride–urea complexes (Chapter 5).

Chapter 4

In this chapter the synthesis of 19 novel hydrogen-bonded tetraalkylammonium fluoride–alcohol complexes is described. For a subset of 15, the solid-state structures as determined by single-crystal X-ray diffraction experiments are presented. Trends of reactivity and selectivity were determined using these complexes as sources of fluoride anion in a model S_N2 reaction. Preliminary results from *in silico* modelling of the fluoride–alcohol system provide a basis for explaining the results.

Chapter 5

This chapter summarises the synthesis and solid-state structures of 20 hydrogen-bonded fluoride complexes using the urea and related squaramide and amide motifs. Also, the size of the tetraalkylammonium counter-cation was varied to study the influence on the solid-state structure. The reactivity and selectivity of a series of complexes was studied using the same model S_N2 reaction as in Chapter 4 and results were compared accordingly. Different UV-vis and NMR spectroscopic techniques were used to study the behaviour of the fluoride–urea system in solution. Preliminary results demonstrate the use of 1,3-diarylureas as organocatalysts for nucleophilic fluorination.

Acknowledgements

The following work would have not been possible without the generous support and input of many outstanding people, to whom I owe special thanks.

When I first started out as a Ph.D. student in the Gouverneur group, Elena Benedetto was charged with the task of helping me settle in and navigate my way through fluorine chemistry. For her advice and patience I am deeply grateful.

In my first year, I teamed up with Keary Engle and George Pidgeon, who had earlier started the work on hydrogen-bonded fluoride complexes, which I was later to continue, after they had left Oxford. Both I would like to thank for the fun times and for the knowledge that they shared with me. I am especially indebted to Keary, whose thoughtful input I could always rely on, even after he had departed Oxford, and whose outstanding passion for chemistry continues to be a great source of inspiration. Soon thereafter, I started working with Enrico Emer on the hydrofluorination of alkenylarenes, a collaboration that is an invaluable part of my first couple of years as a young researcher, and an experience for which I owe Enrico special thanks. Over the past 4 years I have also been lucky to join Samuel Calderwood, Tanatorn Khotavivattana (Plum), Matthew Tredwell and Stefan Verhoog on a variety of ^{18}F-labelling projects. This greatly productive collaboration has allowed me to get a glimpse of a part of chemistry that not everyone gets to see, for which I want to express my gratitude. My work a an X-ray crystallographer also allowed me to join efforts with Miriam Ó Dúill, Raul Pereira, Stefan Gruber, Sean Preshlock, Janis Veliks, Francesco Ibba and Paolo Ricci at various stages during their endeavours, which has greatly enriched my Ph.D experience.

During my time in Oxford, I had the opportunity to supervise Osman Tack during his year as a Part II student as well as Ruchuta Ardkhean (Nod) during one of her first year rotations in the group. Being able to assist them during these times has been a truly inspiring experience. As part of the EU-backed RADIOMI project I have also been able to work with Prof. Olof Solin, Prof. Merja Haaparanta-Solin, Katharina Grafinger, Anna Krzyczmonik (Anja) and Thomas Keller an a set of PET-studies on rats, which has left a deep impression on me, and has helped me realise that it is the preparation of compounds with a specific function that I find most appealing about chemistry.

In terms of Ph.D. supervisor, I could not have asked for a better one than Prof. Véronique Gouverneur. During these past four years she has been an exceptional mentor to me, her guidance and support has been invaluable and crucial for the success of my Ph.D., and I will always feel indebted to her, for giving me this chance.

I am also deeply grateful to Dr. John Brown, whose invaluable input, based on vast experience and knowledge, has been essential to the success of many projects that I have been a part of. Furthermore, I would like to express special thanks to Dr. Amber Thompson, for introducing me to the world of X-ray crystallography and her exceptional patience, when it comes to dealing with my many questions. Thanks also go to Prof. Tim Claridge, Dr. Barbara Odell and the rest of the NMR team as well as Colin Sparrow and Dr. James Wickens from the mass spectrometry facility for their continuous support.

Thanks also go to my examiners Prof. Jeremy Robertson and Prof. David O'Hagan for taking the time and broadening my chemical horizon.

Apart from the work in the Chemistry Department I am exceedingly thankful for the friendships I have forged during my time in Oxford. This includes “The Germans” – Miriam Ó Dúill, Michael Schedler, Gregor Cremosnik and Wanda Stuber (Wendy) – with whom I have spent countless lunchbreaks and pub evenings, explored the UK outside Oxford and shared some of the best moments over the past four years. Similarly, I am indebted to Anne Kornahrens, who has been a great friend ever since I met her. Her different view on life and its challenges has always been very stimulating and our discussions have given me countless precious insights. I am also grateful to Ulrike Filp and Aleksandra Pekošak, for all the good times at the half-yearly RADIOMI meetings. And thanks of course to all the other members of the Gouverneur group, who for lack of space I haven’t mentioned individually, for their daily support in the lab.

I would also like to express my sincere gratitude to Mag. Thomas Heinzel who really stirred up my early interest in chemistry and whose commitment opened up many opportunities.

Lastly, but perhaps most importantly, I would like to thank my family. My parents for raising me in a way that allowed me to get to this point, and for all their love and support, especially over the last 4 years. My brother, with whom I have had the chance to explore our talents together, and who, sometimes willingly and sometimes not, has taught me many invaluable lessons. This is also, where I would like to thank my girlfriend, Emeline, honorary member of “The Germans”, who shares my passion for good food (if not for 2 am soufflés) and diving, has shown remarkable understanding for my many shortcomings, punctuality related and otherwise, and who has never failed to lift me up when I was feeling down.

Table of Contents

Abbreviations and Acronyms

[bmim]	1-Butyl-3-methylimidazolium
°C	Degrees Celsius
1-Ada-OH	1-Adamantanol
5'-FDA	5'-Fluoro-5'-deoxyadenosine
Å	Angstrom
Ac	Acetyl
aq.	Aqueous
Ar	Aryl
Asp	Aspartic Acid
BINAP	2,2'-Bis(diphenylphosphino)-1,1'-binaphthyl
BINOL	1,1'-Bi-2-naphthol
Bn	Benzyl
b.p.	Boiling Point
Bu	Butyl
c	Concentration
C.N.	Coordination Number
Cal	Calorie(s)
Cat	Catechol
CI	Chemical Ionisation
^{Cl}IPr	4,5-Dichloro-1,3-bis(2,6-diisopropylphenyl)2-imidazolidinylidene
cm	Centimetre(s)
COD	1,5-Cyclooctadiene
CSD	Cambridge Structural Database
d	Day(s)
D	Diffusion Coefficient
D_0	Homolytic Bond Dissociation Energy
DABCO	1,4-Diazabicyclo[2.2.2]octane
DAST	Diethylaminosulfur Trichloride
dba	Dibenzylideneacetone
DBH	1,3-Dibromo-5,5-dimethylhydantoin
DBU	1,8-Diazabicyclo(5.4.0)undec7-ene
D_{calc}	Calculated Density
DCC	*N*,*N*'-Dicyclohexylcarbodiimide
DCE	1,2-Dichloroethane
DCH	1,3-Dichloro-5,5-dimethylhydantoin

DCM	Dichloromethane
DFT	Density Functional Theory
DIBAL-H	Diisobutylaluminium Hydride
DIH	1,3-Diiodo-5,5-dimethylhydantoin
DIPEA	*N*,*N*-Diisopropylethylamine
DMAP	4-Dimethylaminopyridine
DME	Dimethoxyethane
DMF	Dimethylformamide
DMIPA	*N*,*N*-Dimethylisopropylamine
DMSO	Dimethyl Sulfoxide
DNP	2',4'-Dinitrophenyl
DOSY	Diffusion-Ordered NMR Spectroscopy
dppb	1,4-Bis(diphenylphosphino)butane
dppf	1,1'-Bis(diphenylphosphino)ferrocene
dppp	1,3-Bis(diphenylphosphino)propane
dr	Diastereomeric Ratio
DXH	1,3-Dihalo-5,5-dimethylhydantoin
e	Elementary Charge
E2	Bimolecular Elimination
ED_{50}	Median Effective Dose
ee	Enantiomeric Excess
E_{ea}	Electron Affinity
EI	Electron Ionisation
equiv.	Equivalent(s)
ESI	Electrospray Ionisation
ESR	Electron Spin Resonance
Et	Ethyl
FI	Field Ionisation
G	Gibbs Free Energy
g	Gram(s)
GC/MS	Gas Chromatography–Mass Spectrometry
Glu	Glutamic Acid
GP	General Procedure
h	Hour(s)
HMPA	Hexamethylphosphoramide
HOESY	Heteronuclear Overhauser Effect Spectroscopy
HOMO	Highest Occupied Molecular Orbital

HPLC	High Performance Liquid Chromatography
HRMS	High Resolution Mass Spectrometry
Hz	Hertz(s)
i	*iso*
IE	Ionisation Energy
IR	Infrared Spectroscopy
J	Coupling Constant
K	Equilibrium Constant
K	Kelvin
k	Rate Constant
kJ	Kilojoule(s)
L	Litre(s)
LFER	Linear Free Energy Relationship
LUMO	Lowest Unoccupied Molecular Orbital
m	*meta*
M	Mole(s) per Litre (mol/L)
M.p.	Melting Point
m/z	Mass-to-Charge Ratio
Me	Methyl
MeCN	Acetonitrile
mim	Methylimidazole
min.	Minute(s)
mL	Millilitre(s)
mol	Mole(s)
mol%	Mole Percent
Ms	Mesylate
MW	Microwave
n	*normal*
NBS	*N*-Bromosuccinimide
NCS	*N*-Chlorosuccinimide
NFSI	*N*-Fluorobenzenesulfonimide
NHS	*N*-Hydroxysuccinimide
NIS	*N*-Iodosuccinimide
NMR	Nuclear Magnetic Resonance
nOe	Nuclear Overhauser Effect
NOESY	Nuclear Overhauser Effect Spectroscopy
NOS	*N*-Oxysuccinimide

NPG	Neopentylglycol
NXS	*N*-Halosuccinimide
o	ortho
OTf	Trifluoromethanesulfonate
ox	Oxalate
P	Distribution Coefficient in *n*-Octanol/Water System
p	*para*
PDB	Protein Structure Database
PERT	Pentaerythritol
Ph	Phenyl
Pin	Pinacol
ppm	Parts per Million
PPY	4-(Pyrrolidin-1-yl)pyridine
Pr	Propyl
PVPHF	Poly[4-vinylpyridinium Poly(hydrogen fluoride)]
pyr	Pyridine
R	Generic Carbogenic Fragment (Aryl or Alkyl Group)
R_f	Generic Perfluorinated Fragment
RMS	Root Mean Square
rt	Room Temperature
s	Second(s)
s	Secondary (*sec*)
SAM	(*S*)-Adenosyl-L-Methionine
sat.	Saturated
Ser	Serine
SIPr	1,3-Bis(2,6-diisopropylphenyl)-2-imidazolidinylidene
S_N2	Bimolecular Nucleophilic Substitution
S_p	Square Planar Symmetry
SU	Standard Uncertainty
T	Temperature
t	Tertiary (*tert*)
t	Time
TASF	Tris(dimethylamino)sulfonium Difluorotrimethylsilicate
TBA	Tetrabutylammonium
TBAT	Tetrabuylammonium Difluorotriphenylsilicate
TBCO	2,4,4,6-Tetrabromo-2,5-cyclohexadienone
T_d	Tetrahedral Symmetry

TEA	Tetraethylammonium
TEMPO	(2,2,6,6-Tetramethylpiperidin-1-yl)oxidanyl
THF	Tetrahydrofuran
Thr	Threonine
TIPS	Triisopropylsilyl
TLC	Thin Layer Chromatography
TMA	Tetramethylammonium
TME	1,1,1-Tris(hydroxymethyl)ethane
TMS	Trimethylsilyl
TOF	Time of Flight
Tol	Tolyl
T_p	Tetragonal Pyramidal Symmetry
Tyr	Tyrosine
UV	Ultraviolet
V	Volume
vis	Visible
VSEPR	Valence Shell Electron Pair Repulsion
WFT	Wave Functional Theory
X	Anionic Ligand
$\Delta G^{\ddagger}$	Activation Free Energy
λ	Wavelength
μ	Dipole Moment
µL	Microlitre(s)

Introduction

Chapter 1 Properties and Synthesis of Organofluorine Compounds

1.1. Properties of Fluorine and the C–F Bond

The properties of fluorine are mostly governed by its high electronegativity and small size.

Fluorine is assigned the highest electronegativity of all the elements, with X = 4.0 on the Pauling scale (Table 1.1).[1]

Table 1.1. Pauling electronegativities of selected elements.[1]

H (2.1)				
Li (1.0)	C (2.5)	N (3.0)	O (3.5)	F (4.0)
Na (0.9)	Si (1.8)	P (2.1)	S (2.5)	Cl (3.0)
K (0.8)				Br (2.8)
Cs (0.7)				I (2.5)

This is based on fluorine having the smallest atomic radius of all the elements in the 2nd Period due to contraction caused by its high nuclear charge. As a result, the positive nucleus exerts a large electrostatically attractive force onto the electrons, which makes the process of removing an electron to generate an F^+ species highly endothermic (IE = –1679 kJ mol^{-1}). This also gives fluorine the highest electron affinity (E_{ea} = 327 kJ mol^{-1}) of

the elements in the 2nd Period, with the incoming electron filling the contracted 2p orbital and the negative charge being stabilised by the electropositive nucleus.

In terms of size, the fluorine atom is in between hydrogen and oxygen but closer to the latter with van der Waals radii of 1.47 Å for fluorine and 1.20 Å and 1.52 Å for hydrogen and oxygen, respectively (Table 1.2).[2] The same is true for the C–X bond lengths, whereby the average C–F bond is 1.35 Å long with values of 1.09 Å and 1.43 Å for C–H and C–O, respectively (Table 1.2).[3–5]

Table 1.2. Van der Waals radii and average C–X bond lengths of selected elements.

Van der Waals radii [Å]	H (1.20)	C (1.70)	N (1.55)	O (1.52)	F (1.47)
	Si (2.10)	P (1.80)	S (1.80)	Cl (1.74)	
Bond lengths [Å]	C–H (1.09)	C–C (1.54)	C–N (1.47)	C–O (1.43)	C–F (1.35)
	C–Si (1.85)	C–P (1.84)	C–S (1.82)	C–Cl (1.77)	

In medicinal chemistry fluorine is often used to replace hydrogen or oxygen. In the former case, although exchanging a C–H bond for a C–F bond is the most conservative form of hydrogen substitution in terms of its steric impact, it greatly changes the electronic properties of the compound. Substituting an oxygen for a fluorine is a more neutral change, as both elements possess high electronegativity. However, substituting a C=O group for C–F or CF_2 leads to a significant change of shape and C–F replacement of C–OH causes the loss of the acidic hydrogen and the hydrogen bond donating ability. Therefore, this kind of substitution can be used to decipher between a C–OH functionality serving as a hydrogen bond donor and its inherent polarity which is preserved in the C–F bond.[6]

The C–F bond is furthermore the strongest single bond in organic chemistry at D_0 = 485 kJ mol^{-1} (compare Table 1.3).

Table 1.3. Homolytic bond dissociation energies of common C–X bonds.

Bond	D_0 [kJ mol^{-1}]
C–F	485
C–H	411
C–O	358
C–C	346
C–Cl	327
C–N	305

The reason lies in the extraordinarily high electronegativity of fluorine. This causes a strong attractive force for the bond electron density towards fluorine, resulting in a highly polarised bond. Therefore, one can attribute the remarkable strength of the C–F bond to a significant contribution from electrostatic interaction between $F^{\delta-}$ and $C^{\delta+}$.[7,8] This argument also explains the gradual C–F bond shortening in the series from fluoromethane to tetrafluoromethane, as an ever more positively charged carbon exerts an increasing attractive force on the negatively polarised fluorine substituents.

1.2. Effect of Fluorination on Physicochemical and Conformational Properties

The introduction of fluorine into organic molecules causes geometric changes. For example, contrary to what one might expect from steric and lone pair repulsion considerations, the H–C–H angle widens upon going from methane (109.5°) to

fluoromethane (110.2°) and difluoromethane (113.8°) with the F–C–H angle narrowing (fluoromethane: 108.7°; difluoromethane: 108.4°).[6,9] This effect can be explained by evoking valence shell electron pair repulsion (VSEPR) theory, where fluorine pulling electron density towards it reduces electron pair repulsion between the electron-rich C–H bonds and causes them to spread out. Alternatively, the C–F bond can be regarded as pulling p-orbital electrons from carbon to fluorine as a consequence of fluorine's low energy 2p orbital, causing the carbon to become more sp^2-like.[6] This is also the reason why fluorine preferentially binds to sp^3 rather than sp^2 hybridised carbons, which can have a profound influence on product selectivity.[10–12] The explained changes in geometry/hybridisation at the fluorine-substituted carbon centre lead to considerable conformational disorder when introducing CF_2 groups into long chain alkanes.[13]

1.2.1. Hyperconjugation

Similar to the C–O bond, the C–F bond has a low lying σ^*_{C-F} antibonding orbital, which can interact with stereoelectronically aligned electron-rich bonds, heteroatom lone pairs or nucleophiles, leading to the stabilisation of certain conformations, intermediates and transition states.

An example of this can be observed in the anomeric effect found for 2-fluoropyran, **1.2** (Figure 1.1).

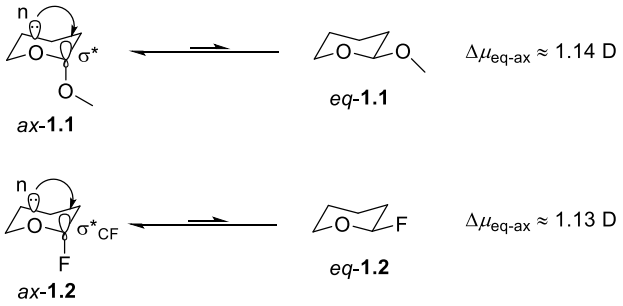

Figure 1.1. Anomeric effect for 2-methoxypyran (**1.1**) and 2-fluoropyran (**1.2**).

In analogy to 2-methoxypyran (**1.1**), **1.2** prefers the conformation featuring the fluorine substituent in the axial rather than the sterically favourable equatorial position by ≈12 kJ mol^{-1}, according to calculations at the density functional level of theory.[14] This can be understood by considering lone pair (HOMO) donation from the ether oxygen into the σ^*_{C-F} orbital (LUMO). For comparison, fluorocyclohexane only has a small equatorial preference (≈0.8–1 kJ mol^{-1}). There is, however, also a reduction in dipole moment (μ) of **1.2** in going from the equatorial to the axial conformer, which also contributes to the overall preference of the latter, albeit to a smaller extent. It is also important to note, that α-fluoropyrans are relatively stable, because the n–σ^*_{C-F} interaction does not have the destabilising effect one might expect, but rather decreases the covalent in favour of the ionic character of the C–F bond, thus leading to an increased electrostatic attraction between $F^{\delta-}$ and $C^{\delta+}$, which makes up for some of the loss.[6]

Related to this finding is the *gauche*-effect, causing the *gauche*-conformation of vicinal difluorides bound to an alkane backbone to be preferred over the alternative, sterically favoured *anti*-conformer. Although in the *gauche*-conformation the two fluorine atoms are expected to repel each other due to their negative polarisation and three lone pairs, the stabilising overlap between two σ_{C-H} orbitals and σ^*_{C-F} orbitals (hyperconjugation)

from neighbouring carbons makes the *gauche*-conformation more stable. This is shown exemplarily for 1,2-difluoroethane (**1.3**) in Figure 1.2.

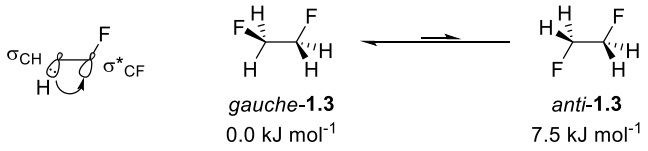

Figure 1.2. *Gauche*-Effect in 1,2-difluoroethane rationalised by hyperconjugation.

Additionally to this effect resulting from hyperconjugation, as Wiberg and co-workers explained in their 'bent bond' analysis, the highly polarised C–F bond leads to geometric changes of the C–C and C–H σ-bonds, ultimately contributing to the relative stabilisation of the *gauche*- over the *anti*-conformer (Figure 1.3).[15]

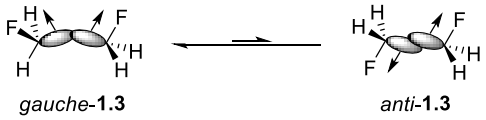

Figure 1.3. 'Bent bond' model of *gauche*-effect in 1,2-difluoroethane.

Due to the electron-deficiency in the C–F bond, which has most of its electron density resting on the fluorine atom, the electron density trajectory from each carbon towards the C–C bond is bent towards the fluorine substituent. As a consequence, a good overlap in the C–C bond is only possible in the *gauche*-conformation, whereas in the *anti*-conformation the electron density is skewed in opposite directions (Figure 1.3). Both hyperconjugation as well as the 'bent bond' model constitute the *gauche*-effect observed in these systems, but the stabilisation resulting from hyperconjugation seems to be the more important factor.[16]

1.2.2. 1,3-C–F Bond Repulsion

For 1,3-difluoroalkanes another destabilising interaction can be observed, which can override the stabilising effect of hyperconjugation. This has been best shown for 1,3-difluoropropane (**1.4**), which can adopt four reasonable staggered conformations (Figure 1.4).[17]

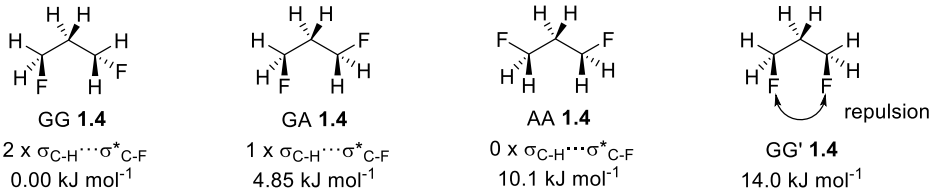

Figure 1.4. The relative energies of the conformers of 1,3-difluoropropane.

Both calculations as well as experimental evidence show their relative stabilities as GG < GA < AA < GG'. This can be largely understood by considering stabilisation by hyperconjugation, assuming that a C–H bond is a better donor than a C–CF bond.[18] The GG conformer has two hyperconjugative interactions of σ^*_{C-F} with σ_{C-H} orbitals, whereas the GA conformer has one and AA has none. The least stable conformer, GG', again has two such interactions, but it suffers from a dominant destabilisation caused by dipole repulsion between the two parallel C–F bonds, making it 14 kJ mol^{-1} higher in energy compared to GG. The overriding effect of the 1,3-dipolar repulsion (≈13 kJ mol^{-1}) illustrates how strong the negative electrostatic field associated with the C–F dipole is.

The combination of 1,2-*gauche*-effect and 1,3-dipolar repulsion also controls the conformation of all-*syn* multivicinal fluorinated alkanes, which preferably display a helical arrangement of the C–F bonds rather than an *anti*-zigzag structure.[19] This allows them to preserve the 1,2-*gauche* relationships between C–F bonds while avoiding destabilising 1,3-dipolar repulsions.

1.2.3. Dipole–Dipole Interactions

The highly ionic nature of the C–F bond gives rise to a large dipole moment (μ), which has to be taken into consideration when determining the conformational behaviour of organofluorine compounds. α-Fluorocarbonyl functionalities like amides (**1.5**), esters (**1.6**), ketones (**1.7**) and aldehydes (**1.8**) all prefer the C–F bond to lie *anti*-planar to the carbonyl, so that the dipoles oppose each other (Figure 1.5). [20–23]

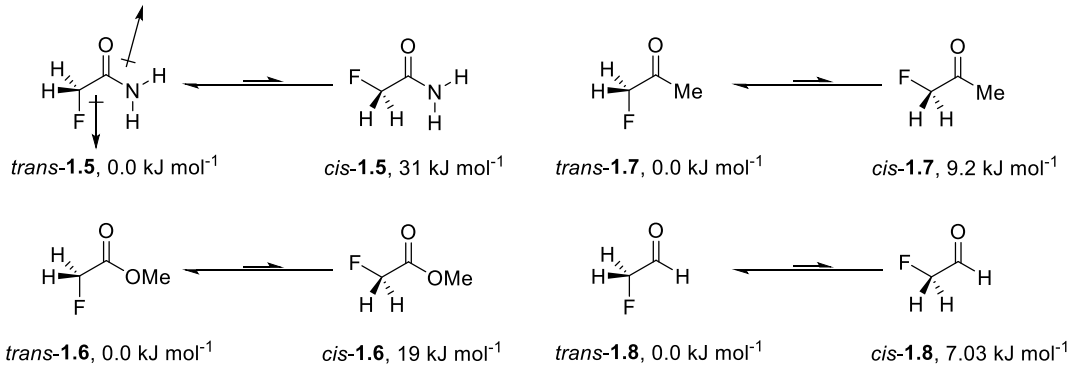

Figure 1.5. Calculated energy differences between the *cis*- and *trans*-isomers of selected α-fluorocarbonyl species.

Furthermore, vinylfluorides have established themselves as reasonable steric and polar hydrophobic mimetics of the amide group, whereby the success appears to be due to the vinylfluoride (**1.9**) dipole being oriented in the same way as the amide (**1.10**) dipole (Figure 1.6)

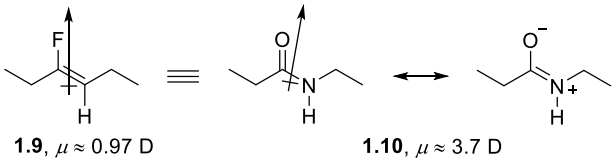

Figure 1.6. Similar dipole orientations in vinylfluoride, **1.9**, and amide, **1.10**.

This is despite the fact that the vinylfluoride dipole is considerably weaker (≈0.97 D *vs*. ≈3.7 D) compared to the amide group, suggesting that shape compatibility must also play

a significant role.[24] Similarly, difluorotoluene can be used as a good analogue for the DNA base thymine.[25]

When studying the orientation of fluorinated drugs on their target proteins using the protein structure database (PDB), it was found that the C–F dipole shows a propensity to adopt a Bürgi-Dunitz-type trajectory to amide carbonyls on the peptide backbone (Figure 1.7).[26]

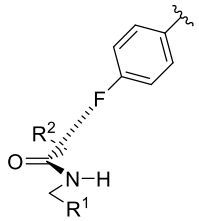

Figure 1.7. Dipole–dipole interaction of aromatic fluoride with peptide amide.

1.2.4. Charge–Dipole Interactions

The polarised C–F bond can also participate in interactions with a formal charge, which are generally significantly stronger than the aforementioned dipole–dipole interactions and can similarly have consequences for the conformation of fluorinated compounds. Examples are the significant preference of the fluorine substituent in 3-fluoropiperidinium ring systems **1.11** and **1.12** to sit in an axial position[27] as well as the large preference for the *gauche*-conformation of protonated fluoroethylamine **1.13** and fluoroethanol **1.14** (Figure 1.8).[28]

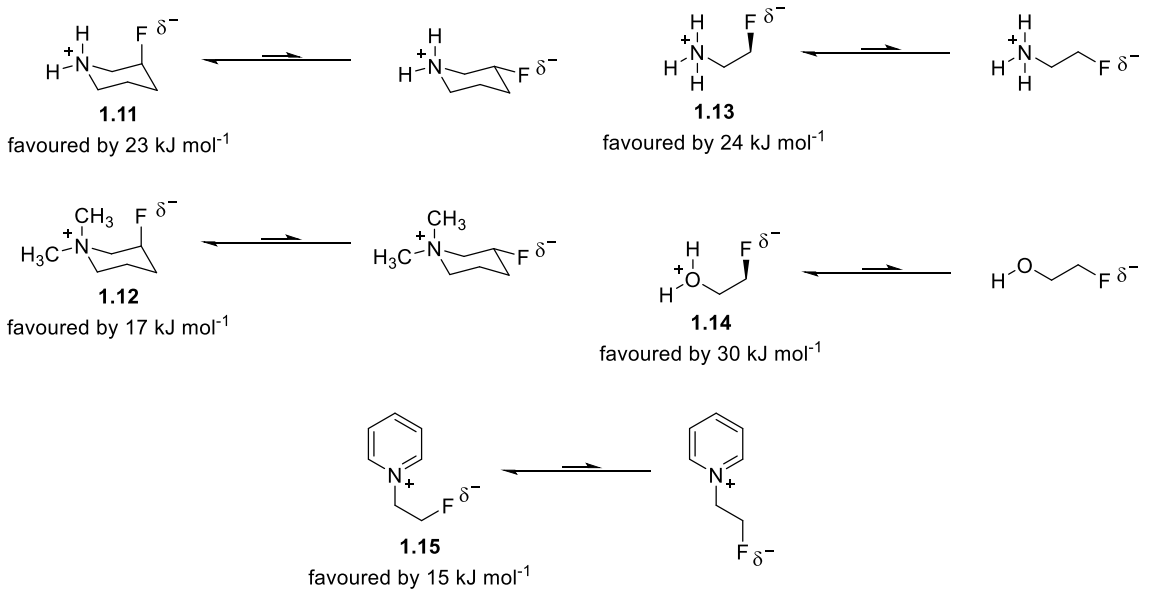

Figure 1.8. Preferred conformations due to intermolecular charge–dipole interactions between C–F and formally charged heteroatoms.

The resulting short C–F···H–N^+ contacts are more accurately described as charge–dipole interactions than hydrogen bonds, due to the unfavourable orientation of the bonds involved. Furthermore, the interaction persists even when there is no acidic hydrogen but still a positive charge as in **1.12** or in fluoroethylpyridinium cation **1.15** (Figure 1.8). This kind of interaction has shown potential as a tool to study the binding conformations of protonated amines to target proteins.[29]

1.2.5. C–F as Hydrogen Bond Acceptor

Despite the high polarisation of the C–F bond and the presence of three lone pairs on fluorine, organic fluorine only sporadically forms weak hydrogen bonds.[30,31] In those crystal structures that show short C–F···H–X contacts, they are often supported by additional factors such as optimal coordination or entropy effects. The reason for this lies in fluorine's poor polarizability, with the residual weak interactions being mostly caused

by through-space electrostatic interaction between $C^{\delta+}$–$F^{\delta-}$ and $H^{\delta+}$–$X^{\delta-}$ and van der Waals dispersion forces.[32] More polarised C(sp^3)–H bonds therefore form stronger hydrogen bonds to C–F compared to less polarised C(sp)–H groups.

On the contrary, fluoride anion is capable of forming very strong hydrogen bonds, for example with HF to give the symmetrical bifluoride anion, which is generally considered to contain the strongest hydrogen bond known. Its energy has been determined by different experimental as well as *in silico* methods, indicating a value of 163 ± 4 kJ mol^{-1}.[33–36] Fluoride's capabilities as a hydrogen bond acceptor are furthermore supported by the high hydration free energy of fluoride anion, which has been calculated to be –436 ± 3 kJ mol^{-1} and helps explain the high hygroscopicity observed for many fluoride salts.[37]

1.2.6. Lowering of pK_a

Due to its high electronegativity, the introduction of a fluorine substituent can influence the pK_as of adjacent functional groups, usually making them more acidic due to an inductively electron withdrawing effect (Table 1.4).[38–40]

Table 1.4. The effect of fluorine substitution on pK_a values of carboxylic acids, alcohols and amines.

Carboxylic Acid	pK_a	Alcohol	pK_a	Amine	pK_a[a]
CH_3CO_2H	4.76	CH_3CH_2OH	15.9	$CH_3CH_2NH_2$	10.7
CH_2FCO_2H	2.59	CF_3CH_2OH	12.4	$CF_3CH_2NH_2$	5.7
CHF_2CO_2H	1.34	$(CH_3)_3COH$	10.2	$C_6H_5NH_2$	4.6
CF_3CO_2H	0.52	$(CF_3)_3COH$	5.1	$C_6F_5NH_2$	–0.36

[a]Of the protonated ammonium form.

This effect can be used to improve the bioavailability (*F*), defined as the % of dose reaching the circulatory system, of orally administered drugs by affecting the absorption process.[41] For example, in a series of 3-piperidinylindole antipsychotic drugs the introduction of a fluorine substituent on the piperidine moiety lowered the basicity of the amine functionality, thereby improving bioavailablity to 18% (Table 1.5, Entry 1 *vs*. Entry 2).[42] Introduction of a second fluorine substituent on the indole group was used to block a site of metabolic functionalisation, which led to further improvement of bioavailability (Table 1.5, Entry 3). Furthermore, these subsequent substitutions also improved the binding affinity for the target 5-HT_{2A} receptor by more than one order of magnitude.

Table 1.5. Selected parameters of a series of 3-piperidinylindole antipsychotic drugs.

Entry	Indole	5-HT_{2A}[a] [nM]	pK_a[b]	*F* [%]
1	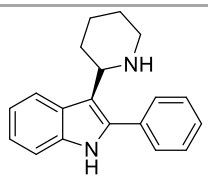	0.99	10.4	Poor
2	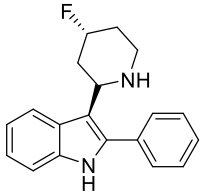	0.43	8.5	18
3	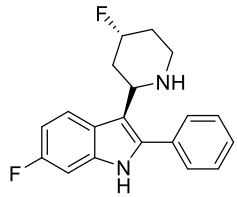	0.06	–	80

[a]Affinities at human cloned 5-HT_{2A} receptor. [b]Bioavailability calculated from intravenous and oral dosing at 0.5–2 mg kg^{-1}.

1.2.7. Modulation of Lipophilicity

By changing the lipophilicity of a compound one can greatly influence its suitability for passive transport through cell membranes. For a molecule to be able to diffuse through the cell membrane it must be lipophilic enough to pass through the lipid core, but not too lipophilic so as to not get trapped in it. Fluorination at different positions of a drug can be used to increase or decrease its lipophilicity, measured by its distribution coefficient between an octanol and a water layer (log(*P*)). Generally, monofluorination or trifluoromethylation of saturated alkyl chains decreases lipophilicity due to induced dipoles caused by fluorine's high electronegativity (Table 1.6).[43]

Table 1.6. Effect of fluorination on lipophilicity of short alkanes.

	log(*P*) (octanol–water)
CH_3CH_3	1.81
CH_3CHF_2	0.75
$CH_3(CH_2)_3CH_3$	3.11
$CH_3(CH_2)_3CH_2F$	2.33

On the other hand, aromatic fluorination, per/polyfluorination and fluorination adjacent to atoms with π-bonds, with the exception of some fluorinated α-carbonyl compounds, increase lipophilicity. This effect is governed by the low polarizability of the fluorine substituents.

The possibility to optimize the lipophilicity of a lead compound has for example been used for the development of leukotriene inhibitors.[44] It was found that lipophilicity could be increased by increasing the chain length of the amide substituent. Because this strategy was limited due to a loss of affinity for longer chains, fluorination was used to address this problem. The introduction of fluorine substituents led to an increase in

potency, and measurement of log(*P*) values revealed an increase in lipophilicity for each fluorinated amide compared to its non-fluorinated parent compound (Table 1.7).

Table 1.7. Lipophilicity for a series of leukotriene receptor inhibitors.

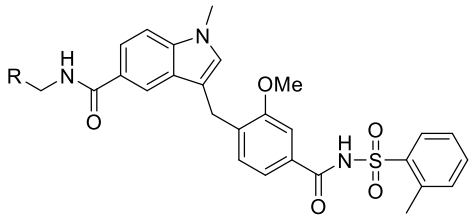

R	log(*P*) (octanol–water)
$CH_3CH_2CH(CH_3)$	5.85
$CF_3CH_2CH(CH_3)$	6.18
$(CH_3CH_2)_2CHCH_2$	6.29
$CF_3CH_2CH(CH_3CH_2)CH_2$	6.45
$CF_3CH(CH_3)CH_2CH_2$	6.30
$CF_3CH(CH_3)CH_2$	5.89

1.2.8. Improvement of Metabolic Stability

Short half-life due to rapid clearance assisted by metabolic instability is a common problem in drug development. The most important group of enzymes responsible for metabolising drugs are the Cytochrome P450 monooxygenases, which oxidise their substrates, in order to make them more hydrophilic thereby allowing for a more rapid clearance. Fluorine substitution can be used to block metabolically labile sites in order to increase a compound's *in vivo* half-life.

This can be exemplified using the lead optimisation study of the cholesterol inhibitor Ezetimib (Figure 1.9).[45,46]

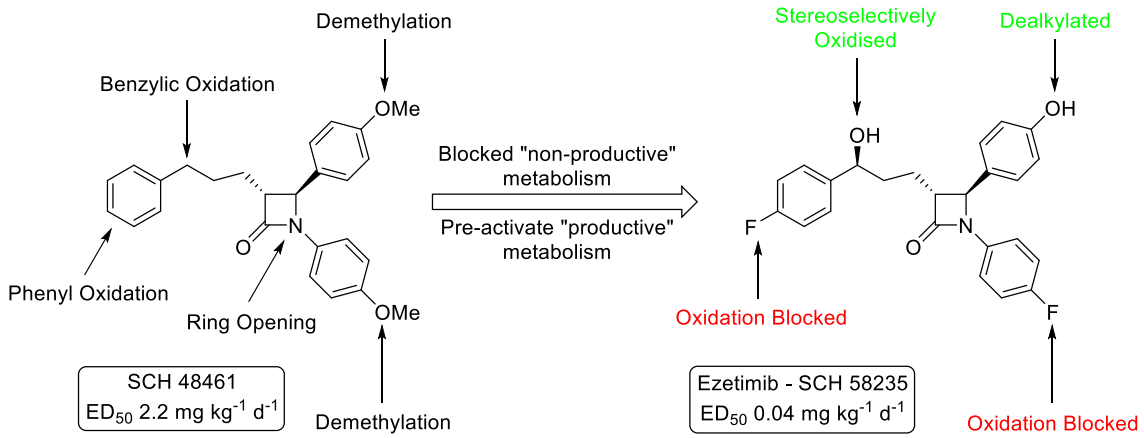

Figure 1.9. Metabolism-inspired lead optimisation of Ezetimib.

Radiolabelling studies of a first generation compound revealed a complex metabolic mixture in the bile of rats, which was found to be more potent than the original drug. Therefore, the introduction of the benzylic (*S*)-hydroxy group and the C4 hydroxy group were identified as beneficial, increasing the potency of the drug. On the other hand, "non-productive" metabolism was blocked by incorporating fluorine substituents at the *para*–positions of the phenyl rings. Generally, aromatic fluorine substituents can be used to block oxidation at the site of substitution, and they furthermore decrease the rate of reaction of the aromatic π-system with activated cytochrome P450(FeO)$^{3+}$.[47,48]

1.3. Strategies for Fluorination

There are three general strategies for the installation of C–F bonds, referred to as nucleophilic, electrophilic and radical fluorination, depending on the mode of reactivity of the fluorine atom source.

1.3.1. Nucleophilic Fluorination

Here, fluorine is introduced by the nucleophilic attack of fluoride anion on an alkyl chain or aryl ring bearing a suitable leaving group (Scheme 1.1).

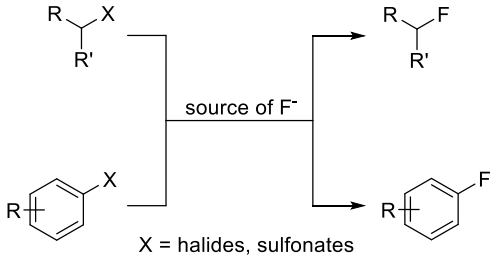

Scheme 1.1. Strategies for nucleophilic fluorination.

In the case of an aryl ring, the aromatic system needs to be highly electron-deficient in order to allow for this substitution to proceed. This strategy for fluorination has the inherent advantage that nucleophilic sources of fluorine are comparably cheap, as they don't require costly preparation.

Fluoride sources that have found wide-spread application in organic synthesis include various alkali-metal fluorides (e.g. KF, CsF), silver fluoride, tetraalkylammonium fluorides (e.g. TBAF), HF-based reagents (e.g. pyr/HF, $Et_3N{\cdot}3HF$),[49–51] hypervalent iodine derivatives (e.g. IPy_2BF_4, *p*-Tol–IF_2)[52,53] as well as fluorinated hypervalent silicates and stannates (e.g. TBAT).[54] See Figure 1.10 for selected examples.

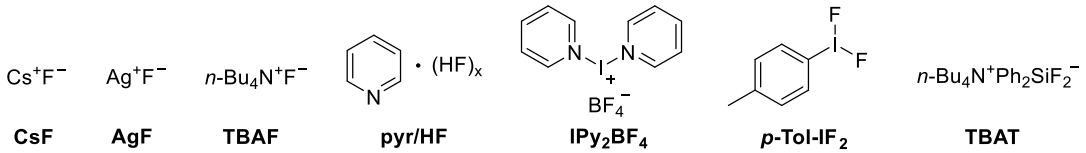

Figure 1.10. Examples of nucleophilic fluorinating reagents.

A specialised variant of the nucleophilic mode of fluorination is the deoxyfluorination reaction (Scheme 1.2).

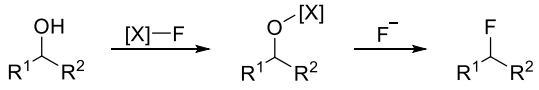

Scheme 1.2. General deoxyfluorination reaction.

Here, different reagents like diethylaminosulfur trifluoride (DAST)[55] and Deoxo-Fluor™[56,57] (Figure 1.11) are employed, which in a first step convert an alcohol functionality into a leaving group, thereby releasing fluoride anion, which in a second step displaces the leaving group, usually in an S_N2-type reaction.[58] Compared to these compounds XtalFluor™ reagents (aminodifluorosulfinium tetrafluoroborate salts), developed by Couturier, have been described as more stable, crystalline alternatives.[59–61] Recently, Ritter and Doyle developed the more selective reagents PhenoFluor[62] and PyFluor (Figure 1.11).[63]

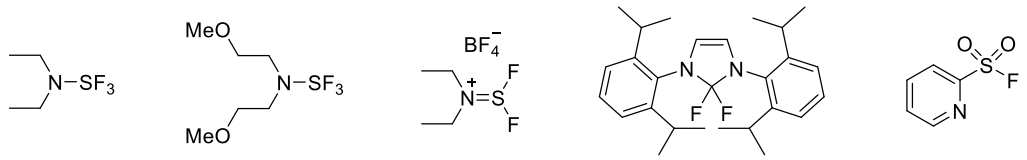

Figure 1.11. Examples of deoxyfluorination reagents.

1.3.2. Electrophilic Fluorination

For this strategy the roles of substrate and fluorinating reagent are reversed, meaning that the former acts as nucleophile and the latter provides formal electrophilic "F^+". Possible substrates include carbanions (e.g.: Grignard reagents), electron-rich

unsaturated systems (e.g.: arenes, alkenes, alkynes), and substrates containing a nucleophilic and labile bond (e.g.: C–Si, C–Sn, C–B) (Scheme 1.3).

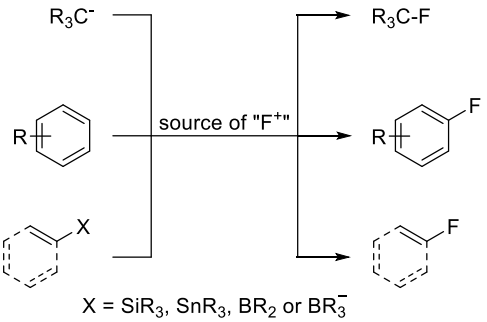

Scheme 1.3. Strategies for electrophilic fluorination.

Following O–F bond based reagents,[64–66] XeF_2[67] and elemental F_2,[68] which all suffer from low selectivity and in most cases an absence of commercial sources, mostly N–F bond containing reagents are used today. These include *N*-fluoropyridinium salts,[69] *N*-fluorobenzenesulfonimide (NFSI)[70] and 1-chloromethyl-4-fluoro-1,4-diazoniabicyclo[2.2.2]octane bis(tetrafluoroborate) (Selectfluor™) (Figure 1.12).[71]

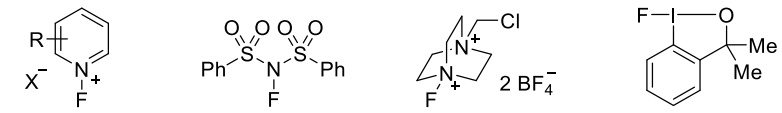

Figure 1.12. Examples of electrophilic fluorinating reagents.

Recently, chiral derivatives of Selectfluor™[72] as well as NFSI[73] have been developed by Gouverneur and Shibata, respectively (Figure 1.13).

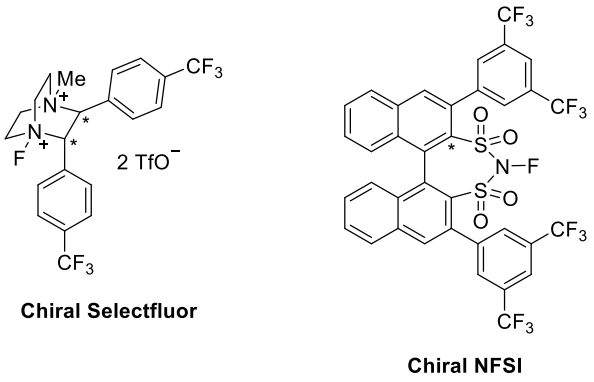

Figure 1.13. Structures of chiral electrophilic fluorinating reagents.

Also, a new class of electrophilic fluorinating reagent has been introduced by Stuart and co-workers in the form of a hypervalent iodine-based fluoroiodane (Figure 1.12).[74]

It is important to point out that these reagents do not form "F^+", which is an unknown species, but rather transfer the fluorine atom *via* single-electron transfer or through an S_N2-type attack. The exact mechanism for each reaction depends on the conditions used, the nature of the nucleophile as well the electrophilic fluorine source.

1.3.3. Radical Fluorination

Carbon-based radicals, which can be prepared by various means, have been shown to react with XeF_2, hypofluorite, and elemental fluorine, or more recently N–F bond-based reagents like NFSI and Selectfluor™ to form C–F bonds (Scheme 1.4).[75–77]

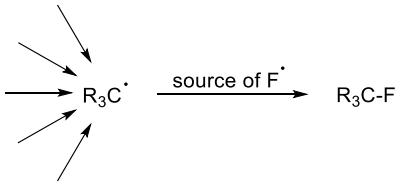

Scheme 1.4. General radical fluorination.

Part A

New Methods for Carbon–Fluorine

Bond Formation

Chapter 2: Hydrofluorination of Alkenylarenes under Pd-Catalysis

2.1. Introduction: Hydrofluorination of Alkenes and Alkynes

In recent years, considerable effort has been put into the development of novel, metal-mediated protocols for the hydrofluorination of alkenes and alkynes, as these reactions allow for the direct transformation of feedstock precursors into valuable, fluorinated alkanes and alkenes respectively.

2.1.1. Alkenes

Although previous studies had suggested the addition of HF to olefins to be impossible,[78] this reaction was first described in 1935 by adding simple alkenes like ethylene and propylene to anhydrous HF, which had first been filled into an autoclave.[79] The authors found 50% aqueous HF not to be reactive towards these substrates.

Olah, in 1973, reported that liquid pyr/HF, as a source of 'tamed HF',[80] can be used to achieve the same transformation on a range of olefinic hydrocarbons in a more convenient manner (Scheme 2.1).[51,81] The products were found to generally follow Markovnikov-type selectivity.

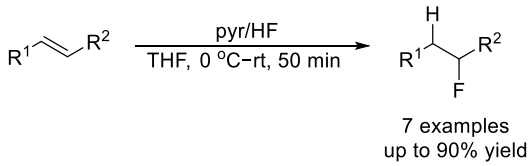

Scheme 2.1. Hydrofluorination of simple alkenes with pyr/HF.

This methodology was later expanded to the use of poly-4-vinylpyridinium poly(hydrogen fluoride), PVPHF, a solid and therefore more easily manageable source of HF.[82]

Moving away from hazardous HF based reagents, Boger, in 2012, presented the hydrofluorination of alkenes mediated by $Fe_2(ox)_3$, using Selectfluor™[71] and $NaBH_4$ as separate sources of atomic hydrogen and fluorine respectively (Scheme 2.2).[83]

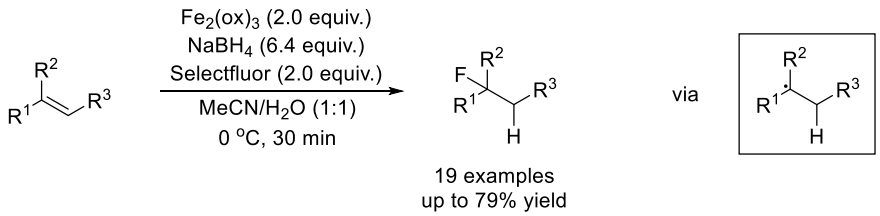

Scheme 2.2. Fe-mediated hydrofluorination of alkenes *via* radical intermediates.

This reaction proceeds *via* free radical intermediates and its outcome is determined by their relative stability, effecting exclusive Markovnikov-type regioselectivity. It was also found to be insensitive to air as well as moisture and to possess an excellent functional group tolerance, including unprotected alcohols, amines and carboxylic acids, esters, amides and epoxides.

Another hydrofluorination *via* radical intermediates was published in 2013 by Shigehisa and Hiroya. This Co-catalysed transformation uses 1,1,3,3-tetramethyldisiloxane and an *N*-fluoropyridinium salt as sources of atomic hydrogen and fluorine, respectively (Scheme 2.3).[84]

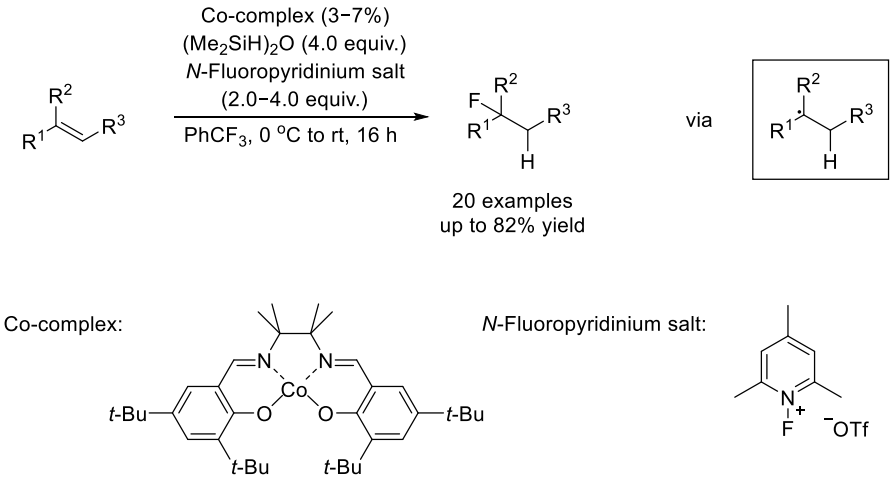

Scheme 2.3. Co-catalysed hydrofluorination of alkenes *via* radical intermediates.

The substrate scope includes examples of free alcohols, acetals, silyl ethers, esters, amides and aromatic halides.

2.1.2. Alkynes

In 1973, Olah first published the hydrofluorination of 1- and 3-hexyne with pyr/HF as liquid source of HF, giving rise to the *gem*-difluorinated alkanes as products of Markovnikov-type additions (Scheme 2.4).[51,81]

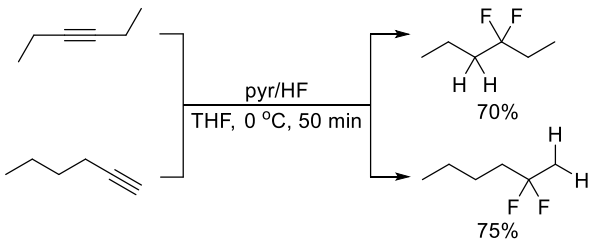

Scheme 2.4. Hydrofluorination of simple alkynes with pyr/HF.

As for alkenes, it was also possible to perform this reaction using PVPHF.[82]

The first Au-catalysed hydrofluorination of alkynes was described in 2007 by Sadighi and co-workers, using $Et_3N{\cdot}3HF$ as a milder source of HF that is comparably easy to handle (Scheme 2.5).[85]

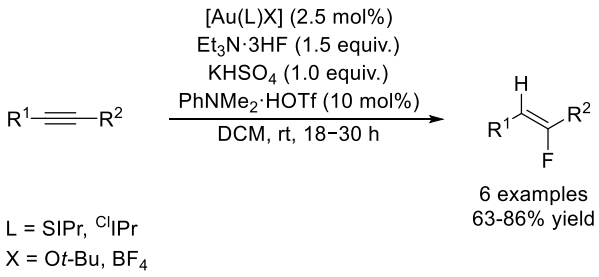

Scheme 2.5. *trans*-Hydrofluorination of internal alkynes under Au-catalysis.

This methodology was found to be limited to internal alkynes and requires the addition of acidic additives to obtain synthetically useful yields. All tested substrates led to the exclusive formation of the *trans*-product, consistent with initial *trans*-specific fluoroauration of the alkyne functionality followed by protodeauration under retention of stereochemistry. Alkynes bearing a phenyl as well as an alkyl substituent predominantly led to the formation of *β*-fluorostyrene products, with electron-poor aryl substituents leading to better selectivities. *gem*-Difluoroalkanes, which are formed by the direct reaction of alkynes with more acidic pyr/HF,[51,81] were not observed as by-products for this reaction.

Later, Miller and co-workers developed a regioselective hydrofluorination of alkynes, using different directing groups based on Sadighi's original reaction (Scheme 2.6).[86]

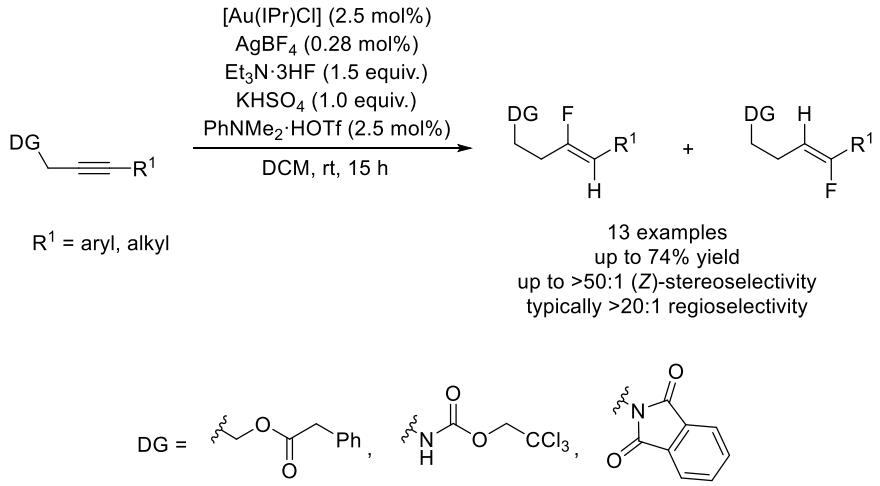

Scheme 2.6. Directed *trans*-hydrofluorination of alkynes under Au-catalysis.

Placing the directing group in an appropriate distance from the alkyne allowed for the reversal of the regioselectivity observed for substrates bearing a phenyl and an alkyl substituent, now giving the benzylic fluoride products in typically >20:1 regioselectivity. Alkynes with two alkyl substituents could also be regioselectively hydrofluorinated according to the spacing of the directing group from the pendant alkyne.

2.2. Results and Discussion

The early work described above, using highly reactive anhydrous HF or pyr/HF, suffers from substrate incompatibilities as well as handling problems, which limits their applicability. More recent contributions concerning the hydrofluorination of alkenes, on the other hand, follow radical pathways, which introduces problems with selectivity, while the Au-catalysed hydrofluorination of alkynes, developed by Sadighi and co-workers, remains limited to this kind of substrates.

In light of this, we sought to develop a novel hydrofluorination of unsaturated systems that would use mild conditions and reagents that are easy to handle, while not following a radical pathway. For this reason, we envisaged a metal-catalysed reaction following an ionic pathway, with separate sources for hydrogen and fluorine atom so as to avoid the use of HF based reagents. Hydropalladation of alkenes and alkynes is a well-known step in transition metal catalysed reactions[87] and could be employed here to form an organopalladium intermediate, which might in turn be susceptible to reaction with an electrophilic or nucleophilic source of fluorine to install the C–F bond.

Grushin and co-workers, in 1997, reported the first successful isolation of a Pd(II) monofluoride complex stabilised by triphenylphosphine,[88–90] while the first Pd(II) difluoride complexes of the general formula $(R_3P)_2PdF_2$ were described by Vigalok, in 2003.[91] Early efforts towards the formation of C–F bonds from organopalladium intermediates focussed on the potential use of Pd(0/II) catalytic cycles and were of limited success.[92] In 2006, the first transition metal catalysed C–F bond formation *via* a putative Pd(II/IV) catalytic cycle using *N*-fluoropyridinium reagents as an electrophilic source of fluorine was published by Sanford.[93] Further $C(sp^2)$–F and $C(sp^3)$–F bond forming reactions, including Pd-catalysed C–H fluorination[94,95] and olefin aminofluorination[96] using "F^+" reagents as well as stoichiometric aryl–F coupling from Pd(II)/"F^+",[97] whose putative catalytic cycles were all believed to include C–F bond formation *via* reductive elimination from transient (alkyl/aryl)–Pd(IV)–F intermediates, were published by different groups. Reductive elimination from a putative Pt(IV) intermediate to yield a $C(sp^3)$–F bond was shown by Gagné in 2011.[98] Finally, in 2012 Sanford and co-workers showed the feasibility of $C(sp^3)$–F bond formation *via* reductive

elimination from a Pd(IV) centre under retention of stereochemistry.[99] This was evidence that an organo–Pd(II) complex, which we would obtain after an initial hydropalladation, is a viable intermediate for subsequent C–F bond formation.

The subsequent work was carried out in collaboration with Dr. Enrico Emer and was published in *Angewandte Chemie* in 2013.[100]

2.2.1. Reaction Development

With this precedent in hand we set out to study the hydrofluorination of alkenylarenes, as they represent a class of activated alkenes, ideal for the development of a challenging, novel transformation. 4-Ethenyl-1,1'-biphenyl (**2.1a**) was chosen to be our test substrate, and we at first looked at different sources of electrophilic fluorine using [$Pd(PPh_3)_4$] as catalyst and *i*-Pr_3SiH as hydride source (Table 2.1). The reactions were stirred in anhydrous MeCN at 0 °C for 2 h before quenching by addition of water.

Table 2.1. Optimisation of hydrofluorination: Screening of "F^+"-sources.

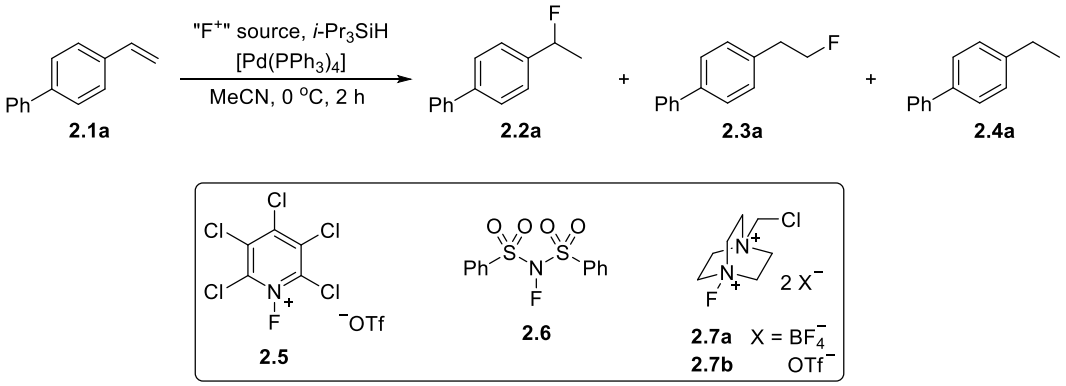

Entry	"F^+" Source	Conversion[a] [%]	**2.2a**[a] [%]	**2.3a**[a] [%]	**2.4a**[a] [%]
1	**2.5**	>95	0	0	23
2	**2.6**	25	11	0	12
3	XeF_2	72	16	11	28
4	**2.7a**	>95	30	0	0
5	**2.7b**	>95	34	0	0
6[b]	**2.7a**	>95	35	0	0

Conditions: 1.0 equiv. **2.1a** (0.10 mmol), 2.0 equiv. "F^+" source (0.20 mmol), 2.0 equiv. *i*-Pr_3SiH (0.20 mmol), 10 mol% [$Pd(PPh_3)_4$] (0.010 mmol), MeCN (2.0 mL). [a]Determined by ^1H NMR of the crude reaction product using 1-fluoro-3-nitrobenzene as internal reference. [b]4.0 mL MeCN.

Using *N*-fluoropyridinium salt **2.5** full consumption of the starting material was observed, but no peak indicative of either fluorinated product, **2.2a** or **2.3a**, was observed in ^{19}F NMR of the crude mixture (Table 2.1, Entry 1); 23% of **2.4a** was found as an unwanted by-product. Albeit NFSI (**2.6**) led to low conversion, a peak at 5.69 ppm (dq, *J* = 47.7, 6.6 Hz, 1H),[101] corresponding to product **2.2a**, was found in the ^1H NMR spectrum, which integrated to 11% relative to the internal reference (Table 2.1, Entry 2). XeF_2 increased the yield of **2.2a** to 16%, but it was obtained in a mixture with 11% of regioisomer **2.3a** (^1H NMR, diagnostic peaks: 4.65 ppm (dt, *J* = 47.2, 6.6 Hz, 2H), 3.11 ppm (dt, *J* = 23.2, 6.6 Hz, 2H))[102] (Table 2.1, Entry 3). With commercial Selectfluor™ (**2.7a**, BF_4^- counter-anion) a significant increase to 30% of **2.2a** was found, with no by-products **2.3a** or **2.4a** being formed (Table 2.1, Entry 4). To prove that the BF_4^- counter-anion was not involved

in this transformation, the reaction was repeated using the OTf^- analogue (**2.7b**), which led to a comparable result (Table 2.1, Entry 5). Since both reactions with **2.7a** and **2.7b** led to full consumption of starting material **2.1a**, but only returned 30% and 34% of $CDCl_3$ soluble products, respectively, we assumed polymerisation side reactions might cause this discrepancy. To test this, we halved the concentration, which increased the yield slightly from 30% to 35% (Table 2.1, Entry 6).

In an attempt to further improve the conversion into the desired benzylic fluoride **2.2a**, a range of different hydride sources was tested (Table 2.2).

Table 2.2. Optimisation of hydrofluorination: Screening of H^--sources.

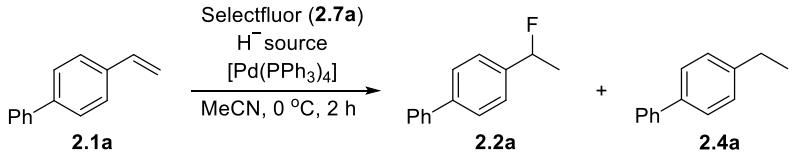

2.1a **2.2a** **2.4a**

Entry	H^--Source	Conversion[a] [%]	**2.2a**[a] [%]	**2.4a**[a] [%]
1	$PhSiH_3$	>95	0	31
2	$NaBH_4$	>95	18	48
3	Bu_3SnH	9	<5	0
4	-	0	0	0

Conditions: 1.0 equiv. **2.1a** (0.10 mmol), 2.0 equiv. Selectfluor™ (0.20 mmol), 2.0 equiv. H^--source (0.20 mmol), 10 mol% $[Pd(PPh_3)_4]$ (0.010 mmol), MeCN (4.0 mL). [a]Determined by ^1H NMR of the crude reaction product using 1-fluoro-3-nitrobenzene as internal reference.

In this study, $PhSiH_3$ as well as $NaBH_4$ were shown to lead to an increased formation of by-product **2.4a**, which was obtained in 31% and 48%, respectively, while 0% and 18% of alkyl fluoride **2.2a** were obtained (Table 2.2, Entries 1 and 2). In both reactions full consumption of starting material was observed. On the other hand, using Bu_3SnH was detrimental for reactivity, leading to a low conversion of 9% and a yield of **2.2a** of <5% (Table 2.2, Entry 3). Performing the reaction without any source of hydride led to full

recovery of starting olefin **2.1a**, proving the indispensability of such a reagent for this transformation (Table 2.2, Entry 4).

In the reactions carried out to this point we had also observed the formation of significant amounts of another fluorinated by-product, showing a signal at –175.6 ppm (sept, J = 6.4 Hz)[103] in ^{19}F NMR, which was identified as Et_3SiF. Because this process must be accompanied by the consumption of Selecfluor™ (**2.7a**), we carried out a series of experiments, varying the amounts of H^-- and "F^+"-sources to increase formation of **2.2a** (Table 2.3).

Table 2.3. Optimisation of hydrofluorination: Screening of H^-- and "F^+"-source amounts.

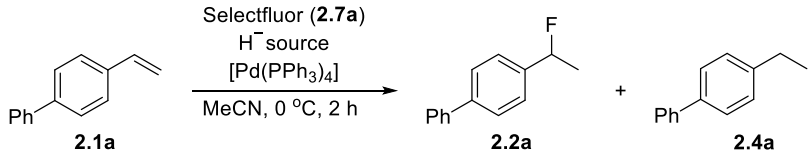

2.1a **2.2a** **2.4a**

Entry	Equiv. Selectfluor™	H^- Source (equiv.)	Conversion[a] [%]	**2.2a**[a] [%]	**2.4a**[a] [%]
1	2.0	*i*-Pr_3SiH (1.5)	>95	41	0
2	1.5	*i*-Pr_3SiH (1.5)	37	22	0
3	3.0	*i*-Pr_3SiH (1.5)	>95	54	0
4	3.0	Et_3SiH (1.5)	>95	69	0
5[b]	3.0	Et_3SiH (1.5)	>95	48	15

Conditions: 1.0 equiv. **2.1a** (0.10 mmol), Selectfluor™ (as in table), H^--source (as in table), 10 mol% $[Pd(PPh_3)_4]$ (0.010 mmol), MeCN (4.0 mL). [a]Determined by ^{1}H NMR of the crude reaction product using 1-fluoro-3-nitrobenzene as internal reference. [b]Reaction carried out at rt.

At first, the amount of *i*-Pr_3SiH was reduced to 1.5 equiv., which increased the yield of **2.2a** from 35% (Table 2.1, Entry 6) to 41% (Table 2.3, Entry 1) Decreasing the amount of Selectfluor™ (**2.7a**) to 1.5 equiv., however, had a detrimental effect on the reaction (22% of **2.2a**) (Table 2.3, Entry 2), while increasing it to 3.0 equiv. improved the yield of **2.2a** to 54% (Table 2.3, Entry 3). Substituting *i*-Pr_3SiH for Et_3SiH improved this yield further to

69% (Table 2.3, Entry 4). Working at low temperature (0 °C) was necessary, as an increase to rt was shown to lead to a lower yield of alkyl fluoride **2.2a** and an increased formation of reduced by-product **2.4a** (Table 2.3, Entry 5).

Finally, we tested whether the use of a different Pd-catalyst could improve the outcome of this reaction (Table 2.4).

Table 2.4. Optimisation of hydrofluorination: Screening of Pd-catalysts.

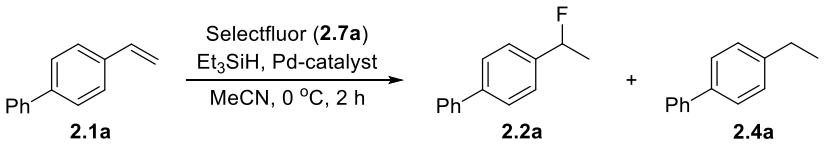

2.1a 2.2a 2.4a

Entry	Pd-catalyst	Conversion[a] [%]	**2.2a**[a] [%]	**2.4a**[a] [%]
1	$Pd(OAc)_2$	>95	27	10
2	$[Pd(MeCN)_2Cl_2]$	>95	38	12
3	$[Pd(dba)_2]$	92	31	16
4	-	10	0	0

Conditions: 1.0 equiv. **2.1a** (0.10 mmol), 3.0 equiv. Selectfluor™ (0.30 mmol), 1.5 equiv. Et_3SiH (0.15 mmol), 10 mol% Pd-catalyst (0.010 mmol), MeCN (4.0 mL). [a]Determined by ^1H NMR of the crude reaction product using 1-fluoro-3-nitrobenzene as internal reference.

PdOAc and $[Pd(MeCN)_2Cl_2]$ as examples of Pd(II)-catalysts reduced the yield of **2.2a** to 27% and 38%, respectively, with 10% and 12% of by-product **2.4a** being formed (Table 2.4, Entries 1 and 2). $Pd(dba)_2$ gave a comparable result with 31% **2.2a** and 16% **2.4a** (Table 2.4, Entry 3). Therefore, we concluded that initially used $[Pd(PPh_3)_4]$ was our optimal catalyst for this reaction. In absence of a source of Pd, however, neither product was observed after 2 h (Table 2.4, Entry 4).

With our optimised reaction conditions in hand (3.0 equiv. Selectfluor™ (**2.7a**), 1.5 equiv. Et_3SiH, 10 mol% $[Pd(PPh_3)_4]$, MeCN, 0 °C, 2 h), we then set out to study the scope of this transformation.

2.2.2 Substrate Scope

To test the substrate scope of this hydrofluorination of alkenylarenes we at first employed a range of styrene derivatives, bearing different aromatic substituents, under our standard conditions, to study the compatibility of different functional groups as well as the effect of varying electronic bias (Scheme 2.7).

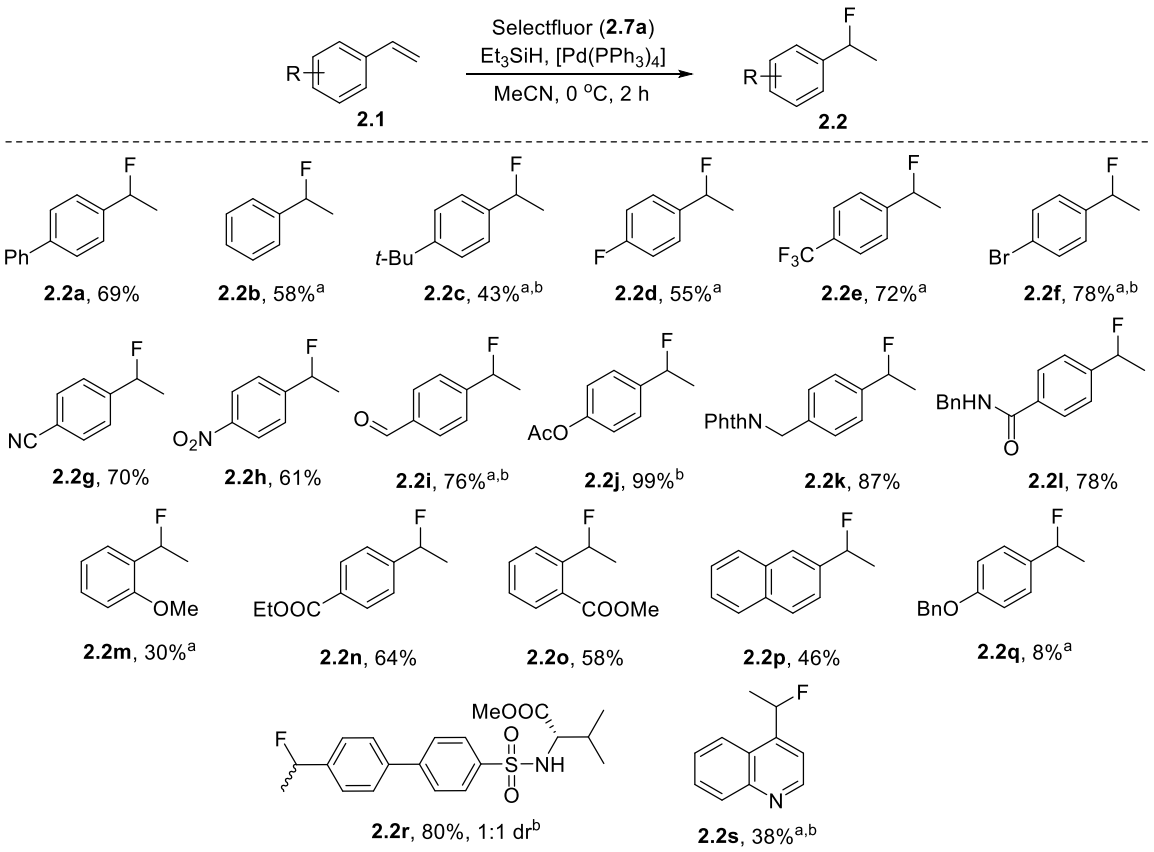

Scheme 2.7. Substrate scope of hydrofluorination of alkenylarenes: Unsubstituted alkenes. Conditions: 1.0 equiv. **2.1** (0.20 mmol), 3.0 equiv. Selectfluor™ (0.60 mmol), 1.5 equiv. Et_3SiH (0.30 mmol), 10 mol% $[Pd(PPh_3)_4]$ (0.020 mmol), MeCN (8.0 mL). [a]Reaction performed with 0.050 mmol **2.1** in MeCN-d_3 (1.0 mL). Yield determined by ^1H NMR using 1-fluoro-3-nitrobenzene as internal reference. [b]Prepared by Dr. E. Emer.

The reaction was found to tolerate a broad range of different functional groups, giving good to excellent yields. Product **2.2f**, bearing an aromatic bromide, which can be used for further functionalisation, was obtained in 78% yield. Also, hydrolysable esters (**2.2j**, **2.2n**, **2.2o** and **2.2r**), amides (**2.2l**), phthalimides (**2.2k**) and sulphonamides (**2.2r**) as well

as reactive aldehydes (**2.2i**) were compatible with this transformation, leading to yields ranging from 58% to 99%. More electron-poor substrates **2.1e** (4-CF_3), **2.1g** (4-CN) and **2.1h** (4-NO_2) give consistent yields between 61% and 72%. Electron-rich styrenes like **2.1c** (4-*t*-Bu), **2.1m** (2-OMe) and **2.1q** (4-OBn), on the other hand, show lower yields between 8% and 43%, with products being unstable to silica due to loss of fluoride, aided by increased stabilisation of positive charge in the benzylic position. **2.2s**, derived from 4-vinylquinoline, was obtained in 38% yield and shows the compatibility of heteroaromatics with this protocol, although the yield was lower compared to related electron-poor styrenes.

2.2k was found to be a crystalline solid and allowed us to obtain a single-crystal X-ray diffraction structure, which unambiguously proved the formation of the benzylic fluoride product. (Figure 2.1).

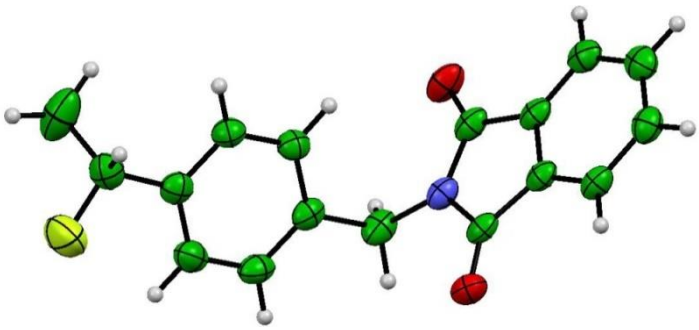

Figure 2.1. Single-crystal X-ray structure of **2.2k**. Displacement ellipsoid plot drawn at 50% probability.

Having determined the electronic limitations of this protocol, we turned our attention to studying the influence of increased steric hindrance by introducing substituents in α- and β-position of the alkene (Scheme 2.8).

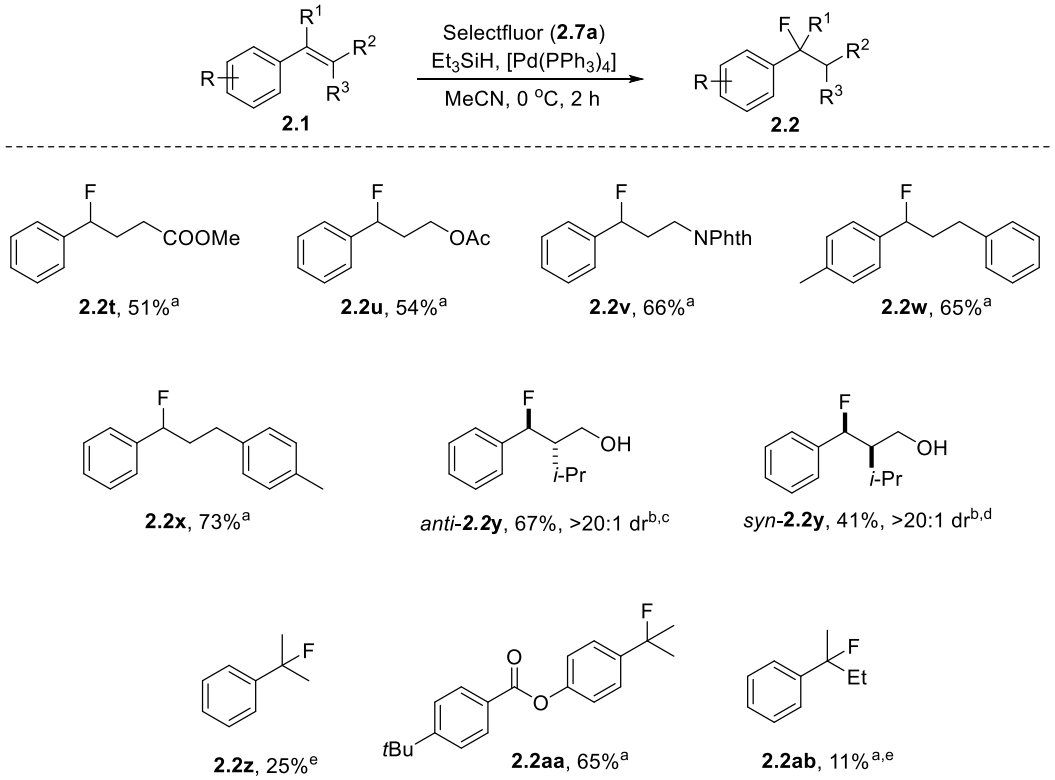

Scheme 2.8. Substrate scope of hydrofluorination of alkenylarenes: Substituted alkenes. Conditions: 1.0 equiv. **2.1** (0.20 mmol), 3.0 equiv. Selectfluor™ (0.60 mmol), 1.5 equiv. Et_3SiH (0.30 mmol), 10 mol% $[Pd(PPh_3)_4]$ (0.020 mmol), MeCN (8.0 mL). [a]Prepared by Dr. E. Emer. [b]Reaction time was 15 h. [c]Prepared from (*E*)-2-benzylidene-3-methyl-butan-1-ol ((*E*)-**2.1y**). [d]Prepared from (*Z*)-**2.1y**. [e]Reaction performed with 0.050 mmol **2.1** in MeCN-d_3 (1.0 mL). Yield determined by ^{1}H NMR using 1-fluoro-3-nitrobenzene as internal reference.

Products **2.2t**–**x** show mono-substitution on the β-carbon to be readily tolerated, as they were obtained in yields comparable to parent styrene **2.2b**. Furthermore, **2.2w** and **2.2x** demonstrate the possibility to selectively introduce fluorine on the former C(sp^2) benzylic carbon. *Anti*- and *syn*-**2.2y** were successfully prepared in 67% and 41% yield with >20:1 dr, proving that also double substitution at β-position is compatible with this reaction. For substrates **2.2z**, **2.2aa** and **2.2ab** we see greatly varying yields between 11% and 65%, but generally α-substitution seems to be detrimental to the outcome of this reaction. The exceptionally high yield obtained for **2.2aa** might be resulting from the fact that it is an esterified phenol derivative, which seems to be a preferred substitution pattern (compare **2.2j** in Scheme 2.7). Comparing **2.2z** and **2.2ab** we see a decrease in yield, going

from 25% to 11%, indicating that the increased steric congestion caused by the α-Et group in **2.2ab** compared to the α-Me-group in **2.2z** has a negative impact on this transformation.

Given the success of this hydrofluorination with alkenylarenes, we sought to also extend it to non-activated alkenes (Scheme 2.9).

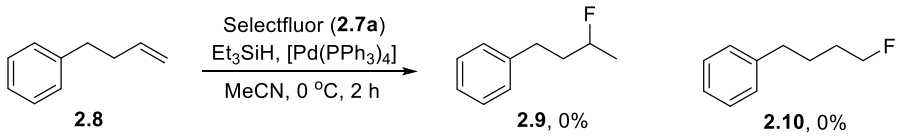

Scheme 2.9. Hydrofluorination of non-activated terminal alkene **2.8**. Conditions: 1.0 equiv. **2.8** (0.10 mmol), 3.0 equiv. Selectfluor™ (0.30 mmol), 1.5 equiv. Et_3SiH (0.15 mmol), 10 mol% $[Pd(PPh_3)_4]$ (0.010 mmol), MeCN (4.0 mL).

Using our standard reaction conditions on substrate **2.8**, however, did not lead to the formation of either of the possible hydrofluorinated products **2.9** or **2.10**. Instead, ^1H NMR showed a mixture of different alkene species, indicating that double bond migration had occurred. This is commonly observed under Pd-catalysis, with a hydropalladation step followed by β-hydride elimination.[104]

This result brought up the question, what would happen if we employed a substrate including both a styrene-type double bond as well as a non-activated one (Scheme 2.10).

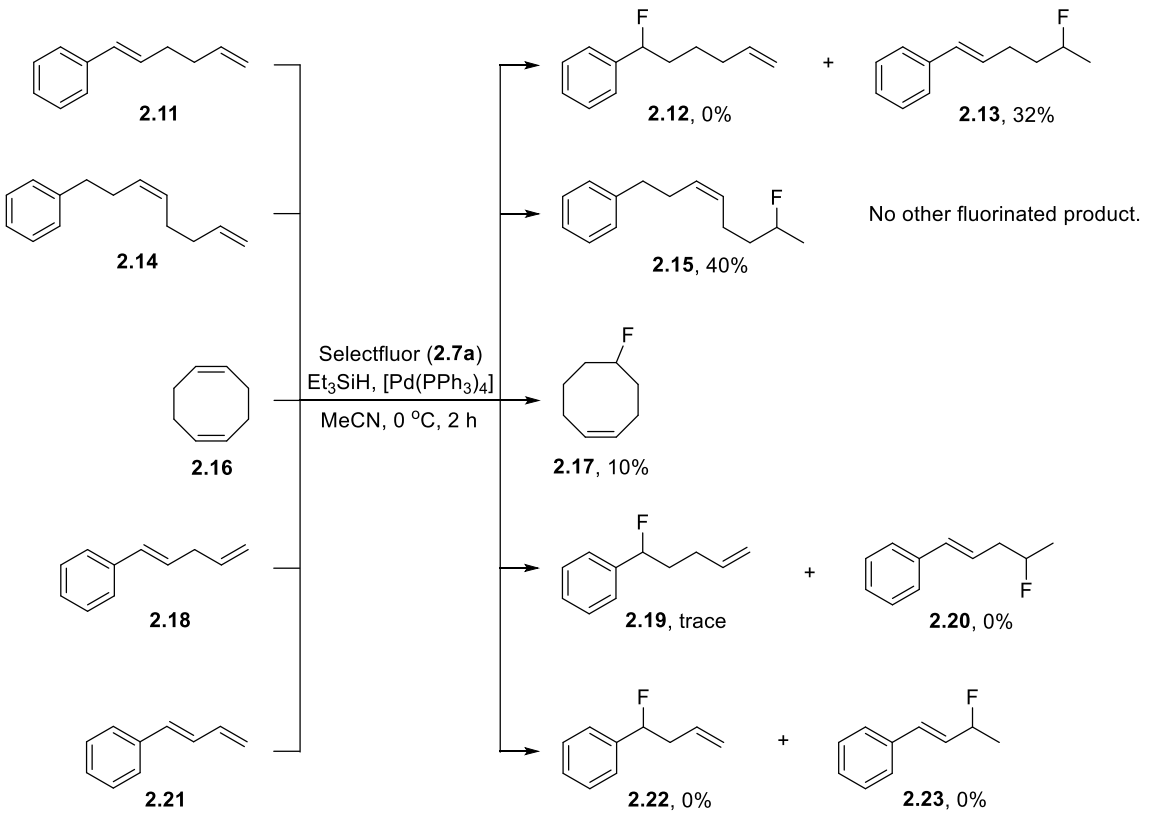

Scheme 2.10. Hydrofluorination of dienes. Conditions: 1.0 equiv. diene (0.10 mmol), 3.0 equiv. Selectfluor™ (0.30 mmol), 1.5 equiv. Et_3SiH (0.15 mmol), 10 mol% $[Pd(PPh_3)_4]$ (0.010 mmol), MeCN (4.0 mL). Yields determined by ^{19}F NMR using 1-fluoro-3-nitrobenzene as internal reference.

We initially performed our reaction on 1,5-diene **2.11** and found no benzylic product **2.12** in the crude reaction mixture, but a new signal at –173.7 ppm (m) in the ^{19}F NMR that integrated to 32% relative to the internal reference, which we assigned to the Markovnikov-type hydrofluorination product of the non-activated terminal double bond, **2.13**. Given the well documented formation of Pd-complexes with 1,5-dienes due to their chelating nature, it is possible that such an intermediate is formed, which then preferentially reacts at the non-activated alkene.[105,106]. $[Pd(COD)Cl_2]$, for example, has been shown to be a viable intermediate for the hydroamination and hydroalkoxylation of one double bond of COD.[107] A similar result was found when using 1,5-diene **2.14** featuring a (*Z*)-configured internal double bond, where the terminal double bond was also selectively hydrofluorinated to give **2.15** in 40% yield as the only fluorinated product.

Using 1,5-diene **2.16** (COD), which forms isolable complexes with Pd(II),[108] only resulted in the formation of 10% of hydrofluorinated product **2.17**. Pd can furthermore form complexes with 1,3- and 1,4-dienes,[105] and these dienes have also been used as substrates in Pd-catalysed transformations.[109–117] Therefore, we carried out reactions with 1,4-diene **2.18** and 1,3-diene **2.21** to study the dependency of this hydrofluorination reaction on the spacing of the double bonds. Neither reaction resulted in the formation of terminally hydrofluorinated products **2.20** and **2.23** and only **2.18** led to trace amounts of benzylic fluoride (**2.19**).

Finally, we also tried to extend this methodology to alkyne substrates and chose 4-ethynyl-1,1'-biphenyl (**2.24**) as test substrate (Scheme 2.11).

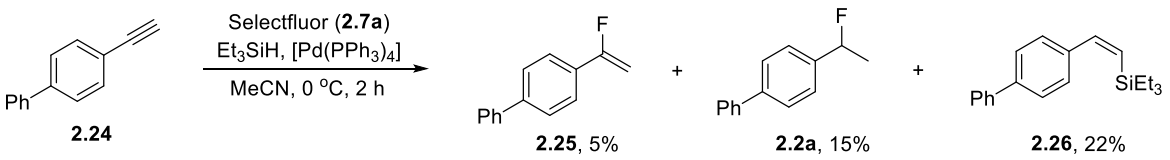

Scheme 2.11. Hydrofluorination of alkyne **2.24**. Conditions: 1.0 equiv. **2.1** (0.10 mmol), 3.0 equiv. Selectfluor™ (0.30 mmol), 1.5 equiv. Et_3SiH (0.15 mmol), 10 mol% $[Pd(PPh_3)_4]$ (0.010 mmol), MeCN (4.0 mL). Yields determined by ^1H NMR using 1-fluoro-3-nitrobenzene as internal reference.

Analysis of the NMR spectrum of the crude product after 2 h reaction time revealed full consumption of starting material and formation of a mixture of products **2.25**, **2.2a** and **2.26** in 5%, 15% and 22% yield relative to our internal reference. The insufficient mass balance, we speculated, might be due to polymerisation as there was no other product detected in ^1H and ^{19}F NMR of the crude mixture. This outcome meant that these conditions were not suitable for the hydrofluorination of alkynes

2.2.3. Mechanistic Experiments

At the outset of our mechanistic studies of this hydrofluorination of alkenylarenes we wanted to prove that the newly introduced hydrogen originates from Et_3SiH. In order to do so, we subjected styrene **2.1b** to reaction conditions using commercially available Et_3SiD instead of protonated Et_3SiH. (Figure 2.2).

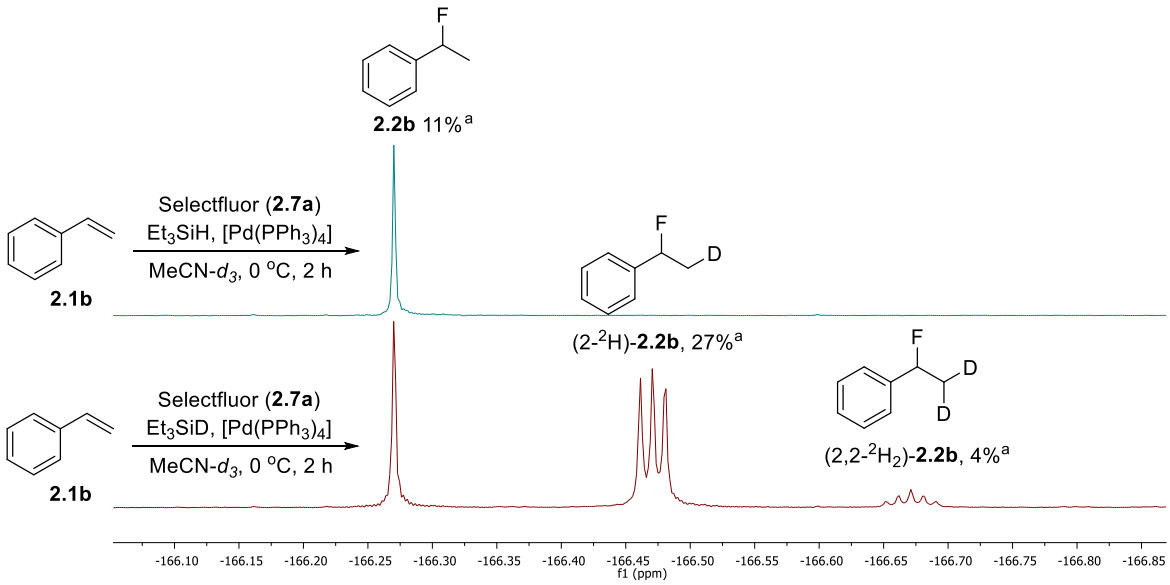

Figure 2.2. Mechanistic studies: Hydrofluorination of **2.1b** with Et_3SiH and Et_3SiD. Regions of interest in ^{19}F-{^1H} NMR spectra of crude reaction mixtures are shown. Conditions: 1.0 equiv. **2.1b** (0.050 mmol), 3.0 equiv. Selectfluor™ (0.15 mmol), 1.5 equiv. Et_3SiH/Et_3SiD (0.075 mmol), 10 mol% [$Pd(PPh_3)_4$] (0.0050 mmol), MeCN-d_3 (1.0 mL). Yields determined by ^{19}F NMR using 1-fluoro-3-nitrobenzene as internal reference. [a]Yields for reaction with Et_3SiD.

Compared to the hydrofluorination under standard conditions (Figure 2.2, top) where benzylic fluoride **2.2b** is the only fluorinated product, there are three such products in the crude reaction mixture of the reaction with Et_3SiD (Figure 2.2, bottom). These are **2.2b** and the mono-as well as *gem*-dideuterated analogues, (2-^2H)-**2.2b** and (2,2-$^2H_2$-**2.2b**), which had been formed in 11%, 27% and 4%, respectively. Firstly, formation of (2-^2H)-**2.2b** confirms that the newly introduced hydrogen is supplied by the silane reagent, which is the only possible source of deuterium in this reaction, as the solvent had been

ruled out before. The additional formation of undeuterated **2.2b** and (2,2-$^2H_2$-**2.2b**) requires the hydropalladation, which is postulated to be the initial step of the catalytic cycle, to be reversible. This would allow for an elimination of a Pd(II)–H species to occur after deuteropalladation to give a deuterated styrene, (2-^{2}H-**2.1b**), which can undergo a second deuteropalladation to give product (2,2-$^2H_2$-**2.2b**). The obtained Pd(II)–H could form **2.2b** upon reaction with **2.1b**. As further evidence for this a trace amount of (2-^{2}H-**2.1b**) was found in ^{1}H NMR. These findings are in line with observations in the literature.[118]

A comparable result was obtained with substrate **2.1g** – Scheme 2.12 shows the product distribution as determined by ^{1}H NMR relative to an internal reference.

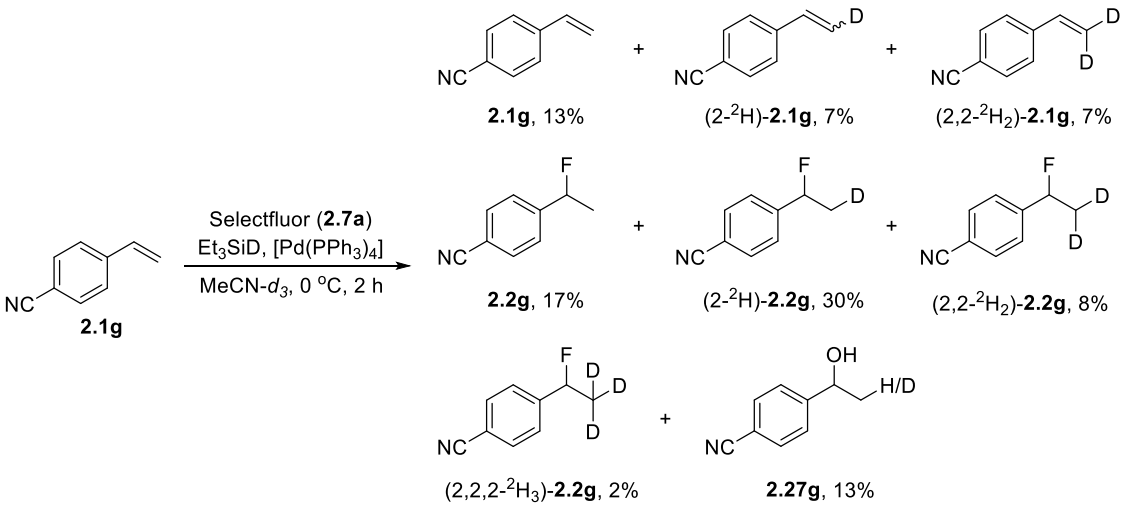

Scheme 2.12. Mechanistic studies: Product distribution after hydrofluorination of **2.1g** with Et_3SiD. Conditions: 1.0 equiv. **2.1g** (0.050 mmol), 3.0 equiv. Selectfluor™ (0.15 mmol), 1.5 equiv. Et_3SiD (0.075 mmol), 10 mol% [$Pd(PPh_3)_4$] (0.0050 mmol), MeCN-d_3 (1.0 mL). Reaction carried out by Dr. E. Emer. Yields determined by ^{19}F NMR using 1-fluoro-3-nitrobenzene as internal reference.

The main product was deuterofluorinated (2-^{2}H-**2.2g**), which was formed in 30% yield alongside 8% of (2,2-$^2H_2$-**2.2g**) and 2% of (2,2,2-$^2H_3$-**2.2g**) as well as 17% of undeuterated **2.2g**. Furthermore, 13% of starting material and 7% of each of the deuterated analogues (2-^{2}H-**2.1g**) and (2,2-$^2H_2$-**2.1g**) were also found. The presence of deuterated benzylic

alcohol **2.27g** suggests that this by-product is also formed *via* an initial hydropalladation step.

We then turned our attention towards establishing whether the addition of HF overall follows *syn*- or *anti*-specificity. To this end, we synthesised substrates (*E*)-**2.1y** and (*Z*)-**2.1y** with two β-substituents, which would contain two adjacent stereogenic centres after hydrofluorination and should therefore give rise to two different diastereoisomers, depending on the double bond geometry in the starting material. Hydrofluorination gave two different products, clearly distinguishable by NMR but with the same mass (Scheme 2.13).

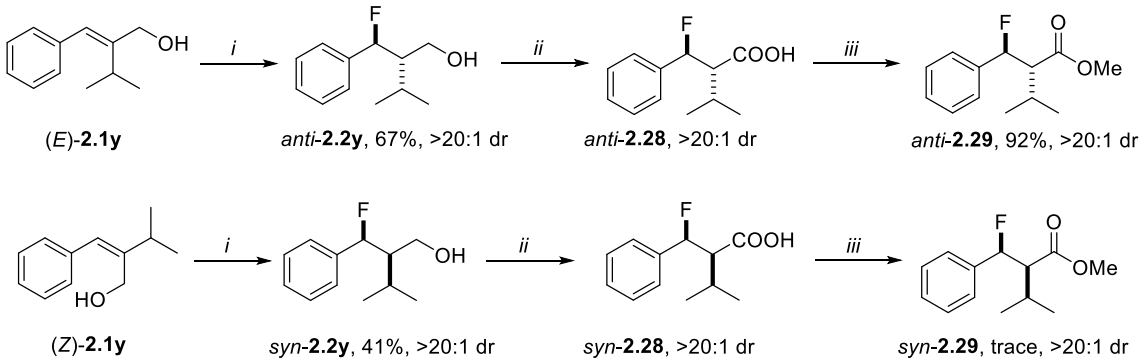

Scheme 2.13. Mechanistic studies: Determination of stereochemistry of **2.2y** derived from hydrofluorination of (*E*)-**2.1y** and (*Z*)-**2.1y**. Conditions: *i*: 1.0 equiv. **2.1y** (0.20 mmol), 3.0 equiv. Selectfluor™ (0.60 mmol), 1.5 equiv. Et_3SiH (0.30 mmol), 10 mol% $[Pd(PPh_3)_4]$ (0.020 mmol), MeCN (8.0 mL). *ii*: 2 mol% TEMPO, 3.0 equiv. $NaClO_2$, 2 mol% NaOCl, MeCN (2.0 mL), sodium phosphate buffer pH 6.7 (0.67 M, 1.5 mL), 35 °C, 15 h. *iii*: Excess of TMS-diazomethane, MeOH (5.0 mL), 0 °C, 15 min. Steps *ii* and *iii* carried out by Dr. E. Emer.

The products (**2.2y**) were at first oxidised to the according carboxylic acids (**2.28**) and then converted into the methyl esters (**2.29**) without altering the relative configuration. *Anti*- and *syn*-**2.29** were known compounds, and comparison of the ^{19}F NMR shifts of our products with the literature values revealed the selective formation of *anti*-**2.29** and *syn*-**2.29** starting from (*E*)-**2.1y** and (*Z*)-**2.1y**, respectively (Figure 2.3).[119]

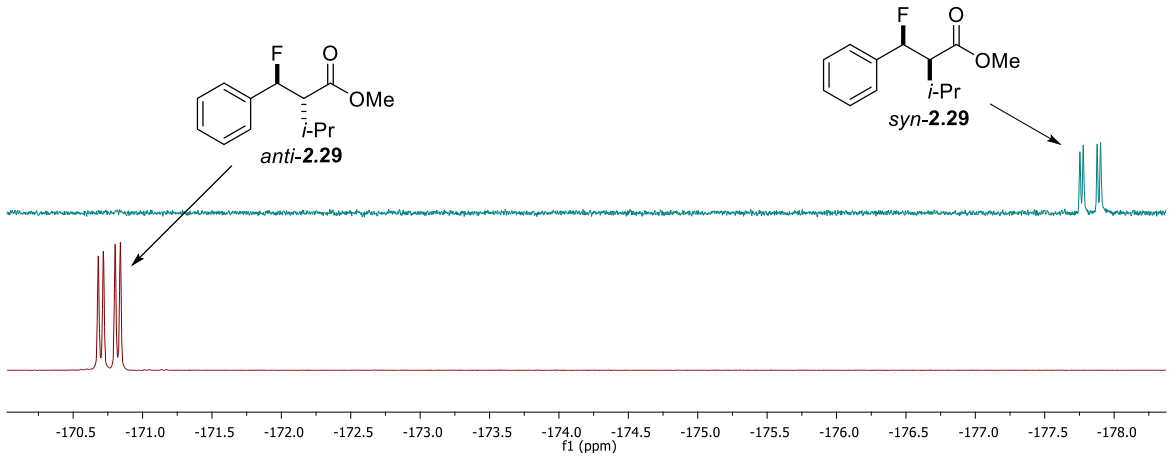

Figure 2.3. Mechanistic studies: ^{19}F NMR shifts of *anti*- and *syn*-**2.29**. Lit.: *anti*-**2.29**: δ –170.8 ppm (dd, *J* = 45.9, 14.0 Hz); *syn*-**2.29**: δ –177.8 ppm (dd, *J* = 47.0, 9.3 Hz).

This stereochemical outcome is indicative of a *syn*-specific addition of HF across the double bond. This is in contrast to earlier results by Hartwig and co-workers, who for their addition of anilines to vinylarenes observed *anti*-specificity.[120]

Further proof of the *syn*-specificity of our reaction was obtained by the deuterofluorination of (*Z*)-stilbene using Et_3SiD, and independent preparation of the expected *anti*-product (*anti*-(2-^{2}H)-**2.31)** from *cis*-stilbene oxide *via* epoxide opening with $LiAlD_4$ to benzylic alcohol *syn*-(2-^{2}H)-**2.30** followed by deoxyfluorination under inversion (Figure 2.4).

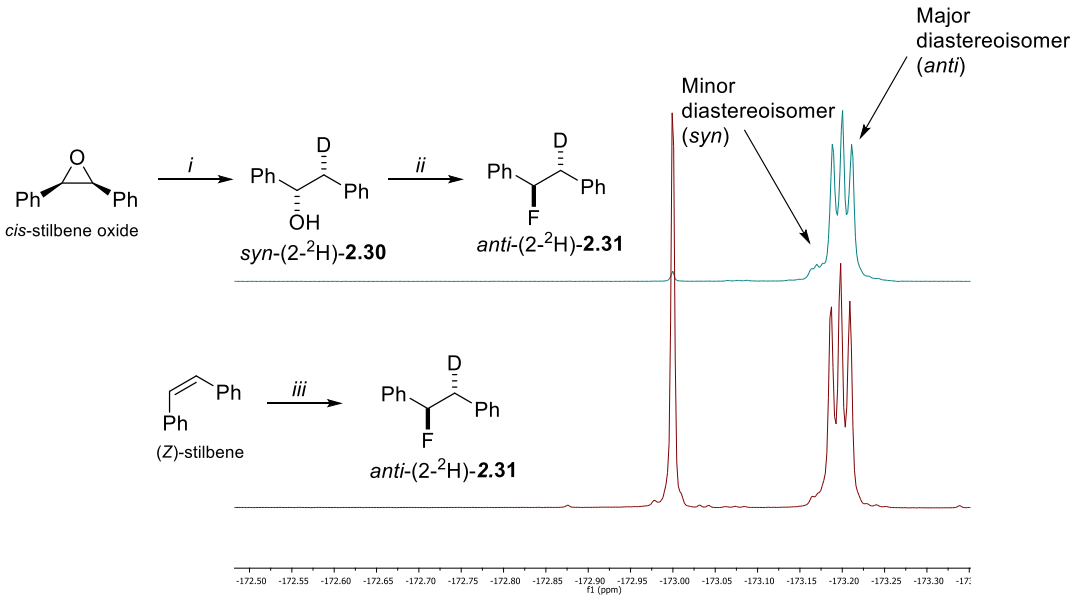

Figure 2.4. Mechanistic studies: Deuterofluorination of (*Z*)-stilbene and comparison of ^{19}F-{^{1}H} NMR with independently prepared product *anti*-(2-^{2}H)-**2.31**. Conditions: *i*: 1.0 equiv. *cis*-stilbene oxide (2.40 mmol), 1.2 equiv. $LiAlD_4$ (2.87 mmol), Et_2O (5.0 mL), 0 °C to rt, 22 h; *ii*: 1.0 equiv. *syn*-(2-^{2}H)-**2.30** (0.37 mmol), 3.4 equiv. *N*-(trimethylsilyl)morpholine (1.25 mmol), 3.3 equiv. DAST (1.22 mmol), DCM (1.6 mL), rt, 15 h; *iii*: 1.0 equiv. (*Z*)-stilbene (0.10 mmol), 3.0 equiv. Selectfluor™ (0.30 mmol), 1.5 equiv. Et_3SiD (0.15 mmol), 10 mol% $[Pd(PPh_3)_4]$ (0.010 mmol), MeCN (4.0 mL).

Comparison of the ^{19}F NMR spectra of the product prepared from (*Z*)-stilbene with the independently prepared reference showed matching peaks. The major *anti*-diastereoisomer thereby resonates at higher field compared to the *syn*- isomer and shows a larger coupling constant, $^{3}J_{F-D}$, due to the different dihedral angles between the C–F and C–D bonds; this is consistent with earlier reports.[121,122]

To prove *syn*-specificity in the case of the hydrofluorination of stilbene the same was done using (*E*)-stilbene and *trans*-stilbene oxide (Figure 2.5).

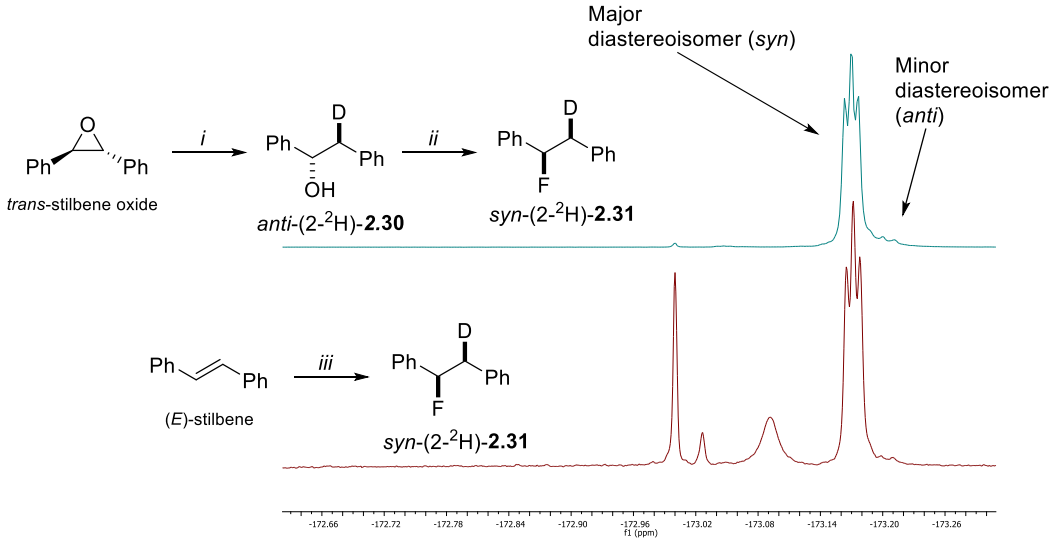

Figure 2.5. Mechanistic studies: Deuterofluorination of (*E*)-stilbene and comparison of ^{19}F-{^{1}H} NMR with independently prepared product *syn*-(2-^{2}H)-**2.31**. Conditions: *i*: 1.0 equiv. *trans*-stilbene oxide (4.00 mmol), 1.2 equiv. $LiAlD_4$ (4.80 mmol), Et_2O (9.0 mL), 0 °C to rt, 22 h; *ii*: 1.0 equiv. *anti*-(2-^{2}H)-**2.30** (0.37 mmol), 3.4 equiv. *N*-(trimethylsilyl)morpholine (1.25 mmol), 3.3 equiv. DAST (1.22 mmol), DCM (1.6 mL), rt, 15 h; *iii*: 1.0 equiv. (*E*)-stilbene (0.10 mmol), 3.0 equiv. Selectfluor™ (0.30 mmol), 1.5 equiv. Et_3SiD (0.15 mmol), 10 mol% $[Pd(PPh_3)_4]$ (0.010 mmol), MeCN (4.0 mL).

Also in this case, the ^{19}F NMR signals of hydrofluorination product and reference compound matched, thereby proving the overall *syn*-specificity of our reaction.

Given the well-established *syn*-specificity of the hydropalladation step[87] this necessitates the C–F bond formation to proceed under retention of stereochemistry, which is consistent with the studies by Gagné[98,123] and Sanford.[99] To demonstrate that this step is possible *via* reductive elimination from an organo–Pd(II) intermediate, we prepared η^3-benzyl Pd-complex **2.32**, ligated with dppp, following a protocol developed by Hartwig and co-workers.[120,124] **2.32** was treated with Selectfluor™, and the reaction was followed by ^{1}H and ^{19}F NMR (Scheme 2.14). dppp was chosen as ligand coordinating to the Pd-centre in **2.29** after attempts of isolating an analogous complex bearing PPh_3 had failed.

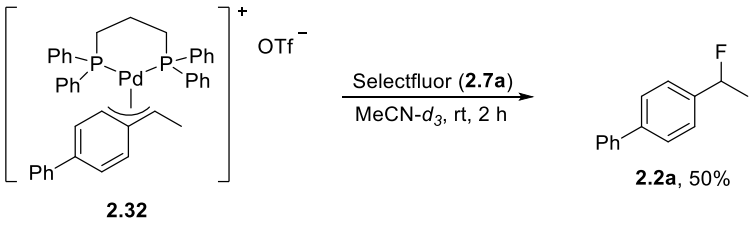

Scheme 2.14. Mechanistic studies: C(sp^3)–F bond formation from η^3-benzyl complex **2.32**. Conditions: 1.0 equiv. **2.32** (0.020 mmol), 1.2 equiv. Selectfluor™ (0.024 mmol), MeCN-d_3 (0.50 mL), rt, 2 h.

2.2a was obtained in 50% yield after 2 h and this result shows the possibility of C–F bond formation in our hydrofluorination protocol to occur from an organo–Pd(II) intermediate. Generally speaking, this can happen following an outer- or inner-sphere mechanism, leading to inversion or retention of stereochemistry at the benzylic carbon. Our previous observations were consistent with the latter and therefore suggested an inner-sphere mechanism, proceeding *via* an organo–Pd(IV)–F. To test this, complex **2.33**, bearing a chiral (*R*)-T-BINAP ligand, was prepared following the aforementioned protocol.[120,124] It was then subjected to Selectfluor™ and XeF_2 and the results were compared with its reaction with aniline, which Hartwig had shown leads to inversion of stereochemistry, as the result of an outer-sphere-type attack of the nucleophile on the benzylic carbon (Scheme 2.15).[120]

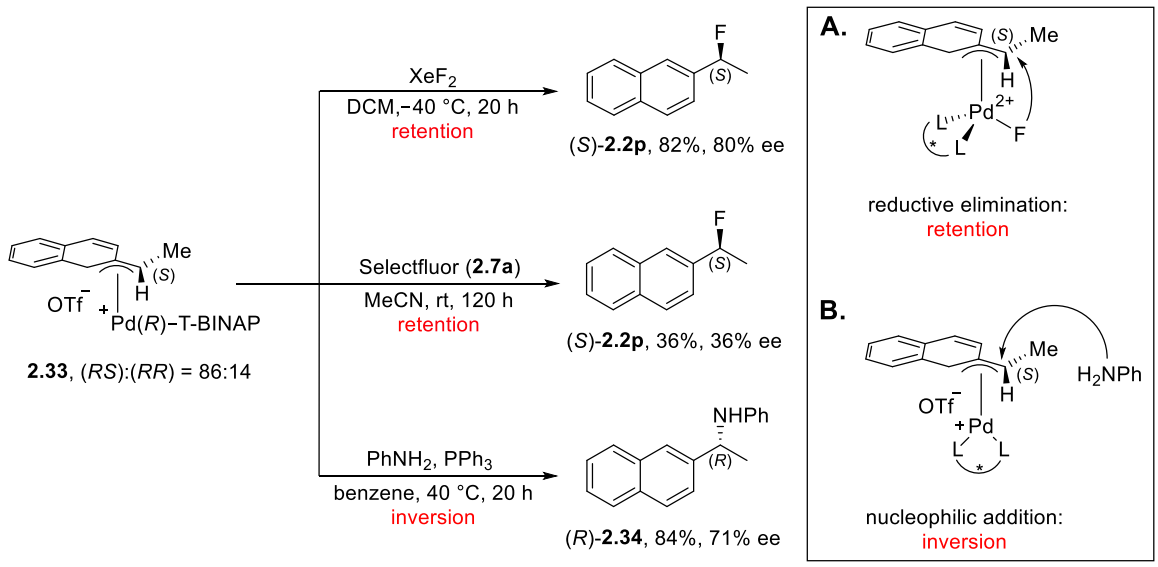

Scheme 2.15. Mechanistic studies: Comparison of benzylic fluorination and amination of η^3-benzyl Pd-complex **2.33** ligated with chiral (*R*)-T-BINAP. Conditions: 1.0 equiv. **2.33** (0.010 mmol), 1.5 equiv. XeF_2 (0.015 mmol), DCM (0.50 mL), –40 °C, 20 h; 1.0 equiv. **2.33** (0.010 mmol), 1.5 equiv. Selectfluor™ (0.015 mmol), MeCN (0.50 mL), rt, 120 h; 1.0 equiv. **2.33** (0.015 mmol), 100 equiv. aniline (1.5 mmol), 3.0 equiv. PPh_3 (0.045 mmol), benzene (0.30 mL), 40 °C, 20 h.[120] Work carried out by Dr. E. Emer. Yields determined by ^{19}F and ^{1}H NMR using 1-fluoro-3-nitrobenzene as internal reference.

Using XeF_2 and Selectfluor™ product **2.2p** was obtained in 82% and 36% yield, respectively, with ees of 80% and 36% favouring (*S*)-configuration. This is consistent with an inner-sphere mechanism, including the oxidation of the Pd(II) centre to a Pd(IV)–F followed by reductive elimination (**A**). When reacting **2.33** with aniline, Hartwig reported the formation of benzylic amine **2.34** in 84% yield and 71% ee favouring the (*R*)-enantiomer.[120] In this case, aniline attacks the benzylic carbon in an S_N2-like fashion, resulting in the observed inversion of configuration.

Putting together all the results from our mechanistic studies and observations made during the development of this hydrofluorination protocol, we were able to outline a catalytic cycle, explaining the stereochemical outcome, the formation of by-products as well as the excess of Selectfluor™ that was necessary to obtain synthetically useful yields (Scheme 2.16).

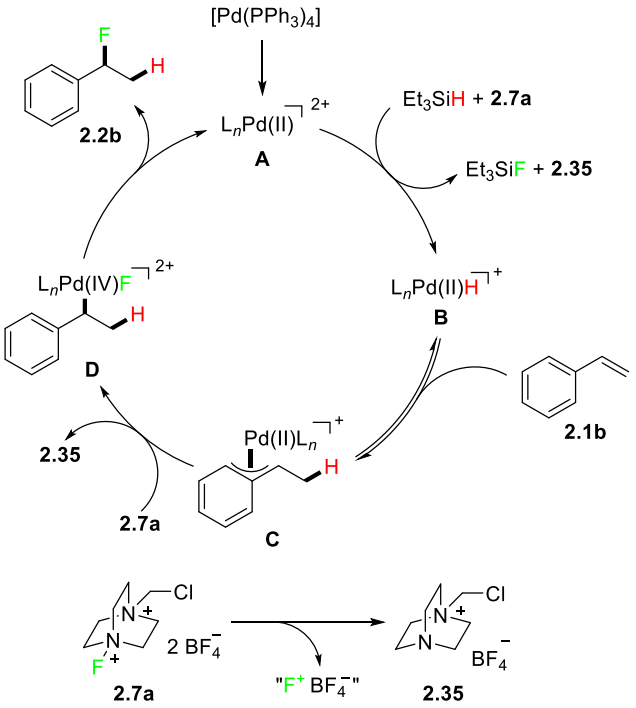

Scheme 2.16. Proposed catalytic cycle for the hydrofluorination of **2.1b**.

Given the high redox potential of Selectfluor™[125,126] we assume the oxidation of Pd(0) in $[Pd(PPh_3)_4]$ to a Pd(II) species **A** to be the first step, with **A** being the starting point of the catalytic cycle. Upon hydride transfer from Et_3SiH to **A** we obtain Pd(II)–H intermediate **B** with Et_3SiF as by-product, which was identified in crude reaction mixtures by its characteristic ^{19}F NMR peak at –175.6 ppm (sept, J = 6.4 Hz).[127] The formation of the strong Si–F bond[3] is believed to serve as a thermodynamic driving force for this transformation. Furthermore, the formation of this by-product also helps to explain the excess of Selectfluor™ that is needed for this transformation as 1.0 equiv. is consumed during this step. Intermediate **B** then undergoes *syn*-specific, reversible hydropalladation of substrate **2.1b** leading to η^3-benzyl Pd(II)-complex **C** or the according η^1 analogue. Subsequently, **C** is oxidised by Selectfluor™ (**2.7a**) giving the benzylic organo–Pd(VI)–F intermediate **D** or the according η^3 analogue, which we have, however, been unable to isolate. **2.35** is obtained as by-product, and it is found in the crude mixtures of this

reaction. Reductive elimination under retention of configuration finally yields the hydrofluorinated product **2.2b**, leading back to the starting point of this catalytic cycle (**A**)

Another by-product that is formed during this reaction is the oxidation product of the PPh_3 ligand, $OPPh_3$. A plausible explanation for this would be the initial formation of F_2PPh_3 under the oxidising reaction conditions with subsequent hydrolysis to HF and $OPPh_3$.[128] F_2PPh_3 has previously been observed after addition of XeF_2 to a solution of PPh_3 in DCM. [129] This also helps to explain the excess of Selectfluor™ needed for this reaction.

By assuming the initial formation of a Pd(II)-diene complex **B** the catalytic cycle could be adapted for the hydrofluorination of 1,5-dienes (Scheme 2.17).

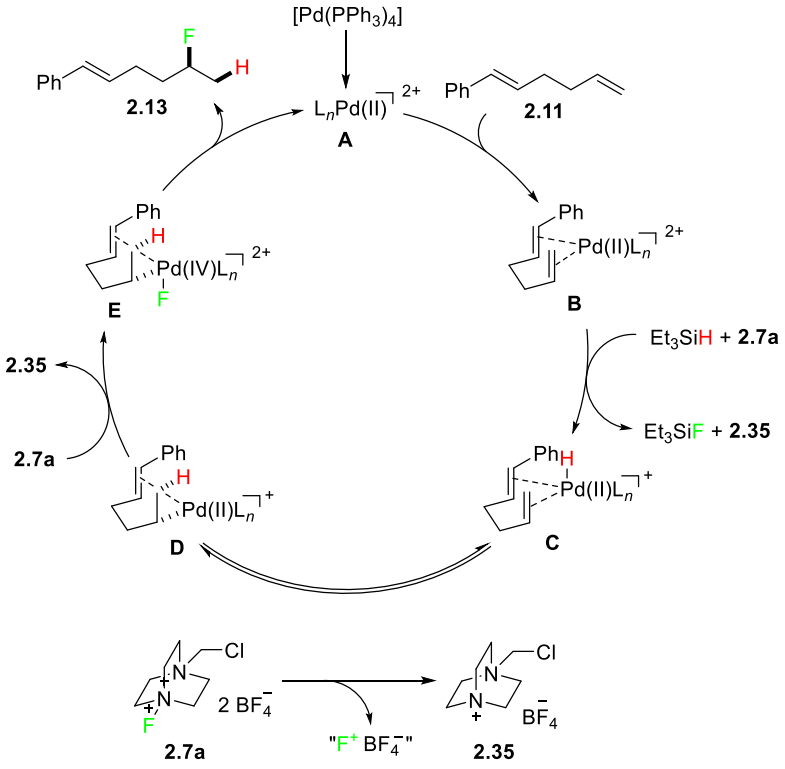

Scheme 2.17. Proposed catalytic cycle for the hydrofluorination of **2.11**.

Subsequently, **B** is converted into the according Pd(II)–H **C**, which after olefin insertion gives organo–Pd(II) complex **D**. Oxidation by Selectfluor™ leads to Pd(IV)–F **E**, which undergoes reductive elimination to give rise to the hydrofluorinated product **2.13** and leads back to the starting point of the catalytic cycle (**A**).

2.3. Conclusion

In summary, we have developed a novel Pd-catalysed hydrofluorination of alkenylarenes using independent sources of H^- and F^+. This polar approach makes it distinctly different from related protocols following radical mechanisms, and it also stands out for its umpolung-type character. The reaction is characterised by the selective formation of benzylic fluoride products and a unique *syn*-specificity.

Mechanistic experiments, including isotopic labelling with Et_3SiD and stoichiometric reactions from isolated Pd-complexes, support a mechanism with sequential, *syn*-specific hydropalladation of the double bond yielding a benzylic Pd-complex, followed by oxidation with Selectfluor™ to a Pd(IV)–F intermediate and reductive elimination under retention of stereochemistry at the benzylic position. Overall, this would lead to the observed *syn*-specificity for net HF-addition.

Preliminary experiments have shown the potential of this protocol to be extended to 1,5-dienes, where the selective hydrofluorination of the unactivated double bond was observed. To the best of our knowledge, this selectivity had not been observed previously for this kind of transformation. The yields, however, would need to be improved for this reaction to be of synthetic value.

Chapter 3: Iodofluorination of Alkynes

3.1. Introduction: Formal Addition of R_f–X and F–X (X = Cl, Br, I) across Alkynes

The development of novel synthetic pathways for the vicinal difunctionalisation of alkynes with halogens and fluorinated groups is of considerable interest, as the resulting alkenes are key intermediates for the synthesis of complex fluorinated molecules.

3.1.1. Halogenoperfluoroalkylation of Alkynes

In 1954, Haszeldine and Leedham developed the first addition of trifluoroiodomethane to propyne (Scheme 3.1).[130]

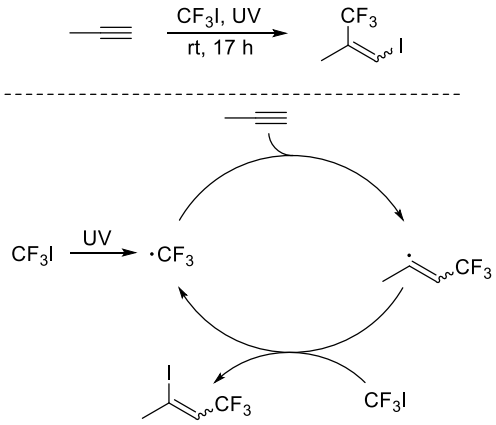

Scheme 3.1. Addition of trifluoroiodomethane to propyne *via* a SET mechanism.

UV light was used as radical initiator for this transformation, but in subsequent studies different inorganic oxidants,[131–145] metals,[146–159] organic initiators[142,160–171] as well as

photolytic,[130,172–178] electrochemical,[179–182] thermal[183–187] and ultrasound[173] activation have also successfully been employed in the addition of perfluoroalkyl iodides to alkynes. The initially formed trifluoromethyl radicals react with the alkyne to give a highly reactive vinyl radical intermediate, which abstracts iodine from trifluoroiodomethane to give the product and a chain propagating trifluoromethyl radical (Scheme 3.1).

Burton and MacNeil used a sequence of carbocupration and subsequent quenching of the intermediate copper species **3.3** with molecular iodine to achieve the *syn*-specific iodoperfluoroalkylation of alkynes. They successfully isolated **3.4** in 46% yield performing this reaction with pentafluorophenyl–copper **3.1** and perfluorinated alkyne **3.2**. (Scheme 3.2).[188]

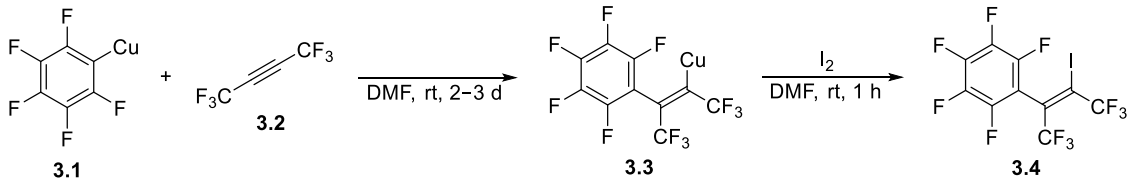

Scheme 3.2. Iodoperfluoroarylation of alkyne **3.2** *via* carbocupration and quenching with molecular iodine.

A similar strategy was used to introduce perfluorinated vinyl moieties instead of aromatic groups.[189]

In 2012, Stephenson and co-workers published the Ru-catalysed photoredox iodoperfluoroalkylation of terminal alkynes **3.5** (Scheme 3.3).[190]

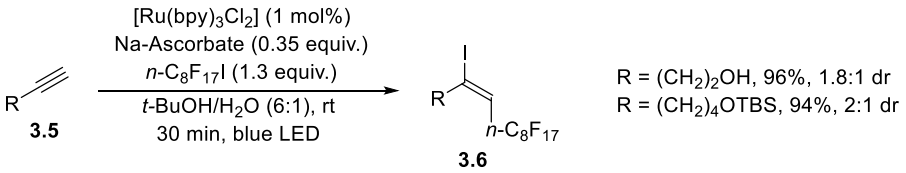

Scheme 3.3. Photocatalysed iodoperfluoroalkylation of terminal alkynes.

By changing the solvent from MeCN/MeOH, which is most commonly used for the perfluoroalkylation of alkenes, to a *t*-BuOH/H_2O mixture the amount of deiodinated alkene by-products could be significantly reduced. This allowed for the perfluoroalkylated iodoalkene products (**3.6**) to be isolated in excellent yields and modest diastereomeric ratios.

Recently, the $FeBr_2$-catalysed 1,2-addition of perfluorinated alkyl iodides to terminal alkynes (**3.5**), using sub-stoichiometric amounts of Cs_2CO_3 as base, was reported by Hu and co-workers (Scheme 3.4).[191]

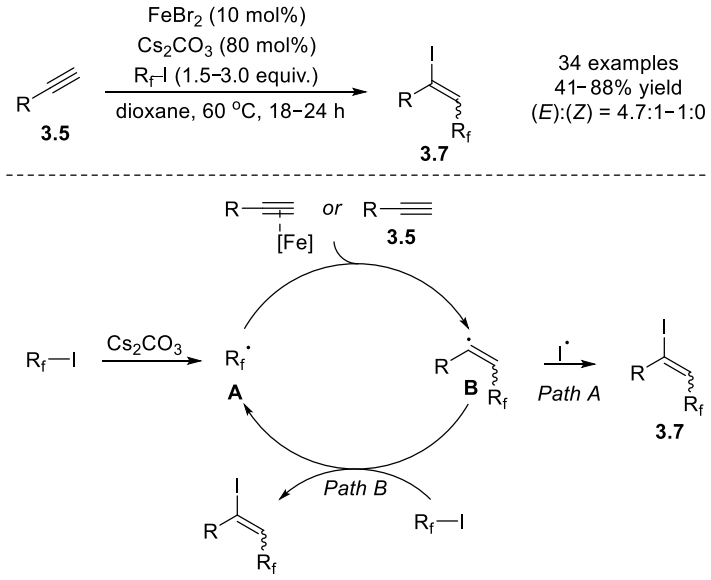

Scheme 3.4. Iodoperfluoroalkylation of terminal alkynes under Fe-catalysis

A large substrate scope was studied and good to excellent yields and (*E*):(*Z*) ratios were found for all reactions. The authors found that for unfunctionalised alkyl alkynes the reaction also proceeded under Fe-free conditions. The proposed catalytic cycle starts with the formation of the perfluorinated radical **A** by reaction of R_f–I with Cs_2CO_3. **A** then reacts with the alkyne to generate vinyl radical **B**. The desired product **3.7** is formed from **B** either by addition of an iodide radical (Path A) or a chain propagation step (Path B). Fe

is thought to activate the alkynes to facilitate the reaction with **A**. This mechanistic proposal is consistent with sub-stoichiometric amounts of Fe and Cs_2CO_3.

In the same year, Liu and co-workers published the iodotrifluoromethylation of terminal alkynes (**3.5**), mediated by I_2O_5, using sodium trifluoromethanesulfinate ($NaSO_2CF_3$) as the CF_3 source (Scheme 3.5).[192] The desired iodotrifluoromethylated alkenes (**3.8**) were obtained in moderate to good yields and moderate (*E*):(*Z*) ratios. Electron spin resonance (ESR) experiments indicated a radical process for the related iodotrifluoromethylation of terminal alkenes.

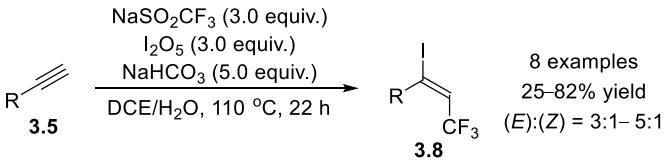

Scheme 3.5. Iodotrifluoromethylation of terminal alkynes mediated by I_2O_5.

Also in 2014, the copper-mediated synthesis of bromo-difluoroalkylated olefins from terminal and internal alkynes (**3.9**) was reported by Besset and Poisson (Scheme 3.6).[193] Varying yields between 23% and 88% were obtained with mostly moderate (*E*):(*Z*) ratios.

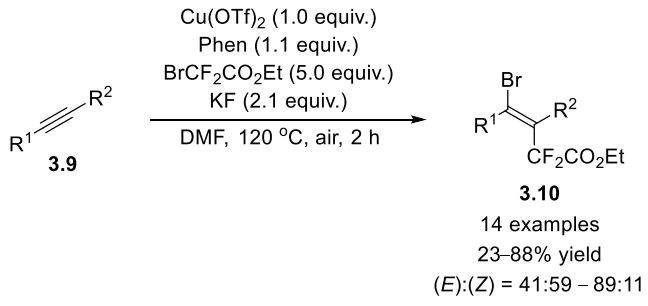

Scheme 3.6. Cu-mediated bromodifluoroalkylation of alkynes.

3.1.2. Halofluorination of Alkynes

In 1973, Olah and co-workers described the formal addition of "XF" (X = Cl, Br, I) across symmetrical internal alkynes (**3.11**), using *N*-halosuccinimides (NXS) in a solution of pyr/HF (Table 3.1).[51,194]

Table 3.1. Halofluorination of internal alkynes with NXS and pyr/HF.

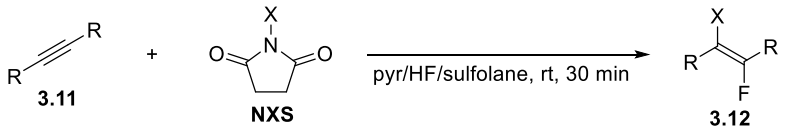

R	X	Yield [%]
Et	Cl	70
	Br	85
	I	70
Ph	Cl	95
	Br	95
	I	90

Zupan showed that polymer-supported pyridinium hydrofluoride can be used for this transformation.[195] Rolando and co-workers also reported that 1,3-dibromo-5,5-dimethylhydantoin (DBH) and bis(pyridine)iodonium(I) tetrafluoroborate (Barluenga's reagent)[52] can be used as alternative electrophilic halogen sources. In the reaction with terminal alkynes (**3.5**) products **3.13** and **3.14** were obtained in good to excellent yields and excellent (*E*):(*Z*) ratios (Scheme 3.7).[196]

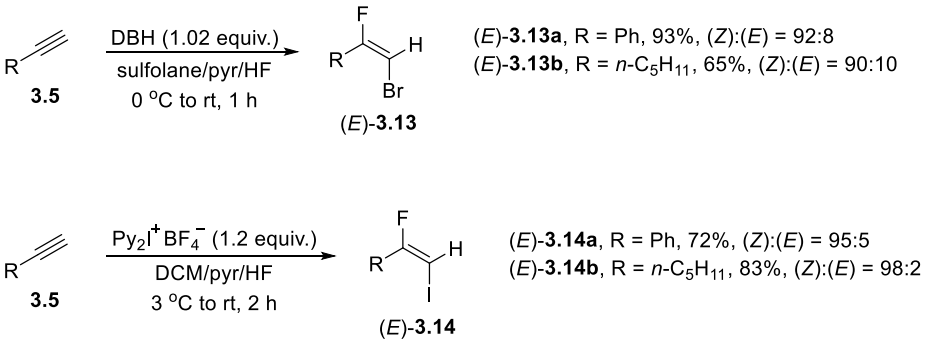

Scheme 3.7. Bromo- and iodofluorination of terminal alkynes, using alternative electrophilic halogen sources.

Another method for the Markovnikov-type iodofluorination of alkynes was published by Zupan in 1976.[197] CH_3IF_2 was used in the presence of catalytic amounts of anhydrous HF to convert several terminal and internal alkynes (**3.9**) into the desired (*Z*)-iodofluoroalkenes ((*Z*)-**3.15**) (Scheme 3.8). The hypervalent iodine reagent was generated *in situ* from CH_3I and XeF_2.

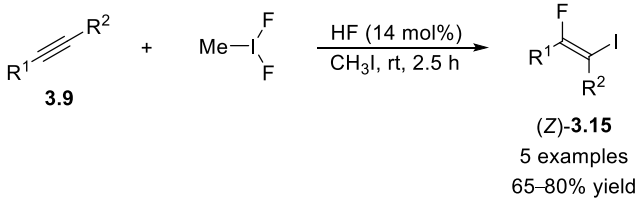

Scheme 3.8. (*Z*)-Specific iodofluorination of alkynes with CH_3IF_2.

In 2006, a related transformation, using more stable 4-iodotoluene difluoride in the presence of 0.5 equiv. I_2, was developed by Tingoli and co-workers (Scheme 3.9).[198]

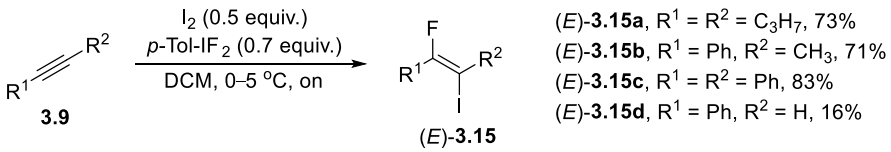

Scheme 3.9. Iodofluorination of terminal and internal alkynes with 4-iodotoluene difluoride and I_2.

In this reaction internal and terminal alkynes (**3.9**) reacted mostly to the (*E*)-isomers ((*E*)-**3.15)**.

When reacting 4-iodotoluene difluoride with terminal alkynes (**3.5**) in a solution of $Et_3N{\cdot}5HF$, Hara and co-workers observed the selective formation of stable λ^3-iodane species **3.16** in good yields (Scheme 3.10).[199–201]

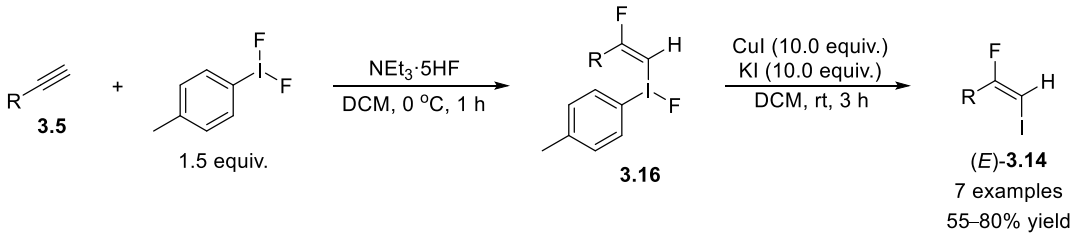

Scheme 3.10. Preparation of β-fluoroalkenyl-λ^3-iodanes **3.4** and subsequent transformation into (*E*)-iodofluorinated alkenes.

These could be transformed into (*E*)-iodofluorinated alkenes ((*E*)-**3.14**) by reaction with a mixture of CuI and KI.

Ochiai and co-workers published the related synthesis of β-fluoroalkenyl-λ^3-bromanes **3.18**, using difluoro-λ^3-bromate **3.17** (Scheme 3.11).[202]

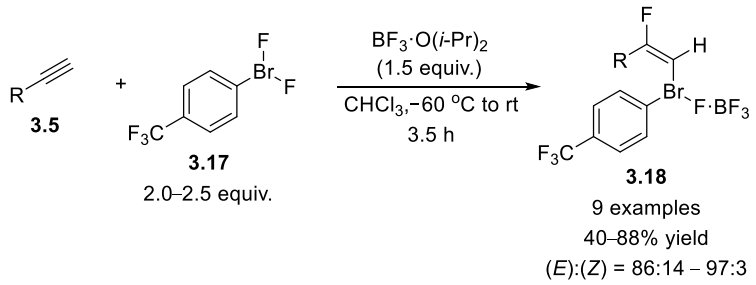

Scheme 3.11. Preparation of β-fluoroalkenyl-λ^3-bromanes **3.18**.

The desired products were obtained as BF_3-adducts in moderate to good yields and (*E*):(*Z*) ratios.

In 1970, Dear described the bromofluorination of 1- and 3-hexyne, using a mixture of anhydrous HF and *N*-bromoacetamide (Scheme 3.12).[203]

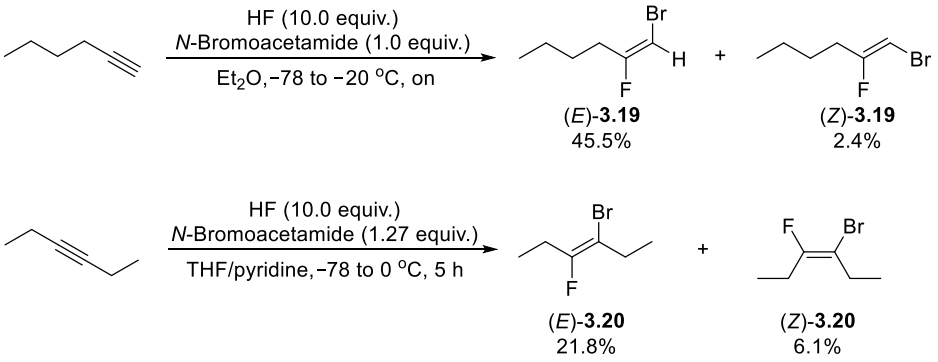

Scheme 3.12. Bromofluorination of alkynes with *N*-bromoacetamide and HF.

The addition of a second equivalent of "BrF" was not observed and the products were predominantly formed as (*E*)-isomers.

In 1986, Barluenga and co-workers published one example of the iodofluorination of 3-hexyne, using Barluenga's reagent and a fluoride salt, to give the according iodofluorinated alkene in 50% NMR yield without specification of the double bond geometry in the product (Scheme 3.13).[204]

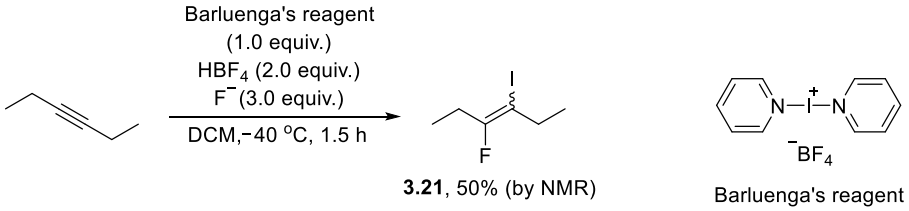

Scheme 3.13. Iodofluorination of 3-hexyne with Barluenga's reagent.

In the same year, Rozen reported the reaction of I–F and Br–F, which had been prepared from the elements, with alkynes. When XF is present in excess, this leads to the formation of double-addition-derived *gem*-difluoroalkanes. However, if 1.0 equiv. of Br–F

is allowed to react with 1-hexyne, (*E*)-1-bromo-2-fluoro-1-hexene (**3.22**) is obtained in 50% yield together with 25% of **3.23** (Scheme 3.14).[205]

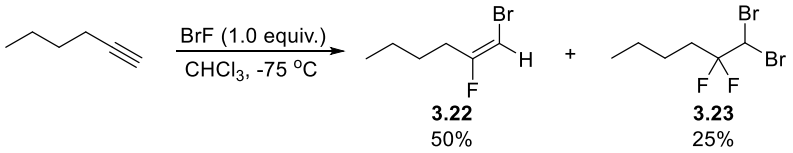

Scheme 3.14. Bromofluorination of 1-hexyne with BrF.

Similarly, Dolenc and Šket published the net addition of "Cl–F" to phenylacetylene and ((prop-1-yn-1-yl)benzene) alkyne using *N*-chlorosaccharin and pyr/HF (Scheme 3.15).[206]

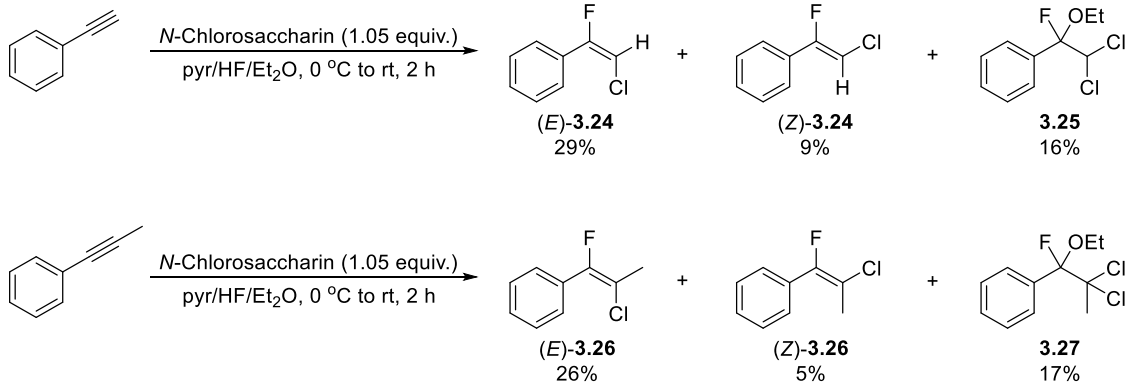

Scheme 3.15. Chlorofluorination of alkynes with *N*-chlorosaccharin and pyr/HF.

The obtained yields for products **3.24** and **3.26** were comparably low with moderate (*E*):(*Z*) selectivities. Significant amounts of by-products **3.25** and **3.27** were formed.

The addition of "I–F" across the triple bond in 3-hexyne, using a combination of XeF_2 and I_2 in apolar solvents, was shown by Shellhamer and co-workers (Scheme 3.16).[207]

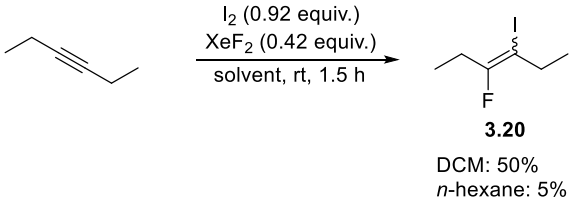

Scheme 3.16. Iodofluorination of 3-hexyne with XeF_2 and I_2.

A 50% yield of **3.20** was obtained in DCM but only 5% of product were formed in *n*-hexane. The authors did not comment on the (*E*):(*Z*) ratio.

In 2012, Jiang and co-workers reported the silver-mediated *cis*-selective bromofluorination of terminal alkynes, using AgF and *N*-bromosuccinimide (NBS) (Scheme 3.17).[208]

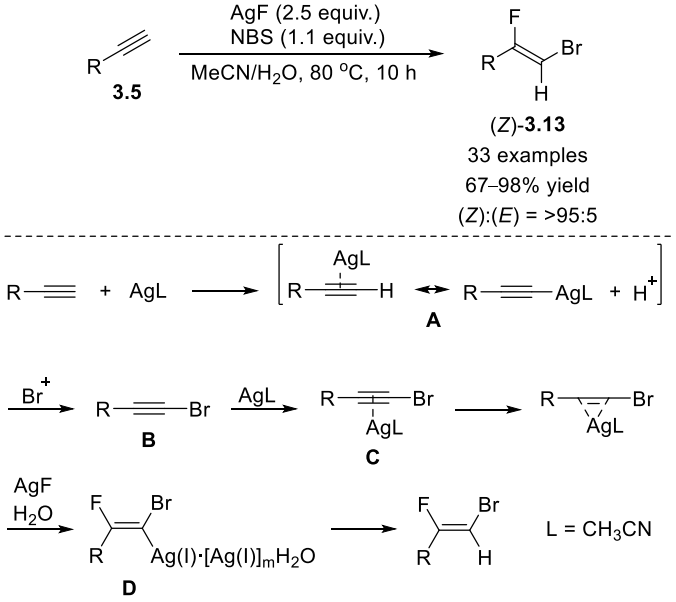

Scheme 3.17. Ag-mediated *cis*-specific bromofluorination of terminal alkynes with AgF and NBS.

Good to excellent yields and (*Z*):(*E*) ratios were observed for all 33 substrates, although the scope of employed functional groups remained limited to ethers, ketones, esters and aromatic halogens,. The reaction proved to be selective for terminal alkynes over internal ones, when both are present in the same substrate. Mechanistically, the authors suggest the formation of the bromoalkyne **B** *via* intermediate **A** as the first step. **B** then forms a π-complex with silver (**C**), which is further converted into fluorinated vinyl-silver intermediate **D**, followed by protonation to give the desired product.

Recently, Hara and co-workers published the iodofluorination of a limited selection of internal and terminal alkynes, using IF_5–pyridine–HF and hydroquinone (Scheme 3.18).[209]

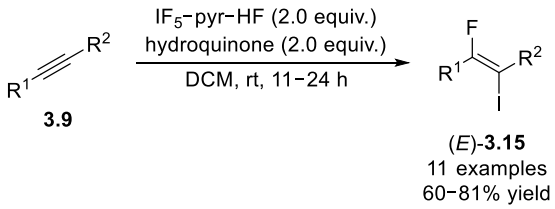

Scheme 3.18. Iodofluorination of alkynes with IF_5–pyridine–HF.

However, in some cases only ^{19}F NMR yields were reported and although good yields had been obtained with α-carbonyl alkynes, functional groups except esters and ketones remained largely unexplored.

3.2. Results and Discussion

The presented literature precedent reveals the absence of a general halofluorination of alkynes, permitting the transformation of a wide range of substrates. We therefore sought to develop a novel method, using readily available reagents and mild conditions, which would display good functional group tolerance.

Halofluorinated alkenes are valuable intermediates for the synthesis of highly substituted fluoroalkenes, which have been widely used as isopolar and isosteric mimics of amides.[24,210–216] Their reduced hydrogen bond donating and accepting ability[217] can be used to improve the lipophilicity and membrane permeability of biological probes.[218] Since they are not recognised as substrates by proteases, they can furthermore help to

improve the metabolic stability of peptides.[218,219] Selective preparation of (*E*)- and (*Z*)-isomers also allows for conducting conformational analyses of amides.[220] Fluoroalkenes have also been used as dienophiles in Diels-Alder reactions,[221] for the preparation of cyclopropane derivatives[222,223] and as substrates for the synthesis of fluorinated polymers.[224–226]

3.2.1. Reaction Development

In order to achieve mild reaction conditions and a broad functional group tolerance we envisioned a metal catalysed halofluorination of alkynes. Hashmi and co-workers had shown before that vinyl gold species, bearing a triphenylphosphine ligand (**3.28**), cleanly react with electrophilic sources of iodine, bromine and chlorine to give the corresponding vinyl halides (Table 3.2).[227]

Table 3.2. Reaction of vinyl gold species with electrophilic halogen sources.

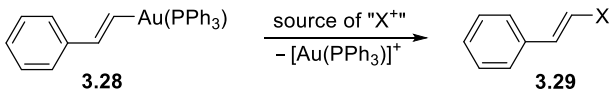

3.28 **3.29**

Source of "X^+"	Product (Yield)
NIS	**3.29a** X = I (96%)
NBS	**3.29b** X = Br (95%)
NCS	**3.29c** X = Cl (95%)

Furthermore, in 2007 Sadighi and co-workers published a protocol for the hydrofluorination of internal alkynes, where they demonstrated that [Au(SIPr)F] (**3.30**) and 3-hexyne reversibly form (*β*-fluorovinyl)gold complex **3.31**, when dissolved in DCM at rt (Scheme 3.19).[85]

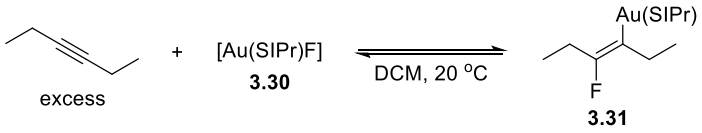

Scheme 3.19. Equilibrium between 3-hexyne, [Au(SIPr)F] (**3.30**) and (*β*-fluorovinyl)gold complex **3.31**.

Therefore, we sought to combine these two observations into a novel Au-catalysed halofluorination of alkynes. In an initial attempt we dissolved [Au(SIPr)F] (**3.30**) and 3-hexyne in CD_2Cl_2, according to Sadighi's protocol (Scheme 3.20).

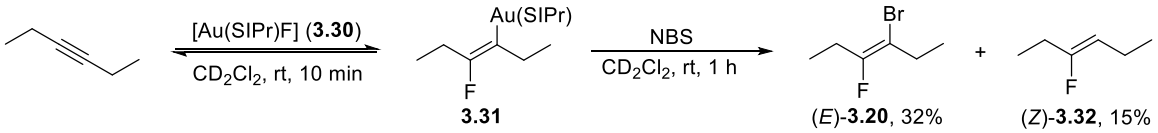

Scheme 3.20. Bromofluorination of 3-hexyne *via* consecutive reaction with [Au(SPIr)F] and NBS. Conditions: 1.1 equiv. 3-hexyne (0.055 mmol), 1.0 equiv. [Au(SIPr)F] (**3.30**) (0.050 mmol), CD_2Cl_2 (0.50 mL), rt, 10 min. 1.0 equiv. NBS (0.050 mmol), CD_2Cl_2 (0.50 mL), rt, 1 h.

As had been reported, after 10 min the reagents were found to be in equilibrium with fluoroaurated alkene **3.31**. Subsequent addition of NBS led to the formation of 32% of the desired fluorobrominated alkene **3.20** (^{19}F NMR: –108.6 ppm (tt, *J* = 23.0, 3.5 Hz)), which was solely obtained as the (*E*)-isomer, together with 15% of the hydrofluorinated analogue, (*Z*)-**3.32** (^{19}F NMR: –110.8 ppm (dtt, *J* = 38.7, 14.6, 1.7 Hz)). This proved the feasibility of the bromodeauration of (*β*-fluorovinyl)gold intermediates.

To show that this overall transformation can also be achieved starting from a gold(I)–alkyne π-complex, which is a common intermediate in gold-catalysed reactions,[228–230] isolated complex **3.33** was treated with a mixture of NBS and NEt_3·3HF as well as TASF (Scheme 3.21). These reactions resulted in the formation of 18% and 64%, respectively, of (*E*)-**3.20** together with 8% of (*Z*)-**3.32** in the reaction with NEt_3·3HF.

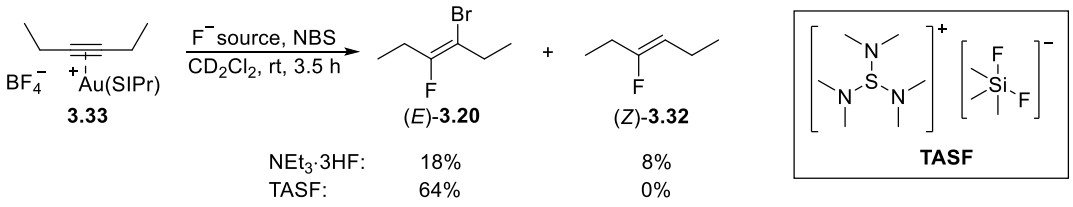

Scheme 3.21. Bromofluorination of 3-hexyne, starting from isolated gold–alkyne complex **3.33**. Conditions: 1.0 equiv. **3.33** (0.040 mmol), 1.0 equiv. F^- source (0.040 mmol), 1.0 equiv. NBS (0.040 mmol), CD_2Cl_2 (0.80 mL), rt, 3.5 h.

Following this lead result, we attempted this transformation starting from free 3-hexyne, using catalytic amounts of [Au(SIPr)BF_4] in combination with different sources of fluoride and electrophilic bromine (Table 3.3).

Table 3.3. Screening of conditions for bromofluorination of 3-hexyne.

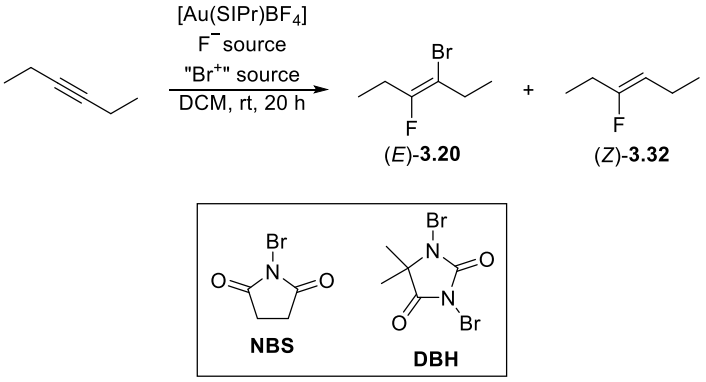

Entry	F^- Source	"Br^+" Source	(*E*)-**3.20**[a] [%]	(*Z*)-**3.32**[a] [%]
1	TASF	NBS	0	0
2	TASF	DBH	0	0
3	NEt_3·3HF	NBS	<5	0
4	NEt_3·3HF	DBH	54	0
5[b]	NEt_3·3HF	DBH	44	0

Conditions: 1.0 equiv. 3-hexyne (0.050 mmol), 5.0 mol% [Au(SIPr)BF_4] ($2.5\cdot10^{-3}$ mmol), 1.0 equiv. F^- source (0.050 mmol), 1.0 equiv. "Br^+" source (0.050 mmol), DCM (0.50 mL), rt, 20 h. [a]Determined by ^{19}F NMR of crude reaction mixture using hexafluorobenzene as internal reference. [b]No [Au(SIPr)BF_4] added to the reaction.

Employing TASF together with NBS, which had given 64% of the desired product in the previous reaction starting from gold–alkyne complex **3.33** (Scheme 3.21), did not lead to

any formation of either (*E*)-**3.20** or (*Z*)-**3.32** (Table 3.3., Entry 1). Exchanging NBS for 1,3-dibromo-5,5-dimethylhydantoin (DBH) gave the same result (Table 3.3, Entry 2), whereas using NEt_3·3HF instead of TASF resulted in the observation of 3% of (*E*)-**3.20** in the crude reaction mixture (Table 3.3, Entry 3). When NEt_3·3HF was used in conjunction with DBH a significantly improved yield of 54% of the desired product was observed (Table 3.3, Entry 4). However, when performing the reaction without the Au-catalyst (*E*)-**3.20** was still formed in 44% yield (Table 3.3, Entry 5).

Therefore, we concluded that the Au-catalyst was not needed for this reaction. On the other hand, DBH, which had already been successfully employed in aromatic bromination[231–233] as well as the bromination of alkenes and alkynes,[234,235] was identified as an electrophilic bromine source of high potential for the bromofluorination of alkynes. This is due to its known activation by acids, making it ideally suited for use in combination with HF-based reagents (Table 3.3, Entries 4 and 5 *vs.* 2), which are among the cheapest fluorinating reagents.[236] Furthermore, the reaction of DBH and related sources of electrophilic halogens with alkenes, for example in halolactonisation reactions, has been shown before to be catalysed by nucleophilic organocatalysts like tertiary amines, which are also used to bind HF in NEt_3·3HF and pyr/HF reagents.[235,237–240]

Consequently, we employed DBH as the electrophilic bromine source in a first optimisation study, varying the source of fluoride, using 5-decyne (**3.34a**) as test substrate (Table 3.4).

Table 3.4. Optimisation of halofluorination: Screening of fluoride sources.

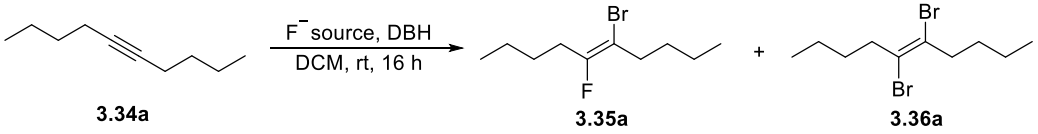

3.34a **3.35a** **3.36a**

Entry	F^- Source (equiv.)	Conversion[a] [%]	**3.35a**[a] [%]	**3.36a**[a] [%]
1	TBAF (1 M in THF) (1.0)	67	0	37
2	TBAF(*N*,*N*'-diphenylurea)$_2$ (1.0)	56	0	trace
3	TBAF(pin)$_2$ (1.0)	91	0	46
4	CsF (1.0)	94	trace	10
5	benzoyl fluoride (1.0)	33	0	5
6	NEt_3·3HF (1.0)	89	45	32
7	pyr/HF (3.0)	>95	29	trace
8	-	23	0	trace

Conditions: 1.0 equiv. **3.34a** (0.050 mmol), 1.0 equiv. DBH (0.050 mmol), fluoride source as in table, DCM (0.50 mL). [a]Determined by ^{1}H and ^{19}F NMR of crude reaction mixture using 1-fluoro-3-nitrobenzene as internal reference.

Reactions with TBAF (Table 3.4, Entry 1), as well as TBAF-complexes, TBAF(*N*,*N*'-diphenylurea)$_2$ (**5.7e**) (Table 3.4, Entry 2) and TBAF(pin)$_2$ (**4.19d**) (Table 3.4, Entry 3), led to varying amounts of dibrominated by-product **3.36a** being formed with no desired bromofluoroalkene **3.35a** being observed after 16 h at rt. The reaction with CsF, although leading to almost full consumption of the starting alkyne **3.34a**, only gave a trace amount of **3.35a**, identified by its ^{19}F NMR signal at –105.4 ppm (tt, *J* = 23.4, 3.4 Hz), alongside 10% of by-product **3.36a** (Table 3.4, Entry 4). Benzoyl fluoride, which had first been used by Doyle and co-workers as a latent source of nucleophilic fluoride for the enantioselective opening of meso epoxides,[241] showed comparably low reactivity with only 5% of by-product **3.36a** being obtained (Table 3.4, Entry 5). Using 1.0 equiv. of NEt_3·3HF, however, allowed for the formation of 45% of the desired bromofluorinated alkene **3.35a** and 32% of dibromo by-product **3.36a**, showing good mass recovery (Table

3.4, Entry 6). CH_2Br_2 was detected as another by-product using GC/MS analysis. When comparing this result to pyr/HF, 3.0 equiv. of this fluorinating reagent were used in order to have an equal amount of fluoride present in the reaction mixture (Table 3.4, Entry 7). This reaction, however, only gave 29% of the desired product **3.35a** accompanied by another species (18%) of the same mass, which showed a ^{19}F NMR signal at –92.5 ppm (t, *J* = 22.7 Hz) consistent with the (*Z*)-isomer. Furthermore, traces of **3.36a** were also detected in the crude reaction product. Importantly, reactions with $NEt_3{\cdot}3HF$ and pyr/HF did not show the formation of hydrofluorinated by-products. It is to be noted that without a source of fluoride low conversion (23%) and only traces of **3.36a** were observed (Table 3.4, Entry 8).

Overall, these results show a remarkably different behaviour for HF-based reagents in the bromofluorination with DBH compared to other fluoride sources, illustrating the double activity of these reagents as activators of DBH as well as sources of fluoride.[236] Therefore, $NEt_3{\cdot}3HF$ was used for further optimisation studies, looking into the effect of different solvents on the outcome of this reaction (Table 3.5).

Table 3.5. Optimisation of halofluorination: Screening of solvents.

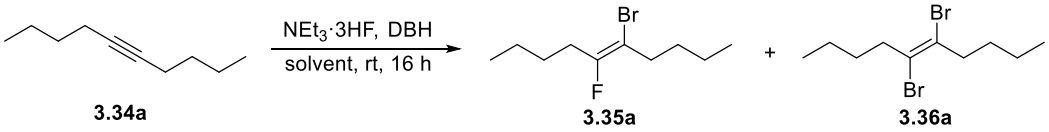

Entry	Solvent	Conversion[a] [%]	**3.35a**[a] [%]	**3.36a**[a] [%]
1	THF	47	0	6
2	MeCN	90	trace	29
3	DMF	>95	0	n.d. (overlap with DMF)
4	Toluene	91	<5	27
5	MeOH	85	0	34
6	DCE	85	32	31
7	$CHCl_3$	87	43	27

Conditions: 1.0 equiv. **3.34a** (0.050 mmol), 1.0 equiv. DBH (0.050 mmol), 1.0 equiv. NEt_3·3HF (0.050 mmol), solvent as in table (0.50 mL). n.d. = not determined. [a]Determined by ^{1}H and ^{19}F NMR of crude reaction mixture using 1-fluoro-3-nitrobenzene as internal reference.

THF as example of an ethereal solvent caused a significantly reduced conversion and 6% of **3.36a** were formed as the only product soluble in $CDCl_3$ (Table 3.5, Entry 1). More polar, aprotic solvents, MeCN and DMF, led to almost full consumption of the starting alkyne but gave only a trace amount of **3.35a** in the case of MeCN and no desired product in the reaction with DMF (Table 3.5, Entries 2 and 3). For the latter reaction the amount of by-product **3.36a** was not determined due to overlap with DMF peaks in the ^{1}H NMR spectrum of the crude product. Apolar toluene also allowed for an almost complete consumption of starting material, but only <5% of fluorobromoalkene **3.35a** and 27% of dibrominated by-product **3.36a** were formed (Table 3.5, Entry 4). A similar result was also obtained with protic MeOH (Table 3.5, Entry 5). Only chlorinated solvents, DCE and $CHCl_3$, led to significant amounts of **3.35a** being formed (Table 3.5, Entries 6 and 7). For the former reaction 32% of **3.35a** were found in the ^{1}H and ^{19}F NMRs of the crude reaction

mixture together with 31% of **3.36a**, whereas for $CHCl_3$ these numbers were 43% and 27%, respectively.

The screening was thus continued with DCM, as it had shown a higher yield of desired product **3.35a** and better mass recovery than the other solvents in this study. In order to improve the yield of **3.35a** and reduce the formation of by-product **3.36a** the amounts of DBH and NEt_3·3HF employed for this transformation as well as the temperature were optimised next (Table 3.6).

Table 3.6. Optimisation of halofluorination: Amounts of DBH and NEt_3·3HF and temperature.

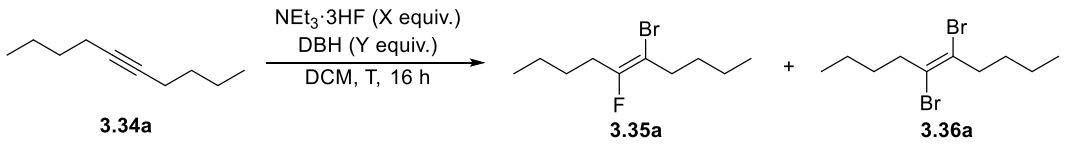

Entry	X	Y	T [°C]	Conversion[a] [%]	**3.35a**[a] [%]	**3.36a**[a] [%]
1	1.0	0.5	rt	45	29	16
2	1.0	1.0	0	>95	53	33
3	1.0	1.0	–40	>95	53	38
4	2.0	1.0	0	>95	72	19
5	3.0	1.0	0	>95	81	14
6	5.0	1.0	0	>95	79	6

Conditions: 1.0 equiv. **3.34a** (0.050 mmol), X equiv. DBH (as in table), Y equiv. NEt_3·3HF (as in table), DCM (0.50 mL). [a]Determined by ^1H and ^{19}F NMR of crude reaction mixture using 1-fluoro-3-nitrobenzene as internal reference.

Lower yields of both **3.35a** (29%) and **3.36a** (16%) were observed when the amount of DBH was reduced to 0.5 equiv. (Table 3.6, Entry 1). Lowering the temperature to 0 °C allowed for complete consumption of starting material and an improved yield of bromofluoroalkene **3.35a** of 53% (Table 3.6, Entry 2). A comparable result was obtained at –40 °C (Table 3.6, Entry 3), so for ease of synthesis further screening was performed at 0 °C. Increasing the amount of NEt_3·3HF to 2.0 equiv. and 3.0 equiv. improved the yield of

3.35a further to 72% and 81%, respectively, with an accordingly reduced yield of by-product **3.36a** (Table 3.6, Entries 4 and 5). However, using more than 3.0 equiv. of $NEt_3 \cdot 3HF$ did not lead to any further improvement (Table 3.6, Entry 6).

With the optimised conditions from Table 3.6 (Entry 5) we went on to study the effect of alternative sources of electrophilic bromine on the outcome of the reaction (Table 3.7).

Table 3.7. Optimisation of halofluorination: Screening of electrophilic bromine sources.

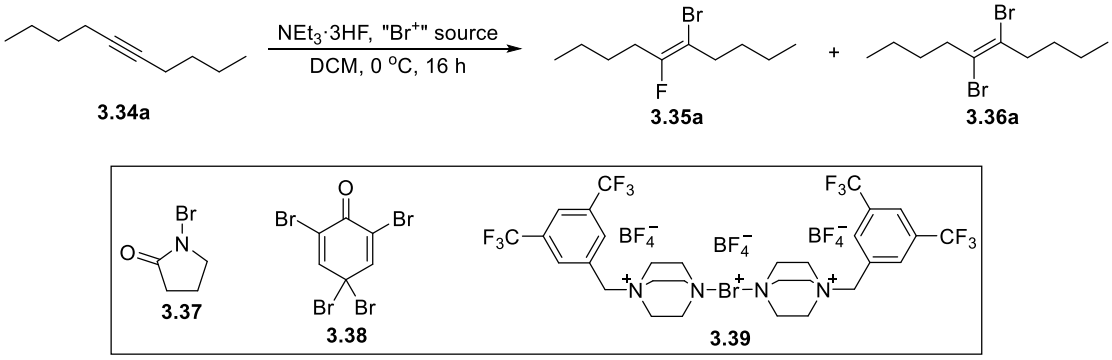

Entry	"Br^+" Source	Conversion[a] [%]	**3.35a**[a] [%]	**3.36a**[a] [%]
1	NBS	70	40	24
2	Br_2	86	0	85
3	**3.37**	>95	16	29
4	**3.38**	51	18	25
5	**3.39**	10	0	trace

Conditions: 1.0 equiv. **3.34a** (0.050 mmol), 1.0 equiv. of "Br^+" source (0.050 mmol), 3.0 equiv. $NEt_3 \cdot 3HF$ (0.15 mmol), DCM (0.50 mL). [a]Determined by ^1H and ^{19}F NMR of crude reaction mixture using 1-fluoro-3-nitrobenzene as internal reference.

NBS, which is structurally closely related to DBH, was found to give a reduced yield of the desired product **3.35a** of 40% (Table 3.7, Entry 1), whereas Br_2 led to the exclusive formation of **3.36a** in 85% yield (Table 3.7, Entry 2). **3.37**, which is the lactam analogue of NBS and was first described by Toste and co-workers for the Au(I)-catalysed enantioselective bromocyclisation of allenes,[242] showed high conversion but only 16% and 29% of products **3.35a** and **3.36a**, respectively, were formed (Table 3.7, Entry 3).

2,4,4,6-Tetrabromo-2,5-cyclohexadienone (TBCO, **3.38**) gave a lower conversion of 51% and comparable yields for **3.35a** and **3.36a** of 18% and 25%, respectively (Table 3.7, Entry 4). Structurally more complex **3.39**, which had also first been used by Toste and co-workers for the development of an enantioselective halocyclisation to obtain 4*H*-3,1-benzoxazines,[243] led to poor conversion of 10% and no formation of desired product **3.35a** (Table 3.7, Entry 5).

Our final optimised conditions for the bromofluorination of **3.34a** were the ones described in Entry 5 of Table 3.6, consisting of 1.0 equiv, of DBH, 3.0 equiv. of $NEt_3 \cdot 3HF$ and a reaction temperature of 0 °C, and so we tried to employ them for the alternative iodo- and chlorofluorinations using the according DBH analogues, DIH and DCH (Table 3.8).

Table 3.8. Optimisation of halofluorination: Iodofluorination and chlorofluorination.

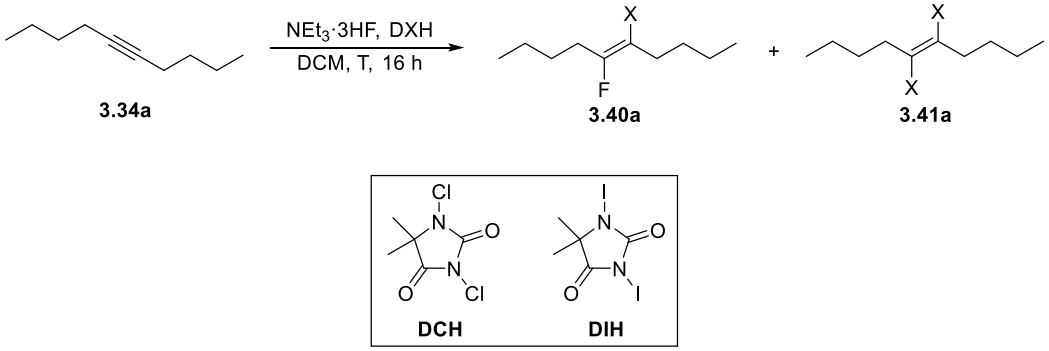

Entry	X	T [°C]	Conversion[a] [%]	**3.40a**[a] [%]	**3.41a**[a] [%]
1	Cl	0	86	22	6
2	Cl	–40	78	27	trace
3	I	0	87	30	30
4	I	40	>95	91	trace

Conditions: 1.0 equiv. **3.34a** (0.050 mmol), 1.0 equiv. DXH (0.050 mmol), 3.0 equiv. $NEt_3 \cdot 3HF$ (0.15 mmol), DCM (0.50 mL). [a]Determined by ^1H and ^{19}F NMR of crude reaction mixture using 1-fluoro-3-nitrobenzene as internal reference.

Entries 1 and 2 in Table 3.8 show the results for chlorofluorination with DCH at 0 °C and –40 °C, respectively. Although high consumption of starting material of 86% and 78% was observed for both reactions, less than 30% were converted into either **3.40a** (X = Cl) or **3.41a** (X = Cl). **3.40a** (X = Cl) was the dominant product in both cases with 22% and 27% being formed at 0 °C and –40 °C, respectively. Therefore, DCH was assumed to either be too reactive or lead to sensitive intermediates, which easily decompose under our reaction conditions and don't lead to formation of either **3.40a** (X = Cl) or **3.41a** (X = Cl). DCH was therefore not considered for further optimisation. Bridged chlorirenium species, which are likely intermediates for this transformation, have previously been shown to be energetically less favourable than their bromo-counterparts.[244]

Performing the reaction with iodinating reagent DIH at 0 °C also led to high conversion, with 30% of both iodofluorinated **3.40a** as well as diiodinated **3.41a** being found in the crude reaction product (Table 3.8, Entry 3). Upon increasing the reaction temperature to 40 °C the yield of **3.40a** (X = I) improved to 91%, 10% more than for related bromofluorination, and only a trace amount of **3.41a** (X = I) was formed (Table 3.8, Entry 4). Further experiments showed that the yield could not be further improved by changing the amounts of DIH or $NEt_3 \cdot 3HF$.

Having established the optimised conditions for the iodofluorination of internal alkyne **3.34a**, we sought to extend this methodology to terminal alkynes using 1-hexyne (**3.42a**) as test substrate (Table 3.9).

Table 3.9. Optimisation of halofluorination: Terminal alkynes.

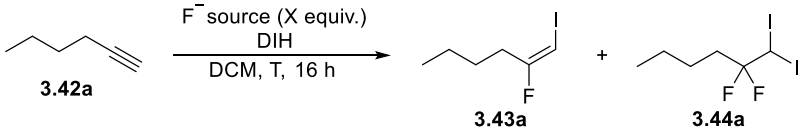

Entry	F^- Source (equiv.)	T [°C]	Conversion[a] [%]	**3.43a**[a] [%]	**3.44a**[a] [%]
1	NEt_3·3HF (3.0)	40	>95	35	0
2	NEt_3·3HF (3.0)	rt	>95	31	0
3	NEt_3·3HF (3.0)	60	>95	33	0
4	NEt_3·3HF (5.0)	40	>95	28	0
5	pyr/HF (3.0)	rt	>95	14	29
6	pyr/HF (3.0)	0	>95	33	20
7	pyr/HF (3.0)	–20	>95	77	8
8	pyr/HF (2.0)	–20	>95	39	0
9	pyr/HF (9.0)	–20	>95	0	87

Conditions: 1.0 equiv. **3.42a** (0.050 mmol), 1.0 equiv. DIH (0.050 mmol), X equiv. of fluoride source (as in table), DCM (0.50 mL). [a]Determined by ^{1}H and ^{19}F NMR of crude reaction mixture using 1-fluoro-3-nitrobenzene as internal reference.

Applying the optimised conditions for the iodofluorination of **3.34a** only led to 35% of Markovnikov-type product **3.43a** as the only fluorinated product observed in crude ^{19}F NMR (–82.3 ppm, td, *J* = 22.7, 17.9 Hz), although full consumption of starting material had occurred (Table 3.9, Entry 1). Neither de- nor increasing the reaction temperature nor increasing the amount of NEt_3·3HF had a beneficial effect on the outcome of the reaction (Table 3.9, Entries 2–4). Therefore, more acidic pyr/HF was tested, but when using 3.0 equiv. at rt only 14% of desired product **3.43a** were found in the crude product alongside 29% of **3.44a** (^{19}F NMR: –96.0 ppm, td, *J* = 16.7, 12.6 Hz), which is obtained after addition of a second equivalent of "IF" (Table 3.9, Entry 7).[245] Upon lowering the reaction temperature incrementally to 0 °C and finally –20 °C, the amount of **3.43a** that was obtained increased to 33% and 77%, respectively, with accordingly less by-product **3.44a** being formed (Table 3.9, Entries 5 and 6). Reducing the amount of pyr/HF to

2.0 equiv. led to a diminished yield of 39% (Table 3.9, Entry 8). Using 9.0 equiv. of pyr/HF, however, led to exclusive formation of **3.44a** in 87% yield (Table 3.9, Entry 9).

Therefore, the optimised conditions for the mono- and double iodofluorination of terminal alkynes are the ones presented in Entry 7 and 9 in Table 3.9, respectively.

Finally, in order to expand the substrate scope for this transformation further, we studied the reaction with electron deficient α-ketoalkyne **3.34v** (Table 3.10).

Table 3.10. Optimisation of halofluorination: α-Ketoalkynes.

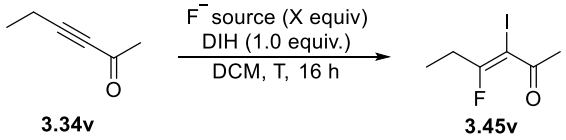

3.34v **3.45v**

Entry	F^- Source (equiv.)	T [°C]	Conversion[a] [%]	**3.45v**[a] [%]
1	$NEt_3 \cdot 3HF$ (3.0)	40	57	5
2	pyr/HF (3.0)	–20	43	9
3	pyr/HF (3.0)	0	76	35
4	pyr/HF (3.0)	rt	85	37
5	pyr/HF (3.0)	40	>95	0
6	pyr/HF (4.0)	rt	92	44
7	pyr/HF (6.0)	rt	>95	43

Conditions: 1.0 equiv. **3.34v** (0.050 mmol), 1.0 equiv. DIH (0.050 mmol), X equiv. of fluoride source (as in table), DCM (0.50 mL). [a]Determined by ^1H and ^{19}F NMR of crude reaction mixture using 1-fluoro-3-nitrobenzene as internal reference.

Applying the optimised conditions for both internal (Table 3.10, Entry 1) as well as terminal alkynes (Table 3,10, Entry 2) led to only 5% and 9% of product **3.45v** (^{19}F NMR: –66.2, tq, *J* = 22.8, 6.6 Hz) as the major fluorinated product alongside traces of unidentified by-products, although conversions of 57% and 43%, respectively, had been achieved. Regioselectivity of the fluoride attack leading to **3.45v** follows the established rules for nucleophilic addition to Michael acceptors. Increasing the temperature for the

reaction with pyr/HF to 0 °C caused an increase in conversion as well as yield to 76% and 35%, respectively (Table 3.10, Entry 3). Performing the reaction at rt gave a similar yield of 37% (Table 3.10, Entry 4) and at 40 °C no product formation was observed although full consumption of the starting material had occurred (Table 3.10, Entry 5). Therefore, further optimisation was performed at rt and more pyr/HF was used in order to let the reaction proceed to completion. Using 4.0 equiv. of the fluorinating reagent an increased yield of 44% was obtained (Table 3.10, Entry 6), with no further improvement being achieved by increasing the amount to 6.0 equiv. (Table 3.10, Entry 7). Consequently, the conditions used in Entry 6 (Table 3.10) were the optimised ones for the iodofluorination of α-ketoalkynes.

This now left us with four sets of conditions for the iodofluorination of different alkynes (Table 3.11) that were subsequently applied to establish the substrate scope of this transformation.

Table 3.11. Summary of conditions for the iodofluorination of alkynes.

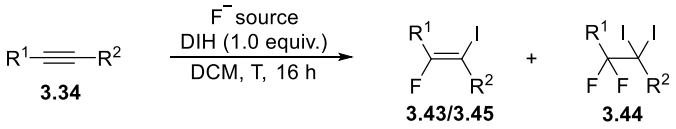

#	F^- Source (equiv.)	T [°C]	Product	Optimised for
Conditions A	$NEt_3 \cdot 3HF$ (3.0)	40	**3.45**	$R^1 = R^2$ = alkyl
Conditions B	pyr/HF (3.0)	–20	**3.43**	R^1 = alkyl, R^2 = H
Conditions C	pyr/HF (9.0)	–20	**3.44**	R^1 = alkyl, R^2 = H
Conditions D	pyr/HF (4.0)	rt	**3.45**	R^1 = alkyl, R^2 = C(O)–alkyl

3.2.2. Substrate Scope

In order to study the scope of our halofluorination of alkynes we at first employed a range of different internal alkynes (Scheme 3.22). Substrates were chosen so as to cover a wide range of functionalities as well as different kinds of electronic and steric bias to direct regioselectivity.

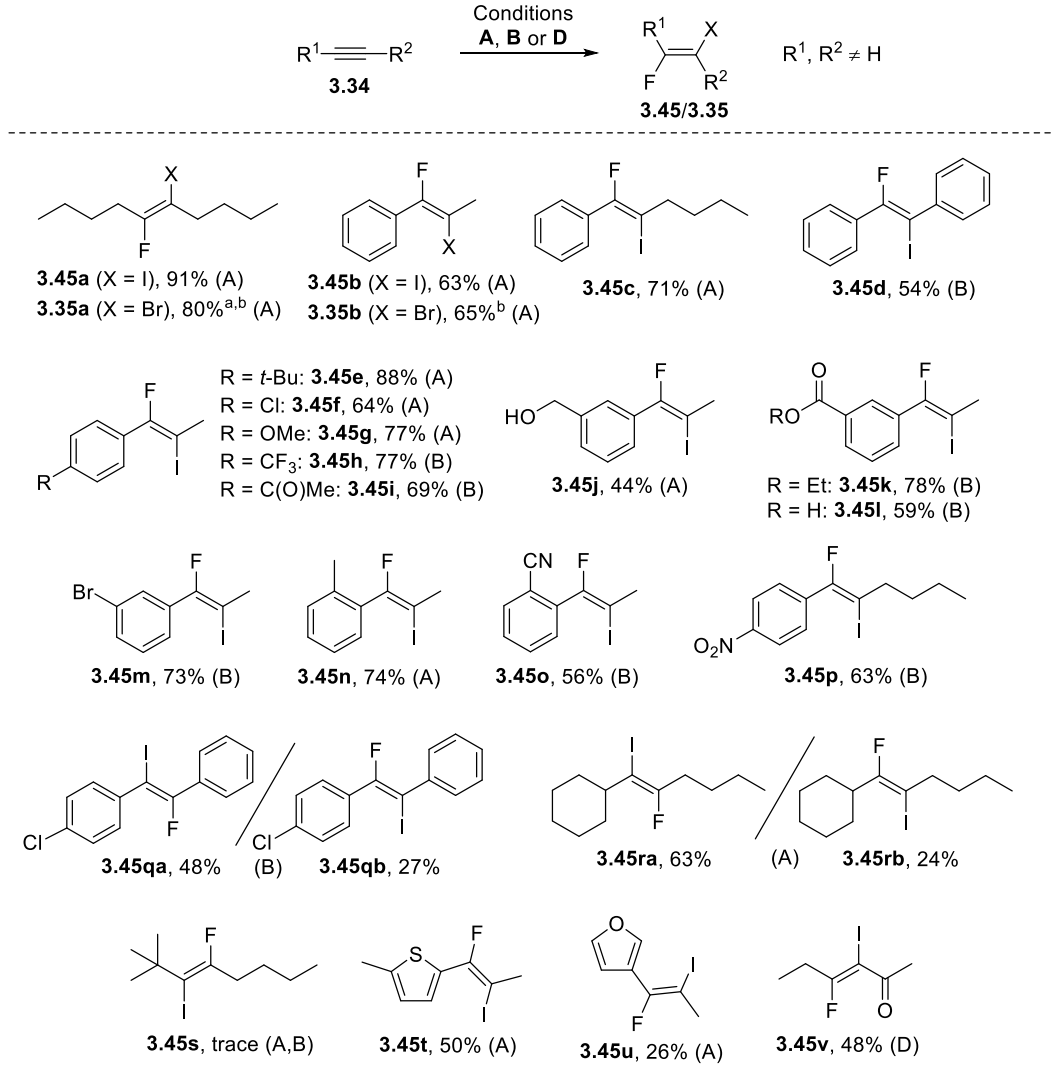

Scheme 3.22. Substrate scope of halofluorination of internal alkynes. Conditions A: 1.0 equiv. internal alkyne (**3.34**) (0.20 mmol), 1.0 equiv. DXH (0.20 mmol), 3.0 equiv. $NEt_3 \cdot 3HF$ (0.60 mmol), DCM (2.0 mL), 40 °C, 16 h. Conditions B: 1.0 equiv. internal alkyne (0.20 mmol), 1.0 equiv. DIH (0.20 mmol), 3.0 equiv. pyr/HF (0.60 mmol), DCM (2.0 mL), –20 °C, 16 h. Conditions D: 1.0 equiv. internal alkyne (0.20 mmol), 1.0 equiv. DIH (0.20 mmol), 4.0 equiv. pyr/HF (0.80 mmol), DCM (2.0 mL), rt, 16 h. Conditions used for each substrate are shown in parentheses. [a]Yield determined by ^{19}F NMR using hexafluorobenzene as internal reference. [b]Reaction was performed at 0 °C.

It was found that the conditions developed for symmetrical, aliphatic alkyne **3.34a** (Conditions A) worked well for electron-neutral (**3.34b**–**c** and **3.34r**), electron-rich (**3.34e**, **3.34g**, **3.34j**, **3.34n**, **3.34t**–**u**) as well as slightly electron-deficient substrates (**3.34f**), not including diaryl substituted ones (**3.34d**). For those bearing more electron deficient aryl substituents (**3.34h**–**i**, **3.34k**–**m**, **3.34o**–**p**) or two aryl substituents (**3.34d**, **3.34q**) Conditions B, which had been optimised for the mono-iodofluorination of terminal alkynes, consistently gave better results. Varying the temperature or the amount of pyr/HF used in these reactions led to diminished yields, suggesting that this was also the optimised set of conditions for these types of substrates. It is to be noted that *p*-Cl-substituted **3.34f** (σ_p = 0.23) gave the same yield within margin of error under Conditions A (64%) as well as Conditions B (63%), whereas *m*-Br-substituted **3.34m** (σ_m = 0.39) showed an almost threefold increase in yield upon changing to the latter (73% compared to 27%).[246]

By applying the appropriate conditions for each substrate, good to excellent yields were obtained for electron rich (e.g.: **3.34g**, **3.34j**), electron neutral (e.g.: **3.34a**–**c**) as well as electron deficient (e.g.: **3.34o**–**p**) internal alkynes. The reaction readily tolerates aromatic halides (**3.45f**, **3.45m**, **3.45q**), ketones (**3.45i**), esters (**3.45k**) unprotected alcohols (**3.45j**) and carboxylic acids (**3.45l**) as well as oxygen and sulphur containing heterocycles (**3.45t**–**u**).

Substrates **3.34a** and **3.34b** were furthermore successfully bromo-fluorinated in 80% and 65% yield, respectively. **3.35a** was thereby obtained in an inseparable mixture with 15% of dibrominated by-product **3.36a**. Generally, it has to be said that Conditions A were more prone to give by-products analogous to **3.36a** than Conditions B or D.

Every substrate tested by us showed exclusive *anti*-addition, in line with the generally accepted mechanism for halogen addition across alkynes. Alkynes bearing one aryl and one aliphatic substituent without exception led to the formation of the benzylic fluoride products, with unsymmetrical diaryl alkyne **3.34q** giving a 1.7:1 mixture of the two possible products **3.45qa** and **3.45qb** in favour of the former, obtained by fluoride attacking the benzylic position, where a positive charge is better stabilised. Iodofluorination of alkyne **3.34r**, bearing one primary and one secondary substituent, resulted in a 2.6:1 ratio of **3.45ra** and **3.45rb**. The formation of the main product includes the attack of fluoride on the less sterically congested alkyne carbon, neighbouring the primary substituent. Employing substrate **3.34s**, with a *t*-butyl group instead of the cyclohexyl, however, led to neither formation of **3.45s** nor its according regioisomer in an isolable yield, suggesting that too sterically demanding substituents can inhibit the intended reaction.

Iodofluorinated enone **3.45v** was isolated in 48% yield, using the previously optimised conditions for this substrate (Conditions D).

After having established the substrate scope for the iodofluorination with internal alkynes, we set out to do the same for the class of terminal alkynes, applying Conditions B summarised in Table 3.11 (Scheme 3.23).

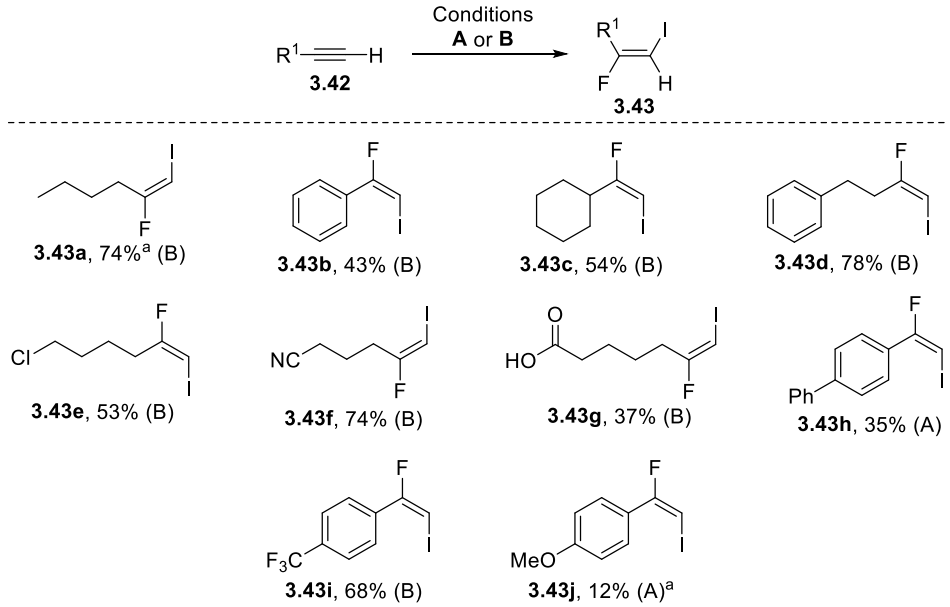

Scheme 3.23. Substrate scope of iodofluorination of terminal alkynes. Conditions A: 1.0 equiv. internal alkyne (**3.42**) (0.20 mmol), 1.0 equiv. DIH (0.20 mmol), 3.0 equiv. $NEt_3 \cdot 3HF$ (0.60 mmol), DCM (2.0 mL), 40 °C, 16 h. Conditions B: 1.0 equiv. internal alkyne (0.20 mmol), 1.0 equiv. DIH (0.20 mmol), 3.0 equiv. pyr/HF (0.60 mmol), DCM (2.0 mL), –20 °C, 16 h. Conditions used for each substrate are shown in parentheses. [a]Yield determined by ^{19}F NMR using hexafluorobenzene as internal reference.

This set of conditions proved to be broadly applicable to alkyl- (**3.42a**, **3.42c**–**g**) as well as aryl-substituted (**3.42b** and **3.42i**), terminal alkynes, bearing different functional groups. Good yields (74–78%) were achieved for primary alkyl substituents with the exception of **3.42g** (37%), whose carboxylic acid functionality might interfere as an alternative nucleophile with the reaction. **3.43c**, bearing a secondary alkyl-group, was obtained in a lower yield (54%) compared to **3.43a**, suggesting a detrimental influence of the increased steric demand. For aryl-substituted alkynes, electron withdrawing substituents on the phenyl core seemed to increase the yield of iodofluorination, as exemplified by the comparison of unsubstituted **3.42b** (43%) with *p*-CF_3-substituted **3.42i** (68%). Biphenyl **3.42h** gave only 5% of the desired monoiodofluorinated product **3.43h**, when employing standard Conditions B, alongside 16% of diiodofluorinated **3.44h**. Using Conditions A, which had previously been used for the iodofluorination of internal alkynes, gave an

increased yield of **3.43h** of 35%. Similarly, for substrate **3.42j** only a trace amount of the desired product was formed using Conditions B, whereas Conditions A gave an increased yield of 12%, as determined by ^{19}F NMR of the crude product mixture. Terminal, aromatic alkynes bearing electron donating substituents therefore seem to consistently give lower yields in this transformation.

Subsequently, we were keen to study whether the double iodofluorination (Conditions C), observed and optimised for 1-hexyne (**3.42a**), could be achieved on a broader scope of substrates. To this end, we performed this transformation on the same selection of terminal alkynes that had been used for the monoiodofluorination described in Scheme 3.23 (Scheme 3.24).

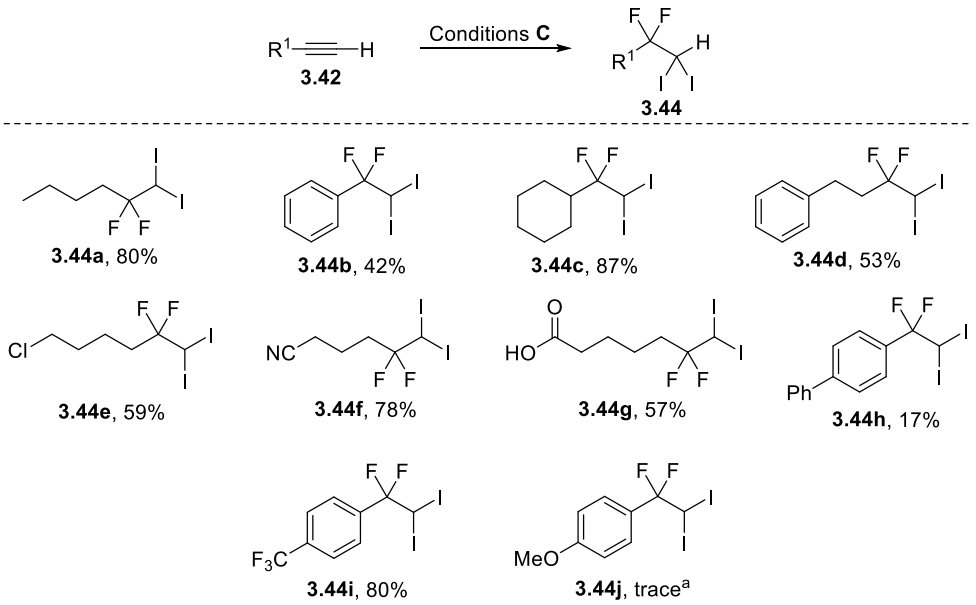

Scheme 3.24. Substrate scope of double iodofluorination of terminal alkynes. Conditions C: 1.0 equiv. internal alkyne (**3.42**) (0.20 mmol), 1.0 equiv. DIH (0.20 mmol), 9.0 equiv. pyr/HF (1.8 mmol), DCM (2.0 mL), –20 °C, 16 h. [a]Yield determined by ^{19}F NMR using hexafluorobenzene as internal reference.

Generally, the yields of the diiodofluorination of **3.42a–j** reflected similar trends as had been observed for the monoiodofluorination (Scheme 3.23). However, greatly increased

yields of 87% and 57%, respectively, compared to the monoiodofluorination, were found for **3.42c** and **3.42g** and a smaller increase, from 68% to 80%, was observed for **3.42i**. By contrast, **3.44d** was obtained in 53% yield compared to 78% that had been achieved for **3.43d**. Also, yields of the diiodofluorinated products of **3.42h** and **3.42j**, which had shown better results in the monoiodofluorination using Conditions A, were lower than for the according monoiodofluorinated products. Trying to prepare **3.44h** using up to 9.0 equiv. of $NEt_3 \cdot 3HF$ in Conditions A failed to produce more than 4% of the desired product with the yield of **3.43h** remaining constant. The obtained terminal diiodides are potential substrates for a Simmons-Smith-type cyclopropanation[247] or the preparation of allylic difluorides *via* olefination.[248,249] Furthermore, one could take advantage of the impossibility of β-hydride elimination after oxidative addition of the C–I bond to a transition metal catalyst for the development of iterative cross-coupling protocols.

In order to show the potential of this protocol for industrial application we prepared **3.45a** on a gram-scale, using the same conditions as for the small scale reaction (Scheme 3.25).

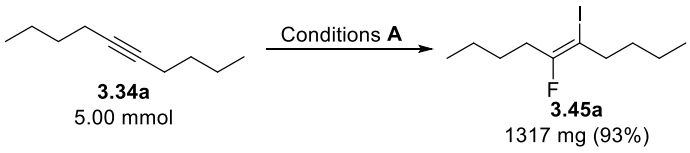

Scheme 3.25. Preparative scale synthesis of **3.45a**. Conditions A: 1.0 equiv. internal alkyne (5.00 mmol), 1.0 equiv. DXH (5.00 mmol), 3.0 equiv. $NEt_3 \cdot 3HF$ (15.00 mmol), DCM (50 mL), 40 °C, 16 h.

This reaction gave more than 1.3 g of **3.45a** starting from 5.00 mmol of alkyne **3.34a**, which is equal to a yield of 93%. This is comparable to the small scale reaction's yield of 91% and demonstrates the robustness of this protocol towards scale-up.

3.2.3. Mechanistic Considerations

As had been suggested before for similar transformations, an ionic mechanism seems the most probable for this reaction.[198,203–205] The general formation of only one iodofluorinated isomer with the observed regio- and stereoselectivity leads us to assume an initial attack of an electrophilic iodine species onto the triple bond, forming a π-complex **A** or cyclic iodonium intermediate **B** (Scheme 3.26). In a second step, this cationic intermediate is then attacked by fluoride nucleophile in an S_N2-like fashion to give the final iodofluorinated alkene in overall *anti*-selectivity. The (*E*)-configuration of the alkenes obtained in this reaction has been shown for internal alkene **3.45b** and terminal alkene **3.43d** using NOESY and HOESY NMR experiments. An nOe correlation was observed in the $^{19}F–^{1}H$ HOESY experiment for both the methyl group as well as *ortho*-hydrogens in **3.45b**, and for the alkene hydrogen substituent as well as the CH_2 group neighbouring the alkene in **3.43d** (Figure 3.1).

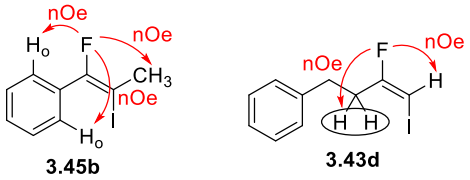

Figure 3.1. nOe signals observed in HOESY NMR experiments on **3.45b** and **3.43d**.

On the other hand, the NOESY experiment revealed no such interaction between the *ortho*-hydrogens and the methyl group in **3.45b**, or the CH_2 and the alkene hydrogen substituent in **3.43d**.

In reactions starting from non-symmetric alkynes fluoride would attack the carbon where a positive charge is better stabilised, resulting in the formation of Markovnikov-type

products. Support for an initial formation of species **A** or **B** followed by nucleophilic attack of fluoride comes from the configuration of the double bond in the final products, showing the two larger substituents *cis* to each other.

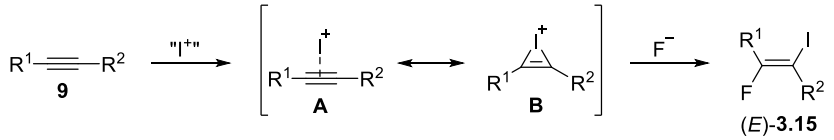

Scheme 3.26. Proposed mechanism of iodofluorination of alkynes with DIH and HF-reagent.

The distinct difference in reactivity between the DIH/NEt_3·3HF compared to the DIH/pyr/HF system could suggest a divergence in terms of mechanism or the intermediate electrophilic iodine species. Activation of DBH by strong acids has been reasoned before to be due to the formation of bromonium ions, Br^+.[236] An analogous pathway may be possible for DIH with acidic pyr/HF (pK_{aH}(pyr) = 5.2) but not NEt_3·3HF (pK_{aH}(NEt_3) = 10.7), which is an almost neutral liquid (Scheme 3.27).[245]

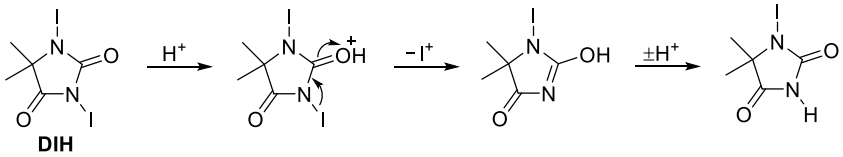

Scheme 3.27. Formation of I^+ *via* acidic activation of DIH.

The released I^+ could subsequently react with the alkyne starting material to give **A**/**B**. Note that in the case of the shown double iodofluorinations (Scheme 3.24) only 1.0 equiv. of DIH is used, suggesting that this reagent is able to also release its second iodine substituent as I^+, presumably *via* an analogous mechanism.

Alternatively, different nucleophilicity of the employed fluoride sources due to the different hydrogen bond accepting potential of pyridine (pK_{BHX} = 1.86) and NEt_3 (pK_{BHX} =

1.98) might play a critical role in explaining an alternative reaction pathway for $NEt_3 \cdot 3HF$.[250] The stronger hydrogen bonds formed by NEt_3 to HF could make a direct attack of fluoride on DIH possible leading to the formation of IF, which would then serve as the electrophilic source of iodine for the formation of **A**/**B** (Scheme 3.28). This might help explain the substantial excess of fluoride needed in order to achieve satisfactory yields.

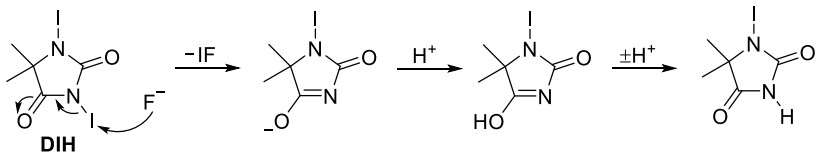

Scheme 3.28. Formation of IF *via* nucleophilic attack of fluoride on DIH.

3.2.4. Post-Fluorination Transformations

The products obtained after iodofluorination are potentially highly valuable intermediates for the synthesis of more complex targets. Vinylic iodides have been shown to readily undergo a plethora of different transformations, among them Suzuki (organoboron),[251–255] Heck (alkene),[256–259] Negishi (organozinc),[252,260–263] Sonogashira (alkyne),[252,264–270] Stille (organotin),[252,271–278] Hiyama (organosilicon),[279–285] as well as Ullmann-type cross-couplings.[286–288]

To show the synthetic potential of our iodofluorinated products we chose to exemplarily elaborate them further, using Suzuki, Sonogashira as well as Ullmann-type reactions. Using dialiphatic product **3.45a** Suzuki-type reactions with different boronic acids were found to proceed smoothly using $[Pd_2(dba)_3]$, PPh_3 and K_2CO_3 (Scheme 3.29).

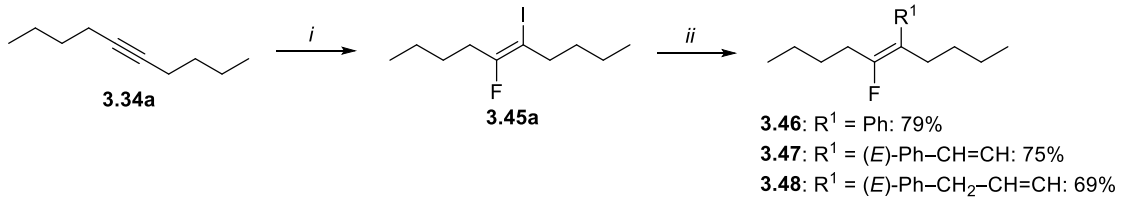

Scheme 3.29. Iodofluorination-Suzuki-coupling sequence starting from **3.34a**. Conditions: *i*: 1.0 equiv. **3.34a** (0.10 mmol), 1.0 equiv. DIH (0.10 mmol), 3.0 equiv. $NEt_3{\cdot}3HF$ (0.30 mmol), DCM (1.0 mL), 40 °C, 16 h. *ii*: 1.5 equiv. R^1–$B(OH)_2$ (0.15 mmol), 5 mol% $[Pd_2(dba)_3]$ (0.0050 mmol), 20 mol% PPh_3 (0.020 mmol), 3.0 equiv. K_2CO_3 (0.30 mmol), 3:1:1 toluene:EtOH:H_2O (1.6 mL), 80 °C, 12 h – amounts calculated assuming quantitative formation of **3.45a**. Isolated yields over two steps are reported.

Intermediate **3.45a** was not isolated, but was directly used for the second step after filtration through a silica plug. This resulted in the formation of products **3.46**–**3.48**, obtained after cross-coupling with phenylboronic acid, ((*E*)-2-phenylethenyl)boronic acid and ((1*E*)-3-phenylprop-1-en-1-yl)boronic acid in 79%, 75% and 69% yield over two steps, respectively. The analogous reaction with (2-phenylethyl)boronic acid, as an example of an alkylboronic acid, did not result in any formation of the desired product with a mixture of starting material and protodeiodinated product (**3.49**) being obtained (Scheme 3.30). In order to get this reaction to work different ligands (e.g. dppf) as well as organoboron reagents would have to be assessed.

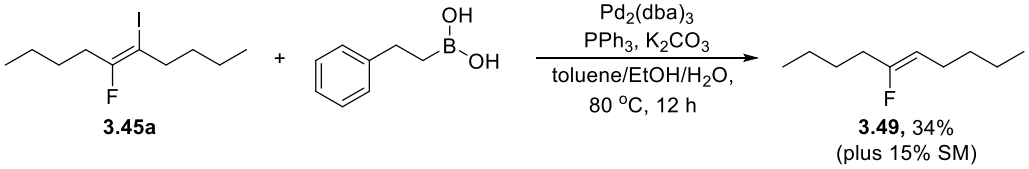

Scheme 3.30. Attempted Suzuki coupling of **3.45a** with alkylboronic acid. Conditions: 1.0 equiv. **3.45a** (0.10 mmol), 1.5 equiv. R^1–$B(OH)_2$ (0.15 mmol), 5 mol% $[Pd_2(dba)_3]$ (0.0050 mmol), 20 mol% PPh_3 (0.020 mmol), 3.0 equiv. K_2CO_3 (0.30 mmol), 3:1:1 toluene:EtOH:H_2O (1.6 mL), 80 °C, 12 h. ^{19}F NMR yields over two steps relative to hexafluorobenzene as internal standard are reported.

The reactions shown in Scheme 3.29 could furthermore be applied to product **3.45b**, containing an activated iodofluorinated styrene-type double bond (Scheme 3.31).

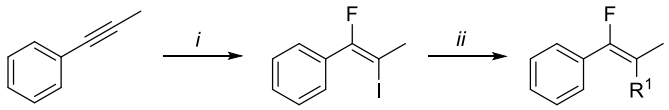

3.50: R^1 = Ph: 52%
3.51: R^1 = (*E*)-Ph–CH=CH: 50%
3.52: R^1 = (*E*)-Ph–CH_2–CH=CH: 55%

Scheme 3.31. Iodofluorination-Suzuki-coupling sequence starting from **3.34b**. Conditions: *i*: 1.0 equiv. **3.34b** (0.10 mmol), 1.0 equiv. DIH (0.10 mmol), 3.0 equiv. NEt_3·3HF (0.30 mmol), DCM (1.0 mL), 40 °C, 16 h. *ii*: 1.5 equiv. R^1–$B(OH)_2$ (0.11 mmol), 5 mol% $[Pd_2(dba)_3]$ (0.0035 mmol), 20 mol% PPh_3 (0.014 mmol), 3.0 equiv. K_2CO_3 (0.21 mmol), 3:1:1 toluene:EtOH:H_2O (1.1 mL), 80 °C, 12 h – amounts calculated assuming a yield of **3.45b** of 70%. Isolated yields over two steps are reported.

Products **3.50**–**3.52** were isolated in 52%, 50% and 55%, respectively, relative to the amount of alkyne **3.34b**.

The reaction sequence using phenylboronic acid in the second step was also successfully performed on iodofluorinated stilbene derivative **3.45d**, which gave **3.53** in 49% yield (Scheme 3.32). It is be noted that the reactions with ((*E*)-2-phenylethenyl)boronic acid and ((1*E*)-3-phenylprop-1-en-1-yl)boronic acid were not attempted for this substrate.

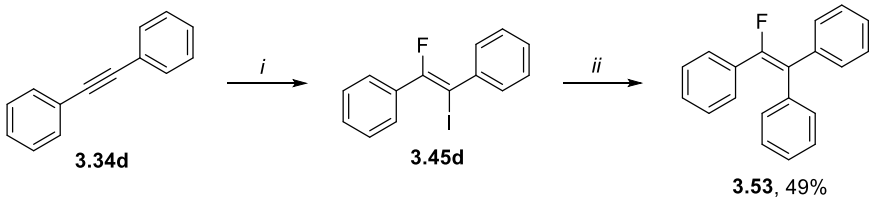

Scheme 3.32. Iodofluorination-Suzuki-coupling sequence starting from **3.34d**. Conditions: *i*: 1.0 equiv. **3.34d** (0.10 mmol), 1.0 equiv. DIH (0.10 mmol), 3.0 equiv. pyr/HF (0.30 mmol), DCM (1.0 mL), –20 °C, 16 h. *ii*: 1.5 equiv. R^1–$B(OH)_2$ (0.083 mmol), 5 mol% $[Pd_2(dba)_3]$ (0.0028 mmol), 20 mol% PPh_3 (0.011 mmol), 3.0 equiv. K_2CO_3 (0.17 mmol), 3:1:1 toluene:EtOH:H_2O (0.90 mL), 80 °C, 12 h – amounts calculated assuming a yield of **3.45d** of 55%. Isolated yield over two steps is reported.

Finally, we also successfully employed this two-step procedure for the synthesis of a fluorinated tamoxifen derivative (**3.56**), which had previously been shown to exhibit higher growth inhibition activity against four tested human cancer cell lines compared to the parent compound (Scheme 3.33).[289]

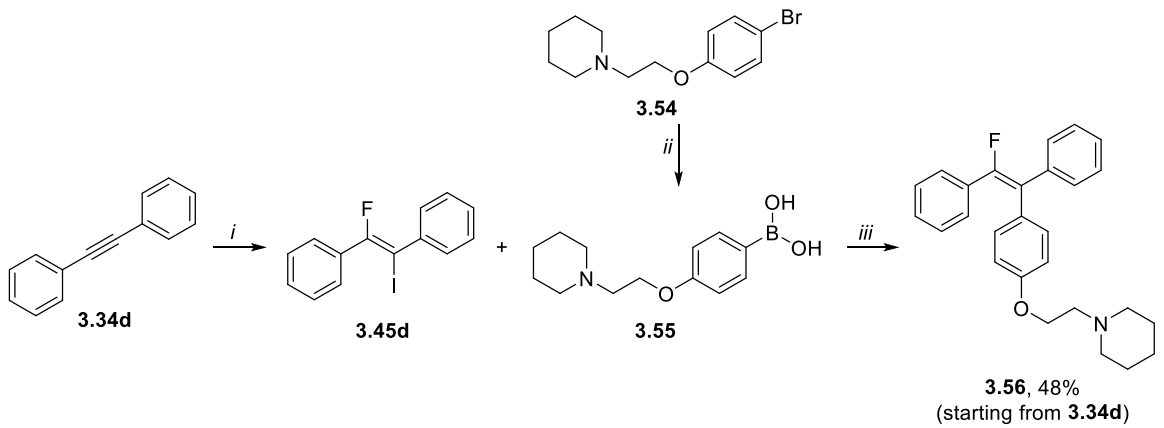

Scheme 3.33. Synthesis of fluorinated tamoxifen derivative **3.56** from commercial starting materials. Conditions: *i*: 1.0 equiv. **3.34d** (0.20 mmol), 1.0 equiv. DIH (0.20 mmol), 3.0 equiv. pyr/HF (0.60 mmol), DCM (2.0 mL), –20 °C, 16 h. *ii*: 1.0 equiv. **3.54** (1.00 mmol), 1.0 equiv. *n*-BuLi (1.00 mmol), 1.0 equiv. $B(O\textit{i}\text{-}Pr)_3$ (1.00 mmol), THF (3.0 mL), –78 °C to rt, 75 min. *iii*: 1.5 equiv. R^1–$B(OH)_2$ (0.17 mmol), 5 mol% $[Pd_2(dba)_3]$ (0.0055 mmol), 20 mol% PPh_3 (0.022 mmol), 3.0 equiv. K_2CO_3 (0.33 mmol), 3:1:1 toluene:EtOH:H_2O (1.8 mL), 80 °C, 12 h – amounts calculated assuming a yield of **3.45d** of 55%. Isolated yield calculated from **3.34d** is reported.

Starting from commercially available alkyne **3.34d** and aryl bromide **3.54**, the two coupling partners for the Suzuki reaction were prepared in one step each without requiring purification by column chromatography. The subsequent cross-coupling was performed under the same conditions as had been used for the synthesis of **3.53**, and **3.56** was obtained in 48% yield over two steps starting from **3.34d**. In comparison, **3.56** had before been prepared in six steps with an unreported overall yield.[289]

In conclusion, this Suzuki cross-coupling protocol could be used for the synthesis of fluorinated stilbene-type double bonds, triaryl-substituted double bonds as well as fluorinated dienes.

In order to also be able to access fluorinated enynes we chose to investigate the possibility of using Sonogashira-type cross-couplings of our iodofluorinated products with different terminal alkynes. The conditions presented in Scheme 3.34 allowed for alkyne

3.34a to be converted into enynes **3.57** and **3.58** using phenylacetylene and ethynyltrimethylsilane *via* **3.45a**, with only a short filtration work-up after the first step.

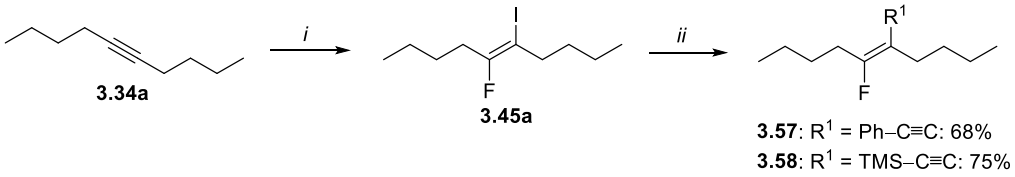

Scheme 3.34. Iodofluorination-Sonogashira-coupling sequence starting from **3.34a**. Conditions: *i*: 1.0 equiv. **3.34a** (0.10 mmol), 1.0 equiv. DIH (0.10 mmol), 3.0 equiv. $NEt_3{\cdot}3HF$ (0.30 mmol), DCM (1.0 mL), 40 °C, 16 h. *ii*: 1.4 equiv. terminal alkyne (0.14 mmol), 2.5 mol% $[Pd_2(PPh_3)_2Cl_2]$ (0.0025 mmol), 5 mol% CuI (0.0050 mmol), NEt_3 (0.50 mL), rt, 12 h – amounts calculated assuming quantitative formation of **3.45a**. Isolated yields over two steps are reported.

Using $[Pd(PPh_3)_2Cl_2]$ and CuI as catalysts and NEt_3 as solvent, fluorinated enynes **3.57** and **3.58** were obtained in 68% and 75%, respectively, over two steps, making this sequence an efficient way of accessing this motif from readily available starting materials.

In order to perform this transformation with aromatic alkyne **3.34b** NEt_3 had to be exchanged for $(i\text{-Pr})_2NH$ in the cross-coupling step (Scheme 3.35).

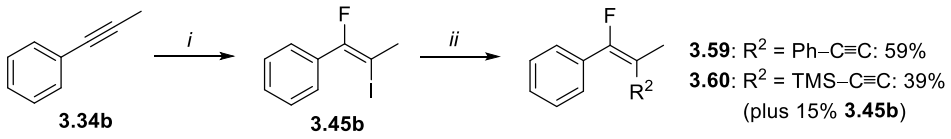

Scheme 3.35. Iodofluorination-Sonogashira-coupling sequence starting from **3.34b**. Conditions: *i*: 1.0 equiv. **3.34b** (0.10 mmol), 1.0 equiv. DIH (0.10 mmol), 3.0 equiv. $NEt_3{\cdot}3HF$ (0.30 mmol), DCM (1.0 mL), 40 °C, 16 h. *ii*: 1.4 equiv. terminal alkyne (0.098 mmol), 2.5 mol% $[Pd_2(PPh_3)_2Cl_2]$ (0.0018 mmol), 5 mol% CuI (0.0035 mmol), $(i\text{-Pr})_2NH$ (0.35 mL), rt, 12 h – amounts calculated assuming a yield of **3.34b** of 70%. Isolated yields over two steps are reported.

This allowed for the preparation of enynes **3.59** and **3.60** in 59% and 39%, respectively, calculated from the starting alkyne. After the reaction with ethynyltrimethylsilane 15% of intermediate **3.45b** were recovered.

The tetrasubstituted alkene products so far prepared *via* these two-step sequences all bear three carbon substituents on the double bond, in addition to the vinylic fluoride. Ullmann-type reactions, which have been less widely reported for vinylic iodides compared to Suzuki and Sonogashira cross-couplings, would give access to a different class of tetrasubstituted alkenes, bearing an additional heteroatom substituent in addition to fluoride (Table 3.12).

Table 3.12. Optimisation of the iodofluorination-Ullmann-coupling sequence starting from **3.34a**.

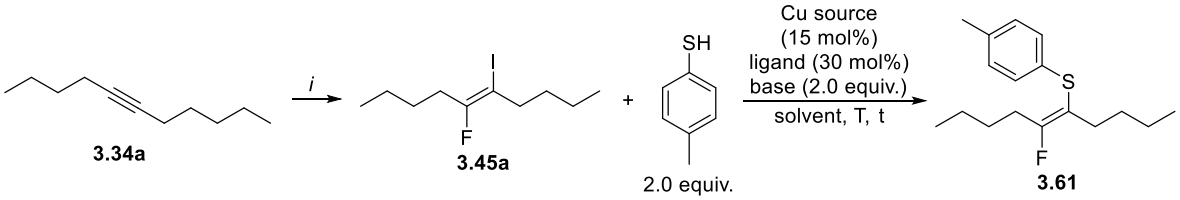

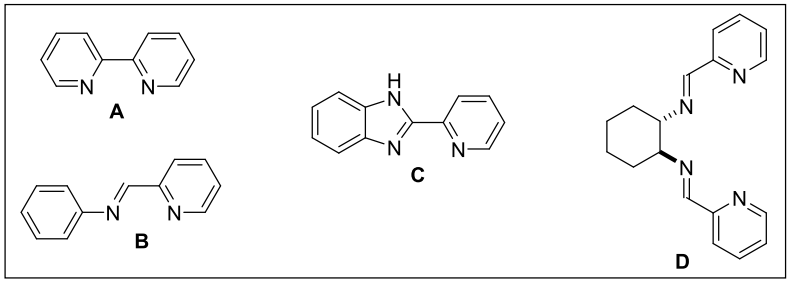

Entry	Cu	Ligand	Base	Solvent	T [°C]	t [h]	Conversion[a] [%]	**3.61**[a] [%]
1	$[Cu(MeCN)_4PF_6]$	**A**	Cs_2CO_3	1,4-Dioxane	100	16	60	29
2	$[Cu(MeCN)_4PF_6]$	**B**	Cs_2CO_3	1,4-Dioxane	100	16	62	37
3	$[Cu(MeCN)_4PF_6]$	**C**	Cs_2CO_3	1,4-Dioxane	100	16	55	43
4	$[Cu(MeCN)_4PF_6]$	**D**	Cs_2CO_3	1,4-Dioxane	100	16	48	38
5	$[Cu(MeCN)_4PF_6]$	**C**	Cs_2CO_3	DMF	100	16	88	46
6	$[Cu(MeCN)_4PF_6]$	**C**	Cs_2CO_3	Toluene	100	16	26	0
7[b]	$[Cu(MeCN)_4PF_6]$	**C**	Cs_2CO_3	MeCN	100	16	61	24
8	$[Cu(MeCN)_4PF_6]$	**C**	Cs_2CO_3	DMSO	100	16	82	47
9	CuI	**C**	Cs_2CO_3	1,4-Dioxane	100	16	67	28

10	$[Cu(MeCN)_4PF_6]$	**C**[c]	Cs_2CO_3	1,4-Dioxane	100	16	53	34
11[d]	$[Cu(MeCN)_4PF_6]$	**C**	Cs_2CO_3	1,4-Dioxane	100	16	57	41
12	$[Cu(MeCN)_4PF_6]$	**C**	Cs_2CO_3[e]	1,4-Dioxane	100	16	62	37
13	$[Cu(MeCN)_4PF_6]$	**C**	K_2CO_3	1,4-Dioxane	100	16	76	49
14	$[Cu(MeCN)_4PF_6]$	**C**	Na_2CO_3	1,4-Dioxane	100	16	18	0
15	$[Cu(MeCN)_4PF_6]$	**C**	K_3PO_4	1,4-Dioxane	100	16	71	50
16	$[Cu(MeCN)_4PF_6]$	**C**	K_3PO_4	1,4-Dioxane	125	16	>95	83 (83)
17[f]	$[Cu(MeCN)_4PF_6]$	**C**	K_3PO_4	1,4-Dioxane	125	16	>95	74
18[f]	$[Cu(MeCN)_4PF_6]$[g]	**C**[h]	K_3PO_4	1,4-Dioxane	125	16	>95	84 (82)
19[f]	$[Cu(MeCN)_4PF_6]$[i]	**C**[g]	K_3PO_4	1,4-Dioxane	125	16	91	72
20	$[Cu(MeCN)_4PF_6]$	-	K_3PO_4	1,4-Dioxane	125	16	>95	62
21	-	-	K_3PO_4	1,4-Dioxane	125	16	21	0

Conditions: *i*: 1.0 equiv. **3.34a** (0.10 mmol), 1.0 equiv. DIH (0.10 mmol), 3.0 equiv. $NEt_3{\cdot}3HF$ (0.30 mmol), DCM (1.0 mL), 40 °C, 16 h. Assuming quantitative formation of **3.45a**: 2.0 equiv. 4-methylthiophenol (0.20 mmol), 15 mol% Cu source (0.015 mmol), 30 mol% ligand (0.030 mmol), 2.0 equiv. base (0.20 mmol), solvent (0.30 mL), 100 °C, 16 h. [a]Determined by ^{19}F NMR of crude reaction mixture using hexafluorobenzene as internal reference. Isolated yields in parentheses. [b]80 °C. [c]15 mol%. [d]3.0 equiv. of 4-methylthiophenol. [e]3.0 equiv. [f]1.5 equiv. of 4-methylthiophenol. [g]10 mol%. [h]20 mol%. [i]5 mol%.

Performing the reactions with $[Cu(MeCN)_4PF_6]$ as precatalyst and Cs_2CO_3 as base in 1,4-dioxane at 100 °C, we at first looked at different nitrogen-based ligands **A**–**D**, which have been used before for similar transformations (Table 3.12, Entries 1–4).[288,290–293] Ligand **C**, consisting of a benzimidazole and a pyridine moiety, gave the best result with a conversion of 55% and desired product **3.61** being obtained in 43% yield. A screening of different solvents (Table 3.12, Entries 5–8), apolar and polar, then revealed slightly better results for DMF and DMSO giving **3.61** in 46% and 47%, respectively. However, whereas for 1,4-dioxane the starting alkene had almost quantitatively been converted into **3.61**,

the conversions observed for DMF as well as DMSO were significantly higher. Since there was no other major by-product isolated from these reactions, this suggests decomposition of starting material, which prompted us to continue this study with 1,4-dioxane. Following this, CuI was tested as a cheaper alternative to $[Cu(MeCN)_4PF_6]$, but was found to give a lower yield of **3.61** of 28% (Table 3.12, Entry 9). Using only 1.0 equiv. of **C** relative to the amount of Cu also resulted in a diminished yield of 34% (Table 3.12, Entry 10). Similarly, increasing the amount of either 4-methylthiophenol or Cs_2CO_3 led to worse yields of 41% and 37%, respectively (Table 3.12, Entries 11 and 12). Varying the counter-cation of the base gave an improved yield of 49% for K_2CO_3 and no formation of **3.61** in the case of Na_2CO_3 (Table 3.12, Entries 13 and 14). K_3PO_4 was found to give a slightly improved yield of 50% compared to K_2CO_3 (Table 3.12, Entry 15). Performing the reaction at 125 °C instead of 100 °C proofed to be highly beneficial, increasing the yield of **3.61** to 83% (isolated yield: 83%) over two steps with no starting material being recovered (Table 3.12, Entry 16). Upon reducing the amount of 4-methylthiophenol nucleophile from 2.0 equiv. to 1.5 equiv. the yield dropped to 74% (Table 3.12, Entry 17), however, when the catalyst loading was also reduced to 10 mol%, **3.61** was again obtained in 84% yield by ^{19}F NMR and 82% isolated yield over two steps (Table 3.12, Entry 18). Reducing the amount of Cu further to 5 mol% caused the yield to drop to 72% (Table 3.12, Entry 19). Control reactions without ligand (Table 3.12, Entry 20) and without Cu as well as ligand (Table 3.12, Entry 21) gave 62% and 0% yield, respectively, showing that Cu is necessary for this reaction to proceed and the ligand improves the conversion into the desired product.

Therefore, the conditions presented in Entry 18 are our optimised ones for the Ullmann-type coupling of iodofluoroalkene **3.45a** with 4-methylthiophenol. These were then also applied to substrate **3.45b** (Scheme 3.36).

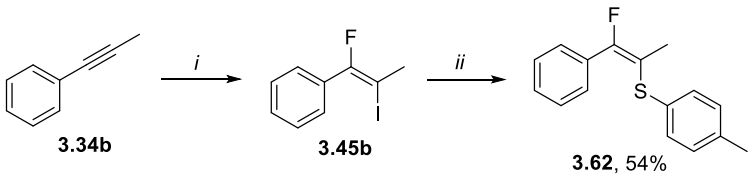

Scheme 3.36. Iodofluorination-Ullmann-coupling sequence starting from **3.34b**. Conditions: *i*: 1.0 equiv. **3.34b** (0.10 mmol), 1.0 equiv. DIH (0.10 mmol), 3.0 equiv. $NEt_3 \cdot 3HF$ (0.30 mmol), DCM (1.0 mL), 40 °C, 16 h. *ii*: 1.5 equiv. 4-methylthiophenol (0.11 mmol), 10 mol% Cu source (0.0070 mmol), 20 mol% ligand (0.014 mmol), 2.0 equiv. base (0.14 mmol), solvent (0.30 mL), 100 °C, 16 h – amounts calculated assuming a yield of **3.45b** of 70%.

The reaction sequence presented in Scheme 3.36 allowed for alkene **3.62** to be isolated in 54% over two steps from alkyne **3.34b**.

3.3. Conclusion

To conclude, we have successfully developed a novel method for the iodofluorination of internal alkynes, giving iodofluorinated alkenes with overall *anti*-selectivity. We have shown its broad applicability by using it to prepare 21 iodofluoroalkenes bearing a wide range of functionalities. This protocol was also successfully employed in a gram-scale reaction, demonstrating its robustness towards scale-up. Furthermore, by lowering the temperature it could be used for related bromofluorination of alkynes.

The conditions could also be altered in such a way as to allow for terminal alkynes as well as an example of an ynone to be used as substrates. In the case of terminal alkynes,

increasing the amount of fluorinating reagent led to the exclusive formation of doubly iodofluorinated products.

The obtained iodofluoroalkenes were successfully shown to be good substrates for Suzuki- as well as Sonogashira- and Ullmann-type cross couplings to access further elaborated fluoroalkenes. Our reaction has furthermore been used as key step in the synthesis of a tamoxifen derivative with improved potency compared to the parent compound, which could be prepared in two linear steps from commercial starting materials.

Part B

Hydrogen-Bonded Fluoride Complexes as Novel Reagents for Carbon–Fluorine Bond Formation

Chapter 4: Structure and Reactivity Study on Fluoride–Alcohol Complexes

4.1. Introduction: Activation of Fluoride Anion

Many of the striking discoveries in fluorine chemistry were made possible due to the development of an extensive library of specialised reagents for electrophilic as well as nucleophilic fluorination. Although these reagents often successfully circumvent drawbacks associated with more easily accessible fluoride sources, many of them require expensive, multi-step syntheses from commercially available starting materials, which makes them unsuitable for large-scale industrial application. Also, due to the small window of reactivity typically tolerated in a certain transformation,[294] many of these reagents remain limited in their potential application. New methods, employing simple metal fluorides as sources of F^-, are highly sought after, as this group of nucleophilic fluorinating reagents is the most cost as well as atom efficient.

The use of fluoride in organic reactions is challenging due to impediments associated with its high electronegativity, low polarizability, small size as well as considerable charge density (see Chapter 1). Currently, the use of metal fluorides is underdeveloped, because their use suffers from a range of drawbacks: Firstly, their ionic character as well as high lattice energy renders them insoluble in most organic solvents, often resulting in incompatibilities with reaction conditions. Secondly, many of these salts are highly hygroscopic, making them challenging reagents when working under anhydrous conditions. The hygroscopicity is a result of the high hydration enthalpy, which has also

been argued to be the reason why fluorine, although being the 13th most abundant element in the earth's crust, is only found in fewer than 10 natural products.[295] Thirdly, most noticeably in its anhydrous state, the free fluoride anion, besides being a nucleophile, can also act as a potent Brønsted as well as Lewis base, potentially leading to unwanted side-reactions.

Therefore, different ways to activate metal fluorides and fluoride anion in general have been explored to obtain more potent and more selective nucleophiles, in an attempt to make these reagents more applicable to organic synthesis.

4.1.1. Crown Ethers

In 1974, Liotta and Harris reported the improved solubility of KF in benzene and MeCN with catalytic amounts of 18-crown-6 by complexation of K^+ (Figure 4.1). [296–298]

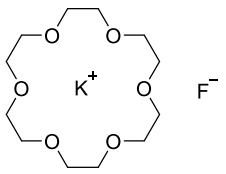

Figure 4.1. Liotta's 'naked' fluoride.

The reactivity profile of this 'naked' fluoride was demonstrated by studying nucleophilic substitutions and their competing eliminations at sp^3-hybridised carbons with leaving groups located at primary, secondary, tertiary as well as benzylic positions, and nucleophilic displacements at sp^2-hybridised carbons. In the cases of benzyl bromide, 2,4-dinitrochlorobenzene and acetyl chloride a clean transformation into the desired fluorinated products was observed, whereas for bromocyclohexane only the olefinic by-

product was detected at the end of the reaction. 1-Bromooctane, 2-bromooctane as well as 2-chloro-2-methylcyclohexanone gave mixtures of the substitution and elimination products.

In further applications of this source of activated fluoride it became apparent that the reactivity did not match that of a truly 'naked' fluoride anion.[297–300] Subsequent ^{39}K NMR studies by Miller and Clark showed peak broadening for solutions of KF–18-crown-6, associated with ion pairing and potential formation of aggregates beyond simple ion pairs.[301]

In 2009, Lee, Chi and Song disclosed the beneficial effect of using bis-terminal hydroxyl polyethers as activators, giving improved results in the nucleophilic substitution of primary alkyl mesylate **4.1** compared to KF–18-crown-6 (Scheme 4.1).[302]

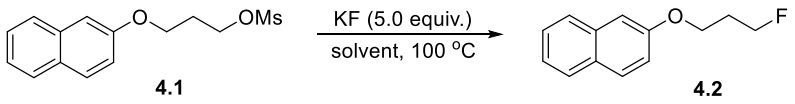

4.1 **4.2**

tetraEG: 92% (1.5 h)
triEG: 93% (1.5 h)
MeCN: 0% (24 h), 40% (24 h with 18-crown-6)

Scheme 4.1. Nucleophilic fluorination with KF using different activators.

After 1.5 h tetraethylene glycol (tetraEG) and triethylene glycol (triEG) returned the desired product **4.2** in 92% and 93% yield, respectively, whereas only 40% were found after 24 h in a reaction with 2.0 equiv. of 18-crown-6 in MeCN. The authors suggested a cooperative mechanism, whereby the ether groups act as Lewis bases towards K^+, thereby weakening its interaction with fluoride and improving the solubility of KF, similar to the effect of 18-crown-6. Additionally, one hydroxyl group would form a hydrogen bond to fluoride, consequently decreasing its basicity and potentially blocking the

formation of aggregates compared to the KF–18-crown-6 system; the second one could simultaneously activate the leaving group (Figure 4.2). [302]

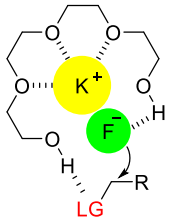

Figure 4.2. Cooperative activation mechanism of tetraEG.

Evidence for this cooperative behaviour was obtained by performing the reaction in triethylene glycol dimethyl ether as well as the monomethyl ether, which led to the formation 0% and 42% of **4.2**, respectively, illustrating the importance of the terminal hydroxyl functionalities. Further support was obtained from quantum chemical calculations, showing a remarkably low energy barrier for the reaction with KF in tetraethylene glycol, which increased upon replacing one hydroxyl for a methoxy group.

This activation approach using oligoethylene glycols was extended to CsF and other carbon, nitrogen, oxygen, sulphur and halogen nucleophiles,[302,303] a variant using polymer supported oligoethylene glycols[304] as well as to an asymmetric variant using BINOL-based chiral analogues of oligoethylene glycols for the activation of KF.[305]

Chiral bis(hydroxyl) polyether (*S*)-**4.3** was found to be capable of promoting the desilylative kinetic resolution of silyl-protected secondary alcohols with KF (Scheme 4.2).[305]

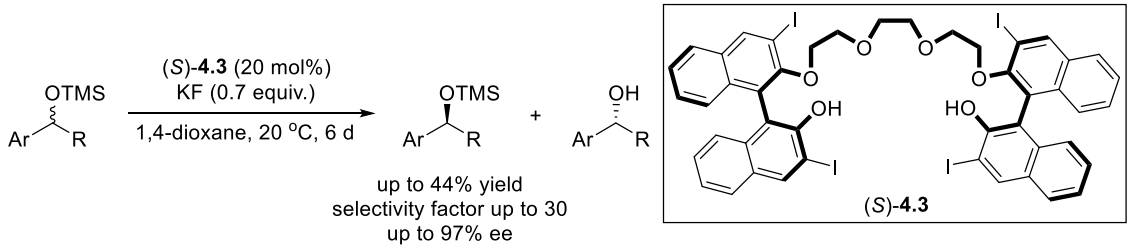

Scheme 4.2. Desilylative kinetic resolution of silyl-protected secondary alcohols with KF and chiral bis(hydroxyl) polyether **4.3**.

Using 20 mol% of (*S*)-**4.3** and 0.7 equiv. of KF, enantioenriched silyl-protected alcohols could be isolated in 91–97% ee. The crystal structure of the complex formed between KF and **4.3** showed hydrogen-bonding of the free BINOL hydroxyl groups to fluoride as well as coordination of ether oxygens as well as aromatic iodides to potassium, reducing the Coulombic interaction between K^+ and F^-. Methylating the free hydroxyl groups led to an unreactive system.

Recently, Kim and co-workers described the use of bis-*t*-alcohol-functionalised crown-6-calix[4]arene (BACCA) as another type of bis-terminal hydroxyl polyether for the activation of CsF.[306] Quantum chemical calculations suggested the formation of free fluoride by separation of cation and anion to a distance >8 Å.

4.1.2. Solid-Supported Fluoride

In 1976, Cainelli and co-workers described the use of fluoride trapped on an anion-exchange resin containing quaternary ammonium groups (Amberlyst-A 26) for nucleophilic substitutions.[307] The F^- form of the resin was formed by washing the OH^- form with dilute aqueous HF (Scheme 4.3).

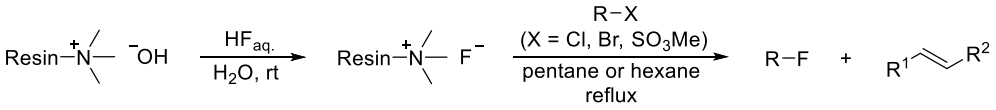

Scheme 4.3. Preparation of fluoride-loaded anion-exchange resin and reaction with alkyl halides/methanesulfonates.

Stirring an excess of the fluoride-loaded resin with different primary and secondary alkyl halides and methanesulfonates in an apolar solvent led to the formation of the according alkyl fluorides and alkene by-products. The effectiveness of this approach relies on the dehydration of fluoride as a consequence of resin incorporation and also allowed for the reaction with 1-bromooctane to be carried out in water, giving as products 1-fluorooctane (24%) and 1-octanol (32%).

In a separate study, Colonna and co-workers used fluoride-loaded anion-exchange resins for the incorporation of fluorine at chiral centres *via* nucleophilic displacement of halide and methanesulfonate leaving groups.[308] Clean S_N2 reactions, leading to epimerically pure 3-fluoro-steroids and both diastereoisomers of ethyl 2-fluoropropionate, were reported, highlighting the stereospecificity of this reaction.

In the context of ^{18}F-radiolabelling, Luxen and co-workers later reported a protocol for the recovery of cyclotron produced [^{18}F]F$^-$ from [^{18}O]H$_2$O to, after elution with MeCN, obtain fluoride with a low water content without the use of an evaporation step.[309]

4.1.3. Spray-Drying

As mentioned earlier, one major drawback of most simple metal fluorides is their hygroscopic character.

In 1981, Ishikawa and co-workers found that spray-dried KF was less hygroscopic and a more effective fluorinating reagent compared to calcine-dried KF.[310] Letting samples of both reagents stand at ambient conditions for 1 h, calcine-dried KF absorbed 26% of its weight in water whereas for spray-dried KF it was only 3%. The reaction with *p*-chloronitrobenzene in refluxing DMSO proceeded considerably faster with spray-dried KF compared to the calcine-dried variant, and the former was also shown to be an effective source of fluoride for the nucleophilic displacement of acyl, aroyl and sulfonyl chlorides as well as alkyl halides. The difference in hygroscopicity, was argued, might be ascribed to differences in the surface structure of the KF crystals.

4.1.4. Ionic Liquids

Ionic liquids are known to be able to stabilise polar transition states and show high solubility for metal salts, which makes them an attractive object of study for fluorination reactions using simple metal fluorides.

In 2002, Song and Chi reported the first example of a nucleophilic fluorination with KF using an ionic liquid, [bmim][BF_4], as activator and water as additive (Scheme 4.4).[311]

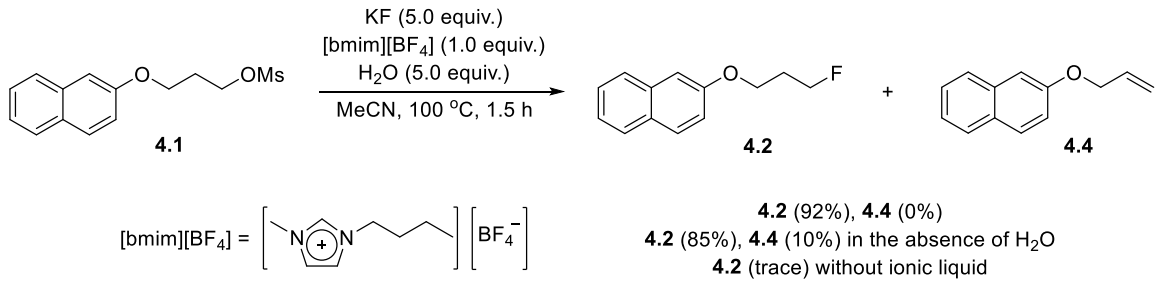

Scheme 4.4. Fluorination of **4.1** with KF in the presence of an ionic liquid and H_2O.

Substrate **4.1** was thereby converted into alkyl fluoride **4.2** in 92% yield over 1.5 h using 1.0 equiv. of [bmim][BF_4] and 5.0 equiv. of KF as well as water in MeCN at 100 °C. In the absence of water, the reaction gave **4.2** in 85% yield with 10% of alkene by-product **4.4** being formed, indicating that water is reducing the basicity of fluoride anion. The reaction without ionic liquid only produced a trace amount of **4.2**. Subsequently published DFT calculations by the same group suggested cooperative activity of the cation and the anion as possible explanation for the improved reactivity.[312] The anion was thought to act as a Lewis base towards K^+, thereby reducing its electrostatic effects on F^-, whereas the acidic C2-proton of the imidazolium cation would activate the mesylate leaving group *via* hydrogen-bonding.

To facilitate product purification use of a Merrifield resin-anchored ionic liquid, **4.5**, was reported (Scheme 4.5).[313]

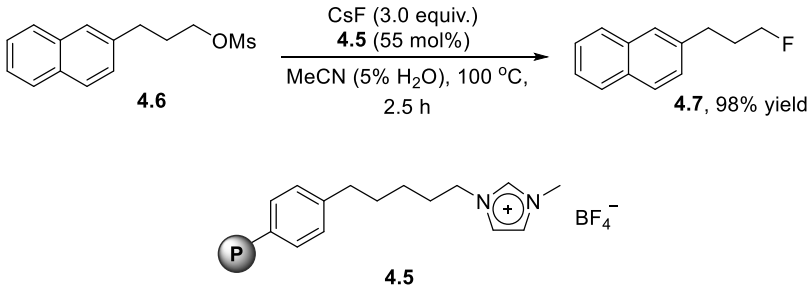

Scheme 4.5. Fluorination of **4.6** with sub-stoichiometric amount of polymer-supported ionic liquid **4.5**.

Performing the fluorination of **4.6** with CsF in the presence of a sub-stoichiometric amount of **4.5** yielded alkyl fluoride **4.7** in 98% yield, a better result than had been obtained with the non-immobilised version of **4.5** under otherwise identical conditions. This effect was related to synergistic effects between neighbouring imidazolium groups, as had been proposed earlier for tetraarylphosphonium salt grafted silica gel.[314]

However, although ionic liquids have been shown to be excellent activators for simple metal fluorides leading to excellent yields in nucleophilic substitutions with little by-product formation, they were found to decompose after prolonged exposure to highly basic fluoride anion, particularly at elevated temperatures, leading to the formation of alkyl imidazoles, fluoroalkanes and alkenes .[315]

4.1.5. Hydrogen-Bonding

In 2001, the Withers group described the synthesis of *β*-mannosides from *α*-D-mannosyl fluoride using a mutant *β*-mannosidase (Man2a Glu519Ser).[316] Moreover, they found that fluoride anion was able to rescue significant glycosidic bond-cleaving ability when 2',4'-dinitrophenyl-*β*-D-mannopyranoside was used as substrate, leading to the *in situ* formation of *α*-D-mannosyl fluoride (Scheme 4.6).

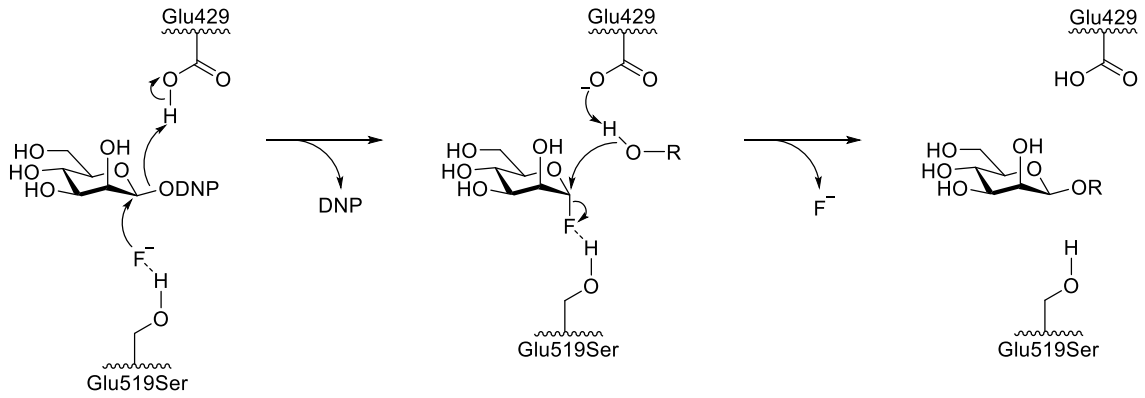

Scheme 4.6. Man2a Glu519Ser mutant catalysed formation of a *β*-mannoside *via* an *α*-D-mannosyl fluoride intermediate.

This was described as the first case, where a fluoride anion acts as a substitute nucleophile in a mutant enzyme system. By using an acid-base mutant of Man2A (E429A) the authors were able to slow down the second step, leading to the accumulation of the

covalent intermediate, which can be detected by ^{19}F NMR.[317] The authors argued that C–F bond formation in this system might be facilitated by hydrogen-bonding interactions and desolvation of fluoride anion.

In 2002, the O'Hagan group published work describing the formation of 5'-fluoro-5'-deoxyadenosine (5'-FDA) from (*S*)-adenosyl-L-methionin (SAM) and fluoride anion when incubated with partially purified protein extract from *Streptomyces cattleya* (Scheme 4.7A).[318] The final product of the associated biosynthetic pathway was fluoroacetate, which was also formed when incubating the protein extract with synthetic 5'-FDA. Later, 5'-fluoro-5'-deoxyadenosine synthase, the enzyme responsible for the formation of 5'-FDA in *S. cattleya*, was isolated as the first enzyme in this organisms biosynthetic pathway to fluoroacetate and 4-fluorothreonine.[319] Subsequent crystallographic characterisation of substrate- as well as product-bound 5'-fluoro-5'-deoxyadenosine synthase suggested fluoride to be bound first, followed by highly specific binding of SAM, which is recognised by a combination of hydrogen bonds and van der Waals contacts (Scheme 4.7B).[320–322]

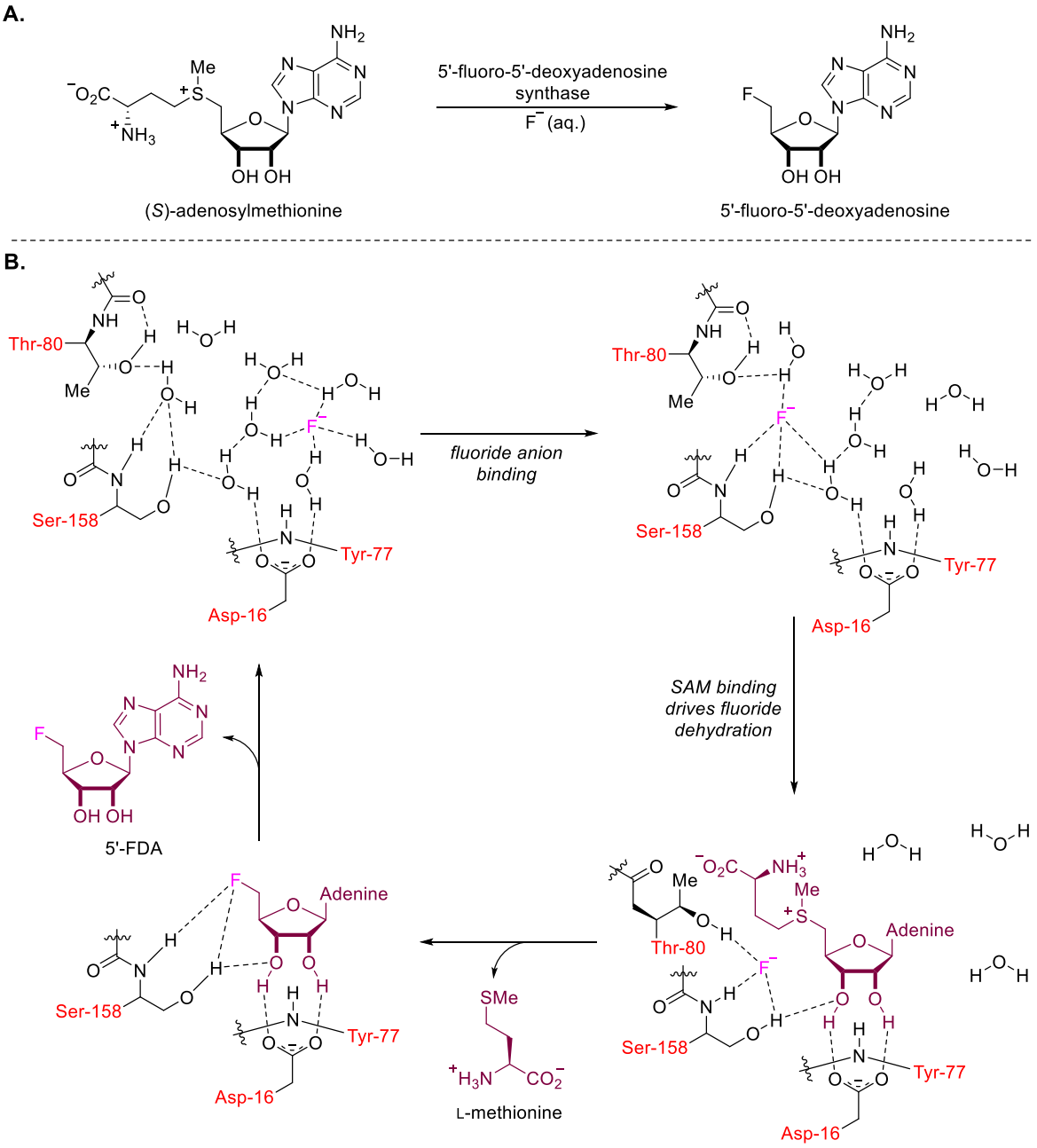

Scheme 4.7. (A) Fluorinase-mediated synthesis of 5'-fluoro-5'-deoxyadenosine. (B) Catalytic cycle of fluorinase, highlighting key hydrogen bonds.

Purification of the enzyme containing SAM from *S. cattleya* hints at strong binding of SAM, which the authors argued is used by the enzyme to achieve dehydration of the bound fluoride. Extrapolating from the orientation of the fluoromethyl of 5'-FDA in the product-bound complex, a strong hydrogen bond to the backbone amide and a bifurcated hydrogen bond to the OH group of Ser-158 are used by the enzyme to reduce the high

activation barrier for full dehydration, similar to what had been suggested by Withers for mutant *β*-mannosidase. Results from isotopic labelling in whole-cell experiments furthermore indicated that the fluorination proceeds with a stereochemical inversion of configuration at the C5' carbon of SAM, in the fashion of an S_N2-type nucleophilic substitution. Computational studies also suggested a third hydrogen bond to the OH side chain of Thr-80 to stabilise the transition state (Scheme 4.7B).[323]

These two examples suggest that hydrogen-bonding interactions can be used by enzymes to dehydrate fluoride anion to create a more potent nucleophile for a subsequent substitution reaction.

Moreover, in 1994 Yonezawa and co-workers characterised a series of hydrogen-bonded fluoride–alcohol complexes, which they had been able to prepare by mixing $TBAF(H_2O)_3$ and the according volatile alcohol solvents at 40 °C under controlled vacuum to effect azeotropic removal of water (Table 4.1).[324]

Table 4.1. Summary of TBAF–alcohol complexes prepared by Yonezawa.

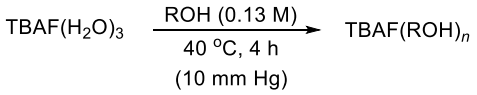

ROH	*n*	H_2O [%]	physical properties
MeOH	2.5	5.0	oil
EtOH	2.5	0.0	oil
n-PrOH	2.5	0.4	crystalline
i-PrOH	3.5	0.1	crystalline
n-BuOH	3.3	0.3	oil
i-BuOH	5.0	0.1	slush
s-BuOH	2.5	2.0	oil
t-BuOH	3.7	0.5	crystalline

The calculated alcohol molecules per fluoride varied between 2.5 and 5.0. Complexes formed with *n*-PrOH, *i*-PrOH and *t*-BuOH were found to be crystalline solids and except MeOH and *s*-BuOH all alcohols formed complexes containing less than 1% water. The authors furthermore found that the hydrogen bond donors influenced the kinetic reactivity of fluoride in the S_N2-type displacement reaction with benzyl bromide (**4.8**) to give the according fluoride **4.9** (Scheme 4.8).

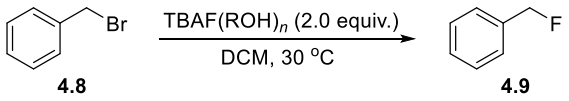

4.8 **4.9**

Rate: *t*-BuOH > *i*-PrOH > *n*-BuOH ~ *n*-PrOH > H_2O

Scheme 4.8. Kinetic study of S_N2 displacement of benzyl bromide with TBAF(ROH)$_n$.

A good agreement was found between increasing steric bulk of the alcohol and increasing reactivity, with TBAF–*t*-BuOH complex showing the best result.

Following up on this work, Kim and co-workers were able to show that S_N2-type fluorination with simple metal fluoride salts (*e.g.* CsF) proceeds with greater kinetic reactivity, as well as improved selectivity over competing E2 pathways when performed in bulky tertiary alcohol solvents (*e.g. t*-BuOH, *t*-AmylOH) compared to polar aprotic solvents like MeCN or DMF (Table 4.2).[325]

Table 4.2. Fluorination of alkyl mesylate **4.1** with CsF in tertiary alcohol solvents.

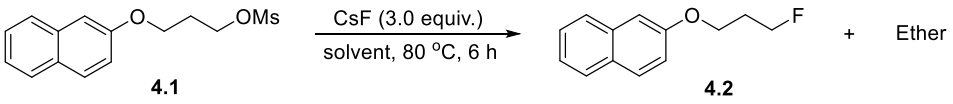

4.1 **4.2**

Solvent	**4.1** [%]	**4.2** [%]	Ether[a] [%]
t-AmylOH	-	93	5
t-BuOH	trace	92	7
n-BuOH	4	64	30
CH_3CN	91	7	-
DMF[b]	33	48	-

[a]Formed by nucleophilic attack of alcohol solvent on primary alkyl carbon substituting mesylate. [b]8% of alcohol and 9% of alkene by-product formed.

Although primary alcohols like *n*-BuOH were also able to promote the fluorination to give **4.2**, they also led to an increased formation of the ether by-product due to their reduced steric bulk.

This protocol using *t*-BuOH as solvent was furthermore extended to radiolabelling of a set of key ^{18}F-labelled radiopharmaceuticals with [^{18}F]F$^-$ and the yields were found to improve significantly compared to the according literature procedures.[325]

The effect of the tertiary alcohol solvent on this reaction was argued to be threefold: (1) By forming hydrogen bonds to fluoride ion in the CsF lattice it might reduce the strength of the CsF ionic bond, thereby improving solubility. (2) The hydrogen-bonded fluoride ion is expected to exhibit a lower basicity, thereby improving the selectivity of this transformation. (3) Hydrogen-bonding of the alcohol solvent molecules to the leaving group should improve its leaving group ability, leading to faster turnover.[325,326]

Evidence for the activation of certain leaving groups as part of the explanation for the beneficial effect of *t*-BuOH on nucleophilic fluorination was provided by the fact that

substrates bearing a mesylate leaving group reacted significantly faster than the corresponding bromides or iodides.[326]

In 2008, Kim published the single-crystal X-ray structure of TBAF(*t*-BuOH)$_4$, which had been obtained from a mixture of commercially available TBAF(H_2O)$_3$ and *t*-BuOH in hexane after refluxing for 30 min and cooling to room temperature. It showed fluoride anion hydrogen-bonding to four alcohol moieties in a tetrahedral arrangement, providing some evidence of how fluoride and *t*-BuOH might interact in solution (Figure 4.3).[327]

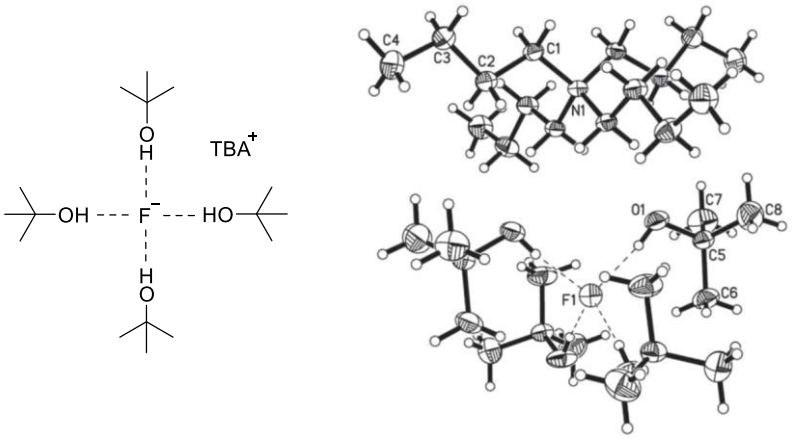

Figure 4.3. Solid state structure of TBAF(*t*-BuOH)$_4$ as determined by single-crystal X-ray crystallography. Reprinted with permission from: D. W. Kim, H.-J. Jeong, S. T. Lim, M-H Sohn, *Angew. Chem. Int. Ed.* **2008**, *47*, 8404–8406. Copyright © 2008 WILEY-VCH Verlag GmbH & Co. KGaA.

Using this isolated hydrogen-bonded complex as fluoride source yielded similar results compared to the reactions with CsF in *t*-BuOH, significantly outperforming anhydrous TBAF as well as TBAF(H_2O)$_3$ (Table 4.3).[327]

Table 4.3. Fluorination of alkyl bromide **4.10** with different TBAF sources.

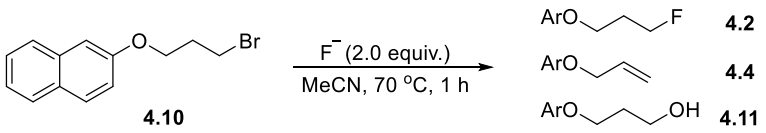

F^--Source	**4.10** [%]	**4.2** [%]	**4.4** [%]	**4.11** [%]
TBAF(*t*-BuOH)$_4$	-	80	20	-
TBAF(H_2O)$_3$	-	63	30	6
TBAF (anhydrous)	-	22	78	-

TBAF(*t*-BuOH)$_4$ also proved to be significantly less hygroscopic compared to commercial TBAF(H_2O)$_3$, making it a potential source of anhydrous fluoride.

In order to combine the beneficial effects of ionic liquids as well as tertiary alcohols, Kim and co-workers prepared *t*-alcohol-tethered ionic liquid **4.12** ([mim-^{t}OH][OMs]) and compared its ability to promote the nucleophilic fluorination of primary alkyl mesylate **4.1** to [bmim][OMs] and *t*-BuOH (Table 4.4).[328]

Table 4.4. Fluorination of primary alkyl mesylate **4.1** with *t*-alcohol-tethered ionic liquid **4.12**.

Additive	**4.1**[a] [%]	**4.2**[a] [%]	**4.4**[a] [%]	**4.11**[a] [%]
t-BuOH	77	23	-	-
[bmim][OMs]	64	32	4	-
[bmim][OMs]/*t*-BuOH	58	40	2	trace
4.12	-	100	-	-

[a]Determined by ^{1}H NMR integration.

The results showed a significant cooperative effect, with quantitative transformation of **4.1** into alkyl fluoride **4.2** with newly developed ionic liquid **4.12**, compared to 40% yield

when using a 1:1 mixture of [bmim][OMs] and *t*-BuOH as promoters, as well as 23% and 32% for the reactions with *t*-BuOH and [bmim][OMs], respectively.

The use of hydrogen-bonding to ameliorate the reactivity of free fluoride also proved crucial for the development of Pd(0)- and Ir(I)-catalysed allylic fluorinations developed by Gouverneur and Brown (Scheme 4.9).[329,330]

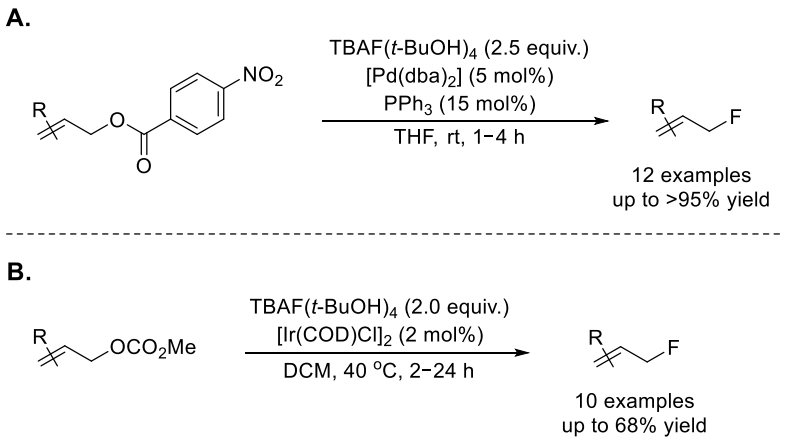

Scheme 4.9. Allylic fluorinations with TBAF(*t*-BuOH)$_4$ under Pd(0)- (A) and Ir(I)-catalysis (B).

For these reactions, TBAF(*t*-BuOH)$_4$ with its high kinetic reactivity, reduced basicity and low water content proved to be the ideal source of fluoride.

Outside the context of C–F bond formation, hydrogen-bonding to fluoride has also been used in a series of stereocontrolled reactions employing alcohols or thioureas as hydrogen bond donors.

In 2006, the Scheidt group found that the combination of TMAF with thiourea derivative **4.13** was beneficial for the direct nucleophilic acylation of nitroalkenes (Scheme 4.10).[331]

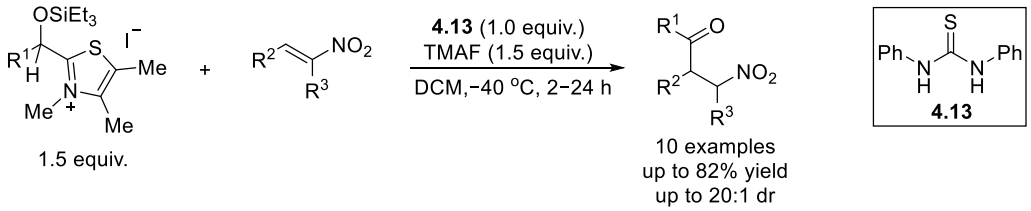

Scheme 4.10. Nucleophilic acylation of nitroalkenes promoted by a fluoride/thiourea combination.

By using chiral quinine-derived thiourea **4.14** this transformation could be rendered asymmetric, giving **4.16** in 67% yield and 74% ee from nitroalkene **4.15** (Scheme 4.11).[331]

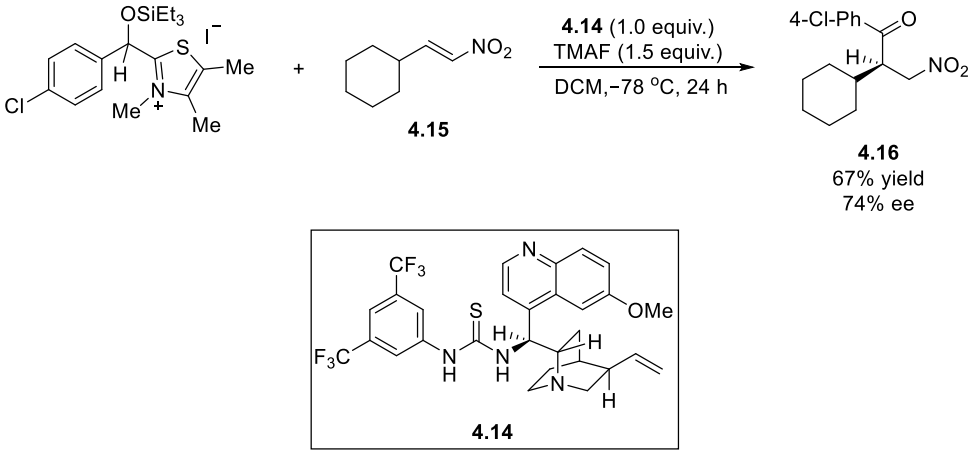

Scheme 4.11. Asymmetric acylation of nitroalkene **4.15**.

In 2011, Jacobsen published a protocol for the organocatalytic, enantioselective acylation of silyl ketene acetals, using acyl fluorides and a dual-functional thiourea (**4.17**) (Scheme 4.12A).[332]

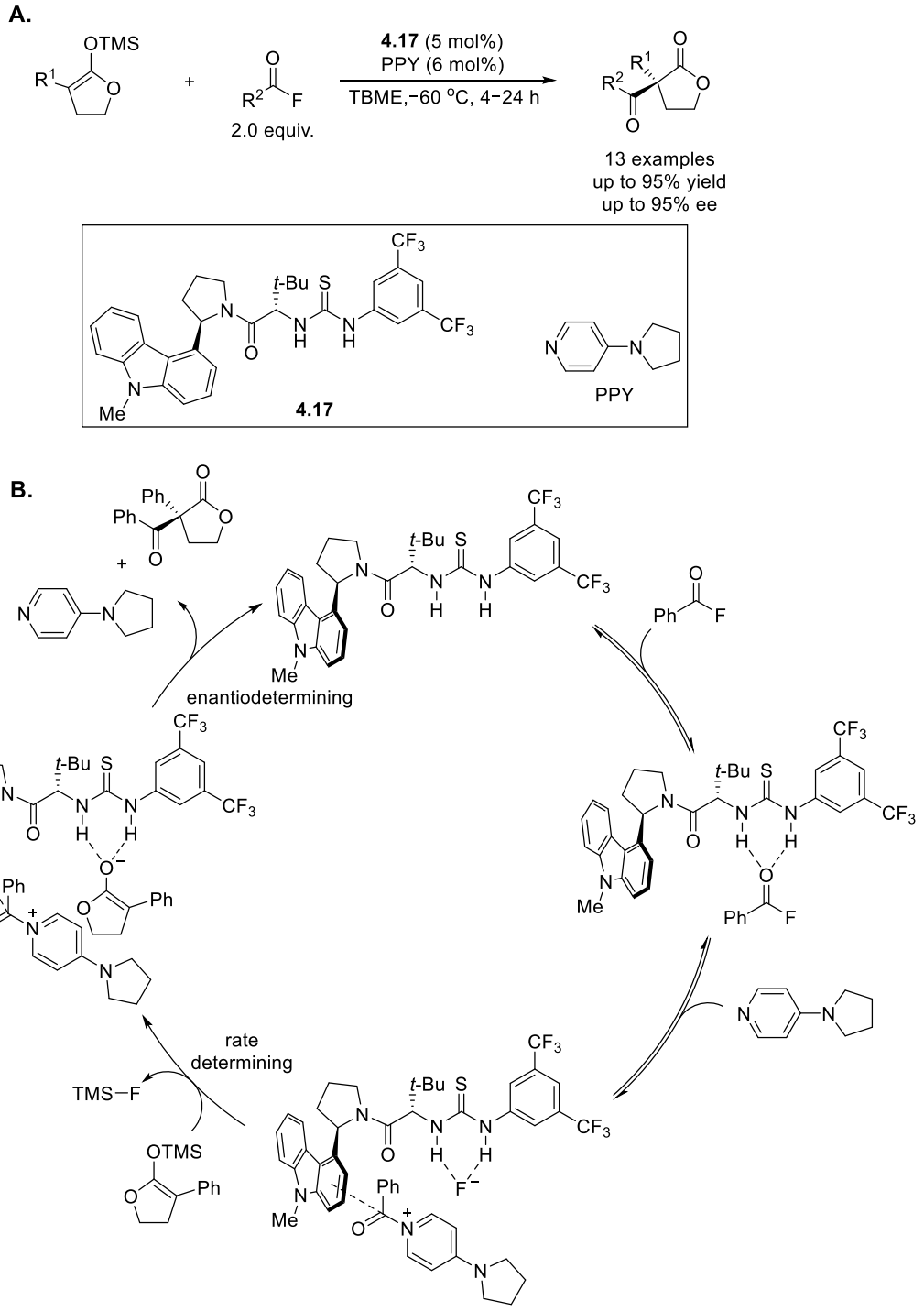

Scheme 4.12. (A) Enantioselective acylation of silyl ketene acetals through hydrogen-bonding catalysis. (B) Suggested catalytic cycle.

The thiourea organocatalyst was expected to play multiple roles in the catalytic cycle of this transformation (Scheme 4.12B). Activation of the acyl fluoride would be followed by C–F bond cleavage to give an *N*-acyl pyridinium fluoride species, stabilised by cation–π

interaction and fluoride–thiourea hydrogen-bonding. From there, rate determining desilylation of silyl ketene acetal yields a hydrogen-bonded enolate, which attacks the stabilised cation in the following enantiodetermining acylation step, leading to formation of the desired product and catalyst recovery.

Given these precedents we sought to further the understanding of the effects of hydrogen-bonding on fluoride reactivity using a combined structural, kinetic as well as computational approach. This should allow us to determine factors that play a crucial role in influencing the reactivity as well as selectivity in reactions, using hydrogen-bonded fluoride sources. The following work was carried out in collaboration with Dr. Keary M. Engle, George W. Pidgeon and Dr. Guy T. Giuffredi and was published in *Chemical Science* in 2015.[333]

4.2. Results and Discussion

With Yonezawa's and Kim's seminal contributions as precedent and also considering that two of the hydrogen-bonding partners of fluoride in the reactive pocket of the fluorinase enzyme are hydroxyl functionalities of amino acids, we started our investigation using alcohols and polyols as hydrogen bond donors.

4.2.1. Complex Synthesis

At the outset of this study our goal was to establish the solid state structures of a wide range of hydrogen-bonded complexes with different alcohols and polyols, which would

later serve as a basis for interpreting observations in solution. For reasons of ease of synthesis and characterisation, as well as favourable expected solubility profiles tetrabutylammonium was used as counter-cation. Alcohols/polyols were chosen on the basis of varying pK_a values as well as steric environments. The synthesis followed an adapted version of Kim's protocol for the preparation of TBAF(*t*-BuOH)$_4$:[327] Commercially available TBAF(H_2O)$_3$ and 1.0–4.0 equiv. of alcohol/polyol (see Experimental Section for details) in hexane were heated to violent reflux for 2 h, so as to azeotropically remove water from the mixture. Depending on the complex, after cooling to room temperature or subsequent removal of solvents under reduced pressure (see Experimental Section for details), solid products were obtained, which were washed with hexane and characterised by ^{1}H and ^{13}C NMR. This revealed a clearly defined stoichiometry of the bulk materials. The crude products were then recrystallised from DCM, EtOAc or THF by gradually reducing their solubility due to slow mixing with hexane either using a layering or vapour diffusion technique (see Experimental Section for details) to obtain single-crystals suitable for X-ray diffraction experiments. An overview of all 15 structures prepared in this way is given in Table 4.5, stating the coordination numbers (C.N.) as found in the solid state structures and NMR.

Table 4.5. Summary of structurally characterised fluoride–alcohol complexes prepared from $TBAF(H_2O)_3$.

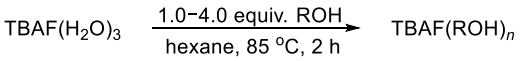

Entry	Alcohol	Yield [%]	Complex	C.N.[a]
1[b,c]	1-Adamantanol **4.18a**	84	**4.19a**	4
2[d]	(*R*,*R*)-di-(*i*-Pr)tartrate **4.18b**	61	**4.19b**	4
3	Mannitol derivative **4.18c**[e]	95	**4.19c**	4
4[d]	Pinacol **4.18d**	93[f]	**4.19d**	4
5[b,g]	Neopentyl glycol **4.18e**	87	**4.19e**	4
6[b,d]	Tris(hydroxymethyl)ethane **4.18f**[e]	95	**4.19f**	4
7[b,c]	Pentaerythritol **4.18g**	77	**4.19g**	4
8[b,c,g]	Catechol **4.18h**	93	**4.19h**	4,3
9[b,c]	Cyclic hemiacetal **4.18i**[e]	89	**4.19i**	3[h]
10	(*R*)-BINOL **4.18j**	88	**4.19j**	3
11[b,d]	Diphenylmethanol **4.18k**	91	**4.19k**	3
12[b,c]	9-Phenylfluoren-9-ol **4.18l**	91	**4.19l**	2, 3
13[c]	Triphenylmethanol **4.18m**	61	**4.19m**	2
14[c]	Tri-(*p*-tolyl)-methanol **4.18n**	76[i]	**4.19n**	2
15	Pyrrolidine **4.18o**[e]	77	**4.19o**	2[j]

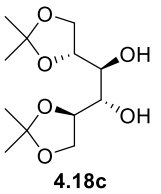

4.18c

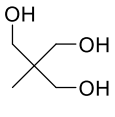

4.18f

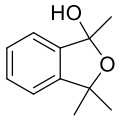

4.18i

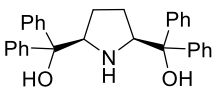

4.18o

Conditions: 1.0 equiv. $TBAF(H_2O)_3$, 1.0–4.0 equiv. **4.18** (see Experimental Part for details), hexane (0.033 M F^-), 80 °C, 2 h. [a]Coordination number *n* in $(ROH)_nF^-$. [b]Complex prepared by Dr. K. M. Engle. [c]Single-crystal X-ray diffraction data collected by G. W. Pidgeon. [d]Single-crystal X-ray diffraction data collected by Dr. G. T. Giuffredi. [e]See formulae block. [f]Yield was 96% when performed on a 12.00 mmol scale. [g]Single-crystal X-ray diffraction data collected by Dr. K. M. Engle. [h]3 ROH, 1 H_2O. [i]Yield was 91% when performed on 15.00 mmol scale. [j]1 $(ROH)_2$, 1 H_2O.

As can be seen from Table 4.5, most complexes featured four fluoride–alcohol hydrogen bonds in the solid state (Table 4.5, Entries 1–7), similar to Kim's structure of TBAF(*t*-BuOH)$_4$.[327] Using catechol, two polymorphic structures were obtained, both containing tri- as well as tetracoordinate fluoride species (Table 4.5, Entry 8). Upon increasing the steric bulk of the alcohol molecules lower coordination numbers could be achieved. (*R*)-

BINOL (**4.18i**), cyclic hemiacetal **4.18j**, diphenylmethanol **4.18k** and 9-phenyl-9-fluorenol (**4.18l**) formed structures with three fluoride–alcohol hydrogen bonds, with the latter also containing a second dicoordinate fluoride species (Table 4.5, Entries 9–12). Complexes **4.19m–o** prepared from triphenylmethanol, tri-(*p*-tolyl)-methanol and pyrrolidine derivative **4.18o**, respectively, only showed two fluoride–alcohol hydrogen bonds (Table 4.5, Entries 13–15). It is to be noted here that this variability in coordination stoichiometry had not been observed previously. All complexes were obtained in good to excellent yields, with those containing sterically more hindered ligands tending to give lower yields (Table 4.5, Entries 13–15).

In order to study the effect of the size of the counter-cation the same procedure was used to prepare analogous complexes to **4.19d** (neopentyl glycol) and **4.19g** (pinacol) using TEAF$(H_2O)_2$ and TMAF$(H_2O)_4$ instead of TBAF$(H_2O)_3$. Again, the crude products were analysed by ^{1}H and ^{13}C NMR and the stoichiometry of the bulk material was found to be clearly defined. In all these cases, however, no single-crystals suitable for X-ray diffraction experiments could be obtained despite multiple attempts. A summary is presented in Table 4.6 with coordination numbers (C.N.) assumed from the stoichiometry found in ^{1}H NMR.

Table 4.6. Summary of fluoride–alcohol complexes obtained from $TEAF(H_2O)_2$ and $TMAF(H_2O)_4$.

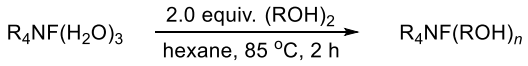

Entry	Alcohol	R	Yield [%]	Complex	C.N.[a]
1[b]	Pinacol **4.18d**	Me	73	**4.19p**	4
2[b]	Pinacol **4.18d**	Et	77	**4.19q**	4
3[b]	Neopentyl glycol **4.18e**	Me	92	**4.19r**	4
4[b]	Neopentyl glycol **4.18e**	Et	87	**4.19s**	4

Conditions: 1.0 equiv. $TBAF(H_2O)_3$ (4.00 mmol), 2.0 equiv. **4.18** (8.00 mmol), hexane (125 mL), 80 °C, 2 h. [a]Coordination number *n* in $(ROH)_nF^-$. [b]Prepared by Dr. K. M. Engle.

Complexes **4.19p** and **4.19q** obtained from pinacol were isolated in 73% and 77% yield (Table 4.6, Entries 1–2), with neopentyl glycol-derived complexes **4.19r** and **4.19s** being formed in higher yields of 92% and 87% (Table 4.6, Entries 3–4), respectively.

Furthermore, when we used *N*-hydroxysuccinimide (NHS, **4.20**) as hydrogen bond donor a white solid was obtained, which did not contain fluoride as was established by ^{19}F NMR. Determining the solid state structure of complex **4.21** after recrystallisation revealed that the acidic hydroxyl group of **4.20** had been deprotonated during complexation, accompanied by the release of HF, and the obtained structure showed the *N*-oxide hydrogen-bonding to two protonated NHS molecules with a TBA^+ counter-cation (Scheme 4.13A). Similarly, the complexation reaction with squaryl amide **4.22** also led to deprotonation and formation of the according TBA^+-salt of the resulting squaramate (**4.23**) (Scheme 4.13B).

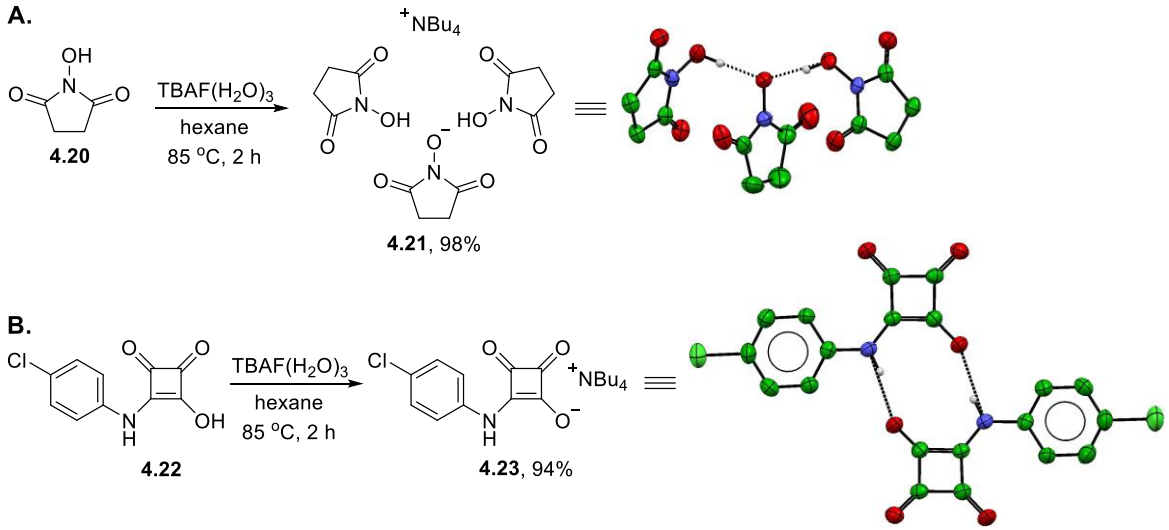

Scheme 4.13. Deprotonation of *N*-hydroxysuccinimide (A) and squaryl amide **4.18q** (B) upon reaction with $TBAF(H_2O)_3$. Displacement ellipsoids are drawn at 50% probability. Cations and hydrogens not involved in hydrogen-bonding are omitted for clarity. Conditions: (A) 1.0 equiv. $TBAF(H_2O)_3$ (4.00 mmol), 3.0 equiv. **4.20** (12.00 mmol), hexane (125 mL), 80 °C, 2 h. (B) 1.0 equiv. $TBAF(H_2O)_3$ (1.00 mmol), 1.0 equiv. **4.22** (1.00 mmol), hexane (30 mL), 80 °C, 2 h. Experiments carried out by Dr. K. M. Engle (**4.21**) and G. W. Pidgeon (**4.23**).

With pK_as of 5.9–6.0 for NHS[334–336] and 0.51 for parent squaric acid[337] these hydrogen bond donors were the most acidic surveyed in this study, and the observed deprotonations indicate that too highly acidic OH functionalities engage in Brønsted acid/base chemistry with fluoride anion rather than forming isolable hydrogen-bonded complexes.

4.2.2. Solid State Structures

As a basis for further studies, the solid state structures of complexes **4.19a**–**o** were determined using single-crystal X-ray diffraction experiments.

The structure found for 1-adamantanol (1-Ada-OH) derived complex **4.19a** was the only one to feature four fluoride–alcohol hydrogen bonds without involving a diol (Figure 4.4).

Two crystallographically distinct but closely related complexed anions (**A** and **B**) were found to make up the unit cell.

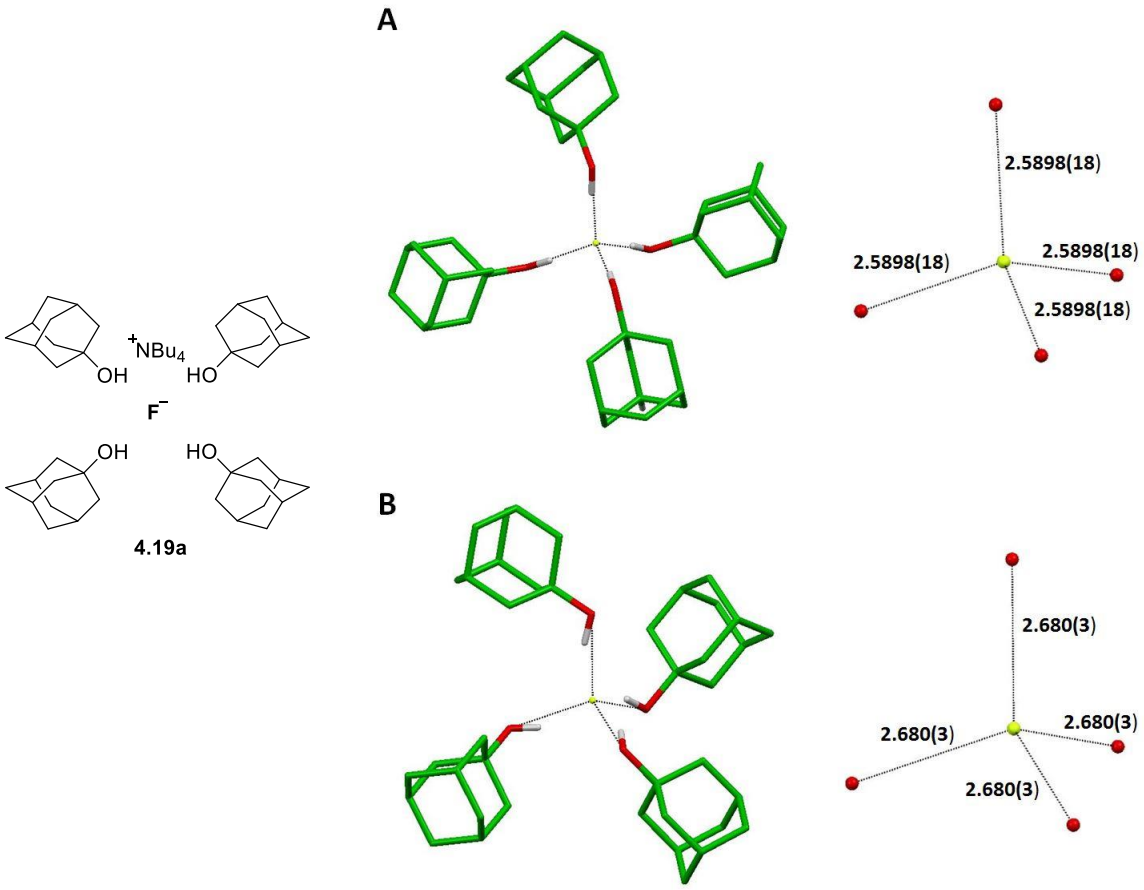

Figure 4.4. Fluoride coordination in TBAF(1-Ada-OH)$_4$ (**4.19a**). O(H)···F$^-$ distances are shown. Cations and hydrogens not involved in hydrogen-bonding are omitted for clarity.

With 1-adamantanol being nearly isosteric with *t*-BuOH around the hydroxyl group and despite its distinct packing requirements, the solid state structure of TBAF(1-Ada-OH)$_4$ is closely related to the only previously studied homoleptic fluoride–alcohol complex, TBAF(*t*-BuOH)$_4$.[327] Both compounds were found to crystallise in tetragonal space groups – P –4 for TBAF(1-Ada-OH)$_4$ and I 41/a for TBAF(*t*-BuOH)$_4$ – and in both structures the fluoride-coordinating hydroxyl groups form an almost perfect tetrahedron around the central fluoride anion. Due to the fluoride anions in TBAF(1-Ada-OH)$_4$ sitting on 4-fold rotation axes, all four hydrogen bonds were equivalent and each coordination

polyhedron can be described with two distinct O···F⁻···O angles. For the two fluorides found in TBAF(1-Ada-OH)$_4$ these values were 2.5898(18) Å, 117.06(6)° and 95.17(6)° as well as 2.680(3) Å, 113.26(9)° and 102.14(9)° for **A** and **B**, respectively.

The structures derived from diols **4.18b**–**e** showed a greater variability of coordination patterns, which can be analysed in terms of their distortion from an ideal tetrahedral (T_d) symmetry, assuming hydrogen bonds of approximately equal length.[338–340] Firstly, two O···F⁻···O angles are fixed at 72.10(4)° and 71.35(5)° for (*R*,*R*)-di-(*i*-Pr)tartrate (**4.18b**), 69.38(3)° for mannitol derivative **4.18c**, 69.11(5)° and 68.24(5)° for pinacol (**4.18d**) and 79.12(6)° and 78.62(5)° for neopentyl glycol (**4.18e**), respectively, due to the chelating nature of the diols. The 1,3-diol neopentyl glycol thereby showed a significantly bigger bite-angle compared to the 1,2-diols, which is also expected to influence the stability of the hydrogen-bonded assembly and therefore its reactivity as a fluoride source. All further distortions from an ideal T_d structure can be described with a combination of twist (**A**), roll (**B**) and glide (**C**) movements of one pair of hydroxyl groups relative to the other (Figure 4.5).

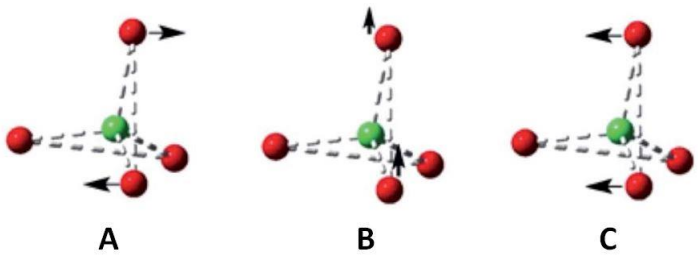

Figure 4.5. Distortions from a tetrahedral (T_d) symmetry for a bis-chelated system with equal ligation distances: (A) C_2 twist, (B) Out-of-plane roll, (C) In-plane glide. K. M. Engle, L. Pfeifer, G. Pidgeon, G. Giuffredi, A. L. Thompson, R. Paton, J. M. Brown, V. Gouverneur, *Chem. Sci.* **2015**, 5293–5302 – Published by The Royal Society of Chemistry.

Complex **4.19b** was prepared from enantiomerically pure (*R*,*R*)-di-(*i*-Pr)tartrate (**4.18b**) and crystallised as a hexane solvate with the complexed anion in this 2:1 complex showing overall C_2 symmetry (Figure 4.6).

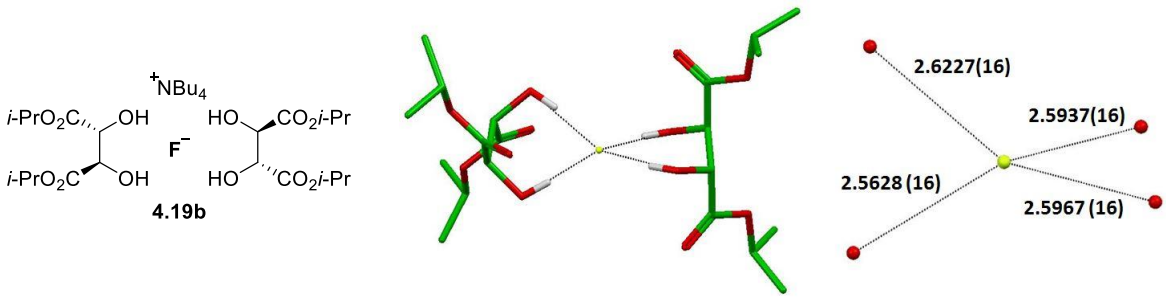

Figure 4.6. Fluoride coordination in TBAF((*R*,*R*)-di-(*i*-Pr)tartrate)$_2$·(hexane) (**4.19b**). O(H)···F$^-$ distances are shown. Cation and hydrogens not involved in hydrogen-bonding are omitted for clarity.

The dihedral angle between the O···F$^-$···O planes, formed by the hydroxyl oxygens of the two tartrate molecules with the central fluoride, was measured to be 60.05(7)°, indicating a C_2-twist (**A**) contribution. The asymmetric hydrogen bond lengths found for one tartrate molecule (Figure 4.6) might indicate an influence by crystal packing forces. The fluoride anion is placed in an almost equidistant position from the two central C–C bonds and is located only 0.1391(11) Å from their mean plane.

A more distorted arrangement of the hydrogen bond donors was found for complex **4.19c**, showing two molecules of enantiomerically pure 1,2,5,6-(*R*,*S*,*S*,*R*)-di-isopropylidene mannitol (**4.18c**) binding to the central fluoride anion (Figure 4.7).

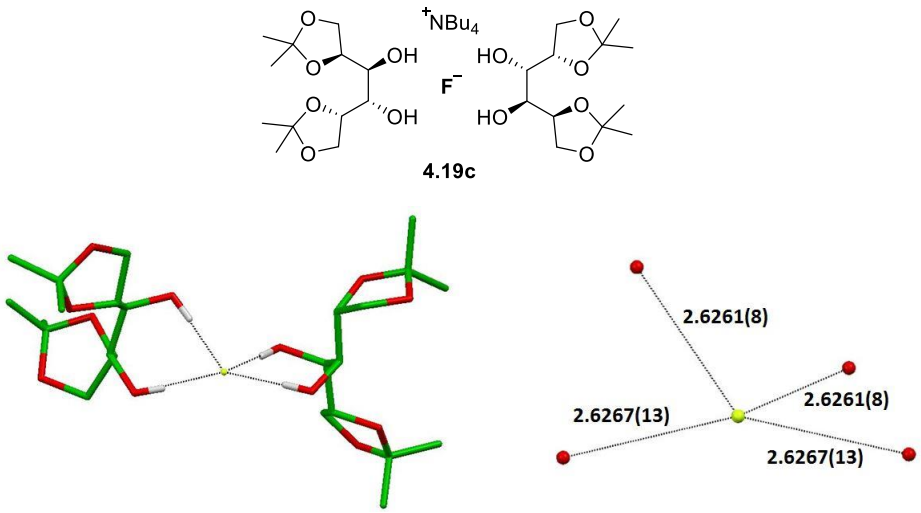

Figure 4.7. Fluoride coordination in TBAF(1,2,5,6-(*R*,*S*,*S*,*R*)-di-isopropylidene mannitol)$_2$·(EtOAc) (**4.19c**). O(H)···F$^-$ distances are shown. Cation and hydrogens not involved in hydrogen-bonding are omitted for clarity.

Complex **4.19c** crystallised as an EtOAc solvate and features a dihedral angle between O···F$^-$···O planes of 61.03(5)° – similar to **4.19b**. The structure of the complexed anion was found to be strongly influenced by out-of-plane roll **B** (Figure 4.5). This is reflected in the significant difference between the distances of the hydroxyl oxygens of one diol from the plane, defined by the hydroxyl oxygens of the second diol and the central fluoride. One of them was located 0.7222(8) Å to one side of the plane, while other one was found 1.7874(9) Å to the other side. This causes the central C–C bonds, connecting the hydroxyl-bearing carbons, to no longer be co-planar.

A combination of C_2 twist **A** and out-of-plane roll **B** shaped the coordination geometry of fluoride in the pinacol derived 2:1 complex **4.19d** (Figure 4.8).

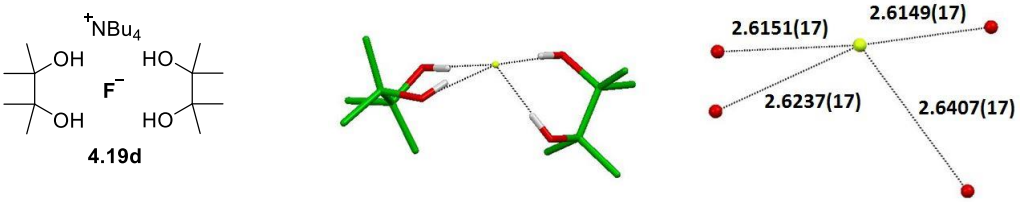

Figure 4.8. Fluoride coordination in TBAF(pinacol)$_2$ (**4.19d**). O(H)···F$^-$ distances are shown. Cation and hydrogens not involved in hydrogen-bonding are omitted for clarity.

Four crystallographically different hydrogen bonds form the complexed anion in **4.19d** and due to the aforementioned distortions all four O···F^- vectors are confined to one coordination hemisphere. The dihedral angle between the O···F^-···O planes, formed by the pairs of hydroxyl oxygens, belonging to one pinacol ligand, and the central fluoride, is 64.96(8)° and therefore slightly larger compared to **4.19b** and **4.19c**. Taking one of these planes, the hydroxyl oxygens of the other pinacol molecule lie 0.7417(13) Å and 2.3880(13) Å both to the same side of it. Although fluoride is comparatively easily accessible from one side, no further short contacts are found. Relatively acidic α-protons on the TBA^+ cation instead show such interactions with pinacol oxygens, forming 1D-ribbons with the complexed anion (Figure 4.9).

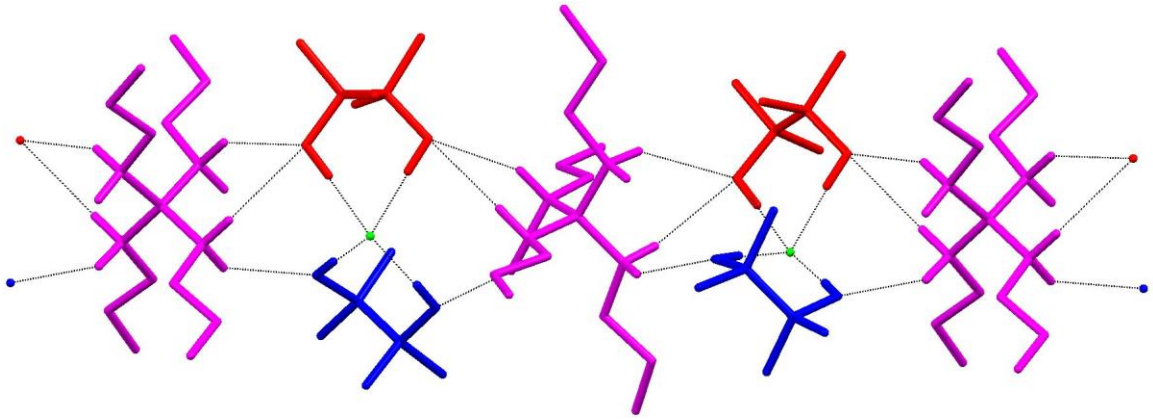

Figure 4.9. 1D ribbon formed by pinacol-complexed fluoride and TBA^+ in **4.19d**. Only hydroxyl protons and TBA^+ α-protons are shown. Symmetry equivalent molecules are depicted in the same colour.

Complex **4.19e** was prepared using 1,3-diol neopentyl glycol to allow for a comparison to the complexes featuring 1,2-diols (**4.19b**–**d**) (Figure 4.10). The successful crystallisation of this compound showed that eight-membered cyclic hydrogen bond networks can be stably incorporated into these complexes.

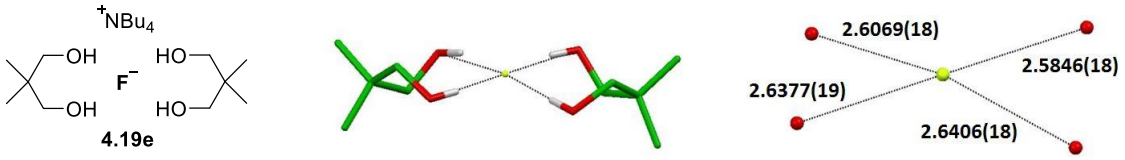

Figure 4.10. Fluoride coordination in TBAF(neopentyl glycol)$_2$ (**4.19e**). O(H)···F$^-$ distances are shown. Cation and hydrogens not involved in hydrogen-bonding are omitted for clarity.

The solid state structure of **4.19e** showed the central fluoride anion hydrogen-bonding to four hydroxyl groups of two different neopentyl glycol molecules, forming an almost square planar arrangement. The dihedral angle between O···F$^-$···O planes was determined to be 11.51(8)°, with fluoride sitting 0.1287(12) Å above the mean plane formed by the four hydroxyl oxygens, comparable to the distance of the oxygens themselves. The O···F$^-$···O angles of 100.84(6)° and 101.43(6)°, involving neighbouring oxygens belonging to different neopentyl glycol molecules, also reflect the overall symmetrical geometry of this complexed anion. The asymmetry found in the hydrogen bond lengths might be due to crystal packing forces. Similar to pinacol derived complex **4.19d** no further short contacts to fluoride are present, but interactions between hydroxyl oxygens and α-protons of the TBA$^+$ cation lead to the formation of a 3D network.

By substituting protons on the terminal carbons of neopentyl glycol for OH groups, tris(hydroxymethyl)ethane (**4.18f**) and pentaerythritol (**4.18g**) are obtained, which were expected to engage in more than two hydrogen bonds to fluoride. The reaction of 2.0 equiv. of **4.18f** with TBAF(H_2O)$_3$ after recrystallisation gave complex **4.19f**, featuring four fluoride–alcohol hydrogen bonds (Figure 4.11).

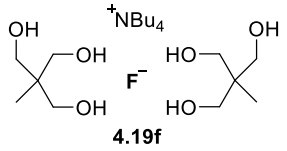

4.19f

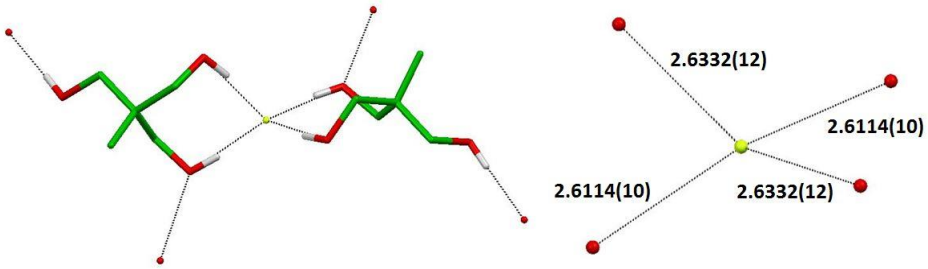

Figure 4.11. Fluoride coordination in TBAF(tris(hydroxymethyl)ethane)$_2$ (**4.19f**). O(H)···F$^-$ distances are shown. Cation and hydrogens not involved in hydrogen-bonding are omitted for clarity.

Similar to diol-complexes **4.19b**–**e**, however, these involved two hydroxyl hydrogen bond donors each from two different tris(hydroxymethyl)ethane molecules, with the third one activating and thereby shortening one of the O–H···F$^-$ bonds of a neighbouring complexed anion. The dihedral angle between the O···F$^-$···O planes of one anion complex is 81.32(6)° – close to what would be expected for an undistorted tetrahedron. Through a combination of roll and glide motions **B** and **C**, however, one hydroxyl group of one ligand almost lies in the O···F$^-$···O plane, spanned by the O···F$^-$ vectors of the second ligand. Fluoride anion is found to lie 0.4287(10) Å to one side of the plane, defined by these three oxygens.

The last complex in this series is **4.19g**, prepared with pentaerythritol as a potential tetra-coordinating hydrogen bond donor. This compound crystallised as a DCM solvate and its solid state structure was made up of 1D ribbons, formed by interconnected [F(diol)$_2$]$^-$ units (Figure 4.12) surrounded by TBA$^+$ cations, which form short contacts to the hydroxyl oxygens with their relatively acidic α- and β-protons, as had been seen before for pinacol (**4.19d**) and neopentyl glycol (**4.19e**) derived complexes.

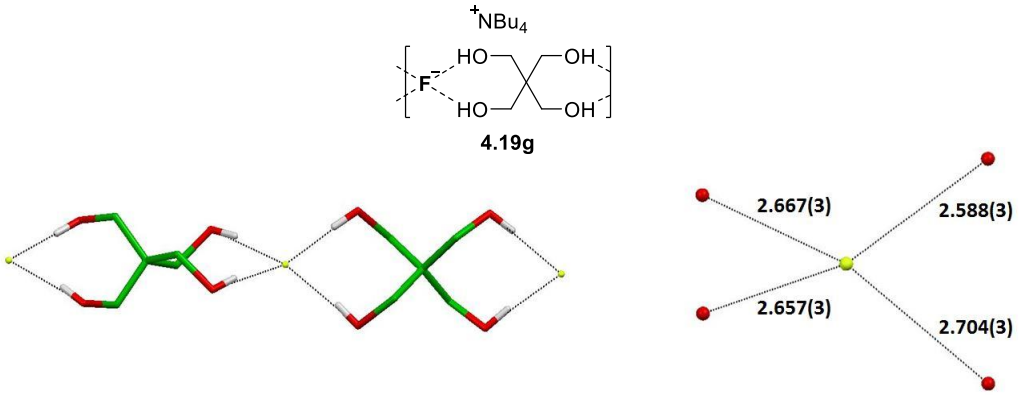

Figure 4.12. Fluoride coordination in TBAF(pentaerythritol)·(DCM) (**4.19g**). O(H)···F^- distances are shown. Cation and hydrogens not involved in hydrogen-bonding are omitted for clarity.

C_2 twist distortion **A** (Figure 4.5) from ideal orthogonal geometry of the two O···F^-···O planes leads to a dihedral angle of 50.54(12)°.

Two closely related polymorphs of TBAF(catechol)$_2$ (**4.19h**) were discovered during our studies. No deprotonation of catechol was observed, suggesting that its pK_a of 9.25[341] is high enough to still allow for preferential formation of hydrogen bonds over deprotonation.

The first polymorph was found in crystals taken directly from the reaction mixture, which exhibited significant disorder. It contained three different fluoride species, one tri- (**A**) and two tetracoordinate (**B** and **C**) ones (Figure 4.13).

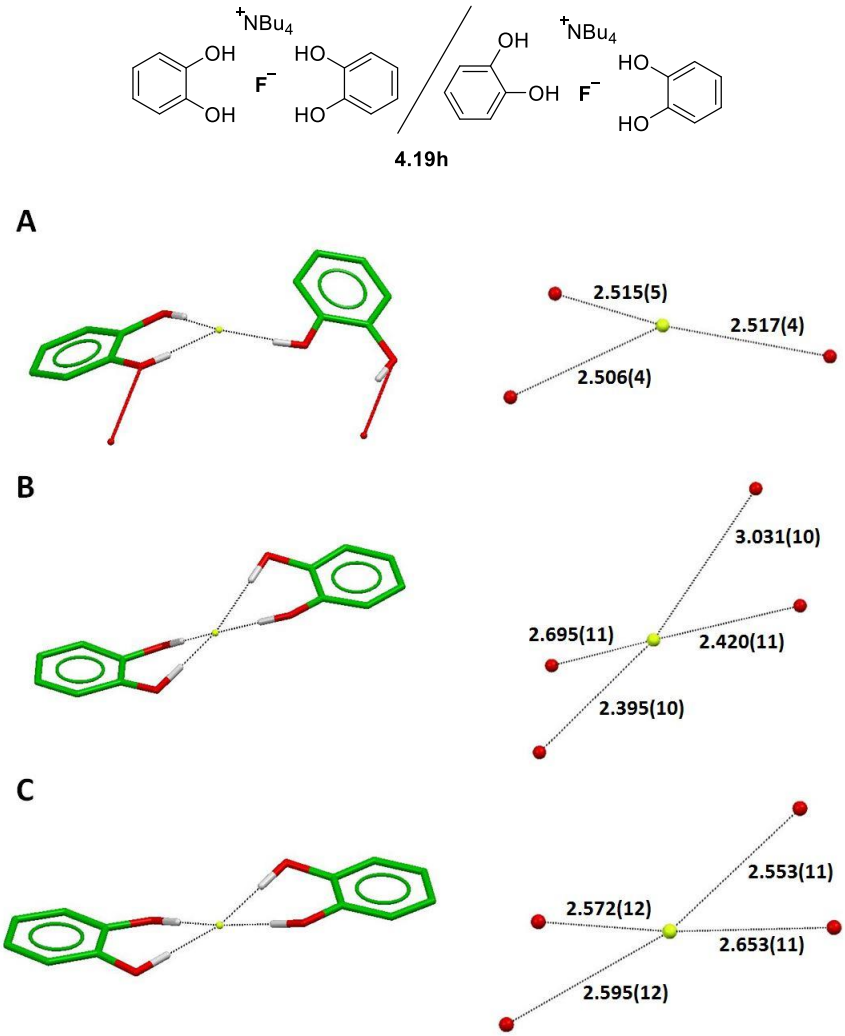

Figure 4.13. Tricoordinate (**A**) and tetracoordinate (**B**, **C**) fluoride species in the first polymorph of TBAF(catechol)$_2$ (**4.19h**). Only major components of disordered molecules are shown. O(H)···F$^-$ distances are shown. Cations and hydrogens not involved in hydrogen-bonding are omitted for clarity.

The mono-dentate catechol ligands in **A** bind to a second tricoordinate fluoride-complex in a head-to-tail fashion, forming a macrocyclic system containing four hydrogen bonds. In this species of complexed fluoride a fourth short contact to the *ortho*-H of the mono-dentate catechol is formed by the anion (C(H)···F$^-$ = 3.256(6) Å). In tetracoordinate fluoride species **B** (Figure 4.13) one hydrogen bond is significantly elongated, indicating that it might be better described as a transition structure between a "truly" tetracoordinate and tricoordinate species. On the other hand, **C** contains hydrogen bonds

of varying lengths between 2.553(11) Å and 2.653(11) Å. In terms of packing, the structure consists of alternating layers of tri- and tetracoordinate complexed fluoride, separated by layers of TBA^+.

Vapour diffusion of hexane into a saturated solution of $TBAF(catechol)_2$ in EtOAc gave the second polymorph, containing four distinct fluoride species – two tri- (**A** and **B**) and two tetracoordinate (**C** and **D**) ones (Figure 4.14).

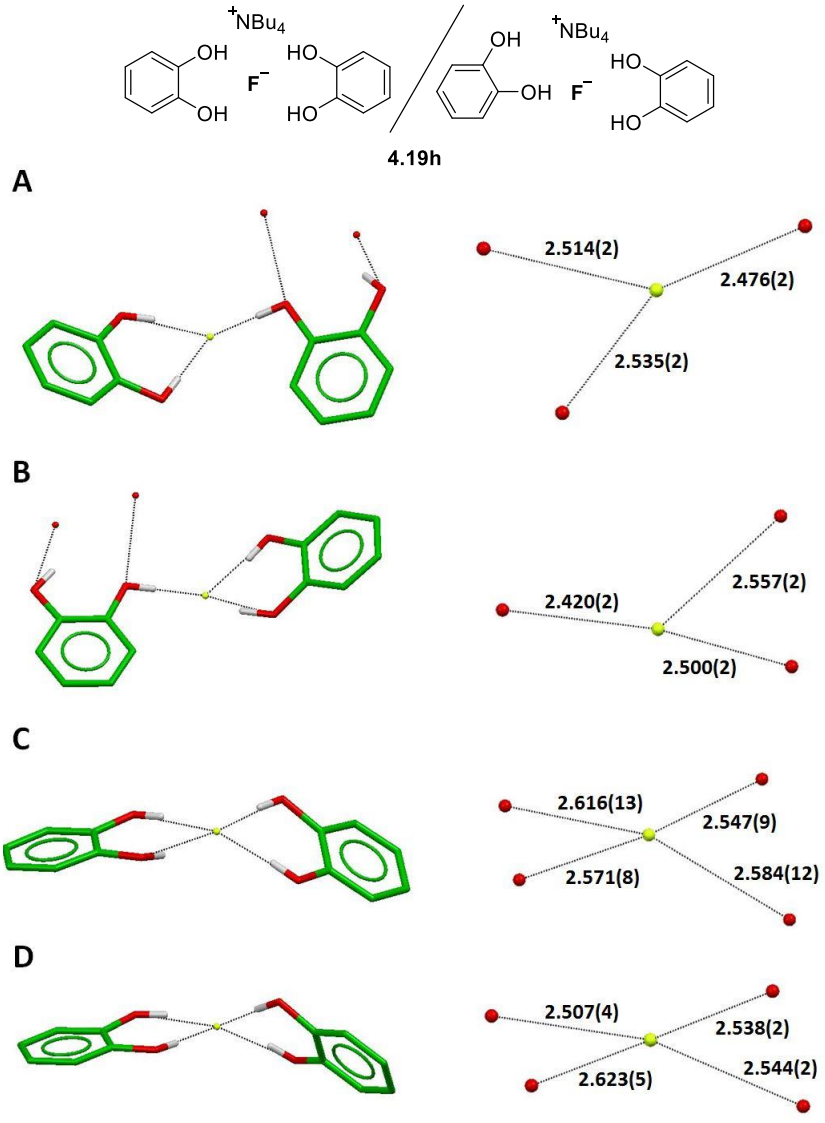

Figure 4.14. Tricoordinate (**A**, **B**) and tetracoordinate (**C**, **D**) fluoride species in the second polymorph of $TBAF(catechol)_2$ (**4.19h**). Only major components of disordered molecules are shown. O(H)···F^- distances are shown. Cations and hydrogens not involved in hydrogen-bonding are omitted for clarity.

The catechol molecules only forming one hydrogen bond to fluoride in the tricoordinate arrangements form a pair with the equivalent catechol of a neighbouring tricoordinate species of the other kind, so that the otherwise free hydroxyl groups now form hydrogen bonds to the fluoride-coordinating hydroxyl oxygen of the opposite catechol. Similar to the first polymorph, fluoride in **A** and **B** forms short contacts to the *ortho*-protons of the mono-dentate catechol with C(H)···F^- distances of 3.226(2) Å and 3.344(3) Å, respectively. The average hydrogen bond length in the tricoordinate fluoride species is RMS = 2.501 ± 0.044 Å, compared to RMS = 2.567 ± 0.037 Å for the tetracoordinate ones. Overall, the structure consists of alternating layers of complexed fluorides of types **A** and **C** as well as **B** and **D**, separated by layers of TBA^+.

Trimethylisobenzofuran-2-ol (**4.18i**) was used for the preparation of **4.19i**, where fluoride is coordinated to three alcohol moieties and an additional water molecule (Figure 4.15).

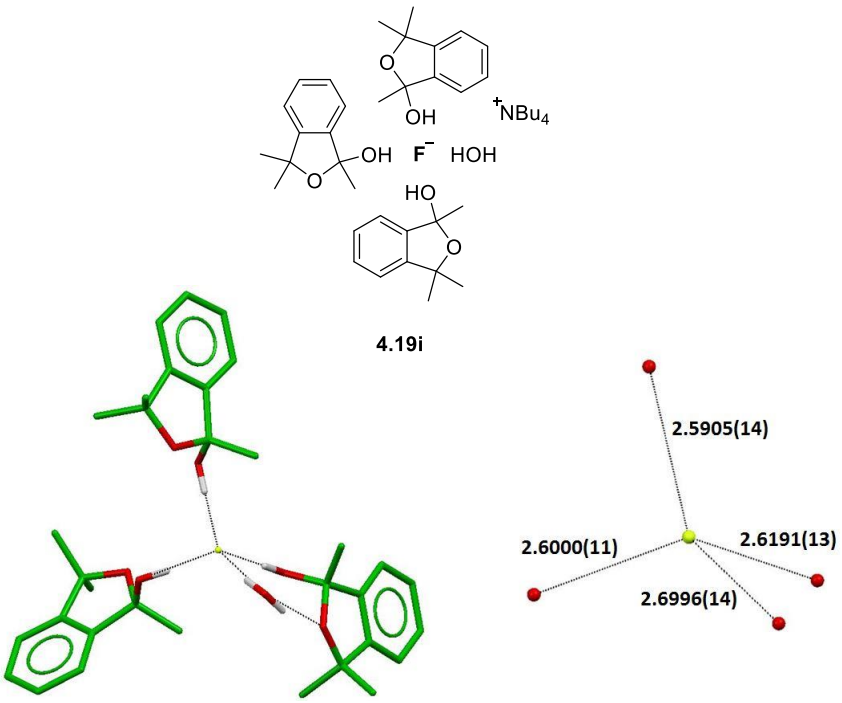

Figure 4.15. Fluoride coordination in TBAF(trimethylisobenzofuran-2-ol)$_3$(H_2O) (**4.19i**). O(H)···F^- distances are shown. Cation and hydrogens not involved in hydrogen-bonding are omitted for clarity.

The four hydrogen bond donor oxygens form an almost perfect tetrahedron around fluoride with O···F⁻···O angles between 90° and 122°. The O(H)···F⁻ hydrogen bond lengths are comparable to other tetracoordinate fluoride structures (**4.19a**–**g**), ranging from 2.5905(14) Å to 2.6996(14) Å, the one involving water being significantly longer than the fluoride–alcohol contacts (Figure 4.15).

Furthermore, a set of purely tricoordinate structures was found for complexes **4.19j** and **4.19k**.

TBAF$(H_2O)_3$ and (*R*)-BINOL gave a complex, **4.19j**, that only contained tricoordinate fluoride, most likely due to the increased steric bulk of the hydrogen bond donor (Figure 4.16).

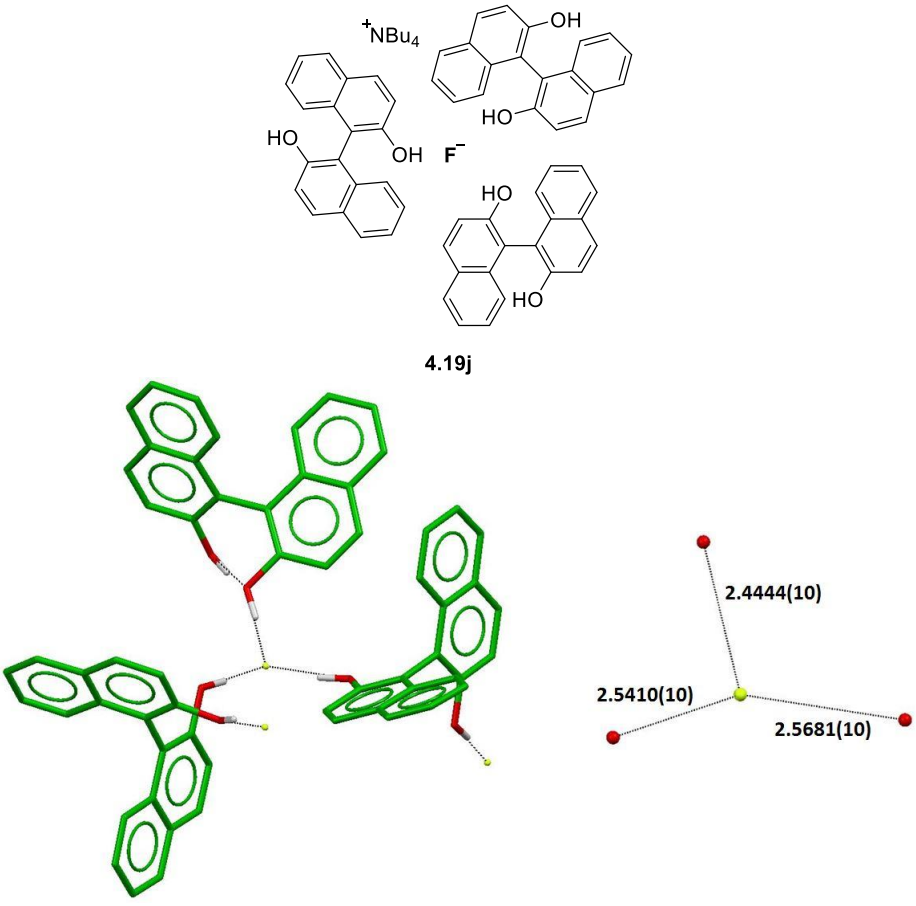

Figure 4.16. Fluoride coordination in TBAF((*R*)-BINOL)$_2$ (**4.19j**). O(H)···F⁻ distances are shown. Cation and hydrogens not involved in hydrogen-bonding are omitted for clarity.

The three hydroxyl groups coordinating to one fluoride stem from three different (*R*)-BINOL molecules, with two of the remaining hydroxyls coordinating to two different fluoride anions, leading to the formation of 1D ribbons of connected anion-complexes. The third hydroxyl group, not coordinating to fluoride, forms a hydrogen bond to the hydroxyl group of the same (*R*)-BINOL that was binding to fluoride. This O–H···F^- hydrogen bond was found to be significantly shorter compared to the other two present in this structure (Figure 4.16). Fluoride was found to lie 0.6501(6) Å outside the plane, described by the three alcohol oxygens. An additional short contact to an aromatic C–H of a neighbouring anion complex is present (C(H)···F^- = 3.4732(12) Å), possibly making up for some of the stabilisation lost, compared to the structures with four fluoride–alcohol hydrogen bonds.

The solid state structure of complex **4.19k**, prepared from diphenylmethanol, also showed fluoride hydrogen-bonding to three alcohol groups (Figure 4.17).

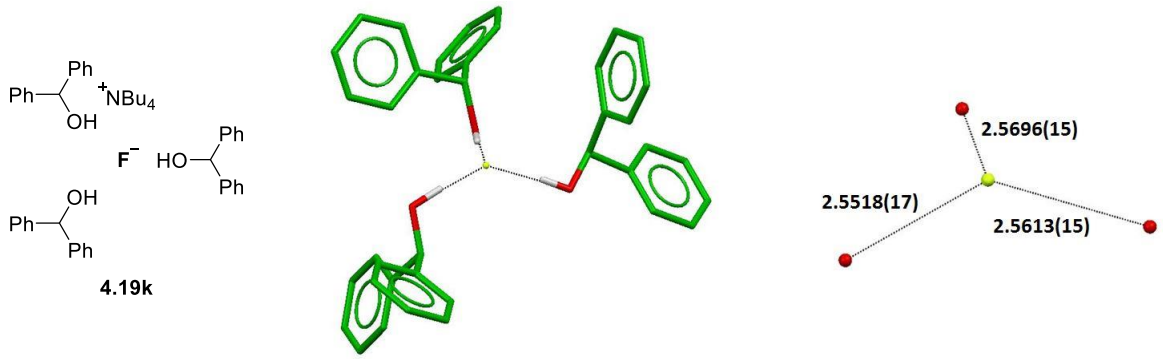

Figure 4.17. Fluoride coordination in TBAF(diphenylmethanol)$_3$ (**4.19k**). O(H)···F^- distances are shown. Cation and hydrogens not involved in hydrogen-bonding are omitted for clarity.

The three donor oxygens form a gently inclining pyramid with the central fluoride anion, which is located 0.6483(11) Å above their mean plane. An additional short contact to an

α-proton of the TBA^+ cation with a C(H)···F^- distance of 3.3331(18) Å and a C–H···F^- angle of 161.92(4)° occupies the fourth apex.

9-Phenylfluoren-9-ol-derived complex **4.19l** showed a tri- as well as a dicoordinate fluoride motif in the solid state (Figure 4.18).

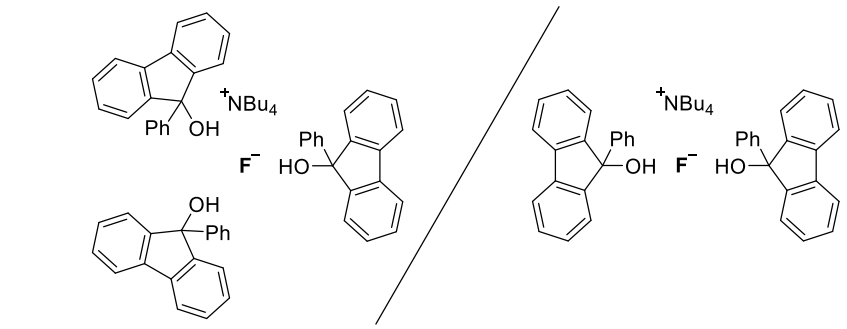

4.19l

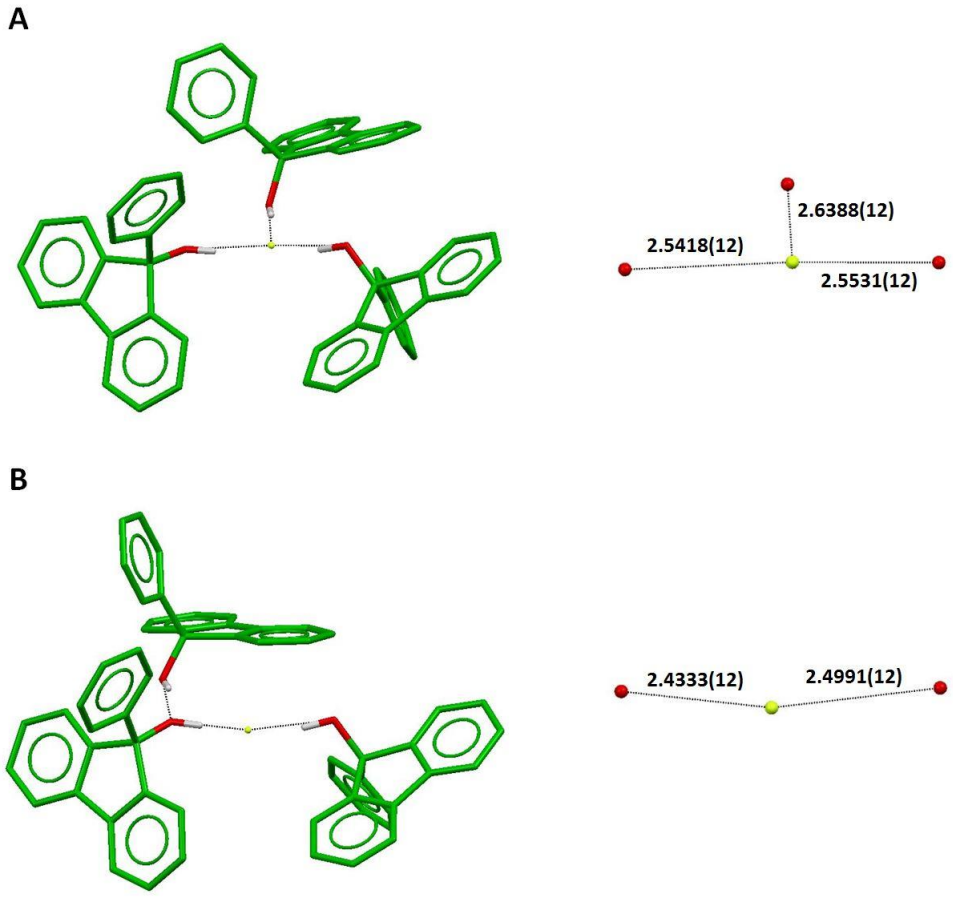

Figure 4.18. Tri- (**A**) and dicoordinate (**B**) fluoride species in TBAF(9-phenylfluoren-9-ol)$_3$ (**4.19l**). O(H)···F^- distances are shown. Cations and hydrogens not involved in hydrogen-bonding are omitted for clarity.

The two hydrogen-bonded structures were found to be closely related, with the "missing" alcohol donor in dicoordinate **B** showing an elongated hydrogen bond in tricoordinate **A** compared to the other ligands. In **B** this alcohol moiety is binding to the hydroxyl oxygen of one of the other 9-phenylfluoren-9-ol molecules, which then displays a shorter hydrogen bond compared to the non-activated hydroxyl group of the second ligand in **B**. Both hydrogen bonds in **B**, however, are significantly shorter than those in **A**. **A** is approximately T-shaped with O···F^-···O angles of 160.40(4)°, 120.00(4)° and 78.30(3)°, whereas **B** is almost linear with an O···F^-···O angle of 151.98(5)°. No further short contacts to fluoride are found in **A**, whereas there is one aromatic proton of one of the 9-phenylfluoren-9-ol ligands within distance of their combined van der Waals radii in **B** (C(H)···F^- = 3.1586(15)), albeit with the C–H bond not being in a favourable spatial orientation with a C–H···F^- angle of 127°.[342]

With its two different fluoride coordination modes, hydrogen bond donor **4.18l** can be seen as a transition between purely tri-coordinating and even more sterically demanding di-coordinating ones.

Triphenylmethanol (**4.18m**) belongs to the latter class and the structure of the complexed fluoride anion found in the solid state of **4.19m**, prepared from **4.18m** and TBAF$(H_2O)_3$, is shown in Figure 4.19.

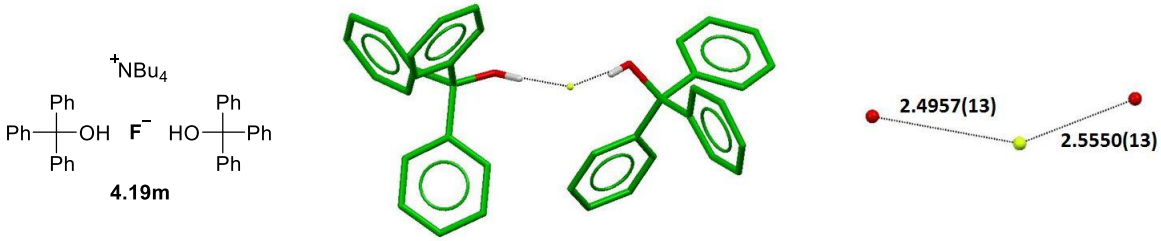

Figure 4.19. Fluoride coordination in TBAF(triphenylmethanol)$_3$ (**4.19m**). O(H)···F^- distances are shown. Cation and hydrogens not involved in hydrogen-bonding are omitted for clarity.

Fluoride forms a bent arrangement with the two hydrogen-bonded hydroxyl groups enclosing an O···F⁻···O angle of 102.94(4)°. It also engages in short contacts with an α-C–H group of the cation with a C(H)···F⁻ distance of 3.181(12) Å and a C–H···F⁻ angle of 165°, as well as two *ortho*-protons of proximal phenyl rings with C(H)···F⁻ distances of 3.247(2) Å and 3.2946(18) Å and favourable spatial orientation with C–H···F⁻ angles of 157° and 152°, respectively.[342] Possibly as a result of this, these two phenyl rings appear well ordered, whereas the other four exhibit librational disorder.

Closely related to **4.19m** is tri-(*p*-tolyl)-methanol-derived (**4.18n**) complex **4.19n**, also showing two fluoride–alcohol interactions (Figure 4.20).

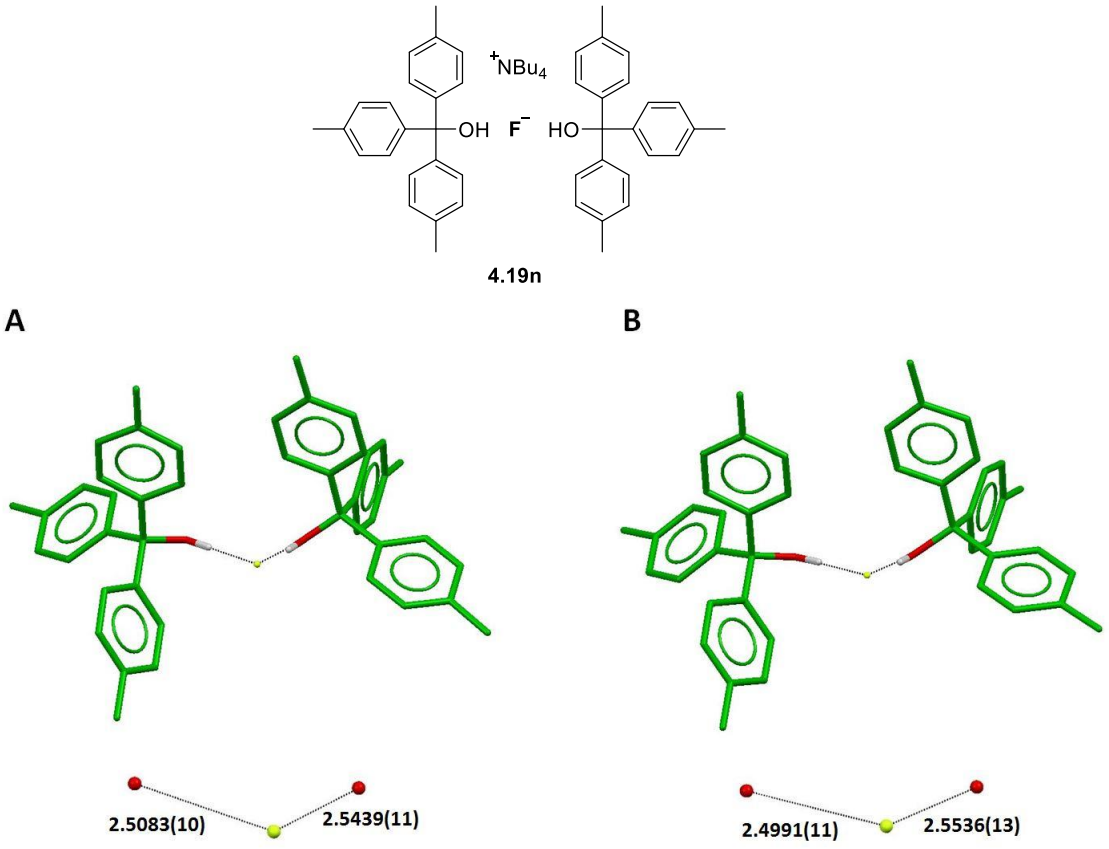

Figure 4.20. Fluoride coordination in TBAF(triphenylmethanol)$_3$ (**4.19n**) (**A**, **B**). O(H)···F⁻ distances are shown. Cations and hydrogens not involved in hydrogen-bonding are omitted for clarity.

Two different fluoride-binding motifs are found in the solid state that both show very similar characteristics to the one found in **4.19m**. The O···F$^-$···O angles are 85.21(3)° and 87.63(3)°, respectively, and additional short contacts to *ortho*-protons on the phenyl rings as well as α- and β-protons in the TBA$^+$ counter-cations are present in both motifs.

Finally, the solid state structure of **4.19o**, with pyrrolidine derivative **4.18o** as hydrogen bond donor, stands out, for it shows fluoride monohydrate with one diol each coordinating to the fluoride and the water oxygen (Figure 4.21).

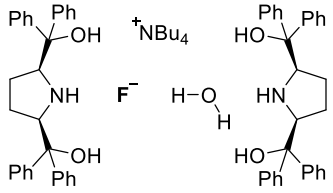

4.19o

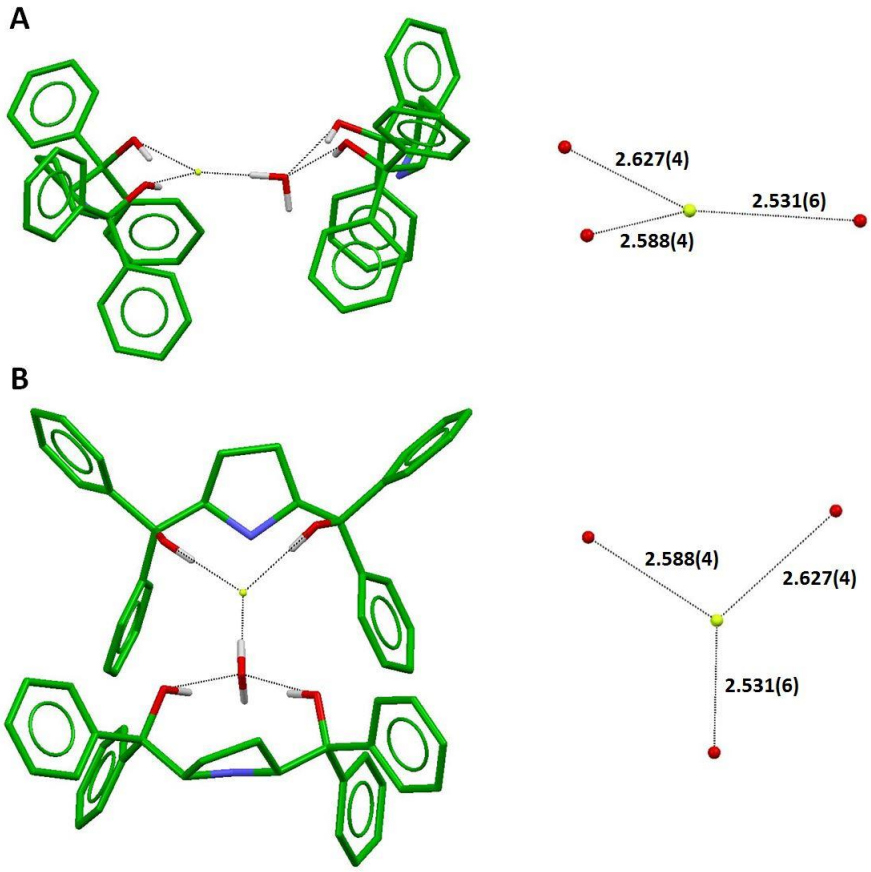

Figure 4.21. Side (**A**) and top view (**B**) of the fluoride coordination motif in TBAF(**4.18o**)$_2$(H_2O). O(H)···F$^-$ distances are shown. Cations and hydrogens not involved in hydrogen-bonding are omitted for clarity.

Fluoride therefore forms three hydrogen bonds to the diol as well as water but the secondary amine is not involved in binding to the anion or water. However, as had been observed before, short contacts to α-protons of the TBA^+ cation were present. The geometry of both diols is almost identical, so that they refine as one with very similar positions for the fluoride and water oxygen.

In summary, if sterically possible, fluoride was found to preferentially form four hydrogen bonds to alcohol moieties, in line with literature precedent on fluoride tetrahydrate species.[343–347] By increasing the steric congestion around the alcohol groups, however, the coordination number can be reduced to three or two hydrogen bonds, the lowest number observed in this study. In most structures with less than four fluoride–alcohol hydrogen bonds fluoride forms weak hydrogen bonds to other relatively acidic protons.[348,349] Generally, we found a correlation between the number and the length of O–H···F^- hydrogen bonds, observing shorter contacts for structures with fewer such interactions (Figure 4.22).

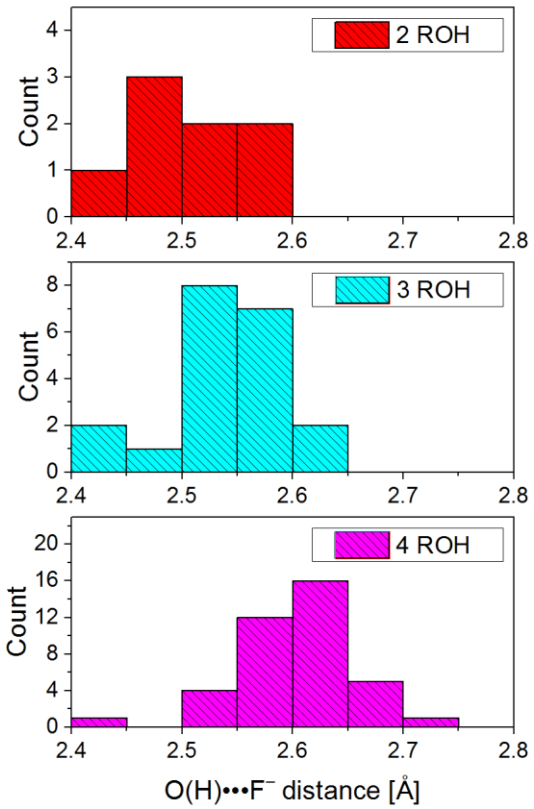

Figure 4.22. Relationship between O(H)···F$^-$ distance and fluoride coordination number for complexes **4.19a**–**o**. The value >3.0 Å for **4.19h** is omitted.

For this set of complexes, we did not observe the preferential formation of ideal coordination geometries, but instead packing forces seem to be the driving force behind the adopted geometry in any given structure.

4.2.3. Reactivity and S_N2/E2 Selectivity of Fluoride–Alcohol Complexes

After having established the solid state structures of these fluoride–alcohol complexes, we wanted to study their behaviour as sources of fluoride in a model S_N2 reaction. Primary alkyl bromide **4.10** was added to 2.0 equiv. of different complexes in MeCN and the mixture was heated to 70 °C for 2 h. The relative amounts of starting material, alkyl

fluoride **4.2** (S_N2) and alkene **4.4** (E2) were determined at different time points over the course of the reaction. These data was used to calculate the rate constants for the formation of **4.2** using the Berkeley Madonna software package, as well as determine the product ratio at the end of the reaction (Table 4.7). These kinetic experiments were performed by Dr. K. M. Engle.

Table 4.7. Reactivity study of fluoride–alcohol complexes in a model S_N2 reaction.

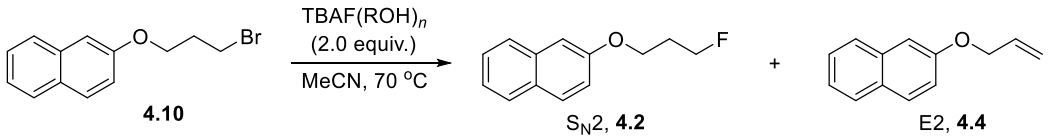

Entry	Complex	C.N.[a]	*c* [M][b]	$k_2(S_N2)$[c] [$M^{-1}s^{-1}$]	k_2*(rel)*	[**4.2**]/[**4.4**][d]
1	TBAF(H_2O)$_3$	3	0.50	0.0061	1.0	1.6
2	**4.19n**	2	0.50	0.0251	4.1	2.1
3	**4.19n**	2	0.13	0.0870	14	1.0
4	**4.19n**	2	0.05	0.123	20	0.74
5	**4.19n**[e]	2	0.50	0.0142	2.3	3.6
6	**4.19l**	2, 3	0.50	0.0032	0.52	3.5
7	TBAF(*t*-BuOH)$_4$	4	0.50	0.0130	2.1	2.0
8	**4.19d**	4	0.50	0.0021	0.35	2.8
9	**4.19e**	4	0.50	0.0004	0.066	3.1
10	**4.19f**	4	0.50	0.0002	0.037	4.2
11	TBAF(H_2O)$_3$[f]	3	0.50	0.0075	1.2	4.2

Standard conditions: 1.0 equiv. **4.10** (0.20 mmol), 2.0 equiv. TBAF(ROH)$_n$ (0.40 mmol), MeCN (0.80 mL). Reactions carried out by Dr. K. M. Engle. [a]Number of fluoride–alcohol hydrogen bonds in TBAF(ROH)$_n$. [b]Concentration of TBAF(ROH)$_n$ in reaction mixture. [c]From ^{1}H NMR analysis by curve fitting. [d]After 2 h. [e]With 4.0 equiv. of additional tri-(*p*-tolyl)-methanol (**4.18n**). [f]In toluene.

The reaction with commercially available TBAF(H_2O)$_3$ resulted in a ratio of 1.6 of alkyl fluoride **4.2** to alkene **4.4** and it was assigned a relative rate constant (k_2*(rel)*) for the formation of **4.2** of 1.0 (Table 4.7, Entry 1). This reaction provided a benchmark to which we could compare the results of our complexes. Complex **4.19n**, prepared from tri-(*p*-tolyl)-methanol (**4.18n**), showed the highest reactivity with a k_2*(rel)* of 4.1 and an

improved product ratio of 2.1 (Table 4.7, Entry 2). The decay of starting material **4.10** followed 2nd order during the first 600 s before slowing down. Both products **4.2** and **4.4** were formed over the entire course of the reaction with **4.2** dominating at every time point. The ratio of **4.2** to **4.4**, however, improved slightly towards the end of the reaction. Performing this reaction under more dilute conditions led to an increased reactivity, accompanied by a decrease and finally a reversal in selectivity (Table 4.7, Entries 3 and 4). This indicates dissociation of the L_2F^- anions, found for **4.19n** in the solid state, under these conditions to give more reactive LF^- and F^- species, which are expected to display lower selectivity for the formation of the S_N2 product **4.2**. Adding additional tri-(*p*-tolyl)-methanol (**4.18n**) to the reaction, therefore, resulted in a lower reactivity but an improved selectivity for the desired alkyl fluoride **4.2** (Table 4.7, Entry 5). The reaction with 9-phenylfluoren-9-ol derived complex **4.19l** under standard conditions exhibited lower reactivity and higher selectivity compared to **4.19n** (Table 4.7, Entries 2 and 6). This is consistent with the higher 3:1 ratio of alcohol:fluoride found in the solid state of **4.19l** compared to **4.19n**. Comparing Kim's TBAF(*t*-BuOH)$_4$ to TBAF(pinacol)$_2$ (**4.19d**), where both hydroxyl groups have similar steric environments and four fluoride–alcohol contacts were found in the solid state, reveals a distinctly lower reactivity and improved selectivity for the latter complex. It is assumed that the chelating pinacol diols form a more stable complex compared to *t*-BuOH, which helps to preserve the less reactive but more selective, higher coordinated fluoride species in solution (Table 4.7, Entries 7 and 8). Going from the 1,2-diol pinacol to the 1,3-diol neopentyl glycol (**4.18e**), we find that the associated complex **4.19e** shows a markedly lower reactivity together with a slightly improved selectivity, indicating that 1,3-diols might form more stable hydrogen-bonded complexes with fluoride due to their larger bite angle (Table 4.7, Entry 9). Reduced steric

bulk in the vicinity of the hydroxyl groups is also expected to contribute to this observation. Complex **4.19f**, prepared from tris(hydroxymethyl)ethane (**4.18f**), shows an even lower reactivity and better selectivity compared to **4.19e**, which might again be attributed to the higher ratio of hydroxyl groups to fluoride in the reaction mixture (Table 4.7, Entry 10). The observed product ratio of alkyl fluoride **4.2** to alkene **4.4** of 4.2 at the end of the reaction was the highest obtained for this set of fluoride–alcohol complexes. When performing the reaction with commercial $TBAF(H_2O)_3$ in toluene instead of MeCN the reactivity as well as selectivity improves, showcasing the influence of the solvent on this transformation (Table 4.7, Entries 1 and 11).

In general, a clear correlation between reactivity and selectivity of reactions performed with different complexes but under otherwise identical conditions can be found (Figure 4.23).

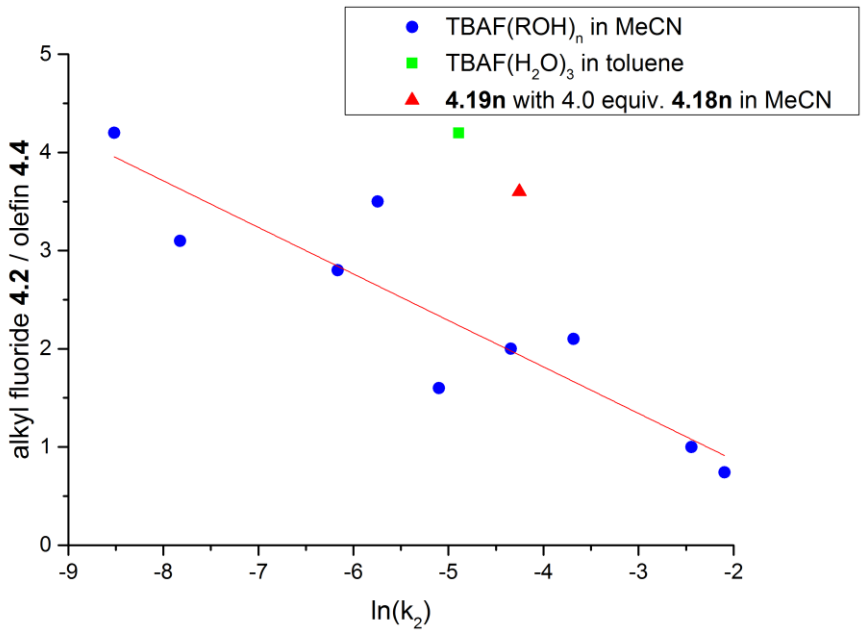

Figure 4.23. Correlation between reaction rate and S_N2/E2 selectivity for reactions in Table 4.7.

The reactions in toluene (Table 4.7, Entry 11) and with additional alcohol (Table 4.7, Entry 5) showed a selectivity that was higher than expected for their reaction rates.

4.2.4. Computational Modelling

In collaboration with the group of Prof. Robert S. Paton, a computational study at the density functional level of theory (DFT) of the effects of hydrogen-bonding to fluoride on the activation barriers of S_N2 and E2 reaction pathways was performed; the results are summarised in Figure 4.24.

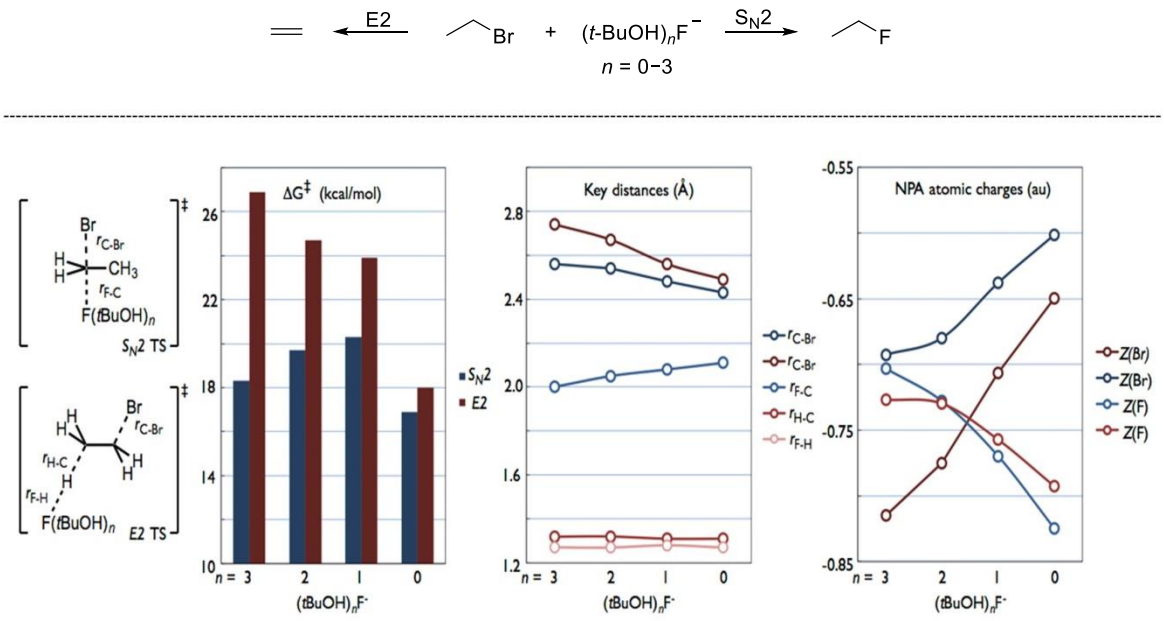

Figure 4.24. Computed activation free energies ($\Delta G^{\ddagger}$), geometric and electronic parameters of S_N2 and E2 transition state structures for F(*t*-BuOH)$_n^-$ reacting with EtBr. Reprinted with permission of Prof R. Paton.

Assuming that at least one alcohol has to dissociate in order to create an accessible fluoride species, reactions of EtBr with F(*t*-BuOH)$_n^-$ species where n = 3–0 were studied. Transition state structures for the S_N2 and antiperiplanar E2 pathways were located, while less favourable *syn*-elimination was not taken into consideration. Bulk solvation by

acetonitrile was modelled by performing optimisations in a surrounding continuum of dielectric medium. Apart from this bulk solvation the Br^- leaving group was assumed to initially be formed in an unsolvated state due to inefficient transfer of alcohol molecules during either reaction.[350] Although the underestimation of S_N2 barriers by DFT is well known,[351] the difference in activation barriers for S_N2 and E2 reaction pathways for the reaction of F^- with EtBr compares favourably for wB97XD ($\Delta\Delta G^{\ddagger}$ = 5.0 kcal/mol) and wave functional theory (WFT) calculations (MP2/CBS ($\Delta\Delta G^{\ddagger}$ = 6.0 kcal/mol)).

Figure 4.24 shows that the highest kinetic reactivity for both S_N2 and E2 mechanisms is found for free, uncoordinated fluoride (*n* = 0). Coordination of fluoride to *t*-BuOH causes a selective stabilisation of the educts relative to the products of both reactions, making them less exergonic. This causes a higher activation barrier ($\Delta G^{\ddagger}$), and therefore a later more product-like transition state according to the Hammond-Leffler postulate.[352–354]

The behaviour of the activation barriers, however, is intriguingly different for the S_N2 and E_2 mechanisms. Whereas $\Delta G^{\ddagger}$ for the elimination pathway incrementally increases from 18 to 27 kcal/mol upon going from *n* = 0 to 3, for the nucleophilic substitution it stays converged between 18–20 kcal/mol after an initial increase on going to *n* = 1 (Figure 4.24, left). It is this increasing difference in activation energy, needed for the competing S_N2 and E2 pathways, which leads to more highly coordinated fluoride species showing better selectivity.

This different behaviour can be explained by taking into account the structural changes, caused to the respective transition state by its backwards shift along the reaction coordinate. For both S_N2 and E2 pathways this means a more elongated C–Br bond in the transition state. This effect is more pronounced in the E2 reaction, where this distance

increases from 2.5 Å to almost 2.8 Å (Figure 4.24, middle). The increased C–Br bond length also comes with a higher charge transfer from F towards Br, with the E2 transition state showing a significantly more negative bromide leaving group compared to the S_N2 pathway (Figure 4.24, right). This in turn means that less negative charge resides on F, where it is stabilised by the coordinated hydrogen bond donors, therefore increasing the relative energy of the transition structure. A similar observation would be expected for the S_N2 pathway, albeit to a smaller extent. The fact that the activation free energy instead stays converged between *n* = 1–3 suggests a mitigating effect that stabilises the transitions state, which might be based on reduced electrostatic repulsion between nucleophile and leaving group.

4.3 Conclusion

In summary, we prepared 19 novel fluoride–alcohol complexes from commercially available $TBAF(H_2O)_3$ using an operationally simple protocol. Single-crystals were successfully grown for a subset of 15, which allowed us to determine their solid state structure using single-crystal X-ray crystallography.

These structures revealed the preferential formation of four fluoride–alcohol hydrogen bonds per fluoride, with the coordination geometries being mainly determined by crystal packing forces. By increasing the steric bulk of the alcohol donors, structures with three and two such hydrogen bonds can be obtained. These tend to form additional short contacts to relatively acidic C–H groups.

When studying the application of these complexes as a fluoride source for a model S_N2 reaction, they consistently showed a better selectivity over the competing E2 pathway than TBAF$(H_2O)_3$. Lowering the concentration of the complexes in this reaction led to increased reactivity but decreased selectivity, which is consistent with complex dissociation. Furthermore, diols exhibited lower reactivity and better selectivity compared to mono-ols and the solvent was found to have a major influence on these reaction parameters.

Computational modelling of the activation barriers for S_N2 and E2 pathways revealed a steady increase of $\Delta G^{\ddagger}$ for E2 upon hydrogen-bonding of up to three *t*-BuOH molecules to fluoride. On the other hand, $\Delta G^{\ddagger}$ for the S_N2 reaction stays converged after addition of the first alcohol. This disparity is rooted in geometric differences of the transition states causing the S_N2 one to be more stabilised compared to the one of the elimination reaction. This increasing difference in activation barriers causes more highly coordinated fluoride species to be more selective for S_N2 over E2 pathways.

Chapter 5: Structure, Reactivity and Coordinating Power of Fluoride–Urea Complexes

5.1. Introduction: Fluoride–Urea Complexes

Although the interaction between fluoride anion and (thio)urea groups has in many cases been utilised for the design of fluoride sensors[355–363] and more recently also in anion binding catalysis,[332] only a comparably small number of characterised fluoride–urea complexes have been published. These studies mostly focussed on the use of di- and tripodal ligands encapsulating fluoride.

In 1998, Mak and co-workers reported the solid state structure of the hydrogen-bonded complex of urea with tetra-*n*-propylammonium fluoride, which they had been able to determine using single-crystal X-ray crystallography.[364] It contained two crystallographically distinct fluoride species that were both coordinated to a mixture of urea and water hydrogen bond donors, with the three different compounds forming a 3D network consisting of twisted urea ribbons, bridged by water molecules and fluoride anions *via* hydrogen-bonding (Figure 5.1).

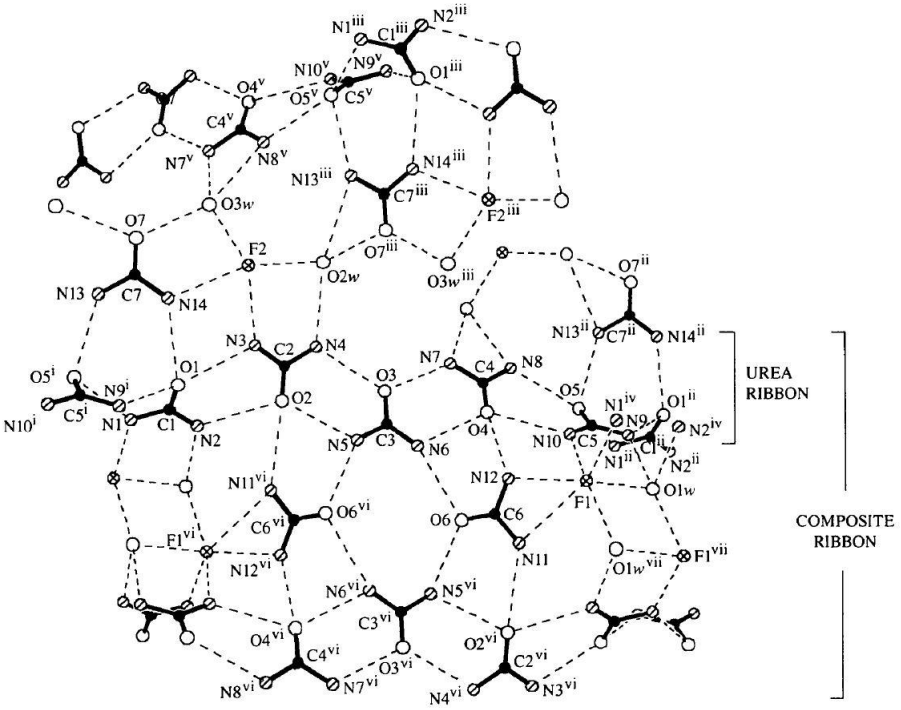

Figure 5.1. Projection drawing of 3D lattice formed by urea molecules, water molecules and fluoride. Reproduced with permission of the International Union of Crystallography from: Q. Li, T. C. W. Mak, *Acta Crystallogr. Sect. B* **1998**, *54*, 180–192.

In 2009, Ghosh and co-workers published a fluoride-complex, derived from tripodal urea-based ligand **5.1** (Figure 5.2).[365]

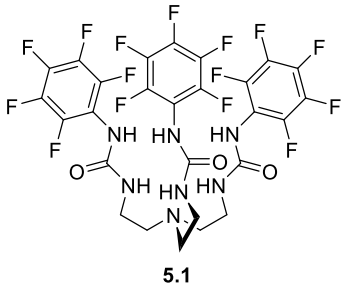

5.1

Figure 5.2. Tripodal ligand **5.1** used for complexation of fluoride.

In the single-crystal X-ray structure (TBA^+ counter-cation) they found fluoride forming six strong hydrogen bonds to all six urea protons ($d_{H\cdots F}$ < 2.2 Å and $d_{N\cdots F}$ < 3.0 Å), overall forming a distorted trigonal prismatic geometry around the anion. The NH···F^- distances,

involving the three NH groups further away from the bridgehead N-atom, are thereby significantly shorter – between 2.700–2.793 Å compared to 2.835–2.834 Å – due to the influence of the perfluorinated phenyl substituents. Binding studies in solution revealed the binding constant for fluoride in DMSO-d_6 at 25 °C to be log(K) = 4.06 (M^{-1}).

Bu and Yang, in 2011, reported a different tripodal urea-based fluoride ligand (**5.2**), bearing ferrocenyl groups on one urea nitrogen (Figure 5.3).[366]

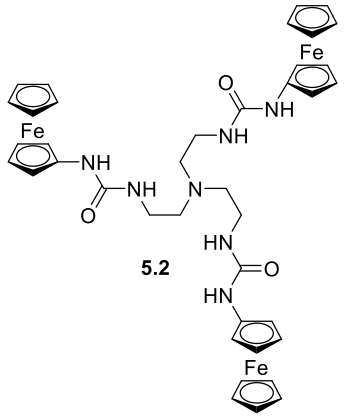

Figure 5.3. Tripodal ligand **5.2** used for complexation of fluoride.

The hydrogen-bonding distances and angles in the solid state (TBA^+ counter-cation) were found to be similar to the earlier example using **5.1**, with fluoride forming six hydrogen bonds to urea NH protons, with NH···F^- distances, involving the three NH groups further away from the bridging N-atom, being significantly shorter (2.757–2.787 Å compared to 2.881–2.925 Å). Negative-ion mode ESI mass-spectrometric studies also proved the formation of this complexed anion in solution. Using UV-vis studies log(K) for the association of fluoride in $CHCl_3$ at 25 °C was determined to be 5.31 (M^{-1}).

The same group reported a related solid state structure of a hydrogen-bonded complex, prepared from tripodal ligand **5.3** and KF (Figure 5.4).[367]

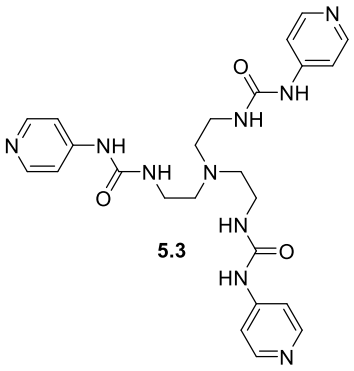

5.3

Figure 5.4. Tripodal ligand **5.3** used for complexation of fluoride.

Similarly to the structures found for ligands **5.1** and **5.2**, **5.3** was encapsulating fluoride, forming six hydrogen bonds with its six NH protons. However, in this case the NH···F^- distances, involving the three NH groups closer to the bridging N-atom, are considerably shorter (2.852(6) Å) than for those further away (3.172(5) Å). The average fluoride–urea hydrogen bond is longer and therefore weaker than in complexes with **5.1** and **5.2**. A possible explanation for this is the presence of three additional hydrogen bonds to three pyridine CH groups of a second, fluoride-encapsulating molecule **5.3**, leading to the formation of [**5.3**·F^-]$_2$ dimers.

In 2012, Dastidar and co-workers published a dipodal ligand, **5.4**, that was found to form crystals suitable for single-crystal X-ray crystallographic analysis upon layering a DMF-ethanol solution of it on top of an aqueous solution of $CuF_2 \cdot xH_2O$ (Figure 5.5).[368]

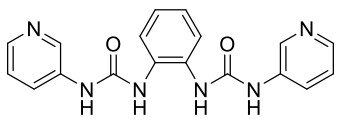

5.4

Figure 5.5. Dipodal ligand **5.4** used for complexation of fluoride.

The solid state structure was found to be best described by the formula [{Cu(μ-**5.4**)$_2$(H$_2$O)$_2$}F·2H$_2$O]$_\infty$, with fluoride coordinating to one urea NH as well as three water molecules. Closely related, isomorphous structures were obtained using the according chloride and bromide salts, CuCl$_2$·2H$_2$O and CuBr$_2$.[369]

In 2013, a different behaviour was reported by Huszthy and co-workers when they studied the effect of fluoride addition to urea-based receptor **5.5** (Figure 5.6).[370]

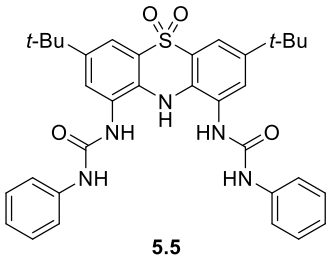

5.5

Figure 5.6. Dipodal ligand **5.5** used for complexation of fluoride.

In this case, fluoride binding was observed up to 1.0 equiv. of fluoride during UV-vis titration studies. This was followed by deprotonation of the 5,5-dioxophenothiazine NH between 1.0–3.0 equiv., leading to the formation of HF_2^-. The remaining anionic ligand was still coordinated to fluoride, which the authors were able to show by obtaining a single-crystal X-ray structure.

In the same year, Coles and Gale reported the solid state structure of TMAF(*N*,*N*'-bis(4-nitrophenyl)urea)$_2$ (Figure 5.7).[371]

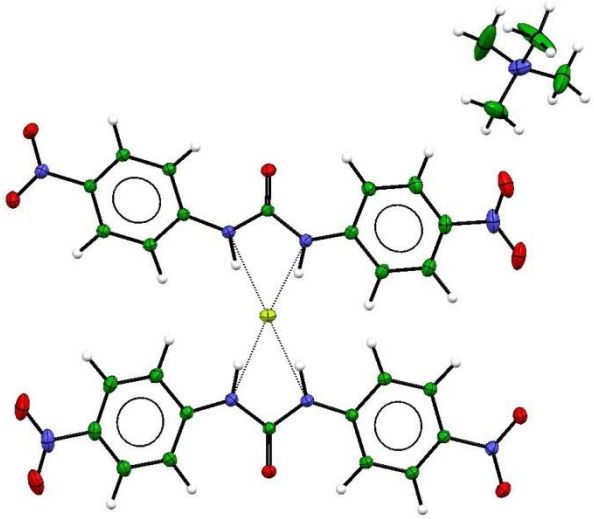

Figure 5.7. Hydrogen-bonding between urea groups and fluoride anion in the solid state structure of TMAF(*N*,*N*'-bis(4-nitrophenyl)urea)$_2$. Displacement ellipsoids are drawn at 50% probability.

As can be seen in Figure 5.7, each F^- was found to be coordinating to both NH functionalities of two urea groups with no short contacts to the TMA^+ cation. This behaviour is in stark contrast to related structures with Cl^- and acetate, where a 1:1 ratio between urea and anion was observed with additional short contacts to TMA^+ methyl groups. The authors suggest that this is mainly due to the smaller size of the fluoride anion, and it might also be the reason for the higher packing efficiency, observed for its structure with *N*,*N*'-bis(4-nitrophenyl)urea compared to the other studied anions.

This precedent showed that in order to study the structure and reactivity of fluoride–urea complexes it was viable to take a similar approach as we had chosen for complexes with alcohols, studying at first the solid state structures before looking at the behaviour in solution. The following work was carried out in collaboration with Dr. Keary M. Engle and George W. Pidgeon and was published in the *Journal of the American Chemical Society* in 2016.[372]

5.2. Results and Discussion

In order to get more insight into the solid state structures of fluoride–urea complexes, which could then be used to better understand their behaviour in solution, including most importantly their reactivity, we started our investigation by synthesising a library of *N*,*N*'-diarylureas and using them to grow crystals of hydrogen-bonded complexes with TBAF.

5.2.1. Solid State Structures

The complexes used in this study were synthesised using a protocol analogous to the one that had been employed for the synthesis of fluoride–alcohol complexes in Chapter 4: TBAF$(H_2O)_3$ was violently refluxed with 2.0 equiv. of *N*,*N*'-diarylurea, **5.6**, for 2 h in hexane in order to azeotropically remove water. Depending on the substitution pattern on the phenyl groups this either led to the formation of a white precipitate, which could be isolated by filtration, or a second liquid phase, which upon drying at elevated temperatures *in vacuo* gave the product as a white solid (see Experimental Section for details). A summary of the complexes, **5.7**, prepared in this manner is given in Table 5.1.

Table 5.1. Summary of prepared fluoride–urea complexes.

Entry	Urea	Yield	Complex	Type	C.N.[a]
1	**5.6a**, R = 3-CH_3	87%	**5.7a**	**A_1**	2
2	**5.6b**, R= 4-CF_3	96%	**5.7b**	**A_1**	2
3	**5.6c**, R= 4-NO_2	96%	**5.7c**	**A_1**	2
4	**5.6d**, R= 4-*n*-Pr	97%	**5.7d**[b]	**A_1**	2
5	**5.6e**, R= 4-H	90%[c]	**5.7e**	**A_2**	2
6	**5.6f**, R = 4-CH_3	97%	**5.7f**	**A_2**	2
7	**5.6g**, R = 4-OCH_3	91%	**5.7g**	**A_2**	2
8	**5.6h**, R= 4-Cl	99%	**5.7h**[b]	**A_2**	2
9[d]	**5.6i**, R= 4-*n*-Bu	77%	**5.7i**	**A_2**	2
10	**5.6j**, R= 4-F	94%[e]	**5.7j**[b]	**B**	2
11[d]	**5.6k**, R = 4-*i*-Pr	94%	**5.7k**	**B**	2
12[d]	**5.6l**, R = 4-I	91%	**5.7l**	**C**	1[f]
13[d]	**5.6m**, R = 4-Br	97%	**5.7m**	**C**	1[f]
14	**5.6n,** R = 4-Et	95%	**5.7n**	**C**	1[f]
15[d]	**5.6k**, R = 4-*i*-Pr	94%	**5.7o**	**C**	1[f]
16[d]	**5.6m**, R = 4-Br	97%	**5.7p**[g]	**C**	1[f]
17[d]	**5.6e**, R = 4-H (NMe_4^+)	99%	**5.7q**[g]	**D**	3
18[d]	**5.6e**, R= 4-H (NEt_4^+)	98%	**5.7r**	**D**	3

Conditions: 1.0 equiv. TBAF(H_2O)$_3$, 2.0 equiv. **5.6**, hexane (0.033 M F^-), 80 °C, 2 h. Single-crystal X-ray diffraction data collected by G. W. Pidgeon. [a]Coordination number *n* for (urea)$_n F^-$. [b]Neutron diffraction structure also obtained. [c]Yield was 93% when performed on a 12.00 mmol scale. [d]Prepared by Dr. K. M. Engle. [e]Yield was 96% when performed on a 12.00 mmol scale. [f][urea:H_2O:F^-] = 1:1:1. [g]CH_2Cl_2 solvate.

Complexes **5.7a**–**r** were mostly obtained in excellent yields >90% and were recrystallised from DCM, EtOAc or THF using a layering or vapour diffusion technique with hexane as the apolar solvent. The obtained single crystals were studied using single-crystal X-ray as well as neutron diffraction (**5.7d**, **5.7h** and **5.7j**) experiments to establish the solid state structures.

Although we were using a relatively restricted set of *N*,*N*'-diarylureas, we observed a series of several distinct modes of coordination (Figure 5.8).

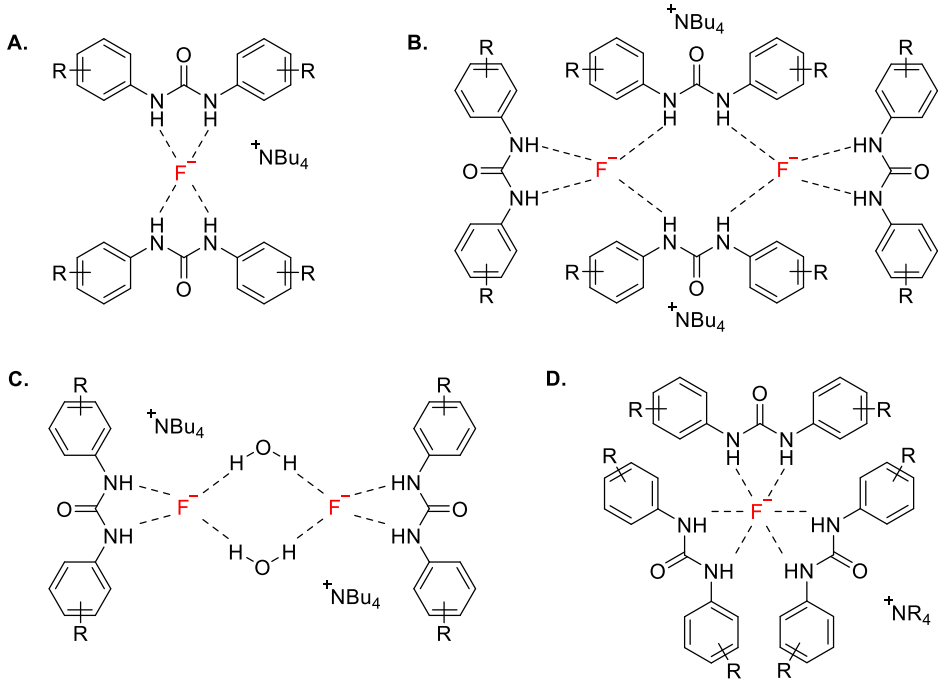

Figure 5.8. Observed coordination modes for fluoride–urea complexes.

9 out of the 18 structures that were analysed featured the $[U_2F]^-$ (U = urea) motif (**A**), which had been described earlier.[371] Due to significant structural variations within this group we further sub-divided it into types $\mathbf{A_1}$ and $\mathbf{A_2}$ (*vide infra*). Three additional modes of complexation of fluoride were observed, each in at least two structures. These included $[U_2F_4]^{2-}$ complexes (**B**), $[U_2(H_2O)_2F_2]^{2-}$ complexes (**C**) as well as $[U_3F]^-$ complexes (**D**).

In the 2:1 urea–fluoride complexes of category **A** the fluoride adopts a position approximately equidistant between the two urea molecules that constitute the $[U_2F]^-$ motif, thereby acting as a doubly bifurcated hydrogen bond acceptor (Figure 5.8A). The geometry of the complexed $[U_2F]^-$ anion can be characterised by the urea–urea interplanar angle (φ) and the O···F$^-$···O angle (ϑ). Due to steric restrictions this can range

from square planar (S_p, φ = 0°, ϑ = 180°) to tetrahedral (T_d, φ = 90°, ϑ = 180°) and tetragonal pyramidal with a vacant apical site (T_p, φ = <90°, ϑ = <180°) (Table 5.2).

Table 5.2. Summary of urea–urea interplanar angles (φ) described by the NNCO motif, and O···F^-···O angles (ϑ) for complexes of types **A** and **C**.

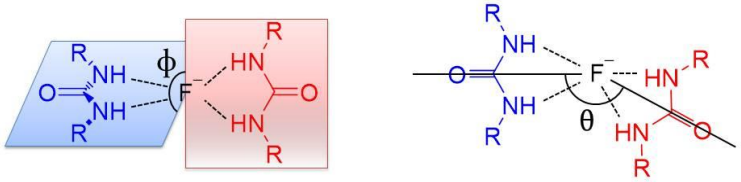

Entry	Complex	φ [°]	ϑ [°]	$S_p/T_d/T_p$[a]
1	**5.7a** (3-CH_3)	59.66(9)	131.88(4)	T_p
2	**5.7b** (4-CF_3)	56.3(4)	137.55(12)	T_p
3	**5.7c** (4-NO_2)	4.26(15)	172.60(5)	S_p
4	**5.7d** (4-*n*-Pr)	15.52(9)	163.11(4)	S_p-T_p
5	**5.7e** (4-H)	43.15(9)	169.87(4)	S_p-T_d
		64.13(7)	173.54(3)	S_p-T_d
6	**5.7f** (4-CH_3)	43.12(12)	174.12(5)	S_p-T_d
		77.58(10)	171.69(5)	T_d
7	**5.7g** (4-OMe)	80.9(2)	174.71(9)	T_d
		maj.: 43.5(4) min.: 38.8(7)	maj.: 177.10(15) min.: 172.49(17)	S_p-T_d
8	**5.7h** (4-Cl)	76.27(7)	172.23(3)	T_d
		40.59(9)	172.71(4)	S_p-T_d
9	**5.7i** (4-*n*-Bu)	27.41(15)	155.00(5)	T_p
		16.52(17)	168.58(7)	T_p
10[b]	**5.7l** (4-I)	60.99(18)	144.51(6)[c]	-
11[b]	**5.7m** (4-Br)	68.5(2)	138.72(7)[c]	-
12[b]	**5.7n** (4-Et)	0[d]	180[c,d]	-
13[b]	**5.7o** (4-*i*-Pr)	6.60(15)	175.55(4)[c]	-
14[b]	**5.7p** (4-Br)	0[d]	180[c,d]	-

[a]S_p = square planar, T_d = tetrahedral, T_p = tetragonal pyramidal with vacant apical site. [b]Two ureas binding to one $(F^-{\cdot}H_2O)_2$ dianion used. [c]Centroid between the two fluorides of the $(F^-{\cdot}H_2O)_2$ dianion used as hinge point. [d]Ureas related by inversion.

Type A_1 2:1 structures: Structures belonging to type **A_1** (**5.7a**–**d**) contain one crystallographically distinct ion pair, with fluoride forming the aforementioned $[U_2F]^-$ motif featuring four NH···F^- hydrogen bonds (Figure 5.9).

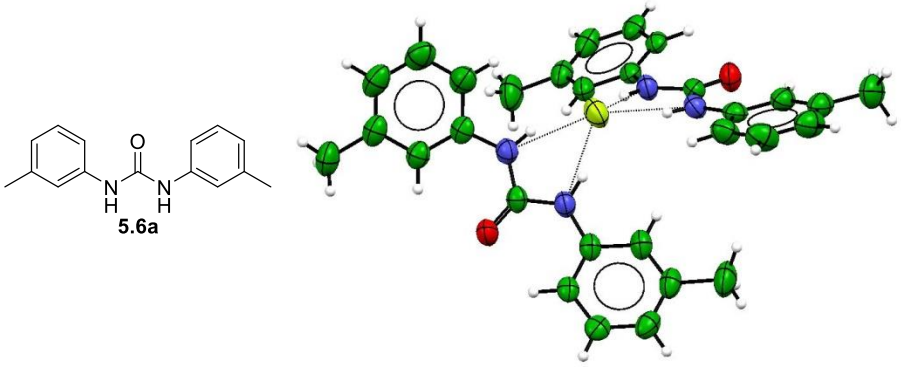

Figure 5.9. Solid state structure of the $[UF_2]^-$ complex anion in **5.7a**, determined using single-crystal X-ray diffraction. Urea-urea interplanar angle and O···F^-···O angle are 59.66(9)° and 131.88(4)°, respectively. Displacement ellipsoids are drawn at 50% probability. Cation is omitted for clarity.

The interplanar angle between the NNCO motifs of the two urea groups varies widely throughout this set of structures, though this seems to be largely due to crystal packing forces. For example, this angle was determined to be 4.26(15)° in **5.7c** (4-NO_2), but 40.30(3)° in the previously mentioned TMA^+ analogue.[371] In the case of 3-Me and 4-CF_3 substituted complexes **5.7a** and **5.7b**, the O···F^-···O angle deviates significantly from linearity, with all four NH hydrogen bond donors lying in the same hemisphere forming a tetragonal pyramid (Table 5.2, Entries 1 and 2), whose vacant site is occupied by weak, long-range contacts to C–H donors. A similar structure had been observed before for the 2:1 pinacol–fluoride complex (**4.19d**).[333] Complexes **5.7c** (4-NO_2) and **5.7d** (4-*n*-Pr) exhibit shallow urea–urea interplanar angles of 4.26(15)° and 15.52(9)°, respectively, effecting a more square planar ensemble (Table 5.2, Entries 3 and 4).

In the case of complex **5.7d** we succeeded in growing a crystal of sufficient size and quality for single-crystal neutron diffraction experiments, which allowed for the accurate placement of hydrogen nuclei in the structure. This made a comparison between geometric hydrogen bond parameters, taken from the solid state structure before and after refinement using the newly obtained neutron data, possible (Table 5.3).

Table 5.3. Summary of geometric hydrogen-bonding parameters for **5.7d**, **5.7h** and **5.7j** from single-crystal X-ray and neutron diffraction data.

Complex	D–H [Å]	H···A [Å]	D···A [Å]	∠ DHA [°]
5.7d, R= 4-*n*-Pr X-ray / neutron	0.863 / 1.049(9)	1.893(2) / 1.696(9)	2.7004(15) / 2.697(6)	155 / 158.0(8)
	0.867 / 1.007(11)	1.880(2) / 1.750(11)	2.6994(16) / 2.704(6)	157 / 156.6(8)
	0.856 / 1.043(10)	1.915(2) / 1.731(10)	2.7261(17) / 2.716(6)	158 / 155.7(9)
	0.838 / 1.013(11)	1.978(2) / 1.796(10)	2.7631(17) / 2.747(6)	156 / 154.8(8)
5.7h, R= 4-Cl X-ray / neutron	0.850 / 1.046(9)	1.834(1) / 1.634(9)	2.6538(11) / 2.648(4)	162 / 161.8(9)
	0.852 / 1.042(10)	2.011(1) / 1.825(10)	2.7945(10) / 2.788(4)	153 / 152.0(8)
	0.848 / 1.013(15)	1.879(1) / 1.719(13)	2.6821(11) / 2.672(6)	157 / 155.2(9)
	0.878 / 1.012(14)	1.872(1) / 1.748(14)	2.6989(11) / 2.697(5)	156 / 154.6(9)
5.7j, R= 4-F X-ray / neutron	0.856 / 1.030(10)	1.853(2) / 1.674(10)	2.6866(19) / 2.676(6)	164 / 162.8(9)
	0.861 / 1.062(8)	1.858(2) / 1.659(9)	2.700(2) / 2.700(6)	165 / 165.7(10)
	0.856 / 1.031(15)	1.881(2) / 1.703(14)	2.7086(19) / 2.698(8)	162 / 160.8(9)
	0.862 / 1.062(13)	2.002(2) / 1.820(13)	2.811(2) / 2.807(8)	156 / 153.0(9)

Thereby, it was found that the N(H)···F^- (D···A) distances as well as N–H···F^- angles (∠ DHA) largely remained unchanged, whereas significant deviations were found for the

N–H bond lengths (D–H) as well as (N)H···F$^-$ distances (H···A). The former increased by 14.0–18.7 pm with the latter decreasing accordingly by 13.0–19.7 pm, illustrating the weakening of the N–H bonds in favour of strong NH···F$^-$ hydrogen bonds.

Type A_2 2:1 structures: Compared to **A_1**-type structures, those belonging to type **A_2** (**5.7e**–**i**) possess two crystallographically distinct ion pairs with different twist geometries (Figure 5.10).

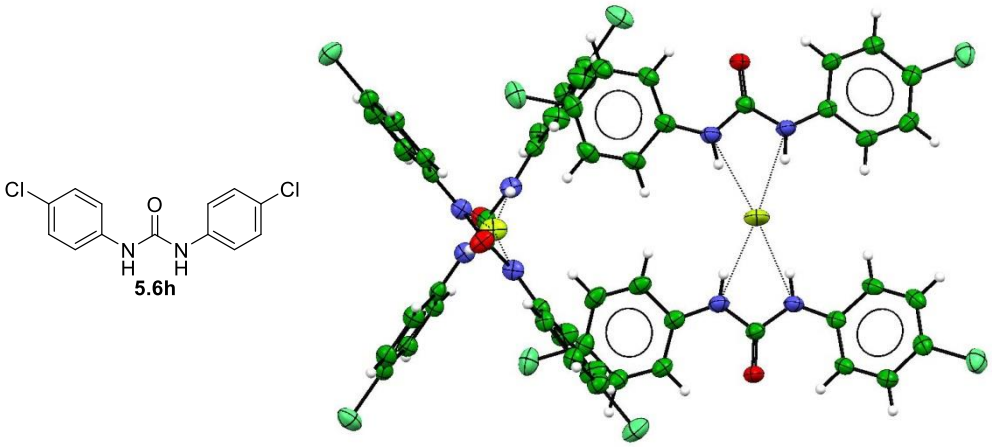

Figure 5.10. Solid state structure of the two independent $[U_2F]^-$ anions in **5.7h**, determined using single-crystal X-ray diffraction. Urea–urea interplanar angles are 40.59(9)˚ and 76.27(7)˚ degrees. Displacement ellipsoids are drawn at 50% probability. Cations are omitted for clarity.

Upon substitution of 4-Me (**5.7f**) for 4-Cl (**5.7h**) an isomorphous pair of structures was obtained, an observation that is consistent with the previously described "chloro-methyl exchange rule".[373] Furthermore, the solid state structures of **5.7e** (4-H) and **5.7g** (4-OMe) are very similar and are considered to be isostructural.[369] The O···F$^-$···O angles (ϑ) determined for this sub-set of fluoride–urea complexes are all close to linearity, and with urea-urea interplanar angles between 40–81° their coordination geometries can either be described as tetrahedral, or as being intermediary between square planar and tetrahedral (Table 5.2, Entries 5–8). Complex **5.7i** (4-*n*-Bu) stands out, as the two urea pairs of the

two different complexed anions describe a shallow V-shape, forming a tetragonal pyramidal coordination geometry with urea–urea interplanar angles of 16.52(17)° and 27.41(15)°, respectively, and O···F^-···O angles that deviate significantly from linearity (Table 5.2, Entry 9).

Crystals suitable for neutron diffraction experiments could be grown from complex **5.7h** (Table 5.3). As had been the case for complex **5.7d**, the overall N(H)···F^- (D···A) distances as well as N–H···F^- angles (∠ DHA) were found to be very similar in the structure before and after refinement with the newly obtained neutron data. Also in line with earlier observations, the N–H bond lengths (D–H) and (N)H···F^- (H···A) distances were significantly longer and shorter, respectively, after the refinement.

Type B 4:2 structures: This class of structures (**5.7j** and **5.7k**) comprises a supramolecular 4:2 cluster dianion (Figure 5.11).

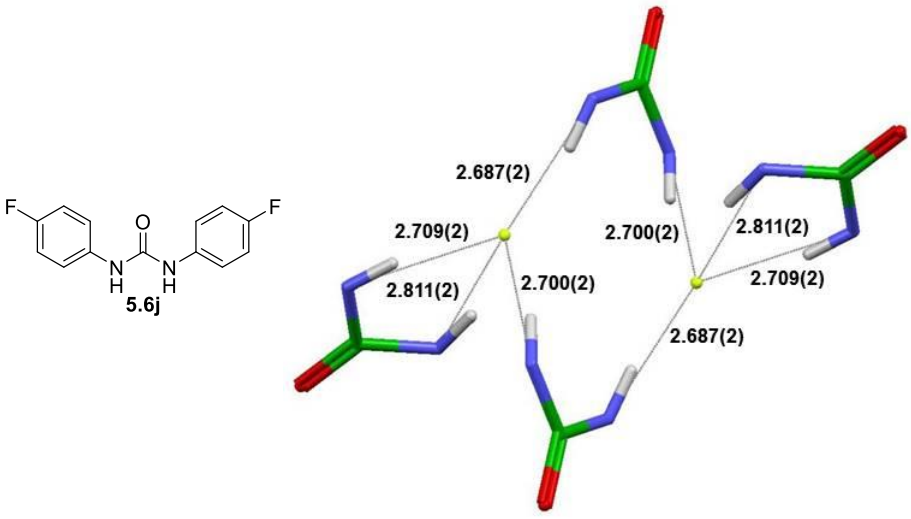

Figure 5.11. Bridging and terminal fluoride–urea hydrogen-bonding in the 4:2 supramolecular dianion in complex **5.7j**, featuring 1,3-bis(4-fluorophenyl)urea (**5.6j**). N(H)···F^- distances are shown. Aryl groups and cations are omitted for clarity.

Both fluorides engage in four hydrogen bonds to NH groups of three different urea molecules. Two are provided by a terminal urea with the other two coming from two ureas that by binding with one NH group each to the two fluorides serve as bridges. All hydrogen bonds in **5.7j** (4-F) and **5.7k** (4-*i*-Pr) are short with N(H)···F^- distances ≤2.82 Å. Complex **5.7k** has an $F^-\cdots F^{-\prime}$ distance of 3.2632(16) Å, which is significantly longer compared to the 3.045(3) Å found in **5.7j**. This type of $[U_4F_2]^{2-}$ complex anion with two bridging hydrogen-bonding ureas is without precedent in the Cambridge Structural Database (CSD).[374]

As before for **5.7d** and **5.7h**, it was possible to grow a crystal of suitable size and quality for single-crystal neutron diffraction of compound **5.7j** (Table 5.3). Once again the results showed a shortening of the (N)H···F^- (H···A) distances with N–H bond lengths (D–H) being elongated accordingly upon refinement of the X-ray solution with neutron data.

Type C 2:2 dihydrate structures: All structures presented so far had an overall 2:1 ratio of urea:fluoride. By contrast, employing ligand **5.6l** (4-I) under the same reaction conditions as before gave **5.7l**, which, although prepared under azeotropic water removal, contained water of crystallisation, hydrogen-bonding to fluoride anion (Figure 5.12). The most likely source for this is incomplete water removal during the complexation reaction, but water binding during recrystallisation is also possible.

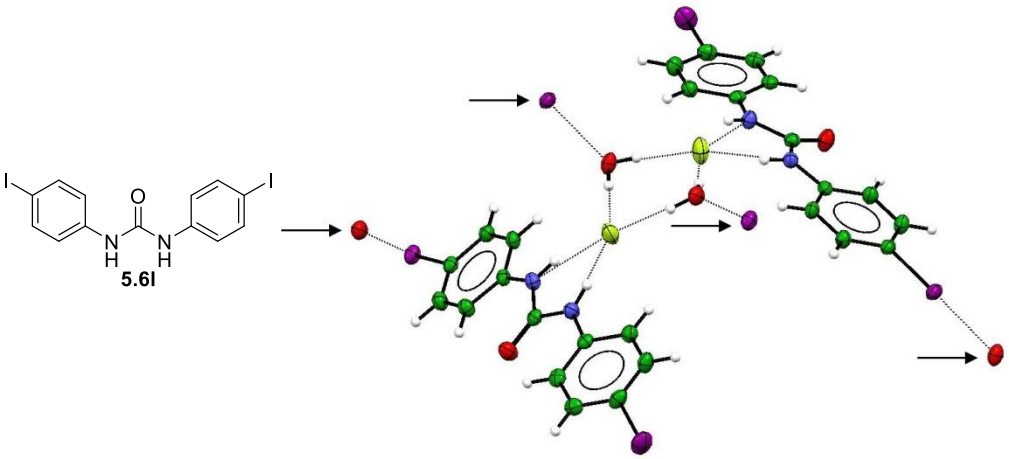

Figure 5.12. Complex anion of **5.7l**; ⟶ marks halogen-bonding interactions. Displacement ellipsoids are drawn at 50% probability. Cations are omitted for clarity.

Similarly, **5.7m** is obtained after the reaction with the corresponding bromide **5.6m**. Both structures comprise single I···O and Br···O halogen-bonding interactions between neighbouring urea ligands and both water molecules, involving the positively polarised aromatic halogen substituents and the negatively polarised water oxygens.[375,376] The Hal···O distance is 3.037(2) Å (**5.7l**) and 3.090(3) Å (**5.7m**), respectively, with C–Hal···O angles of 174.37(10)° and 170.84(15)°, indicative of an approximately linear arrangement. Of **5.6m** a second related hydrogen-bonded fluoride complex, **5.7p**, was obtained, featuring CH_2Cl_2 of crystallisation. **5.7p** does not display the aforementioned halogen-bonding interactions found in **5.7m**. Another related structure, **5.7o**, was obtained from 4-*i*-Pr-substituted urea (**5.6k**), whose first fluoride complex structure **5.7k** contained the $[U_4F_2]^{2-}$ cluster dianion. The fifth structure belonging to this category, **5.7n**, prepared from 4-Et-substituted urea **5.6n**, stood out as the crystal was found to be aperiodic.[377] The $[U_2(H_2O)_2F_2]^{2-}$ dianion displays an approximately planar geometry with an average F^- ···F^-' distance of 4.17 ± 0.03 Å. The dihedral angles between urea planes (φ) in **5.7l** and **5.7m** are 60.99(18)° and 68.5(2)°, and by using the centroid of the two fluorides as hinge point ϑ angles were determined to be 144.51(6)° and 138.72(7)° (Table 5.2, Entries 10

and 11). As can be taken from these values, overall, the hydrogen-bonded assemblies describe shallow U-shapes. On the other hand, urea planes in structures **5.7n**–**p** are parallel or almost parallel, and ϑ values show a perfectly or almost linear relationship between the centroid of the two fluorides and the two urea carbonyl oxygens (Table 5.2, Entries 12–14). Several other examples of $(F^{-}\cdot H_2O)_2$ dianionic clusters can be found in the CSD[374] although their generality has not been well recognised.[364,378–381] In our examples their formation in an isolated unit is partly encouraged by the combination of bulky *p*-substituents on the 1,3-diarylureas with a bulky counter-cation. Furthermore, the presence of the bridging water molecules offers the possibility of additional interactions, as observed in **5.7l** and **5.7m**.

Type D 3:1 structures: So far we only looked at complexes comprising spatially demanding *n*-Bu_4N^+ as counter-cation. To answer the question, what would happen upon exchanging this for a smaller tetraalkylammonium analogue, we prepared complexes **5.7q** and **5.7r** from parent *N*,*N*'-diphenylurea (**5.6e**) using TMAF·$4H_2O$ and TEAF·$2H_2O$ as the respective fluoride source, following the same procedure as had been described earlier. Contrary to all previous structures in this study, these two derivatives contain a hexacoordinate fluoride species in the solid state (Figure 5.13).

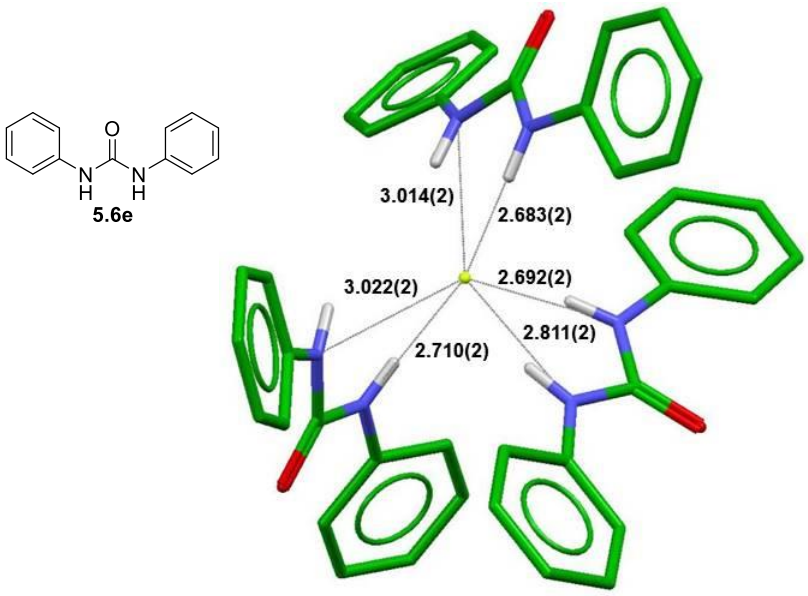

Figure 5.13. Hydrogen-bonded fluoride anion in complex **5.7q**, featuring a TMA^+ counter-cation. N(H)···F^- distances are shown. Aromatic protons and cation are omitted for clarity.

These six hydrogen-bonding contacts involve three different ureas and the arrangement of the three pairs of donor atoms forms a distorted paddle-wheel motif. Two hydrogen bonds, involving different urea donor molecules, are significantly longer compared to the remaining four (Figure 5.13).

Other ligated fluoride complexes: Having seen the variety of binding arrangements in this rather narrow set of urea-derived complexes, we wondered whether it would be possible to replace the urea unit with a different hydrogen-bonding functionality. We therefore chose amide **5.8** and squaramides **5.10a**–**c** to synthesise four additional complexes following our standard procedure (Table 5.4).

Table 5.4. Amide (**5.9**) and squaramide (**5.11a–c**) complexes characterised by single-crystal X-ray diffraction.

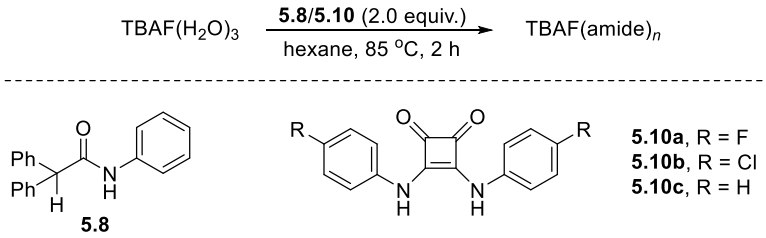

Entry	Amide	Yield	Complex	Type[a]	C.N.[b]
1	**5.8**	93%	**5.9**	$\mathbf{A_1}$[c]	2
2	**5.10a**	98%	**5.11a**[d]	$\mathbf{A_1}$	2
3[e]	**5.10b**	95%	**5.11b**	$\mathbf{A_1}$	2
4	**5.10c**	96%	**5.11c**	[f]	1

Conditions: 1.0 equiv. $TBAF(H_2O)_3$ (2.00 mmol), 2.0 equiv. **5.8/5.10** (4.00 mmol), hexane (60 mL), 80 °C, 2 h. Single-crystal X-ray diffraction data collected by G. W. Pidgeon. [a]See Table 5.1. [b]Coordination number *n* for $(amide)_nF^-$. [c]With one C–H replacing an N–H. [d]THF solvate. [e]Prepared by Dr. K. M. Engle. [f]1:1:2 fluoride:squaramide:H_2O.

Complex **5.9** was prepared from amide **5.8** and single-crystal X-ray diffraction analysis after recrystallisation revealed fluoride anion hydrogen-bonding to two amides. The N–H···F^- bonds in the resulting 2:1 structure are nearly co-linear, and four additional C–H···F^- contacts, two major ones from the benzhydryl unit and two minor ones from the proximal *o*-C–H of the *N*-arylamide, are found in the solid state (Figure 5.14).

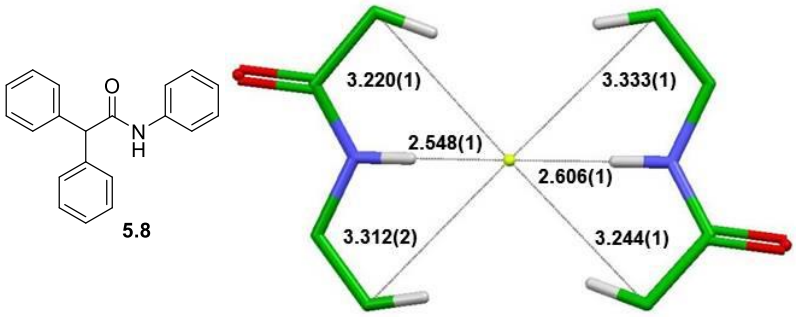

Figure 5.14. Hydrogen-bonding to fluoride in complex **5.9** derived from amide **5.8**. N(H)···F^- and C(H)···F^- distances are shown. Aryl groups and cation are omitted for clarity.

Hydrogen-bonding to acidic C(sp^3)–H groups had previously been shown to be a possible determinant of conformation.[382] The amido N(H)···F^- distances were determined to be 2.5475(11) Å and 2.6060(11) Å, respectively, and therefore significantly shorter than the values found in urea derived complexes. All six hydrogen bonds lie in approximately the same plane.

Squaramides, derived from the parent 1,2-diaminocyclobuten-3,4-dione, have found broad application in molecular recognition and catalysis.[383–386] Furthermore, in a direct comparison, transmembrane transport of chloride or bicarbonate anions is more efficient with squaramides compared to analogous ureas and thioureas.[387] This prompted us to study the solid state structures of three complexes **5.11a–c**, derived from prototypical *N*,*N*'-diarylsquaramides **5.10a–c**. Prior to this work, no solid state structure of a fluoride–squaramide complex had been reported, although several 1:1 complexes with chloride and one 1:1 complex with bromide are known.[384,388] 4-Fluoro- (**5.10a**) and 4-chloro-substituted (**5.10b**) *N*,*N*'-diarylsquaramides were found to form 2:1 complexes (**5.11a** and **5.11b**) analogous to type $\mathbf{A_1}$ (Figure 5.15).

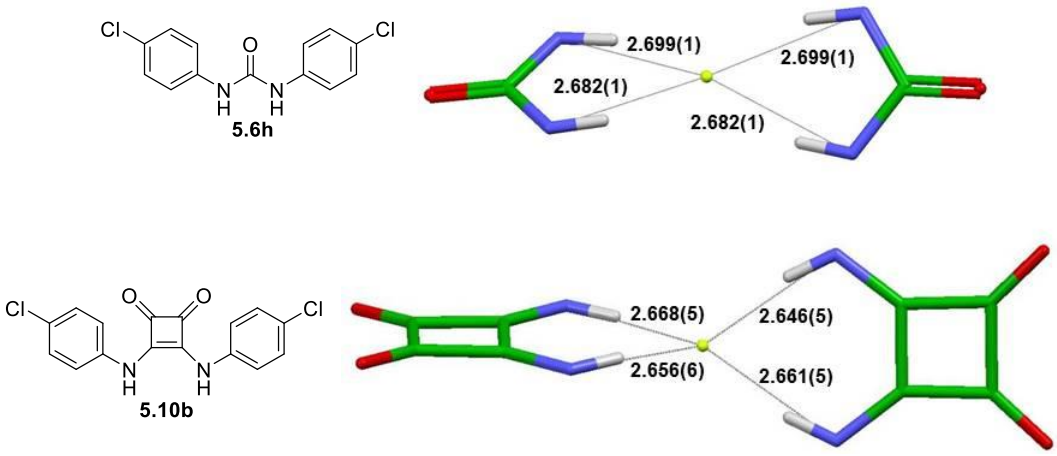

Figure 5.15. Comparison of the coordination geometry of a typical 2:1 urea (**5.7h**) and squaramide (**5.11b**) complex. N(H)···F^- distances are shown. Aryl groups and cations are omitted for clarity.

Co-planarity of the two squaramide ligands in **5.11a** and **5.11b** is disfavoured as, contrary to urea-derived complexes **5.7a**–**i** (types $\mathbf{A_1}$ and $\mathbf{A_2}$), the aryl substituents would have to rotate out of conjugation in order to avoid a steric clash. Consequently, they form twisted arrangements with squaramide–squaramide interplanar angles of 61.48(5)° for **5.11a** and 78.8(2)° for **5.11b**. On the other hand, the parent, unsubstituted *N*,*N*'-diphenylsquaramide **5.10c** forms a 1:1:2 squaramide–fluoride–H_2O structure, with fluoride hydrogen-bonding to both NH groups of a squaramide as well as two water molecules. The latter also form a second set of hydrogen bonds to the carbonyl groups of the neighbouring squaramide, thereby linking the individual complexed fluoride anions into a 1D ribbon-like structure. All three structures contain four (**5.11a** and **5.11b**) or two (**5.11c**) distinct hydrogen bonds, with N(H)···F^- distances between 2.625–2.709 Å.

Putting everything together, the presented structures provide an extensive set of data on N(H)···F^- hydrogen bonds for ureas and related analogues. The distribution of hydrogen bond lengths is relatively narrow across all urea-based complexes. For 2:1 and 4:2 urea–fluoride complexes of types **A** and **B** the average hydrogen bond length was RMS = 2.711 ± 0.062 Å, with no significant difference between electron-rich and electron poor ureas. Similarly, there is no significant difference in hydrogen bond lengths to 1:1:2 urea–fluoride–H_2O complexes of type **C** (RMS = 2.706 ± 0.034 Å). However, 3:1 urea–fluoride complexes (**D**) have longer average hydrogen bonds at RMS = 2.830 ± 0.135 Å (2.754 ± 0.049 Å omitting the three N(H)···F^- contacts >3.0 Å), whereas the average N(H)···F^- hydrogen bond in squaramide-based complexes is significantly shorter (RMS = 2.662 ± 0.024 Å). Figure 5.16 shows the overall distribution of N(H)···F^- hydrogen bond lengths of the complexes used in this study.

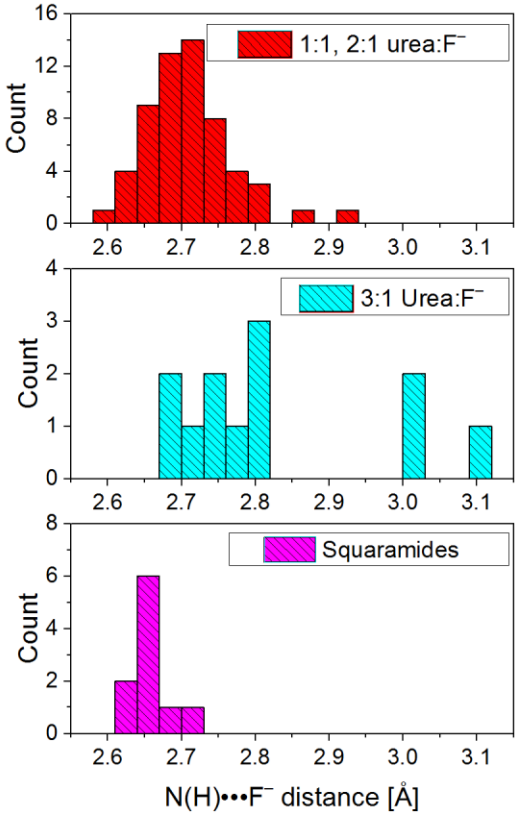

Figure 5.16. Summary of N(H)···F⁻ hydrogen bond lengths of the complexes used in this study. Only the major components of disordered structures **5.7g** and **5.7k** are included.

5.2.2. Reactivity Study

In order to be able to assess the capabilities of fluoride–urea complexes as sources of fluoride compared to fluoride–alcohol complexes, we performed the same reactivity study as we had done for the latter (see Chapter 4). In this case, aliquots were taken from the same model reaction, now using fluoride–urea complexes, over the course of 48 h. These samples were again analysed by ^{1}H NMR to follow the consumption of alkyl bromide **4.10** and the concomitant formation of alkyl fluoride **4.2** and olefin **4.4**. These

data was used to determine rate constants for the competing S_N2 and E2 processes using Berkeley Madonna software. The results are summarised in Table 5.5.

Table 5.5. Reactivity study of fluoride–urea, –amide and –squaramide complexes with alkyl bromide **4.10**.

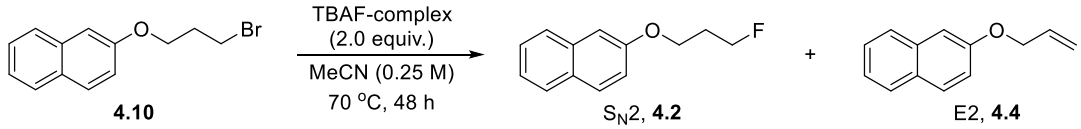

4.10 S_N2, **4.2** E2, **4.4**

Entry[a]	Complex	$k_2(S_N2)$[b] [$\cdot 10^{-5}$ $M^{-1}s^{-1}$]	$k'_2(E2)$[b] [$\cdot 10^{-5}$ $M^{-1}s^{-1}$]	$k_2(S_N2)/k'_2(E2)$[c]
1; 3-Me	**5.7a**	5.95	1.07	5.6
2; 4-OMe[d]	**5.7g**	12.7	2.45	5.2
3; 4-Me[d]	**5.7f**	9.8	1.65	5.7
4; H[d]	**5.7e**	5.76	0.85	6.8
5; H[d,e]	**5.7e**	18.8	4.63	4.1
6; H[d,f]	**5.7e**	42.4	12.9	3.3
7; 4-F[d]	**5.7j**	5.67	0.80	7.1
8; 4-Cl[d]	**5.7h**	5.83	0.84	6.9
9; 4-NO_2[d]	**5.7c**	3.2	0.38	8.4
10; 4-CF_3[g]	**5.7b**	1.65	0.19	8.7
11[h,i]	**5.9**	178	112	1.6
12[d,h,j]	**5.11a**	(2)	(0.7)	2.8
13[k]	TBAF$(H_2O)_3$	607	378	1.6

Conditions: 1.0 equiv. **4.10** (0.20 mmol), 2.0 equiv. hydrogen-bonded complex (0.40 mmol), MeCN (0.80 mL), 70 °C, aliquots taken over course of 48 h. [a]Substituent of urea. [b]From ^{1}H NMR analysis by curve fitting. [c]For comparison, the ratio $k_2(S_N2)/k'_2(E2)$ for TBAF(*t*-BuOH)$_4$ was 2.1.[333] [d]Reactions carried out by Dr. K. M. Engle. [e]0.063 M. [f]0.025 M. [g]In a separate reaction under identical conditions, yields of **4.2** and **4.4** after 48 h were determined to be 45% and 4%, respectively, using ^{19}F and ^{1}H NMR with 1-fluoro-3-nitrobenzene as internal reference. [h]See Table 5.4. [i]2 h reaction time. [j]Slow reaction accompanied by decomposition of diamide **5.10a**. [k]From Table 4.7.

In general, fluoride–urea complexes proved to be significantly less reactive compared to the fluoride–alcohol complexes in Chapter 4. This, however, comes with an improved S_N2:E2 selectivity, where even the least selective urea, **5.7g** (4-OMe; Table 5.5, Entry 2)), trumps the most selective alcohol complex, **4.19f** (Table 4.7, Entry 10). At long reaction

times, side-reactions that consumed bromide **4.10** but did not lead to either **4.2** or **4.4** were observed. When comparing the reactions involving ureas with different *para*-substituents, one can see a general trend of decreasing reactivity and increasing selectivity, when going from electron donating to electron withdrawing ones (Table 5.5, Entries 2–4 and 7–10). This is only a qualitative observation, as the halide substituents in ureas **5.6h** and **5.6j** show a comparable reactivity and selectivity to unsubstituted **5.6e**. Furthermore, 4-CF_3-substituted urea **5.6b** resulted in a 2-fold reactivity decrease and an improved S_N2:E2 selectivity (8.7 *vs.* 8.4) relative to 4-NO_2-bearing **5.6c**. Comparing 3-Me-substituted complex (**5.7a**) with its 4-Me-substituted analogue (**5.7f**), one can see a marked increase in reactivity affecting both pathways to the same extent (Table 5.5, Entries 1 and 3). With electronic differences generally also affecting selectivity, this increase seems to be caused by the changed steric hindrance of the urea. In analogy to the fluoride–alcohol complexes, we again see a clear correlation between reactivity and selectivity, with less reactive complexes giving better selectivities and *vice versa*. To the best of our knowledge, selectivities for both complexes **5.7b** and **5.7c** are the highest that have been observed for this type of substrate to date (Table 5.5, Entries 9 and 10).[303] The spread of S_N2 reactivity is relatively narrow, about 8-fold, across this set of compounds.

Amide complex **5.9** was more similar to alcohol-based complexes, with an approximately 100-fold higher S_N2 rate constant and an S_N2:E2 selectivity of 1.6 (Table 5.5, Entry 11). The reaction with fluoride–squaramide complex **5.11a** was slow in terms of both S_N2 as well as E2 pathways and was accompanied by decomposition of diamide ligand **5.10a** (Table 5.5, Entry 12).

Similarly to the fluoride–alcohol complexes, the rate constants for urea-based complexes were found to increase significantly upon lowering the reaction concentration. This could imply that partial or full dissociation of one urea ligand might be required to obtain a reactive fluoride–urea species (Table 5.5, Entries 5 and 6 *vs.* Entry 4). Subsequent dissociation of the second urea to give free fluoride would increase reactivity and decrease selectivity. Overall, a two-stage dissociation sequence can be envisioned, where both products of dissociation starting from 2:1 urea–fluoride complex can react to give alkyl fluoride **4.2** and olefin **4.4** (Scheme 5.1). The two species, $[UF]^-$ and F^-, would thereby show different selectivities for the two products.

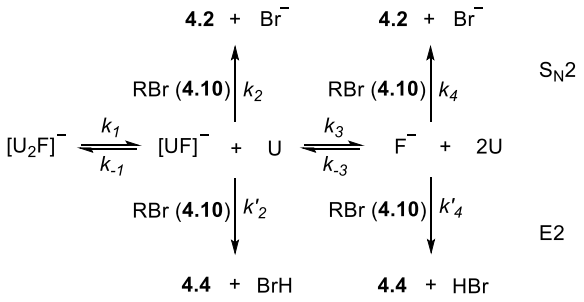

Scheme 5.1. Working model for activity of $[U_2F]^-$ in solution.

5.2.3. Fluoride–Urea Binding in Solution

In order to get further insight we decided to examine fluoride–urea complexation in solution. This binding interaction is known to alter the electronic character of the compounds involved and can therefore be followed by UV-vis spectroscopy.

We performed a series of UV-vis titrations of 8.0 μM solutions of selected ureas in MeCN using a solution of $TBAF(H_2O)_3$, without changing the concentration of the urea over the course of the titration. The exact concentration of the TBAF solution had previously been

determined by titrating a TIPS-protected coumarin derivative, which is known to be a highly sensitive fluorescence "turn-on" indicator for fluoride anion.[389] Upon adding fluoride to different ureas a bathochromic shift of the absorption band with a urea-dependent maximum between 250–264 nm was observed (Figure 5.17).

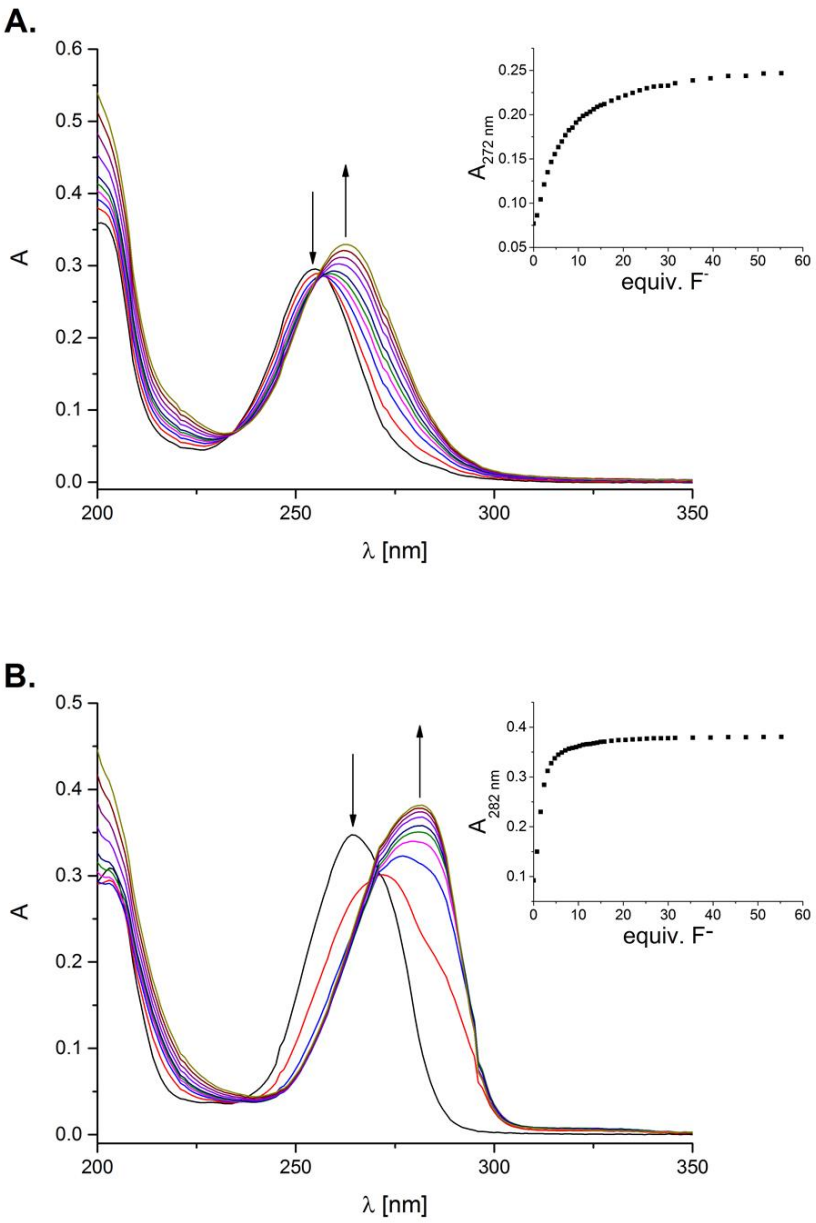

Figure 5.17. (A) Series of UV-vis spectra, recorded over the course of a titration of an 8.0 µM solution of **5.6e** (4-H) in MeCN with a 1.58 mM solution of TBAF$(H_2O)_3$. *Inset*: Titration profile at 272 nm. (B) Same for **5.6b** (4-CF_3). *Inset*: Titration profile at 282 nm.

The absorption at the new maximum between 259–282 nm was then plotted against the concentration of added fluoride. In a first step, a simple binding model, assuming only the formation of 1:1 complexes, was fitted to the obtained data *via* non-linear least-squares regression using DynaFit4 software (Figure 5.18).[390]

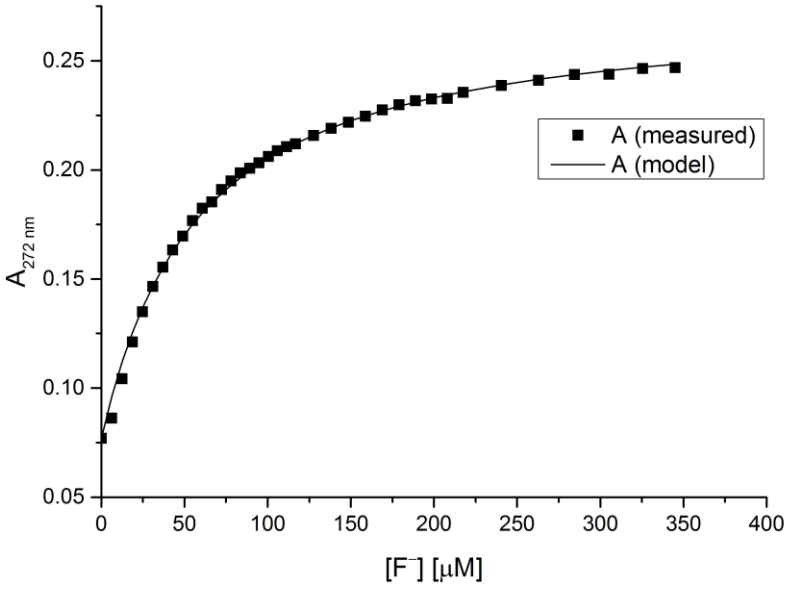

Figure 5.18. Fitting of a 1:1 binding model to the observed absorption at 272 nm from a series of UV-vis spectra, recorded over the course of a titration of an 8.0 μM solution of **5.6e** (4-H) in MeCN with a 1.58 mM solution of TBAF$(H_2O)_3$.

This could be used to obtain the association constants for the formation of 1:1 urea–fluoride complexes, $K_{a,1:1}$, and also calculate the free energies of complexation, $\Delta G_{1:1}$ (Table 5.6).

Table 5.6. Association constants, $K_{a,1:1}$, and free energies, $\Delta G_{1:1}$, for the formation of $[UF]^-$ complexes.

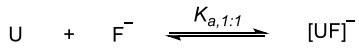

	4-H (**5.6e**)	4-Me (**5.6f**)	4-OMe (**5.6g**)	4-F (**5.6j**)	4-Cl (**5.6h**)	4-CF_3 (**5.6b**)
$\log(K_{a,1:1})$ $[M^{-1}]$	4.29(1)	4.20(2)	4.09(2)	4.38(2)	4.53(2)	4.93(1)
$\Delta G_{1:1}$ [kJ mol^{-1}]	24.5(1)	24.0(1)	23.3(1)	25.0(1)	25.8(1)	28.1(1)

For electron-rich 1,3-diarylureas, taking only this complexation into account returned good results. Further evidence for the clean transition is provided by the presence of two isosbestic points (Figure 5.17A) as well as band deconvolution analysis which also indicated the presence of two species over the course of the titration (Figure 5.19).

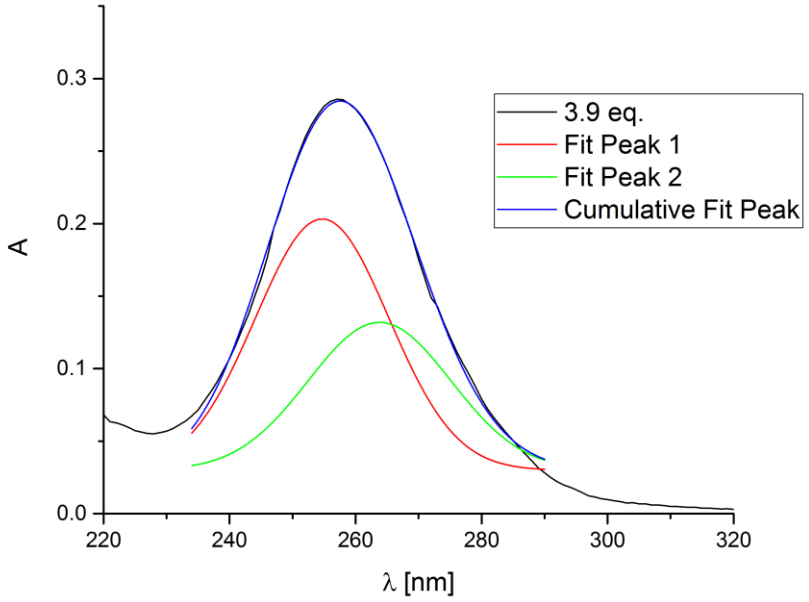

Figure 5.19. Gaussian deconvolution analysis of UV-vis absorption spectrum after 3.9 equiv. of fluoride had been added during the titration of an 8.0 µM solution of **5.6e** (4-H) in MeCN with a 1.58 mM solution of $TBAF(H_2O)_3$.

In the case of electron-deficient 1,3-diarylureas, however, a more intricate behaviour was observed. These titrations lack the presence of clean isosbestic points (Figure 5.17B) and

band deconvolution suggested the presence of a third species, which becomes dominant at higher fluoride concentrations (Figure 5.20).

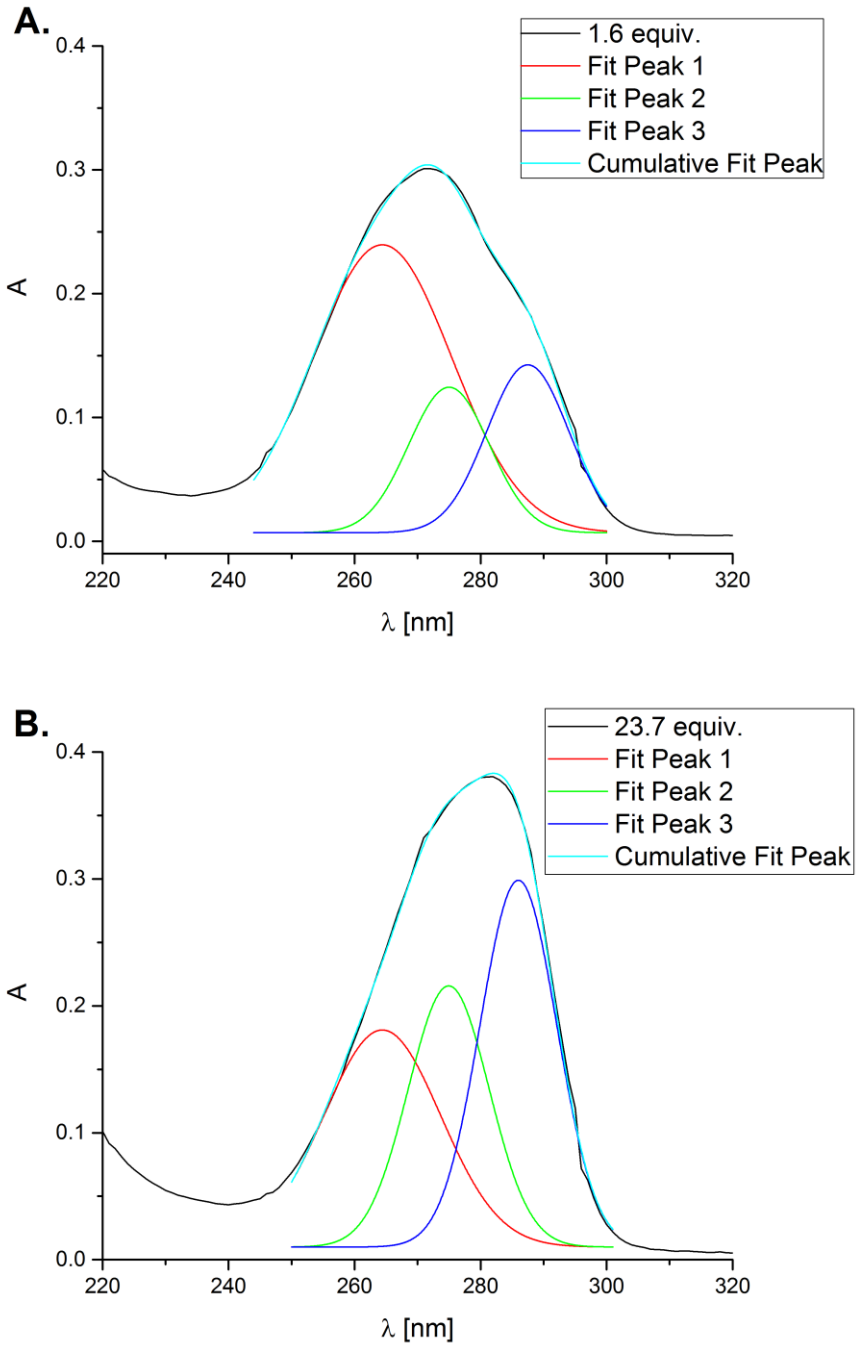

Figure 5.20. Gaussian deconvolution analysis of UV-vis absorption spectrum after 1.6 equiv. (A) and 23.7 equiv. (B) of fluoride had been added during the titration of an 8.0 µM solution of **5.6b** (4-CF_3) in MeCN with a 1.58 mM solution of TBAF$(H_2O)_3$.

By only using the early data points of these titrations (up to ca. 10 equiv.) to obtain approximated values, which were then refined using the whole dataset, while also taking into account a possible deprotonation of the ureas (*vide infra*), a reasonable fit of the 1:1 binding model was obtained. This allowed for the determination of the according association constants, $K_{a,1:1}$. At higher fluoride concentrations significant deviations from this model were observed. In a related study, the UV-vis titration of 4-NO_2-substituted urea **5.6c** had shown an intense band at 475 nm, which, similarly, became dominant at higher fluoride concentrations. The authors associated this band with the deprotonated urea, making this a likely possibility in our study, especially for the more N–H acidic ureas like **5.6b** (4-CF_3).[363]

The calculated association constants, although including highly electron-rich (4-OMe, **5.6g**) as well as electron-deficient (4-CF_3, **5.6b**) ureas, all lie within one order of magnitude (Table 5.6). Hammett analysis (*vs.* $2\sigma_p$) of $K_{a,1:1}$ shows a linear correlation with a *ρ*-value of 0.43 ± 0.03, indicating stronger binding with electron-deficient ureas (Figure 5.21).

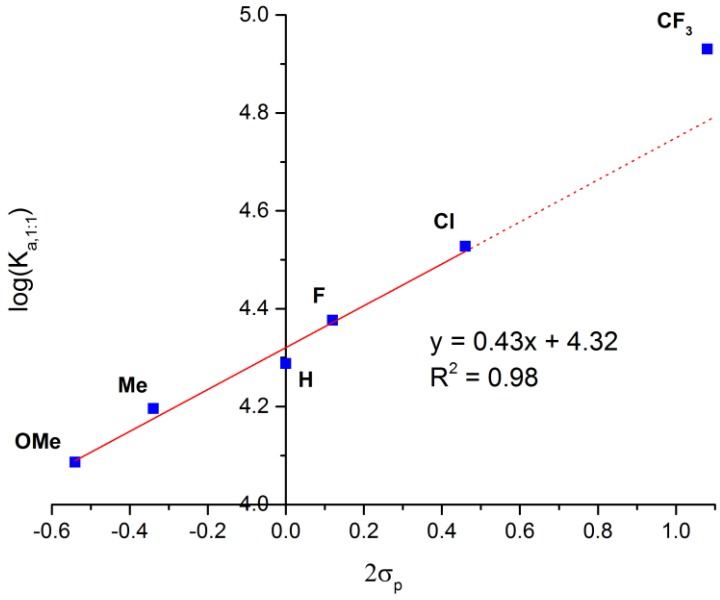

Figure 5.21. Hammett plot based on association constants, $K_{a,1:1}$, for the formation of 1:1 urea–fluoride complexes, obtained by UV-vis titration of 1,3-diarylureas with TBAF$(H_2O)_3$ in MeCN.

The free energies associated with the formation of the 1:1 complexes, $\Delta G_{1:1}$, range from 23.3–28.1 kJ/mol (Table 5.6).

Since UV-vis titrations are limited to low µM concentrations of the analyte, where the results we obtained all seemed to fit a 1:1 binding model, we followed them up by a series of ^{1}H NMR titrations using the same ureas in 1.0–2.0 mM starting concentrations. Figure 5.22 shows the aromatic region of a representative set of spectra that were recorded over the course of a titration of unsubstituted urea **5.6e**.

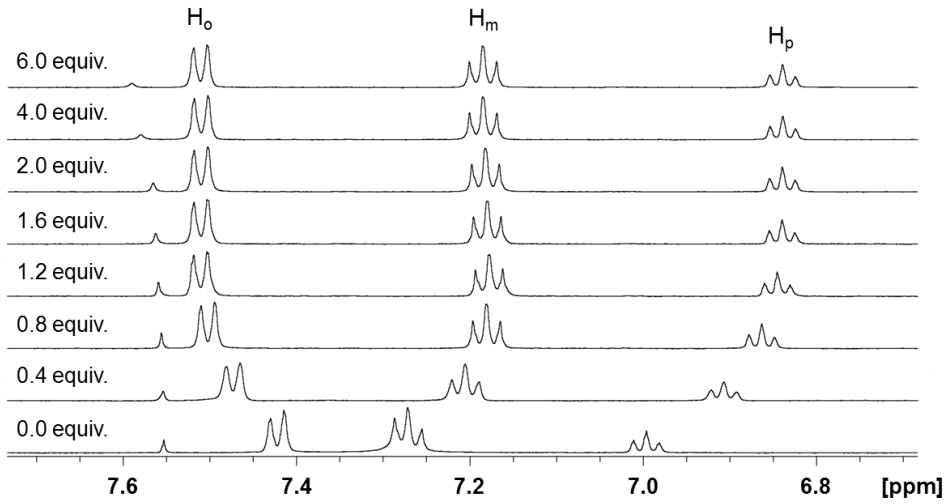

Figure 5.22. Aromatic region of ^{1}H NMR spectra, recorded over the course of a titration of 2.0 mM **5.6e** (4-H) in 8:2 MeCN/MeCN-d_3 with 78.9 mM TBAF$(H_2O)_3$.

Fluoride addition led to a pronounced, urea-dependent broadening and downfield shift of the N–H proton signal for the first 1.0–1.5 equiv., before forming a plateau. For more electron-deficient 1,3-diarylureas this signal was invisible at >1.0 equiv. of fluoride, again hinting at their more intricate behaviour. The addition of fluoride also influenced the three sets of aromatic protons, causing a deshielding of *ortho*-protons and a shielding of *meta*- and *para*-protons by about 0.1 ppm over the range of added TBAF. This observation can be rationalised by an increased electron density in the phenyl rings of fluoride–urea complexes due to through-bond propagation, exerting a shielding influence on all aromatic protons. In the case of the protons in *ortho*-position to the urea group this is accompanied by a dominant deshielding through-space effect.

In a first attempt to analyse the obtained data the same 1:1 binding model that had been successful in explaining the results of the UV-vis titrations was tested (Figure 5.23). In this case, however, it failed as it was not able to explain the rapid changes in the ^{1}H NMR spectra for the early parts of the titrations, especially up to 0.5 equiv. of added fluoride. This suggested the formation of higher coordinated fluoride species at low fluoride

concentrations, and upon including the formation of solid state-like 2:1 urea–fluoride complexes to our binding model a good agreement with the experimental data was achieved (Figure 5.23).

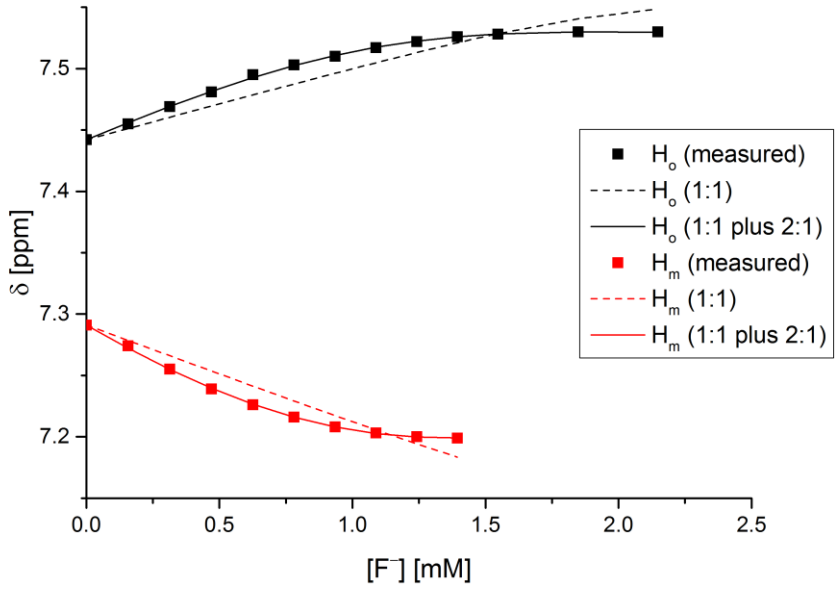

Figure 5.23. Fitting of 1:1 and (1:1 + 2:1) binding models to aromatic C–H chemical shifts taken from a series of ^{1}H NMR spectra, recorded over the course of a titration of 2.0 mM **5.6e** (4-H) in 8:2 MeCN/MeCN-d_3 with 78.9 mM TBAF$(H_2O)_3$.

This allowed for the determination of association constants, $K_{a,2:1}$, and free energies, $\Delta G_{2:1}$, for the formation of these 2:1 complexes from their 1:1 precursors for more electron-rich ureas (Table 5.7).

Table 5.7. Association constants, $K_{a,2:1}$, and free energies, $\Delta G_{2:1}$, for the formation of $[U_2F]^-$ complexes.

$$U + [UF]^- \underset{}{\overset{K_{a,2:1}}{\rightleftharpoons}} [U_2F]^-$$

	4-H (**5.6e**)	4-Me (**5.6f**)	4-OMe (**5.6g**)
$\log(K_{a,2:1})$ [M^{-1}]	2.4(1)	2.7(1)	2.40(6)
$\Delta G_{2:1}$ [kJ mol^{-1}]	13.6(8)	15.3(6)	13.7(3)

In the case of electron-deficient ureas, however, there was no plateau formation towards the end of the titrations, again displaying their more complex behaviour, which had already been observed in the UV-vis titrations (Figure 5.24).

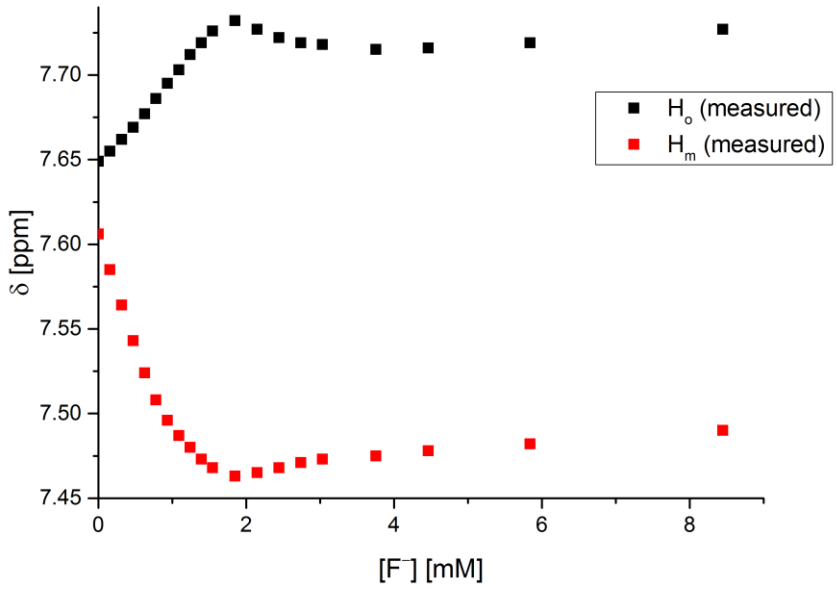

Figure 5.24. C–H chemical shifts taken from a series of ^{1}H NMR spectra, recorded over the course of a titration of 2.0 mM **5.6b** (4-CF_3) in 8:2 MeCN/MeCN-d_3 with 78.9 mM TBAF$(H_2O)_3$.

This prevented us from determining $K_{a,2:1}$ association constants for these ureas.

Since we were using commercially available TBAF$(H_2O)_3$ as fluoride source in all our titrations, we then moved on to study a possible influence of water on their outcome (Figure 5.25).

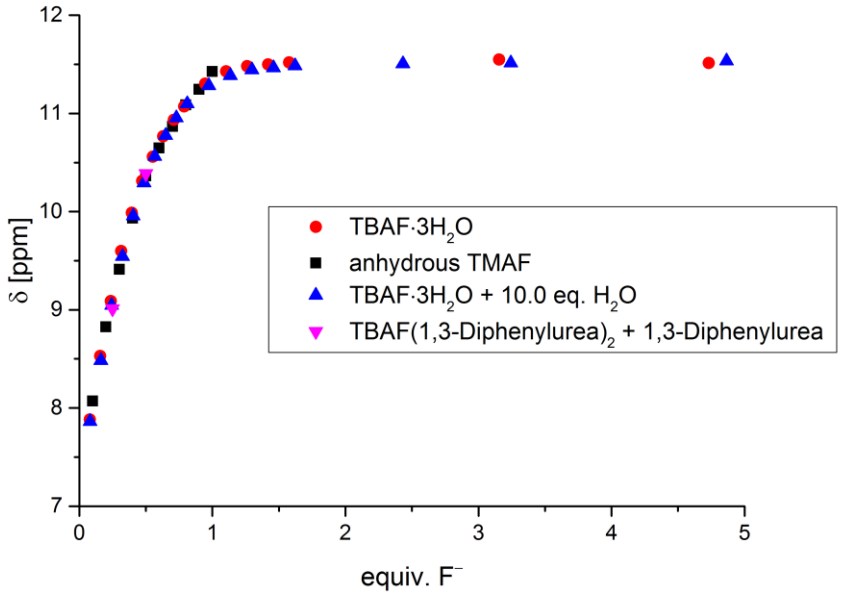

Figure 5.25. Proton chemical shift of N–H as a function of added fluoride ($TBAF(H_2O)_3$: 78.9 mM in 8:2 MeCN/MeCN-d_3; TMAF: 100 mM in anhydrous DMSO) to a 2.0 mM solution of **5.6e** (4-H) in 8:2 MeCN/MeCN-d_3 with and without additives – as in caption. Control samples (pink triangles) were prepared from isolated $TBAF(1,3\text{-diphenylurea})_2$ (**5.7e**) and free 1,3-diphenylurea (**5.6e**).

In addition to the standard conditions, we therefore also performed the ^{1}H NMR titration of parent 1,3-diphenylurea (**5.6e**) with anhydrous TMAF as well as in the presence of 10.0 equiv. of additional H_2O. Both titration profiles were found to match the original one. Furthermore, we prepared two independent samples from 1,3-diphenylurea and isolated 2:1 complex **5.7e** and the measured ^{1}H NMR shifts also agreed with the results of the titrations.

In order to obtain additional evidence for the formation of $[UF]^-$ as well as $[U_2F]^-$ complexes, ^{1}H diffusion-ordered NMR spectroscopy (DOSY) experiments were performed over the course of a titration of **5.6e** (4-H) with $TBAF(H_2O)_3$ in MeCN-d_3.[391,392] The obtained diffusion coefficients, *D*, for the average urea species during this titration were then compared to the species distribution between free urea, 1:1 and 2:1 urea–fluoride

complexes, which was calculated from the previously determined association constants, $K_{a,1:1}$ and $K_{a,2:1}$, using the HYPERQUAD software package (Figure 5.26).[393]

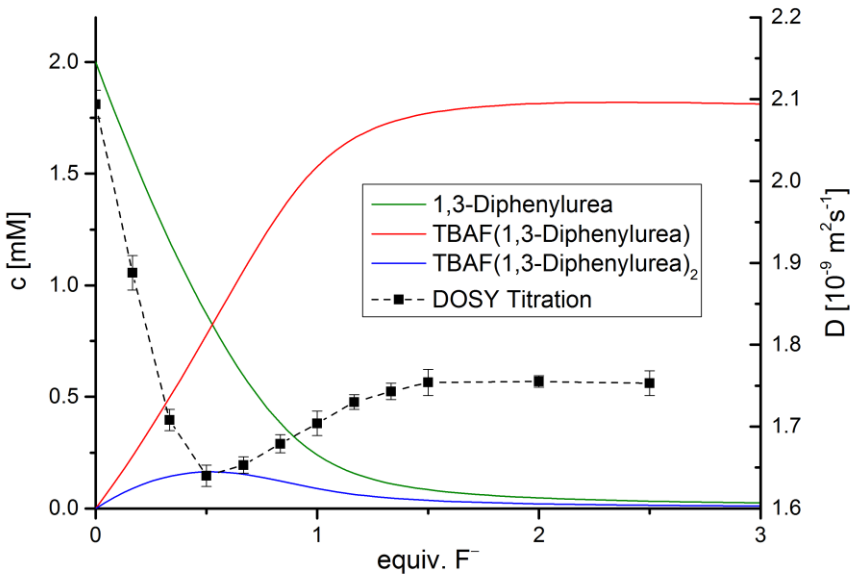

Figure 5.26. Simulated species distribution and diffusion coefficient, *D*, over course of titration of 2.0 mM **5.6e** (4-H) in MeCN-d_3 with 81.1 mM TBAF$(H_2O)_3$. Error bars show standard deviation determined from three independent experiments.

As can be seen in Figure 5.26, the diffusion coefficient of the average urea species steadily decreased, from (2.09 ± 0.02)·10^{-9} m^{2}s^{-1} for free urea before fluoride addition, to a minimum of (1.64 ± 0.01)·10^{-9} m^{2}s^{-1} after 0.5 equiv. of fluoride had been added. This corresponds to an increase of the hydrodynamic radius of the average urea molecule, and is matched in the species distribution by the increasing presence of both 1:1 as well as 2:1 urea–fluoride complex. The amount of the latter, however, reaches a maximum at 0.5 equiv. of fluoride, before it starts to be consumed in favour of the former. This was found to be reflected in *D* by its increase until 1.5 equiv. of fluoride had been added, before it reached a plateau at (1.75 ± 0.02)·10^{-9} m^{2}s^{-1}. This increase corresponds to a decreasing hydrodynamic radius during this part of the titration, which is what one would

expect for the formation of $[UF]^-$ from $[U_2F]^-$ species. At 1.5 equiv. of fluoride, all urea is bound as 1:1 complex causing *D* to plateau. A possible influence of changing viscosity over the course of the titration was ruled out by following the diffusion coefficient, *D*, of a trace amount of pentane, which had been added to the sample (see Experimental Section).

The successful characterisation of **5.7j**, derived from 1,3-bis(4-fluorophenyl)urea, by neutron diffraction analysis enabled the precise determination of the average (N)H···F^- distance in the solid state to be 1.732 ± 0068 Å. For comparison, 1D ^{19}F–^{1}H heteronuclear nOe (HOESY) experiments were performed on this fluoride–urea complex to estimate the (N)H···F^- distance in solution. In order to be able to do so, the average distance between the aromatic fluoride and its neighbouring protons was also determined from the neutron diffraction data and used as reference (2.599 ± 0.012 Å). It was assumed that the spin-pair (initial rate) approximation would hold and that isotropic molecular tumbling occurs in solution. HOESY build-up curves for both (N)H···F^- and aromatic *para*-F···*meta*-H pairs were recorded to identify the regions, in which the initial rate approximation was valid, and the slopes of the linear build-ups were determined (Figure 5.27).

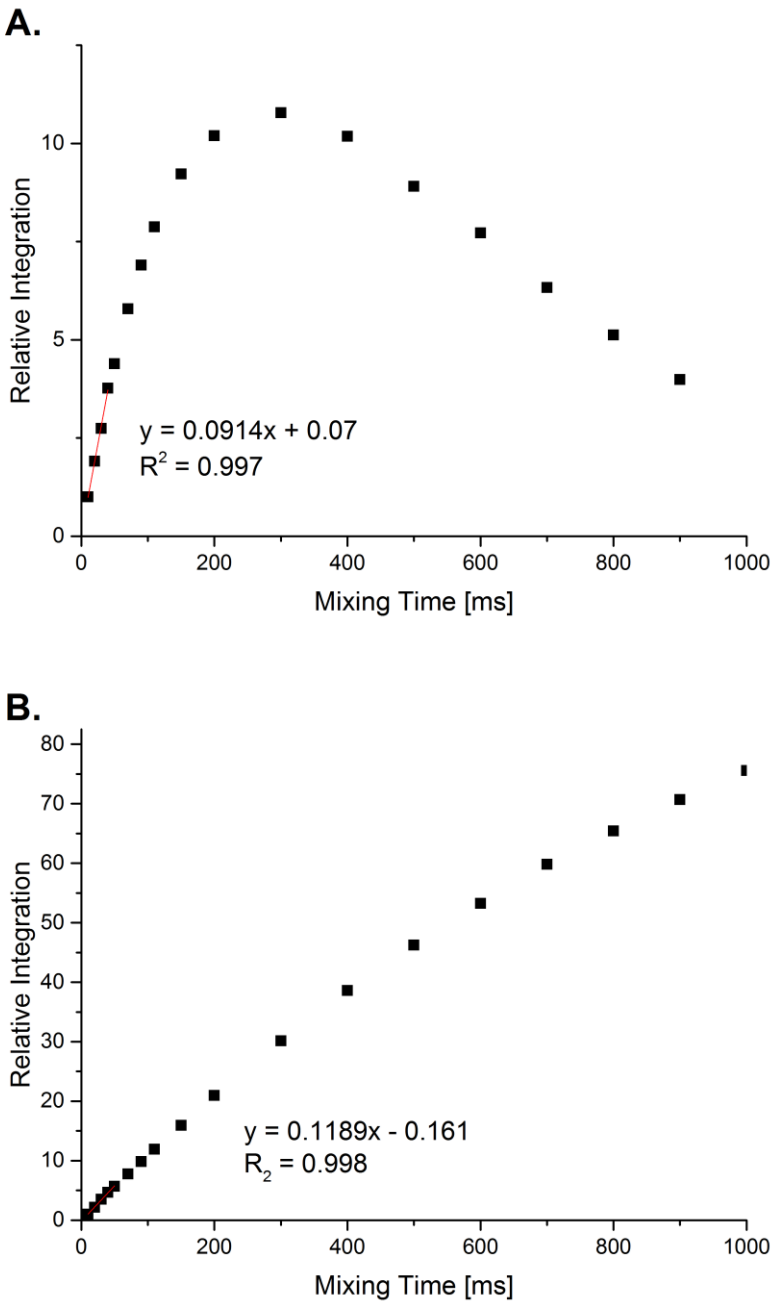

Figure 5.27. $^{19}F–^{1}H$ heteronuclear nOe build-up curves for (N)H···F^- (A) and *para*-F···*meta*-H (B) of a 0.26 M solution of **5.7j** in MeCN-d_3.

In relatively non-polar DCM-d_2 the average (N)H···F^- distance in a sample of isolated **5.7j** was found to be 1.86 ± 0.01 Å, which compares well with 1.732 ± 0.068 Å, derived from neutron diffraction data. In more polar solvents the same procedure found longer hydrogen bond lengths of 2.03 ± 0.01 Å for DMSO-d_6, 2.23 ± 0.01 Å for THF-d_8 and 2.42 ±

0.01 Å for MeCN-d_3, respectively. Since these values reflect the average (N)H···F^- distance, the apparent elongation could also be due to faster ligand exchange.

5.2.4. Organocatalytic Fluorination with 1,3-Diarylureas

Given the beneficial influence of 1,3-diarylureas on the reaction of alkyl bromide **4.10** with fluoride, we were keen to investigate the possibility of catalytic use of ureas in the fluorination of this compound. In order to avoid background reactions, metal fluorides, with no or very low solubility in organic solvents, were chosen as fluoride sources. The presence of a 1,3-diarylurea was thought to increase the solubility of fluoride salts by hydrogen-bonding to fluoride anion, and the hydrogen-bonded fluoride species in solution was assumed to show the improved S_N2 *vs.* E2 selectivity (*vide supra*). Since more electron-deficient 1,3-diarylureas had been shown to have higher association constants, $K_{a,1:1}$, for the formation of hydrogen-bonded 1:1 urea–fluoride complexes, *p*-CF_3-substituted **5.6b** was chosen for this investigative study (Table 5.8).

Table 5.8. Study into the 1,3-diarylurea-catalysed fluorination of alkyl bromide **4.10**.

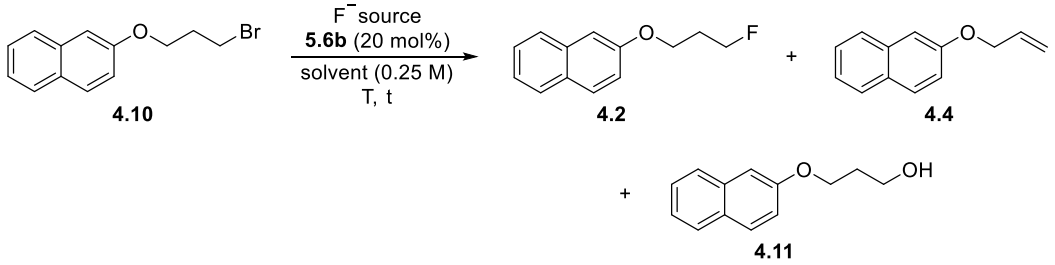

Entry	F^- Source	Solvent	T [°C]	t [h]	Conversion[a] [%]	**4.2**[a] [%]	**4.4**[a] [%]	**4.11**[a] [%]
1	CsF	MeCN	70	48	68	46	20	<5
2	CsF[b]	MeCN	70	48	24	7	16	<5
3	RbF	MeCN	70	48	13	12	trace	0
4	RbF[b]	MeCN	70	48	<5	trace	<5	0
5	AgF	MeCN	70	23	48	43	<5	<5
6	AgF[b]	MeCN	70	28	48	43	<5	<5
7	CsF	Toluene	70	48	0	0	0	0
8	CsF	DCM	70	48	0	0	0	0
9	CsF	THF	70	48	<5	trace	trace	0
10	CsF	DMSO	70	48	>95	27	72	<5
11	CsF	MeCN	40	48	9	6	<5	<5

Conditions: 1.0 equiv. **4.10** (0.10 mmol), 2.0 equiv. fluoride source (0.20 mmol), 20 mol% **5.6b** (0.020 mmol); solvent (1.0 mL), T and t as in table. [a]Determined by ^{1}H and ^{19}F NMR using 1-fluoro-3-nitrobenzene as internal reference. [b]Without **5.6b**.

Using CsF as fluoride source in MeCN at 70 °C resulted in the formation of 46% of the desired alkyl fluoride **4.2** alongside 20% of olefin by-product **4.4** (Table 5.8, Entry 1). 32% of the starting alkyl bromide **4.10** were also recovered. In the control reaction without **5.6b** a lower conversion of 24% was obtained. The amount of E2 product being formed (16%) is similar to the first reaction, whereas the amount of alkyl fluoride is significantly smaller (7%) (Table 5.8, Entry 2). This illustrates the dual role of **5.6b** in this reaction, improving the solubility and therefore reactivity of CsF as well as the selectivity of fluoride anion. A similar but more pronounced trend was observed with RbF. In this case,

in the presence of **5.6b**, 12% of S_N2 product **4.2** were found in the crude reaction mixture alongside a trace amount of **4.4** (Table 5.8, Entry 3). Without urea the amount of alkyl fluoride dropped to just a trace amount in the crude reaction mixture, whereas <5% of olefin **4.4** were found (Table 5.8, Entry 4). These observations can be rationalised using the lower solubility of RbF compared to CsF.[394] Contrary to this, AgF led to a conversion of 48% and a yield of **4.2** of 43% with and without **5.6b** being present during the reaction (Table 5.8, Entries 5 and 6). This indicates an involvement of Ag^+ cations in the abstraction of the bromide leaving group, as had been reported before for nucleophilic substitution of alkyl halides.[395] This makes AgF a non-suitable fluoride source for this study, and further experiments were performed with CsF. The effect of different solvents was studied by performing the reaction in toluene, DCM, THF and DMSO in addition to MeCN (Table 5.8, Entries 7–10). In apolar solvents, toluene and DCM, no product was formed and the starting material was quantitatively recovered after 48 h reaction time. Using THF led to trace amounts of both S_N2 and E2 products. **4.10** was fully consumed in the reaction in DMSO, but with 27% of alkyl fluoride **4.2** and 71% of olefin **4.4** being detected in the crude reaction mixture this can most likely be explained with a dominant background reaction, due to improved solubility of CsF in DMSO compared to MeCN. Overall, MeCN showed the best balance between fluoride salt solubility and a limited background reaction. However, upon reducing the reaction temperature from 70 °C to 40 °C a significant reduction of both the conversion of starting material and obtained product **4.2** to 9% and 6%, respectively, was observed (Table 5.8, Entry 11).

5.3. Conclusion

In conclusion, we prepared 16 novel fluoride–urea complexes and determined their solid state structures, whereby two different structures were found for two of these complexes. Furthermore, we prepared 4 additional hydrogen-bonded complexes from squaramide and amide ligands, whose solid state structures were also elucidated.

In the structures of the urea-based complexes a surprisingly rich diversity of structural arrangements was encountered. Besides the previously reported 2:1 urea–fluoride complexes, 4:2 supramolecular structures as well as hydrated structures of the general formula $[U_2(H_2O)_2F_2]^{2-}$ and hexacoordinate structures were found. We documented that the counter-cation can impose structural changes in the solid state, as exemplified by the synthesis of hexacoordinate fluoride species featuring fluoride anions hydrogen-bonding to three urea ligands. These were formed when TBA^+ ($(n\text{-}Bu)_4N^+$) counter-cation was exchanged for either TMA^+ (Me_4N^+) or TEA^+ (Et_4N^+). Furthermore, two complexes, derived from 4-bromo- and 4-iodo-substituted ureas, contained halogen-bonding contacts as additional, non-covalent interactions. The homoleptic complex $[A_2F]^-$ (A = amide), derived from *N*,2,2-triphenylacetamide, also includes hexacoordinate fluoride anions, which besides the strong hydrogen bonds to the amide NH groups also form weak hydrogen bonds to phenyl as well as benzyl C–H groups. Two of the squaramide-based structures also featured 2:1 squaramide–fluoride arrangements, with the third one forming a hydrated structure, where each fluoride forms two hydrogen bonds to the two N–H groups of one squaramide and two additional hydrogen bonds to two water molecules.

In this study we also for the first time employed fluoride–urea complexes as sources of fluoride for C–F bond formation in the S_N2 reaction with a model alkyl bromide.

Compared to fluoride–alcohol complexes, the reaction was found to proceed significantly slower with these urea-based complexes. On the other hand, the latter favoured the S_N2 over the E2 pathway at a previously undocumented level. This reactivity-selectivity trend is most strikingly manifested in the complex, derived from 1,3-bis(4-(trifluoromethyl)phenyl)urea. Increasing second order rate constants as well as a reduced selectivities at lower concentrations support the hypothesis that the active species is a partially dissociated complex, $[UF]^-$, which dissociates further at lower concentration to give free fluoride.

UV-vis and ^{1}H NMR titrations were performed in order to calculate association constants, $K_{a1:1}$ and $K_{a2:1}$. It was found that the strength of the fluoride–urea interaction is tunable by modifying substituents on the urea phenyl groups of *N*,*N*'-diarylureas. Hammett LFER analysis of $K_{a,1:1}$ shows a positive ρ-value, indicating that stronger binding is seen with electron-deficient aryl groups.

Over the course of a ^{1}H NMR titration of 1,3-diphenylurea with TBAF$(H_2O)_3$, DOSY experiments showed a decrease of the diffusion coefficient, *D*, going from 0–0.5 equiv., followed by an increase between 0.5–1.5 equiv. of fluoride, before forming a plateau. This is in line with the formation of a mixture of $[U_2F]^-$ and $[UF]^-$ complexes at the beginning of the titration, when an excess of urea is present, followed by consumption of the former in favour of the latter. An important finding is the ability of 1,3-diarylureas to outcompete water as hydrogen bond donor to fluoride.

Furthermore, we also presented the first single-crystal neutron diffraction studies of fluoride–urea complexes. These were used to obtain accurate information on the geometry of the hydrogen bonds in the solid state. The distance between the aromatic

fluoride and neighbouring aromatic hydrogens in TBAF(1,3-bis(4-fluorophenyl)urea)$_2$ was used as basis for the calculation of apparent hydrogen bond lengths in solution using 1D ^{19}F–^{1}H HOESY NMR experiments. These showed longer NH···F$^-$ distances, when the complex was dissolved in polar solvents like DMSO, THF or MeCN, compared to apolar DCM. This might be due to TBAF(1,3-bis(4-fluorophenyl)urea)$_2$ forming more dynamic systems in polar solvents, which can themselves also participate in hydrogen-bonding.

Finally, we have been able to show that the fluoride–urea system also holds great potential for the development of organocatalytic C–F bond forming reactions from cheap alkali fluoride salts. This is currently being developed further in the group.

Experimental Data and Analysis

General Experimental Information

Unless otherwise noted, all materials were used as received from commercial sources without further purification. Spectrophotometric grade MeCN was obtained from Alfa Aesar. MeCN-d_3 for NMR titrations was bought from Euriso-Top. NBS was recrystallised from boiling water, and aldehydes were distilled before use.

All NMR spectra were recorded on Bruker DPX200, AVIII 400 nanobay, AVII 500 and AVIIIHD 500 spectrometers. ^{1}H and ^{13}C spectra are reported as chemical shifts (δ) in parts per million (ppm) relative to the solvent peak using the Bruker internal referencing procedure (edlock). ^{19}F NMR spectra are referenced relative to $CFCl_3$ in $CDCl_3$. Coupling constants (*J*) are reported in units of hertz (Hz). The following abbreviations are used to describe multiplicities: s (singlet), d (doublet), t (triplet), q (quartet), qn (quintet), sx (sextet), sept (septet), m (multiplet), bs (broad singlet), ad (aromatic doublet). The relaxation time D1 for quantitative ^{19}F NMR experiments was set to 10 s. NMR data were processed using TOPSPIN 3.1 and 3.2 as well as MestReNova 10.0 and 11.0 software. High resolution mass spectra (HRMS, *m/z*) were recorded on a Bruker MicroTOF spectrometer using positive electrospray ionisation (ESI^+), or an Agilent 7200 QTOF spectrometer fitted with a direct insertion probe (Scientific Instruments Manufacturer GmbH) using electron (EI^+) or chemical ionisation (CI^+) with ammonia or on a Micromass GCT spectrometer using field ionisation (FI^+). Infrared spectra were recorded either using the neat compound or a solution using a Bruker Tensor 27 FT-IR spectrometer. Absorptions are reported in wavenumbers (cm^{-1}). Melting points of solids were measured on a Griffin apparatus and are uncorrected. UV-vis spectra were recorded using a PG instruments T60 UV-vis spectrophotometer.

IUPAC names were obtained using ChemDraw Professional 15.1 software or the ACD I-Lab 2.0 service. Unless otherwise specified, all reactions were performed in flame dried glass apparatus with magnetic stirring under an inert atmosphere of nitrogen or argon, and solvents were dried by passing through a column of activated alumina built according to the specifications of Pangborn and Grubbs.[396] Thin layer chromatography (TLC) was carried out on aluminium foil supported Merck Kiesegel 60 F254 plates and compounds were visualised UV fluorescence (254 nm) or $KMnO_4$ stain. Silica gel column chromatography was performed over Merck silica gel C60 (40–60 µm).

X-ray diffraction data were collected variously on a Nonius Kappa CCD and Agilent SuperNova diffractometer at 150 K.[397] Data were reduced using the instrument manufacturer software, DENZO-SMN[398] and CrysAlisPro.[399] All structures could be solved *ab initio* using SIR92[400] or SuperFlip,[401] however, the final refinements used a common model to provide the initial phases and the structure was refined using CRYSTALS.[402–404] In general, all non-hydrogen atoms were refined using anisotropic displacement ellipsoids, and hydrogen atoms were visible in the difference map. Once the heavy atoms structure was complete, hydrogen atoms were positioned geometrically then refined separately using soft restraints prior to inclusion in the final refinement using a riding model.[405] Where disorder was identified, the structure was modelled with multiple sites using same distance and thermal similarity restraints to maintain a sensible model. On refinement of **5.7b** it became apparent that the CF_3 groups were disordered. A multicomponent model proved to be inadequate, so the major component was modelled with conventional anisotropic displacement parameters, and the residual electron density was fitted as described by Schröder *et al*.[406] Structure **4.19n** and **5.7k** were found to

exhibit diffuse disordered solvent which was modelled using PLATON/SQUEEZE within CRYSTALS.[407,408] On refinement of **4.19d**, there was a poor agreement between the observed and calculated structure factor amplitudes. Examination of the data and model using ROTAX[409] suggested the crystal was a pseudo-merohedral twin which was included in the refinement.

Neutron diffraction data were collected at several orientations at 150 K in a top-loading closed-cycle refrigerator on the SXD time-of-flight Laue diffractometer at the ISIS spallation neutron source.[410] Data were reduced using SXD2001[411] and the atomic positions obtained from the X-ray solutions were refined against the neutron data using SHELXL.[412]

C···F distances, N(H)···F^- distances, F^-···F^- distances and dihedral angles, DHA angles as well as O···F^-···O angles were calculated using PLATON,[407,413] whereby for complexes **5.7l**–**5.7p** the geometrically placed centroid between fluoride anions was used to determine ϑ in Table 4.2 with standard uncertainties being taken from the O···F^-···O angles. F^-···O as well as NH···F^- and N–H distances were calculated with CRYSTALS using the full variance-covariance matrix, though they are displayed herein as images generated in Mercury.[414] All discussed structures except of for **4.19h**, **4.21** and **4.23** have been deposited with the Cambridge Crystallographic Data Centre (reference codes: CCDC 984222 (Chapter 2), CCDC 1401765–1401778 (Chapter 3), CCDC 1493410-1493434 (Chapter 4)); these data can be obtained free of charge via www.ccdc.cam.ac.uk/data_request/cif.

Chapter 2

S.2.1. Synthesis and Characterisation of Compounds

S.2.1.1. Substrate Preparation

General Procedure (GP) 1: Preparation of Substituted Styrene Derivatives[415]

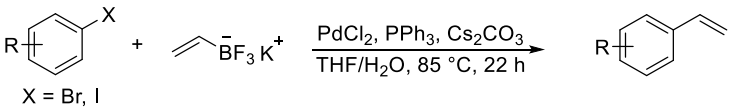

Scheme S.2.1. Synthesis of substituted styrenes.

In a sealed tube, a solution of potassium vinyltrifluoroborate (134 mg, 1.00 mmol), $PdCl_2$ (3.5 mg, 0.020 mmol), PPh_3 (15.7 mg, 0.060 mmol), Cs_2CO_3 (978 mg, 3.00 mmol), and the according substituted halobenzene (1.00 mmol) in THF/H_2O (9:1, 2.0 mL) was heated to 85 °C under an inert atmosphere. The reaction mixture was stirred at 85 °C for 22 h, then cooled to rt and diluted with H_2O followed by extraction with DCM. The solvent was removed *in vacuo*, and the crude product was purified by column chromatography.

4-Ethenylbenzonitrile (2.1g)

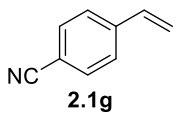

2.1g

The title compound was prepared according to GP1 using 4-iodobenzonitrile (229 mg, 1.00 mmol). After column chromatography (SiO_2, 5% EtOAc in hexane) the desired product (112 mg, 87%) was obtained as a colourless oil. **^{1}H NMR** (400 MHz, $CDCl_3$) δ 7.63 (ad, *J* = 8.4 Hz, 2H), 7.49 (ad, *J* = 8.4 Hz, 2H), 6.74 (dd, *J* = 17.6, 11.1 Hz, 1H), 5.88 (d, *J* = 17.6 Hz, 1H), 5.46 (d, *J* = 11.1 Hz, 1H); **^{13}C**

NMR (100 MHz, $CDCl_3$) δ 141.8, 135.3, 132.3, 126.7, 118.9, 117.7, 111.0. The spectroscopic data were identical in all respects to those previously reported.[416]

1-Ethenyl-4-nitrobenzene (2.1h)

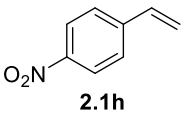

2.1h

The title compound was prepared according to GP1 using 1-iodo-4-nitrobenzene (249 mg, 1.00 mmol). After column chromatography (SiO_2, 0–5% EtOAc in hexane) the desired product (113 mg, 76%) was obtained as a yellow oil. **^{1}H NMR** (400 MHz, $CDCl_3$) δ 8.18 (ad, *J* = 8.9 Hz, 2H), 7.54 (ad, *J* = 8.9 Hz, 2H), 6.78 (dd, *J* = 17.6, 10.9 Hz, 1H), 5.93 (d, *J* = 17.6 Hz, 1H), 5.50 (d, *J* = 10.9 Hz, 1H); **^{13}C NMR** (100 MHz, $CDCl_3$) δ 147.2, 143.8, 135.0, 126.8, 124.0, 118.6. The spectroscopic data were identical in all respects to those previously reported.[417]

2-(4-Ethenylbenzyl)-1H-isoindole-1,3(2H)-dione (2.1k)[418]

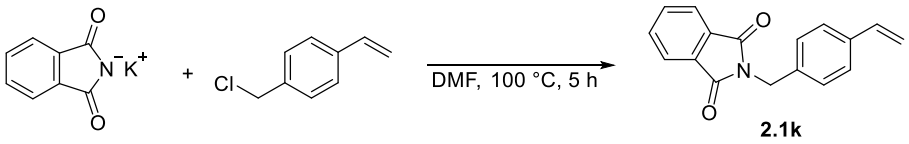

2.1k

Scheme S.2.2. Synthesis of substrate **2.1k**.

A suspension of potassium phthalimide (926 mg, 5.00 mmol) in DMF (5.0 mL) was prepared. 4-vinylbenzyl chloride (732 µL, 5.20 mmol) was added and the resulting mixture was heated to 100 °C for 5 h. After cooling to rt, EtOAc and H_2O were added, the layers were separated and the aqueous layer was extracted with EtOAc. The combined organic layers were washed with water and brine, dried over $MgSO_4$ and the solvent was removed under reduced pressure. The obtained residue was dissolved in hot EtOAc (1.6 mL) before adding pentane (10 mL) to the mixture, which caused the formation of a

white precipitate. The white solid was filtered off, washed with pentane and found to be pure 2-(4-ethenylbenzyl)-1H-isoindole-1,3(2H)-dione, **2.1k** (960 mg, 73%).

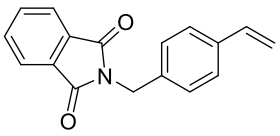

2.1k

^{1}H NMR (400 MHz, $CDCl_3$) δ 7.86 (dd, *J* = 5.5, 3.0 Hz, 2H), 7.72 (dd, *J* = 5.5, 3.0 Hz, 2H), 7.43–7.37 (m, 4H), 6.69 (dd, *J* = 17.9, 11.0 Hz, 1H), 5.74 (d, *J* = 17.9 Hz, 1H), 5.25 (d, *J* = 11.0 Hz, 1H), 4.85 (s, 2H); **^{13}C NMR** (100 MHz, $CDCl_3$) δ 168.1, 137.2, 136.3, 135.9, 134.0, 132.1, 128.9, 126.5, 123.4, 114.2, 41.4. The spectroscopic data were identical in all respects to those previously reported.[418]

_N_-Benzyl-4-vinylbenzamide (2.1l)

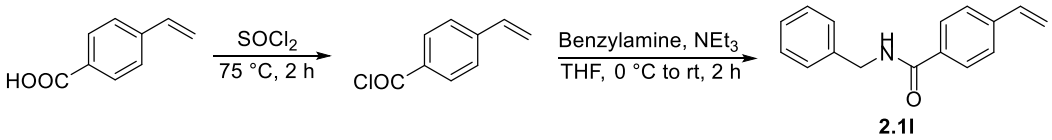

2.1l

Scheme S.2.3. Synthesis of substrate **2.1l**.

A solution of 4-vinylbenzoic acid (250 mg, 1.69 mmol) in $SOCl_2$ (15 mL) was refluxed for 2 h before excess $SOCl_2$ was removed under reduced pressure. The obtained crude acid chloride was dissolved in THF (10.0 mL) and cooled to 0 °C. Triethylamine (1.0 mL) and benzylamine (185 µL, 1.69 mmol) were added successively and the resulting mixture was stirred at 0 °C for 15 min before it was allowed to warm to rt. After 2 h at rt the reaction was quenched with H_2O, the layers were separated and the aqueous layer was extracted three times with DCM. The combined organic layers were dried over $MgSO_4$ before the solvent was removed under reduced pressure. Column chromatography (SiO_2, 40% EtOAc in hexane) yielded pure *N*-benzyl-4-vinylbenzamide, **2.1l** (231 mg, 58%), as a white solid.

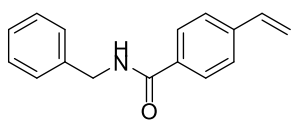
2.1l

^{1}H NMR (400 MHz, $CDCl_3$) δ 7.65 (ad, *J* = 8.2 Hz, 2H), 7.3 (ad, *J* = 8.2 Hz, 2H), 7.23–7.15 (m, 5H), 6.78 (bs, 1H), 6.62 (dd, *J* = 17.6, 11.0 Hz, 1H), 5.71 (dd, *J* = 17.6, 0.7 Hz, 1H), 5.24 (dd, *J* = 11.0, 0.7 Hz, 1H), 4.48 (d, *J* = 5.9 Hz, 2H); **^{13}C NMR** (100 MHz, $CDCl_3$) δ 167.2, 140.7, 138.4, 136.0, 133.4, 128.8, 127.9, 127.5, 127.4, 126.3, 116.0, 44.1. The spectroscopic data were identical in all respects to those previously reported.[419]

1-Ethenyl-2-methoxybenzene (2.1m)

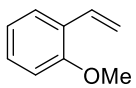
2.1m

The title compound was prepared according to GP1 using 2-iodoanisole (130 µL, 1.00 mmol). After column chromatography (SiO_2, 0–5% EtOAc in hexane) the desired product (95 mg, 71%) was obtained as a colourless oil. **^{1}H NMR** (400 Hz, $CDCl_3$) δ 7.54 (dd, *J* = 7.6, 1.7 Hz, 1H), 7.32–7.27 (m, 1H), 7.13 (dd, *J* = 17.7, 11.1 Hz, 1H), 7.02–6.98 (m, 1H), 6.93–6.91 (m, 1H), 5.80 (dd, *J* = 17.7, 1.6 Hz, 1H), 5.33 (dd, *J* = 11.1, 1.6 Hz, 1H), 3.89 (s, 3H); **^{13}C NMR** (100 MHz, $CDCl_3$) δ 156.8, 131.7, 128.9, 126.8, 126.6, 120.7, 114.5, 110.9, 55.5. The spectroscopic data were identical in all respects to those previously reported.[420]

Ethyl 4-ethenylbenzoate (2.1n)[421]

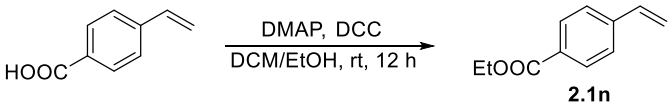

2.1n

Scheme S.2.4. Synthesis of substrate **2.1n**.

EtOH (780 µL, 13.5 mmol) was added to a solution of 4-vinylbenzoic acid (200 mg, 1.40 mmol), DCC (334 mg, 1.60 mmol) and DMAP (17 mg, 0.14 mmol) in DCM (10 mL) at rt. After stirring the reaction mixture for 12 h the solvent was removed under reduced pressure. Purification by column chromatography (SiO_2, 10% EtOAc in hexane) yielded pure ethyl-4-ethenylbenzoate, **2.1n** (198 mg, 83%), as a colourless oil.

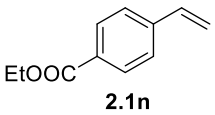

2.1n

^{1}H NMR (400 MHz, $CDCl_3$) δ 8.01 (ad, *J* = 8.2 Hz, 2H), 7.47 (ad, *J* = 8.2 Hz, 2H), 6.77 (dd, *J* = 17.6, 10.9 Hz, 1H), 5.87 (dd, *J* = 17.6, 0.7 Hz, 1H), 5.39 (dd, *J* = 10.9, 0.7 Hz, 1H), 4.38 (q, *J* = 7.2 Hz, 2H), 1.41 (t, *J* = 7.2 Hz, 3H); **^{13}C NMR** (100 MHz, $CDCl_3$) δ 166.4, 141.8, 136.1, 129.9, 129.7, 126.1, 116.4, 60.9, 14.4. The spectroscopic data were identical in all respects to those previously reported.[422]

Methyl 2-ethenylbenzoate (2.1o)

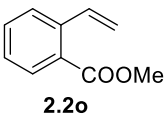

2.2o

The title compound was prepared according to GP1 using methyl 2-iodobenzoate (147 µL, 1.00 mmol). After column chromatography (SiO_2, 0–10% EtOAc in hexane) the desired product (141 mg, 87%) was obtained as a colourless oil. **^{1}H NMR** (400 MHz, $CDCl_3$) δ 7.90–7.88 (m, 1H), 7.60–7.58 (m, 1H), 7.53–7.46 (m, 2H), 7.32 (td, *J* = 7.6, 1.2 Hz, 1H), 5.66 (dd, *J* = 17.5, 1.3 Hz, 1H), 5.36 (dd, *J* = 10.9, 1.3 Hz, 1H) 3.90 (s, 3H); **^{13}C NMR** (100 MHz, $CDCl_3$) δ 167.7, 139.4, 135.8, 132.0, 130.2, 128.4, 127.3, 127.1, 116.3, 51.9. The spectroscopic data were identical in all respects to those previously reported.[423]

1-(Benzyloxy)-4-ethenylbenzene (2.1q)

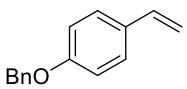

2.1q

The title compound was prepared according to GP1 using 4-benzyloxybromobenzene (263 mg, 1.00 mmol). After column chromatography (SiO_2, 0–5% EtOAc in hexane) the desired product (78 mg, 37%) was obtained as a white solid. **^{1}H NMR** (400 MHz, $CDCl_3$) δ 7.49–7.32 (m, 7H), 6.99–6.94 (m, 2H), 6.69 (dd, *J* = 17.6, 10.9 Hz, 1H), 5.65 (dd, *J* = 17.6, 0.9 Hz, 1H), 5.16 (dd, *J* = 10.9, 0.9 Hz, 1H), 5.08 (s, 2H); **^{13}C NMR** (100 MHz, $CDCl_3$) δ 158.7, 137.1, 136.4, 130.8, 128.8, 128.2, 127.6, 127.6, 115.0, 111.9, 70.2. The spectroscopic data were identical in all respects to those previously reported.[424]

(2*E*)-2-Benzylidene-3-methylbutan-1-ol ((*E*)-2.1y)[425]

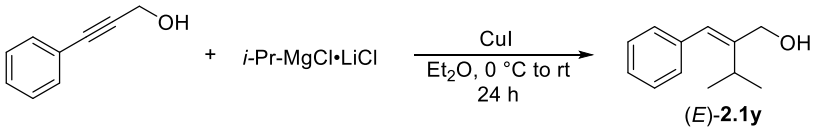

(*E*)-**2.1y**

Scheme S.2.5. Synthesis of substrate (*E*)-**2.1y**.

i-Pr–MgCl·LiCl (1.3 M in THF, 30 mL, 38.9 mmol) was added dropwise to a stirred solution of 3-phenylprop-2-yn-1-ol (1.47 g, 11.1 mmol) and CuI (211 mg, 1.11 mmol) in dry Et_2O (50 mL) under an inert atmosphere at 0 °C. The resulting mixture was allowed to warm to rt and stirred for 24 h, then cooled to 0 °C, quenched with sat. aq. NH_4Cl and extracted with Et_2O. The combined organic layers were dried over $MgSO_4$ and the solvent removed under reduced pressure. Purification by column chromatography (SiO_2, 10% EtOAc in hexane) afforded the title compound (*E*)-**2.1y** (1.86 g, 95%) as a colourless oil.

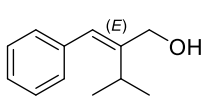

(*E*)-**2.1y**

^{1}H NMR (400 MHz, $CDCl_3$) δ 7.39–7.31 (m, 2H), 7.27–7.20 (m, 3H), 6.56 (s, 1H), 4.31 (d, *J* = 1.5 Hz, 2H), 3.12 (sept, *J* = 7.2 Hz, 1H), 1.37 (bs, 1H), 1.12 (d, *J* = 7.2 Hz, 6H); **^{13}C NMR** (100 MHz, $CDCl_3$) δ 147.0, 137.7, 128.7, 128.1, 126.4, 124.4, 63.1, 28.1, 21.5. The spectroscopic data were identical in all respect to those previously reported.[425]

Synthesis of Substrate (*Z*)-2.1y

Ethyl (diphenylphosphono)acetate[426]

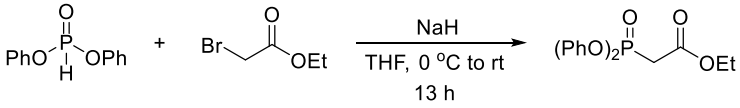

Scheme S.2.6. Synthesis of ethyl (diphenylphosphono)acetate.

Diphenyl phosphite (3.00 g, 12.8 mmol) was added dropwise to a vigorously stirred suspension of NaH (512 mg, 12.8 mmol) in THF (20 mL) under an inert atmosphere at 0 °C. The reaction mixture was stirred for 1 h at 0 °C, which led to the formation of a clear, orange solution. Now, ethyl bromoacetate (1.42 mL, 12.8 mmol) was added dropwise before the cooling bath was removed. After stirring the reaction for 12 h at rt it was quenched with sat. aq. NH_4Cl. The layers were separated and the aqueous one was extracted with Et_2O. The combined organic layers were washed with H_2O and brine, before being dried over $MgSO_4$. The crude product was purified by column chromatography (SiO_2, 20–50% Et_2O in pentane) to yield the title compound (2.44 g, 60%) as a colourless oil.

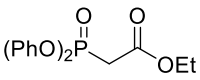

^{1}H NMR (400 MHz, $CDCl_3$) δ 7.26–7.20 (m, 4H), 7.17–7.05 (m, 6H), 4.13 (q, *J* = 7.1 Hz, 2H), 3.17 (d, *J* = 21.6 Hz, 2H), 1.17 (t, *J* = 7.1 Hz, 3H); **^{13}C NMR** (100 MHz, $CDCl_3$) δ 164.6 (d, $J_{C–P}$ = 6.4 Hz), 149.9 (d, $J_{C–P}$ = 8.5 Hz), 129.7 (d, $J_{C–P}$ = 0.7 Hz), 125.4 (d, $J_{C–P}$ = 1.1 Hz), 120.4 (d, $J_{C–P}$ = 6.3 Hz), 61.9 (d, $J_{C–P}$ = 22.8 Hz), 34.0 (d, $J_{C–P}$ = 137.1 Hz), 13.9 (d, $J_{C–P}$ = 6.7 Hz); **^{31}P NMR** (162 MHz, $CDCl_3$) δ 12.8 (t, *J* = 21.6 Hz). The spectroscopic data were identical in all respect to those previously reported.[426]

Ethyl 2-(diphenylphosphono)isopropylacetate[427]

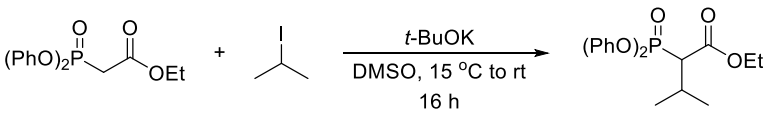

Scheme S.2.7. Synthesis of ethyl 2-(diphenylphosphono)-isopropylacetate.

t-BuOK (733 mg, 6.53 mmol) was added to a solution of ethyl (diphenylphosphono)acetate (1.90 g, 5.93 mmol) in DMSO (6.0 mL) at 15 °C. The resulting suspension was allowed to warm to rt where it was stirred for 20 min before isopropyl iodide (622 µL, 6.23 mmol) was added. After stirring the reaction over night at rt it was quenched with sat. aq. NH_4Cl. The layers were separated and the aqueous one was extracted with EtOAc. The combined organic layers were washed with H_2O and brine before being dried over $MgSO_4$. Column chromatography (SiO_2, 20–40% Et_2O in pentane) gave the title compound (1.27 g, 59%) as a colourless oil.

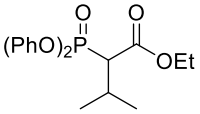

^{1}H NMR (400 MHz, $CDCl_3$) δ 7.26–7.18 (m, 4H), 7.15–7.04 (m, 6H), 4.13 (dq, *J* = 7.0, 1.2 Hz, 2H), 3.01 (dd, *J* = 20.5, 8.9 Hz, 1H), 2.64–2.47 (m, 1H), 1.20 (d, *J* = 6.6 Hz, 3H), 1.17 (t, *J* = 7.1 Hz, 3H), 1.05 (dd, *J* = 7.0, 1.2 Hz, 3H); **^{13}C NMR** (100 MHz, $CDCl_3$) δ 168.1 (d, $J_{C–P}$ = 4.3 Hz), 150.3 (d, $J_{C–P}$ = 7.1 Hz), 150.2 (d, $J_{C–P}$ = 7.1 Hz),

129.7, 129.4, 125.1, 120.6 (d, J_{C-P} = 4.4 Hz), 120.5 (d, J_{C-P} = 4.4 Hz), 61.5, 54.3, 52.9, 28.5 (d, J_{C-P} = 4.6 Hz), 23.3, 21.8 (d, J_{C-P} = 5.7 Hz), 21.5 (d, J_{C-P} = 14.8 Hz), 15.2, 14.0; **^{31}P NMR** (162 MHz, $CDCl_3$) δ 15.5 (dd, *J* = 20.5, 10.2 Hz). The spectroscopic data were identical in all respect to those previously reported.[427]

(*Z*)-2-Benzylidene-3-methylbutanoate[427]

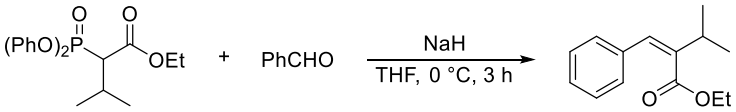

Scheme S.2.8. Synthesis of ethyl (*Z*)-2-benzylidene-3-methylbutanoate.

Ethyl 2-(diphenylphosphono)isopropylacetate (1.00 g, 2.76 mmol) was added dropwise to a suspension of NaH (144 mg, 3.59 mmol) in THF (50 mL) at 0 °C. After stirring the reaction mixture for 1 h at 0 °C benzaldehyde (287 µL, 2.84 mmol) was added dropwise and the mixture was stirred for 2 h at 0 °C. It was then quenched with sat. aq. NH_4Cl. The organic layer was separated and the aqueous one was extracted with EtOAc. The combined organic layers were washed with H_2O and brine before being dried over $MgSO_4$. Column chromatography (SiO_2, 0–5% Et_2O in pentane) gave the title compound (509 mg, 88%) as a colourless oil.

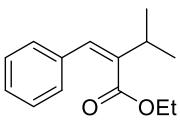

^{1}H NMR (400 MHz, $CDCl_3$) δ 7.34–7.22 (m, 5H), 6.57 (d, *J* = 1.3 Hz, 1H), 4.16 (q, *J* = 7.1 Hz, 2H), 2.81 (septd, *J* = 6.8, 1.3 Hz, 1H), 1.22 (d, *J* = 6.8 Hz, 6H), 1.13 (t, *J* = 7.1 Hz, 3H); **^{13}C NMR** (100 MHz, $CDCl_3$) δ 170.0, 141.5, 136.4, 128.5, 128.0, 127.8, 127.3, 60.4, 33.1, 21.3, 13.7. The spectroscopic data were identical in all respect to those previously reported.[427]

(2*Z*)-2-Benzylidene-3-methylbutan-1-ol ((*Z*)-2.1y)

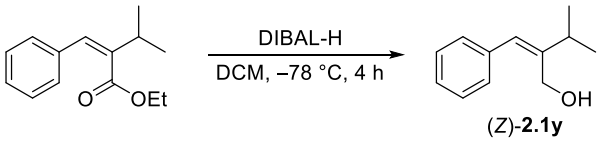

Scheme S.2.9. Synthesis of substrate (*Z*)-**2.1y**.

DIBAL-H (1.0 M in hexane, 2.31 mL, 2.31 mmol) was added dropwise to a solution of ethyl (*Z*)-2-benzylidene-3-methylbutanoate (200 mg, 1.05 mmol) in DCM (5.0 mL) at –78 °C. After stirring the reaction for 4 h at –78 °C the cooling bath was removed and the reaction was quenched with a sat. aq. solution of Rochelle salt. It was now vigorously stirred over night before H_2O and DCM were added. The layers were separated and the aqueous one was extracted with DCM. The combined organic layers were dried over $MgSO_4$. Column chromatography (SiO_2, 10–30% Et_2O in pentane) gave the title compound, (*Z*)-**2.1y** (151 mg, 81%), as a colourless oil.

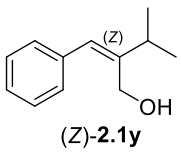

(*Z*)-**2.1y**

^{1}H NMR (400 MHz, $CDCl_3$) δ 7.36–7.17 (m, 5H), 6.46 (d, *J* = 0.8 Hz, 1H), 4.25 (s, 2H), 3.12 (septd, *J* = 6.9, 0.8 Hz, 1H), 1.52 (s, 1H), 1.16 (d, *J* = 6.9 Hz, 6H); **^{13}C NMR** (100 MHz, $CDCl_3$) δ 147.0, 137.4, 129.0, 128.2, 126.7, 126.6, 60.0, 32.1, 22.0. **IR** (film, $CDCl_3$) ν 3325, 2959, 2360, 1464, 1075, 1010, 921, 775, 7.25, 699 cm^{-1}; **HRMS** (ESI-TOF): *m/z* Calcd for $C_{12}H_{16}NaO$ $[M+Na]^+$ 199.1093, found 199.1097.

[(1*E*)-Hexa-1,5-dien-1-yl]benzene (2.11)[428]

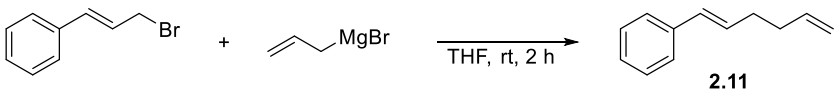

Scheme S.2.10. Synthesis of substrate **2.11**.

Allylmagnesium bromide (1.0 M in Et_2O, 10.1 mL, 10.1 mmol) was added to a solution of cinnamyl bromide (1.00 mL, 6.76 mmol) in THF (20 mL) and the resulting mixture was stirred for 2 h at rt. The reaction was then quenched with water and the mixture was extracted with Et_2O. The combined organic layers were washed with water and brine and dried over $MgSO_4$ before removing volatiles *in vacuo*. Column chromatography (SiO_2, pentane) gave the desired product **2.11** (726 mg, 68%), as a colourless oil.

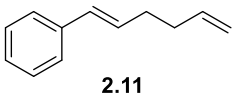

^{1}H NMR (400 MHz, $CDCl_3$) δ 7.37–7.35 (m, 2H), 7.31 (dd, *J* = 8.5, 6.9 Hz, 2H), 7.23–7.19 (m, 1H), 6.42 (d, *J* = 15.8 Hz, 1H), 6.25 (dt, *J* = 15.8, 6.6 Hz, 1H), 5.89 (ddt, *J* = 17.0, 10.3, 6.5 Hz, 1H), 5.11–5.05 (m, 1H), 5.01 (ddt, *J* = 10.3, 2.1, 1.1 Hz, 1H), 2.37–2.31 (m, 2H), 2.28–2.22 (m, 2H); **^{13}C NMR** (100 MHz, $CDCl_3$) δ 138.1, 137.7, 130.16, 130.11, 128.5, 126.9, 125.9, 114.9, 33.5, 32.4. The spectroscopic data were identical in all respects to those previously reported.[428]

[(2*Z*)-Octa-3,7-dien-1-yl]benzene (2.14)[429]

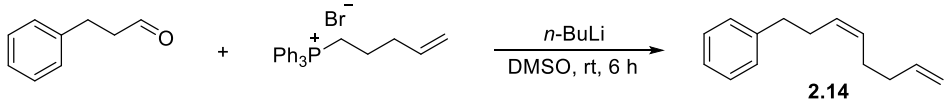

Scheme S.2.11. Synthesis of substrate **2.14**.

(Pent-4-en-1-yl)(triphenyl)phosphonium bromide (1.23 g, 3.00 mmol) dissolved in DMSO (3.75 mL) was added dropwise to a solution of *n*-BuLi (2.5 M in hexane, 1.32 mL,

3.75 mmol) in DMSO (2.25 mL), which had before been stirred at rt for 30 min. The resulting solution was stirred for 1 h at rt, before a solution of 3-phenylpropionaldehyde (495 µL, 3.75 mmol) in DMSO (500 µL) was added. The mixture was stirred for 5 h at rt, before it was quenched with ice water. The mixture was extracted with 10% Et_2O in hexane and the combined organic layers were dried over $MgSO_4$. Volatiles were removed *in vacuo* and column chromatography (SiO_2, hexane) was used to obtain the desired product **2.14** (382 mg, 68%) as a colourless oil.

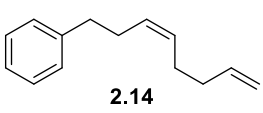

2.14

^{1}H NMR (400 MHz, $CDCl_3$) δ 7.36–7.29 (m, 2H), 7.26–7.20 (m, 3H), 5.88–5.76 (m, 1H), 5.54–5.38 (m, 2H), 5.10–4.96 (m, 2H), 2.74–2.68 (m, 2H), 2.45–2.37 (m, 2H), 2.17–2.03 (m, 4H); **^{13}C NMR** (100 MHz, $CDCl_3$) δ 142.0, 138.4, 129.7, 129.1, 128.4, 128.2, 125.7, 114.6, 35.9, 33.7, 29.2, 26.6. The spectroscopic data were identical in all respects to those previously reported.[430]

[(1*E*)-Penta-1,4-diene-1-yl]benzene (2.18)[431]

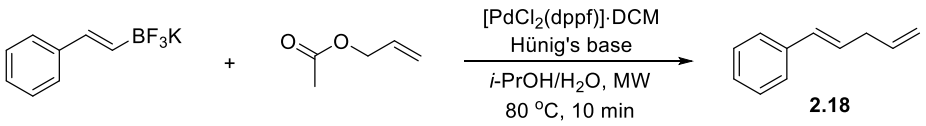

Scheme S.2.12. Synthesis of substrate **2.18**.

A microwave reactor flask flushed with Ar was charged with potassium *trans*-styryl trifluoroborate (210 mg, 1.00 mmol) and $[PdCl_2(dppf)]$·DCM (16.3 mg, 0.020 mmol). This was followed by the addition of allyl acetate (108 µL, 1.00 mmol), Hünig's base (523 µL, 3.00 mmol) and *i*-PrOH/H_2O (2:1, 5.0 mL). The mixture was placed in a microwave reactor and allowed to react at 80 °C for 10 min. It was then diluted with Et_2O and H_2O, the

phases were separated and the aqueous layer was extracted with Et_2O. The combined organic layers were dried over $MgSO_4$ and after column chromatography (SiO_2, pentane) **2.18** (107 mg, 82%) was obtained as a colourless oil.

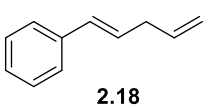

2.18

^{1}H NMR (400 MHz, $CDCl_3$) δ 7.41–7.19 (m, 5H), 6.42 (dt, *J* = 15.9, 1.2 Hz, 1H), 6.23 (dt, *J* = 15.9, 6.4 Hz, 1H), 5.92 (ddt, *J* = 17.2, 10.1, 6.4 Hz, 1H), 5.21–5.01 (m, 2H), 2.97 (tq, *J* = 6.4, 1.4 Hz, 2H); **^{13}C NMR** (100 MHz, $CDCl_3$) δ 137.8, 136.6, 131.0, 128.6, 128.4, 127.2, 126.1, 115.8, 37.2. The spectroscopic data were identical in all respects to those previously reported.[431]

[(1*E*)-Buta-1,3-dien-1-yl]benzene (2.21)[432]

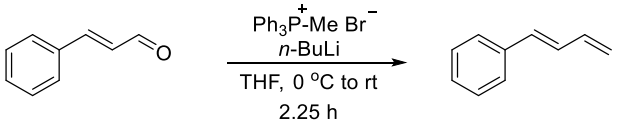

Scheme S.2.13. Synthesis of substrate **2.21**.

n-BuLi (2.5 M in hexane, 4.00 mL, 10.0 mmol) was added dropwise to a suspension of methyltriphenylphosphonium bromide (3.57 g, 10.0 mmol) in THF (50 mL) under an inert atmosphere at 0 °C. After stirring the mixture for 15 min at 0 °C a solution of (*E*)-cinnamaldehyde (1.00 mL, 8.00 mmol) in THF (10 mL) was added. It was then stirred for 1 h at 0 °C, warmed to rt, and then stirred for 1 h at rt before being quenched with sat. aq. NH_4Cl. The mixture was extracted with Et_2O and the combined organic layers were dried over $MgSO_4$. Column chromatography (SiO_2, pentane) afforded product **2.21** (968 mg, 93%) as a colourless oil.

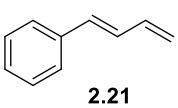

2.21

^{1}H NMR (400 MHz, $CDCl_3$) 7.41–7.37 (m, 2H), 7.32–7.26 (m, 2H), 7.24–7.18 (m, 1H), 6.78 (ddt, *J* = 15.6, 10.3, 0.9 Hz, 1H), 6.54 (d, *J* = 15.6 Hz, 1H), 6.56–6.44 (m, 1H), 5.32 (ddt, *J* = 16.9, 1.6, 0.9 Hz, 1H), 5.16 (ddd, *J* = 10.3, 1.6, 0.9 Hz, 1H); **^{13}C NMR** (100 MHz, $CDCl_3$) 137.1, 137.1, 132.8, 129.6, 128.6, 127.6, 126.4, 117.6. The spectroscopic data were identical in all respects to those previously reported.[433]

S.2.1.2. Hydrofluorination

General Procedure (GP) 3: Hydrofluorination of Alkenylarenes

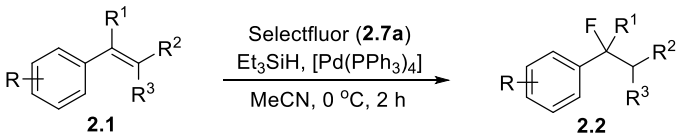

Scheme S.2.14. Hydrofluorination of alkenylarenes.

$[Pd(PPh_3)_4]$ (23.2 mg, 0.020 mmol), Selectfluor™ (213 mg, 0.60 mmol) and Et_3SiH (48 µL, 0.30 mmol) were added to a solution of alkenylarene **2.1** (0.20 mmol) in dry MeCN (8.0 mL) in a screw-top vial, which had been flushed with Ar. The solution was stirred for 2 h at 0 °C before it was diluted with water and extracted with DCM. The combined organic layers were dried over $MgSO_4$ and the solvent removed under reduced pressure. Purification by column chromatography afforded the title compounds.

General Procedure (GP) 4: Hydrofluorination of Alkenylarenes for NMR Yields

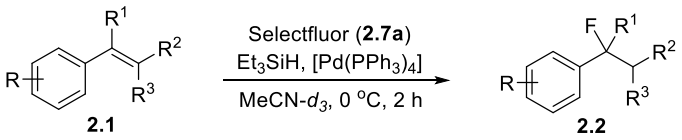

Scheme S.2.15. Hydrofluorination of alkenylarenes leading to non-isolable benzylic fluorides.

$[Pd(PPh_3)_4]$ (5.8 mg, 0.005 mmol), Selectfluor™ (53.2 mg, 0.15 mmol) and Et_3SiH (12.0 µL, 0.075 mmol) were added to a solution of alkenylarene **2.1** (0.050 mmol) in MeCN-d_3 (1.0 mL) in a screw-top vial, which had been flushed with Ar. 1-Fluoro-3-nitrobenzene (5.3 µL, 0.050 mmol) was added as internal standard and the solution was stirred for 2 h at 0 °C before being transferred into a NMR tube and submitted for NMR analysis.

General Procedure (GP) 5: Hydrofluorination of Dienes

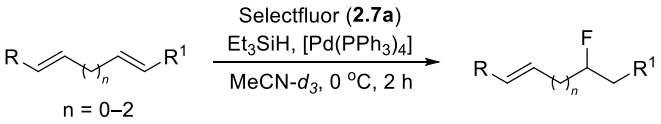

Scheme S.2.16. Hydrofluorination of dienes.

$[Pd(PPh_3)_4]$ (5.8 mg, 0.010 mmol), Selectfluor™ (53.2 mg, 0.30 mmol) and Et_3SiH (24.0 µL, 0.15 mmol) were added to a solution of diene (0.10 mmol) in MeCN (4.0 mL) in a screw-top vial, which had been flushed with Ar. The solution was stirred for 2 h at 0 °C before it was diluted with water and extracted with DCM. The combined organic layers were dried over $MgSO_4$ and the solvent was removed under reduced pressure. The crude product was taken up in $CDCl_3$, 1-fluoro-3-nitrobenzene (10.6 µL, 0.10 mmol) was added as internal standard and the resulting solution was submitted for NMR analysis.

4-(1-Fluoroethyl)-1,1'-biphenyl (2.2a)

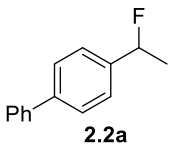

2.2a

The title compound was prepared following GP3 using 4-ethenyl-1,1'-biphenyl, **2.1a** (36.1 mg, 0.20 mmol). Column chromatography (SiO_2, 5% EtOAc in hexane) gave **2.2a** (27.6 mg, 69%) as a white solid. **^{1}H NMR** (400 MHz, $CDCl_3$) δ 7.56–7.49 (m, 4H), 7.40–7.34 (m, 4H), 7.31–7.26 (m, 1H), 5.69 (dq, *J* = 48.0, 6.5 Hz, 1H), 1.69 (dd, *J* = 23.7, 6.5 Hz, 3H); **^{13}C NMR** (100 MHz, $CDCl_3$) δ 141.2, 140.7, 140.3 (d, $J_{C–F}$ = 19.1 Hz), 128.8, 127.4, 127.2 (d, $J_{C–F}$ = 12.0 Hz), 125.7 (d, $J_{C–F}$ = 6.5 Hz), 125.7, 90.8 (d, $J_{C–F}$ = 166.9 Hz), 22.9 (d, $J_{C–F}$ = 25.4 Hz); **^{19}F NMR** (377 MHz, $CDCl_3$) δ –166.6 (dq, *J* = 48.0, 23.7 Hz). The spectroscopic data were identical in all respects to those previously reported.[434]

4-(2-Fluoroethyl)-1,1'-biphenyl (2.3a)

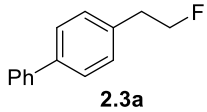

2.3a

The title compound was obtained as a by-product during the optimisation of this hydrofluorination reaction using 4-ethenyl-1,1'-biphenyl, **2.1a** (18.0 mg, 0.10 mmol) as starting material. Characteristic peaks: **^{1}H NMR** (400 MHz, $CDCl_3$) δ 4.65 (dt, *J* = 47.2, 6.6 Hz, 2H), 3.11 (dt, *J* = 23.2, 6.6 Hz, 2H); **^{19}F NMR** (377 MHz, $CDCl_3$) δ –215.8 (tt, *J* = 47.2, 23.2 Hz). The spectroscopic data were identical in all respects to those previously reported.[102]

4-Ethyl-1,1'-biphenyl (2.4a)

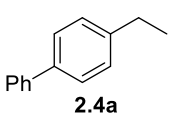

2.4a

The title compound was obtained as a by-product during the optimisation of this hydrofluorination reaction using 4-ethenyl-1,1'-biphenyl, **2.1a** (18.0 mg, 0.10 mmol) as starting material. Characteristic peaks: **^{1}H NMR** (400 MHz, $CDCl_3$) δ 2.71 (q, *J* = 7.6 Hz, 2H), 1.29 (t, *J* = 7.6 Hz, 3H). The spectroscopic data were identical in all respects to those previously reported.[435]

(1-Fluoroethyl)benzene (2.2b)

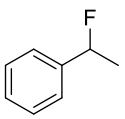

2.2b

The title compound was prepared following GP4 using styrene, **2.1b** (5.7 µL, 0.050 mmol). ^{1}H and ^{19}F NMR analysis showed 58% of **2.2b** had been formed. **^{1}H NMR** (400 MHz, MeCN-d_3) δ 7.39–7.29 (m, 5H), 5.61 (dq, *J* = 48.1, 6.5 Hz, 1H), 1.62 (dd, *J* = 23.5, 6.5 Hz, 3H); **^{19}F NMR** (377 MHz, MeCN-d_3) δ –166.6 (dq, *J* = 48.1, 23.5 Hz). The spectroscopic data were identical in all respects to those previously reported.[436]

1-Fluoro-4-(1-fluoroethyl)benzene (2.2d)

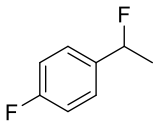

2.2d

The title compound was prepared following GP4 using 1-ethenyl-4-fluorobenzene, **2.1d** (6.0 µL, 0.050 mmol). ^{1}H and ^{19}F NMR analysis showed 55% of **2.2d** had been formed. **^{1}H NMR** (400 MHz, MeCN-d_3) δ 7.44–7.38 (m, 2H), 7.16–7.10 (m, 2H), 5.65 (dq, *J* = 48.2, 6.4 Hz, 1H), 1.59 (dd, *J* = 24.2, 6.4 Hz, 3H); **^{19}F NMR** (377 MHz, MeCN-d_3) δ –115.6 (m), –164.3 (dq, *J* = 48.2, 24.2 Hz). The spectroscopic data were identical in all respects to those previously reported.[437]

1-(1-Fluoroethyl)-4-(trifluoromethyl)benzene (2.2e)

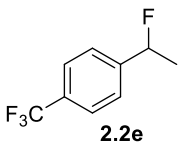

2.2e

The title compound was prepared following GP4 using 1-ethenyl-4-(trifluoromethyl)benzene, **2.1e** (7.4 µL, 0.050 mmol). ^{1}H and ^{19}F NMR analysis showed 72% of **2.2e** had been formed. **^{1}H NMR** (400 MHz, MeCN-d_3) δ 7.65 (ad, *J* = 8.4 Hz, 2H), 7.47 (ad, *J* = 8.4 Hz, 2H), 5.75 (dq, *J* = 47.9, 6.6 Hz, 1H), 1.61 (dd, *J* = 24.1, 6.6 Hz, 3H); **^{19}F NMR** (377 MHz, MeCN-d_3) δ –63.1, –171.0 (dq, *J* = 47.9, 24.1 Hz). The spectroscopic data were identical in all respects to those previously reported.[438]

4-(1-Fluoroethyl)benzonitrile (2.2g)

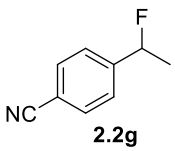

2.2g

The title compound was prepared following GP3 using 4-ethenylbenzonitrile, **2.1g** (25.8 mg, 0.20 mmol). Column chromatography (SiO_2, 5% EtOAc in hexane) gave **2.2g** (20.9 mg, 70%) as a colourless oil. **^{1}H NMR** (400 MHz, $CDCl_3$) δ 7.69 (ad, *J* = 8.0 Hz, 2H), 7.46 (ad, *J* = 8.0 Hz, 2H), 5.68 (dq, *J* = 47.3, 6.6 Hz, 1H), 1.65 (dd, *J* = 24.1, 6.6 Hz, 3H); **^{13}C NMR** (100 MHz, $CDCl_3$) δ 146.7 (d, J_{C-F} = 20.7 Hz), 132.4, 125.6 (d, J_{C-F} = 7.5 Hz), 118.6, 112.0, 90.0 (d, J_{C-F} = 171.7 Hz), 22.9 (d, J_{C-F} = 23.8 Hz); **^{19}F NMR** (377 MHz, $CDCl_3$) δ –172.7 (dq, *J* = 47.3, 24.1 Hz). The spectroscopic data were identical in all respects to those previously reported.[439]

1-(1-Fluoroethyl)-4-nitrobenzene (2.2h)

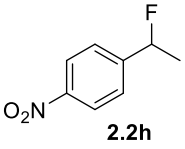

2.2h

The title compound was prepared following GP3 using 1-ethenyl-4-nitrobenzene, **2.1h** (29.8 mg, 0.20 mmol). Column chromatography (SiO_2, 2–5% EtOAc in hexane) gave **2.2h** (20.7 mg, 61%) as a yellow oil. **^{1}H NMR** (400 MHz, $CDCl_3$) δ 8.25 (ad, *J* = 8.6 Hz, 2H), 7.52 (ad, *J* = 8.6 Hz, 2H), 5.74 (dq, *J* = 48.1,

6.4 Hz, 1H), 1.67 (dd, *J* = 24.1, 6.4 Hz, 3H); **^{13}C NMR** (100 MHz, $CDCl_3$) δ 148.6 (d, $J_{C–F}$ = 19.1 Hz), 147.6, 125.7 (d, $J_{C–F}$ = 166.9 Hz), 123.8, 89.7 (d, $J_{C–F}$ = 171.7 Hz), 23.0 (d, $J_{C–F}$ = 23.8 Hz); **^{19}F NMR** (377 MHz, $CDCl_3$) δ –172.7 (dq, *J* = 48.1, 24.1 Hz). The spectroscopic data were identical in all respects to those previously reported.[436]

2-(4-(1-Fluoroethyl)benzyl)isoindoline-1,3-dione (2.2k)

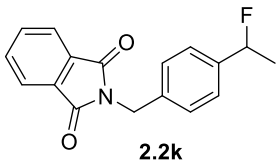

2.2k

The title compound was prepared following GP3 using 2-(4-ethenylbenzyl)-1H-isoindole-1,3(2H)-dione, **2.1k** (52.7 mg, 0.20 mmol). Column chromatography (SiO_2, 10% EtOAc in hexane) gave **2.2k** (49.3 mg, 87%) as a white solid. **M.p.** (toluene) 88 °C; **^{1}H NMR** (400 MHz, $CDCl_3$) δ 7.85 (dd, *J* = 5.5, 3.0 Hz, 2H), 7.71 (dd, *J* = 5.5, 3.0 Hz, 2H), 7.46 (ad, *J* = 7.6 Hz, 2H), 7.31 (ad, *J* = 7.6 Hz, 2H), 5.59 (dq, *J* = 47.5, 6.5 Hz, 1H), 4.86 (s, 2H), 1.6 (dd, *J* = 24.0, 6.5 Hz, 3H); **^{13}C NMR** (100 MHz, $CDCl_3$) δ 168.0, 141.0, 136.4, 134.1, 132.1, 128.8, 125.6 (d, $J_{C–F}$ = 6.4 Hz), 123.4, 90.7 (d, $J_{C–F}$ = 166.9 Hz), 41.3, 22.9 (d, $J_{C–F}$ = 25.4 Hz); **^{19}F NMR** (377 MHz, $CDCl_3$) δ –167.4 (dq, *J* = 47.5, 24.0 Hz); **IR** (solid) ν 1770, 1708, 1468, 1428, 1392, 1346, 1302, 1185, 1068, 1006, 938, 854, 810, 715, 625 cm^{-1}; **HRMS** (ESI) *m/z* Calcd for $C_{17}H_{14}FNNaO_2$ $[M+Na]^+$ 306.0901, found 306.0901.

***N*-Benzyl-4-(1-fluoroethyl)benzamide (2.2l)**

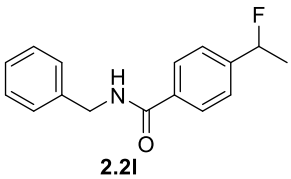

2.2l

The title compound was prepared following GP3 using *N*-benzyl-4-vinylbenzamide, **2.1l** (47.5 mg, 0.20 mmol). Column chromatography (SiO_2, 30% EtOAc in hexane) gave **2.2l** (40.1 mg, 78%) as a white solid. **M.p.** (toluene) 118 °C; **^{1}H NMR** (400 MHz, $CDCl_3$) δ 7.71 (ad, *J* = 8.2 Hz, 2H), 7.28 (ad, *J* = 8.2 Hz, 2H), 7.25–7.17 (m, 5H), 6.66 (bs, 1H), 5.56 (dq, *J* = 47.5, 6.4 Hz, 1H), 4.25 (d, *J* = 5.9 Hz, 2H), 1.54 (dd, *J* = 24.0, 6.4 Hz, 3H); **^{13}C NMR** (100 MHz,

$CDCl_3$) δ 167.0, 145.1 (d, $J_{C–F}$ = 19.1 Hz), 138.2, 134.1, 128.8, 127.9, 127.6, 127.3, 125.2 (d, $J_{C–F}$ = 6.4 Hz), 90.4 (d, $J_{C–F}$ = 168.5 Hz), 44.1, 23.0 (d, $J_{C–F}$ = 23.8 Hz); **^{19}F NMR** (377 MHz, $CDCl_3$) δ –170.3 (dq, *J* = 47.5, 24.0 Hz); **IR** (solid) ν 3326, 2361, 1639, 1549, 1497, 1452, 1420, 1319, 1259, 1068, 990, 884, 856, 725, 695, 670 cm^{-1}; **HRMS** (ESI-TOF) *m/z* Calcd for $C_{16}H_{16}FNNaO$ $[M+Na]^+$ 280.1108, found 280.1115.

1-(1-Fluoroethyl)-2-methoxybenzene (2.2m)

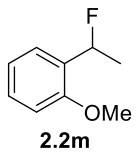

2.2m

The title compound was prepared following GP4 using 4-ethenylbenzaldehyde, **2.1m** (6.7 mg, 0.050 mmol). ^{1}H and ^{19}F NMR analysis showed 30% of **2.2m** had been formed. **^{1}H NMR** (400 MHz, MeCN-d_3) δ 7.38 (d, *J* = 7.6 Hz, 1H), 7.31 (t, *J* = 7.6 Hz, 1H), 7.14 (t, *J* = 7.6 Hz, 1H), 6.98 (d, *J* = 7.6 Hz, 1H), 5.93 (dq, *J* = 47.6, 6.4 Hz, 1H), 3.81 (s, 3H), 1.55 (dd, *J* = 24.1 6.4 Hz, 3H); **^{19}F NMR** (377 MHz, MeCN-d_3) δ –173.6 (dq, *J* = 47.6, 24.1 Hz).

Ethyl 4-(1-fluoroethyl)benzoate (2.2n)

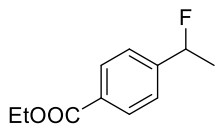

2.2n

The title compound was prepared following GP3 using ethyl 4-ethenylbenzoate, **2.1n** (35.2 mg, 0.20 mmol). Column chromatography (SiO_2, 10% EtOAc in hexane) gave **2.2n** (25.1 mg, 64%) as a colourless oil. **^{1}H NMR** (500 MHz, $CDCl_3$) δ 8.06 (ad, *J* = 8.4 Hz, 2H), 7.42 (ad, *J* = 8.4 Hz, 2H), 5.69 (dq, *J* = 47.5, 6.6 Hz, 1H), 4.39 (q, *J* = 7.0 Hz, 2H), 1.65 (dd, *J* = 24.0, 6.6 Hz, 3H), 1.41 (t, *J* = 7.0 Hz, 3H); **^{13}C NMR** (126 MHz, $CDCl_3$) δ 166.3, 146.4 (d, $J_{C–F}$ = 20.0 Hz), 130.2 (d, $J_{C–F}$ = 1.9 Hz), 129.8, 124.8 (d, $J_{C–F}$ = 7.6 Hz), 90.4 (d, $J_{C–F}$ = 169.8 Hz), 61.0, 23.0 (d, $J_{C–F}$ = 24.8 Hz), 14.3; **^{19}F NMR** (377 MHz, $CDCl_3$) δ –167.4 (dq, *J* = 47.5, 24.0 Hz); **IR** (film, $CDCl_3$) ν 2984, 1716, 1416, 1367, 1272, 1179, 1107, 1071, 1021, 888, 857, 773, 705 cm^{-1}; **HRMS** (ESI-TOF) *m/z* Calcd for $C_{11}H_{13}FNaO_2$ $[M+Na]^+$ 219.0792, found 219.0798.

Methyl 2-(1-fluoroethyl)benzoate (2.2o)

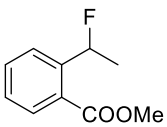

2.2o

The title compound was prepared following GP3 using methyl 2-ethenylbenzoate, **2.1o** (32.4 mg, 0.20 mmol). Column chromatography (SiO_2, 10% EtOAc in hexane) gave **2.2o** (21.1 mg, 58%) as a colourless oil. **^{1}H NMR** (400 MHz, $CDCl_3$) δ 7.96 (dt, *J* = 7.7, 1.3 Hz, 1H), 7.71 (ddd, *J* = 7.7, 1.3, 0.7 Hz, 1H), 7.60 (td, *J* = 7.7, 1.3 Hz, 1H), 7.38 (td, *J* = 7.7, 1.3 Hz, 1H), 6.45 (dq, *J* = 48.9, 6.3 Hz, 1H), 3.91 (s, 3H), 1.66 (dd, *J* = 24.1, 6.3 Hz, 3H); **^{13}C NMR** (100 MHz, $CDCl_3$) δ 167.0, 144.7 (d, $J_{C–F}$ = 20.7 Hz), 132.8, 130.3, 127.5, 126.6 (d, $J_{C–F}$ = 4.8 Hz), 125.4 (d, $J_{C–F}$ = 12.7 Hz), 88.6 (d, $J_{C–F}$ = 165.3 Hz), 52.2, 23.6 (d, $J_{C–F}$ = 25.4 Hz); **^{19}F NMR** (377 MHz, $CDCl_3$) δ –172.0 (dq, *J* = 48.9, 24.1 Hz); **IR** (film, $CDCl_3$) ν 2954, 1720, 1436, 1372, 1262, 1203, 1142, 1109, 1060, 1003, 884, 757, 710, 613 cm^{-1}; **HRMS** (ESI-TOF) *m/z* Calcd for $C_{10}H_{11}FO_2$ 205.0635 $[M+Na]^+$, found 205.0635.

2-(1-Fluoroethyl)naphthalene (2.2p)

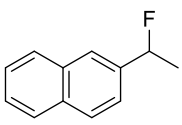

2.2p

The title compound was prepared following GP3 using 1-ethenylnaphthalene, **2.1p** (29.7 µL, 0.20 mmol). Column chromatography (SiO_2, 0–5% EtOAc in hexane) gave **2.2p** (16.0 mg, 46%) as a white solid. **^{1}H NMR** (400 MHz, $CDCl_3$) δ 7.97–7.81 (m, 4H), 7.61–7.46 (m, 3H), 5.80 (dq, *J* = 48.1, 6.6 Hz, 1H), 1.74 (dd, *J* = 24.1, 6.6 Hz, 3H); **^{13}C NMR** (100 MHz, $CDCl_3$) δ 138.8 (d, $J_{C–F}$ = 19.2 Hz), 133.1, 133.0, 128.3, 128.1, 127.7, 126.3 (d, $J_{C–F}$ = 12.1 Hz), 126.2, 124.1, 123.1, 91.1 (d, $J_{C–F}$ = 167.0 Hz), 22.9 (d, $J_{C–F}$ = 25.6 Hz); **^{19}F NMR** (377 MHz, $CDCl_3$) δ –167.0 (dq, *J* = 48.1, 24.1 Hz). The spectroscopic data were identical in all respects to those previously reported.[436]

1-(Benzyloxy)-4-(1-fluoroethyl)benzene (2.2q)

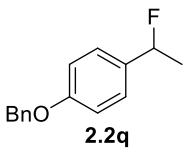

2.2q

The title compound was prepared following GP4 using 1-(benzyloxy)-4-ethenylbenzene, **2.1q** (10.5 mg, 0.050 mmol) and MeCN (2.0 mL). The reaction was worked up according to GP1 and the crude product was taken up in $CDCl_3$ and 1-fluoro-3-nitrobenzene (10.6 µL, 0.1 mmol) was added as NMR standard. ^{1}H and ^{19}F NMR analysis showed 8% of **2.2q** had been formed. Characteristic peaks: **^{1}H NMR** (400 MHz, $CDCl_3$) δ 5.55 (dq, *J* = 47.7, 6.4 Hz, 1H), 1.61 (dd, *J* = 23.7, 6.4 Hz, 3H); **^{19}F NMR** (377 MHz, $CDCl_3$) δ –161.4 (dq, *J* = 47.7, 23.7 Hz).

(2*S*)-2-[(*S*)-Fluoro(phenyl)methyl]-3-methylbutan-1-ol (*anti*-2.2y)

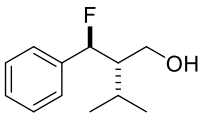

anti-**2.2y**

The title compound was prepared following GP3 using (2*E*)-2-benzylidene-3-methylbutan-1-ol, (*E*)-**2.1y** (35.3 mg, 0.20 mmol). Column chromatography (SiO_2, 10% EtOAc in hexane) gave *anti*-**2.2y** (26.3 mg, 67%) as a colourless oil. **^{1}H NMR** (400 MHz, $CDCl_3$) δ 7.45–7.32 (m, 5H), 5.70 (dd, *J* = 47.4, 6.4 Hz, 1H), 3.91–3.77 (m, 2H), 1.87 (dm, *J* = 22.8 Hz, 1H), 1.83–1.73 (m, 1H), 1.58 (bs, 1H), 1.04 (dd, *J* = 6.9, 1.0 Hz, 3H), 0.96 (d, *J* = 6.9 Hz, 3H); **^{13}C NMR** (100 MHz, $CDCl_3$) δ 139.2 (d, $J_{C–F}$ = 19.8 Hz), 128.6, 128.2 (d, $J_{C–F}$ = 1.6 Hz), 125.8 (d, $J_{C–F}$ = 7.5 Hz), 96.6 (d, $J_{C–F}$ = 170.1 Hz), 61.4 (d, $J_{C–F}$ = 4.8 Hz), 52.4 (d, $J_{C–F}$ = 18.3 Hz), 26.4 (d, $J_{C–F}$ = 4.0 Hz), 21.0 (d, $J_{C–F}$ = 0.9 Hz), 18.9; **^{19}F NMR** (376 MHz, $CDCl_3$) δ –183.3 (dd, *J* = 47.4, 22.8 Hz); **IR** (film, $CDCl_3$) ν 3393, 2960, 2360, 1454, 1390, 1043, 762, 700 cm^{-1}; **HRMS** (ESI-TOF) *m/z* Calcd for $C_{12}H_{17}FNaO$ $[M+Na]^+$ 219.1156, found 219.1162.

(2*R*)-2-[(*S*)-Fluoro(phenyl)methyl]-3-methylbutan-1-ol (*syn*-2.2y)

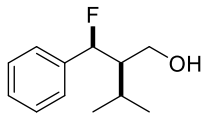

syn-**2.2y**

The title compound was prepared following GP3 using (2*Z*)-2-benzylidene-3-methylbutan-1-ol, (*Z*)-**2.1y** (35.3 mg, 0.20 mmol). Column chromatography (SiO_2, 10% EtOAc in hexane) gave *syn*-**2.2y** (16.1 mg, 41%) as a colourless oil. **^{1}H NMR** (400 MHz, $CDCl_3$) δ 7.42–7.31 (m, 5H), 5.68 (dd, *J* = 46.9, 6.9 Hz, 1H), 3.69 (dd, *J* = 11.3, 6.9 Hz, 1H), 3.62 (dd, *J* = 11.3, 4.2 Hz, 1H), 2.14–2.02 (m, 1H), 1.94 (dm, *J* = 21.5 Hz, 1H), 1.58 (bs, 1H), 1.04 (d, *J* = 7.1 Hz, 3H), 1.01 (dd, *J* = 6.9, 0.7 Hz, 3H); **^{13}C NMR** (100 MHz, $CDCl_3$) δ 139.5 (d, $J_{C–F}$ = 20.5 Hz), 128.5, 128.2 (d, $J_{C–F}$ = 1.7 Hz), 125.9 (d, $J_{C–F}$ = 7.4 Hz), 94.4 (d, $J_{C–F}$ = 173.7 Hz), 59.7 (d, $J_{C–F}$ = 6.7 Hz), 52.3 (d, $J_{C–F}$ = 20.7 Hz), 25.9 (d, $J_{C–F}$ = 2.4 Hz), 21.6, 18.9 (d, $J_{C–F}$ = 2.4 Hz); **^{19}F NMR** (376 MHz, $CDCl_3$) δ –183.8 (dd, *J* = 46.9, 21.5 Hz); **IR** (film, $CDCl_3$) ν 3364, 2959, 2360, 1452, 1369, 1041, 981, 756, 700, 670 cm^{-1}; **HRMS** (ESI) *m/z* Calcd for $C_{12}H_{17}FNaO$ $[M+Na]^+$ 219.1156, found 219.1163.

(2-Fluoropropan-2-yl)benzene (2.2z)

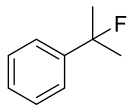

2.2z

The title compound was prepared following GP4 using (prop-1-en-2-yl)benzene, **2.1z** (6.5 µL, 0.050 mmol). ^{1}H and ^{19}F NMR analysis showed 25% of **2.2z** had been formed. Characteristic Peaks: **^{1}H NMR** (400 MHz, MeCN-d_3) δ 1.69 (d, *J* = 22.2 Hz, 1H); **^{19}F NMR** (377 MHz, MeCN-d_3) δ –136.8 (sept, *J* = 22.2 Hz). The spectroscopic data were identical in all respects to those previously reported.[440]

[(1*E*)-5-Fluorohex-1-en-1-yl]benzene (2.13)

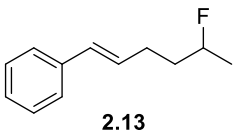

2.13

The title compound was prepared following GP5 using [(1*E*)-hexa-1,5-dien-1-yl]benzene, **2.11** (15.8 mg, 0.1 mmol). ^{1}H and ^{19}F NMR analysis showed 32% of **2.13** had been formed. Characteristic peaks: **^{1}H NMR** (400 MHz, $CDCl_3$) δ 4.64 (dm, *J* = 48.6 Hz, 1H), 1.28 (dd, *J* = 24.0, 6.2 Hz, 3H); **^{19}F NMR** (377 MHz, $CDCl_3$) δ –173.7 (ddqd, *J* = 48.6, 30.0, 24.0, 16.1 Hz).

[(3*E*)-7-Fluorooct-3-en-1-yl]benzene (2.15)

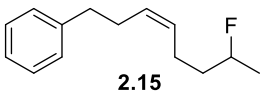

2.15

The title compound was prepared following GP5 using [(2*Z*)-octa-3,7-dien-1-yl]benzene, **2.14** (18.6 mg, 0.1 mmol). ^{1}H and ^{19}F NMR analysis showed 40% of **2.15** had been formed. Characteristic peaks: **^{1}H NMR** (400 MHz, $CDCl_3$) δ 4.56 (dm, *J* = 48.7 Hz, 1H), 1.27 (dd, *J* = 23.9, 6.1 Hz, 3H); **^{19}F NMR** (377 MHz, $CDCl_3$) δ –173.6 (ddqd, *J* = 48.7, 30.3, 23.9, 15.9 Hz).

(1*Z*)-5-Fluorocyclooct-1-ene (2.17)

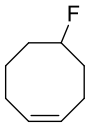

2.17

The title compound was prepared following GP5 using (1*Z*,5*Z*)-cycloocta-1,5-diene, **2.16** (12.2 µL, 0.1 mmol). ^{1}H and ^{19}F NMR analysis showed 10% of **2.17** had been formed. Characteristic peaks: **^{1}H NMR** (400 MHz, $CDCl_3$) δ 4.82 (dm, *J* = 52.6 Hz, 1H); **^{19}F NMR** (377 MHz, $CDCl_3$) δ –164.3–164.8 (m).

(1-Fluoropent-4-en-1-yl)benzene (2.19)

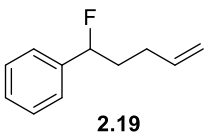

2.19

The title compound was prepared following GP5 using [(1*E*)-penta-1,4-diene-1-yl]benzene, **2.18** (14.4 µL, 0.1 mmol). ^{1}H and ^{19}F NMR analysis showed a trace of **2.19** had been formed. Characteristic peak: **^{19}F NMR** (377 MHz, $CDCl_3$) δ –173.9 (ddd, *J* = 45.2, 27.2, 17.5 Hz).

Hydrofluorination of Alkyne 2.24

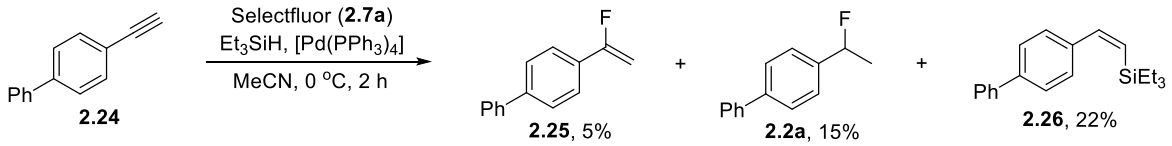

Scheme S.2.17. Hydrofluorination of alkyne **2.24**.

$[Pd(PPh_3)_4]$ (5.8 mg, 0.01 mmol), Selectfluor™ (53.2 mg, 0.30 mmol) and Et_3SiH (24.0 µL, 0.15 mmol) were added to a solution of 4-ethynyl-1,1'-biphenyl, **2.24** (17.8 mg, 0.1 mmol), in MeCN (4.0 mL) in a screw-top vial, which had been flushed with Ar. The solution was stirred for 2 h at 0 °C before it was diluted with water and extracted with DCM. The combined organic layers were dried over $MgSO_4$ and the solvent removed under reduced pressure. The crude product was taken up in $CDCl_3$, 1-fluoro-3-nitrobenzene (10.6 µL, 0.1 mmol) was added as internal standard and the resulting solution was submitted for NMR analysis. This revealed that 5% of **2.25**, 15% of **2.2a** and 22% of **2.26** relative to the internal standard had been formed.

4-(1-Fluoroethenyl)-1,1'-biphenyl (2.25)

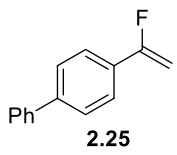

Characteristic peaks: **^{1}H NMR** (400 MHz, $CDCl_3$) δ 5.09 (dd, *J* = 49.9, 3.5 Hz, 1H), 4.88 (dd, *J* = 18.1, 3.5 Hz, 1H); **^{19}F NMR** (377 MHz, $CDCl_3$) δ –108.0 (dd, *J* = 49.9, 18.1 Hz). The spectroscopic data were identical in all respects to those previously reported.[441]

(*Z*)-(2-([1,1'-biphenyl]-4-yl)vinyl)triethylsilane (2.26)

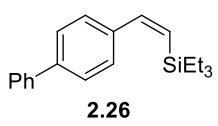

Characteristic peaks: **^{1}H NMR** (400 MHz, $CDCl_3$) δ 7.68–7.60 (m, 2H), 7.61–7.53 (m, 2H), 7.49 (d, *J* = 15.3 Hz, 1H), 7.47–7.43 (m, 2H), 7.39–7.33 (m, 3H), 5.81 (d, *J* = 15.3 Hz, 1H), 0.88 (t, *J* = 7.8 Hz, 1H), 0.58 (q, *J* = 7.8 Hz, 1H).

S.2.2. Deuterium Labelling Experiments

S.2.2.1. Deuterofluorination of 2.1b

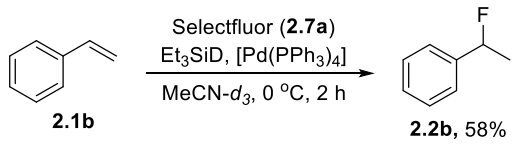

Scheme S.2.18. Hydrofluorination of **2.1b**.

$[Pd(PPh_3)_4]$ (5.8 mg, 0.0050 mmol), Selectfluor™ (53.2 mg, 0.15 mmol) and Et_3SiH (12.0 µL, 0.075 mmol) were added to a solution of **2.1b** (5.2 mg, 0.050 mmol) in MeCN-d_3 (1.0 mL) in a screw-top vial, which had been flushed with Ar. 1-Fluoro-3-nitrobenzene (5.3 µL, 0.050 mmol) was added as internal standard and the solution was stirred for 2 h at 0 °C before being transferred into a NMR tube and submitted for NMR analysis.

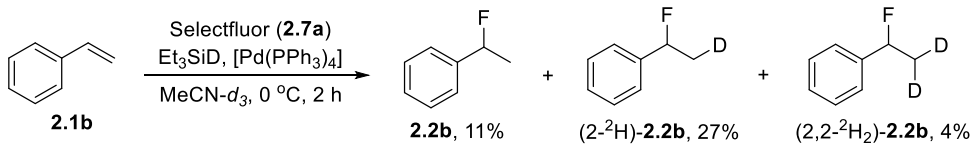

Scheme S.2.19. Deuterofluorination of **2.1b**.

$[Pd(PPh_3)_4]$ (5.8 mg, 0.0050 mmol), Selectfluor™ (53.2 mg, 0.15 mmol) and Et_3SiD (11.9 µL, 0.075 mmol) were added to a solution of **2.1b** (5.2 mg, 0.050 mmol) in MeCN-d_3 (1.0 mL) in a screw-top vial, which had been flushed with Ar. 1-Fluoro-3-nitrobenzene (5.3 µL, 0.050 mmol) was added as internal standard and the solution was stirred for 2 h at 0 °C before being transferred into a NMR tube and submitted for NMR analysis.

(1-Fluoroethyl-2-*d*)benzene (2-^{2}H)-2.2b

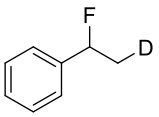

(2-^{2}H)-**2.2b**

NMR analysis revealed that the title compound had been formed in 27% yield. Characteristic peaks: **^{1}H NMR** (400 MHz, MeCN-d_3) δ 5.65 (ddd, *J* = 47.2, 5.9, 5.4 Hz, 1H), 1.57 (ddt, *J* = 24.2, 6.4, 2.0 Hz, 2H). **^{19}F-{^{1}H} NMR** (377 MHz, MeCN-d_3) δ –166.5 (t, *J* = 4.0 Hz).

(1-Fluoroethyl-2,2-d_2)benzene (2,2-^{2}H$_2$)-2.2b

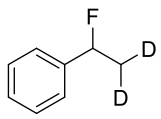

(2,2-^{2}H$_2$)-**2.2b**

NMR analysis revealed that the title compound had been formed in 4% yield. Characteristic peaks: **^{19}F-{^{1}H} NMR** (377 MHz, MeCN-d_3) δ –166.7 (sept, *J* = 3.9 Hz).

S.2.2.2. Hydrofluorination of *E*- and *Z*-Stilbene

Synthesis of *anti*-(2-^{2}H)-2.31 from *cis*-stilbene oxide

(1*S*,2*R*)-1,2-Diphenylethan-2-*d*-1-ol (*syn*-(2-^{2}H)-2.30)[442]

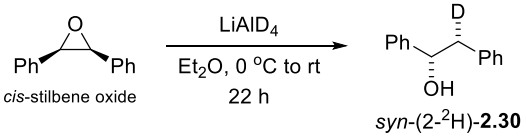

Scheme S.2.20. Synthesis of *syn*-(2-^{2}H)-**2.30** from *cis*-stilbene oxide.

cis-Stilbene oxide (470 mg, 2.40 mmol) dissolved in Et_2O (4.0 mL) was added to a suspension of $LiAlD_4$ (202 mg, 4.80 mmol) in Et_2O (5.0 mL) under an inert atmosphere at 0 °C. The mixture was stirred for 20 min at 0 °C before warming to rt. After 22 h of stirring at rt the reaction was quenched by slow addition of ice. The product was extracted with Et_2O and the combined organic layers were dried over $MgSO_4$ before the solvent was

removed under reduced pressure. Purification by column chromatography (SiO_2, 30% Et_2O in pentane) gave the product (417 mg, 87%) as a white solid.

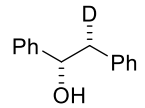

syn-(2-^{2}H)-**2.30**

^{1}H NMR (400 MHz, $CDCl_3$) 7.25–7.23 (d, 4H), 7.22–7.17 (m, 3H), 7.16–7.11 (m, 1H), 7.10–7.06 (m, 2H), 4.76 (d, *J* = 4.4 Hz, 1H), 2.91 (dt, *J* = 4.4, 1.9 Hz, 1H), 1.98 (s, 1H); **^{13}C NMR** (100 MHz, $CDCl_3$) δ 143.7, 137.9, 129.4, 128.4, 128.3, 127.5, 126.5, 125.9, 75.2, 45.6 (t, J_{C-D} = 19.4 Hz). The spectroscopic data were identical in all respects to those previously reported.[443]

anti-(1-Fluoroethane-1,2-diyl-2-*d*)dibenzene (*anti*-(2-^{2}H)-2.31)[444]

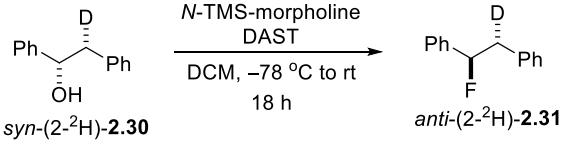

syn-(2-^{2}H)-**2.30** → *anti*-(2-^{2}H)-**2.31**

Scheme S.2.21. Synthesis of *anti*-(2-^{2}H)-**2.31** from *syn*-(2-^{2}H)-**2.30**.

A solution of DAST (159 µL, 1.20 mmol) in DCM (0.50 mL) was prepared under an inert atmosphere and cooled to –78 °C. After adding *N*-(trimethylsilyl)morpholine (229 µL, 1.30 mmol) the reaction mixture was warmed to rt and stirred for 2.5 h. It was then again cooled to –78 °C before adding *syn*-(2-^{2}H)-**2.30** (79.7 mg, 0.40 mmol) dissolved in DCM (1.1 mL). The mixture was now allowed to warm to rt and was then stirred for 15 h. To quench it the reaction was poured into sat. aq. $NaHCO_3$. The layers were separated and the aqueous one was extracted with DCM. The combined organic layers were dried over $MgSO_4$ before the solvent was removed under reduced pressure. Due to degradation the product could not be isolated.

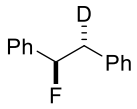
anti-(2-^{2}H)-**2.31**

Characteristic peaks: **^{1}H NMR** (400 MHz, $CDCl_3$) δ 5.65 (dd, *J* = 47.4, 8.2 Hz, 1H), 3.29 (ddt, *J* = 17.4, 8.2, 2.0 Hz, 1H); **^{19}F NMR** (377 MHz, $CDCl_3$) δ –173.3 (ddt, *J* = 47.4, 17.4, 4.4 Hz); **^{19}F-{^{1}H} NMR** (377 MHz, $CDCl_3$) δ –173.3 (t, *J* = 4.3 Hz).

Synthesis of *syn*-(2-^{2}H)-2.31 from *trans*-stilbene oxide

(1*S*,2*S*)-1,2-Diphenylethan-2-*d*-1-ol (*anti*-(2-^{2}H)-2.30)[442]

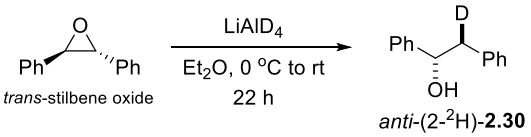
trans-stilbene oxide

Scheme S.2.22. Synthesis of *anti*-(2-^{2}H)-**2.30** from *trans*-stilbene oxide.

trans-Stilbene oxide (785 mg, 4.00 mmol) dissolved in Et_2O (4.0 mL) was added to a suspension of $LiAlD_4$ (202 mg, 4.80 mmol) in Et_2O (5.0 mL) under an inert atmosphere at 0 °C. The mixture was stirred for 20 min at 0 °C before warming it to rt. After 22 h of stirring at rt the reaction was quenched by slow addition of ice. The product was extracted with Et_2O and the combined organic layers were dried over $MgSO_4$ before the solvent was removed under reduced pressure. Purification by column chromatography (SiO_2, 20% Et_2O in pentane) gave the product (697 mg, 87%) as a white solid.

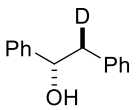
anti-(2-^{2}H)-**2.30**

^{1}H NMR (400 MHz, $CDCl_3$) 7.26–7.24 (m, 4H), 7.23–7.17 (m, 3H), 7.17–7.11 (m, 1H), 7.11–7.07 (m, 2H), 4.77 (d, *J* = 8.7 Hz, 1H), 2.87 (dt, *J* = 8.7, 1.9 Hz, 1H), 1.91 (s, 1H); **^{13}C NMR** (100 MHz, $CDCl_3$) δ 143.7, 138.0, 129.5, 128.4, 128.3, 127.5, 126.5, 125.8, 75.2, 45.7 (t, $J_{C–D}$ = 19.5 Hz). The spectroscopic data were identical in all respects to those previously reported.[443]

syn-(1-Fluoroethane-1,2-diyl-2-*d*)dibenzene (*syn*-(2-^{2}H)-2.31)[444]

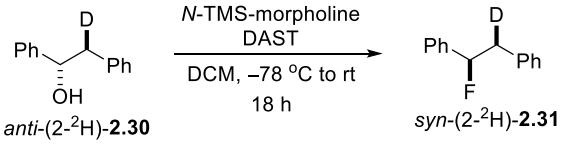

Scheme S.2.23. Synthesis of *syn*-(2-^{2}H)-**2.31** from *anti*-(2-^{2}H)-**2.30**.

A solution of DAST (159 µL, 1.20 mmol) in DCM (0.50 mL) was prepared under an inert atmosphere and cooled to –78 °C. After adding *N*-(trimethylsilyl)morpholine (229 µL, 1.30 mmol) it was warmed to rt and stirred for 2.5 h. It was then again cooled to –78 °C before adding *anti*-(2-^{2}H)-**2.30** (79.7 mg, 0.40 mmol) dissolved in DCM (1.1 mL). The mixture was now allowed to warm to rt and was then stirred for 15 h. To quench it the reaction was poured sat. aq. $NaHCO_3$. The layers were separated and the aqueous one was extracted with DCM. The combined organic layers were dried over $MgSO_4$ before the solvent was removed under reduced pressure. Due to degradation the product could not be isolated.

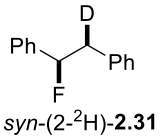

syn-(2-^{2}H)-**2.31**

Characteristic peaks: **^{1}H NMR** (400 MHz, $CDCl_3$) δ 5.65 (dd, *J* = 47.3, 4.6 Hz, 1H), 3.13 (ddt, *J* = 29.0, 4.6, 1.9 Hz, 1H); **^{19}F NMR** (377 MHz, $CDCl_3$) δ–173.3 (ddt, *J* = 47.3, 29.0, 2.5 Hz); **^{19}F-{^{1}H} NMR** (377 MHz, $CDCl_3$) δ–173.3 (t, *J* = 2.5 Hz).

Deuterofluorination of (*E*)-Stilbene

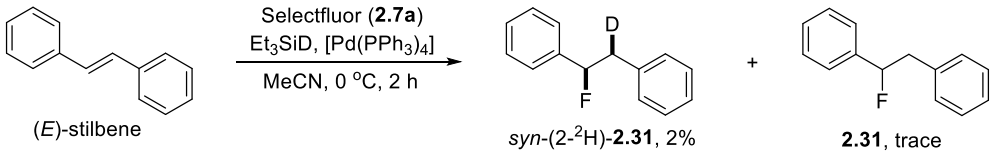

Scheme S.2.24. Deuterofluorination of (*E*)-stilbene.

Selectfluor™ (106 mg, 0.30 mmol) and $[Pd(PPh_3)_4]$ (11.6 mg, 0.010 mmol) were dissolved in MeCN (4.0 mL) in a screw-top vial, which had been flushed with Ar. To this solution was added (*E*)-stilbene (18.0 mg, 0.10 mmol), before it was cooled to 0 °C, followed by the addition of Et_3SiD (23.9 µL, 0.15 mmol). After stirring the reaction mixture for 2 h at 0 °C it was diluted with H_2O and extracted with DCM. The combined organic layers were dried over $MgSO_4$ and the solvent removed under reduced pressure. The crude product was taken up in $CDCl_3$, 1-fluoro-3-nitrobenzene (10.6 µL, 0.10 mmol) was added as internal standard and the resulting solution was submitted for NMR analysis. In this mixture 2% *syn*-(2-^{2}H)-**2.31** were found alongside a trace amount of **2.31** relative to the internal standard.

(1-Fluoroethane-1,2-diyl)dibenzene (2.31)

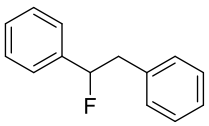

2.31

Characteristic peaks: **^{1}H NMR** (400 MHz, $CDCl_3$) δ 5.65 (ddd, *J* = 46.7, 8.0, 4.8 Hz, 1H); **^{19}F NMR** (377 MHz, $CDCl_3$) δ–173.2 (ddd, *J* = 46.7, 28.7, 17.5 Hz). The spectroscopic data were identical in all respects to those previously reported.[445]

Deuterofluorination of (*Z*)-Stilbene

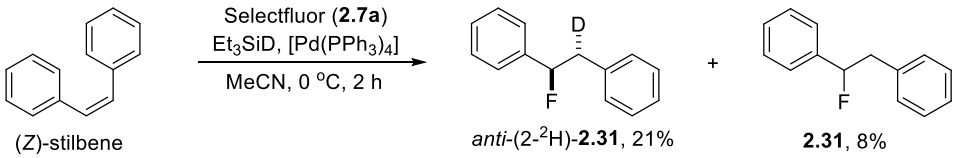

Scheme S.2.25. Deuterofluorination of (*Z*)-stilbene.

Selectfluor™ (106 mg, 0.30 mmol) and $[Pd(PPh_3)_4]$ (11.6 mg, 0.010 mmol) were dissolved in MeCN (4.0 mL) in a screw-top vial, which had been flushed with Ar. To this solution was added (*Z*)-stilbene (17.8 µL, 0.10 mmol), before it was cooled to 0 °C, followed by the addition of Et_3SiD (23.9 µL, 0.15 mmol). After stirring the reaction mixture for 2 h at 0 °C it was diluted with H_2O and extracted with DCM. The combined organic layers were dried over $MgSO_4$ and the solvent removed under reduced pressure. The crude product was taken up in $CDCl_3$, 1-fluoro-3-nitrobenzene (10.6 µL, 0.10 mmol) was added as internal standard and the resulting solution was submitted for NMR analysis. In this mixture 21% *anti*-(2-^{2}H)-**2.31** were found alongside 8% of **2.31** relative to the internal standard.

S.2.3. Reaction of 2.32 with Selectfluor™

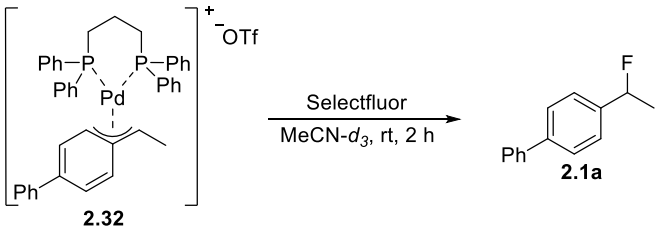

Scheme S.2.26. Reaction of **2.32** with Selectfluor™.

Selectfluor™ (8.6 mg, 0.024 mmol) was added to a solution of palladacomplex **2.32** (16.8 mg, 0.020 mmol) in MeCN-d_3 (1.0 mL) in an NMR tube at rt. 1-Fluoro-3-

nitrobenzene (2.1 µL, 0.020 mmol) was added as internal standard and the reaction was followed by ^{1}H NMR (Figure S.2.1.) After 2 h 50% of **2.1a** relative to the internal standard had been formed.

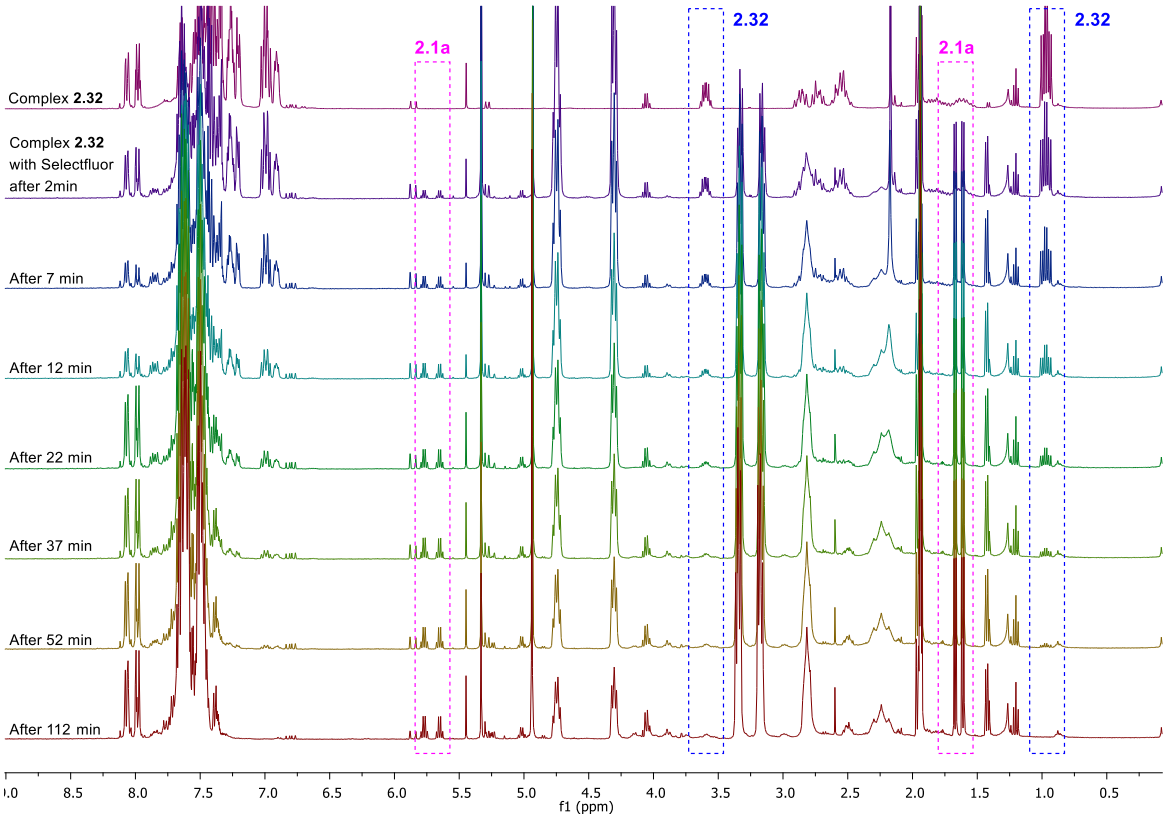

Figure S.2.1. A series of ^{1}H NMR spectra collected during the reaction of **2.32** with Selectfluor™ in MeCN-d_3.

S.2.4. Single-Crystal X-Ray Structure

Table S.2.1. Summary of single-crystal X-ray structure of **2.2k**.

Nr.	**2.2k**
Formula	$C_{17}H_{14}F_1N_1O_2$
Molecular Weight	283.30
Crystal System	monoclinic
T [K]	150
Space Group	P 21/n
a [Å]	12.7659(6)
b [Å]	7.5133(3)
c [Å]	14.5265(8)
α [°]	90
β [°]	99.441(5)
γ [°]	90
V [Å^3]	1374.42(12)
Z	4
D_{calc} [g cm^{-3}]	1.369
F(0 0 0)	592
μ [mm^{-1}]	0.820
Crystal Size [mm]	0.18 * 0.28 * 0.30
Colour, Shape	clear_pale_colourless, plate
R_{int}	6.78
θ_{min}, θ_{max} [deg]	4.277 – 77.197
Total Reflections (before merge)	21326
Data (I>–3.0/sigma(I)) [Reflections, Restraints, Parameters]	2892, 0, 190
S (=GooF)	0.998
Min. and Max. Residual Dens., [e/Å^3]	–0.45
	0.86
Threshold Expression	I>2sigma(I)
R_1	0.0667
wR_2	0.1666

Chapter 3

S.3.1. Synthesis and Characterisation of Compounds

S.3.1.1. Preparation of and Reactions with Au-Complexes

[Au(SIPr)Cl][446]

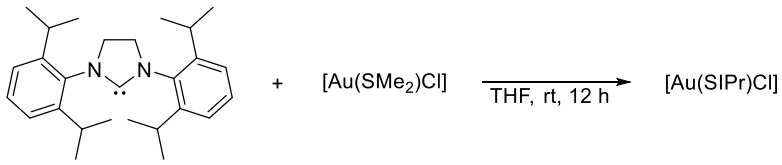

Scheme S.3.1. Synthesis of [Au(SIPr)Cl].

A flame dried Schlenk tube under an inert atmosphere was charged with 1,3-bis(2.6-di-*i*-propylphenyl)imidazolidin-2-ylidene (500 mg, 1.28 mmol), [Au(SMe_2)Cl] (400 mg, 1.36 mmol) and THF (90 mL). The mixture was stirred at rt in the dark for 12 h before it was filtered through celite. Activated carbon was added to the filtrate and the mixture was stirred in the dark for 4 h. It was then filtered through celite, THF was removed *in vacuo* and the remaining solid was taken up in DCM (13 mL). Pentane (33 mL) was added to cause precipitation of the product, which was collected by filtration, washed with pentane and dried under high vacuum to give the title compound (560 mg, 72%) as a white solid.

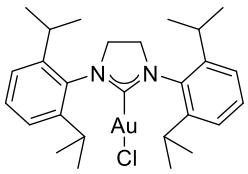

^{1}H NMR (400 MHz, $CDCl_3$) δ 7.39 (t, *J* = 7.8 Hz, 2H), 7.21 (d, *J* = 7.8 Hz, 4H), 4.02 (s, 4H), 3.03 (sept, *J* = 6.9 Hz, 4H), 1.40 (d, *J* = 6.9 Hz, 12H), 1.31 (d, *J* = 6.9 Hz, 12H); **^{13}C NMR** (100 MHz, $CDCl_3$) δ 196.1, 146.5, 134.0, 130.0, 124.6, 53.5, 29.0, 25.1, 24.1. The spectroscopic data were identical in all respects to those previously reported.[447]

[Au(SIPr)BF_4][448]

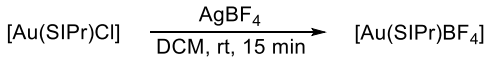

Scheme S.3.2. Synthesis of [Au(SIPr)BF_4].

A flame dried Schlenk tube under an inert atmosphere was charged with [Au(SIPr)Cl] (108 mg, 0.17 mmol), $AgBF_4$ (33.7 mg, 0.17 mmol) and DCM (2.4 mL). The resulting mixture was stirred at rt in the dark for 15 min, filtered through celite and the filtrate concentrated *in vacuo* (≈1.0 mL). Et_2O (8.0 mL) and hexane (5.5 mL) were added to the solution and the mixture was stirred for 30 min at rt. The formed precipitate was collected by filtration, washed with pentane and dried under high vacuum. The title compound (95 mg, 83%) was obtained as a white solid.

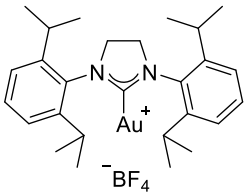

^{1}H NMR (500 MHz, $CDCl_3$) δ 7.42 (t, *J* = 7.8 Hz, 2H), 7.20 (d, *J* = 7.8 Hz, 4H), 4.02 (s, 4H), 2.89 (hept, *J* = 6.9 Hz, 4H), 1.29 (d, *J* = 6.9 Hz, 12H), 1.17 (d, *J* = 6.9 Hz, 12H); **^{19}F NMR** (471 MHz, $CDCl_3$) δ –153.5 (BF_4^-), –153.6 (BF_4^-); **^{13}C NMR** (126 MHz, $CDCl_3$) δ 186.4, 147.1, 134.3, 130.6, 125.1, 54.1, 29.4, 25.4, 24.3; **IR** (solid) ν 2959, 2927, 2868, 2163, 1491, 1460, 1384, 1364, 1345, 1322, 1275, 1177, 1100, 1060, 1020, 809, 763, 623, 608 cm^{-1}; **HRMS** (ESI-TOF) *m/z*

Calcd for $C_{27}H_{38}N_2Au$ $[Au(SIPr)]^+$ 578.2695, found 587.2675; Calcd for BF_4 $[BF_4]^-$ 86.0071, found 86.0070.

[Au(SIPr)F] (3.30)[449,450]

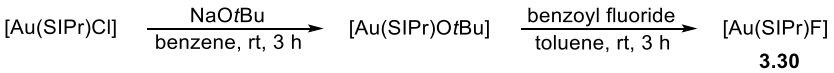

Scheme S.3.3. Synthesis of [Au(SIPr)F] (**3.30**).

A flame dried Schlenk tube under an inert atmosphere was charged with [Au(SIPr)Cl] (500 mg, 0.80 mmol), NaO*t*Bu (80.7 mg, 0.84 mmol) and benzene (37 mL), which had been degassed using three freeze-pump-thaw cycles. The resulting mixture was stirred at rt in the dark for 3 h before it was filtered through celite into a second flame dried Schlenk tube. Benzene was evaporated *in vacuo* and crude [Au(SIPr)O*t*Bu] was taken up in toluene (8.0 mL), which had been degassed using three freeze-pump-thaw cycles. Benzoyl fluoride (131 µL, 1.20 mmol) was added and the reaction was left to stir at rt in the dark for 3 h. During this time a white precipitate formed which was filtered off, washed with toluene and pentane and found to be analytically clean [Au(SIPr)F] (394 mg, 81%).

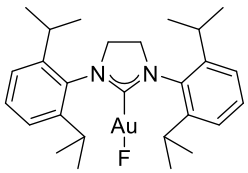

3.30

^{1}H NMR (500 MHz, CD_2Cl_2) δ 7.48 (t, *J* = 7.8 Hz, 2H), 7.30 (d, *J* = 7.8 Hz, 4H), 4.06 (s, 4H), 3.05 (hept, *J* = 6.9 Hz, 4H), 1.42 (d, *J* = 6.9 Hz, 12H), 1.34 (d, *J* = 6.9 Hz, 12H); **^{13}C NMR** (126 MHz, CD_2Cl_2) δ 186.0 (d, J_{C-F} = 60.5 Hz), 147.3, 134.9, 130.5, 125.2, 53.9 (d, J_{C-F} = 1.7 Hz), 29.5, 25.3, 24.5; **^{19}F NMR** (471 MHz, CD_2Cl_2) δ –247.3. The spectroscopic data were identical in all respects to those previously reported.[451]

{[1,3-Bis(2,6-diisopropylphenyl)imidazolin-2-ylidene]gold(I)[η^2-(3-hexyne)]} tetrafluoroborate (3.33)[85]

3.33

Scheme S.3.4. Synthesis of **3.33**.

A flame dried Schlenk tube under an inert atmosphere was charged with [Au(SIPr)Cl] (112 mg, 0.18 mmol), $AgBF_4$ (35.0 mg, 0.18 mmol) and DCM (2.0 mL). 3-Hexyne (30.7 µL, 0.27 mmol) was added to this mixture before it was stirred at rt in the dark for 10 min. Solids were removed by filtration through celite, the obtained solution was concentrated *in vacuo* (≈0.66 mL) and hexane (2.0 mL) was added to cause precipitation of the product. The white solid was filtered off, washed with hexane and dried under high vacuum to give analytically clean **3.33** (107 mg, 77%).

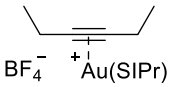

3.33

^{1}H NMR (500 MHz, CD_2Cl_2) δ 7.48 (t, *J* = 7.8 Hz, 2H), 7.31 (d, *J* = 7.8 Hz, 4H), 4.28 (s, 4H), 3.08 (hept, *J* = 6.9 Hz, 4H), 2.09 (q, *J* = 7.5 Hz, 4H), 1.38 (d, *J* = 6.9 Hz, 12H), 1.36 (d, *J* = 6.9 Hz, 12H), 0.51 (t, *J* = 7.5 Hz, 6H); **^{13}C NMR** (126 MHz, CD_2Cl_2) δ 199.4, 147.6, 133.5, 131.3, 125.5, 87.8, 54.9, 29.6, 25.6, 24.5, 15.2, 13.5; **^{19}F NMR** (471 MHz, CD_2Cl_2) δ –153.2 (BF_4^-), –153.3 (BF_4^-). The spectroscopic data were identical in all respects to those previously reported.[85]

Bromofluorination of 3-Hexyne with [Au(SIPr)F] and NBS

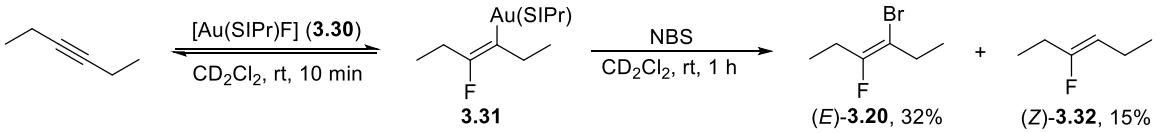

Scheme. S.3.5. Bromofluorination of 3-hexyne with [Au(SIPr)F] (**3.30**) and NBS.

In a flame dried Schlenk tube under an inert atmosphere [Au(SIPr)F] (30.3 mg, 0.050 mmol) was dissolved in CD_2Cl_2 (0.50 mL). 3-Hexyne (6.2 µL, 0.055 mmol) and C_6F_6 (5.8 µL, 0.050 mmol) were added to the resulting solution, which was then transferred into an NMR tube. After 10 min a stable amount of intermediate **3.31**, which was identified by its characteristic ^{19}F NMR peak at –97.4 ppm (t, *J* = 20.9 Hz), was present in the reaction. At this point NBS (8.9 mg, 0.050 mmol) dissolved in CD_2Cl_2 (0.50 mL) was added and after 1 h 32% of (*E*)-**3.20** and 15% of (*Z*)-**3.32** relative to the internal reference were found in the reaction mixture.

(*E*)-3-Bromo-4-fluorohex-3-ene ((*E*)-3.20)

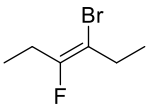

(*E*)-**3.20**

^{1}H NMR (500 MHz, CD_2Cl_2) δ 2.46–2.35 (m, 4H), 1.02 (t, *J* = 7.6 Hz, 3H), 1.00 (t, *J* = 7.5 Hz, 3H); **^{19}F NMR** (471 MHz, CD_2Cl_2) δ –108.6 (tt, *J* = 23.0, 3.5 Hz); **HRMS** (EI) *m/z* Calcd for C_7H_6FIO $[M]^+$ 179.9950, found 179.9947. The spectroscopic data were identical in all respects to those previously reported.[452]

(*Z*)-3-Fluorohex-3-ene ((*Z*)-3.32)

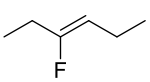

(*Z*)-**3.32**

Characteristic peaks: **^{1}H NMR** (500 MHz, CD_2Cl_2) δ 4.50 (dtt, *J* = 38.7, 7.6, 0.9 Hz 1H); **^{19}F NMR** (471 MHz, CD_2Cl_2) δ –110.8 (dtt, *J* = 38.7, 14.6, 1.7 Hz). The spectroscopic data were identical in all respects to those previously reported.[453]

Bromofluorination of 3.33

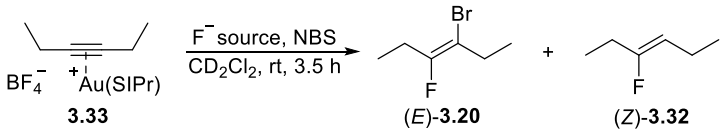

3.33 (*E*)-**3.20** (*Z*)-**3.32**

Scheme S.3.6. Bromofluorination of **3.33**.

Two flame dried Schlenk tubes under an inert atmosphere were charged with **3.33** (30.3 mg, 0.040 mmol) and CD_2Cl_2 (0.40 mL). In two separate flame dried Schlenk tubes NBS (7.1 mg, 0.040 mmol) was dissolved in CD_2Cl_2 (0.40 mL). $NEt_3{\cdot}3HF$ (6.5 µL, 0.040 mmol) was added to one NBS solution and TASF (11.0 mg, 0.040 mmol) to the other. Both of the resulting mixtures were added to a solution of **3.33** and the two reactions were stirred at rt in the dark for 3.5 h. They were then transferred into NMR tubes and analysed by ^{1}H and quantitative ^{19}F NMR. This revealed that in the reaction with $NEt_3{\cdot}3HF$ 18% of (*E*)-**3.20** and 8% of (*Z*)-**3.32** relative to BF_4^- had been formed whereas in the reaction with TASF 64% of (*E*)-**3.20** were found as the only fluorinated product.

Bromofluorination of 3-Hexyne with [Au(SIPr)BF_4] (Table 3.3)

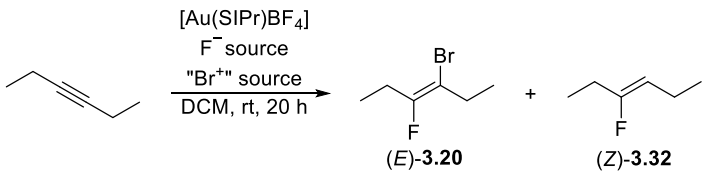

(*E*)-**3.20** (*Z*)-**3.32**

Scheme S.3.7. Bromofluorination of 3-hexyne with [Au(SIPr)BF_4].

A flame dried Schlenk tube under an inert atmosphere was charged with [Au(SIPr)BF_4] (1.7 mg, 0.0025 mmol) and the according fluoride source (0.050 mmol) as well as source

of electrophilic bromine (0.050 mmol). DCM (0.50 mL) was added and the mixture was stirred at rt for 20 h. Then, CD_2Cl_2 (0.30 mL) and C_6F_6 (5.8 µL, 0.050 mmol) were added and the solution was transferred into an NMR tube and analysed by ^1H and quantitative ^{19}F NMR.

S.3.1.2. Preparation of Brominating Reagents

1-Bromopyrrolidin-2-one (3.37)[242]

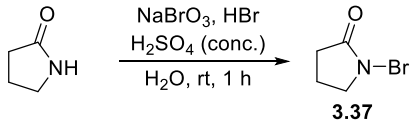

3.37

Scheme S.3.8. Synthesis of **3.37**.

HBr (48% in H_2O, 1.78 mL, 15.7 mmol) was added dropwise over 5 min to a mixture of pyrrolidin-2-one (2.00 g, 23.5 mmol), $NaBrO_3$ (1.77 g, 11.8 mmol) and conc. H_2SO_4 (313 µL, 5.87 mmol) in H_2O (7.0 mL) at rt. The reaction mixture was stirred for 1 h at rt in the dark before it was cooled to –78 °C for 5 min. It was then allowed to warm to rt. The product was filtered off, washed with H_2O and dried under high vacuum. **3.37** (891 mg, 23%) was obtained as a white solid.

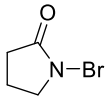

3.37

^{1}H NMR (400 MHz, $CDCl_3$) δ 3.57 (t, *J* = 7.7 Hz, 2H), 2.36 (t, *J* = 7.7 Hz, 2H), 2.20 (qn, *J* = 7.7 Hz, 2H); **^{13}C NMR** (100 MHz, $CDCl_3$) δ 174.37, 53.45, 26.61, 19.90. The spectroscopic data were identical in all respects to those previously reported.[242]

Synthesis of 3.39

1-(3,5-Bis(trifluoromethyl)benzyl)-1,4-diazabicyclo[2.2.2]octan-1-ium chloride[243]

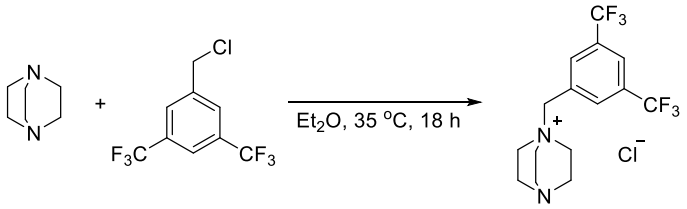

Scheme S.3.9. Synthesis of 1-(3,5-bis(trifluoromethyl)benzyl)-1,4-diazabicyclo[2.2.2]octan-1-ium chloride.

A flame dried flask under an inert atmosphere was charged with DABCO (2.46 g, 21.9 mmol) as well as 3,5-bis(trifluoromethyl)benzyl chloride (5.75 g, 21.9 mmol) and Et_2O (100 mL). The mixture was refluxed for 18 h during which the formation of a white precipitate was observed. After cooling to rt the product was filtered off, washed with Et_2O and dried under high vacuum. 1-(3,5-Bis(trifluoromethyl)benzyl)-1,4-diazabicyclo[2.2.2]octan-1-ium chloride (4.24 g, 52%) was obtained as a white solid.

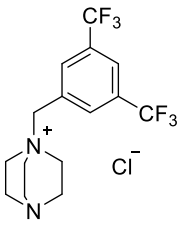

^{1}H NMR (400 MHz, MeOH-d_4) δ 8.25 (s, 2H), 8.22 (s, 1H), 4.87 (s, 2H), 3.48 (t, J = 7.6 Hz, 6H), 3.20 (t, J = 7.6 Hz, 6H); **^{13}C NMR** (100 MHz, MeOH-d_4) δ 135.1 (q, $J_{C–F}$ = 2.5 Hz), 133.9 (q, $J_{C–F}$ = 33.7 Hz), 131.3, 125.9 (q, $J_{C–F}$ = 3.6 Hz), 124.6 (q, $J_{C–F}$ = 272.4 Hz), 67.3, 53.8, 46.3; **^{19}F NMR** (377 MHz, MeOH-d_4) δ –64.3. The spectroscopic data were identical in all respects to those previously reported.[243]

1-(3,5-Bis(trifluoromethyl)benzyl)-1,4-diazabicyclo[2.2.2]octan-1-ium tetrafluoroborate[243]

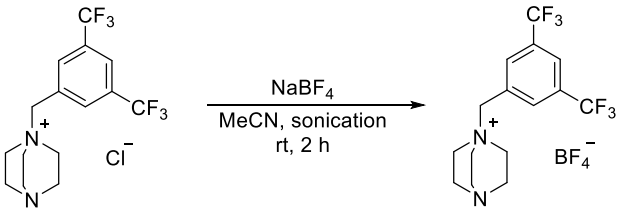

Scheme S.3.10. Synthesis of 1-(3,5-Bis(trifluoromethyl)benzyl)-1,4-diazabicyclo[2.2.2]octan-1-ium tetrafluoroborate.

A flame dried flask under an inert atmosphere was charged with 1-(3,5-bis(trifluoromethyl)benzyl)-1,4-diazabicyclo[2.2.2]octan-1-ium chloride (4.00 g, 10.7 mmol), $NaBF_4$ (11.72 g, 10.7 mmol) and MeCN (150 mL). The mixture was sonicated for 2 h with occasional swirling, before it was filtered through a pad of celite. The celite was rinsed with MeCN and the combined filtrate was evaporated to dryness under reduced pressure. The crude product was recrystallised from EtOH/MeCN (2:1) to give 1-(3,5-bis(trifluoromethyl)benzyl)-1,4-diazabicyclo[2.2.2]octan-1-ium tetrafluoroborate (3.99 g, 88%) as a white crystalline solid.

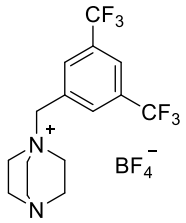

^{1}H NMR (400 MHz, MeOH-d_4) δ 8.18 (s, 2H), 8.14 (s, 1H), 4.68 (s, 2H), 3.46 (t, J = 7.6 Hz, 6H), 3.20 (t, J = 7.6 Hz, 6H); **^{13}C NMR** (100 MHz, MeOH-d_4) δ 135.0 (q, J_{C-F} = 3.1 Hz), 133.8 (q, J_{C-F} = 33.8 Hz), 131.1, 125.7 (sept, J_{C-F} = 3.8 Hz), 124.5 (q, J_{C-F} = 272.2 Hz), 67.3, 53.6, 46.1; **^{19}F NMR** (377 MHz, MeOH-d_4) δ –64.4, –155.4 (BF_4^-), –155.5 (BF_4^-). The spectroscopic data were identical in all respects to those previously reported.[243]

4,4'-Bromonium-bis(1-(3,5-bis(trifluoromethyl)benzyl)-1,4-λ^4-diazabicyclo[2.2.2]octan-1-ium) tetrafluoroborate (3.39)[243]

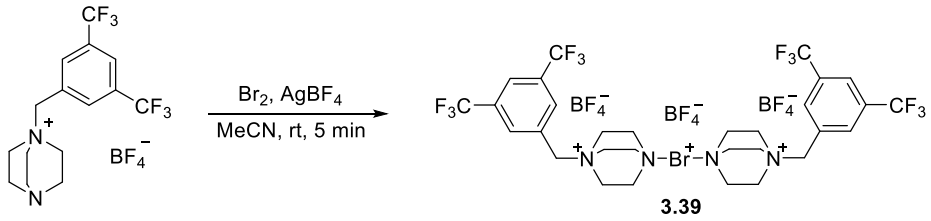

Scheme S.3.11. Synthesis of **3.39**.

Fume hood lights need to be switched off for this reaction. Br_2 (53 µL, 1.03 mmol) dissolved in MeCN (7.0 mL) was added dropwise over 3 min to a solution of 1-(3,5-bis(trifluoromethyl)benzyl)-1,4-diazabicyclo[2.2.2]octan-1-ium tetrafluoroborate (710 mg, 1.67 mmol) and $AgBF_4$ (178 mg, 0.92 mmol) in MeCN (70 mL) in an open flask. After the addition the flask was capped and the mixture stirred for 5 min. It was then filtered through celite, which was rinsed with MeCN. Volatiles were removed *in vacuo* and the resulting solid was taken up in a minimum amount of MeCN. DCM (70 mL) and hexane (140 mL) were added and the mixture was sonicated for 5 min. The formed solid was filtered off, rinsed with hexane and dried on the sinter funnel. It was then taken up in $MeNO_2$ (17 mL) to give a cloudy solution, which was filtered through celite. The celite was rinsed with additional $MeNO_2$ (17 mL), and DCM (60 mL) and hexane (70 mL) were added to cause precipitation of **3.39**. The mixture was sonicated for 5 min, before the solid product was filtered off, rinsed with hexane and dried under high vacuum. **3.39** (393 mg, 23%) was obtained as a white solid.

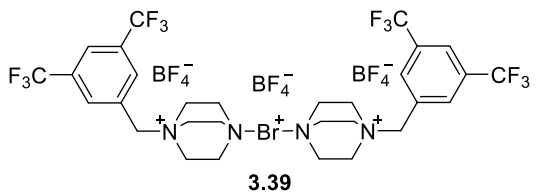

3.39

^{1}H NMR (400 MHz, MeCN-d_3) δ 8.24 (s, 2H), 8.09 (s, 4H), 4.65 (s, 4H), 3.69–3.60 (m, 12H), 3.58–3.53 (m, 12H); **^{13}C NMR** (100 MHz, MeCN-d_3) δ 135.1 (q, $J_{C–F}$ = 3.7 Hz), 133.6 (q, $J_{C–F}$ = 33.9 Hz), 129.9, 126.6 (sept, $J_{C–F}$ = 3.7 Hz), 124.5 (q, $J_{C–F}$ = 272.2 Hz), 67.5, 54.2, 51.4; **^{19}F NMR** (377 MHz, MeCN-d_3) δ –63.5, –151.2 (BF_4^-), –151.2 (BF_4^-). The spectroscopic data were identical in all respects to those previously reported.[243]

S.3.1.3. Synthesis of Ligands for Ullmann Coupling

(*E*)-*N*-Phenyl-1-(pyridin-2-yl)methanimine (B)[454]

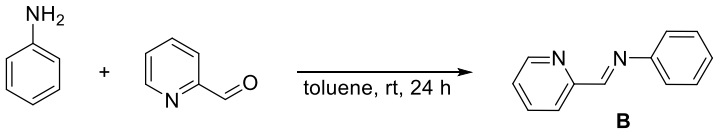

B

Scheme S.3.12. Preparation of ligand **B**.

A solution of aniline (456 µL, 5.00 mmol) and 2-pyridinecarboxaldehyde (476 µL, 5.00 mmol) in toluene (2.5 mL) was stirred at rt for 24 h. Volatiles were removed *in vacuo* and residual water was removed by co-evaporation with toluene. Drying under high vacuum gave the title compound (909 mg, quant.) as a yellow oil.

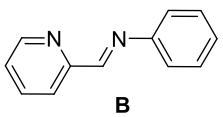

B

^{1}H NMR (400 MHz, $CDCl_3$) δ 8.70 (ddd, *J* = 4.9, 1.7, 1.1 Hz, 1H), 8.59 (s, 1H), 8.19 (dt, *J* = 7.7, 1.1 Hz, 1H), 7.80 (td, *J* = 7.7, 1.7 Hz, 1H), 7.43–7.37 (m, 2H), 7.35 (ddd, *J* = 7.7, 4.9, 1.1 Hz, 1H), 7.30–7.25 (m, 3H); **^{13}C NMR** (100 MHz, $CDCl_3$) δ 160.6, 154.5, 150.9, 149.7, 136.7, 129.2, 126.7, 125.1, 121.9, 121.1. The spectroscopic data were identical in all respects to those previously reported.[454]

2-(Pyridin-2-yl)-1*H*-benzo[*d*]imidazole (C)[455]

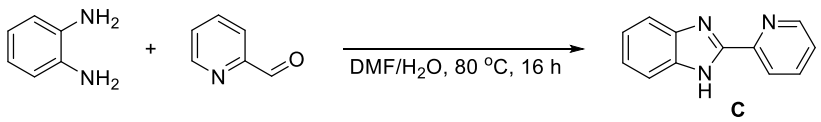

Scheme S.3.13. Preparation of ligand **C**.

A solution of benzene-1,2-diamine (433 mg, 4.00 mmol) and 2-pyridinecarboxaldehyde (380 µL, 4.00 mmol) in a mixture of DMF (36 mL) and H_2O (4.0 mL) was heated to 80 °C for 16 h under air. It was then cooled to rt, solvents were removed *in vacuo* and subsequent column chromatography (SiO_2, DCM) gave the title compound (581 mg, 74%) as a white solid.

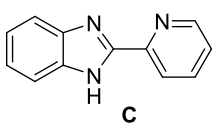

^{1}H NMR (500 MHz, DMSO-d_6) δ 13.09 (s, 1H), 8.73 (ddd, *J* = 4.8, 1.8, 1.2 Hz, 1H), 8.33 (dt, *J* = 7.8, 1.2 Hz, 1H), 8.00 (td, *J* = 7.8, 1.8 Hz, 1H), 7.70 (d, *J* = 7.7 Hz, 1H), 7.54 (d, *J* = 7.7 Hz, 1H), 7.52 (ddd, *J* = 7.8, 4.8, 1.2 Hz, 1H), 7.26–7.18 (m, 2H); **^{13}C NMR** (126 MHz, DMSO-d_6) δ 150.7, 149.3, 148.5, 143.8, 137.5, 134.9, 124.7, 123.1, 121.9, 121.4, 119.3, 112.0. The spectroscopic data were identical in all respects to those previously reported.[455]

(±)-(*N*,*N*'-Bis(pyridin-2-ylmethylene)cyclohexane-1,2-diamine[420] **(D)**

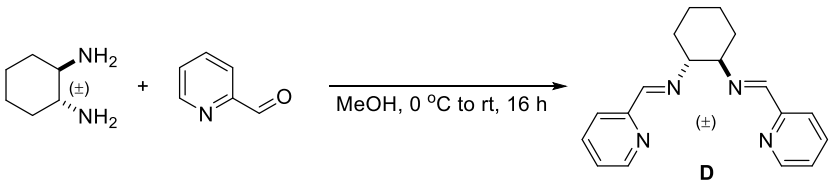

Scheme S.3.14. Preparation of ligand **D**.

A flame dried flask was charged with molecular sieves (3 Å), MeOH (20 mL) and (±)-trans-diaminocyclohexane (480 µL, 4.00 mmol). The mixture was cooled to 0 °C and a solution of 2-pyridinecarboxaldehyde (837 µL, 8.80 mmol) in MeOH (20 mL) was added. It was then slowly warmed to rt over the course of 16 h and filtered through a plug of celite. Removing solvents *in vacuo* gave **D** (1.17 g, quant.) as a yellow solid.

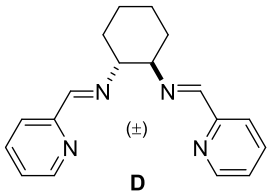

D

^{1}H NMR (400 MHz, $CDCl_3$) δ 8.50 (ddd, *J* = 4.9, 1.8, 1.1 Hz, 2H), 8.27 (s, 2H), 7.84 (dt, *J* = 7.7, 1.1 Hz, 2H), 7.62–7.57 (m, 2H), 7.17 (ddd, *J* = 7.7, 4.9, 1.1 Hz, 2H), 3.54–3.45 (m, 2H), 1.88–1.74 (m, 6H), 1.51–1.42 (m, 2H); **^{13}C NMR** (100 MHz, $CDCl_3$) δ 161.4, 154.5, 149.2, 136.4, 124.4, 121.3, 73.5, 32.7, 24.3. The spectroscopic data were identical in all respects to those previously reported.[420]

S.3.1.4. Synthesis of Alkyne Substrates

General Procedure (GP) 1: Preparation of (1-Propynyl)arenes[456]

3.34

Scheme S.3.15. General procedure for the preparation of (1-propynyl)arenes

A flame dried Schlenk tube under an inert atmosphere was charged with $[Pd(PPh_3)_2Cl_2]$ (21.1 mg, 1.0 mol%), dppb (25.6 mg, 2.0 mol%), 2-butynoic acid (303 mg, 3.60 mmol) and the accordingly substituted iodobenzene (3.00 mmol). DMSO (9.0 mL) was added followed by DBU (1.35 mL, 9.00 mmol) before the resulting solution was degassed (three

freeze-pump-thaw cycles). The reaction mixture was stirred at 110 °C for 12 h before letting it cool to rt. Sat. aq. NH_4Cl was added to quench the reaction and the aqueous mixture was extracted with DCM. The combined organic layers were washed with H_2O and brine before being dried over $MgSO_4$. Volatiles were removed *in vacuo* and clean products were obtained after subsequent column chromatography.

General Procedure (GP) 2: Preparation of (1-Hexynyl)arenes[457]

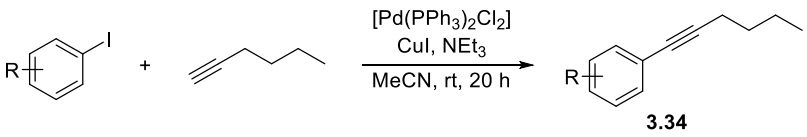

3.34

Scheme S.3.16. General procedure for the preparation of (1-hexynyl)arenes.

A flame dried Schlenk tube under an inert atmosphere was charged with $[Pd(PPh_3)_2Cl_2]$ (14.7 mg, 0.021 mmol) and CuI (28.6 mg, 0.15 mmol). Degassed MeCN/NEt_3 (1:4, 10 mL; three freeze-pump-thaw cycles), the accordingly substituted iodobenzene (6.00 mmol) as well as 1-hexyne (345 µL, 3.00 mmol) were added to the mixture before it was stirred for 20 h at rt. H_2O and DCM were then added, the layers were separated and the aqueous layer was extracted with DCM. The combined organic layers were dried over $MgSO_4$ and concentrated *in vacuo*. Clean products were obtained after column chromatography.

Hex-1-yn-1-ylbenzene (3.34c)

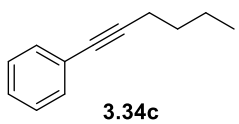
3.34c

The title compound was prepared according to GP2 using iodobenzene (671 µL, 6.00 mmol). Column chromatography (SiO_2, pentane) gave **3.34c** (468 mg, 99%) as a colourless oil. **^{1}H NMR** (400 MHz, $CDCl_3$) δ 7.39–7.33 (m, 2H), 7.28–7.21 (m, 3H), 2.38 (t, *J* = 7.0 Hz, 2H), 1.60–1.52 (m, 2H), 1.50–1.40 (m, 2H), 0.92 (t, *J* = 7.3 Hz, 3H); **^{13}C NMR** (100 MHz, $CDCl_3$) δ 131.5, 128.1, 127.4, 124.1, 90.4, 80.5, 30.8, 22.0, 19.1, 13.6. The spectroscopic data were identical in all respects to those previously reported.[458]

1-(*t*-Butyl)-4-(prop-1-yn-1-yl)benzene (3.34e)

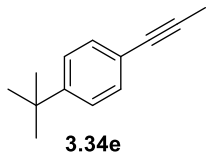
3.34e

The title compound was prepared according to GP1 using 1-*t*-butyl-4-iodobenzene (532 µL, 3.00 mmol). Column chromatography (SiO_2, pentane) gave **3.34e** (446 mg, 87%) as a colourless oil, which crystallised upon standing at rt for a prolonged time to give a white solid. **^{1}H NMR** (400 MHz, $CDCl_3$) δ 7.31 (ad, *J* = 8.9 Hz, 2H), 7.28 (ad, *J* = 8.9 Hz, 2H), 2.02 (s, 3H), 1.28 (s, 9H); **^{13}C NMR** (100 MHz, $CDCl_3$) δ 150.6, 131.1, 125.2, 121.0, 84.9, 79.7, 34.7, 31.2, 4.4. The spectroscopic data were identical in all respects to those previously reported.[456]

1-Chloro-4-(prop-1-yn-1-yl)benzene (3.34f)

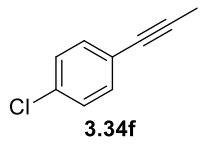

3.34f

The title compound was prepared according to GP1 using 1-chloro-4-iodobenzene (715 mg, 3.00 mmol). Column chromatography (SiO_2, pentane) gave **3.34f** (327 mg, 72%) as a colourless oil. **^{1}H NMR** (400 MHz, $CDCl_3$) δ 7.29 (ad, *J* = 8.6 Hz, 2H), 7.23 (ad, *J* = 8.6 Hz, 2H), 2.02 (s, 3H); **^{13}C NMR** (100 MHz, $CDCl_3$) δ

133.4, 132.7, 128.5, 122.5, 86.9, 78.7, 4.3. The spectroscopic data were identical in all respects to those previously reported.[459]

1-Methoxy-4-(prop-1-yn-1-yl)benzene (3.34g)

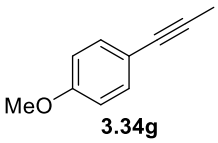

3.34g

The title compound was prepared according to GP1 using 1-iodo-4-methoxybenzene (702 mg, 3.00 mmol). Column chromatography (SiO_2, 0–5% Et_2O in pentane) gave **3.34g** (364 mg, 83%) as a colourless oil. **^{1}H NMR** (400 MHz, $CDCl_3$) δ 7.30 (ad, *J* = 8.9 Hz, 2H), 6.79 (ad, *J* = 8.9 Hz, 2H), 3.78 (s, 3H), 2.01 (s, 3H); **^{13}C NMR** (100 MHz, $CDCl_3$) δ 159.0, 132.8, 116.1, 113.8, 84.1, 79.4, 55.2, 4.3. The spectroscopic data were identical in all respects to those previously reported.[459]

1-(Prop-1-yn-1-yl)-4-(trifluoromethyl)benzene (3.34h)

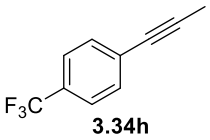

3.34h

The title compound was prepared according to GP1 using 1-iodo-4-(trifluoromethyl)benzene (441 µL, 3.00 mmol). Column chromatography (SiO_2, pentane) gave **3.34h** (394 mg, 71%) as a colourless oil. **^{1}H NMR** (500 MHz, $CDCl_3$) δ 7.51 (ad, *J* = 8.2 Hz, 2H), 7.46 (ad, *J* = 8.2 Hz, 2H), 2.05 (s, 3H); **^{13}C NMR** (126 MHz, $CDCl_3$) δ 131.7, 129.3 (q, $J_{C–F}$ = 32.6 Hz), 127.9 (q, $J_{C–F}$ = 0.9 Hz), 125.1 (q, $J_{C–F}$ = 3.8 Hz), 124.0 (q, $J_{C–F}$ = 271.9 Hz) 88.7, 78.7, 4.4; **^{19}F NMR** (471 MHz, $CDCl_3$) δ –62.8. The spectroscopic data were identical in all respects to those previously reported.[460]

1-(4-(Prop-1-yn-1-yl)phenyl)ethan-1-one (3.34i)

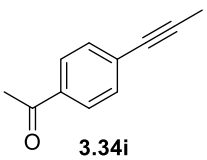

3.34i

The title compound was prepared according to GP1 using 4'-iodoacetophenone (738 mg, 3.00 mmol). Column chromatography (SiO_2, 10% Et_2O in pentane) gave **3.34i** (435 mg, 92%) as a white solid. **^{1}H NMR** (400 MHz, $CDCl_3$) δ 7.85 (ad, *J* = 8.5 Hz, 2H), 7.43 (ad, *J* = 8.5 Hz, 2H), 2.56 (s, 3H),

2.06 (s, 3H); **^{13}C NMR** (100 MHz, $CDCl_3$) δ 197.4, 135.7, 131.6, 129.0, 128.2, 89.8, 79.2, 26.6, 4.5. The spectroscopic data were identical in all respects to those previously reported.[461]

(3-(Prop-1-yn-1-yl)phenyl)methanol (3.34j)

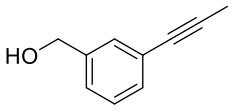

3.34j

The title compound was prepared according to GP1 using (3-iodophenyl)methanol (381 µL, 3.00 mmol). Column chromatography (SiO_2, 25% Et_2O in pentane) gave **3.34j** (429 mg, 98%) as a yellow oil. **^{1}H NMR** (400 MHz, $CDCl_3$) δ 7.40–7.38 (m, 1H), 7.34–7.30 (m, 1H), 7.29–7.26 (m, 2H), 4.65 (s, 2H), 2.05 (s, 3H), 1.79 (bs, 1H); **^{13}C NMR** (100 MHz, $CDCl_3$) δ 140.9, 130.7, 129.9, 128.4, 126.1, 124.2, 86.0, 79.5, 64.9, 4.3; **IR** (neat) ν 3320, 2916, 2874, 1603, 1581, 1483, 1431, 1282, 1170, 1025, 1002, 895, 788, 689 cm^{-1}; **HRMS** (CI) *m/z* Calcd for $C_{10}H_{14}NO$ $[M+NH_4]^+$ 164.1070, found 164.1075.

Ethyl 3-(prop-1-yn-1-yl)benzoate (3.34k)

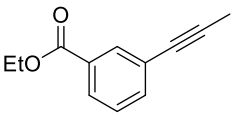

3.34k

The title compound was prepared according to GP1 using ethyl 3-iodobenzoate (505 µL, 3.00 mmol). Column chromatography (SiO_2, 3% Et_2O in pentane) gave **3.34k** (530 mg, 94%) as a colourless oil. **^{1}H NMR** (400 MHz, $CDCl_3$) δ 8.04 (t, *J* = 1.5 Hz, 1H), 7.92 (dt, *J* = 7.8, 1.5 Hz, 1H), 7.53 (dt, *J* = 7.8, 1.5 Hz, 1H), 7.33 (td, *J* = 7.8, 0.6 Hz, 1H), 4.35 (q, *J* = 7.1 Hz, 2H), 2.04 (s, 3H), 1.37 (t, *J* = 7.1 Hz, 3H); **^{13}C NMR** (100 MHz, $CDCl_3$) δ 166.0, 135.6, 132.6, 130.6, 128.5, 128.3, 124.3, 86.8, 78.9, 61.1, 14.3, 4.3. The spectroscopic data were identical in all respects to those previously reported.[462]

3-(Prop-1-yn-1-yl)benzoic acid (3.34l)

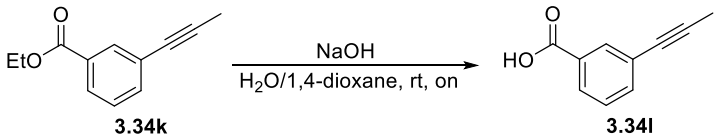

3.34k 3.34l

Scheme S.3.17. Synthesis of substrate **3.34l**.

A flask was charged with 1,4-dioxane (3.0 mL), **3.34k** (282 mg, 1.50 mmol) and 2 M aq. NaOH (3.0 mL) and the mixture was stirred at rt over night. It was then extracted with DCM and the DCM layers were discarded. The aqueous layer was acidified with 6 M aq. HCl until pH 1 and again extracted with DCM. The combined organic layers were dried over $MgSO_4$ and volatiles were removed *in vacuo* to give the title compound (230 mg, 96%) as a white solid.

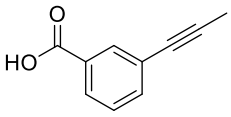

3.34l

M.p. (DCM) = 127–128 °C; **^{1}H NMR** (400 MHz, $CDCl_3$) δ 8.12 (t, *J* = 1.5 Hz, 1H), 7.99 (dt, *J* = 7.8, 1.5 Hz, 1H), 7.59 (dt, *J* = 7.8, 1.5 Hz, 1H), 7.38 (td, *J* = 7.8, 0.6 Hz, 1H), 2.05 (s, 3H); **^{13}C NMR** (100 MHz, $CDCl_3$) δ 171.5, 136.5, 133.2, 129.4, 129.1, 128.4, 124.7, 87.2, 78.6, 4.3; **IR** (solid) ν 2963, 2922, 2845, 2226, 1682, 1599, 1578, 1441, 1414, 1302, 1244, 1082, 930, 914, 810, 750, 718, 679, 660, 571 cm^{-1}; **HRMS** (ESI-TOF) *m/z* Calcd for $C_{10}H_7O_2$ $[M–H]^-$ 159.0452, found 159.0451.

1-Bromo-3-(prop-1-yn-1-yl)benzene (3.34m)[463]

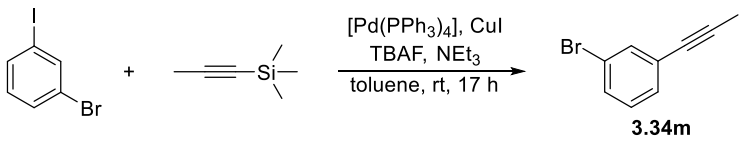

3.34m

Scheme S.3.18. Synthesis of substrate **3.34m**.

A flame dried Schlenk tube under an inert atmosphere was charged with $[Pd(PPh_3)_4]$ (173 mg, 0.15 mmol) and CuI (171 mg, 0.90 mmol). Toluene (6.0 mL), 3-bromoiodobenzene (382 µL, 3.00 mmol), 1-trimethylsilylpropyne (444 µL, 3.00 mmol), NEt_3 (1.38 mL, 9.90 mmol) and TBAF (1.0 M in THF, 3.00 mL, 3.00 mmol) were added. The resulting mixture was stirred at rt for 17 h before it was partitioned between Et_2O and H_2O. The layers were separated and the aqueous layer was extracted with Et_2O. The combined organic layers were dried over $MgSO_4$. Column chromatography (SiO_2, pentane) gave the title compound (571 mg, 98%) as a colourless oil.

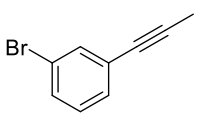

3.34m

^{1}H NMR (500 MHz, $CDCl_3$) δ 7.52 (t, *J* = 1.9 Hz, 1H), 7.38 (ddd, *J* = 7.8, 1.9, 1.2 Hz, 1H), 7.28 (dt, *J* = 7.8, 1.2 Hz, 1H), 7.12 (t, *J* = 7.8 Hz, 1H), 2.02 (s, 3H); **^{13}C NMR** (126 MHz, $CDCl_3$) δ 134.3, 130.7, 130.0, 129.6, 126.0, 122.0, 87.4, 78.3, 4.3; **IR** (neat) ν 3063, 2916, 2849, 2361, 1589, 1555, 1472, 1402, 1076, 995, 988, 880, 777, 746, 679, 660 cm^{-1}; **HRMS** (CI) *m/z* Calcd for $C_9H_{11}{}^{79}BrN$ $[M+NH_4]^+$ 212.0069, found 212.0061. The spectroscopic data were identical in all respects to those previously reported.[463]

1-Methyl-2-(prop-1-yn-1-yl)benzene (3.34n)

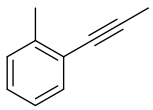
3.34n

The title compound was prepared according to GP1 using 2-iodotoluene (382 µL, 3.00 mmol). Column chromatography (SiO_2, pentane) gave **3.34n** (355 mg, 91%) as a colourless oil. **^{1}H NMR** (400 MHz, $CDCl_3$) δ 7.34 (dt, *J* = 7.4, 1.2 Hz, 1H), 7.16–7.13 (m, 2H), 7.11–7.05 (m, 1H), 2.39 (s, 3H), 2.08 (s, 3H); **^{13}C NMR** (100 MHz, $CDCl_3$)

δ 139.9, 131.8, 129.3, 127.5, 125.4, 123.8, 89.6, 78.5, 20.7, 4.5. The spectroscopic data were identical in all respects to those previously reported.[462]

2-(Prop-1-yn-1-yl)benzonitrile (3.34o)

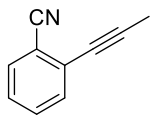

3.34o

The title compound was prepared according to GP1 using 2-iodobenzonitrile (687 mg, 3.00 mmol). Column chromatography (SiO_2, 2% Et_2O in pentane) gave **3.34o** (403 mg, 95%) as a white solid. **M.p.** (pentane) = 34 °C; **^{1}H NMR** (500 MHz, $CDCl_3$) δ 7.58 (dt, *J* = 7.8, 0.9 Hz, 1H), 7.50–7.44 (m, 2H), 7.32 (ddd, *J* = 7.8, 6.3, 2.5 Hz, 1H), 2.12 (s, 3H); **^{13}C NMR** (126 MHz, $CDCl_3$) δ 132.5, 132.3, 132.2, 128.0, 127.6, 117.8, 115.2, 93.4, 76.3, 4.6; **IR** (solid) ν 3102, 3069, 2924, 2845, 2361, 2222, 1595, 1564, 1483, 1445, 1371, 1281, 1167, 953, 756, 733, 677 cm^{-1}; **HRMS** (ESI-TOF) *m/z* Calcd for $C_{10}H_7NNa$ $[M+Na]^+$ 164.0471, found 164.0472.

1-(Hex-1-yn-1-yl)-4-nitrobenzene (3.34p)

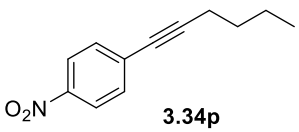

3.34p

The title compound was prepared according to GP2 using 1-iodo-4-nitrobenzene (1.49 g, 6.00 mmol). Column chromatography (SiO_2, 0–2% Et_2O in pentane) gave **3.34p** (547 mg, 90%) as a light yellow oil. **^{1}H NMR** (400 MHz, $CDCl_3$) δ 8.13 (ad, *J* = 8.9 Hz, 2H), 7.49 (ad, *J* = 8.9 Hz, 2H), 2.43 (t, *J* = 7.0 Hz, 2H), 1.63–1.54 (m, 2H), 1.52–1.41 (m, 2H), 0.94 (t, *J* = 7.3 Hz, 3H); **^{13}C NMR** (100 MHz, $CDCl_3$) δ 140.9, 130.7, 129.9, 128.4, 126.1, 124.2, 86.0, 79.5, 64.9, 4.3. The spectroscopic data were identical in all respects to those previously reported.[464]

Hex-1-yn-1-ylcyclohexane (3.34r)[465]

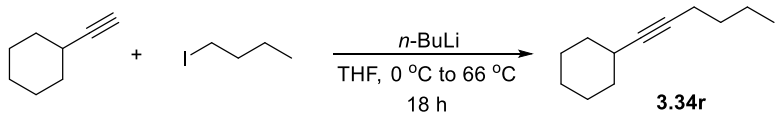

Scheme S.3.19. Synthesis of substrate **3.34r**.

A flame dried flask under an inert atmosphere was charged with THF (10 mL) and cyclohexylacetylene (392 µL, 3.00 mmol), and the resulting solution was cooled to 0 °C. *n*-BuLi (2.5 M in hexanes, 1.20 mL, 3.00 mmol) was added dropwise and the mixture was stirred at 0 °C for 20 min. before it was warmed to rt. 1-Iodobutane (512 µL, 4.50 mmol) was added and the reaction was refluxed for 18 h. It was then diluted with Et_2O, washed with H_2O and brine and dried over $MgSO_4$. Volatiles were removed *in vacuo* and column chromatography (SiO_2, pentane) was used to obtain the pure title compound (454 mg, 92%) as a colourless oil.

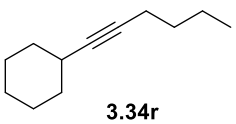
3.34r

^{1}H NMR (400 MHz, $CDCl_3$) δ 2.29 (tdd, *J* = 9.0, 4.7, 2.1 Hz, 1H), 2.14 (td, *J* = 6.9, 2.1 Hz, 2H), 1.79–1.71 (m, 2H), 1.71–1.60 (m, 2H), 1.52–1.31 (m, 7H), 1.33–1.17 (m, 3H), 0.88 (t, *J* = 7.2 Hz, 3H); **^{13}C NMR** (100 MHz, $CDCl_3$) δ 84.6, 80.0, 33.2, 31.4, 29.2, 26.0, 25.0, 21.9, 18.4, 13.7. The spectroscopic data were identical in all respects to those previously reported.[465]

2,2-Dimethyloct-3-yne (3.34s)[466]

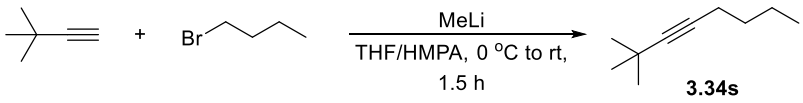

Scheme S.3.20. Preparation of substrate **3.34s**.

A flame dried Schlenk tube under an inert atmosphere was charged with THF (2.1 mL) and *t*-butylacetylene (369 µL, 3.00 mmol). The resulting solution was cooled to 0 °C before MeLi (1.6 M in THF, 2.06 mL, 3.30 mmol) was added dropwise. Then a solution of 1-bromobutane (322 µL, 3.00 mmol) in HMPA (4.0 mL) was added dropwise, the reaction was allowed to warm to rt and stirred for 1.5 h. The mixture was partitioned between H_2O and pentane, the layers were separated and the aqueous one was extracted with pentane. The combined organic layers were dried over $MgSO_4$ and solvents were removed *in vacuo*. Subsequent column chromatography (SiO_2, pentane) gave **3.34s** (213 mg, 51%) as a colourless oil.

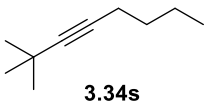

3.34s

^{1}H NMR (500 MHz, $CDCl_3$) δ 2.11 (t, *J* = 7.0 Hz, 2H), 1.46–1.40 (m, 2H), 1.40–1.33 (m, 2H), 1.17 (s, 9H), 0.88 (t, *J* = 7.2 Hz, 3H); **^{13}C NMR** (126 MHz, $CDCl_3$) δ 88.9, 78.5, 31.4, 31.4, 27.3, 21.9, 18.4, 13.7. The spectroscopic data were identical in all respects to those previously reported.[466]

2-Methyl-5-(prop-1-yn-1-yl)thiophene (3.34t)

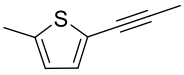

3.34t

The title compound was prepared according to GP1 using (2-iodo-5-methylthiophene (363 µL, 3.00 mmol). Column chromatography (SiO_2, pentane) gave **3.34t** (369 mg, 90%) as a colourless oil. **^{1}H NMR** (500 MHz, $CDCl_3$) δ 6.89 (d, *J* = 3.5 Hz, 1H), 6.55 (dq, *J* = 3.5, 1.1 Hz, 1H), 2.42 (d, *J* = 1.1 Hz, 3H), 2.04 (s, 3H); **^{13}C NMR** (126 MHz, $CDCl_3$) δ 140.5, 131.0, 124.9, 121.7, 89.0, 73.2, 15.3, 4.6; **IR** (neat) ν 3075, 2914, 2847, 2735, 2361, 2342, 1541, 1474, 1437, 1375, 1244, 1196, 1161, 1045, 908, 893 cm^{-1}; **HRMS** (CI) *m/z* Calcd for C_8H_9S $[M+H]^+$ 137.0419, found 137.0419.

3-(Prop-1-yn-1-yl)furan (3.34u)

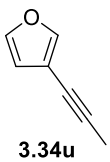

3.34u

The title compound was prepared according to GP1 using 3-bromofuran (270 µL, 3.00 mmol). Column chromatography (SiO_2, pentane) gave **3.34u** (105 mg, 33%) as a volatile colourless oil. **^{1}H NMR** (500 MHz, $CDCl_3$) δ 7.51 (t, *J* = 0.7 Hz, 1H), 7.31 (t, *J* = 1.8 Hz, 1H), 6.37 (dd, *J* = 1.8, 0.7 Hz, 1H), 1.99 (s, 3H); **^{13}C NMR** (126 MHz, $CDCl_3$) δ 144.9, 142.5, 112.6, 108.0, 87.4, 70.5, 4.3; **IR** (neat) ν 3148, 3132, 2918, 2853, 2361, 1506, 1441, 1352, 1290, 1161, 1082, 1036, 1005, 870, 783, 729, 635, 594 cm^{-1}; **HRMS** (CI) *m/z* Calcd for C_7H_7O $[M+H]^+$ 107.0491, found 107.0492.

S.3.1.5. Halofluorination of Alkynes

General Procedure (GP) 3: Halofluorination of Electron-Rich Alkynes (Conditions A)

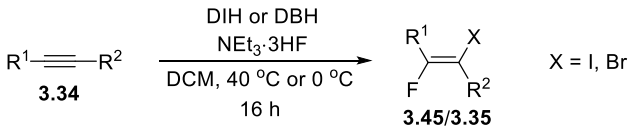

Scheme S.3.21. General procedure for the halofluorination of electron-rich alkynes.

In a flask flushed with Ar, a solution of alkyne, **3.34** (0.20 mmol), and 1,3-diiodo-5,5-dimethylhydantoin (DIH) (76.0 mg, 0.20 mmol) or 1,3-dibromo-5,5-dimethylhydantoin (DBH) (57.2 mg, 0.20 mmol) in HPLC-grade DCM (2.0 mL) was prepared. If DIH is used, NEt_3·3HF (98 µL, 0.60 mmol) was now added to the reaction before it was heated to 40 °C for 16 h. In the case of bromofluorination using DBH, the reaction was at first cooled to 0 °C before NEt_3·3HF (98 µL, 0.60 mmol) was added. It was then stirred at 0 °C for 16 h. In both cases, after 16 h the reaction was brought to rt, diluted with DCM and quenched with sat. aq. $NaHCO_3$. The layers were separated and the aqueous one was extracted with

DCM. The combined organic layers were dried over $MgSO_4$ and volatiles were removed *in vacuo*. If impurities were present at this stage column chromatography was used to obtain clean products.

General Procedure (GP) 4: Iodofluorination of Electron-Poor Alkynes (Conditions B)

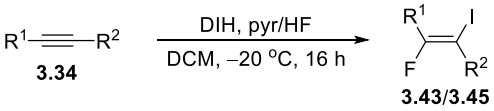

Scheme S.3.22. General procedure for the iodofluorination of electron-poor alkynes.

In a plastic falcon tube flushed with Ar, a solution of alkyne (0.20 mmol) and 1,3-diiodo-5,5-dimethylhydantoin (DIH) (76.0 mg, 0.20 mmol) in DCM (2.0 mL) was prepared. After cooling to –20 °C, pyr/HF (15.6 µL, 0.60 mmol) was added and the reaction was stirred for 16 h. It was then warmed to rt, diluted with DCM and quenched with sat. aq. $NaHCO_3$. The layers were separated and the aqueous one was extracted with DCM. The combined organic layers were dried over $MgSO_4$ and volatiles were removed *in vacuo*. Column chromatography was used to obtain clean products.

General Procedure (GP) 5: Double Iodofluorination of Terminal Alkynes (Conditions C)

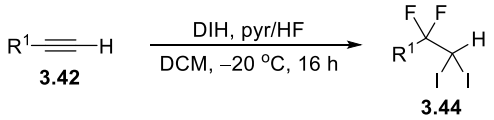

Scheme S.3.23. Double iodofluorination of terminal alkynes.

In a plastic falcon tube flushed with Ar, a solution of alkyne (0.20 mmol) and 1,3-diiodo-5,5-dimethylhydantoin (DIH) (76.0 mg, 0.20 mmol) in DCM (2.0 mL) was prepared. After cooling to –20 °C pyr/HF (46.8 µL, 1.80 mmol) was added and the reaction was stirred for 16 h. It was then warmed to rt, diluted with DCM and quenched with sat. aq. $NaHCO_3$. The layers were separated and the aqueous one was extracted with DCM. The combined organic layers were dried over $MgSO_4$ and volatiles were removed *in vacuo*. Column chromatography was used to obtain clean products.

(*E*)-5-Fluoro-6-iododec-5-ene (3.45a)

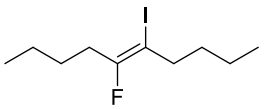

3.45a

The title compound was prepared according to GP3 using dec-5-yne (36.1 µL, 0.20 mmol) and DIH (76.0 mg, 0.20 mmol). **3.45a** was obtained as an analytically clean colourless oil after work-up. **3.45a** was also prepared on a 5.00 mmol scale following the same procedure. **^{1}H NMR** (500 MHz, $CDCl_3$) δ 2.53 (dt, *J* = 23.3, 7.4 Hz, 2H), 2.43 (td, *J* = 7.4, 3.0 Hz, 2H), 1.52–1.46 (m, 2H), 1.46–1.38 (m, 2H), 1.38–1.32 (m, 2H), 1.32–1.23 (m, 2H), 0.91 (t, *J* = 7.4 Hz, 3H), 0.89 (t, *J* = 7.4 Hz, 3H); **^{13}C NMR** (126 MHz, $CDCl_3$) δ 158.1 (d, $J_{C–F}$ = 259.5 Hz), 83.7 (d, $J_{C–F}$ = 33.1 Hz), 34.6 (d, $J_{C–F}$ = 6.5 Hz), 33.2 (d, $J_{C–F}$ = 28.1 Hz), 31.1 (d, $J_{C–F}$ = 1.7 Hz), 28.3, 21.9, 21.4, 13.8, 13.8; **^{19}F NMR** (471 MHz, $CDCl_3$) δ –93.9 (tt, *J* = 23.3, 3.0 Hz); **IR** (neat) ν 2958, 2928, 2872, 2862, 2361, 2341, 1671, 1465, 1431, 1379, 1219, 1179, 1104, 963, 946, 864, 842, 744 cm^{-1}; **HRMS** (EI) *m/z* Calcd for $C_{10}H_{18}FI$ $[M]^+$ 284.0437, found 284.0434.

(*E*)-(1-Fluoro-2-iodoprop-1-en-1-yl)benzene (3.45b)

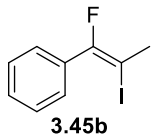

3.45b

The title compound was prepared according to GP3 using prop-1-yn-1-ylbenzene (25.0 µL, 0.20 mmol) and DIH (76.0 mg, 0.20 mmol). Column chromatography (SiO_2, pentane) gave **3.45b** (33.0 mg, 63%) as a colourless oil. **^{1}H NMR** (500 MHz, $CDCl_3$) δ 7.63–7.58 (m, 2H), 7.39–7.35 (m, 3H), 2.58 (d, *J* = 3.6 Hz, 3H); **^{13}C NMR** (126 MHz, $CDCl_3$) δ 154.8 (d, $J_{C–F}$ = 254.7 Hz), 133.2 (d, $J_{C–F}$ = 28.9 Hz), 129.6 (d, $J_{C–F}$ = 1.9 Hz), 129.4 (d, $J_{C–F}$ = 3.6 Hz), 127.9, 74.8 (d, $J_{C–F}$ = 36.9 Hz), 25.4 (d, $J_{C–F}$ = 7.1 Hz); **^{19}F NMR** (471 MHz, $CDCl_3$) δ –82.8 (q, *J* = 3.6 Hz); **IR** (neat) ν 3058, 2951, 2919, 2853, 1665, 1492, 1443, 1259, 1052, 983, 794, 764, 692, 651, 629, 606 cm^{-1}; **HRMS** (EI) *m/z* Calcd for C_9H_8FI $[M]^+$ 261.9655, found 261.9655.

(*E*)-(1-Fluoro-2-iodohex-1-en-1-yl)benzene (3.45c)

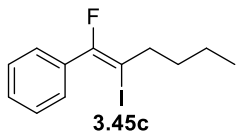

3.45c

The title compound was prepared according to GP3 using hex-1-yn-1-ylbenzene (31.6 mg, 0.20 mmol) and DIH (76.0 mg, 0.20 mmol). Column chromatography (SiO_2, pentane) gave **3.45c** (43.3 mg, 71%) as a colourless oil. **^{1}H NMR** (500 MHz, $CDCl_3$) δ 7.63–7.57 (m, 2H), 7.41–7.35 (m, 3H), 2.69 (td, *J* = 7.4, 3.1 Hz, 2H), 1.57 (tt, *J* = 7.4, 6.3 Hz, 2H), 1.44–1.36 (m, 2H), 0.96 (t, *J* = 7.3 Hz, 3H); **^{13}C NMR** (126 MHz, $CDCl_3$) δ 154.6 (d, $J_{C–F}$ = 254.7 Hz), 133.4 (d, $J_{C–F}$ = 29.1 Hz), 129.6 (d, $J_{C–F}$ = 2.1 Hz), 129.5 (d, $J_{C–F}$ = 3.3 Hz), 127.9, 84.4 (d, $J_{C–F}$ = 35.6 Hz), 36.0 (d, $J_{C–F}$ = 5.7 Hz), 31.1 (d, $J_{C–F}$ = 1.8 Hz), 21.5, 13.9; **^{19}F NMR** (471 MHz, $CDCl_3$) δ –82.1 (t, *J* = 3.1 Hz); **IR** (neat) ν 3059, 2957, 2927, 2860, 1659, 1492, 1445, 1290, 1259, 963, 828, 764, 693, 637 cm^{-1}; **HRMS** (EI) *m/z* Calcd for $C_{12}H_{14}FI$ $[M]^+$ 304.0124, found 304.0116.

(*E*)-(1-Fluoro-2-iodoethene-1,2-diyl)dibenzene (3.45d)

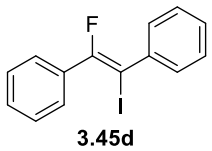

3.45d

The title compound was prepared according to GP4 using diphenylacetylene (35.6 mg, 0.20 mmol). Column chromatography (SiO_2, pentane) gave **3.45d** (35.0 mg, 54%) as a light yellow oil. **^{1}H NMR** (500 MHz, $CDCl_3$) δ 7.77–7.72 (m, 2H), 7.55 (dt, *J* = 8.1, 1.3 Hz, 2H), 7.46–7.41 (m, 3H), 7.39–7.35 (m, 2H), 7.28 (tt, *J* = 7.2, 1.3 Hz, 1H); **^{13}C NMR** (126 MHz, $CDCl_3$) δ 154.7 (d, $J_{C–F}$ = 261.0 Hz), 138.7, 133.5 (d, $J_{C–F}$ = 28.6 Hz), 130.1 (d, $J_{C–F}$ = 1.9 Hz), 129.7 (d, $J_{C–F}$ = 2.7 Hz), 129.6 (d, $J_{C–F}$ = 3.6 Hz), 128.4, 128.2, 128.1, 78.0 (d, $J_{C–F}$ = 32.7 Hz); **^{19}F NMR** (471 MHz, $CDCl_3$) δ –76.3; **IR** (neat) ν 3057, 3029, 2923, 2852, 1640, 1491, 1443, 1258, 1049, 1023, 880, 764, 750 cm^{-1}; **HRMS** (EI) *m/z* Calcd for $C_{14}H_{10}FI$ $[M]^+$ 323.9811, found 323.9810.

(*E*)-1-(*t*-Butyl)-4-(1-fluoro-2-iodoprop-1-en-1-yl)benzene (3.45e)

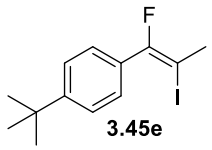

3.45e

The title compound was prepared according to GP3 using 1-(*t*-butyl)-4-(prop-1-yn-1-yl)benzene (34.5 mg, 0.20 mmol) and DIH (76.0 mg, 0.20 mmol). Column chromatography (SiO_2, pentane) gave **3.45e** (56.0 mg, 88%) as a colourless oil. **^{1}H NMR** (500 MHz, $CDCl_3$) δ 7.55 (ad, *J* = 8.2 Hz, 2H), 7.38 (ad, *J* = 8.2 Hz, 2H), 2.57 (d, *J* = 3.5 Hz, 3H), 1.32 (s, 9H); **^{13}C NMR** (126 MHz, $CDCl_3$) δ 154.9 (d, $J_{C–F}$ = 253.9 Hz), 152.7, 130.2 (d, $J_{C–F}$ = 29.1 Hz), 129.0 (d, $J_{C–F}$ = 3.7 Hz), 124.8, 74.1 (d, $J_{C–F}$ = 37.7 Hz), 34.8, 31.2, 25.4 (d, $J_{C–F}$ = 7.3 Hz); **^{19}F NMR** (471 MHz, $CDCl_3$) δ –83.0 (q, *J* = 3.5 Hz); **IR** (neat) ν 3038, 2963, 2868, 1741, 1364, 1267, 1111, 1056, 986, 908, 836, 797, 734, 708, 611 cm^{-1}; **HRMS** (EI) *m/z* Calcd for $C_{13}H_{16}FI$ $[M]^+$ 318.0281, found 318.0279.

(*E*)-1-Chloro-4-(1-fluoro-2-iodoprop-1-en-1-yl)benzene (3.45f)

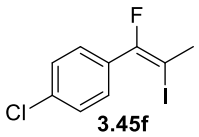

3.45f

The title compound was prepared according to GP3 using 1-chloro-4-(prop-1-yn-1-yl)benzene (30.1 mg, 0.20 mmol) and DIH (76.0 mg, 0.20 mmol). Column chromatography (SiO_2, pentane) gave **3.45f** (38.0 mg, 64%) as a colourless oil. **^{1}H NMR** (500 MHz, $CDCl_3$) δ 7.55 (ad, *J* = 8.5 Hz, 2H), 7.34 (ad, *J* = 8.5 Hz, 2H), 2.56 (d, *J* = 3.6 Hz, 3H); **^{13}C NMR** (126 MHz, $CDCl_3$) δ 153.8 (d, $J_{C–F}$ = 254.2 Hz), 135.5, 131.6 (d, $J_{C–F}$ = 29.6 Hz), 130.8 (d, $J_{C–F}$ = 3.6 Hz), 128.2, 75.4 (d, $J_{C–F}$ = 36.4 Hz), 25.3 (d, $J_{C–F}$ = 7.2 Hz); **^{19}F NMR** (471 MHz, $CDCl_3$) δ –83.6 (q, *J* = 3.6 Hz); **IR** (neat) ν 2920, 2854, 1661, 1596, 1490, 1437, 1254, 1094, 1058, 1016, 985, 829, 799, 719, 706 cm^{-1}; **HRMS** no successful HRMS analysis could be performed using ESI, CI and EI techniques.

(E)-1-(1-Fluoro-2-iodoprop-1-en-1-yl)-4-methoxybenzene (3.45g)

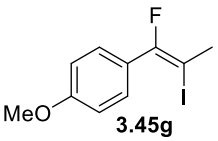

3.45g

The title compound was prepared according to GP3 using 1-methoxy-4-(prop-1-yn-1-yl)benzene (29.2 mg, 0.20 mmol) and DIH (76.0 mg, 0.20 mmol). Column chromatography (SiO_2, 1% Et_2O in pentane) gave **3.45g** (45.0 mg, 77%) as a colourless oil. **^{1}H NMR** (500 MHz, $CDCl_3$) δ 7.55 (ad, *J* = 8.5 Hz, 2H), 6.88 (ad, *J* = 8.5 Hz, 2H), 3.82 (s, 3H), 2.55 (d, *J* = 3.5 Hz, 3H); **^{13}C NMR** (126 MHz, $CDCl_3$) δ 160.3 (d, $J_{C–F}$ = 1.8 Hz), 154.8 (d, $J_{C–F}$ = 254.0 Hz), 130.9 (d, $J_{C–F}$ = 3.4 Hz), 125.6 (d, $J_{C–F}$ = 29.6 Hz), 113.2, 73.9 (d, $J_{C–F}$ = 38.5 Hz), 55.3, 25.2 (d, $J_{C–F}$ = 7.1 Hz); **^{19}F NMR** (471 MHz, $CDCl_3$) δ –82.4 (q, *J* = 3.5 Hz); **IR** (neat) ν 2981, 2917, 2837, 1662, 1608, 1509, 1463, 1440, 1302, 1246, 1176, 1053, 1033, 831, 813, 761 cm^{-1}; **HRMS** (CI) *m/z* Calcd for $C_{10}H_{11}FIO$ $[M+H]^+$ 292.9833, found 292.9829.

(*E*)-1-(1-Fluoro-2-iodoprop-1-en-1-yl)-4-(trifluoromethyl)benzene (3.45h)

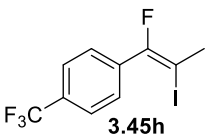

3.45h

The title compound was prepared according to GP4 using 1-(prop-1-yn-1-yl)-4-(trifluoromethyl)benzene (36.8 mg, 0.20 mmol). Column chromatography (SiO_2, pentane) gave **3.45h** (50.8 mg, 77%) as a colourless oil. **^{1}H NMR** (500 MHz, $CDCl_3$) δ 7.74 (ad, *J* = 8.1 Hz, 2H), 7.63 (ad, *J* = 8.1 Hz, 2H), 2.60 (d, *J* = 3.7 Hz, 3H); **^{13}C NMR** (126 MHz, $CDCl_3$) δ 153.3 (d, $J_{C–F}$ = 254.0 Hz), 136.5 (d, $J_{C–F}$ = 29.5 Hz), 131.4 (qd, $J_{C–F}$ = 32.6, 1.6 Hz), 129.8 (d, $J_{C–F}$ = 3.8 Hz), 125.0 (q, $J_{C–F}$ = 3.8 Hz), 123.7 (q, $J_{C–F}$ = 272.4 Hz), 76.4 (d, $J_{C–F}$ = 35.2 Hz), 25.4 (d, $J_{C–F}$ = 7.2 Hz); **^{19}F NMR** (471 MHz, $CDCl_3$) δ –62.9, –84.1 (q, *J* = 3.7 Hz); **IR** (neat) ν 2923, 1662, 1618, 1407, 1322, 1167, 1126, 1060, 1018, 987, 843, 812, 761, 675, 614 cm^{-1}; **HRMS** (EI) *m/z* Calcd for $C_{10}H_7F_4I$ $[M]^+$ 329.9529, found 329.9520.

(*E*)-1-(4-(1-Fluoro-2-iodoprop-1-en-1-yl)phenyl)ethan-1-one (3.45i)

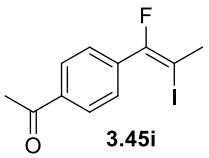

3.45i

The title compound was prepared according to GP4 using 1-(4-(prop-1-yn-1-yl)phenyl)ethan-1-one (31.6 mg, 0.20 mmol). Column chromatography (SiO_2, 5–10% Et_2O in pentane) gave **3.45i** (41.9 mg, 69%) as a colourless oil. **^{1}H NMR** (500 MHz, $CDCl_3$) δ 7.94 (ad, *J* = 8.1 Hz, 2H), 7.73 (ad, *J* = 8.1 Hz, 2H), 2.60 (s, 3H), 2.59 (d, *J* = 3.8 Hz, 3H); **^{13}C NMR** (126 MHz, $CDCl_3$) δ 197.3, 153.6 (d, $J_{C–F}$ = 254.1 Hz), 137.5, 137.4 (d, $J_{C–F}$ = 29.9 Hz), 129.6 (d, $J_{C–F}$ = 3.8 Hz), 127.9, 76.4 (d, $J_{C–F}$ = 35.4 Hz), 26.7, 25.5 (d, $J_{C–F}$ = 7.3 Hz); **^{19}F NMR** (471 MHz, $CDCl_3$) δ –84.3 (q, *J* = 3.8 Hz); **IR** (neat) ν 3003, 2954, 2919, 1683, 1606, 1429, 1403, 1357, 1264, 1058, 985, 957, 840, 803, 724, 607 cm^{-1}; **HRMS** (CI) *m/z* Calcd for $C_{11}H_{11}FIO$ $[M+H]^+$ 304.9833, found 304.9838.

(*E*)-(3-(1-Fluoro-2-iodoprop-1-en-1-yl)phenyl)methanol (3.45j)

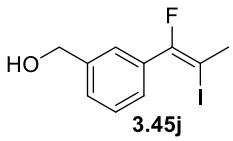

3.45j

The title compound was prepared according to GP3 using (3-(prop-1-yn-1-yl)phenyl)methanol (29.2 mg, 0.20 mmol) and DIH (76.0 mg, 0.20 mmol). Column chromatography (SiO_2, 10–40% Et_2O in pentane) gave **3.45j** (25.5 mg, 44%) as a colourless oil. **^{1}H NMR** (500 MHz, $CDCl_3$) δ 7.60–7.58 (m, 1H), 7.54 (td, *J* = 3.9, 1.5 Hz, 1H), 7.39–7.34 (m, 2H), 4.70 (s, 2H), 2.57 (d, *J* = 3.6 Hz, 3H), 1.79 (bs, 1H); **^{13}C NMR** (126 MHz, $CDCl_3$) δ 154.6 (d, J_{C-F} = 254.8 Hz), 140.7, 133.4 (d, J_{C-F} = 28.9 Hz), 128.8 (d, J_{C-F} = 3.5 Hz), 128.2, 128.1 (d, J_{C-F} = 1.9 Hz), 127.8 (d, J_{C-F} = 3.4 Hz), 75.0 (d, J_{C-F} = 36.6 Hz), 64.9, 25.2 (d, J_{C-F} = 7.1 Hz); **^{19}F NMR** (471 MHz, $CDCl_3$) δ –82.9 (q, *J* = 3.6 Hz); **IR** (neat) ν 3310, 2919, 2873, 1665, 1434, 1180, 1055, 906, 873, 793, 762, 732, 699, 655 cm^{-1}; **HRMS** (CI) *m/z* Calcd for $C_{10}H_{14}FINO$ $[M+NH_4]^+$ 310.0099, found 310.0097.

Ethyl (*E*)-3-(1-fluoro-2-iodoprop-1-en-1-yl)benzoate (3.45k)

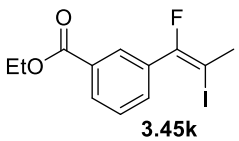

3.45k

The title compound was prepared according to GP4 using ethyl 3-(prop-1-yn-1-yl)benzoate (37.6 mg, 0.20 mmol). Column chromatography (SiO_2, 0–4% Et_2O in pentane) gave **3.45k** (52.2 mg, 78%) as a colourless oil. **^{1}H NMR** (500 MHz, $CDCl_3$) δ 8.31–8.26 (m, 1H), 8.04–8.02 (m, 1H), 7.83–7.75 (m, 1H), 7.50–7.40 (m, 1H), 4.37 (q, *J* = 7.1 Hz, 2H), 2.58 (d, *J* = 3.6 Hz, 3H), 1.38 (t, *J* = 7.1 Hz, 3H); **^{13}C NMR** (126 MHz, $CDCl_3$) δ 165.8, 153.8 (d, J_{C-F} = 254.7 Hz), 133.6 (d, J_{C-F} = 3.4 Hz), 133.4 (d, J_{C-F} = 29.5 Hz), 130.6 (d, J_{C-F} = 1.9 Hz), 130.5, 130.4, 128.1, 75.7 (d, J_{C-F} = 35.8 Hz), 61.2, 25.2 (d, J_{C-F} = 7.1 Hz), 14.3; **^{19}F NMR** (471 MHz, $CDCl_3$) δ –83.7 (q, *J* = 3.6 Hz); **IR** (neat) ν 2982, 2921, 1719, 1439, 1297, 1227, 1058, 1024, 756, 696 cm^{-1}; **HRMS** (CI) *m/z* Calcd for $C_{12}H_{13}FIO_2$ $[M+H]^+$ 334.9939, found 334.9944.

(*E*)-3-(1-Fluoro-2-iodoprop-1-en-1-yl)benzoic acid (3.45l)

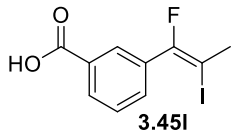

3.45l

The title compound was prepared according to GP4 using 3-(prop-1-yn-1-yl)benzoic acid (32.0 mg, 0.20 mmol). Column chromatography (SiO_2, 20–40% Et_2O in pentane) gave **3.45l** (36.1 mg, 59%) as a white solid. **M.p.** (Et_2O) = 139–140 °C; **^{1}H NMR** (400 MHz, $CDCl_3$) δ 8.41–8.37 (m, 1H), 8.16–8.08 (m, 1H), 7.93–7.82 (m, 1H), 7.57–7.45 (m, 1H), 2.60 (d, *J* = 3.6 Hz, 3H); **^{13}C NMR** (100 MHz, $CDCl_3$) δ 171.5, 153.6 (d, $J_{C–F}$ = 254.5 Hz), 134.6 (d, $J_{C–F}$ = 3.2 Hz), 133.7 (d, $J_{C–F}$ = 29.6 Hz), 131.3 (d, $J_{C–F}$ = 3.5 Hz), 131.2, 129.2, 128.3, 76.0 (d, $J_{C–F}$ = 35.4 Hz), 25.3 (d, $J_{C–F}$ = 7.1 Hz); **^{19}F NMR** (377 MHz, $CDCl_3$) δ –84.1 (q, *J* = 3.6 Hz); **IR** (solid) ν 2944, 2910, 2840, 1683, 1667, 1585, 1442, 1411, 1308, 1286, 1246, 1054, 758, 691, 681 cm^{-1}; **HRMS** (ESI-TOF) *m/z* Calcd for $C_{10}H_7FIO_2$ $[M–H]^-$ 304.9480, found 304.9478.

(*E*)-1-Bromo-3-(1-fluoro-2-iodoprop-1-en-1-yl)benzene (3.45m)

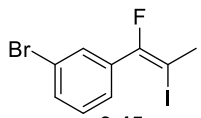

3.45m

The title compound was prepared according to GP4 using 1-bromo-3-(prop-1-yn-1-yl)benzene (39.0 mg, 0.20 mmol). Column chromatography (SiO_2, pentane) gave **3.45m** (49.8 mg, 73%) as a colourless oil. **^{1}H NMR** (400 MHz, $CDCl_3$) δ 7.74 (t, *J* = 1.7 Hz, 1H), 7.55 (ddt, *J* = 7.8, 1.7, 1.0 Hz, 1H), 7.49 (ddt, *J* = 7.8, 1.7, 1.0 Hz, 1H), 7.24 (td, *J* = 7.8, 0.6 Hz, 1H), 2.57 (d, *J* = 3.7 Hz, 3H); **^{13}C NMR** (100 MHz, $CDCl_3$) δ 153.2 (d, $J_{C–F}$ = 254.8 Hz), 135.0 (d, $J_{C–F}$ = 29.3 Hz), 132.6 (d, $J_{C–F}$ = 1.5 Hz), 132.3 (d, $J_{C–F}$ = 3.5 Hz), 129.5, 128.1 (d, $J_{C–F}$ = 3.6 Hz), 121.8, 75.9 (d, $J_{C–F}$ = 35.6 Hz), 25.3 (d, $J_{C–F}$ = 7.1 Hz); **^{19}F NMR** (377 MHz, $CDCl_3$) δ –83.6 (q, *J* = 3.7 Hz); **IR** (neat) ν 2918, 2361, 1663, 1591, 1562, 1474, 1406, 1254, 1244, 1055, 995, 885, 816, 783, 698, 687 cm^{-1}; **HRMS** (EI) *m/z* Calcd for $C_9H_7{}^{79}BrFI$ $[M]^+$ 339.8760, found 339.8757.

(*E*)-1-(1-Fluoro-2-iodoprop-1-en-1-yl)-2-methylbenzene (3.45n)

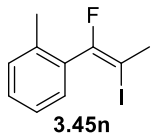

3.45n

The title compound was prepared according to GP3 using 1-methyl-2-(prop-1-yn-1-yl)benzene (26.0 mg, 0.20 mmol) and DIH (76.0 mg, 0.20 mmol). Column chromatography (SiO_2, pentane) gave **3.45n** (40.9 mg, 74%) as a colourless oil. **^{1}H NMR** (500 MHz, $CDCl_3$) δ 7.35–7.27 (m, 2H), 7.27–7.17 (m, 2H), 2.57 (d, *J* = 3.5 Hz, 3H), 2.34 (d, *J* = 2.3 Hz, 3H); **^{13}C NMR** (126 MHz, $CDCl_3$) δ 155.6 (d, $J_{C–F}$ = 259.8 Hz), 137.5, 133.6 (d, $J_{C–F}$ = 26.2 Hz), 130.9 (d, $J_{C–F}$ = 1.7 Hz), 130.1 (d, $J_{C–F}$ = 1.9 Hz), 129.9 (d, $J_{C–F}$ = 2.8 Hz), 125.5 (d, $J_{C–F}$ = 2.0 Hz), 77.6 (d, $J_{C–F}$ = 36.3 Hz), 24.0 (d, $J_{C–F}$ = 5.5 Hz), 19.3; **^{19}F NMR** (471 MHz, $CDCl_3$) δ –79.3 (q, *J* = 3.5 Hz); **IR** (neat) ν 3065, 3024, 2981, 2954, 2920, 2855, 1678, 1486, 1437, 1254, 1053, 983, 819, 759, 725, 650 cm^{-1}; **HRMS** (EI) *m/z* Calcd for $C_{10}H_{10}FI$ $[M]^+$ 275.9811, found 275.9804.

(*E*)-2-(1-Fluoro-2-iodoprop-1-en-1-yl)benzonitrile (3.45o)

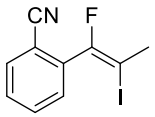

3.45o

The title compound was prepared according to GP4 using 2-(prop-1-yn-1-yl)benzonitrile (28.2 mg, 0.20 mmol). Column chromatography (SiO_2, 1% Et_2O in pentane) gave **3.45o** (32.2 mg, 56%) as a colourless oil. **^{1}H NMR** (500 MHz, $CDCl_3$) δ 7.72 (ddt, *J* = 7.6, 1.5, 0.6 Hz, 1H), 7.63 (tt, *J* = 7.6, 1.5 Hz, 1H), 7.59 (dtd, *J* = 7.6, 1.5, 0.6 Hz, 1H), 7.50 (tt, *J* = 7.6, 1.5 Hz, 1H), 2.61 (d, *J* = 3.6 Hz, 3H); **^{13}C NMR** (126 MHz, $CDCl_3$) δ 151.8 (d, $J_{C–F}$ = 258.1 Hz), 137.2 (d, $J_{C–F}$ = 28.2 Hz), 133.1 (d, $J_{C–F}$ = 1.9 Hz), 132.5 (d, $J_{C–F}$ = 1.1 Hz), 131.7 (d, $J_{C–F}$ = 0.8 Hz), 130.2 (d, $J_{C–F}$ = 2.3 Hz), 116.8, 113.3, 80.1 (d, $J_{C–F}$ = 33.1 Hz), 24.5 (d, $J_{C–F}$ = 5.4 Hz); **^{19}F NMR** (471 MHz, $CDCl_3$) δ –79.6 (q, *J* = 3.6 Hz); **IR** (neat) ν 2920, 2361, 2342, 2232, 1678, 1595, 1481, 1447, 1285, 1248, 1057, 986, 910, 812, 764, 731, 648 cm^{-1}; **HRMS** (EI) *m/z* Calcd for $C_{10}H_7FIN$ $[M]^+$ 286.9607, found 286.9600.

(*E*)-1-(1-Fluoro-2-iodohex-1-en-1-yl)-4-nitrobenzene (3.45p)

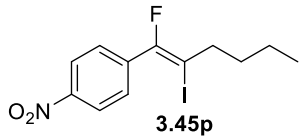

3.45p

The title compound was prepared according to GP4 using 1-(hex-1-yn-1-yl)-4-nitrobenzene (40.6 mg, 0.20 mmol). Column chromatography (SiO_2, pentane) gave **3.45p** (44.0 mg, 63%) as a light yellow oil. **^{1}H NMR** (500 MHz, $CDCl_3$) δ 8.22 (ad, *J* = 8.4 Hz, 2H), 7.82 (ad, *J* = 8.4 Hz, 2H), 2.72 (td, *J* = 7.4, 3.2 Hz, 2H), 1.60–1.53 (m, 2H), 1.44–1.34 (m, 2H), 0.96 (t, *J* = 7.3 Hz, 3H); **^{13}C NMR** (126 MHz, $CDCl_3$) δ 152.2 (d, J_{C-F} = 253.7 Hz), 148.0 (d, J_{C-F} = 1.3 Hz), 139.3 (d, J_{C-F} = 29.8 Hz), 130.5 (d, J_{C-F} = 3.8 Hz), 123.2, 87.3 (d, J_{C-F} = 33.2 Hz), 36.4 (d, J_{C-F} = 5.7 Hz), 31.0 (d, J_{C-F} = 1.7 Hz), 21.6, 13.8; **^{19}F NMR** (471 MHz, $CDCl_3$) δ –84.2 (t, *J* = 3.2 Hz); **IR** (neat) ν 2957, 2928, 2860, 1597, 1522, 1342, 1260, 1107, 1086, 964, 856, 756, 694 cm^{-1}; **HRMS** (EI) *m/z* Calcd for $C_{12}H_{13}FINO_2$ $[M]^+$ 348.9975, found 348.9967.

(*E*)-1-Chloro-4-(2-fluoro-1-iodo-2-phenylvinyl)benzene (3.45qa) / (*E*)-1-Chloro-4-(1-fluoro-2-iodo-2-phenylvinyl)benzene (3.45qb)

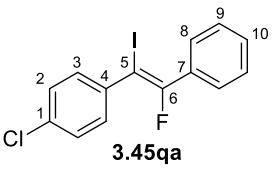

3.45qa

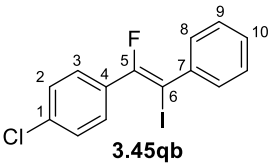

3.45qb

The title compounds were prepared according to GP4 using 1-chloro-4-(phenylethynyl)benzene (42.5 mg, 0.20 mmol). Column chromatography (SiO_2, pentane) gave a mixture (53.8 mg, 75%) of **3.45qa** (48%) and **3.45qb** (27%) as a colourless oil. Major isomer, **3.45qa**: **^{1}H NMR** (500 MHz, $CDCl_3$) δ 7.74–7.71 (m, $2H_8$), 7.48 (ad, *J* = 8.1 Hz, $2H_3$), 7.44–7.41 (m, $2H_9$ and $1H_{10}$), 7.33 (ad, *J* = 8.1 Hz, $2H_2$); **^{13}C NMR** (126 MHz, $CDCl_3$) δ 155.1 (d, J_{C-F} = 262.0 Hz, C_6), 137.1 (C_4), 134.1 (C_1), 133.2 (d, J_{C-F} = 28.4 Hz, C_7), 131.1 (d, J_{C-F} = 2.8 Hz, C_3), 130.2 (d, J_{C-F} = 1.7 Hz, C_{10}), 129.6 (d, *J* = 3.6 Hz, C_8), 128.4 (C_2), 128.1 (C_9), 76.4 (d, J_{C-F} = 32.3 Hz, C_5); **^{19}F NMR** (471 MHz, $CDCl_3$) δ –75.6. Minor isomer, **3.45qb**: **^{1}H NMR** (500 MHz, $CDCl_3$) δ 7.69 (ad, *J* = 8.4 Hz, $2H_3$), 7.52 (d, *J* = 8.2 Hz, $2H_8$),

7.40 (ad, *J* = 8.4 Hz, $2H_2$), 7.38–7.33 (m, $2H_9$), 7.30–7.26 (m, $1H_{10}$); **^{13}C NMR** (126 MHz, $CDCl_3$) δ 153.6 (d, $J_{C–F}$ = 260.3 Hz, C_5), 138.4 (C_7), 136.0 (d, $J_{C–F}$ = 2.1 Hz, C_1), 131.8 (d, $J_{C–F}$ = 29.3 Hz, C_4), 131.0 (d, $J_{C–F}$ = 3.6 Hz, C_3), 129.6 (d, $J_{C–F}$ = 2.6 Hz, C_8), 128.5 (C_{10}), 128.4 (C_2), 128.2 (C_9), 78.7 (d, $J_{C–F}$ = 32.2 Hz, C_6); **^{19}F NMR** (471 MHz, $CDCl_3$) δ –77.3. As a mixture: **IR** (neat) ν 3059, 3033, 1810, 1638, 1591, 1492, 1443, 1398, 1253, 1091, 1048, 1013, 963, 945, 919, 907, 883, 837, 813, 764, 755, 731, 722, 710, 692 cm^{-1}; **HRMS** (EI) *m/z* Calcd for $C_{14}H_9ClFI$ $[M]^+$ 357.9421, found 357.9413.

(*E*)-(2-Fluoro-1-iodohex-1-en-1-yl)cyclohexane (3.45ra) / (*E*)-(1-fluoro-2-iodohex-1-en-1-yl)cyclohexane (3.45rb)

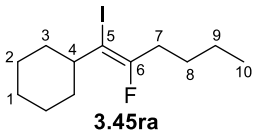

3.45ra

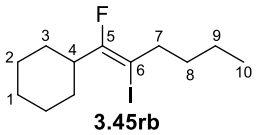

3.45rb

The title compounds were prepared according to GP3 using hex-1-yn-1-ylcyclohexane (32.9 mg, 0.20 mmol) and DIH (76.0 mg, 0.20 mmol). Column chromatography (SiO_2, pentane) gave a mixture (54.1 mg, 87%) of **3.45ra** (63%) and **3.45rb** (24%) as a colourless oil. Major isomer, **3.45ra**: **^{1}H NMR** (500 MHz, $CDCl_3$) δ 2.54 (dt, *J* = 23.8, 7.5 Hz, $2H_7$), 2.19 (ttd, *J* = 11.2, 3.6, 1.7 Hz, $1H_4$), 1.79–1.68 (m, $4H_3$), 1.53–1.20 (m, $1H_1$, $4H_2$, $2H_8$ and $2H_9$), 1.18–1.10 (m, $1H_1$), 0.91 (t, *J* = 7.3 Hz, $3H_{10}$); **^{13}C NMR** (126 MHz, $CDCl_3$) δ 156.6 (d, $J_{C–F}$ = 258.9 Hz, C_6), 94.5 (d, $J_{C–F}$ = 30.1 Hz, C_5), 38.9 (d, $J_{C–F}$ = 6.7 Hz, C_4), 33.5 (d, $J_{C–F}$ = 28.4 Hz, C_7), 33.3 (d, $J_{C–F}$ = 1.2 Hz, C_3), 28.4 (C_8), 25.7 (C_2), 25.6 (C_1), 21.9 (C_9), 13.9 (C_{10}); **^{19}F NMR** (471 MHz, $CDCl_3$) δ –91.2 (t, *J* = 23.8 Hz). Minor isomer, **3.45rb**: **^{1}H NMR** (500 MHz, $CDCl_3$) δ 2.81 (dtt, *J* = 28.9, 11.9, 3.4 Hz, $1H_4$), 2.42 (td, *J* = 7.3, 3.0 Hz, $2H_7$), 1.67–1.60 (m, $4H_3$), 1.50–1.20 (m, $1H_1$, $4H_2$, $2H_8$ and $2H_9$), 1.19–1.08 (m, $1H_1$), 0.89 (t, *J* = 7.3 Hz, $3H_{10}$); **^{13}C NMR** (126 MHz, $CDCl_3$) δ 160.6 (d, $J_{C–F}$ = 262.8 Hz, C_5), 82.1 (d, $J_{C–F}$ = 34.1 Hz, C_6), 42.6 (d, $J_{C–F}$ = 25.7 Hz, C_4), 34.6 (d, $J_{C–F}$ = 6.8 Hz, C_7), 31.1 (d, $J_{C–F}$ = 1.8 Hz, C_8), 28.8

(C_3), 25.9 (C_2), 25.7 (C_1), 21.3 (C_9), 13.9 (C_{10}); **^{19}F NMR** (471 MHz, $CDCl_3$) δ –105.3 (d, *J* = 28.9 Hz). As a mixture: **IR** (neat) ν 2957, 2928, 2855, 2361, 1661, 1449, 1302, 1236, 1105, 905, 891, 870, 841 cm^{-1}; **HRMS** (EI) *m/z* Calcd for $C_{12}H_{20}FI$ $[M]^+$ 310.0594, found 310.0592.

(*E*)-4-Fluoro-3-iodo-2,2-dimethyloct-3-ene (3.45s)

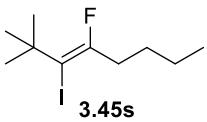

3.45s

The title compound was prepared according to GP3 using 2,2-dimethyloct-3-yne (27.7 mg, 0.20 mmol) and DIH (76.0 mg, 0.20 mmol). After work-up C_6F_6 (5.8 µL, 0.050 mmol) was added as internal reference and quantitative ^{19}F NMR revealed that a trace amount of **3.45s** had been formed. Characteristic peak: **^{19}F NMR** (377 MHz, $CDCl_3$) δ –84.2 (t, *J* = 23.7 Hz).

(*E*)-2-(1-Fluoro-2-iodoprop-1-en-1-yl)-5-methylthiophene (3.45t)

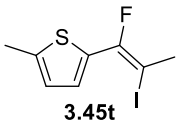

3.45t

The title compound was prepared according to GP3 using 2-methyl-5-(prop-1-yn-1-yl)thiophene (27.2 mg, 0.20 mmol) and DIH (76.0 mg, 0.20 mmol). Column chromatography (SiO_2, pentane) gave **3.45t** (28.3 mg, 50%) as a colourless oil. **^{1}H NMR** (400 MHz, $CDCl_3$) δ 7.34 (d, *J* = 3.6 Hz, 1H), 6.72 (dqn, *J* = 3.6, 1.1 Hz, 1H), 2.59 (d, *J* = 3.8 Hz, 3H), 2.46 (bs, 3H); **^{13}C NMR** (100 MHz, $CDCl_3$) δ 150.5 (d, J_{C-F} = 245.7 Hz), 142.2, 131.5 (d, J_{C-F} = 35.0 Hz), 129.3 (d, J_{C-F} = 6.6 Hz), 125.1, 72.8 (d, J_{C-F} = 37.7 Hz), 25.8 (d, J_{C-F} = 8.0 Hz), 15.3; **^{19}F NMR** (377 MHz, $CDCl_3$) δ –84.7 (q, *J* = 3.8 Hz); **IR** (neat) ν 2947, 2918, 2853, 1638, 1537, 1458, 1435, 1246, 1227, 1165, 1045, 953, 797, 766, 754, 621 cm^{-1}; **HRMS** (EI) *m/z* Calcd for C_8H_8FIS $[M]^+$ 281.9375, found 281.9374.

(*E*)-3-(1-Fluoro-2-iodoprop-1-en-1-yl)furan (3.45u)

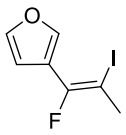

3.45u

The title compound was prepared according to GP3 using 3-(prop-1-yn-1-yl)furan (21.2 mg, 0.20 mmol) and DIH (76.0 mg, 0.20 mmol). Column chromatography (SiO_2, pentane) gave **3.45u** (13.1 mg, 26%) as a colourless oil. **^{1}H NMR** (500 MHz, $CDCl_3$) δ 7.99 (bs, 1H), 7.40 (q, *J* = 1.7 Hz, 1H), 6.84 (dd, *J* = 1.7, 1.0 Hz, 1H), 2.55 (d, *J* = 3.7 Hz, 3H); **^{13}C NMR** (126 MHz, $CDCl_3$) δ 149.4 (d, $J_{C–F}$ = 244.4 Hz), 143.5 (d, $J_{C–F}$ = 8.8 Hz), 142.5, 119.3 (d, $J_{C–F}$ = 35.8 Hz), 110.1 (d, $J_{C–F}$ = 5.6 Hz), 73.9 (d, $J_{C–F}$ = 36.3 Hz), 25.3 (d, $J_{C–F}$ = 7.9 Hz); **^{19}F NMR** (471 MHz, $CDCl_3$) δ –88.9 (qd, *J* = 3.7, 1.0 Hz); **IR** (neat) ν 2953, 2922, 2853, 1665, 1462, 1377, 1167, 1061, 1038, 924, 874, 795, 768, 756, 729, 662, 596 cm^{-1}; **HRMS** (EI) *m/z* Calcd for C_7H_6FIO $[M]^+$ 251.9447, found 251.9439.

(*E*)-4-Fluoro-3-iodohex-3-en-2-one (3.45v) (Conditions D)

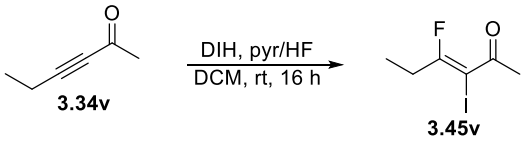

3.34v **3.45v**

Scheme S.3.24. Iodofluorination of α-keto alkyne **3.33v**.

In a plastic falcon tube flushed with Ar, a solution of hex-3-yn-2-one (21.8 µL, 0.20 mmol) and 1,3-diiodo-5,5-dimethylhydantoin (DIH) (76.0 mg, 0.20 mmol) in DCM (2.0 mL) was prepared. Pyr/HF (20.8 µL, 0.80 mmol) was added and the reaction was stirred for 16 h at rt. It was then diluted with DCM and quenched with sat. aq. $NaHCO_3$, the layers were separated and the aqueous one was extracted with DCM. The combined organic layers were dried over $MgSO_4$ and volatiles were removed *in vacuo*. After purification by column

chromatography (SiO_2, 0–2% Et_2O in pentane), **3.45v** (23.1 mg, 48%) was obtained as a volatile colourless oil.

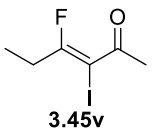

3.45v

^{1}H NMR (500 MHz, $CDCl_3$) δ 2.87 (dq, *J* = 22.8, 7.5 Hz, 2H), 2.54 (d, *J* = 6.6 Hz, 3H), 1.20 (t, *J* = 7.5 Hz, 3H); **^{13}C NMR** (126 MHz, $CDCl_3$) δ 192.3, 170.7 (d, $J_{C–F}$ = 287.8 Hz), 88.3 (d, $J_{C–F}$ = 21.9 Hz), 30.3 (d, $J_{C–F}$ = 27.6 Hz), 29.6 (d, $J_{C–F}$ = 9.1 Hz), 10.0; **^{19}F NMR** (471 MHz, $CDCl_3$) δ –66.3 (tq, *J* = 22.8, 6.6 Hz); **IR** (film, $CDCl_3$) ν 2980, 2941, 2361, 2342, 1678, 1612, 1460, 1425, 1358, 1275, 1229, 1169, 978, 889, 868, 579 cm^{-1}; **HRMS** no successful HRMS analysis could be performed using ESI, CI and EI techniques.

(*E*)-5-Bromo-6-fluorodec-5-ene (3.35a) / (*E*)-5,6-Dibromodec-5-ene (3.36a)

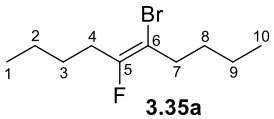

3.35a

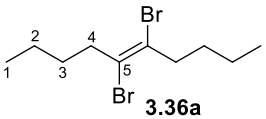

3.36a

The title compounds were prepared according to GP3 using dec-5-yne (36.1 µL, 0.20 mmol) and DBH (57.2 mg, 0.20 mmol). Column chromatography (SiO_2, pentane) gave a mixture (46.9 mg, 95%) of **3.35a** (80%) and **3.36a** (15%) as a colourless oil. Major product, **3.35a**: **^{1}H NMR** (500 MHz, $CDCl_3$) δ 2.45 (td, *J* = 7.2, 3.5 Hz, $2H_7$) 2.44 (dt, *J* = 23.4, 7.6 Hz, $2H_4$), 1.54–1.42 (m, $2H_3$ and $2H_8$), 1.34–1.25 (m, $2H_2$ and $2H_9$), 0.91 (t, *J* = 7.2 Hz, $3H_{10}$), 0.89 (t, *J* = 7.3 Hz, $3H_1$); **^{13}C NMR** (126 MHz, $CDCl_3$) δ 157.3 (d, $J_{C–F}$ = 254.2 Hz, C_5), 109.0 (d, $J_{C–F}$ = 40.9 Hz, C_6), 32.0 (d, $J_{C–F}$ = 4.2 Hz, C_7), 30.3 (d, $J_{C–F}$ = 26.8 Hz, C_4), 29.8 (d, $J_{C–F}$ = 1.9 Hz, C_8), 28.0 (C_3), 22.0 (C_9), 21.5 (C_2), 13.8 (C_{10}), 13.8 (C_1); **^{19}F NMR** (471 MHz, $CDCl_3$) δ –105.4 (tt, *J* = 23.4, 3.5 Hz); **HRMS** (EI) *m/z* Calcd for $C_{10}H_{18}{}^{79}BrF$ $[M]^+$ 236.0576, found 236.0572. Minor product, **3.36a**:[467] **^{1}H NMR** (500 MHz, $CDCl_3$) δ 2.65 (t, *J* = 7.5 Hz, $4H_4$), 1.58–1.48 (m, $4H_3$), 1.40–1.28 (m, $4H_2$), 0.92 (t, *J* = 7.3 Hz, $6H_1$); **^{13}C NMR** (126 MHz,

$CDCl_3$) δ 121.7 (C_5), 40.6 (C_4), 29.6 (C_3), 21.7 (C_2), 13.9 (C_1); As a mixture: **IR** (neat) ν 2958, 2929, 2873, 2862, 2361, 2342, 1686, 1465, 1431, 1380, 1112, 1082, 967, 948, 873, 744, 731, 618 cm^{-1}.

(*E*)-(2-Bromo-1-fluoroprop-1-en-1-yl)benzene (3.35b)

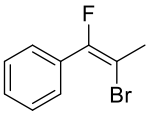

3.35b

The title compound was prepared according to GP3 using prop-1-yn-1-ylbenzene (25.0 µL, 0.20 mmol) and DBH (57.2 mg, 0.20 mmol). Column chromatography (SiO_2, pentane) gave **3.35b** (28.0 mg, 65%) as a colourless oil. **^{1}H NMR** (500 MHz, $CDCl_3$) δ 7.44–7.37 (m, 5H), 2.35 (d, *J* = 3.5 Hz, 3H); **^{13}C NMR** (126 MHz, $CDCl_3$) δ 154.0 (d, $J_{C–F}$ = 246.4 Hz), 130.7 (d, $J_{C–F}$ = 28.8 Hz), 129.5 (d, $J_{C–F}$ = 1.4 Hz), 128.4, 128.1 (d, $J_{C–F}$ = 3.5 Hz), 101.8 (d, $J_{C–F}$ = 26.9 Hz), 22.8; **^{19}F NMR** (471 MHz, $CDCl_3$) δ –86.1 (q, *J* = 3.5 Hz); **IR** (neat) ν 3061, 2920, 2850, 1671, 1443, 1381, 1274, 1107, 1074, 1003, 995, 769, 758, 695, 618 cm^{-1}; **HRMS** (EI) *m/z* Calcd for $C_9H_8{}^{79}BrF$ $[M]^+$ 213.9793, found 213.9788.

(*E*)-5-chloro-6-fluorodec-5-ene (3.40a, X = Cl)

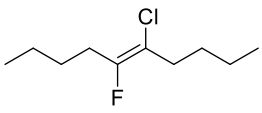

3.40a

The title compound was observed in NMRs of the crude reaction mixture of chlorofluorination reactions described in Table 3.8: In a flask flushed with Ar, a solution of dec-5-yne (9.0 µL, 0.050 mmol), and 1,3-dichloro-5,5-dimethylhydantoin (DCH) (9.9 mg, 0.050 mmol) in DCM (0.50 mL) was prepared. The mixture was then cooled to the specified temperature before NEt_3·3HF (24.5 µL, 0.15 mmol) was added. It was then stirred at this temperature for 16 h before CD_2Cl_2 (0.30 mL) and C_6F_6 (5.8 µL, 0.050 mmol) were added and the solution was transferred into an NMR tube and analysed by ^{1}H and quantitative ^{19}F NMR. Characteristic peaks: **^{1}H NMR**

(400 MHz, $CDCl_3$) δ 2.40 (dt, *J* = 23.2, 7.5 Hz, 2H), 2.38 (td, *J* = 7.5, 3.9 Hz, 2H); **^{19}F NMR** (377 MHz, $CDCl_3$) δ –113.0 (tt, *J* = 23.2, 3.9 Hz); **HRMS** (EI) *m/z* Calcd for $C_{10}H_{18}{}^{35}ClF$ $[M]^+$ 192.1081, found 192.1075.

(*E*)-5,6-Dichlorodec-5-ene (3.41a, X = Cl)

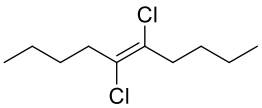

3.41a

The title compound was observed in NMRs of crude reaction mixtures as a by-product during the development of the halofluorination of internal alkynes. Characteristic peak: **^{1}H NMR** (400 MHz, $CDCl_3$) δ 2.57 (t, *J* = 7.3 Hz, 4H); **HRMS** (EI) *m/z* Calcd for $C_{10}H_{18}{}^{35}Cl_2$ $[M]^+$ 208.0786, found 208.0775.

(*E*)-5,6-Diiododec-5-ene (3.41a, X = I)

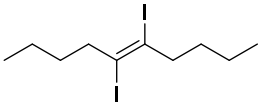
3.41a

The title compound was observed in NMRs of crude reaction mixtures as a by-product during the development of the halofluorination of internal alkynes. Characteristic peak: **^{1}H NMR** (400 MHz, $CDCl_3$) δ 2.71 (t, *J* = 7.7 Hz, 4H); **HRMS** (EI) *m/z* Calcd for $C_{10}H_{18}I_2$ $[M]^+$ 391.9498, found 391.9488.

(*E*)-2-Fluoro-1-iodohex-1-ene (3.43a)

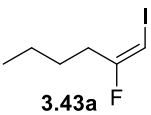
3.43a

The title compound was prepared according to GP4 using 1-hexyne (23.0 µL, 0.20 mmol). Due to the volatility of this compound the yield (74%) was determined by quantitative ^{19}F NMR using C_6F_6 (5.8 µL, 0.050 mmol) as internal standard. Column chromatography (SiO_2, pentane) gave **3.43a** as a volatile colourless oil. **^{1}H NMR** (500 MHz, $CDCl_3$) δ 5.64 (d, *J* = 17.8 Hz, 1H), 2.49 (dt, *J* = 22.6, 7.5 Hz, 2H), 1.42–

1.33 (m, 2H), 1.31–1.24 (m, 2H), 0.92 (t, *J* = 7.3 Hz, 3H); **^{13}C NMR** (126 MHz, $CDCl_3$) δ 164.2 (d, $J_{C–F}$ = 264.4 Hz), 54.6 (d, $J_{C–F}$ = 40.2 Hz), 30.7 (d, $J_{C–F}$ = 26.4 Hz), 27.8, 21.9, 13.8; **^{19}F NMR** (471 MHz, $CDCl_3$) δ –81.9 (td, *J* = 22.6, 17.8 Hz); **IR** (neat) ν 2956, 2922, 2852, 2361, 2342, 1463, 1092, 1068, 1017, 801, 769 cm^{-1}; **HRMS** (EI) *m/z* Calcd for $C_6H_{10}FI$ $[M]^+$ 227.9811, found 227.9803.

(*E*)-(1-Fluoro-2-iodovinyl)benzene (3.43b)

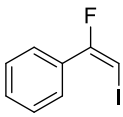

3.43b

The title compound was prepared according to GP4 using ethynylbenzene (22.0 µL, 0.20 mmol). Column chromatography (SiO_2, pentane) gave **3.43b** (22.5 mg, 43%) as a colourless oil. **^{1}H NMR** (500 MHz, $CDCl_3$) δ 7.80–7.76 (m, 2H), 7.44–7.39 (m, 3H), 6.12 (d, *J* = 19.6 Hz, 1H); **^{13}C NMR** (126 MHz, $CDCl_3$) δ 158.9 (d, $J_{C–F}$ = 256.1 Hz), 131.1 (d, $J_{C–F}$ = 28.5 Hz), 130.2 (d, $J_{C–F}$ = 1.1 Hz), 128.6 (d, $J_{C–F}$ = 5.2 Hz), 128.1, 53.8 (d, $J_{C–F}$ = 44.7 Hz); **^{19}F NMR** (471 MHz, $CDCl_3$) δ –75.9 (d, *J* = 19.6 Hz). The spectroscopic data were identical in all respects to those previously reported.[196,468]

(*E*)-(1-Fluoro-2-iodovinyl)cyclohexane (3.43c)

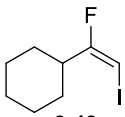

3.43c

The title compound was prepared according to GP4 using ethynylcyclohexane (26.1 µL, 0.20 mmol). Column chromatography (SiO_2, pentane) gave **3.43c** (27.4 mg, 54%) as a colourless oil. **^{1}H NMR** (500 MHz, $CDCl_3$) δ 5.53 (d, *J* = 18.1 Hz, 1H), 2.77 (dtt, *J* = 29.3, 11.9, 3.4 Hz, 1H), 1.81–1.74 (m, 2H), 1.74–1.69 (m, 2H), 1.69–1.63 (m, 1H), 1.43–1.34 (m, 2H), 1.34–1.23 (m, 2H), 1.22–1.11 (m, 1H); **^{13}C NMR** (126 MHz, $CDCl_3$) δ 166.7 (d, $J_{C–F}$ = 267.6 Hz), 52.8 (d, $J_{C–F}$ = 41.3 Hz), 40.1 (d, $J_{C–F}$ = 24.5 Hz), 28.4, 25.7, 25.6; **^{19}F NMR** (471 MHz, $CDCl_3$) δ –92.5 (dd, *J* = 29.3, 18.1 Hz); **IR** (neat) ν 3075, 2930, 2854, 1644, 1449, 1258, 1104, 996, 908, 893, 873, 840, 769, 721 cm^{-1}; **HRMS** (EI) *m/z* Calcd for $C_8H_{12}ClFI$ $[M]^+$ 253.9968, found 253.9969.

(*E*)-(3-Fluoro-4-iodobut-3-en-1-yl)benzene (3.43d)

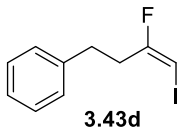

3.43d

The title compound was prepared according to GP4 using but-3-yn-1-ylbenzene (28.1 µL, 0.20 mmol). Column chromatography (SiO_2, pentane) gave **3.43d** (43.1 mg, 78%) as a colourless oil. **^{1}H NMR** (500 MHz, $CDCl_3$) δ 7.32–7.28 (m, 2H), 7.24–7.19 (m, 3H), 5.70 (d, *J* = 17.6 Hz, 1H), 2.88–2.75 (m, 4H); **^{13}C NMR** (126 MHz, $CDCl_3$) δ 162.9 (d, J_{C-F} = 264.6 Hz), 140.0, 128.5, 128.4, 126.3, 55.6 (d, J_{C-F} = 39.0 Hz), 33.1 (d, J_{C-F} = 26.2 Hz), 31.9; **^{19}F NMR** (471 MHz, $CDCl_3$) δ –82.4 (td, *J* = 21.3, 17.6 Hz); **IR** (neat) ν 3074, 3028, 2929, 2863, 2361, 2341, 1650, 1496, 1454, 1427, 1092, 1069, 881, 823, 773, 747, 712, 696 cm^{-1}; **HRMS** (CI) *m/z* Calcd for $C_{10}H_{14}FIN$ $[M+NH_4]^+$ 294.0149, found 294.0155.

(*E*)-6-Chloro-2-fluoro-1-iodohex-1-ene (3.43e)

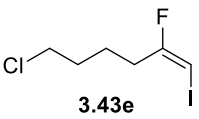

3.43e

The title compound was prepared according to GP4 using 6-chlorohex-1-yne (24.2 µL, 0.20 mmol). Column chromatography (SiO_2, pentane) gave **3.43e** (27.9 mg, 53%) as a colourless oil. **^{1}H NMR** (500 MHz, $CDCl_3$) δ 5.71 (d, *J* = 17.8 Hz, 1H), 3.55 (t, *J* = 6.5 Hz, 2H), 2.54 (dt, *J* = 22.2, 7.3 Hz, 2H), 1.88–1.79 (m, 2H), 1.76–1.65 (m, 2H); **^{13}C NMR** (126 MHz, $CDCl_3$) δ 163.3 (d, J_{C-F} = 264.5 Hz), 55.5 (d, J_{C-F} = 39.4 Hz), 44.4, 31.4, 30.1 (d, J_{C-F} = 26.6 Hz), 23.0; **^{19}F NMR** (471 MHz, $CDCl_3$) δ –82.1 (td, *J* = 22.2, 17.8 Hz); **IR** (neat) ν 3076, 2957, 2870, 2361, 1649, 1454, 1431, 1146, 1094, 868, 849, 772, 714, 652 cm^{-1}; **HRMS** (EI) *m/z* Calcd for $C_6H_9{}^{35}ClFI$ $[M]^+$ 261.9421, found 261.9412.

(*E*)-5-Fluoro-6-iodohex-5-enenitrile (3.43f)

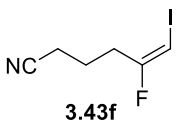

3.43f

The title compound was prepared according to GP4 using hex-5-ynenitrile (21.0 µL, 0.20 mmol). Column chromatography (SiO_2, 10% Et_2O in pentane) gave **3.43f** (35.5 mg, 74%) as a colourless oil. **^{1}H NMR** (500 MHz, $CDCl_3$) δ 5.82 (d, *J* = 17.6 Hz, 1H), 2.67 (dt, *J* = 21.3, 7.2 Hz, 2H), 2.41 (t, *J* = 7.2 Hz, 2H), 1.93 (qn, *J* = 7.2 Hz, 2H); **^{13}C NMR** (126 MHz, $CDCl_3$) δ 161.5 (d, $J_{C–F}$ = 264.1 Hz), 118.9, 56.9 (d, $J_{C–F}$ = 38.0 Hz), 29.8 (d, $J_{C–F}$ = 26.9 Hz), 21.9, 16.3; **^{19}F NMR** (471 MHz, $CDCl_3$) δ –84.4 (td, *J* = 21.3, 17.6 Hz); **IR** (neat) ν 3075, 2968, 2943, 2924, 2361, 2249, 2232, 1651, 1429, 1250, 1173, 1096, 1061, 988, 895, 766 cm^{-1}; **HRMS** (EI) *m/z* Calcd for C_6H_7FIN $[M]^+$ 238.9607, found 238.9607.

(*E*)-6-Fluoro-7-iodohept-6-enoic acid (3.43g)

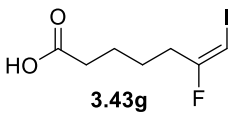

3.43g

The title compound was prepared according to GP4 using hept-6-ynoic acid (25.3 µL, 0.20 mmol). Column chromatography (SiO_2, 20–40% Et_2O in pentane) gave **3.43g** (20.1 mg, 78%) as a colourless oil. **^{1}H NMR** (500 MHz, $CDCl_3$) δ 5.69 (d, *J* = 17.7 Hz, 1H), 2.53 (dt, *J* = 22.1, 7.2 Hz, 2H), 2.39 (t, *J* = 7.3 Hz, 2H), 1.74–1.66 (m, 2H), 1.65–1.58 (m, 2H); **^{13}C NMR** (126 MHz, $CDCl_3$) δ 178.9, 163.4 (d, $J_{C–F}$ = 264.5 Hz), 55.3 (d, $J_{C–F}$ = 39.5 Hz), 33.5, 30.6 (d, $J_{C–F}$ = 26.5 Hz), 25.1, 23.7; **^{19}F NMR** (471 MHz, $CDCl_3$) δ –82.0 (td, *J* = 22.1, 17.7 Hz); **IR** (neat) ν 3076, 2926, 2869, 2673, 2360, 2342, 1704, 1650, 1429, 1413, 1291, 1259, 1100, 1055, 871, 773 cm^{-1}; **HRMS** (ESI-TOF) *m/z* Calcd for $C_7H_9FIO_2$ $[M–H]^-$ 270.9637, found 270.9639.

(*E*)-4-(1-Fluoro-2-iodovinyl)-1,1'-biphenyl (3.43h)

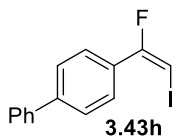

3.43h

The title compound was prepared according to GP3 using 4-ethynyl-1,1'-biphenyl (35.6 mg, 0.20 mmol) and DIH (76.0 mg, 0.20 mmol). Column chromatography (SiO_2, pentane) gave **3.43h** (22.7 mg, 35%) as a white solid. **M.p.** (pentane) = 59–60 °C; **^{1}H NMR** (500 MHz, $CDCl_3$) δ 7.89 (ad, *J* = 8.2 Hz, 2H), 7.64 (ad, *J* = 8.2 Hz, 2H), 7.62–7.60 (m, 2H), 7.48–7.43 (m, 2H), 7.40–7.35 (m, 1H), 6.15 (d, *J* = 19.7 Hz, 1H); **^{13}C NMR** (126 MHz, $CDCl_3$) δ 158.6 (d, $J_{C–F}$ = 255.3 Hz), 142.9 (d, $J_{C–F}$ = 1.1 Hz), 140.1, 129.9 (d, $J_{C–F}$ = 28.8 Hz), 129.0 (d, $J_{C–F}$ = 5.4 Hz), 128.9, 127.9, 127.1, 126.8, 53.7 (d, $J_{C–F}$ = 45.0 Hz); **^{19}F NMR** (471 MHz, $CDCl_3$) δ –76.7 (d, *J* = 19.7 Hz); **IR** (solid) ν 3072, 2920, 1608, 1483, 1404, 1302, 1278, 1154, 1046, 1017, 1003, 841, 813, 763, 742, 722, 690 cm^{-1}; **HRMS** (EI) *m/z* Calcd for $C_{14}H_{10}FI$ $[M]^+$ 323.9811, found 323.9809.

(*E*)-1-(1-Fluoro-2-iodovinyl)-4-(trifluoromethyl)benzene (3.43i)

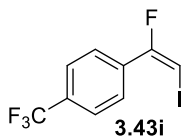

3.43i

The title compound was prepared according to GP4 using 1-ethynyl-4-(trifluoromethyl)benzene (32.6 µL, 0.20 mmol). Column chromatography (SiO_2, pentane) gave **3.43i** (43.1 mg, 68%) as a colourless oil. **^{1}H NMR** (500 MHz, $CDCl_3$) δ 7.92 (ad, *J* = 8.2 Hz, 2H), 7.67 (ad, *J* = 8.2 Hz, 2H), 6.28 (d, *J* = 19.7 Hz, 1H); **^{13}C NMR** (126 MHz, $CDCl_3$) δ 157.4 (d, $J_{C–F}$ = 256.1 Hz), 134.5 (d, $J_{C–F}$ = 29.1 Hz), 131.9 (qd, $J_{C–F}$ = 32.8, 0.8 Hz), 129.0 (d, $J_{C–F}$ = 5.3 Hz), 125.2 (q, $J_{C–F}$ = 3.7 Hz), 123.7 (q, $J_{C–F}$ = 272.4 Hz), 55.9 (d, $J_{C–F}$ = 43.0 Hz); **^{19}F NMR** (471 MHz, $CDCl_3$) δ –63.0, –77.1 (d, *J* = 19.7 Hz); **IR** (neat) ν 3071, 1618, 1408, 1324, 1169, 1126, 1114, 1067, 1047, 1015, 845, 817, 779, 764, 613 cm^{-1}; **HRMS** (EI) *m/z* Calcd for $C_9H_5F_4I$ $[M]^+$ 315.9372, found 315.9372.

(*E*)-1-(1-Fluoro-2-iodovinyl)-4-methoxybenzene (3.43j)

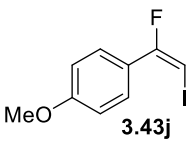

3.43j

The title compound was prepared according to GP3 using 1-ethynyl-4-methoxybenzene (35.6 mg, 0.20 mmol) and DIH (76.0 mg, 0.20 mmol). After work-up the crude product was dissolved in $CDCl_3$, C_6F_6 (5.8 µL, 0.050 mmol) was added as internal reference and quantitative ^{19}F NMR revealed that 12% of **3.43j** had been formed. Characteristic peaks: **^{1}H NMR** (400 MHz, $CDCl_3$) δ 5.90 (d, *J* = 19.6 Hz, 1H); **^{19}F NMR** (377 MHz, $CDCl_3$) δ –76.2 (d, *J* = 19.6 Hz).

2,2-Difluoro-1,1-diiodohexane (3.44a)

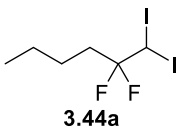

3.44a

The title compound was prepared according to GP5 using hex-1-yne (23.0 µL, 0.20 mmol). Column chromatography (SiO_2, pentane) gave **3.44a** (59.8 mg, 80%) as a colourless oil. **^{1}H NMR** (500 MHz, $CDCl_3$) δ 5.24 (t, *J* = 12.2 Hz, 1H), 2.36–2.22 (m, 2H), 1.50–1.42 (m, 2H), 1.37 (sext, *J* = 7.2 Hz, 2H), 0.92 (t, *J* = 7.2 Hz, 3H); **^{13}C NMR** (126 MHz, $CDCl_3$) δ 119.4 (t, $J_{C–F}$ = 247.9 Hz), 32.7 (t, $J_{C–F}$ = 24.7 Hz), 24.1 (t, $J_{C–F}$ = 3.9 Hz), 22.2, 13.7, –31.0 (t, $J_{C–F}$ = 33.8 Hz); **^{19}F NMR** (471 MHz, $CDCl_3$) δ –95.9 (td, *J* = 16.6, 12.2 Hz); **IR** (neat) ν 2960, 2933, 2872, 2361, 2342, 1466, 1268, 1251, 1179, 1156, 1076, 995, 914, 812, 688, 637 cm^{-1}; **HRMS** (EI) *m/z* Calcd for $C_6H_{10}F_2I_2$ $[M]^+$ 373.8840, found 373.8828.

(1,1-Difluoro-2,2-diiodoethyl)benzene (3.44b)

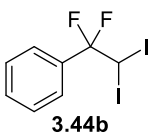

3.44b

The title compound was prepared according to GP5 using ethynylbenzene (22.0 µL, 0.20 mmol). Column chromatography (SiO_2, pentane) gave **3.44b** (31.5 mg, 42%) as a colourless oil. **^{1}H NMR** (500 MHz, $CDCl_3$) δ 7.56–7.52 (m, 2H), 7.50–

7.46 (m, 1H), 7.45–7.40 (m, 2H), 5.39 (t, *J* = 13.4 Hz, 1H); **^{13}C NMR** (126 MHz, $CDCl_3$) δ 131.3 (t, $J_{C–F}$ = 26.8 Hz), 130.9 (t, $J_{C–F}$ = 1.2 Hz), 128.4, 126.4 (t, $J_{C–F}$ = 5.8 Hz), 117.1 (t, $J_{C–F}$ = 248.6 Hz), –28.6 (t, $J_{C–F}$ = 38.2 Hz); **^{19}F NMR** (471 MHz, $CDCl_3$) δ –92.1 (d, *J* = 13.4 Hz); **IR** (neat) ν 2989, 2921, 1452, 1276, 1202, 1146, 1075, 1043, 1028, 987, 906, 766, 731, 695, 681, 640, 609 cm^{-1}; **HRMS** (EI) *m/z* Calcd for $C_8H_6F_2I_2$ $[M]^+$ 393.8527, found 393.8532.

(1,1-Difluoro-2,2-diiodoethyl)cyclohexane (3.44c)

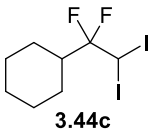

3.44c

The title compound was prepared according to GP5 using ethynylcyclohexane (26.1 µL, 0.20 mmol). Column chromatography (SiO_2, pentane) gave **3.44c** (69.7 mg, 87%) as a colourless oil. **^{1}H NMR** (500 MHz, $CDCl_3$) δ 5.28 (t, *J* = 14.1 Hz, 1H), 2.57–2.44 (tm, *J* = 14.3 Hz, 1H), 1.83–1.75 (m, 4H), 1.70–1.63 (m, 1H), 1.31–1.08 (m, 5H); **^{13}C NMR** (126 MHz, $CDCl_3$) δ 119.5 (t, $J_{C–F}$ = 250.0 Hz), 40.3 (t, $J_{C–F}$ = 23.3 Hz), 25.6, 25.4, 25.2 (t, $J_{C–F}$ = 3.9 Hz), –30.6 (t, $J_{C–F}$ = 34.4 Hz); **^{19}F NMR** (471 MHz, $CDCl_3$) δ –103.0 (dd, *J* = 14.3, 14.1 Hz); **IR** (neat) ν 3001, 2931, 2854, 1450, 1317, 1203, 1169, 1137, 1085, 1073, 998, 987, 895, 859, 830, 782, 708, 649, 606 cm^{-1}; **HRMS** (EI) *m/z* Calcd for $C_8H_{12}F_2I_2$ $[M]^+$ 399.8996, found 399.8995.

(3,3-Difluoro-4,4-diiodobutyl)benzene (3.44d)

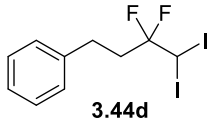

3.44d

The title compound was prepared according to GP5 using but-3-yn-1-ylbenzene (28.1 µL, 0.20 mmol). Column chromatography (SiO_2, pentane) gave **3.44d** (44.7 mg, 53%) as a colourless oil. **^{1}H NMR** (500 MHz, $CDCl_3$) δ 7.34–7.27 (m, 2H), 7.26–7.18 (m, 3H), 5.25 (t, *J* = 12.1 Hz, 1H), 2.85–2.80 (m, 2H), 2.68–2.57 (m, 2H); **^{13}C NMR** (126 MHz, $CDCl_3$) δ 139.6, 128.6, 128.3, 126.5, 118.9 (t, $J_{C–F}$ = 248.5 Hz), 35.1 (t, $J_{C–F}$ = 24.7 Hz), 28.4 (t, $J_{C–F}$ = 4.4 Hz), –31.7 (t, $J_{C–F}$ = 33.3 Hz); **^{19}F NMR** (471 MHz, $CDCl_3$) δ –96.3 (td, *J* = 16.2, 12.1 Hz); **IR** (neat) ν 3063, 3027, 2991, 2938, 1603, 1496,

1454, 1371, 1294, 1168, 1078, 1042, 946, 909, 840, 748, 699, 642 cm^{-1}; **HRMS** (EI) *m/z* Calcd for $C_{10}H_{10}F_2I_2$ $[M]^+$ 421.8840, found 421.8841.

6-Chloro-2,2-difluoro-1,1-diiodohexane (3.44e)

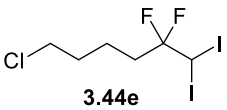

3.44e

The title compound was prepared according to GP5 using 6-chlorohex-1-yne (24.2 µL, 0.20 mmol). Column chromatography (SiO_2, 0–1% Et_2O in pentane) gave **3.44e** (48.3 mg, 59%) as a colourless oil. **^{1}H NMR** (500 MHz, $CDCl_3$) δ 5.25 (t, *J* = 11.9 Hz, 1H), 3.55 (t, *J* = 6.5 Hz, 2H), 2.40–2.29 (m, 2H), 1.88–1.80 (m, 2H), 1.72–1.63 (m, 2H); **^{13}C NMR** (126 MHz, $CDCl_3$) δ 119.1 (t, $J_{C–F}$ = 248.2 Hz), 44.3, 32.3 (t, $J_{C–F}$ = 24.9 Hz), 31.7, 19.6 (t, $J_{C–F}$ = 4.0 Hz), –31.7 (t, $J_{C–F}$ = 33.5 Hz); **^{19}F NMR** (471 MHz, $CDCl_3$) δ –96.2 (td, *J* = 16.5, 11.9 Hz); **IR** (neat) ν 2957, 2872, 1459, 1434, 1381, 1360, 1311, 1270, 1238, 1175, 1111, 1078, 987, 970, 907, 811, 731, 689, 649, 637 cm^{-1}; **HRMS** (EI) *m/z* Calcd for $C_6H_9{}^{35}ClF_2I_2$ $[M]^+$ 407.8450, found 407.8450.

5,5-Difluoro-6,6-diiodohexanenitrile (3.44f)

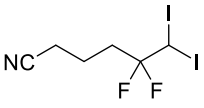

3.44f

The title compound was prepared according to GP5 using hex-5-ynenitrile (21.0 µL, 0.20 mmol). Column chromatography (SiO_2, 10–20% Et_2O in pentane) gave **3.44f** (60.0 mg, 78%) as a colourless oil. **^{1}H NMR** (500 MHz, $CDCl_3$) δ 5.24 (t, *J* = 11.7 Hz, 1H), 2.56–2.47 (m, 2H), 2.46 (t, *J* = 7.1 Hz, 2H), 1.98–1.90 (m, 2H); **^{13}C NMR** (126 MHz, $CDCl_3$) δ 118.8 (t, $J_{C–F}$ = 248.5 Hz), 118.6, 31.8 (t, $J_{C–F}$ = 25.0 Hz), 18.6 (t, $J_{C–F}$ = 4.0 Hz), 16.7, –32.8 (t, $J_{C–F}$ = 32.9 Hz); **^{19}F NMR** (471 MHz, $CDCl_3$) δ –96.8 (td, *J* = 16.8, 11.7 Hz); **IR** (neat) ν 2993, 2949, 2248, 1458, 1426, 1386, 1169, 1125, 1076, 968, 908, 809, 729, 690, 642 cm^{-1}; **HRMS** (EI) *m/z* Calcd for $C_6H_7F_2I_2N$ $[M]^+$ 384.8636, found 384.8632.

6,6-Difluoro-7,7-diiodoheptanoic acid (3.44g)

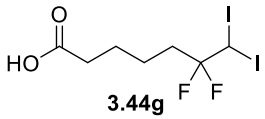

3.44g

The title compound was prepared according to GP5 using hept-6-ynoic acid (25.3 µL, 0.20 mmol). Column chromatography (SiO_2, 20–30% Et_2O in pentane) gave **3.44g** (47.7 mg, 57%) as a white solid. **M.p.** (pentane) = 92–93 °C; **^{1}H NMR** (500 MHz, $CDCl_3$) δ 5.23 (t, *J* = 12.0 Hz, 1H), 2.39 (t, *J* = 7.3 Hz, 2H), 2.38–2.28 (m, 2H), 1.70 (qn, *J* = 7.3 Hz, 2H), 1.61–1.53 (m, 2H); **^{13}C NMR** (126 MHz, $CDCl_3$) δ 179.5, 119.1 (t, $J_{C–F}$ = 248.1 Hz), 33.6, 32.7 (t, $J_{C–F}$ = 24.9 Hz), 24.0, 21.5 (t, $J_{C–F}$ = 3.9 Hz), –31.5 (t, $J_{C–F}$ = 33.5 Hz); **^{19}F NMR** (471 MHz, $CDCl_3$) δ –96.2 (td, *J* = 16.6, 12.0 Hz); **IR** (solid) ν 3014, 2947, 2921, 2878, 1689, 1429, 1267, 1160, 1092, 1074, 983, 931, 895, 812, 791, 731, 686, 637 cm^{-1}; **HRMS** (ESI-TOF) *m/z* Calcd for $C_7H_9F_2I_2O_2$ $[M–H]^-$ 416.8666, found 416.8662.

4-(1,1-Difluoro-2,2-diiodoethyl)-1,1'-biphenyl (3.44h)

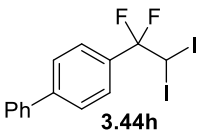

3.44h

The title compound was prepared according to GP5 using 4-ethynyl-1,1'-biphenyl (35.6 mg, 0.20 mmol). Column chromatography (SiO_2, 5% DCM in pentane) gave **3.44h** (16.0 mg, 17%) as a colourless oil. **^{1}H NMR** (500 MHz, $CDCl_3$) δ 7.65 (ad, *J* = 8.5 Hz, 2H), 7.62–7.58 (m, 3H), 7.48–7.43 (m, 2H), 7.40–7.36 (m, 1H), 5.42 (t, *J* = 13.2 Hz, 1H); **^{13}C NMR** (126 MHz, $CDCl_3$) δ 143.7 (t, $J_{C–F}$ = 1.0 Hz), 139.8, 130.1 (t, $J_{C–F}$ = 27.0 Hz), 128.9, 128.0, 127.2, 127.1, 127.0 (t, $J_{C–F}$ = 5.7 Hz), 117.2 (t, $J_{C–F}$ = 248.6 Hz), –28.6 (t, $J_{C–F}$ = 38.5 Hz); **^{19}F NMR** (471 MHz, $CDCl_3$) δ –91.8 (d, *J* = 13.2 Hz); **IR** (solid) ν 3031, 2987, 2924, 1611, 1487, 1405, 1276, 1196, 1147, 1046, 986, 908, 840, 765, 732, 695, 664, 612 cm^{-1}; **HRMS** (EI) *m/z* Calcd for $C_{14}H_{10}F_2I_2$ $[M]^+$ 469.8840, found 469.8841.

1-(1,1-Difluoro-2,2-diiodoethyl)-4-(trifluoromethyl)benzene (3.44i)

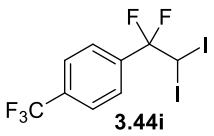

3.44i

The title compound was prepared according to GP5 using 1-ethynyl-4-(trifluoromethyl)benzene (32.6 µL, 0.20 mmol). Column chromatography (SiO_2, pentane) gave **3.44i** (70.2 mg, 76%) as a volatile colourless oil. **^{1}H NMR** (500 MHz, $CDCl_3$) δ 7.74–7.66 (m, 4H), 5.38 (t, *J* = 12.9 Hz, 1H); **^{13}C NMR** (126 MHz, $CDCl_3$) δ 135.1 (tq, $J_{C–F}$ = 27.5, 1.3 Hz), 133.0 (qt, $J_{C–F}$ = 32.9, 1.0 Hz), 127.2 (t, $J_{C–F}$ = 5.7 Hz), 125.5 (q, $J_{C–F}$ = 3.9 Hz), 123.5 (q, $J_{C–F}$ = 272.7 Hz), 116.5 (t, $J_{C–F}$ = 249.1 Hz), –30.6 (t, $J_{C–F}$ = 37.1 Hz); **^{19}F NMR** (471 MHz, $CDCl_3$) δ –63.0, –92.0 (d, *J* = 12.9 Hz); **IR** (neat) ν 2957, 2872, 1459, 1434, 1381, 1360, 1311, 1270, 1238, 1175, 1111, 1078, 987, 970, 907, 811, 731, 689, 649, 637 cm^{-1}; **HRMS** (EI) *m/z* Calcd for $C_9H_5F_5I_2$ $[M]^+$ 407.8450, found 407.8450.

1-(1,1-Difluoro-2,2-diiodoethyl)-4-methoxybenzene (3.44j)

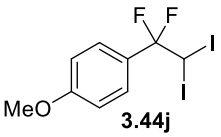

3.44j

The title compound was prepared according to GP5 using 1-ethynyl-4-methoxybenzene (26.4 mg, 0.20 mmol). After work-up, the crude product was taken up in $CDCl_3$, C_6F_6 (5.8 µL, 0.050 mmol) was added as internal reference and quantitative ^{19}F NMR revealed that a trace amount of **3.44j** had been formed. Characteristic peaks: **^{1}H NMR** (400 MHz, $CDCl_3$) δ 5.32 (t, *J* = 13.2 Hz, 1H); **^{19}F NMR** (377 MHz, $CDCl_3$) δ –91.4 (d, *J* = 13.2 Hz).

S.3.1.6. Iodofluorination-Cross-Coupling Sequences

General Procedure (GP) 6: Iodofluorination-Suzuki-Coupling Sequence

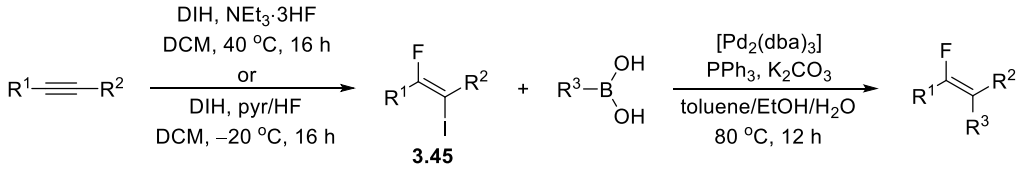

Scheme S.3.25. Preparation of trisubstituted fluoroalkenes *via* an iodofluorination-Suzuki-coupling sequence.

The iodofluorinated intermediate **3.45** was prepared using GP3 or GP4 as specified earlier using 1.00 equiv. of alkyne as well as DIH and 3.00 equiv. of the according fluorinating reagent (NEt_3·3HF, pyr/HF) in DCM. Instead of the work-up described for GP3 and GP4 the reaction mixture was filtered through silica gel, rinsing with 5% DCM in pentane, volatiles were removed *in vacuo* and the filtrate was used for the second step without further purification. The according boronic acid (1.50 equiv.), $[Pd_2(dba)_3]$ (5.0 mol%), PPh_3 (20 mol%), K_2CO_3 (3.00 equiv.) as well as degassed (three freeze-pump-thaw cycles) toluene, EtOH and H_2O were added to the filtrate. The mixture was warmed to 80 °C for 12 h, cooled to rt and diluted with DCM and H_2O. The layers were separated and the aqueous layer was extracted with DCM. The combined organic layers were dried over $MgSO_4$ and volatiles were removed under reduced pressure. Pure products were obtained after subsequent column chromatography.

(*E*)-(6-Fluorodec-5-en-5-yl)benzene (3.46)

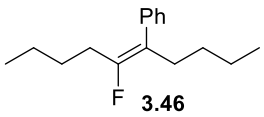

3.46

The title compound was prepared according to GP6 using dec-5-yne (18.0 µL, 0.10 mmol), DIH (38.0 mg, 0.10 mmol), NEt_3·3HF (48.9 µL, 0.30 mmol) and DCM (1.0 mL) for the first step. A quantitative yield of intermediate **3.45a** was assumed and for the second step phenylboronic acid (18.3 mg, 0.15 mmol), [$Pd_2(dba)_3$] (4.6 mg, 0.0050 mmol), PPh_3 (5.2 mg, 0.020 mmol), K_2CO_3 (41.5 mg, 0.30 mmol), toluene (1.0 mL), EtOH (0.30 mL) and H_2O (0.30 mL) were used. Column chromatography (SiO_2, pentane) gave **3.46** (18.5 mg, 79% over two steps) as a colourless oil. **^{1}H NMR** (400 MHz, $CDCl_3$) δ 7.33–7.27 (m, 2H), 7.26–7.20 (m, 1H), 7.15–7.10 (m, 2H), 2.39 (td, *J* = 7.4, 2.9 Hz, 2H), 2.10 (dt, *J* = 23.2, 7.4 Hz, 2H), 1.45 (tt, *J* = 8.6, 7.4 Hz, 2H), 1.33–1.16 (m, 6H), 0.84 (t, *J* = 7.2 Hz, 3H), 0.80 (t, *J* = 7.2 Hz, 3H); **^{13}C NMR** (100 MHz, $CDCl_3$) δ 157.0 (d, J_{C-F} = 251.0 Hz), 139.4 (d, J_{C-F} = 9.3 Hz), 129.0 (d, J_{C-F} = 2.9 Hz), 128.1, 126.6, 119.3 (d, J_{C-F} = 19.5 Hz), 30.0 (d, J_{C-F} = 1.4 Hz), 29.7 (d, J_{C-F} = 6.2 Hz), 29.0 (d, J_{C-F} = 28.4 Hz), 29.0, 22.3, 22.1, 13.9, 13.8; **^{19}F NMR** (377 MHz, $CDCl_3$) δ –111.4 (tt, *J* = 23.2, 2.9 Hz); **IR** (neat) ν 2958, 2928, 2861, 1688, 1493, 1466, 1443, 1220, 1181, 952, 880, 768, 741, 700 cm^{-1}; **HRMS** (EI) *m/z* Calcd for $C_{16}H_{23}F$ $[M]^+$ 234.1784, found 234.1781.

((1*E*,3*E*)-3-Butyl-4-fluoroocta-1,3-dien-1-yl)benzene (3.47)

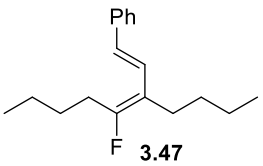

3.47

The title compound was prepared according to GP6 using dec-5-yne (18.0 µL, 0.10 mmol), DIH (38.0 mg, 0.10 mmol), NEt_3·3HF (48.9 µL, 0.30 mmol) and DCM (1.0 mL) for the first step. A quantitative yield of intermediate **3.45a** was assumed and for the second step (*E*)-styrylboronic acid (22.2 mg, 0.15 mmol), [$Pd_2(dba)_3$] (4.6 mg, 0.0050 mmol), PPh_3 (5.2 mg, 0.020 mmol), K_2CO_3 (41.5 mg, 0.30 mmol), toluene (1.0 mL), EtOH (0.30 mL) and H_2O (0.30 mL) were

used. Column chromatography (SiO_2, pentane) gave **3.47** (19.5 mg, 75% over two steps) as a yellow oil. **^{1}H NMR** (400 MHz, $CDCl_3$) δ 7.41–7.37 (m, 2H), 7.35–7.26 (m, 2H), 7.22–7.17 (m, 1H), 6.78 (dd, *J* = 16.1, 2.0 Hz, 1H), 6.50 (d, *J* = 16.1 Hz, 1H), 2.46 (dt, *J* = 24.5, 7.4 Hz, 2H), 2.36 (td, *J* = 7.6, 3.3 Hz, 2H), 1.60–1.51 (m, 2H), 1.49–1.31 (m, 6H), 0.93 (t, *J* = 7.2 Hz, 3H), 0.92 (t *J* = 7.2 Hz, 3H); **^{13}C NMR** (100 MHz, $CDCl_3$) δ 160.6 (d, $J_{C–F}$ = 256.6 Hz), 138.0, 128.6, 127.0, 127.0 (d, $J_{C–F}$ = 10.8 Hz), 126.0, 124.5 (d, $J_{C–F}$ = 7.5 Hz), 117.5 (d, $J_{C–F}$ = 20.0 Hz), 30.9, 29.1, 28.3 (d, $J_{C–F}$ = 28.5 Hz), 24.0 (d, $J_{C–F}$ = 7.4 Hz), 22.7, 22.1, 14.0, 13.9; **^{19}F NMR** (377 MHz, $CDCl_3$) δ –100.1 (ttd, *J* = 24.5, 3.3, 2.0 Hz); **IR** (neat) ν 3026, 2957, 2930, 2872, 2361, 1707, 1653, 1599, 1494, 1465, 1163, 952, 748, 692 cm^{-1}; **HRMS** (CI) *m/z* Calcd for $C_{18}H_{26}F$ $[M+H]^+$ 261.2013, found 261.2019.

((2*E*,4*E*)-4-Butyl-5-fluorononа-2,4-dien-1-yl)benzene (3.48)

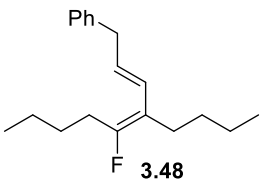

3.48

The title compound was prepared according to GP6 using dec-5-yne (18.0 µL, 0.10 mmol), DIH (38.0 mg, 0.10 mmol), NEt_3·3HF (48.9 µL, 0.30 mmol) and DCM (1.0 mL) for the first step. A quantitative yield of intermediate **3.45a** was assumed and for the second step (*E*)-(3-phenylprop-1-en-1-yl)boronic acid (24.3 mg, 0.15 mmol), $[Pd_2(dba)_3]$ (4.6 mg, 0.0050 mmol), PPh_3 (5.2 mg, 0.020 mmol), K_2CO_3 (41.5 mg, 0.30 mmol), toluene (1.0 mL), EtOH (0.30 mL) and H_2O (0.30 mL) were used. Column chromatography (SiO_2, pentane) gave **3.48** (19.0 mg, 69% over two steps) as a colourless oil. **^{1}H NMR** (400 MHz, $CDCl_3$) δ 7.32–7.26 (m, 2H), 7.24–7.14 (m, 3H), 6.07 (dq, *J* = 15.5, 1.6 Hz, 1H), 5.74 (dt, *J* = 15.5, 7.0 Hz, 1H), 3.45 (d, *J* = 7.0 Hz, 2H), 2.33 (dt, *J* = 24.6, 7.5 Hz, 2H), 2.22 (td, *J* = 7.5, 3.2 Hz, 2H), 1.54–1.45 (m, 2H), 1.41–1.24 (m, 6H), 0.90 (t, *J* = 7.3 Hz, 3H), 0.88 (t, *J* = 7.2 Hz, 3H); **^{13}C NMR** (100 MHz, $CDCl_3$) δ 159.0 (d, $J_{C–F}$ = 253.1 Hz), 140.6, 128.5, 128.4, 127.2 (d, $J_{C–F}$ = 10.6 Hz), 126.6 (d,

J_{C-F} = 7.4 Hz), 126.0, 116.6 (d, J_{C-F} = 19.1 Hz), 39.6, 30.9, 29.0, 28.1 (d, J_{C-F} = 28.6 Hz), 24.2 (d, J_{C-F} = 7.3 Hz), 22.7, 22.1, 14.0, 13.8; **^{19}F NMR** (377 MHz, $CDCl_3$) δ –104.3 (t, *J* = 24.6 Hz); **IR** (neat) ν 3029, 2957, 2930, 2872, 1666, 1495, 1454, 1160, 1079, 957, 735, 697 cm^{-1}; **HRMS** (CI) *m/z* Calcd for $C_{19}H_{28}F$ $[M+H]^+$ 275.2170, found 275.2177.

(*Z*)-5-Fluorodec-5-ene (3.49)

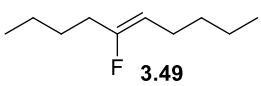

3.49

The title compound was obtained as by-product in a two-step reaction sequence according to GP6 using dec-5-yne (18.0 µL, 0.10 mmol), DIH (38.0 mg, 0.10 mmol), NEt_3·3HF (48.9 µL, 0.30 mmol) and DCM (1.0 mL) for the first step. A quantitative yield of intermediate **3.45a** was assumed and for the second step (3-phenylpropyl)boronic acid (22.5 mg, 0.15 mmol), $[Pd_2(dba)_3]$ (4.6 mg, 0.0050 mmol), PPh_3 (5.2 mg, 0.020 mmol), K_2CO_3 (41.5 mg, 0.30 mmol), toluene (1.0 mL), EtOH (0.30 mL) and H_2O (0.30 mL) were used. After work-up the crude product was dissolved in $CDCl_3$, C_6F_6 (5.8 µL, 0.050 mmol) was added as internal reference and quantitative ^{19}F NMR revealed that no cross-coupled product but instead 34% of **3.49** had been formed. Characteristic peaks: **^{1}H NMR** (400 MHz, $CDCl_3$) δ 4.43 (dtt, *J* = 38.2, 7.5, 0.7 Hz, 1H); **^{19}F NMR** (377 MHz, $CDCl_3$) δ –110.0 (dtt, *J* = 38.2, 17.6, 1.6 Hz). The spectroscopic data were identical in all respects to those previously reported.[469]

(*E*)-(1-fluoroprop-1-ene-1,2-diyl)dibenzene (3.50)

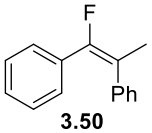

3.50

The title compound was prepared according to GP6 using prop-1-yn-1-ylbenzene (12.5 µL, 0.10 mmol), DIH (38.0 mg, 0.10 mmol), NEt_3·3HF (48.9 µL, 0.30 mmol) and DCM (1.0 mL) for the first step. A 70% yield of intermediate **3.45b** was assumed and for the second step phenylboronic acid (12.8 mg, 0.105 mmol), $[Pd_2(dba)_3]$ (3.2 mg, 0.0035 mmol), PPh_3 (3.7 mg, 0.014 mmol), K_2CO_3 (29.0 mg,

0.21 mmol), toluene (0.70 mL), EtOH (0.21 mL) and H_2O (0.21 mL) were used. Column chromatography (SiO_2, pentane) gave **3.50** (11.1 mg, 52% over two steps) as a colourless oil. **^{1}H NMR** (500 MHz, $CDCl_3$) δ 7.25–7.19 (m, 3H), 7.16–7.11 (m, 7H), 2.16 (d, *J* = 3.9 Hz, 3H); **^{13}C NMR** (126 MHz, $CDCl_3$) δ 153.4 (d, $J_{C–F}$ = 243.7 Hz), 140.0 (d, $J_{C–F}$ = 8.1 Hz), 132.8 (d, $J_{C–F}$ = 29.3 Hz), 128.9 (d, $J_{C–F}$ = 3.0 Hz), 128.5, 128.1 (d, $J_{C–F}$ = 5.7 Hz), 128.1, 127.7, 127.0, 116.9 (d, $J_{C–F}$ = 22.5 Hz), 17.7 (d, $J_{C–F}$ = 7.8 Hz); **^{19}F NMR** (377 MHz, $CDCl_3$) δ –104.7 (q, *J* = 3.9 Hz); **IR** (neat) ν 3058, 3025, 2922, 2854, 2360, 2341, 1668, 1495, 1443, 1237, 1116, 1058, 1025, 978, 801, 762, 692, 630 cm^{-1}; **HRMS** (EI) *m/z* Calcd for $C_{15}H_{13}F$ $[M]^+$ 212.1001, found 212.0995.

((1*E*,3*E*)-1-Fluoro-2-methylbuta-1,3-diene-1,4-diyl)dibenzene (3.51)

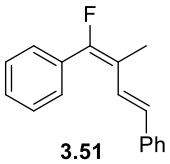

3.51

The title compound was prepared according to GP6 using prop-1-yn-1-ylbenzene (12.5 µL, 0.10 mmol), DIH (38.0 mg, 0.10 mmol), NEt_3·3HF (48.9 µL, 0.30 mmol) and DCM (1.0 mL) for the first step. A 70% yield of intermediate **3.45b** was assumed and for the second step (*E*)-styrylboronic acid (15.5 mg, 0.105 mmol), $[Pd_2(dba)_3]$ (3.2 mg, 0.0035 mmol), PPh_3 (3.7 mg, 0.014 mmol), K_2CO_3 (29.0 mg, 0.21 mmol), toluene (0.70 mL), EtOH (0.21 mL) and H_2O (0.21 mL) were used. Column chromatography (SiO_2, pentane) gave **3.51** (12.0 mg, 50% over two steps) as a light-yellow oil. **^{1}H NMR** (500 MHz, $CDCl_3$) δ 7.50–7.46 (m, 2H), 7.46–7.35 (m, 3H), 7.33–7.30 (m, 2H), 7.29–7.25 (m, 2H), 7.20–7.16 (m, 1H), 7.01 (dd, *J* = 16.0, 1.8 Hz, 1H), 6.63 (d, *J* = 16.0 Hz, 1H), 2.07 (d, *J* = 3.5 Hz, 3H); **^{13}C NMR** (126 MHz, $CDCl_3$) δ 157.4 (d, $J_{C–F}$ = 250.1 Hz), 137.6, 132.4 (d, $J_{C–F}$ = 28.7 Hz), 129.1 (d, $J_{C–F}$ = 4.5 Hz), 129.1, 128.9 (d, $J_{C–F}$ = 11.3 Hz), 128.6, 128.2, 127.2, 126.4 (d, $J_{C–F}$ = 5.3 Hz), 126.2, 114.9 (d, $J_{C–F}$ = 21.6 Hz), 11.0 (d, $J_{C–F}$ = 8.2 Hz); **^{19}F NMR** (471 MHz, $CDCl_3$) δ –94.4 (q, *J* = 3.5 Hz); **IR** (neat) ν 3058, 3025,

2924, 2853, 1642, 1597, 1491, 1446, 1244, 1091, 1067, 1016, 959, 922, 767, 749, 692 cm^{-1}; **HRMS** (CI) *m/z* Calcd for $C_{17}H_{16}F$ $[M+H]^+$ 239.1231, found 239.1229.

((1*E*,3*E*)-1-Fluoro-2-methylpenta-1,3-diene-1,5-diyl)dibenzene (3.52)

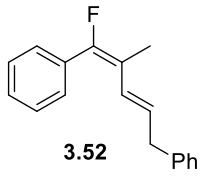

3.52

The title compound was prepared according to GP6 using prop-1-yn-1-ylbenzene (12.5 µL, 0.10 mmol), DIH (38.0 mg, 0.10 mmol), $NEt_3{\cdot}3HF$ (48.9 µL, 0.30 mmol) and DCM (1.0 mL) for the first step. A 70% yield of intermediate **3.45b** was assumed and for the second step (*E*)-(3-phenylprop-1-en-1-yl)boronic acid (17.0 mg, 0.105 mmol), $[Pd_2(dba)_3]$ (3.2 mg, 0.0035 mmol), PPh_3 (3.7 mg, 0.014 mmol), K_2CO_3 (29.0 mg, 0.21 mmol), toluene (0.70 mL), EtOH (0.21 mL) and H_2O (0.21 mL) were used. Column chromatography (SiO_2, pentane) gave **3.52** (13.9 mg, 55% over two steps) as a colourless oil. **^{1}H NMR** (500 MHz, $CDCl_3$) δ 7.44–7.41 (m, 2H), 7.40–7.32 (m, 3H), 7.30–7.26 (m, 2H), 7.21–7.15 (m, 3H), 6.35 (dq, *J* = 15.5, 1.7 Hz, 1H), 5.89 (dt, *J* = 15.5, 7.0 Hz, 1H), 3.42 (d, *J* = 7.0 Hz, 2H), 1.94 (d, *J* = 3.4 Hz, 3H); **^{13}C NMR** (126 MHz, $CDCl_3$) δ 155.9 (d, J_{C-F} = 246.8 Hz), 140.5, 132.5 (d, J_{C-F} = 29.1 Hz), 129.5 (d, J_{C-F} = 10.8 Hz), 129.0 (d, J_{C-F} = 4.4 Hz), 128.8 (d, J_{C-F} = 1.6 Hz), 128.5, 128.5, 128.4 (d, J_{C-F} = 5.4 Hz), 128.1, 126.1, 114.3 (d, J_{C-F} = 20.9 Hz), 39.5, 11.1 (d, J_{C-F} = 8.4 Hz); **^{19}F NMR** (471 MHz, $CDCl_3$) δ –100.6 (bs); **IR** (neat) ν 2084, 3061, 3027, 2922, 2361, 2341, 1600, 1493, 1445, 1238, 1100, 1069, 1050, 766, 695, 635 cm^{-1}; **HRMS** (CI) *m/z* Calcd for $C_{18}H_{18}F$ $[M+H]^+$ 253.1387, found 253.1390.

(2-Fluoroethene-1,1,2-triyl)tribenzene (3.53)

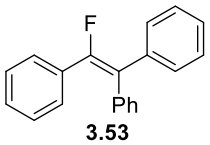

3.53

The title compound was prepared according to GP6 using 1,2-diphenylethyne (17.8 mg, 0.10 mmol), DIH (38.0 mg, 0.10 mmol), pyr/HF (7.8 µL, 0.30 mmol) and DCM (1.0 mL) for the first step. A 55% yield of intermediate **3.45d** was assumed and for the second step phenylboronic acid (10.1 mg, 0.0825 mmol), $[Pd_2(dba)_3]$ (2.5 mg, 0.0028 mmol), PPh_3 (2.9 mg, 0.011 mmol), K_2CO_3 (22.8 mg, 0.165 mmol), toluene (0.55 mL), EtOH (0.17 mL) and H_2O (0.17 mL) were used. Column chromatography (SiO_2, pentane) gave **3.53** (13.5 mg, 49% over two steps) as a white solid. **M.p.** (pentane) = 92–93 °C; **^{1}H NMR** (500 MHz, $CDCl_3$) δ 7.35–7.29 (m, 4H), 7.26–7.10 (m, 11H); **^{13}C NMR** (126 MHz, $CDCl_3$) δ 153.9 (d, J_{C-F} = 252.4 Hz), 139.0 (d, J_{C-F} = 6.8 Hz), 138.4, 133.0 (d, J_{C-F} = 28.8 Hz), 131.1 (d, J_{C-F} = 3.1 Hz), 129.9 (d, J_{C-F} = 4.6 Hz), 128.6, 128.5, 128.5 (d, J_{C-F} = 5.9 Hz), 128.0, 127.8, 127.4, 127.3, 122.3 (d, J_{C-F} = 18.4 Hz); **^{19}F NMR** (471 MHz, $CDCl_3$) δ –102.9; **IR** (solid) ν 3082, 3061, 3023, 2923, 2852, 1637, 1597, 1494, 1443, 1258, 1182, 1052, 1024, 933, 914, 757, 695, 644, 606 cm^{-1}; **HRMS** (CI) *m/z* Calcd for $C_{20}H_{19}FN$ $[M+NH_4]^+$ 292.1496, found 292.1497.

(4-(2-(Piperidin-1-yl)ethoxy)phenyl)boronic acid (3.55)[470]

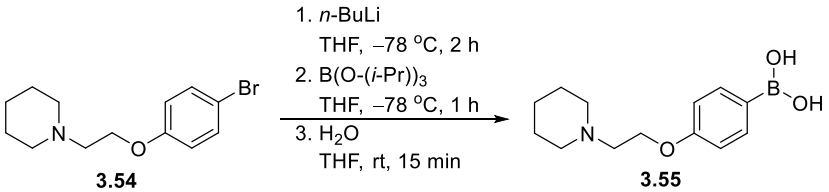

3.54 **3.55**

Scheme S.3.26. Preparation of boronic acid **3.55**.

A flame dried flask under an inert atmosphere was charged with THF (2.75 mL) and aryl bromide **3.54** (284 mg, 1.00 mmol). The resulting solution was cooled to –78 °C before *n*-BuLi (2.5 M in hexane, 400 µL, 1.00 mmol) was added dropwise. It was then stirred for 2 h at –78 °C before B(O-(*i*-Pr))$_3$ (231 µL, 1.00 mmol) was added dropwise and the reaction was stirred for 1 h at –78 °C. After warming to rt the reaction was diluted with H_2O (2.0 mL) and sat. aq. NH_4Cl (0.50 mL) and stirred for 15 min. The mixture was then extracted with DCM, the combined organic layers were dried over $MgSO_4$ and volatiles were removed *in vacuo*. The crude product was dissolved in a minimum amount of DCM and pentane was added causing the product to form a separate oily layer. The DCM layer was taken off and the remaining product (220 mg, 88%) was obtained as a yellow oil after drying under reduced pressure.

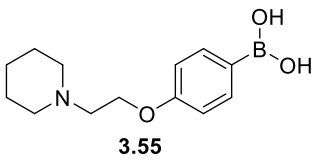

3.55

^{1}H NMR (500 MHz, MeOH-d_4) δ 7.58 (bs, 2H), 6.90 (ad, *J* = 8.5 Hz, 2H), 4.16 (t, *J* = 5.5 Hz, 2H), 2.87 (t, *J* = 5.5 Hz, 2H), 2.68–2.62 (bs, 4H), 1.67 (qn, *J* = 5.7 Hz, 4H), 1.51 (qn, *J* = 5.7 Hz, 2H); **^{13}C NMR** (126 MHz, MeOH-d_4) δ 161.1, 136.6, 114.8, 65.9, 58.9, 56.0, 26.3, 24.9; **IR** (neat) ν 3314, 3029, 2934, 2856, 2791, 2361, 2342, 1600, 1570, 1426, 1371, 1351, 1280, 1231, 1168, 1115, 1035, 833, 732, 676 cm^{-1}; **HRMS** (ESI-TOF) *m/z* Calcd for $C_{13}H_{21}{}^{11}BNO_3$ $[M+H]^+$ 250.1609, found 250.1610.

(*E*)-1-(2-(4-(2-Fluoro-1,2-diphenylvinyl)phenoxy)ethyl)piperidine (3.56)

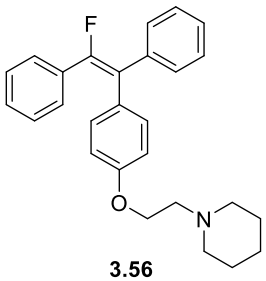

3.56

The title compound was prepared according to GP6 using 1,2-diphenylethyne (35.6 mg, 0.20 mmol), DIH (76.0 mg, 0.20 mmol), pyr/HF (15.6 µL, 0.60 mmol) and DCM (2.0 mL) for the first step. A 55% yield of intermediate **3.45d** was assumed and for the second step (4-(2-(piperidin-1-yl)ethoxy)phenyl)boronic acid, **3.55** (41.1 mg, 0.165 mmol), $[Pd_2(dba)_3]$ (5.0 mg, 0.0055 mmol), PPh_3 (5.8 mg, 0.022 mmol), K_2CO_3 (45.6 mg, 0.33 mmol), toluene (1.10 mL), EtOH (0.33 mL) and H_2O (0.33 mL) were used. Column chromatography (SiO_2, 1–2% MeOH in DCM) gave **3.56** (38.5 mg, 48% over two steps) as a colourless oil. **^{1}H NMR** (500 MHz, $CDCl_3$) δ 7.34–7.27 (m, 4H), 7.25–7.20 (m, 3H), 7.20–7.13 (m, 3H), 7.00 (ad, *J* = 8.7 Hz, 2H), 6.74 (ad, *J* = 8.7 Hz, 2H), 4.05 (t, *J* = 6.1 Hz, 2H), 2.74 (t, *J* = 6.1 Hz, 2H), 2.48 (bs, 4H), 1.58 (qn, *J* = 5.9 Hz, 4H), 1.42 (qn, *J* = 5.9 Hz, 2H); **^{13}C NMR** (126 MHz, $CDCl_3$) δ 158.2, 153.5 (d, J_{C-F} = 251.5 Hz), 138.7, 133.2 (d, J_{C-F} = 28.9 Hz), 132.1 (d, J_{C-F} = 3.1 Hz), 131.2 (d, J_{C-F} = 6.9 Hz), 129.9 (d, J_{C-F} = 4.6 Hz), 128.4, 128.4 (d, J_{C-F} = 6.1 Hz), 128.0, 127.9, 127.2, 121.8 (d, J_{C-F} = 18.5 Hz), 114.6, 65.9, 57.9, 55.1, 25.9, 24.1; **^{19}F NMR** (471 MHz, $CDCl_3$) δ –103.8; **IR** (neat) ν 2934, 2853, 2785, 1607, 1509, 1444, 1243, 1173, 1056, 1034, 935, 908, 825, 761, 730, 694, 606 cm^{-1}; **HRMS** (ESI-TOF) *m/z* Calcd for $C_{27}H_{29}FNO$ $[M+H]^+$ 402.2228, found 402.2223.

General Procedure (GP) 7: Iodofluorination-Sonogashira-Coupling Sequence

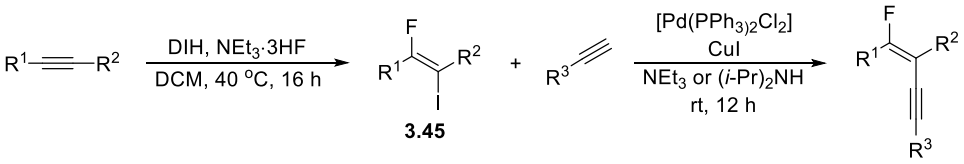

Scheme S.3.27. Preparation of enynes *via* an iodofluorination-Sonogashira-coupling sequence.

The iodofluorinated intermediate **3.45** was prepared using GP3 as described earlier using 1.00 equiv. of alkyne as well as DIH and 3.00 equiv. of NEt_3·3HF in DCM. Instead of the work-up described for GP3 the reaction mixture was filtered through silica gel rinsing with 5% DCM in pentane. Volatiles were removed *in vacuo* and the filtrate was used for the second step without further purification. $[Pd(PPh_3)_2Cl_2]$ (2.5 mol%), CuI (5.0 mol%), degassed (three freeze-pump-thaw cycles) NEt_3 or $(i\text{-}Pr)_2NH$ (see individual compounds) and the according alkyne (1.4 equiv.) were added to the filtrate. The mixture was stirred at rt for 12 h before being diluted with DCM and H_2O. The layers were separated and the aqueous layer was extracted with DCM. The combined organic layers were dried over $MgSO_4$ and volatiles were removed under reduced pressure. Pure products were obtained after subsequent column chromatography.

(*E*)-(3-Butyl-4-fluorooct-3-en-1-yn-1-yl)benzene (3.57)

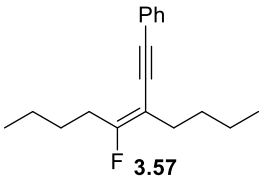

3.57

The title compound was prepared according to GP7 using dec-5-yne (18.0 µL, 0.10 mmol), DIH (38.0 mg, 0.10 mmol), NEt_3·3HF (48.9 µL, 0.30 mmol) and DCM (1.0 mL) for the first step. A quantitative yield of intermediate **3.45a** was assumed and for the second step phenylacetylene (15.4 µL, 0.14 mmol), $[Pd(PPh_3)_2Cl_2]$ (1.8 mg, 0.0025 mmol), CuI (1.0 mg,

0.0050 mmol) and NEt_3 (0.50 mL) were used. Column chromatography (SiO_2, pentane) gave **3.57** (17.5 mg, 68% over two steps) as a colourless oil. **^{1}H NMR** (400 MHz, $CDCl_3$) δ 7.42–7.37 (m, 2H), 7.33–7.26 (m, 3H), 2.55 (dt, *J* = 22.4, 7.3 Hz, 2H), 2.23 (td, *J* = 7.5, 2.9 Hz, 2H), 1.60–1.48 (m, 4H), 1.45–1.30 (m, 4H), 0.94 (t, *J* = 7.2 Hz, 3H), 0.92 (t, *J* = 7.2 Hz, 3H); **^{13}C NMR** (100 MHz, $CDCl_3$) δ 166.1 (d, $J_{C–F}$ = 263.6 Hz), 131.1, 128.3, 127.8, 123.8, 103.3 (d, $J_{C–F}$ = 30.8 Hz), 92.5 (d, $J_{C–F}$ = 7.9 Hz), 86.8 (d, $J_{C–F}$ = 14.3 Hz), 30.5, 30.3, 28.4, 27.5 (d, $J_{C–F}$ = 3.3 Hz), 22.1, 22.0, 13.9, 13.8; **^{19}F NMR** (377 MHz, $CDCl_3$) δ –100.3 (tt, *J* = 22.4, 2.9 Hz); **IR** (neat) ν 2958, 2929, 2862, 1660, 1598, 1490, 1466, 1232, 1193, 1144, 1010, 912, 753, 689 cm^{-1}; **HRMS** (EI) *m/z* Calcd for $C_{18}H_{23}F$ $[M]^+$ 258.1784, found 258.1780.

(*E*)-(3-Butyl-4-fluorooct-3-en-1-yn-1-yl)trimethylsilane (3.58)

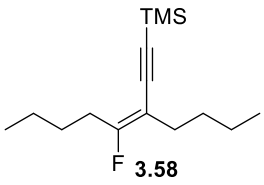

3.58

The title compound was prepared according to GP7 using dec-5-yne (18.0 µL, 0.10 mmol), DIH (38.0 mg, 0.10 mmol), NEt_3·3HF (48.9 µL, 0.30 mmol) and DCM (1.0 mL) for the first step. A quantitative yield of intermediate **3.45a** was assumed and for the second step ethynyltrimethylsilane (19.8 µL, 0.14 mmol), $[Pd(PPh_3)_2Cl_2]$ (1.8 mg, 0.0025 mmol), CuI (1.0 mg, 0.0050 mmol) and NEt_3 (0.50 mL) were used. Column chromatography (SiO_2, pentane) gave **3.58** (19.1 mg, 75% over two steps) as a colourless oil. **^{1}H NMR** (400 MHz, $CDCl_3$) δ 2.47 (dt, *J* = 22.5, 7.4 Hz, 2H), 2.10 (td, *J* = 7.4, 2.7 Hz, 2H), 1.55–1.48 (m, 2H), 1.47–1.38 (m, 2H), 1.38–1.25 (m, 4H), 0.91 (t, *J* = 7.3 Hz, 3H), 0.89 (t, *J* = 7.3 Hz, 3H), 0.16 (s, 9H); **^{13}C NMR** (100 MHz, $CDCl_3$) δ 167.3 (d, $J_{C–F}$ = 264.4 Hz), 103.4 (d, $J_{C–F}$ = 30.0 Hz), 102.8 (d, $J_{C–F}$ = 13.3 Hz), 97.3 (d, $J_{C–F}$ = 7.0 Hz), 30.2 (d, $J_{C–F}$ = 28.1 Hz), 30.1, 28.2, 27.2 (d, $J_{C–F}$ = 3.3 Hz), 22.0, 21.9, 13.9, 13.7, 0.0; **^{19}F NMR** (377 MHz, $CDCl_3$) δ –99.8 (tt, *J* = 22.5, 2.7 Hz); **IR**

(neat) ν 2959, 2930, 2863, 2360, 2145, 1659, 1466, 1249, 1223, 1171, 1014, 839, 758, 698 cm^{-1}; **HRMS** (CI) *m/z* Calcd for $C_{15}H_{28}FSi$ $[M+H]^+$ 255.1939, found 255.1939.

(*E*)-(1-Fluoro-2-methylbut-1-en-3-yne-1,4-diyl)dibenzene (3.59)

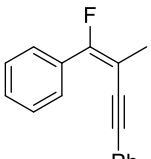

3.59

The title compound was prepared according to GP7 using prop-1-yn-1-ylbenzene (12.5 µL, 0.10 mmol), DIH (38.0 mg, 0.10 mmol), NEt_3·3HF (48.9 µL, 0.30 mmol) and DCM (1.0 mL) for the first step. A 70% yield of intermediate **3.45b** was assumed and for the second step phenylacetylene (10.8 µL, 0.098 mmol), $[Pd(PPh_3)_2Cl_2]$ (1.2 mg, 0.0018 mmol), CuI (0.7 mg, 0.004 mmol) and $(i\text{-Pr})_2NH$ (0.35 mL) were used. Column chromatography (SiO_2, pentane) gave **3.59** (14.0 mg, 59% over two steps) as a light yellow oil. **^{1}H NMR** (500 MHz, $CDCl_3$) δ 8.02–7.95 (m, 2H), 7.43–7.29 (m, 8H), 2.09 (d, *J* = 4.3 Hz, 3H); **^{13}C NMR** (126 MHz, $CDCl_3$) δ 160.8 (d, J_{C-F} = 251.1 Hz), 131.9 (d, J_{C-F} = 27.6 Hz), 131.2, 129.2, 128.4, 128.1 (d, J_{C-F} = 21.9 Hz), 128.0, 126.7 (d, J_{C-F} = 7.3 Hz), 123.4, 99.1 (d, J_{C-F} = 35.6 Hz), 94.3 (d, J_{C-F} = 9.0 Hz), 88.4 (d, J_{C-F} = 13.4 Hz), 16.5 (d, J_{C-F} = 5.8 Hz); **^{19}F NMR** (377 MHz, $CDCl_3$) δ –102.9 (q, *J* = 4.3 Hz); **IR** (neat) ν 3060, 2959, 2361, 2341, 2145, 1494, 1446, 1250, 1211, 1117, 1096, 1071, 1014, 909, 839, 761, 689, 634 cm^{-1}; **HRMS** (CI) *m/z* Calcd for $C_{17}H_{14}F$ $[M+H]^+$ 237.1074, found 237.1079.

(*E*)-(4-Fluoro-3-methyl-4-phenylbut-3-en-1-yn-1-yl)trimethylsilane (3.60)

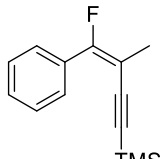

3.60

The title compound was prepared according to GP7 using prop-1-yn-1-ylbenzene (12.5 µL, 0.10 mmol), DIH (38.0 mg, 0.10 mmol), NEt_3·3HF (48.9 µL, 0.30 mmol) and DCM (1.0 mL) for the first step. A 70% yield of intermediate **3.45b** was assumed and for the second step ethynyltrimethylsilane (13.8 µL, 0.098 mmol), $[Pd(PPh_3)_2Cl_2]$ (1.2 mg, 0.0018 mmol), CuI (0.7 mg, 0.004 mmol) and (*i*-

$Pr)_2NH$ (0.35 mL) were used. Column chromatography (SiO_2, pentane) gave **3.60** (9.1 mg, 39% over two steps) as a colourless oil. **^{1}H NMR** (500 MHz, $CDCl_3$) δ 7.99–7.95 (m, 2H), 7.39–7.30 (m, 3H), 1.98 (d, *J* = 4.3 Hz, 3H), 0.19 (s, 9H); **^{13}C NMR** (126 MHz, $CDCl_3$) δ 161.7 (d, J_{C-F} = 251.8 Hz), 131.6 (d, J_{C-F} = 27.5 Hz), 129.2, 127.8 (d, J_{C-F} = 1.8 Hz), 126.7 (d, J_{C-F} = 7.5 Hz), 104.1 (d, J_{C-F} = 12.5 Hz), 100.3 (d, J_{C-F} = 8.1 Hz), 99.0 (d, J_{C-F} = 34.8 Hz), 16.4 (d, J_{C-F} = 6.2 Hz), –0.3; **^{19}F NMR** (471 MHz, $CDCl_3$) δ –103.0 (q, *J* = 4.3 Hz); **IR** (neat) ν 3058, 3033, 2956, 2925, 2830, 2360, 2341, 1596, 1489, 1443, 1260, 1114, 1096, 1070, 915, 765, 753, 687, 631 cm^{-1}; **HRMS** (CI) *m/z* Calcd for $C_{14}H_{18}FSi$ $[M+H]^+$ 233.1156, found 233.1152.

General Procedure (GP) 8: Iodofluorination-Ullmann-Coupling Sequence

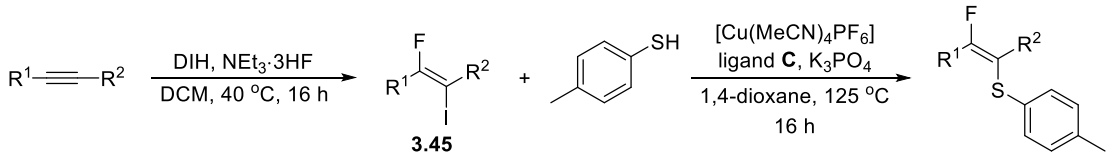

Scheme S.3.28. Synthesis of (*E*)-(β-fluorovinyl)-sulfides *via* an iodofluorination-Ullmann-coupling sequence.

The iodofluorinated intermediate **3.45** was prepared using GP3 as described earlier using 1.00 equiv. of alkyne as well as DIH and 3.00 equiv. of NEt_3·3HF in DCM. Instead of the work-up described for GP3 the reaction mixture was filtered through silica gel, rinsing with 5% DCM in pentane, volatiles were removed *in vacuo* and the filtrate was used for the second step without further purification. A screw-top vial was flushed with Ar and $[Cu(MeCN)_4PF_6]$ (10 mol%), ligand **C** (20 mol%), K_3PO_4 (2.00 equiv.) and 1,4-dioxane were added subsequently. The vial was again flushed with Ar, and the suspension was stirred at rt for 10 min during which the mixture turned dark grey. 4-Methylbenzenethiol (1.50 equiv.) and a solution of intermediate **3.45** in 1,4-dioxane were added, causing the

mixture to turn light yellow. The vial was again flushed with Ar and then placed in a 125 °C oil bath for 16 h. Subsequently, the mixture was cooled to rt and separated between H_2O and DCM. The layers were separated and the aqueous layer was extracted with DCM. The combined organic layers were dried over $MgSO_4$ and volatiles removed under reduced pressure. Column chromatography was used to isolate the desired products.

(*E*)-(6-Fluorodec-5-en-5-yl)(p-tolyl)sulfane (3.61)

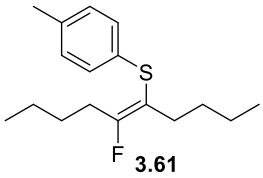

3.61

The title compound was prepared according to GP8 using dec-5-yne (18.0 µL, 0.10 mmol), DIH (38.0 mg, 0.10 mmol), NEt_3·3HF (48.9 µL, 0.30 mmol) and DCM (1.0 mL) for the first step. A quantitative yield of intermediate **3.45a** was assumed and for the second step [$Cu(MeCN)_4PF_6$] (3.7 mg, 0.010 mmol), ligand **C** (3.9 mg, 0.020 mmol), K_3PO_4 (42.5 mg, 0.20 mmol) and 1,4-dioxane (0.15 mL) were at first added followed by 4-methylbenzenethiol (18.6 mg, 0.15 mmol) and a solution of intermediate **3.45a** (from first step) in 1,4-dioxane (0.15 mL). Column chromatography (SiO_2, pentane) gave **3.61** (23.6 mg, 82% over two steps) as a colourless oil. **^{1}H NMR** (500 MHz, $CDCl_3$) δ 7.11 (ad, *J* = 8.2 Hz, 2H), 7.07 (ad, *J* = 8.2 Hz, 2H), 2.61 (dt, *J* = 23.3, 7.5 Hz, 2H), 2.30 (s, 3H), 2.20 (td, *J* = 7.5, 3.2 Hz, 2H), 1.56–1.49 (m, 2H), 1.46–1.39 (m, 2H), 1.34 (sext, *J* = 7.3 Hz, 2H), 1.24 (sext, *J* = 7.3 Hz, 2H), 0.90 (t, *J* = 7.3 Hz, 3H), 0.84 (t, *J* = 7.3 Hz, 3H); **^{13}C NMR** (126 MHz, $CDCl_3$) δ 164.4 (d, J_{C-F} = 265.2 Hz), 135.6, 132.1 (d, J_{C-F} = 2.6 Hz), 129.7, 128.1, 112.2 (d, J_{C-F} = 24.8 Hz), 30.1 (d, J_{C-F} = 1.4 Hz), 29.6 (d, J_{C-F} = 27.3 Hz), 28.9, 28.4 (d, J_{C-F} = 4.6 Hz), 22.1, 22.1, 21.0, 13.9, 13.8; **^{19}F NMR** (471 MHz, $CDCl_3$) δ –93.3 (tt, *J* = 23.3, 3.2 Hz); **IR** (neat) ν

3020, 2957, 2928, 2861, 1647, 1660, 1492, 1465, 1378, 1225, 1181, 1125, 1115, 1087, 1017, 976, 955, 886, 804 cm^{-1}; **HRMS** (CI) *m/z* Calcd for $C_{17}H_{26}FS$ $[M+H]^+$ 281.1734, found 281.1737.

(*E*)-(1-Fluoro-1-phenylprop-1-en-2-yl)(p-tolyl)sulfane (3.62)

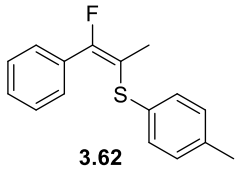

3.62

The title compound was prepared according to GP8 using prop-1-yn-1-ylbenzene (12.5 µL, 0.10 mmol), DIH (38.0 mg, 0.10 mmol), $NEt_3 \cdot 3HF$ (48.9 µL, 0.30 mmol) and DCM (1.0 mL) for the first step. A 70% yield of intermediate **3.45b** was assumed and for the second step $[Cu(MeCN)_4PF_6]$ (2.6 mg, 0.0070 mmol), ligand **C** (2.7 mg, 0.014 mmol), K_3PO_4 (29.7 mg, 0.14 mmol) and 1,4-dioxane (0.15 mL) were at first added followed by 4-methylbenzenethiol (13.0 mg, 0.105 mmol) and a solution of intermediate **3.45b** (from first step) in 1,4-dioxane (0.15 mL). Column chromatography (SiO_2, pentane) gave **3.62** (14.0 mg, 54% over two steps) as a colourless oil. **^{1}H NMR** (500 MHz, $CDCl_3$) δ 7.69–7.64 (m, 2H), 7.37–7.32 (m, 3H), 7.18 (ad, *J* = 8.2 Hz, 2H), 7.10 (ad, *J* = 8.2 Hz, 2H), 2.31 (s, 3H), 2.04 (d, *J* = 4.2 Hz, 3H); **^{13}C NMR** (126 MHz, $CDCl_3$) δ 158.7 (d, *J* = 255.9 Hz), 136.3, 131.9 (d, *J* = 28.7 Hz), 131.0 (d, *J* = 2.4 Hz), 129.9, 129.3 (d, *J* = 1.2 Hz), 129.0, 128.5 (d, *J* = 5.1 Hz), 127.9, 109.9 (d, *J* = 28.5 Hz), 21.0, 17.1 (d, *J* = 6.0 Hz); **^{19}F NMR** (471 MHz, $CDCl_3$) δ –87.8 (q, *J* = 4.2 Hz); **IR** (neat) v 3057, 3023, 2919, 2850, 2361, 2341, 1647, 1600, 1491, 1444, 1262, 1083, 1061, 830, 804, 765, 692 cm^{-1}; **HRMS** (CI) *m/z* Calcd for $C_{16}H_{16}FS$ $[M+H]^+$ 259.0951, found 259.0956.

S.3.2. Determination of Configuration of Iodofluoroalkenes

S.3.2.1. Internal Iodofluoroalkenes

In order to determine the configuration of internal iodofluorinated alkenes, 1D $^{19}F–^{1}H$ HOESY as well as 2D $^{1}H–^{1}H$ NOESY experiments were performed on **3.45b** (Figure S.3.1.–S.3.2.).

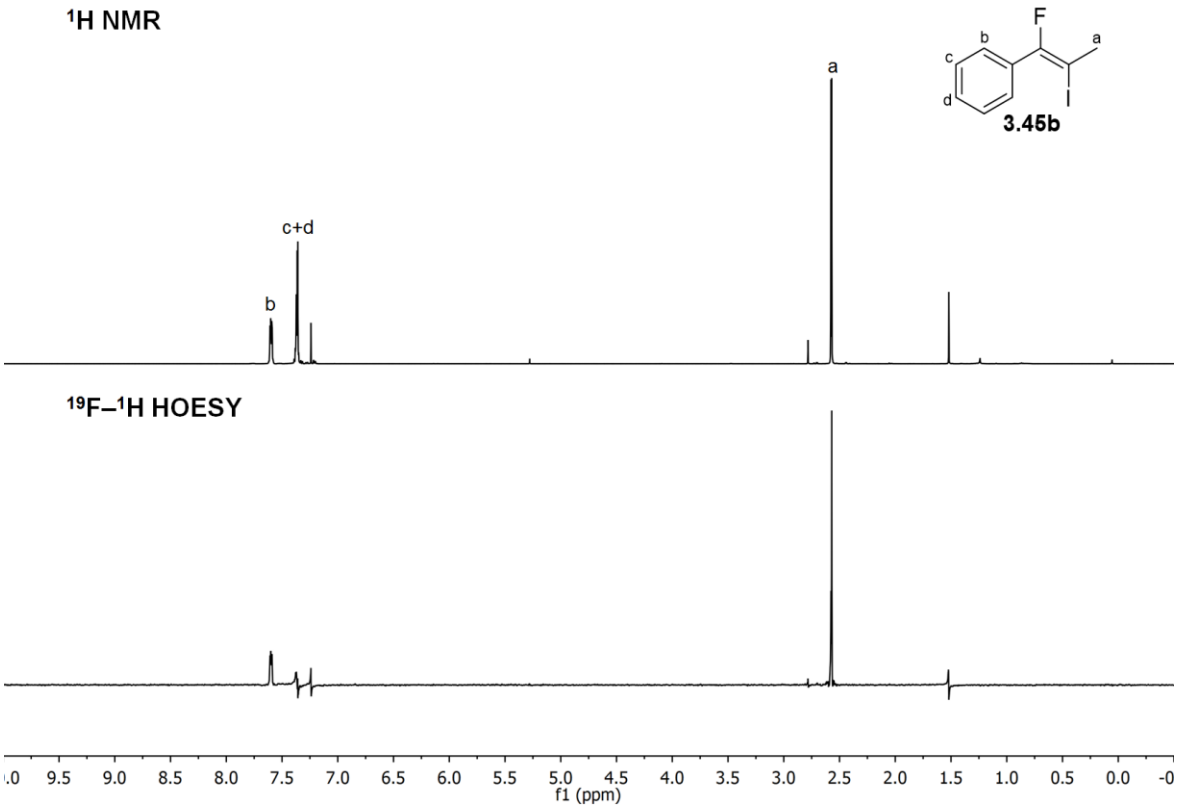

Figure S.3.1. 1D $^{19}F–^{1}H$ HOESY NMR of **3.45b**.

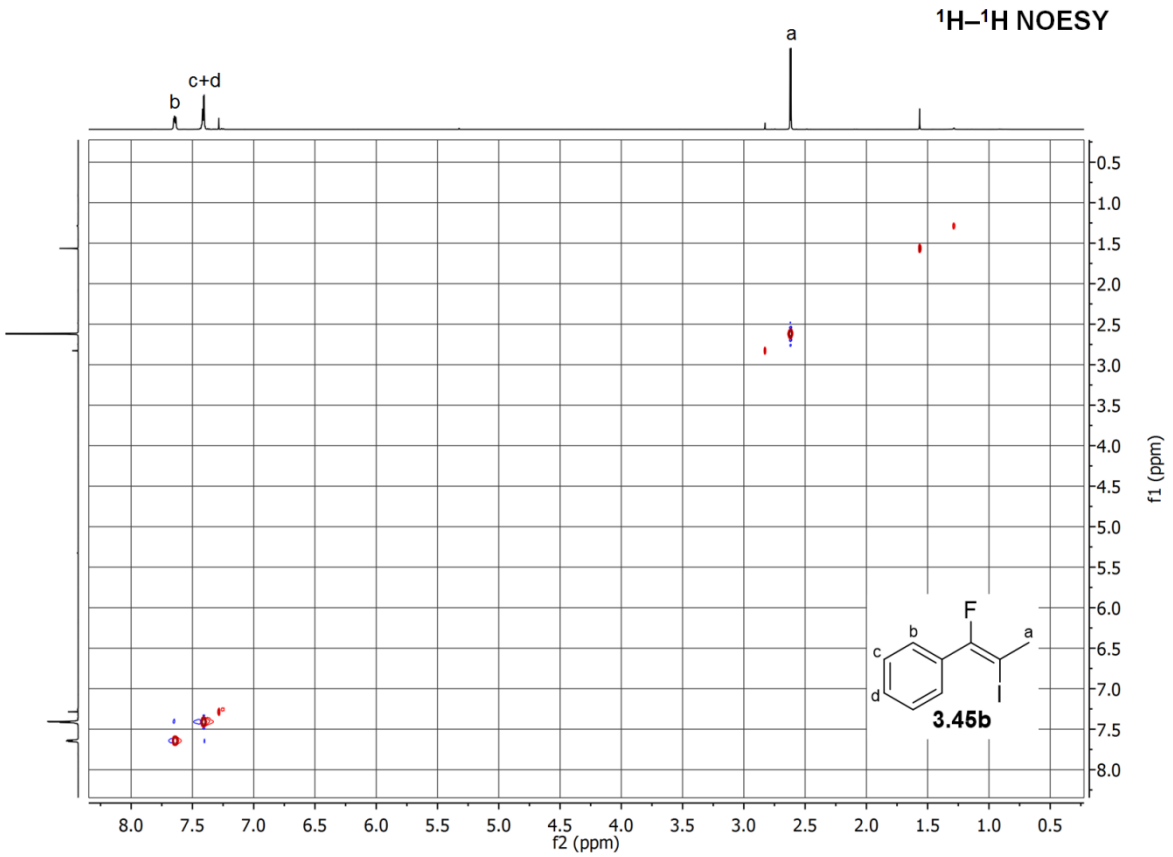

Figure S.3.2. 2D ^{1}H–^{1}H NOESY NMR of **3.45b**.

S.3.2.2. Terminal Iodofluoroalkenes

Similarly to internal iodofluoroalkenes also for terminal iodofluoroalkenes the configuration was determined using 1D ^{19}F–^{1}H HOESY as well as 2D ^{1}H–^{1}H NOESY experiments on **3.43d** (Figure S.3.3.–S.3.4.).

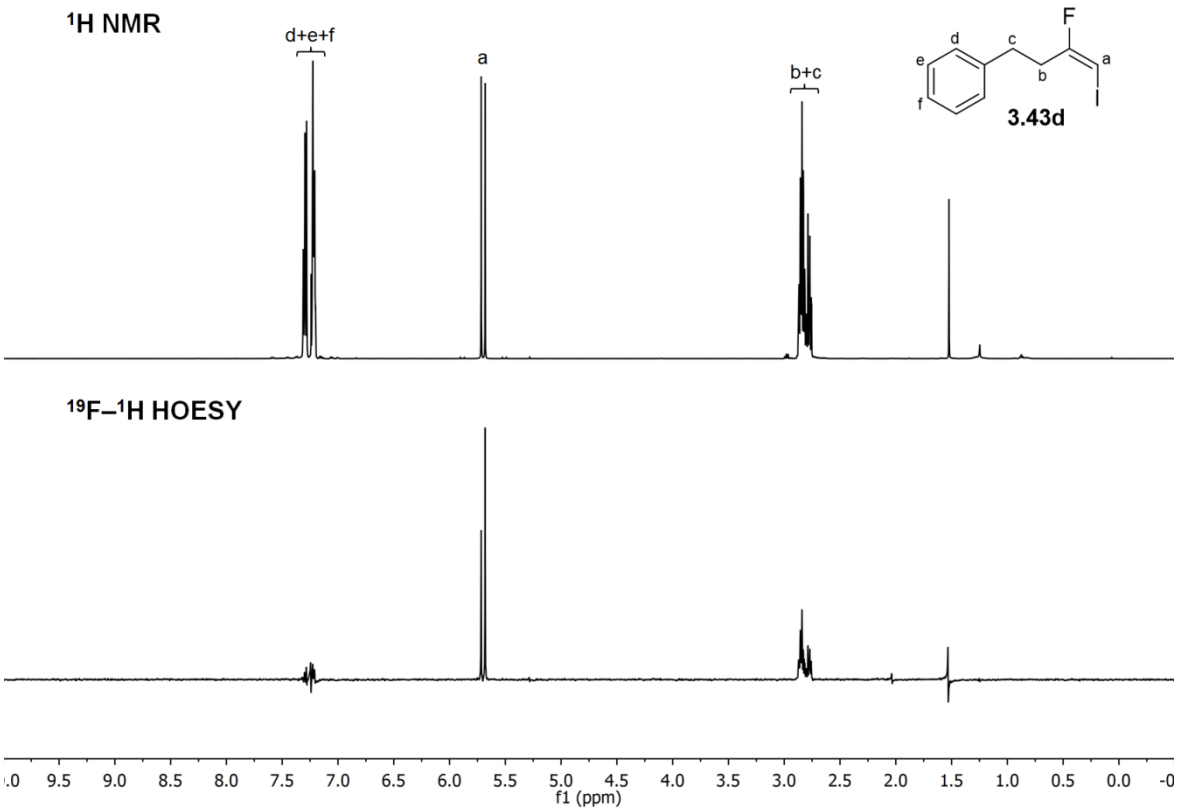

Figure S.3.3. 1D $^{19}F–^{1}H$ HOESY NMR of **3.43d**.

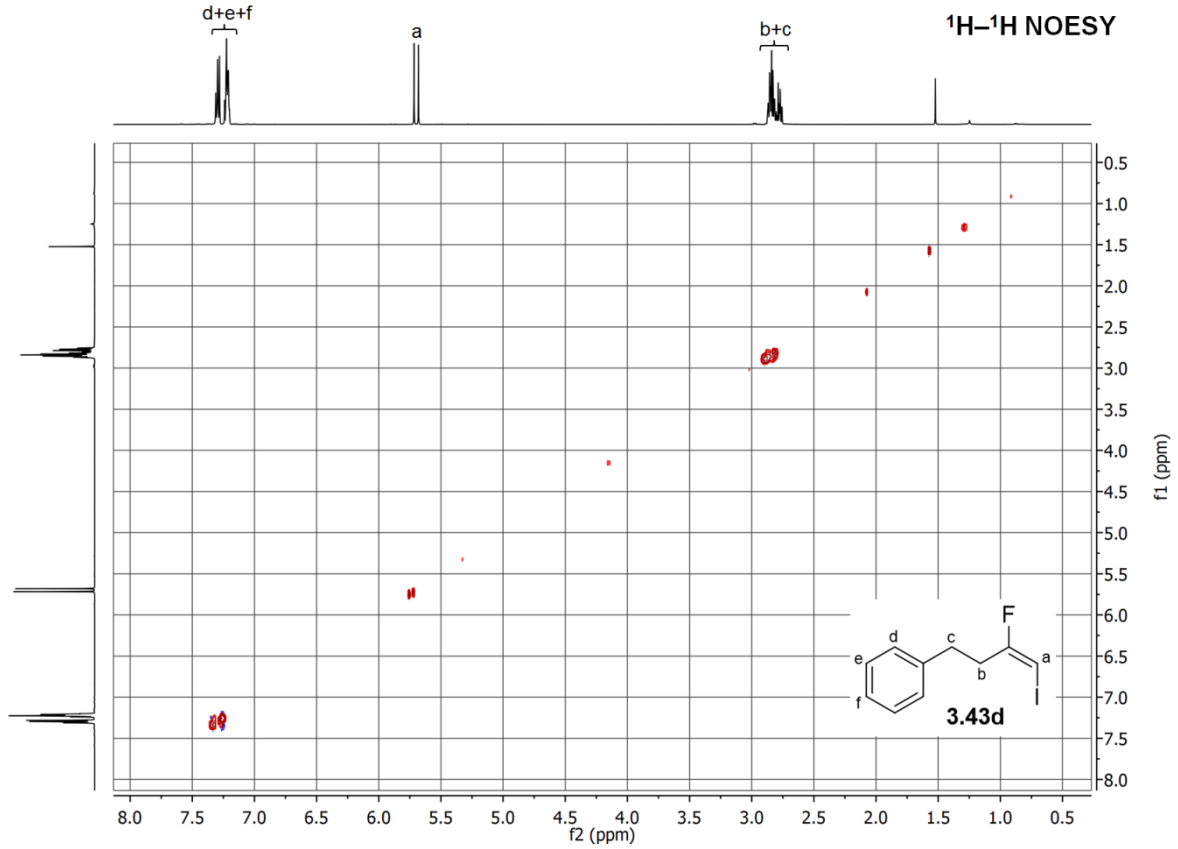

Figure S.3.4. 2D $^{1}H–^{1}H$ NOESY NMR of **3.43d**.

Chapter 4

S.4.1. Synthesis and Characterisation of Compounds

S.4.1.1. Hydrogen Bond Donors

Synthesis of 4.18o

cis-Diethyl 1-benzylpyrrolidine-2,5-dicarboxylate[471]

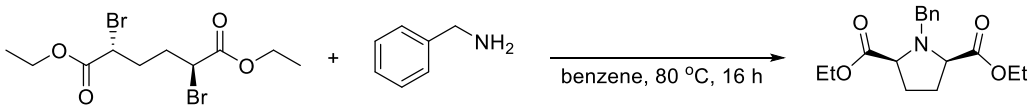

Scheme S.4.1. Synthesis of diethyl 1-benzylpyrrolidine-2,5-dicarboxylate.

A flame dried flask was charged with diethyl *meso*-2,5-dibromoadipate (10.0 g, 27.8 mmol). Benzene (30 mL) was added to dissolve the starting material before the resulting solution was heated to gentle reflux. The heat was removed and benzylamine (10.6 mL, 97.2 mmol) was added dropwise maintaining reflux. After complete addition the mixture was stirred at reflux for 16 h. After cooling to rt solids were removed by filtration, the mixture was concentrated *in vacuo* and column chromatography (SiO_2, 10–15% EtOAc in hexane) gave the title compound (3.26 g, 38%) as a colourless oil.

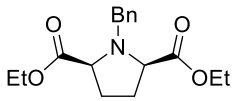

^{1}H NMR (400 MHz, $CDCl_3$) δ 7.35–7.30 (m, 2H), 7.30–7.24 (m, 2H), 7.24–7.18 (m, 1H), 4.07–3.95 (m, 4H), 3.93 (s, 2H), 3.45–3.37 (m, 2H), 2.11–2.00 (m, 4H), 1.18 (t, *J* = 7.2 Hz, 6H); **^{13}C NMR** (100 MHz, $CDCl_3$) δ 173.2, 137.4, 129.4, 127.8, 127.0, 65.4, 60.4, 57.6, 28.5, 14.0; **IR** (neat) ν 3086, 3063, 3028, 2981, 2939, 2904, 2874, 2831, 2361, 2340, 1741, 1727, 1604, 1586, 1495, 1454, 1447, 1371, 1349, 1272, 1178, 1148, 1097, 1072, 1028, 969, 913, 852, 811, 751, 700, 619 cm^{-1}; **HRMS** (ESI-

TOF) *m/z* Calcd for $C_{17}H_{24}NO_4$ $[M+H]^+$ 306.1700, found 306.1699. The spectroscopic data were identical in all respects to those previously reported.[471]

cis-(1-Benzylpyrrolidine-2,5-diyl)bis(diphenylmethanol)

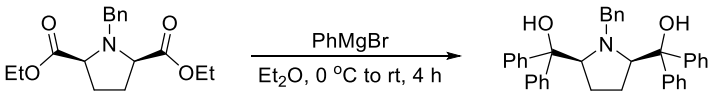

Scheme S.4.2. Synthesis of (1-benzylpyrrolidine-2,5-diyl)bis(diphenylmethanol).

A flask was charged with phenylmagnesium bromide (2.8 M in Et_2O, 7.72 mL, 21.6 mmol), before it was cooled to 0 °C. Diethyl 1-benzylpyrrolidine-2,5-dicarboxylate (1.50 g, 4.90 mmol) dissolved in Et_2O (20 mL) was added dropwise, and the resulting mixture was heated to reflux for 4 h. It was then cooled to 0 °C and quenched with sat. aq. NH_4Cl solution (20 mL). The phases were separated, and the aqueous layer was extracted with DCM. The combined organic layers were dried over $MgSO_4$, filtered and concentrated *in vacuo*. Column chromatography (SiO_2, 5–10% EtOAc in hexane) gave the title compound (1.94 g, 75%) as a white solid.

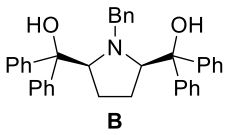

B

M.p. = 175 °C; **^{1}H NMR** (400 MHz, $CDCl_3$) δ 7.63 (d, *J* = 7.6 Hz, 4H), 7.53 (d, *J* = 7.3 Hz, 4H), 7.35–7.25 (m, 11H), 7.23–7.14 (m, 4H), 6.95–6.90 (m, 2H), 4.74 (s, 2H), 4.55–4.48 (m, 2H), 2.39 (s, 2H), 1.96–1.84 (m, 4H); **^{13}C NMR** (100 MHz, $CDCl_3$) δ 147.0, 146.4, 138.4, 128.7, 128.2, 128.1, 127.9, 126.7, 126.6, 126.4, 126.1. 126.0, 80.2, 70.3, 55.8, 28.9; **IR** (solid) ν 3411, 3293, 3085, 3060, 3029, 2959, 2930, 2879, 2361, 2341, 1599, 1493, 1447, 1389, 1360, 1325, 1312, 1255, 1226, 1188, 1156, 1128, 1078, 1066, 1043, 1032, 1001, 979, 929, 891, 859, 846, 805, 769, 747, 696, 659, 636 cm^{-1}; **HRMS** (ESI-TOF) *m/z* Calcd for $C_{37}H_{36}NO_2$ $[M+H]^+$ 526.2741, found 526.2732.

cis-Pyrrolidine-2,5-diylbis(diphenylmethanol) (4.18o)[472]

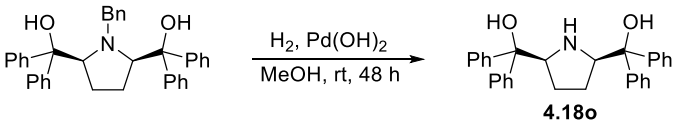

Scheme S.4.3. Synthesis of substrate **4.18o**.

A flask was charged with (1-benzylpyrrolidine-2,5-diyl)bis(diphenylmethanol) (1.60 g, 3.04 mmol), $Pd(OH)_2$ (20% on C, 395 mg, 0.56 mmol) and MeOH (40 mL). The flask was evacuated and backfilled with H_2, and the reaction was left to stir under a H_2 atmosphere at rt for 48 h. The catalyst was removed by filtration through celite, and the filter cake was washed with MeOH (80 mL) to remove impurities. Washing with EtOAc (210 mL) and removing this solvent *in vacuo* gave the crude product which was purified by column chromatography (SiO_2, 10–20% EtOAc in hexane) to give **4.18o** (730 mg, 55%) as a white solid.

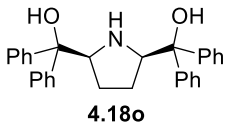

M.p. = 148–149 °C; **^{1}H NMR** (400 MHz, $CDCl_3$) δ 7.52 (d, *J* = 7.6 Hz, 4H), 7.45 (d, *J* = 7.6 Hz, 4H), 7.31–7.24 (m, 8H), 7.20–7.13 (m, 4H), 4.42 (t, *J* = 5.4 Hz, 2H), 3.69 (s, 2H), 1.89 (bs, 1H), 1.80–1.68 (m, 2H), 1.54–1.43 (m, 2H); **^{13}C NMR** (100 MHz, $CDCl_3$) δ 147.0, 144.9, 128.4, 128.0, 126.8, 126.5, 125.8, 125.3, 77.4, 64.1, 25.3; **IR** (solid) ν 3421, 3059, 3025, 2960, 2874, 2361, 2341, 2186, 2163, 1620, 1598, 1582, 1491, 1448, 1401, 1340, 1302, 1275, 1244, 1185, 1130, 1059, 1032, 1011, 1004, 986, 970, 910, 874, 820, 793, 747, 695, 667, 660, 633 cm^{-1}; **HRMS** (ESI-TOF) *m/z* Calcd for $C_{30}H_{30}NO_2$ $[M+H]^+$ 436.2271, found 436.2268.

S.4.1.2. Hydrogen-Bonded Complexes

General Procedure (GP) 1: Preparation of [Tetraalkylammonium Fluoride–Alcohol] Complexes

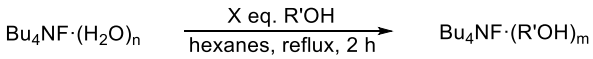

Scheme S.4.4: General procedure for synthesizing [tetraalkylammonium fluoride–alcohol] complexes.

A flame dried round bottom flask under an inert atmosphere was charged with hexane (0.033 M F^-), tetraalkylammonium fluoride hydrate (1.0 equiv.) and the alcohol hydrogen-bond donor (1.0–4.0 equiv.). The resulting suspension was allowed to stir in an oil bath at vigorous reflux (80–85 °C) for 2 h, during which time the formation of droplets of water was observed on the inside walls of the reflux condenser. During the course of the reaction either the persistent presence of a white solid precipitate or the formation of a biphasic system was observed. The solution was allowed to cool to rt, and in the case of solid products they were filtered off, washed with hexane, and dried under high vacuum, giving the desired [tetraalkylammonium fluoride–alcohol] complexes, which were used without further purification. If instead the formation of a second layer had occurred the upper hexane layer was carefully removed and the lower product layer was dried at an elevated temperature under reduced pressure until it solidified. The solid product was then placed on a sinter funnel, washed with hexane and dried under high vacuum. See individual compounds for details.

Note: In all ^{13}C NMR spectra of [tetraalkylammonium fluoride–alcohol] complexes taken in $CDCl_3$, a singlet was observed at approximately 77.2 ppm, which we attribute to $CHCl_3$. We surmise that $CHCl_3$ is formed *in situ* from $CDCl_3$ *via* proton exchange, which is

presumably mediated by fluoride acting as a Brønsted base. This signal has been omitted from the peak listings below.

The structural depictions of complexes in this section reflect the stoichiometry observed in ^{1}H NMR spectra, which is not necessarily the same as is observed in the solid-state structures.

Tetra-*N*-butylammonium fluoride bis((+)-diisopropyl L-tartrate)) (TBAF((+)-DIPT)$_2$, 4.19b)

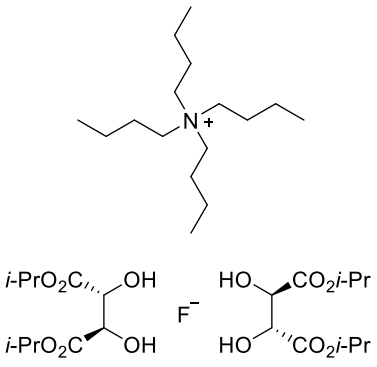

4.19b

The title compound was prepared according to GP1 with TBAF(H_2O)$_3$ (1.26 g, 4.00 mmol) and (+)-diisopropyl tartrate (1.87 g, 8.00 mmol). After heating at reflux for 2 h, a viscous colourless oil was observed at the bottom of the reaction vessel. The reaction was allowed to cool to rt, and the solvent was removed *in vacuo*. After further drying under high vacuum for 8 h, the complex was transferred to –20 °C for 8 h, at which point it was observed to have solidified. The resulting material was warmed to rt and washed with hexane on a sinter funnel, then dried under high vacuum. The complex **4.19b** (1.79 g, 61%) was thus obtained as a sticky colourless solid. **^{1}H NMR** (400 MHz, $CDCl_3$) δ 5.09–5.01 (m, 4H), 4.45 (s, 4H), 3.29–3.25 (m, 8H), 1.61 (qn, *J* = 7.5 Hz, 8H), 1.39 (sx, *J* = 7.5 Hz, 8H), 1.25–1.21 (m, 24H), 0.95 (t, *J* = 7.5 Hz, 12H); **^{13}C NMR** (100 MHz, $CDCl_3$) δ 171.4, 72.8, 69.3, 58.5, 23.9, 21.7, 21.7, 19.6, 13.6; **IR** (solid) ν 3143, 2962, 2875, 1744, 1468, 1375, 1265, 1217, 1197, 1150, 1096 cm^{-1}; **X-ray** (single crystal) Colourless block

crystals of X-ray diffraction quality were obtained by carefully layering hexane onto a saturated solution of **4.19b** in THF, which had previously been prepared by dissolving **4.19b** in refluxing THF (approximately 66 °C) until visibly saturated, filtering while hot, and then allowing to stand for approximately 1 min to cool to near rt. The crystal was found to be an *n*-hexane solvate. Experimental details are provided below.

Tetra-*N*-butylammonium fluoride bis(1,2:5,6-Di-*O*-isopropylidene-D-mannitol) (TBAF(1,2:5,6-Di-*O*-isopropylidene-D-mannitol)$_2$, 4.19c)

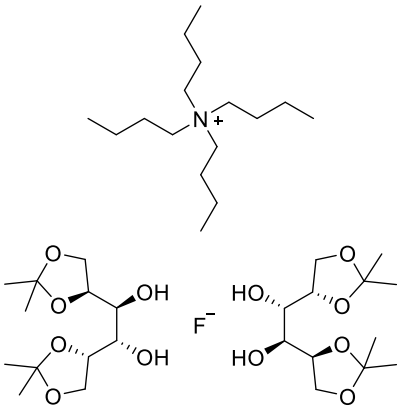

4.19c

The title compound was prepared according to GP1 with TBAF$(H_2O)_3$ (316 mg, 1.00 mmol) and 1,2:5,6-Di-*O*-isopropylidene-D-mannitol (525 mg, 2.00 mmol). After heating at reflux for 2 h, a viscous colourless oil was observed at the bottom of the reaction vessel. The reaction was allowed to cool to room temperature, and the solvent was removed *in vacuo*. Upon further drying under high vacuum for 8 h, solidification was observed. The resulting material was warmed to room temperature and washed with hexane on a sinter funnel, then dried under high vacuum. The complex **4.19c** (795 mg, 95%) was thus obtained as chalky white solid. **^{1}H NMR** (400 MHz, $CDCl_3$) δ 4.18 (td, *J* = 5.6, 8.6 Hz, 4H), 4.07–3.97 (m, 8H), 3.54 (d, *J* = 8.6 Hz, 4H), 3.24–3.11 (m, 8H), 1.57 (qn, *J* = 7.4 Hz, 8H), 1.40 (sx, *J* = 7.4 Hz, 8H), 1.33 (s, 12H), 1.28 (s, 12H), 0.98 (t, *J* = 7.4 Hz, 12H); **^{13}C NMR** (100 MHz, $CDCl_3$) δ 108.7, 75.5, 71.9, 67.6, 58.3, 26.9, 25.5, 23.7, 19.6, 13.6; **IR** (solid) ν 3462, 3302, 3201, 2982, 2960, 2936, 2875, 2360, 2342, 1492, 1456, 1431, 1381, 1370, 1327, 1251, 1214, 1149, 1113, 1064, 988, 948, 919, 884, 844, 783, 738, 692, 669, 651 cm^{-1}; **X-ray** (single-crystal) Colourless block crystals of X-ray diffraction

quality were obtained by carefully layering hexane onto a saturated solution of **4.19c** in EtOAc, which had previously been prepared by dissolving **4.19c** in refluxing EtOAc (approximately 77 °C) until visibly saturated, filtering while hot, and then allowing to stand for approximately 1 min to cool to near rt. The crystal was found to be an EtOAc solvate. Vapour diffusion of hexane into a saturated solution of **4.19c** in EtOAc, which had previously been prepared by dissolving **4.19c** in EtOAc at rt and filtering to remove residual solid, also gave crystals of suitable quality. Experimental details are provided below.

Tetra-*N*-butylammonium fluoride bis(pinacol) (TBAF(Pin)$_2$, 4.19d)

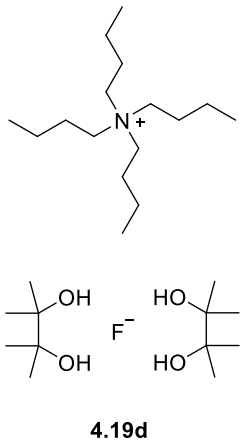

4.19d

The title compound was prepared according to GP1 with TBAF(H_2O)$_3$ (1.26 g, 4.00 mmol) and pinacol (945 mg, 8.00 mmol). The complex **4.19d** (1.86 g, 93%) was thus obtained as flocculent white solid. **^{1}H NMR** (400 MHz, $CDCl_3$) δ 3.28–3.24 (m, 8H), 1.64–1.56 (m, 8H), 1.40 (sx, *J* = 7.4 Hz, 8H), 1.15 (s, 24H), 0.96 (t, *J* = 7.4 Hz, 12H); **^{13}C NMR** (100 MHz, $CDCl_3$) δ 74.5, 58.4, 25.2, 24.0, 19.6, 13.6; **IR** (solid) ν 3159, 2965, 2944, 2878, 1463, 1380, 1150, 953, 887 cm^{-1}. **X-ray** (single-crystal) Colourless needles of X-ray diffraction quality were obtained by carefully layering hexane onto a saturated solution of **4.19d** in THF, which had previously been prepared by dissolving **4.19d** in refluxing THF (approximately 66 °C) until visibly saturated, filtering while hot, and then allowing to stand for approximately 1 min to cool to near rt. Experimental details are provided below.

Tetra-*N*-butylammonium fluoride bis((*R*)-(+)-1,1'-bi(naphthol)) (TBAF((*R*)-BINOL)$_2$, 4.19j)

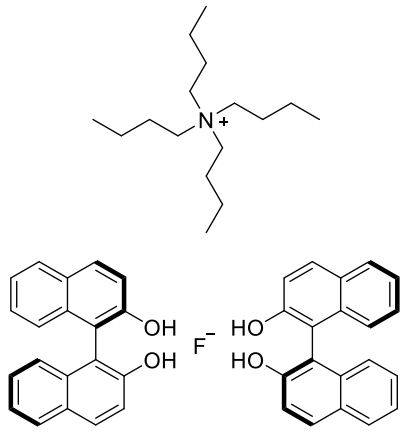

4.19j

The title compound was prepared according to GP1 with TBAF(H_2O)$_3$ (316 mg, 1.00 mmol) and (*R*)-BINOL (573 mg, 2.00 mmol). The complex **4.19j** (736 mg, 88%) was thus obtained as a white solid. **^{1}H NMR** (400 MHz, $CDCl_3$) δ 8.73 (bs, 4H), 7.80–7.73 (m, 8H), 7.52 (d, *J* = 8.7 Hz, 4H), 7.23 (ddd, *J* = 8.1, 6.6, 1.5 Hz, 4H), 7.14 (ddd, *J* = 8.7, 6.6, 1.2 Hz, 4H), 7.12–7.08 (m, 4H), 2.23–2.04 (m, 8H), 1.03–0.83 (m, 16H), 0.67 (t, *J* = 7.1 Hz, 12H); **^{13}C NMR** (100 MHz, $CDCl_3$) δ 154.1, 134.3, 129.4, 128.5, 127.9, 125.9, 125.3, 122.4, 119.1, 114.2, 57.7, 23.0, 19.1, 13.4; **IR** (solid) ν 3052, 2959, 2930, 2872, 2732, 2656, 2360, 2341, 2164, 1857, 1620, 1582, 1505, 1480, 1459, 1432, 1400, 1339, 1302, 1276, 1244, 1213, 1179, 1145, 1129, 1071, 1024, 986, 968, 945, 934, 872, 864, 828, 821, 816, 792, 784, 774, 749, 690, 678, 667, 629 cm^{-1}. **X-ray** (single-crystal) Colourless block crystals of X-ray diffraction quality were obtained by carefully layering hexane onto a saturated solution of **4.19j** in EtOAc, which had previously been prepared by dissolving **4.19j** in refluxing EtOAc (approximately 77 °C) until visibly saturated, filtering while hot, and then allowing to stand for approximately 1 min to cool to near rt. Experimental details are provided below.

Tetra-*N*-butylammonium fluoride bis(triphenylmethanol) (TBAF(Ph$_3$COH)$_2$, 4.19m)

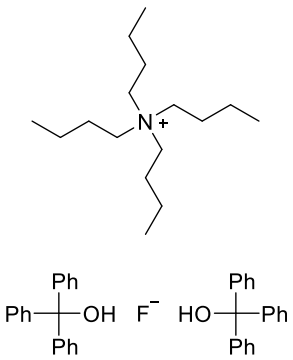

4.19m

The title compound was prepared according to GP1 with TBAF$(H_2O)_3$ (631 mg, 2.00 mmol) and triphenylmethanol (1.04 g, 4.00 mmol). After heating at reflux for 2 h, a viscous yellow oil was observed at the bottom of the reaction vessel, which solidified when allowed to stand at rt for 2 h. The reaction mixture was filtered, the obtained solid washed quickly with acetone and hexane, and dried under high vacuum. The complex **4.19m** (954 mg, 61%) was thus obtained as a crystalline yellow solid. **^{1}H NMR** (400 MHz, $CDCl_3$) δ 7.27–7.24 (m, 30H), 3.31–3.27 (m, 8H), 1.62 (qn, *J* = 7.2 Hz, 8H), 1.40 (sx, *J* = 7.2 Hz, 8H), 0.97 (t, *J* = 7.2 Hz, 12H); **^{13}C NMR** (100 MHz, $CDCl_3$) δ 147.0, 127.9, 127.7, 126.9, 81.6, 58.5, 23.9, 19.6, 13.7; **IR** (solid) ν 3059, 2960, 2932, 2874, 2451, 1488, 1444, 1380, 1162, 1050, 1031, 884, 757, 698, 638 cm^{-1}. **X-ray** (single-crystal) A distinct sample of TBAF(Ph$_3$COH)$_n$ was synthesised using GP1 with a 1:4 ratio of TBAF$(H_2O)_3$ and triphenylmethanol (**4.18m**). After being filtered, washed with hexane, and dried under high vacuum, ^{1}H NMR analysis of this material revealed a ratio of 3.8:1 of alcohol:fluoride. This material was used to grow single crystals of the 2:1 complex. Colourless needles of X-ray diffraction quality were obtained by carefully layering hexane onto a saturated solution of TBAF(Ph$_3$COH)$_n$ in EtOAc, which had previously been prepared by dissolving TBAF(Ph$_3$COH)$_n$ in refluxing EtOAc (approximately 77 °C) until visibly saturated, filtering while hot, and then allowing to stand for 1 min to cool to near rt. The crystal was found to be an *n*-hexane solvate. Experimental details are provided below.

Tetra-*N*-butylammonium fluoride bis(tri-*p*-tolylmethanol) (TBAF(*p*-Tol$_3$COH)$_2$, 4.19n)

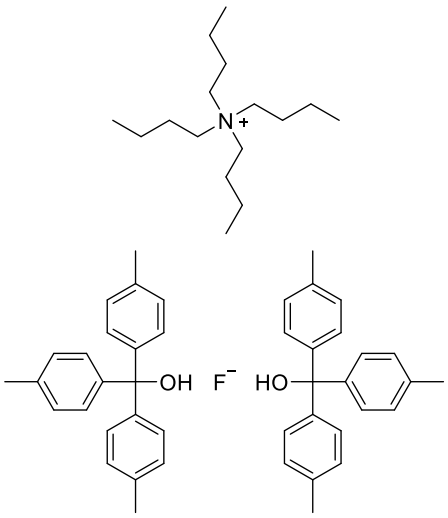

4.19n

The title compound was prepared according to GP1 with TBAF(H_2O)$_3$ (1.26 g, 4.00 mmol) and tri-*p*-tolylmethanol (4.84 g, 16.0 mmol). Over the course of the reaction, the solution became homogenous. After 2 h of heating at reflux, the flask was removed from the oil bath and allowed to stand at rt for 4 h, during which time the formation of a pale yellow precipitate was observed. Following the standard work-up, **4.19n** (2.62 g, 76%) was obtained as a crystalline pale-yellow solid. **^{1}H NMR** (400 MHz, $CDCl_3$) δ 7.15 (ad, *J* = 8.0 Hz, 12H), 7.09 (ad, *J* = 8.0 Hz, 12H), 3.39–3.34 (m, 8H), 2.33 (s, 18H), 1.67 (qn, *J* = 7.2 Hz, 8H), 1.45 (sx, *J* = 7.2 Hz, 8H), 1.01 (t, *J* = 7.2 Hz, 12H); **^{13}C NMR** (100 MHz, $CDCl_3$) δ 144.3, 136.7, 128.5, 127.7, 81.1, 58.9, 24.1, 21.0, 19.8, 13.7; **IR** (solid) ν 2962, 2935, 2874, 2482, 1508, 1488, 1456, 1380, 1182, 1155, 1063, 916, 886, 812, 781 cm^{-1}; **X-ray** (single-crystal) Colourless needles of X-ray diffraction quality were obtained by vapour diffusion of hexane into a saturated solution of **4.19n** in Et_2O, which had previously been prepared by dissolving **4.19n** in refluxing Et_2O (approximately 35 °C) until visibly saturated, filtering while hot, and then allowing to stand for approximately 1 min to cool to near rt. Experimental details are provided below.

Tetra-*N*-butylammonium fluoride (*cis*-pyrrolidine-2,5-diyl(diphenylmethanol) hydrate (TBAF(*cis*-pyrrolidine-2,5-diyl(diphenylmethanol))·(H_2O), (4.19o)

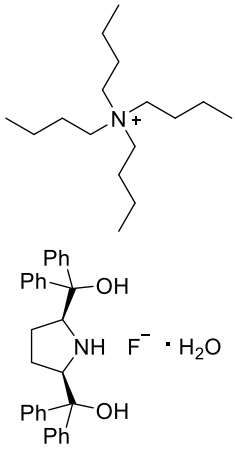

4.19o

The title compound was prepared according to GP1 with TBAF(H_2O)$_3$ (316 mg, 1.00 mmol) and **4.18o** (436 mg, 1.00 mmol). The complex **4.19o** (608 mg, 85%) was thus obtained as a white solid. **^{1}H NMR** (400 MHz, $CDCl_3$) δ 7.51–7.47 (m, 4H), 7.44–7.39 (m, 4H), 7.22 (t, *J* = 7.7 Hz, 8H), 7.14–7.08 (m, 4H), 4.36 (ddd, *J* = 7.2, 5.3, 2.0 Hz, 2H), 3.33–3.25 (m, 8H), 1.76–1.67 (m, 2H), 1.67–1.57 (m, 8H), 1.49–1.35 (m, 10H), 0.97 (t, *J* = 7.3 Hz, 12H); **^{13}C NMR** (100 MHz, $CDCl_3$) δ 147.1, 145.1, 128.2, 127.8, 126.5, 126.3, 125.8, 125.3, 77.3, 64.0, 58.6, 25.3, 23.9, 19.6, 13.5; **IR** (solid) ν 3289, 3086, 3058, 3022, 2959, 2933, 2874, 2581, 2361, 2341, 1653, 1598, 1489, 1467, 1448, 1379, 1350, 1317, 1263, 1181, 1172, 1149, 1106, 1065, 1052, 1033, 998, 978, 940, 885, 840, 800, 745, 697, 666, 636 cm^{-1}; **X-ray** (single-crystal) Colourless block crystals of X-ray diffraction quality were obtained by vapour diffusion of hexane into a saturated solution of **4.19o** in EtOAc, which had previously been prepared by dissolving **4.19o** in refluxing EtOAc (approximately 77 °C) until visibly saturated, filtering while hot, and then allowing to stand for approximately 1 min to cool to near rt. Experimental details are provided below.

S.4.1.3. Compounds for Kinetic Studies with Fluoride–Alcohol Complexes

2-(3-Bromopropoxy)naphthalene (4.10)[473]

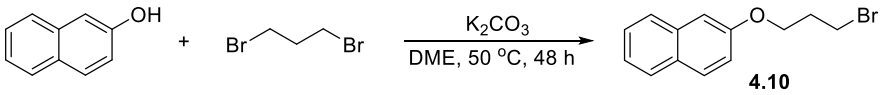

Scheme S.4.5. Synthesis of alkylbromide **4.10**.

A flask was charged with 2-naphthol (2.02 g, 14.0 mmol), 1,3-dibromopropane (280 mmol, 28.6 mL), K_2CO_3 (140 mmol, 19.3 g), and DMF (2.0 mL). The resulting slurry was stirred at 50 °C for 48 h. The reaction mixture was cooled to rt, and water was added. The resulting biphasic mixture was extracted with DCM. The combined organic layers were washed with brine, dried over $MgSO_4$, filtered, and concentrated *in vacuo*. Excess 1,3-dibromopropane (b.p. = 166–167 °C) was removed using a rotary evaporator connected to a well-maintained vacuum pump and a water bath at elevated temperature (70–80 °C). The resulting residue was further dried under high vacuum for several hours. Purification *via* column chromatography (SiO_2, 10–20% DCM in hexane) delivered analytically pure **4.10** (2.56 g, 69% yield) as a colourless oil, which over time transformed into a white crystalline solid.

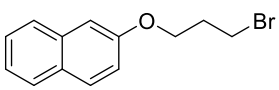

4.10

^{1}H NMR (400 MHz, $CDCl_3$) δ 7.78–7.72 (m, 3H), 7.45 (ddd, *J* = 8.4, 7.2, 1.2 Hz, 1H), 7.35 (ddd, *J* = 8.0, 6.8, 1.2 Hz, 1H), 7.17–7.13 (m, 2H), 4.23 (t, *J* = 6.2 Hz, 2H), 3.66 (t, *J* = 6.2 Hz, 2H), 2.39 (qn, *J* = 6.2 Hz, 2H); **^{13}C NMR** (100 MHz, $CDCl_3$) δ 156.6, 134.5, 129.4, 129.0, 127.6, 126.7, 126.4, 123.6, 118.8, 106.7, 65.3, 32.3, 30.1. **IR** (solid) ν 3060, 2949, 2899, 1629, 1599, 1510, 1461, 1390, 1254, 1215, 1182, 1027, 841, 816, 748 cm^{-1}; **HRMS** (FI) *m/z* Calcd for $C_{13}H_{13}{}^{79}BrO$ $[M]^+$ 264.0150,

$[(M+2)]^+$ 266.0130, found 264.0146, 266.0153, $[M]^+$: $[(M+2)]^+$ = 1:1. The spectroscopic data were identical in all respects to those previously reported.[474]

Representative Procedure for Nucleophilic Fluorination (Preparative Scale):

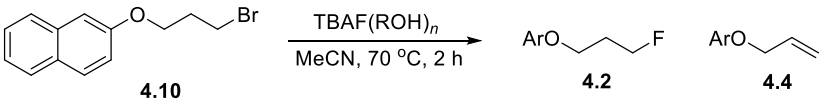

4.10 **4.2** **4.4**

Scheme S.4.6. Nucleophilic fluorination of alkyl bromide **4.10**.

A screw-top vial was charged with **4.10** (53.0 mg, 0.20 mmol), MeCN (0.80 mL) and TBAF(*t*-BuOH)$_4$ (223 mg, 0.80 mmol). The vial was capped and heated to 70 °C. After 1 h, the reaction mixture was allowed to cool to rt and Et_2O (4.0 mL) and H_2O (4.0 mL) were added to quench the reaction. The layers were separated and the aqueous one was further extracted with Et_2O. The combined organic layers were dried over Na_2SO_4, filtered, and concentrated *in vacuo*. Subsequent purification was carried out using column chromatography (SiO_2, 0–10% EtOAc in hexane) to give the fluorinated product and olefin by-product as pure compounds.

2-(3-Fluoropropoxy)naphthalene (4.2)

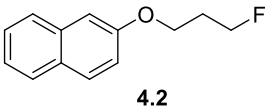

4.2

The title compound **4.2** (25.7 mg, 63%) was obtained as a colourless oil. **^{1}H NMR** (400 MHz, $CDCl_3$) δ 7.78–7.71 (m, 3H), 7.44 (ddd, *J* = 8.0, 6.8, 1.2 Hz, 1H), 7.34 (ddd, *J* = 8.0, 6.8, 1.2 Hz, 1H), 7.15–7.13 (m, 2H), 4.70 (dt, *J* = 47.2, 6.0 Hz, 2H), 4.23 (t, *J* = 6.0 Hz, 2H), 2.25 (dqn, *J* = 26.0, 6.0 Hz, 2H); **^{13}C NMR** (100 MHz, $CDCl_3$) δ 156.7, 134.5, 129.4, 129.0, 127.6, 126.7, 126.4, 123.6, 118.8, 106.6, 80.8 (d, $J_{C–F}$ = 163.5 Hz), 63.5 (d, $J_{C–F}$ = 5.2 Hz), 30.4 (d, $J_{C–F}$ = 19.9 Hz); **^{19}F NMR** (377 MHz,

$CDCl_3$) δ –222.11 (tt, *J* = 47.2, 26.0 Hz); **IR** (film, $CDCl_3$) ν 3058, 2969, 1629, 1601, 1510, 1465, 1390, 1258, 1216, 1181, 1097, 1052, 838, 747cm^{-1}; **HRMS** (FI) *m/z* Calcd for $C_{13}H_{13}FO$ $[M]^+$ 204.0950, found 204.0957. The spectroscopic data were identical in all respects to those previously reported.[474]

2-(Allyloxy)naphthalene (4.4)

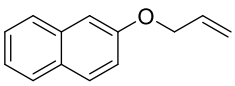
4.4

The title compound **4.4** (10.7 mg, 29%) was isolated as a colourless oil. **^{1}H NMR** (400 MHz, $CDCl_3$) δ 7.78–7.71 (m, 3H), 7.43 (td, *J* = 8.0, 1.2 Hz, 1H), 7.33 (td, *J* = 8.0, 1.2 Hz, 1H), 7.18 (dd, *J* = 8.8, 2.8 Hz, 1H), 7.15–7.14 (m, 1H), 6.14 (ddt, *J* = 17.4, 10.6, 5.6 Hz, 1H), 5.51–5.45 (m, 1H), 5.35–5.31 (m, 1H), 4.66 (dt, *J* = 5.6, 1.2 Hz, 2H); **^{13}C NMR** (100 MHz, $CDCl_3$) δ 156.5, 134.5, 133.2, 129.4, 129.0, 127.6, 126.7, 126.3, 123.6, 119.0, 117.8, 107.0, 68.8; **IR** (film, $CDCl_3$) ν 3058, 1630, 1600, 1258, 1217, 1182, 1017, 837, 747 cm^{-1}; **HRMS** (FI) *m/z* Calcd for $C_{13}H_{12}O$ $[M]^+$ 184.0888, found 184.0891. The spectroscopic data were identical in all respects to those previously reported.[475]

S.4.2. Single-Crystal X-Ray Structures

Table S.4.1. Summary of single-crystal X-ray structures **4.19a**–**o, 4.21** and **4.23** (continued on following pages).

Nr.	4.19a	4.19b	4.19c	4.19d	4.19e	4.19f	4.19g
Formula	$C_{56}H_{100}F_1N_1O_4$	$C_{36}H_{72}F_1N_1O_{12}$	$C_{40}H_{80}F_1N_1O_{12}$	$C_{28}H_{64}F_1N_1O_4$	$C_{26}H_{60}F_1N_1O_4$	$C_{26}H_{60}F_1N_1O_6$	$C_{22}H_{46}Cl_2F_1N_1O_4$
Molecular Weight	870.41	764.3	437.09	497.82	469.76	501.76	482.55
Crystal System	tetragonal	orthorhombic	monoclinic	orthorhombic	monoclinic	orthorhombic	monoclinic
T [K]	150	150	150	150	150	150	150
Space Group	P –4	P 21 21 2	C 2	P b c a	C 1 2/c 1	P b c n	P 21/c
a [Å]	15.6111(1)	18.9780(2)	25.1923(1)	18.6017(3)	22.5166(1)	9.9133(1)	9.9446(3)
b [Å]	15.6111(1)	24.2645(2)	9.6565(1)	18.6158(3)	14.2863(1)	17.3454(3)	18.0891(7)
c [Å]	10.5050(1)	10.3218(1)	10.6715(1)	19.1084(3)	19.8783(1)	18.3631(3)	15.7361(6)
α [°]	90	90	90	90	90	90	90
β [°]	90	90	92.246(1)	90	103.6255(5)	90	103.523(4)
γ [°]	90	90	90	90	90	90	90
V [Å^3]	2560.14(3)	4753.10(8)	2594.1(1)	6616.96(18)	6214.47(6)	3157.54(8)	2752.27(18)
Z	4	4	2	8	8	8	4
D_{calc} [g cm^{-3}]	1.129	1.068	1.119	0.999	1.004	1.055	1.164
F(0 0 0)	968	1679.681	960	2240	2112	1120	1056
μ [mm^{-1}]	0.546	0.080	0.689	0.068	0.549	0.076	2.380
Crystal Size [mm]	0.20 * 0.21 * 0.23	0.10 * 0.10 * 0.43	0.15 * 0.15 * 0.20	0.08 * 0.10 * 0.49	0.18 * 0.20 * 0.28	0.10 * 0.20 * 0.35	0.04 * 0.15 * 0.18
Colour, Shape	clear_pale_colourless, block	clear_pale_colourless, prism	clear_pale_colourless, block	clear_pale_colourless, prism	clear_pale_colourless, block	clear_pale_colourless, plate	clear_pale_colourless, plate
R_{int}	5.82	6.75	3.27	5.58	5.82	6.23	6.93
θ_{min}, θ_{max} [deg]	2.831 – 75.425	5.098 – 26.381	3.511 – 76.028	5.115 – 26.020	3.695 – 75.176	5.200 – 26.942	3.784 – 72.237
Total Reflections (before merge)	5329	65091	49863	96568	66092	46870	19286
Data (I>–3.0/sigma(I)) [Reflections, Restraints, Parameters]	3520, 1255, 406	10798, 201, 525	5353, 623, 321	6466, 0, 308	5509, 0, 289	3597, 0, 155	4548, 32, 293
S (=GooF)	1.011	0.981	1.004	0.986	0.994	0.962	0.986
Min. and Max. Residual Dens., [e/Å^3]	–0.26	–0.25	–0.20	–0.14	–0.24	–0.25	–0.47
	0.29	0.30	0.26	0.20	0.49	0.34	0.60
Threshold Expression	I>2sigma(I)	I>2sigma(I)	I>2sigma(I)	I>2sigma(I)	I>2sigma(I)	I>2sigma(I)	I>2sigma(I)
R_1	0.0574	0.0448	0.0326	0.0427	0.0556	0.0431	0.0572
wR_2	0.1551	0.0884	0.0889	0.0979	0.1490	0.0972	0.1408

Nr.	**4.19h**, 1st Polymorph	**4.19h**, 2nd Polymorph	**4.19i**	**4.19j**	**4.19k**	**4.19l**	**4.19m**
Formula	$C_{28}H_{48}F_1N_1O_4$	$C_{28}H_{48}F_1N_1O_4$	$C_{49}H_{80}F_1N_1O_7$	$C_{56}H_{64}F_1N_1O_4$	$C_{55}H_{72}F_1N_1O_3$	$C_{73}H_{73}F_1N_1O_3$	$C_{54}H_{68}F_1N_1O_2$
Molecular Weight	481.69	481.69	814.17	834.13	814.18	1036.43	782.14
Crystal System	triclinic	monoclinic	monoclinic	orthorhombic	triclinic	triclinic	monoclinic
T [K]	150	150	150	150	150	150	150
Space Group	P –1	C c	P c	P 21 21 21	P –1	P –1	P 21/n
a [Å]	13.2624(3)	27.2660(3)	8.75510(1)	10.6869(1)	9.4953(1)	14.5683(1)	11.2887(1)
b [Å]	13.9265(4)	27.8831(2)	12.74630(1)	12.6528(1)	12.1501(2)	19.9837(2)	17.6025(1)
c [Å]	17.0611(4)	15.9412(2)	22.1115(2)	34.7970(3)	21.4618(4)	20.7534(2)	24.9660(2)
α [°]	67.629(2)	90	90	90	81.8444(6)	91.2454(7)	90
β [°]	74.866(2)	110.3660(11)	92.0698(6)	90	89.1604(6)	94.4191(8)	98.4318(7)
γ [°]	87.898(2)	90	90	90	78.5486(7)	103.9009(9)	90
V [Å^3]	2806.00(13)	11361.9(2)	2465.93(4)	4704.78(7)	2401.96(7)	5842.46(9)	4907.35(7)
Z	2	4	2	4	2	2	4
D_{calc} [g cm^{-3}]	1.140	1.126	1.096	1.178	1.126	1.178	1.059
F(0 0 0)	1056	4224	892	1792	884	2224	1696
μ [mm^{-1}]	0.632	0.625	0.589	0.592	0.070	0.561	0.504
Crystal Size [mm]	0.01 * 0.02 * 0.09	0.03 * 0.09 * 0.15	0.16 * 0.17 * 0.19	0.18 * 0.20 * 0.20	0.14 * 0.18 * 0.65	0.21 * 0.24 * 0.26	0.22 * 0.24 * 0.30
Colour, Shape	clear_pale_pink, needle	clear_pale_pink, plate	clear_pale_colourless, block	clear_pale_colourless, block	clear_pale_colourless, block	clear_pale_colourless, block	clear_pale_colourless, block
R_{int}	10.13	3.81	3.00	2.74	6.11	4.29	6.14
θ_{min}, θ_{max} [deg]	3.440 – 74.966	3.170 – 76.839	3.467 – 75.196	3.717 – 76.149	5.114 – 25.087	3.060 – 75.122	3.083 – 76.917
Total Reflections (before merge)	116266	131227	53899	52468	40263	227665	117478
Data (I>–3.0/sigma(I)) [Reflections, Restraints, Parameters]	7698, 592, 766	22810, 594, 1381	9828, 2, 544	9732, 0, 560	8998, 256, 597	20878, 0, 1406	10304, 1269, 836
S (=GooF)	1.018	0.990	0.998	0.964	0.997	0.986	0.982
Min. and Max. Residual Dens., [e/Å^3]	–1.09	–0.22	–0.16	–0.14	–0.35	–0.30	–0.60
	0.84	0.28	0.33	0.15	0.53	0.52	0.69
Threshold Expression	I>2sigma(I)	I>2sigma(I)	I>2sigma(I)	I>2sigma(I)	I>2sigma(I)	I>2sigma(I)	I>2sigma(I)
R_1	0.0899	0.0354	0.0296	0.0263	0.0480	0.0408	0.0553
wR_2	0.2020	0.0904	0.0793	0.0662	0.1166	0.0976	0.1394

Nr.	4.19n	4.19o	4.21	4.23
Formula	$C_{60}H_{80}F_1N_1O_2$	$C_{38}H_{48}F_{0.5}N_{1.5}O_{2.5}$	$C_{28}H_{50}N_4O_9$	$C_{26}H_{41}C_{11}N_2O_3$
Molecular Weight	866.3	575.31	586.73	465.08
Crystal System	triclinic	monoclinic	monoclinic	orthorhombic
T [K]	150	150	150	150
Space Group	P –1	C 2/c	P 1 21/n 1	P c c n
a [Å]	13.4717(3)	27.7157(6)	9.8919(2)	17.4111(6)
b [Å]	17.5643(4)	9.7374(2)	20.5429(4)	20.7877(6)
c [Å]	24.8506(5)	25.2072(5)	16.0649(3)	14.7572(7)
α [°]	78.8655(19)	90	90	90
β [°]	80.5422(17)	105.664(2)	98.5668(10)	90
γ [°]	69.645(2)	90	90	90
V [$Å^3$]	5379.0(2)	6550.2(2)	3228.10(11)	5341.2(3)
Z	2	8	4	8
D_{calc} [g cm^{-3}]	1.070	1.167	1.207	1.157
F(0 0 0)	1888	2488	1272	2016
μ [mm^{-1}]	0.500	0.576	0.090	1.477
Crystal Size [mm]	0.18 * 0.20 * 0.21	0.20 * 0.20 * 0.24	0.16 * 0.20 * 0.40	0.02 * 0.04 * 0.20
Colour, Shape	clear_pale_colourless, block	clear_pale_colourless, block	clear_pale_colourless, prism	clear_pale_colourless, needle
R_{int}	5.02	4.99	8.36	10.07
θ_{min}, θ_{max} [deg]	3.038 – 74.851	3.312 – 74.463	5.123 – 25.314	3.311 – 75.532
Total Reflections (before merge)	110583	26899	39670	10427
Data (I>–3.0/sigma(I)) [Reflections, Restraints, Parameters]	22370, 0, 1154	6762, 950, 443	5935, 0, 370	5592, 0, 289
S (=GooF)	0.991	0.994	1.052	1.075
Min. and Max. Residual Dens., [e/$Å^3$]	–0.21	–0.17	–0.43	–0.53
	0.33	0.94	0.36	0.51
Threshold Expression	I>2sigma(I)	I>2sigma(I)	I>2sigma(I)	I>2sigma(I)
R_1	0.0439	0.0469	0.0581	0.0677
wR_2	0.1141	0.1322	0.1243	0.1580

S.4.3. Computational Methods

Optimisations were performed with *Gaussian09*, rev C.1 at the density functional level of theory.[476] Stationary points were optimised with the dispersion-corrected range-separated wB97XD functional[477] in combination with the 6-31G(d) basis set for C, H and O, 6-31+G(d) for F, and the LANL08 scalar relativistic effective core potential[478] and associated triple zeta valence + diffuse basis set for Br. All optimisations were performed with a conductor-like polarisable continuum model of the reaction solvent, acetonitrile.[476,479] Free energies calculated in the solution phase incorporate a correction factor of RTLn(24.5) = 2.1 kcal/mol to account for the change from a standard state of 1 atm to 1 mol/L. Stationary points were confirmed as minima and transition structures by the presence of zero and exactly one imaginary harmonic vibrational frequency, respectively. Free energies include unscaled zero point vibrational energies and are corrected for the presence of low frequencies (<50 cm^{-1}), which are unlikely to be well described by a harmonic oscillator, by scaling these values to 50 cm^{-1} in the evaluation of vibrational components to the entropy.[480] Calculation of natural atomic charges was performed using *NBO v3.1*.31 Unless otherwise stated, Gibbs free energies are quoted in kcal/mol at 298 K at a standard state of 1 mol/L.

Chapter 5

S.5.1. Synthesis and Characterisation of Compounds

S.5.1.1. Hydrogen Bond Donors

General Procedure (GP) 1: Preparation of Symmetrical 1,3-Diarylureas from Aryl Isocyanates and Substituted Anilines[481]

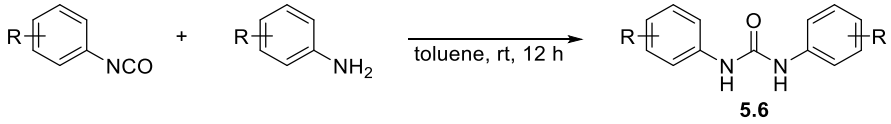

5.6

Scheme S.5.1. General one-step procedure for the preparation of symmetrical 1,3-diarylureas.

A flame dried flask was charged with anhydrous toluene (100 mL), aryl isocyanate (30.0 mmol) and substituted aniline (30.0 mmol). The reaction was allowed to stir at rt for 12 h, during which time the formation of a white precipitate was observed. The mixture was filtered, and the precipitate was washed sequentially with EtOH and hexane, giving the 1,3-diarylurea (**5.6**) as a white solid, which was used without further purification.

Note: Each 1,3-diarylurea has a distinct solubility profile, so the solvents used for washing the crude filtrate vary from case to case, as noted below.

General Procedure (GP) 2: Preparation of Symmetrical 1,3-Diarylureas from Substituted Anilines and 1,1'-Carbonyldiimidazole (CDI)[482]

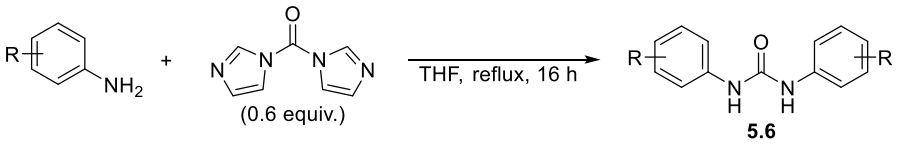

Scheme S.5.2. General one-step procedure for the preparation of symmetrical 1,3-diarylureas.

A flame dried flask was charged with anhydrous THF (50 mL), the substituted aniline (20.0 mmol), and 1,1'-carbonyldiimidazole (1.95 g, 12.0 mmol). The reaction mixture was allowed to stir at reflux for 16 h. It was then allowed to cool to rt and the solvent was removed *in vacuo*, giving a pale yellow solid, which could be dissolved in copious amounts of EtOAc (500 mL). The solution was washed with 1.0 M aq. HCl and brine, dried over Na_2SO_4, filtered, and concentrated *in vacuo*. The resulting off-white solid was washed with a 20:1 EtOAc:MeOH solution and hexane, giving the 1,3-diarylurea product (**5.6**), which was used without further purification.

1,3-Di-*m*-tolylurea (5.6a)

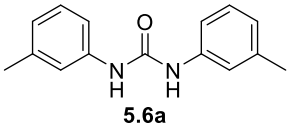

The title compound was prepared according to GP1 using *m*-tolyl isocyanate (3.87 mL, 30.0 mmol) and *m*-toluidine (3.22 mL, 30.0 mmol). Following completion of the reaction, the solution was filtered, and the precipitate was washed sequentially with MeOH and hexane, giving **5.6a** (6.73 g, 93%) as a white solid. **M.p.** (toluene) = 221–223 °C; **^{1}H NMR** (400 MHz, DMSO-d_6) δ 8.56 (s, 2H), 7.31 (s, 2H), 7.22 (d, *J* = 8.0 Hz, 2H), 7.15 (t, *J* = 7.2 Hz, 2H), 6.78 (d, *J* = 7.2 Hz, 2H), 2.27 (s, 6H); **^{13}C NMR** (100 MHz, DMSO-d_6) δ 152.5, 139.7, 137.9, 128.6, 122.5, 118.7, 115.3, 21.2;

IR (solid) ν 3295, 1739, 1633, 1610, 1550, 1487, 1293, 1228, 1217, 879, 781 cm^{-1}; **HRMS** (ESI-TOF) *m/z* Calcd for $C_{15}H_{16}N_2NaO$ $[M+Na]^+$ 263.1155, found 263.1151. The spectroscopic data were identical in all respects to those previously reported.[483]

1,3-Bis(4-(trifluoromethyl)phenyl)urea (5.6b)

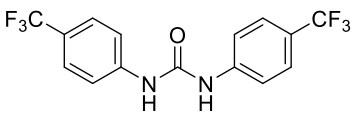

5.6b

The title compound was prepared according to GP1 using 4-(trifluoromethyl)phenyl isocyanate (3.83 mL, 26.8 mmol) and 4-(trifluoromethyl)aniline (3.37 mL, 26.8 mmol). Following completion of the reaction, the solution was filtered, and the precipitate was washed with hexane, giving **5.6b** (5.13 g, 55%) as a white solid. **M.p.** (toluene) = 241–242 °C (decomposition); **^{1}H NMR** (400 MHz, DMSO-d_6) δ 9.24 (s, 2H), 7.70–7.64 (m, 8H); **^{13}C NMR** (125 MHz, DMSO-d_6) δ 152.1, 143.1, 126.1 (q, J_{C-F} =3.8 Hz), 124.5 (q, J_{C-F} = 269.3 Hz), 122.2 (q, J_{C-F} = 31.8 Hz), 118.1; **^{19}F NMR** (377 MHz, DMSO-d_6) δ –60.11; **IR** (solid) ν 3321, 1651, 1600, 1543, 1324, 1160, 1119, 1110, 1066, 840 cm^{-1}; **HRMS** (FI) *m/z* Calcd for $C_{15}H_{10}F_6N_2O$ $[M]^+$ 348.0697, found 348.0713. The spectroscopic data were identical in all respects to those previously reported.[387]

1,3-Bis(4-*n*-propylphenyl)urea (5.6d)

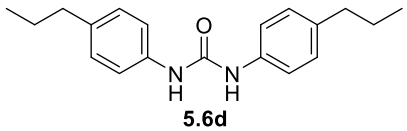

5.6d

The title compound was prepared according to GP2 using 4-*n*-propylaniline (2.94 mL, 20.0 mmol) and 1,1'-carbonyldiimidazole (1.95 g, 12.0 mmol). Following the standard work-up, **5.6d** (1.69 g, 57%) was obtained as a white solid. **M.p.** (EtOAc) = 219–222 °C; **^{1}H NMR** (400 MHz, DMSO-d_6) δ 8.52 (s, 2H), 7.35 (ad, *J* = 7.6 Hz, 4H), 7.09 (ad, *J* = 7.6 Hz, 4H), 2.50 (t, *J* = 7.5 Hz, 4H), 1.57 (sx, *J* = 7.5 Hz, 4H), 0.90 (t, *J* = 7.5 Hz, 6H); **^{13}C NMR** (100 MHz, DMSO-d_6) δ 152.6, 137.5, 135.4, 128.6, 118.2, 36.6, 24.2, 13.6; **IR** (solid) ν 3309, 2954, 1638, 1592,

1552, 1514, 1411, 1303, 1235 cm^{-1}; **HRMS** (ESI-TOF) *m/z* Calcd for $C_{19}H_{24}N_2NaO$ $[M+Na]^+$ 319.1781, found 319.1775.

1,3-Bis(4-methylphenyl)urea (5.6f)

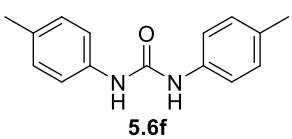
5.6f

The title compound was prepared according to GP1 using *p*-tolyl isocyanate (4.02 mL, 31.9 mmol) and *p*-toluidine (3.42 g, 31.9 mmol). Following completion of the reaction, the solution was filtered, and the precipitate was washed sequentially with EtOH and hexane, giving **5.6f** (7.21 g, 94%) as a white solid. **M.p.** (toluene) = 281–282 °C; **^{1}H NMR** (400 MHz, DMSO-d_6) δ 8.49 (s, 2H), 7.32 (ad, *J* = 8.0 Hz, 4H), 7.07 (ad, *J* = 8.0 Hz, 4H), 2.23 (s, 6H); **^{13}C NMR** (100 MHz, DMSO-d_6) δ 152.6, 137.2, 130.5, 129.2, 118.2, 20.4; **IR** (solid) ν 3302, 2914, 1638, 1591, 1558, 1514, 1308, 1290, 1235, 814 cm^{-1}; **HRMS** (FI) *m/z* Calcd for $C_{15}H_{16}N_2O$ $[M]^+$ 240.1263, found 240.1272. The spectroscopic data were identical in all respects to those previously reported.[483]

1,3-Bis(4-methoxyphenyl)urea (5.6g)

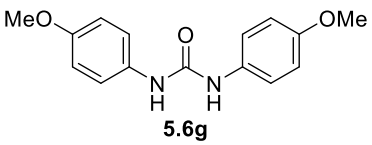
5.6g

The title compound was prepared according to GP1 using 4-methoxyphenyl isocyanate (1.58 mL, 12.2 mmol) and *p*-anisidine (1.50 g, 12.2 mmol). Following completion of the reaction, the solution was filtered, and the precipitate was washed sequentially with EtOH and hexane, giving **5.6g** (2.85 g, 86%) as a white solid. **M.p.** (toluene) = 249–250 °C; **^{1}H NMR** (400 MHz, DMSO-d_6) δ 8.37 (s, 2H), 7.35–7.33 (m, 4H), 6.86–6.84 (m, 4H), 3.71 (s, 6H); **^{13}C NMR** (100 MHz, DMSO-d_6) δ 154.3, 153.0, 132.9, 119.9, 114.0, 55.2; **IR** (solid) ν 3322, 3290, 1645, 1602, 1562, 1509, 1241, 1029, 806 cm^{-1}; **HRMS** (FI) *m/z* Calcd for $C_{15}H_{16}N_2O_3$ $[M]^+$ 272.1161,

found 272.1158. The spectroscopic data were identical in all respects to those previously reported.[483]

1,3-Bis(4-chlorophenyl)urea (5.6h)

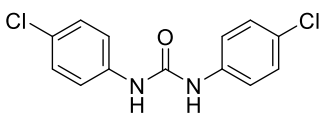
5.6h

The title compound was prepared according to GP1 using 4-chlorophenyl isocyanate (4.20 mL, 32.8 mmol) and 4-chloroaniline (4.18 g, 32.8 mmol). Following completion of the reaction, the solution was filtered, and the precipitate was washed sequentially with EtOH and hexane, giving **5.6h** (8.24 g, 89%) as a white solid. **M.p.** (toluene) = 322–325 °C; **^{1}H NMR** (400 MHz, DMSO-d_6) δ 8.85 (s, 2H), 7.48 (ad, J = 8.8 Hz, 4H), 7.32 (ad, J = 8.8 Hz, 4H); **^{13}C NMR** (400 MHz, DMSO-d_6) δ 152.3, 138.6, 128.7, 125.5, 119.8; **IR** (solid) ν 3292, 1630, 1588, 1556, 1489, 1397, 1297, 1231, 1083, 822 cm^{-1}; **HRMS** (FI) *m/z* Calcd for $C_{13}H_{10}{}^{35}Cl_2N_2O$ $[M]^+$ 280.0170, $[M+2]^+$ 282.0141, $[M+4]^+$ 284.0111, found 280.0162, 282.0222, 284.0212, $[M]^+$: $[M+2]^+$: $[M+4]^+$= 9:6:1. The spectroscopic data were identical in all respects to those previously reported.[483]

1,3-Bis(4-fluorophenyl)urea (5.6j)

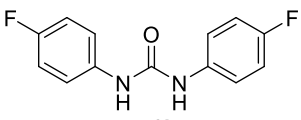
5.6j

The title compound was prepared according to GP1 using 4-fluorophenyl isocyanate (4.33 mL, 38.1 mmol) and 4-fluoroaniline (3.61 mL, 38.1 mmol). Following completion of the reaction, the solution was filtered, and the precipitate was washed sequentially with EtOAc and hexane, giving **5.6j** (8.56 g, 91%) as a white solid. **M.p.** (toluene) = 274–275 °C; **^{1}H NMR** (400 MHz, DMSO-d_6) δ 9.23 (s, 2H), 7.69–7.65 (m, 8H); **^{13}C NMR** (100 MHz, DMSO-d_6) δ 157.4 (d, J_{C-F} = 236.6 Hz), 152.8, 136.1 (d, J_{C-F} = 2.0 Hz), 120.1 (d, J_{C-F} = 7.6 Hz), 115.3 (d, J_{C-F} = 22.0 Hz); **^{19}F NMR** (377 MHz, DMSO-d_6) δ –121.48 (m); **IR** (solid) ν 3301, 1651, 1600, 1543, 1409,

1324, 1119, 1110, 1066, 1016, 840 cm^{-1}; **HRMS** (FI) *m/z* Calcd for $C_{13}H_{10}F_2N_2O$ $[M]^+$ 248.0761, found 248.0763. The spectroscopic data were identical in all respects to those previously reported.[483]

1,3-Bis(4-ethylphenyl)urea (5.6n)

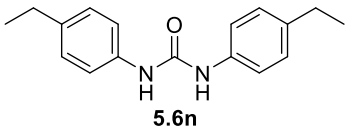

5.6n

The title compound was prepared according to GP1 using 4-ethylphenyl isocyanate (4.86 mL, 33.8 mmol) and 4-ethylaniline (4.20 mL, 33.8 mmol). Following completion of the reaction, the solution was filtered, and the precipitate was washed sequentially with EtOAc and hexane, giving **5.6n** (7.39 g, 81%) as a white solid. **M.p.** (toluene) = 229–231 °C. **^{1}H NMR** (400 MHz, DMSO-d_6) δ 8.52 (s, 2H), 7.35 (ad, *J* = 7.6 Hz, 4H), 7.11 (ad, *J* = 7.6 Hz, 4H), 2.54 (q, *J* = 7.6 Hz, 4H), 1.16 (t, *J* = 7.6 Hz, 6H); **^{13}C NMR** (100 MHz, DMSO-d_6) δ 152.7, 137.5, 137.1, 128.0, 118.3, 27.6, 15.9; **IR** (solid) ν 3299, 2961, 2930, 2869, 1633, 1587, 1550, 1513, 1459, 1297, 1230, 828 cm^{-1}; **HRMS** (ESI-TOF) *m/z* Calcd for $C_{17}H_{20}N_2NaO$ $[M+Na]^+$ 291.1468, found 291.1464. The spectroscopic data were identical in all respects to those previously reported.[484]

***N*,2,2-Triphenylacetamide (5.8)**[485]

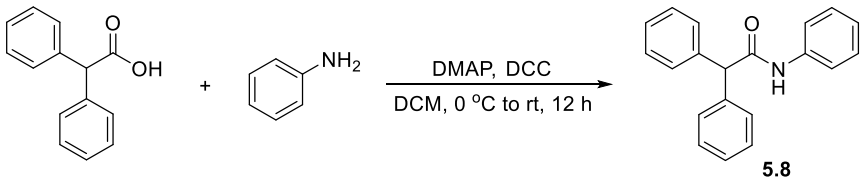

5.8

Scheme S.5.3. Synthesis of amide **5.8**.

A flame dried flask was charged with diphenylacetic acid (2.12 g, 10.0 mmol), aniline (911 µL, 10.0 mmol), DMAP (122 mg, 1.00 mmol), and anhydrous DCM (20 mL). The solution was cooled to 0 °C in an ice bath. DCC (2.27 g, 11.0 mmol) dissolved in anhydrous DCM (20 mL) was added dropwise. The solution was allowed to warm to rt and stirred for 12 h, during which time the formation of a cloudy white precipitate was observed. The crude reaction mixture was then loaded directly onto a bed of silica gel for purification *via* column chromatography (SiO_2, 20–30% EtOAc in hexane), which gave **5.8** (2.15 g, 75%) as a white solid.

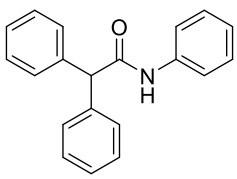

5.8

M.p. (EtOAc) = 177–179 °C; **^{1}H NMR** (400 MHz, $CDCl_3$) δ 7.52 (bs, 1H), 7.37 (d, *J* = 7.6 Hz, 2H), 7.24–7.16 (m, 12H), 7.00 (t, *J* = 7.2 Hz, 1H), 4.99 (s, 1H); **^{13}C NMR** (100 MHz, $CDCl_3$) δ 170.2, 139.1, 137.7, 128.9, 128.9, 128.8, 127.4, 124.4, 119.8, 59.9; **IR** (film, $CDCl_3$) ν 3305, 3059, 3032, 2931, 2854, 1656, 1600, 1548, 1495, 1444, 1360, 1314, 1249, 1170, 740, 692 cm^{-1}; **HRMS** (ESI-TOF) *m/z* Calcd for $C_{20}H_{17}NNaO$ $[M+Na]^+$ 310.1202, found 310.1206. The spectroscopic data were identical in all respects to those previously reported.[486]

General Procedure (GP) 3: Preparation of Symmetrical *N,N'*-Diarylsquaramides from Diethyl Squarate and Substituted Anilines[487]

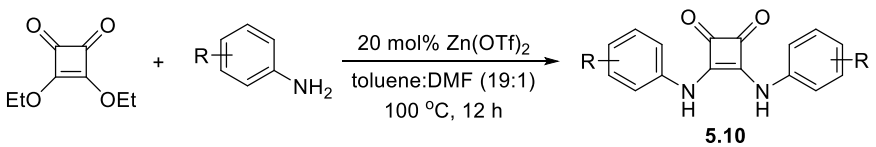

5.10

Scheme S.5.4. General one-step procedure for the preparation of symmetrical *N,N'*-diarylsquaramides.

A flame dried flask was charged with anhydrous toluene (38 mL), anhydrous DMF

(2.0 mL), 3,4-diethoxycyclobut-3-ene-1,2-dione (5.11 g, 30.0 mmol), and zinc triflate (2.18 g, 6.00 mmol). The resulting suspension was stirred at rt, and the substituted aniline (60.0 mmol) was added. The solution was heated to 100 °C and allowed to stir for 18 h, at which point a yellow precipitate was observed. The reaction mixture was cooled to rt, filtered, washed sequentially with methanol and hexane, and dried under high vacuum to give the desired product **5.10**.

3,4-Bis((4-fluorophenyl)amino)cyclobut-3-ene-1,2-dione (5.10a)

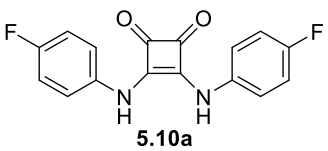

5.10a

The title compound was prepared according to GP3 using 3,4-diethoxycyclobut-3-ene-1,2-dione (5.11 g, 30.0 mmol) and 4-fluoroaniline (6.67 g, 60.0 mmol). **5.10a** (8.65 g, 96%) was obtained as a chalky, pale yellow solid. **M.p.** (toluene) = 321–323 °C (decomposition); **^{1}H NMR** (400 MHz, DMSO-d_6) δ 9.87 (s, 2H), 7.58–7.35 (m, 4H), 7.31–7.08 (m, 4H); **^{13}C NMR** (125 MHz, DMSO-d_6) δ 181.7, 165.4, 158.5 (d, $J_{C–F}$ = 239.8 Hz), 135.0 (d, $J_{C–F}$ = 2.3 Hz), 120.5 (d, $J_{C–F}$ = 8.2 Hz), 116.0 (d, $J_{C–F}$ = 22.7 Hz); **^{19}F NMR** (377 MHz, DMSO-d_6) δ –119.93 (m); **IR** (solid) ν 3130, 3087, 3011, 2951, 1797, 1666, 1616, 1547, 1505, 1405, 1829, 731 cm^{-1}; **HRMS** (ESI-TOF) *m/z* Calcd for $C_{16}H_9F_2N_2O_2$ $[M–H]^-$ 299.0638, found 299.0648.

Note: By ^{19}F NMR, the product appeared to contain trace quantities of an impurity, tentatively assigned as OTf^-. Integration of the product signal and the impurity signal (–77.79 ppm, 3F) suggests <2% OTf^-. The product was used without further purification.

3,4-Bis(phenylamino)cyclobut-3-ene-1,2-dione (5.10c)

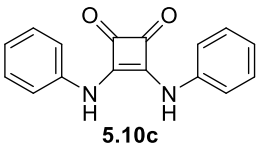

5.10c

The title compound was prepared according to GP3 using 3,4-diethoxycyclobut-3-ene-1,2-dione (5.11 g, 30.0 mmol) and aniline (5.59 g, 60.0 mmol). **5.10c** (7.85 g, 99%) was obtained as a chalky pale-yellow solid. **M.p.** (toluene) = 271–272 °C (decomposition); **^{1}H NMR** (400 MHz, DMSO-d_6) δ 9.89 (s, 2H), 7.50 (d, *J* = 7.6 Hz, 4H), 7.39 (t, *J* = 7.6 Hz, 4H), 7.09 (t, *J* = 7.6 Hz, 2H); **^{13}C NMR** (100 MHz, DMSO-d_6) δ 181.6, 165.7, 138.6, 129.5, 123.4, 118.5; **IR** (solid) ν 3144, 3086, 3037, 2960, 2913, 1797, 1669, 16021539, 1439, 1493, 1449, 1433, 750, 732, 688 cm^{-1}; **HRMS** (ESI-TOF) *m/z* Calcd for $C_{16}H_{12}N_2NaO_2$ $[M+Na]^+$ 287.0791, found 287.0782. The spectroscopic data were identical in all respects to those previously reported.[387]

S.5.1.2. Hydrogen-Bonded Complexes

General Procedure (GP) 4: Preparation of Hydrogen-Bonded Tetraalkylammonium Fluoride–Complexes

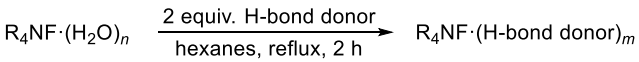

Scheme S.5.5. General procedure for the preparation of hydrogen-bonded tetraalkylammonium fluoride complexes.

A flame dried flask under an inert atmosphere and equipped with a reflux condenser was charged with hexane (0.033 M F^-), tetraalkylammonium fluoride hydrate (1.0 equiv.) and the hydrogen-bond donor (2.0 equiv.). The resulting suspension was allowed to stir in an oil bath at vigorous reflux (80–85 °C) for 2 h, during which time the formation of droplets

of water was observed on the inside walls of the reflux condenser. Over the course of the reaction either the persistent presence of a white solid precipitate or the formation of a biphasic system was observed. The solution was allowed to cool to rt causing some initially liquid products to solidify. In the case of solid products at this stage they were filtered off, washed with hexane, and dried under high vacuum, giving the desired hydrogen-bonded tetraalkylammonium fluoride complexes, which were used without further purification. If instead the formation of a second layer had occurred, which did not give a solid product upon cooling to rt, the upper hexane layer was carefully removed and the lower product layer was dried at an elevated temperature under reduced pressure until it solidified. The solid product was then placed on a sinter funnel, washed with hexane and dried under high vacuum. See individual compounds for details.

Note: In all ^{13}C NMR spectra of hydrogen-bonded tetraalkylammonium fluoride complexes taken in $CDCl_3$, we observed a singlet at approximately 77.20 ppm, which we attribute to $CHCl_3$. We surmise that $CHCl_3$ is formed *in situ* from $CDCl_3$ *via* proton exchange, which is presumably mediated by fluoride acting as a Brønsted base. This signal has been omitted from the peak listings below. Also, some ^{13}C NMR spectra showed a triplet for the carbons in α-position to the TBA^+ nitrogen, which is due to coupling to ^{14}N, as quadrupolar relaxation is slow due to the symmetrical environment of the TBA^+ nitrogen.[488]

The structural depictions of complexes in this section reflect the stoichiometry observed in ^1H NMR spectra, which is not necessarily the same as is observed in the solid-state structures.

TBAF(1,3-di-*m*-tolylurea)$_2$ (5.7a)

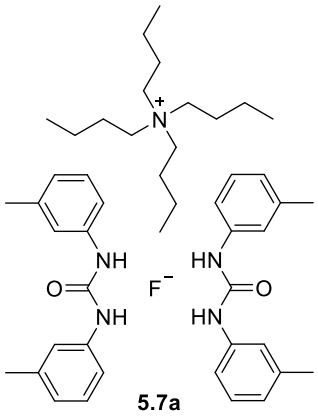

5.7a

The title compound was prepared according to GP4 using TBAF(H_2O)$_3$ (631 mg, 2.00 mmol) and 1,3-di-*m*-tolylurea (**5.6a**) (961 mg, 4.00 mmol). Complex **5.7a** (1.29 g, 87%) was thus obtained as a crystalline white solid. **^{1}H NMR** (400 MHz, $CDCl_3$) δ 7.41 (d, *J* = 7.6 Hz, 4H), 7.32 (s, 4H), 7.01 (t, *J* = 7.6 Hz, 4H), 6.68 (d, *J* = 7.6 Hz, 4H), 2.72–2.68 (m, 8H), 2.13 (s, 12H), 1.20–1.07 (m, 16H), 0.78 (t, *J* = 6.8 Hz, 12H); **^{13}C NMR** (100 MHz, $CDCl_3$) δ 154.4, 140.3, 138.4, 128.4, 128.5, 122.1, 118.9, 58.1, 23.5, 21.3, 19.4, 13.5; **IR** (solid) ν 3296, 3017, 2874, 1712, 1614. 1593, 1560, 1480, 1289, 1204, 1160, 1204, 1160, 794, 774, 755 cm^{-1}; **X-ray** (single-crystal) Colourless needless of X-ray diffraction quality were obtained by vapour diffusion of hexane into a saturated solution of **5.7a** in EtOAc, which had previously been prepared by dissolving **5.7a** in refluxing EtOAc (approximately 77 °C) until visibly saturated, filtering while hot, and then allowing to stand for approximately 1 min to cool to near rt. Experimental details are provided below.

TBAF(1,3-bis(4-(trifluoromethyl)phenyl)urea)$_2$ (5.7b)

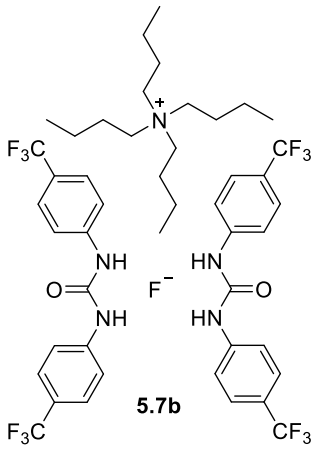

5.7b

The title compound was prepared according to GP4 using TBAF(H_2O)$_3$ (631 mg, 2.00 mmol) and 1,3-bis(4-(trifluoromethyl)phenyl)urea (**5.6b**) (1.39 g, 4.00 mmol). Complex **5.7b** (1.84 g, 96%) was thus obtained as a crystalline white solid. **^{1}H NMR** (400 MHz, $CDCl_3$) δ 7.65 (ad, *J* = 8.4 Hz, 8H), 7.41 (ad, *J* = 8.4 Hz, 8H), 2.93–2.89 (m, 8H), 1.42 (qn, *J* = 7.4 Hz, 8H), 1.26 (sx, *J* = 7.4 Hz, 8H), 0.90 (t, *J* = 7.4 Hz, 12H); **^{13}C NMR** (100 MHz, $CDCl_3$) δ

153.8, 143.3, 125.8 (q, $J_{C–F}$ = 3.6 Hz), 124.5 (q, $J_{C–F}$ = 269.4 Hz), 123.1 (q, $J_{C–F}$ = 32.2 Hz), 117.9, 58.6 (t, $J_{C–N}$ = 2.8 Hz), 23.6, 19.4, 13.3; **^{19}F NMR** (377 MHz, $CDCl_3$) δ –61.61; **IR** (solid) ν 2969, 2880, 1710, 1633, 1602, 1551, 1323, 1307, 1247, 1202, 1178, 1154, 1106, 1066, 823 cm^{-1}; **X-ray** (single-crystal) Colourless block crystals of X-ray diffraction quality were obtained by layering hexane onto a saturated solution of **5.7b** in DCM, which had previously been prepared by dissolving **5.7b** in refluxing DCM (approximately 40 °C) until visibly saturated, filtering while hot, and then allowing to stand for approximately 1 min to cool to near rt. Experimental details are provided below.

TBAF(1,3-bis(4-nitrophenyl)urea)$_2$ (5.7c)

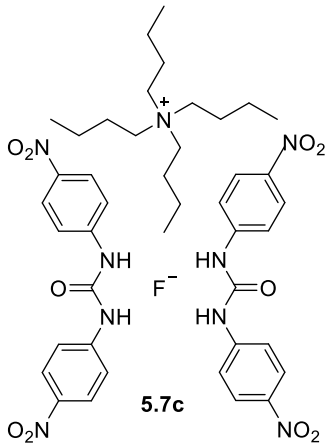

5.7c

The title compound was prepared according to GP4 using TBAF(H_2O)$_3$ (1.26 g, 4.00 mmol) and 1,3-bis(4-nitrophenyl)urea (**5.6c**) (2.54 g, 8.00 mmol). Complex **5.7c** (3.38 g, 96%) was thus obtained as a chalky yellow solid. **^{1}H NMR** (400 MHz, $CDCl_3$) δ 8.07 (ad, *J* = 9.2 Hz, 8H), 7.75 (ad, *J* = 9.2 Hz, 8H), 3.18–3.13 (m, 8H), 1.61 (qn, *J* = 7.2 Hz, 8H), 1.40 (sx, *J* = 7.2 Hz, 8H) 0.98 (t, *J* = 7.2 Hz, 12H); **^{13}C NMR** (100 MHz, $CDCl_3$) δ 153.3, 146.7, 141.4, 125.0, 117.7, 58.9 (t, $J_{C–N}$ = 2.7 Hz), 23.8, 19.7, 13.5; **IR** (solid) ν 2963, 2876, 1723, 1617, 1599, 1571, 1323, 1299, 1252, 1202, 1170, 1109, 846, 751 cm^{-1}; **X-ray** (single-crystal) Yellow block crystals of X-ray diffraction quality were obtained by vapour diffusion of hexane into a saturated solution of **5.7c** in EtOAc, which had previously been prepared by dissolving **5.7c** in refluxing EtOAc (approximately 77 °C) until visibly saturated, filtering while hot, and then allowing to stand for approximately 1 min to cool to near rt. Experimental details are provided below.

Note: During the complexation reaction, small quantities of a deep orange/red solid were observed, possible due to deprotonation of the acidic N–H bond.[363]

TBAF(1,3-bis(4-*n*-propylphenyl)urea)$_2$ (5.7d)

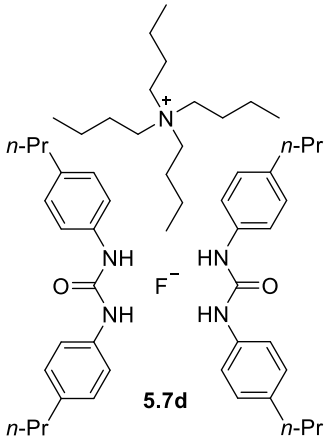

5.7d

The title compound was prepared according to GP4 using TBAF(H_2O)$_3$ (631 mg, 2.00 mmol) and 1,3-bis(4-propylphenyl) urea (**5.6d**) (1.19 g, 4.00 mmol). Complex **5.7d** (1.66 g, 97%) was thus obtained as a chalky white solid. **^{1}H NMR** (400 MHz, $CDCl_3$) δ 7.43–7.41 (m, 8H), 6.93 (ad, *J* = 8.4 Hz, 8H), 2.75–2.71 (m, 8H), 2.45 (t, *J* = 7.2 Hz, 8H), 1.55 (sx, *J* = 7.2 Hz, 8H), 1.18–1.07 (m, 16H), 0.89 (t, *J* = 7.2 Hz, 12H), 0.77–0.74 (m, 12H); **^{13}C NMR** (100 MHz, $CDCl_3$) δ 154.6, 138.2, 135.3, 128.5, 118.4, 58.0, 37.3, 24.7, 23.5, 19.4, 13.7, 13.5; **IR** (solid) ν 2956, 2930, 2869, 1699, 1598, 1554, 1510, 1303, 1239, 1210, 1196, 815 cm^{-1}; **X-ray** (single-crystal) Colourless block crystals of X-ray diffraction quality were obtained by carefully layering hexane onto a saturated solution of **5.7d** in EtOAc, which had previously been prepared by dissolving **5.7d** in refluxing EtOAc (approximately 77 °C) until visibly saturated, filtering while hot, and then allowing to stand for approximately 1 min to cool to near rt. Experimental details are provided below. **Neutron** (single-crystal) Crystals of suitable size and quality for neutron diffraction were grown by placing a single-crystal of the title compound in a saturated solution of **5.7d** in EtOAc, which had previously been prepared by dissolving **5.7d** in refluxing EtOAc (approximately 77 °C) until visibly saturated, filtering while hot, and then allowing to stand for approximately 1 min to cool to near rt. Crystal growth was achieved by vapour diffusion of hexane into this seeded

solution. The process was repeated until a crystal of suitable size was obtained (Figure S.5.2).

TBAF(1,3-diphenylurea)$_2$ (5.7e)

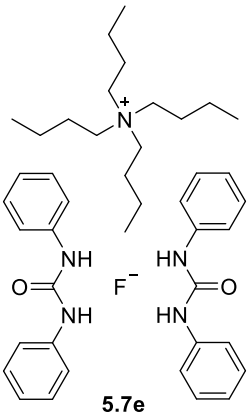

5.7e

The title compound was prepared according to GP4 using TBAF(H_2O)$_3$ (1.26 g, 4.00 mmol) and 1,3-diphenylurea (**5.6e**) (1.70 g, 8.00 mmol). After heating at reflux for 2 h, a viscous pale brown oil was observed at the bottom of the reaction vessel. The reaction was allowed to cool to rt, and the solvent was removed *in vacuo*. After further drying under high vacuum for 8 h, the complex solidified. The resulting material was washed with hexane on a sinter funnel then dried under high vacuum. Complex **5.7e** (2.48 g, 90%) was thus obtained as chalky off-white solid. **^{1}H NMR** (400 MHz, $CDCl_3$) δ 7.55 (d, *J* = 7.6 Hz, 8H), 7.14 (t, *J* = 7.6 Hz, 8H), 6.87 (t, *J* = 7.6 Hz, 4H), 2.76–2.72 (m, 8H), 1.25–1.16 (m, 8H), 1.13 (sx, *J* = 7.2 Hz, 8H), 0.80 (t, *J* = 7.2 Hz, 12H); **^{13}C NMR** (100 MHz, $CDCl_3$) δ 154.4, 140.5, 128.6, 121.2, 118.4, 58.2 (t, $J_{C–N}$ = 2.5 Hz), 23.5, 19.4, 13.5; **IR** (solid) ν 3027, 2962, 2873, 1697, 1617, 1593, 1545, 1497, 1484, 1444, 1299, 1229, 1198, 1173, 884, 756, 695 cm^{-1}; **X-ray** (single-crystal) Colourless plate-like crystals of X-ray diffraction quality were obtained by carefully layering hexane onto a saturated solution of **5.7e** in EtOAc, which had previously been prepared by dissolving **5.7e** in refluxing EtOAc (approximately 77 °C) until visibly saturated, filtering while hot, and then allowing to stand for approximately 1 min to cool to near rt. Experimental details are provided below.

TBAF(1,3-di-*p*-tolylurea)$_2$ (5.7f)

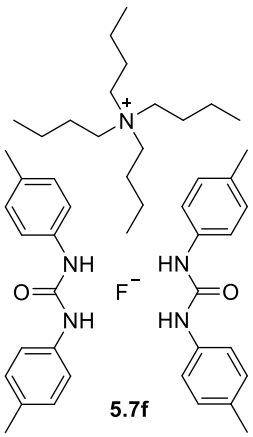

5.7f

The title compound was prepared according to GP4 using TBAF$(H_2O)_3$ (1.26 g, 4.00 mmol) and 1,3-di-*p*-tolylurea (**5.6f**) (1.92 g, 8.00 mmol). Complex **5.7f** (2.87 g, 97%) was thus obtained as a chalky white solid. **^{1}H NMR** (400 MHz, $CDCl_3$) δ 7.42 (ad, *J* = 8.0 Hz, 8H), 6.94 (ad, *J* = 8.0 Hz, 8H), 2.76–2.72 (m, 8H), 2.22 (s, 12H), 1.24–1.17 (m, 8H), 1.12–1.09 (m, 8H), 0.80 (t, *J* = 7.2 Hz, 12H); **^{13}C NMR** (100 MHz, $CDCl_3$) δ 154.6, 138.0, 130.3, 129.1, 118.4, 58.1, 23.5, 20.7, 19.4, 13.5; **IR** (solid) ν 2960, 2926, 2872, 1702, 1600, 1552, 1509, 1310, 1290, 1234, 1215, 1194, 1177 883, 820, 756 cm^{-1}; **X-ray** (single-crystal) Colourless block crystals of X-ray diffraction quality were obtained by vapour diffusion of hexane into a saturated solution of **5.7f** in THF, which had previously been prepared by dissolving **5.7f** in refluxing THF (approximately 66 °C) until visibly saturated, filtering while hot, and then allowing to stand for approximately 1 min to cool to near rt. Experimental details are provided below.

TBAF(1,3-bis(4-methoxyphenyl)urea)$_2$ (5.7g)

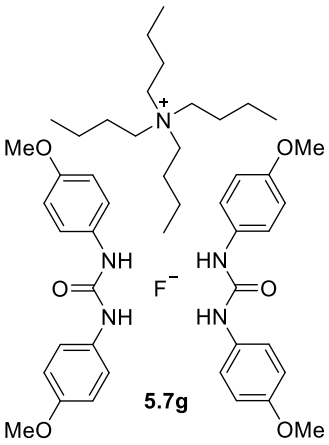

5.7g

The title compound was prepared according to GP4 using TBAF$(H_2O)_3$ (631 mg, 2.00 mmol) and 1,3-bis(4-methoxyphenyl)urea (**5.6g**) (1.09 g, 4.00 mmol). Complex **5.7g** (1.47 g, 91%) was thus obtained as a flocculent white solid. **^{1}H NMR** (400 MHz, DMSO-d_6) δ 10.60 (bs, 4H), 7.35 (ad, *J* = 8.8 Hz, 8H), 6.79 (ad, *J* =8.8 Hz, 8H), 3.69 (s, 12H), 3.16–3.12 (m, 8H), 1.58–1.50 (m, 8H), 1.29 (sx, *J* = 7.2 Hz, 8H), 0.92 (t, *J* = 7.2 Hz, 12H); **^{13}C NMR** (100 MHz, DMSO-d_6) δ 153.9, 153.6, 134.1, 119.0, 113.9, 57.5 (t, $J_{C–N}$ = 2.8 Hz), 55.1, 23.0,

19.2, 13.5; **IR** (solid) ν 3290, 3005, 2874, 2835, 1703, 1605, 1558, 1504, 1297, 1225, 1202, 1178, 1029, 829, 724 cm^{-1}; **X-ray** (single-crystal) Colourless plate-like crystals of X-ray diffraction quality were obtained by vapour diffusion of hexane into a saturated solution of **5.7g** in DCM, which had previously been prepared by dissolving **5.7g** in refluxing DCM (approximately 40 °C) until visibly saturated, filtering while hot, and then allowing to stand for approximately 1 min to cool to near rt. Experimental details are provided below.

TBAF(1,3-bis(4-chlorophenyl)urea)$_2$ (5.7h)

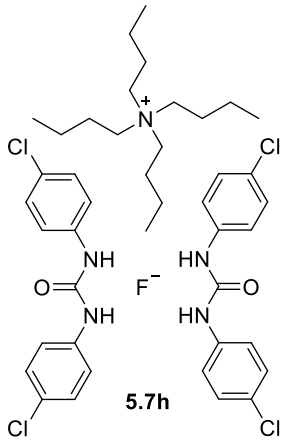

5.7h

The title compound was prepared according to GP4 using $TBAF(H_2O)_3$ (1.26 g, 4.00 mmol) and 1,3-bis(4-chlorophenyl)urea (**5.6h**) (2.25 g, 8.00 mmol). Complex **5.7h** (3.26 g, 99%) was thus obtained as a crystalline white solid. **^{1}H NMR** (400 MHz, DMSO-d_6) δ 11.55 (bs, 4H), 7.52 (ad, *J* = 8.8 Hz, 8H), 7.26 (ad, *J* = 8.8 Hz, 8H), 3.12–3.08 (m, 8H), 1.51 (qn, *J* = 7.2 Hz, 8H), 1.26 (sx, *J* = 7.2 Hz, 8H), 0.89 (t, *J* = 7.2 Hz, 12H); **^{13}C NMR** (100 MHz, DMSO-d_6) δ 153.3, 139.3, 128.5, 124.8, 119.3, 57.5, 23.0, 19.2, 13.4; **IR** (solid) ν 3292, 2961, 2873, 1696, 1591, 1547, 1487, 1400, 1302, 1282, 1234, 1198, 1171, 1086, 1034, 883, 830, 776 cm^{-1}; **X-ray** (single-crystal) Colourless block crystals of X-ray diffraction quality were obtained by layering hexane onto a saturated solution of **5.7h** in EtOAc, which had previously been prepared by dissolving **5.7h** in refluxing EtOAc (approximately 77 °C) until visibly saturated, filtering while hot, and then allowing to stand for approximately 1 min to cool to near rt. Experimental details are provided below. **Neutron** (single-crystal) Crystals of suitable size and quality for neutron diffraction were grown by placing a single-crystal of the title compound in a saturated solution of **5.7h** in EtOAc, which had previously been prepared

by dissolving **5.7h** in refluxing EtOAc (approximately 77 °C) until visibly saturated, filtering while hot, and then allowing to stand for approximately 1 min to cool to near rt. Crystal growth was achieved by vapour diffusion of hexane into this seeded solution. The process was repeated until a crystal of suitable size was obtained (Figure S.5.2).

TBAF(1,3-bis(4-fluorophenyl)urea)$_2$ (5.7j)

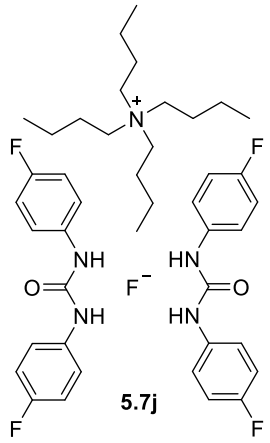

5.7j

The title compound was prepared according to GP4 using TBAF$(H_2O)_3$ (631 mg, 2.00 mmol) and 1,3-bis(4-fluorophenyl)urea (**5.6j**) (993 mg, 4.00 mmol). After heating at reflux for 2 h, a viscous colourless oil was observed at the bottom of the reaction vessel, which solidified when allowed to stand at rt for 2 h. Following the standard work-up, complex **5.7j** (2.86 g, 94%) was obtained as a crystalline white solid. **^{1}H NMR** (400 MHz, $CDCl_3$) δ 7.47–7.43 (m, 8H), 6.84 (ad, *J* = 7.6 Hz, 8H), 2.85 (m, 8H), 1.34 (qn, *J* = 7.2 Hz, 8H), 1.20 (sx, *J* = 7.2 Hz, 8H), 0.87 (t, *J* = 7.2 Hz, 12H); **^{13}C NMR** (100 MHz, $CDCl_3$) δ 157.7 (d, $J_{C–F}$ = 238.2 Hz), 154.5, 136.4, 119.9 (d, $J_{C–F}$ = 7.3 Hz), 115.0 (d, $J_{C–F}$ = 22.0 Hz), 58.4, 23.6, 19.5, 13.4; **^{19}F NMR** (377 MHz, $CDCl_3$) δ –122.31 (m); **IR** (solid) ν 2962, 2876, 1712, 1673, 1618, 1574, 1503, 1410, 1315, 1194, 833, 735 cm^{-1}; **X-ray** (single-crystal) Colourless block crystals of X-ray diffraction quality were obtained by layering hexane onto a saturated solution of **5.7j** in Et_2O which had previously been prepared by dissolving **5.7j** in refluxing Et_2O (approximately 35 °C) until visibly saturated, filtering while hot, and then allowing to stand for approximately 1 min to cool to near rt. Experimental details are provided below. **Neutron** (single-crystal) Crystals of suitable size and quality for neutron diffraction were grown by placing a single-crystal of the title compound in a saturated solution of **5.7j** in Et_2O, which had

previously been prepared by dissolving **5.7j** in refluxing Et_2O (approximately 35 °C) until visibly saturated, filtering while hot, and then allowing to stand for approximately 1 min to cool to near rt. Crystal growth was achieved by vapour diffusion of hexane into this seeded solution. The process was repeated until a crystal of suitable size was obtained (Figure S.5.2).

TBAF(1,3-bis(4-ethylphenyl)urea)$_2$ (5.7n)

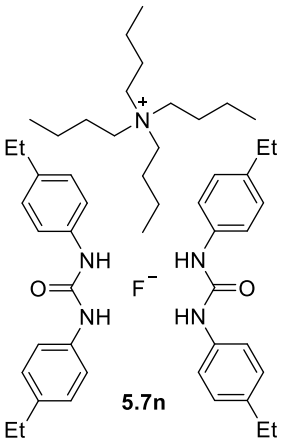

5.7n

The title compound was prepared according to GP4 using $TBAF(H_2O)_3$ (631 mg, 2.00 mmol) and 1,3-bis(4-ethylphenyl)urea (**5.6n**) (1.07 g, 4.00 mmol). Complex **5.7n** (1.52 g, 95%) was thus obtained as a chalky white solid. **^{1}H NMR** (400 MHz, $CDCl_3$) δ 7.46–7.43 (m, 8H), 6.99–6.95 (m, 8H), 2.80–2.70 (m, 8H), 2.53 (q, *J* = 7.2 Hz, 8H), 1.27–1.05 (m, 28H), 0.80 (t, *J* = 7.2 Hz, 12H); **^{13}C NMR** (100 MHz, $CDCl_3$) δ 154.5, 138.0, 137.0, 127.9, 118.6, 58.1, 28.1, 23.6, 19.4, 15.8, 13.5; **IR** (solid) ν 3302, 2962, 2931, 2873, 1699, 1599, 1550, 1509, 1413, 1305, 1246, 1233, 1208, 1194, 1177, 835 cm^{-1}; **X-ray** (single-crystal) Colourless needles of X-ray diffraction quality were obtained by layering hexane on top of a saturated solution of **5.7n** in EtOAc, which had previously been prepared by dissolving **5.7n** in refluxing EtOAc (approximately 77 °C) until visibly saturated, filtering while hot, and then allowing to stand for approximately 1 min to cool to near rt. The observed single-crystal X-ray structure was found to be modulated (Figure S.5.1). Experimental details are provided below.

TBAF(*N*,2,2-triphenylacetamide)$_2$ (5.9)

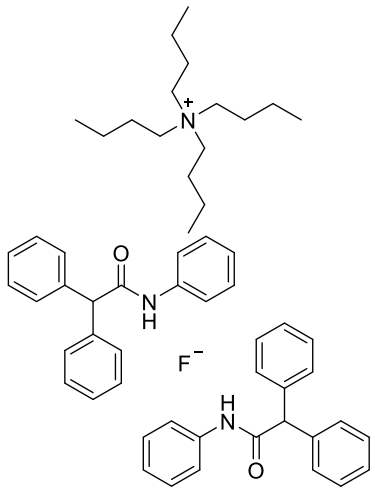

5.9

The title compound was prepared according to GP4 using TBAF$(H_2O)_3$ (631 mg, 2.00 mmol) and *N*,2,2-triphenylacetamide (**5.8**) (1.15 g, 4.00 mmol). Complex **5.9** (1.56 g, 93%) was thus obtained as a chalky white solid. **^{1}H NMR** (400 MHz, $CDCl_3$) δ 7.74 (d, *J* = 7.6 Hz, 4H), 7.40 (d, *J* = 7.2 Hz, 8H), 7.21 (t, *J* = 7.2 Hz, 8H), 7.17–7.12 (m, 8H), 6.95 (t, *J* = 7.6 Hz, 2H), 5.52 (s, 2H), 2.89–2.85 (m, 8H), 1.32 (qn, *J* = 7.2 Hz, 8H), 1.22 (sx, *J* = 7.2 Hz, 8H), 0.88 (t, *J* = 7.2 Hz, 12H); **^{13}C NMR** (100 MHz, $CDCl_3$) δ 171.1, 140.4, 139.5, 129.1, 128.4, 128.2, 126.6, 123.2, 120.2, 58.1, 38.8, 23.7, 19.5, 13.5; **IR** (solid) ν 2963, 2932, 2875, 1882, 1673, 1627, 1596, 1566, 1489, 1444, 1380, 1316, 1299, 1259, 1191, 1173, 1031, 966, 881, 862, 761, 742, 723, 697 cm^{-1}; **X-ray** (single-crystal) Colourless plate-like crystals of X-ray diffraction quality were obtained by carefully layering hexane onto a saturated solution of **5.9** in EtOAc, which had previously been prepared by dissolving **5.9** in refluxing EtOAc (approximately 77 °C) until visibly saturated, filtering while hot, and then allowing to stand for approximately 1 min to cool to near rt. Experimental details are provided below.

TBAF(*N*,*N'*-bis(4-fluorophenyl)squaramide)$_2$ (5.11a)

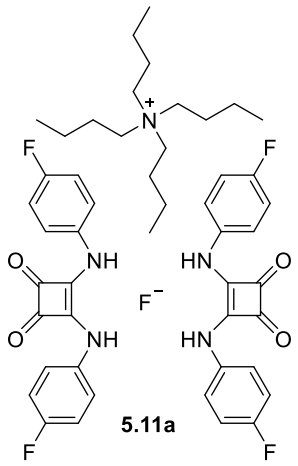

5.11a

The title compound was prepared according to GP4 using TBAF$(H_2O)_3$ (631 mg, 2.00 mmol) and *N*,*N'*-bis(4-fluorophenyl)squaramide (**5.10a**) (1.20 g, 4.00 mmol). Complex **5.11a** (1.69 g, 98%) was thus obtained as a chalky pale yellow solid. **^{1}H NMR** (400 MHz, Acetone-d_6) δ 7.72–7.67 (m, 8H), 7.03 (t, J = 8.8 Hz, 8H), 3.46–3.41 (m, 8H), 1.81 (qn, J = 7.3 Hz, 8H), 1.42 (sx, J = 7.3 Hz, 8H), 0.96 (t, J = 7.3 Hz, 12H); **^{13}C NMR** (100 MHz, Acetone-d_6) δ 183.0, 167.4, 159.5 (d, $J_{C–F}$ = 239.4 Hz), 137.6, 120.7 (d, $J_{C–F}$ = 7.6 Hz), 116.6 (d, $J_{C–F}$ = 22.9 Hz), 59.5 (t, $J_{C–N}$ = 2.7 Hz), 24.5, 20.5, 13.9; **^{19}F NMR** (377 MHz, Acetone-d_6) δ –122.87 (m); **IR** (solid) ν 3131, 2960, 2876, 1797, 1778, 1667, 1551, 1508, 1432, 1404, 1212, 829, 733 cm^{-1}; **X-ray** (single crystal) Yellow plate-like crystals of X-ray diffraction quality were obtained by vapour diffusion of hexane into a saturated solution of **5.11a** in THF, which had previously been prepared by dissolving **5.11a** in refluxing THF (approximately 66 °C) until visibly saturated, filtering while hot, and then allowing to stand for approximately 1 min to cool to near rt. The crystal was found to be a THF solvate. Experimental details are provided below.

TBAF(*N*,*N*'-diphenylsquaramide)$_2$ (5.11c)

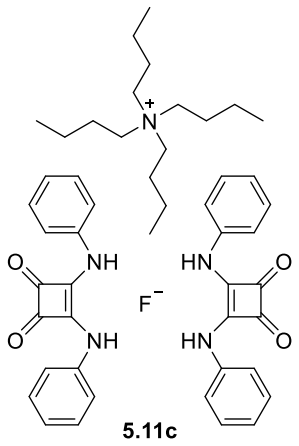

5.11c

The title compound was prepared according to GP4 using TBAF(H_2O)$_3$ (631 mg, 2.00 mmol) and *N*,*N*'-diphenylsquaramide (**5.10c**) (1.06 g, 4.00 mmol). Complex **5.11c** (1.51 g, 96%) was thus obtained as a chalky pale yellow solid. **^{1}H NMR** (400 MHz, Acetone-d_6) δ 7.71 (d, *J* = 7.8 Hz, 8H), 7.24 (t, *J* = 7.8 Hz, 8H), 6.95 (t, *J* = 7.8 Hz, 4H), 3.45–3.39 (m, 8H), 1.81 (qn, *J* = 7.4 Hz, 8H), 1,42 (sx, *J* = 7.4 Hz, 8H), 0.97 (t, *J* = 7.4 Hz, 12H); **^{13}C NMR** (100 MHz, Acetone-d_6) δ 183.1, 167.7, 141.1, 130.1, 123.4, 119.2, 59.5 (t, $J_{C–N}$ = 2.9 Hz), 24.5, 20.5, 13.9; **IR** (solid) ν 3546, 3142, 2962, 2874, 1779, 1669, 1600, 1550, 1499, 1415, 751, 689 cm^{-1}; **X-ray** (single crystal). Yellow needles of X-ray diffraction quality were obtained by carefully layering hexane onto a saturated solution of **5.11c** in THF, which had previously been prepared by dissolving **5.11c** in refluxing THF (approximately 66 °C) until visibly saturated, filtering while hot, and then allowing to stand for approximately 1 min at room temperature to cool to near rt. Experimental details are provided below.

S.5.2. Single-Crystal X-Ray and Neutron Structures

Table S.5.1. Summary of single-crystal X-ray and neutron structures of complexes **5.7a**–**r**, **5.9** and **5.11a**–**c** (continued on following pages).

Nr.	5.7a	5.7b	5.7c	5.7d	5.7e	5.7f	5.7g
Formula	$C_{46}H_{68}F_1N_5O_2$	$C_{46}H_{56}F_{13}N_5O_2$	$C_{42}H_{56}F_1N_9O_{10}$	$C_{54}H_{84}F_1N_5O_2$	$C_{42}H_{60}F_1N_5O_2$	$C_{46}H_{68}F_1N_5O_2$	$C_{46}H_{68}F_1N_5O_6$
Molecular Weight	742.08	957.96	865.96	854.29	685.97	742.08	806.07
Crystal System	monoclinic	monoclinic	triclinic	monoclinic	monoclinic	monoclinic	monoclinic
T [K]	150	150	150	150	150	150	150
Space Group	P 1 2/n 1	P 21/n	P –1	P 1 21/c 1	C 1 2/c 1	C 2/c	C 2/c
a [Å]	11.0040(2)	10.9971(2)	8.6153(2)	13.0796(1)	24.0170(4)	23.8541(2)	23.6270(8)
b [Å]	8.3440(1)	17.0640(4)	14.6367(3)	15.7385(2)	14.3831(2)	15.0254(2)	15.1483(4)
c [Å]	24.0042(4)	24.9997(6)	18.1464(5)	25.2838(3)	26.8362(4)	25.4496(3)	26.7686(5)
α [°]	90	90	91.7994(9)	90	90	90	90
β [°]	97.4468(15)	92.7108(9)	103.2496(10)	102.0084(10)	121.301(2)	107.3282(4)	110.213(5)
γ [°]	90	90	102.4776(8)	90	90	90	90
V [Å^3]	2185.41(6)	4686.06(18)	2166.84(9)	5090.86(10)	7921.0(3)	8707.59(17)	8990.7(6)
Z	2	4	2	4	8	8	8
D_{calc} [g cm^{-3}]	1.128	1.358	1.327	1.115	1.150	1.132	1.191
F(0 0 0)	808	2000	920	1872	2976	3232	3488
μ [mm^{-1}]	0.563	0.119	0.099	0.541	0.584	0.072	0.656
Crystal Size [mm]	0.11 * 0.21 * 0.28	0.11 * 0.22 * 0.34	0.18 * 0.30 * 0.38	0.19 * 0.20 * 0.21	0.03 * 0.10 * 0.17	0.31 * 0.38 * 0.41	0.03 * 0.18 * 0.21
Colour, Shape	clear_pale_colourless, plate	clear_pale_colourless, block	yellow, block	clear_pale_colourless, block	clear_pale_colourless, plate	clear_pale_colourless, block	clear_plate_colourless, plate
R_{int}	5.37	13.42	7.9	6.05	5.03	9.64	10.67
θ_{min}, θ_{max} [deg]	3.714 – 67.011	5.127 – 25.039	5.122 – 25.529	3.328 – 76.856	3.672 – 76.604	5.108 – 26.903	3.534 – 73.485
Total Reflections (before merge)	14195	47775	27473	121582	85948	62224	76871
Data (I>–3.0/sigma(I)) [Reflections, Restraints, Parameters]	4020, 208, 319	5811, 336, 608	6954, 34, 563	10665, 0, 559	8277, 0, 452	9869, 0, 488	9146, 1878, 677
S (=GooF)	0.993	1.019	0.952	0.990	0.972	0.990	1.002
Min. and Max. Residual Dens., [e/Å^3]	–0.22	–0.97	–0.36	–0.51	–0.23	–0.38	–0.51
	0.24	1.340	0.35	0.64	0.38	0.37	0.45
Threshold Expression	I>2sigma(I)	I>2sigma(I)	I>2sigma(I)	I>2sigma(I)	I>2sigma(I)	I>2sigma(I)	I>2sigma(I)
R_1	0.0468	0.0831	0.0500	0.0567	0.0394	0.0573	0.0925
wR_2	0.1242	0.1829	0.1158	0.1498	0.0935	0.1154	0.2450

Nr.	5.7h	5.7i	5.7j	5.7k	5.7l	5.7m	5.7n
Formula	$C_{42}H_{56}Cl_4F_1N_5O_2$	$C_{58}H_{92}F_1N_5O_2$	$C_{42}H_{56}F_5N_5O_2$	$C_{54}H_{84}F_1N_5O_2$	$C_{29}H_{48}F_1I_1N_3O_2$	$C_{30}H_{50}Br_2Cl_2F_1N_3O_2$	$C_{33}H_{58}F_1N_3O_2$
Molecular Weight	823.75	910.40	757.93	854.29	743.53	734.46	547.84
Crystal System	monoclinic	monoclinic	monoclinic	trigonal	monoclinic	monoclinic	monoclinic
T [K]	150	150	150	150	150	150	150
Space Group	C 2/c	P n	P 21/n	R –3	C 2	P 1 21/c 1	P 21/c
a [Å]	23.8256(2)	12.8854(1)	13.2102(3)	36.1165(4)	24.2255(6)	13.7989(2)	12.36670(6)
b [Å]	14.9792(1)	16.5136(1)	14.7340(3)	36.1165(4)	8.1758(2)	17.0778(3)	17.56165(9)
c [Å]	25.1935(2)	26.1896(2)	21.0702(5)	45.7915(5)	16.4519(5)	15.4612(3)	15.47775(8)
α [°]	90	90	90	90	90	90	90
β [°]	107.9175(9)	98.5587(7)	96.2452(10)	90	99.107(3)	104.5476(6)	94.2660(5)
γ [°]	90	90	90	120	90	90	90
V [$Å^3$]	8555.20(12)	5510.68(7)	4076.75(16)	51728.1(10)	3217.44(15)	3526.69(11)	3352.14(3)
Z	8	4	4	36	4	4	4
D_{calc} [g cm^{-3}]	1.279	1.097	1.235	0.987	1.535	1.383	1.085
F(0 0 0)	3488	2000	1616	16848	1496	1520	1208
μ [mm^{-1}]	2.875	0.526	0.092	0.479	15.623	2.485	0.552
Crystal Size [mm]	0.14 * 0.24 * 0.32	0.07 * 0.15 * 0.18	0.22 * 0.23 * 0.25	0.05 * 0.09 * 0.13	0.10 * 0.20 * 0.22	0.20 * 0.22 * 0.30	0.05 * 0.16 * 0.18
Colour, Shape	clear_pale_colourless, block	clear_pale_colourless, lath	clear_pale_colourless, block	clear_pale_colourless, plate	clear_pale_colourless, block	clear_pale_colourless, block	clear_pale_colourless, block
R_{int}	3.40	5.86	10.65	9.71	2.50	7.16	12.90
θ_{min}, θ_{max} [deg]	3.537 – 76.575	3.174 – 75.435	5.135 – 25.290	3.422 – 61.147	3.696 – 72.873	5.108 – 26.939	3.584 – 76.433
Total Reflections (before merge)	100518	131171	28777	18178	27688	66254	69661
Data (I>–3.0/sigma(I)) [Reflections, Restraints, Parameters]	8934, 0, 489	22471, 194, 1282	8232, 0, 487	9610, 4028, 1770	5701, 1, 337	5228, 747, 398	6985, 0, 352
S (=GooF)	0.990	0.996	0.968	1.148	1.008	0.962	2.991
Min. and Max. Residual Dens., [e/$Å^3$]	–0.37	–0.47	–0.48	–0.60	–0.93	–0.54	–0.99
	0.50	0.55	0.47	0.54	1.40	0.79	1.03
Threshold Expression	I>2sigma(I)	I>2sigma(I)	I>2sigma(I)	I>2sigma(I)	I>2sigma(I)	I>2sigma(I)	I>2sigma(I)
R_1	0.0319	0.0558	0.0571	0.0971	0.0249	0.0716	12.25
wR_2	0.0823	0.1654	0.1033	0.0863	0.0662	0.1108	0.5334

Nr.	5.7o	5.7p	5.7q	5.7r	5.9	5.11a	5.11b
Formula	$C_{35}H_{62}F_1N_3O_2$	$C_{29}H_{48}Br_2F_1N_3O_2$	$C_{44}H_{50}Cl_2F_1N_7O_3$	$C_{47}H_{56}F_1N_7O_3$	$C_{56}H_{70}F_1N_3O_2$	$C_{52}H_{64}F_5N_5O_5$	$C_{48}H_{56}Cl_4F_1N_5O_4$
Molecular Weight	575.89	649.52	814.83	786.00	836.19	934.10	927.81
Crystal System	monoclinic	monoclinic	orthorhombic	monoclinic	monoclinic	triclinic	monoclinic
T [K]	150	150	150	150	150	150	150
Space Group	P 1 21/n 1	C 2	P b c a	P 21/c	P 1 21/c 1	P –1	P 21/c
a [Å]	15.9606(5)	23.8588(6)	22.8897(2)	12.4349(2)	14.2788(1)	12.6627(4)	17.3563(4)
b [Å]	17.2439(4)	8.1744(2)	15.1701(1)	22.5589(3)	15.3802(2)	14.9489(5)	15.9395(3)
c [Å]	26.6482(8)	16.1922(4)	24.7223(2)	15.5250(2)	22.0076(2)	15.0370(4)	17.7772(4)
α [°]	90	90	90	90	90	114.772(3)	90
β [°]	103.648	96.692(3)	90	90.6731(12)	95.0763(9)	103.341(3)	108.149(2)
γ [°]	90	90	90	90	90	94.373(3)	90
V [$Å^3$]	7127.1(4)	3136.47(14)	8584.55(12)	4354.74(11)	4814.15(8)	2466.09(16)	4673.40(18)
Z	8	4	8	4	4	2	4
D_{calc} [g cm^{-3}]	1.073	1.375	1.261	1.199	1.154	1.258	1.319
F(0 0 0)	2544	1352	3440	1680	1808	992	1952
μ [mm^{-1}]	0.54	3.553	1.779	0.632	0.557	0.778	2.73
Crystal Size [mm]	0.11 * 0.18 * 0.20	0.04 * 0.15 * 0.18	0.06 * 0.12 * 0.24	0.02 * 0.24 * 0.25	0.08* 0.12 * 0.14	0.20 * 0.22 * 0.24	0.06 * 0.14 * 0.24
Colour, Shape	clear_pale_colourless, block	clear_pale_colourless, plate	clear_pale_colourless, plate	clear_pale_colourless, plate	clear_pale_colourless, block	clear_pale_colourless, block	clear_pale_colourless, block
R_{int}	9.32	3.59	5.97	4.87	4.76	4.16	8.25
θ_{min}, θ_{max} [deg]	2.955 – 74.727	3.731 – 69.913	3.862 – 73.603	3.456 – 76.840	3.107 – 72.043	3.320 – 73.741	3.813 – 75.318
Total Reflections (before merge)	45181	11075	61961	94211	35428	24864	47157
Data (I>–3.0/sigma(I)) [Reflections, Restraints, Parameters]	13140, 216, 759	4926, 1, 336	8720, 0, 514	9115, 2430, 642	9752, 8, 560	10182, 0, 605	8318, 0, 560
S (=GooF)	0.971	1.000	0.978	0.985	0.972	0.994	1.005
Min. and Max. Residual Dens., [e/$Å^3$]	–0.61	–0.81	–0.87	–0.28	–0.22	–0.34	–0.70
	0.83	0.83	0.48	0.28	0.37	0.26	0.88
Threshold Expression	I>2sigma(I)	I>2sigma(I)	I>2sigma(I)	I>2sigma(I)	I>2sigma(I)	I>2sigma(I)	I>2sigma(I)
R_1	0.0606	0.0344	0.0518	0.0380	0.0392	0.0381	0.0780
wR_2	0.1517	0.0882	0.1457	0.0923	0.0970	0.1000	0.2897

Nr.	5.11c	5.7d-neutron	5.7h-neutron	5.7j-neutron
Formula	$C_{32}H_{52}F_1N_3O_4$	$C_{54}H_{84}F_1N_5O_2$	$C_{42}H_{56}Cl_4F_1N_5O_2$	$C_{42}H_{56}F_5N_5O_2$
Molecular Weight	561.78	854.30	823.74	757.93
Crystal System	monoclinic	monoclinic	monoclinic	monoclinic
T [K]	150	150	150	150
Space Group	C c	P 1 21/c 1	C 2/c	P 21/n
a [Å]	22.2441(16)	13.071(4)	23.787(7)	13.209(4)
b [Å]	8.1479(4)	15.712(5)	14.962(5)	14.686(6)
c [Å]	20.0331(17)	25.244(8)	25.156(8)	21.024(8)
α [°]	90	90	90	90
β [°]	120.67(1)	101.98(2)	107.93(2)	96.11(3)
γ [°]	90	90	90	90
V [$Å^3$]	3123.0(5)	5072(3)	8518(5)	4055(3)
Z	4	4	8	4
D_{calc} [g cm^{-3}]	1.195	1.119	1.285	1.241
F(0 0 0)	1224	435	1377	626
μ [mm^{-1}]	0.659	0.227	0.188	0.190
Crystal Size [mm]	0.12 * 0.16 * 0.20	8.0 * 7.0 * 7.0	8.0 * 6.0 * 4.0	10.0 * 9.0 * 8.0
Colour, Shape	clear_pale_yellow, needle	clear_pale_colourless, block	clear_pale_colourless, block	clear_pale_colourless, block
R_{int}	2.47	-	-	-
θ_{min}, θ_{max} [deg]	4.622 – 75.418	7.99 – 84.88	8.59 – 84.92	8.05 – 83.90
Total Reflections (before merge)	16318	13466	13180	10529
Data (I>–3.0/sigma(I)) [Reflections, Restraints, Parameters]	4519, 2, 363	13466, 317, 1315	13180, 0, 1001	10529, 0, 998
S (=GooF)	1.002	1.056	1.067	1.319
Min. and Max. Residual Dens., [e/$Å^3$]	–0.14	–1.279	–0.884	–1.266
	0.16	0.810	1.100	1.766
Threshold Expression	I>2sigma(I)	I>2sigma(I)	I>2sigma(I)	I>2sigma(I)
R_1	0.0246	0.0764	0.0929	0.1031
wR_2	0.0676	0.1893	0.2381	0.2639

Modulation in 5.7n

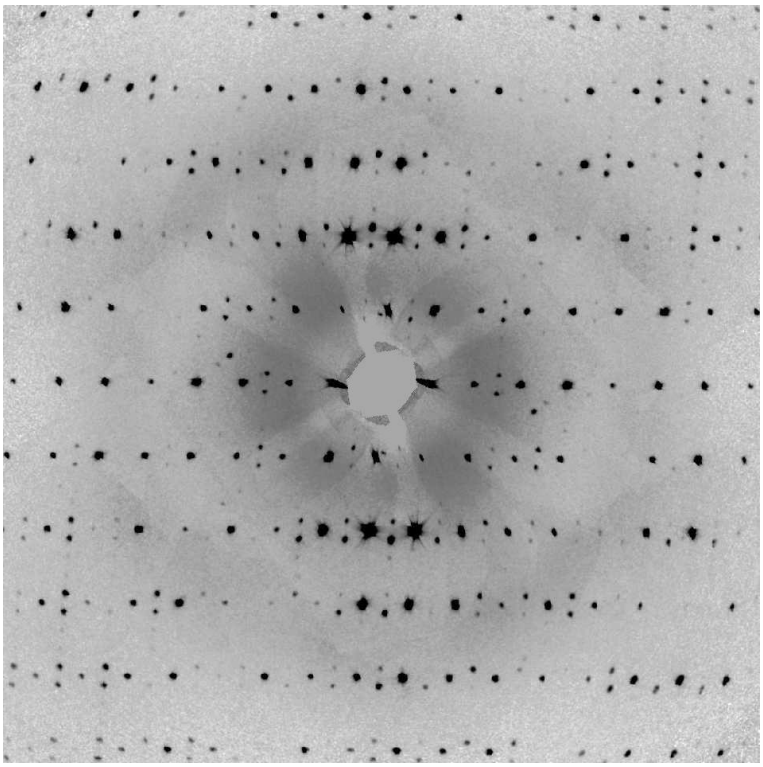

Figure S.5.1. h0l layer showing modulation in **5.7n**.

Single-Crystals for Neutron Diffraction Experiments

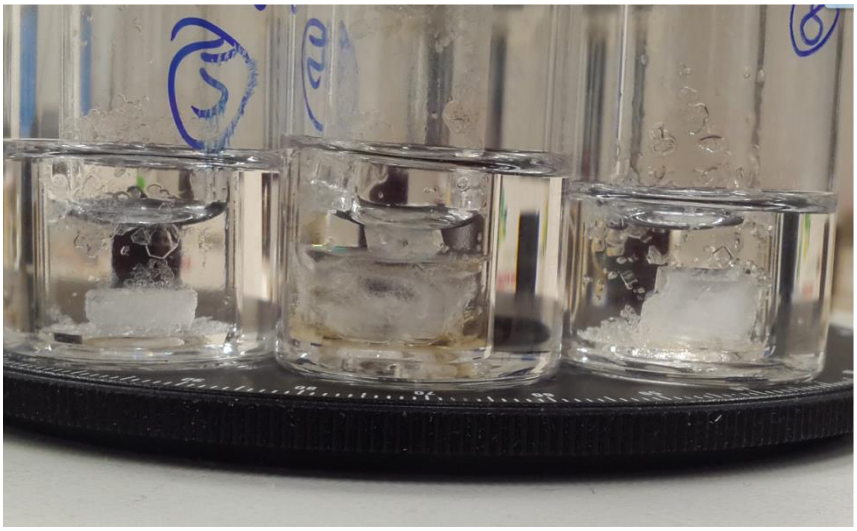

Figure S.5.2. Large crystals of TBAF[1,3-bis(4-chlorophenyl)urea]$_2$ (**5.7h**), TBAF[1,3-bis(4-fluorophenyl)urea]$_2$ (**5.7j**) and TBAF[1,3-bis(4-*n*-propylphenyl)urea]$_2$ (**5.7d**) used for neutron diffraction experiments.

S.5.3. Kinetic Experiments

A 14-mL screw-top vial was charged with **4.10** (53.0 mg, 0.20 mmol), MeCN (0.80 mL), and the hydrogen-bonded tetra-*n*-butylammonium fluoride complex (0.40 mmol). The vial was capped with a rubber septum, then stirred at 70 °C for 48 h (2 h in reaction with **5.9**). At the indicated time points, a small aliquot (<80 µL) was taken with a syringe and needle. Each aliquot was filtered through a short plug of silica gel to quench the reaction, and the silica gel was washed with EtOAc (3 × 2 mL). The combined rinsings were concentrated *in vacuo*, the resulting solid was dissolved in $CDCl_3$, filtered through a pad of cotton wool to remove excess 1,3-diarylurea, and analysed by ^{1}H NMR. The conversion at each time point was determined by integration of the methylene/allylic proton signals depicted in Figure S.5.3, which were then divided by the sum of these integrals. The procedure was repeated three times for each complex, except of for **5.11a** with which only one trial was conducted. The averaged compositions of the reactions after 48 h are summarised in Table S.5.2. Details for individual complexes are shown in Tables S.5.3–S.5.8 and Figures S.5.4–S.5.6. Rate constants, k_2(S_N2) and k'_2(E2), were determined using Berkeley Madonna software.

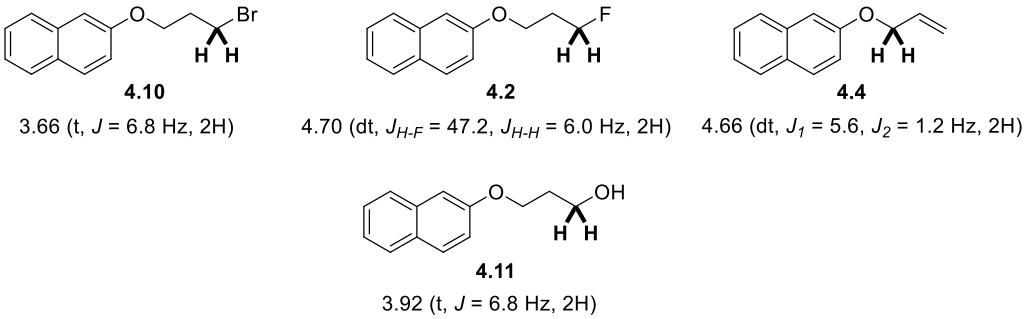

Figure S.5.3. Summary of key peaks for integration. The chemical shifts shown here are based on pure, isolated samples of these compounds. The corresponding alkoxylated products were generally not observed in measurable amounts. In the reaction mixture, the signal for the alcohol product can appear as a broad triplet or broad quartet, depending on the concentration and pH of the solution.

Table S.5.2. Summary of end-point compositions of kinetic experiments under standard conditions.

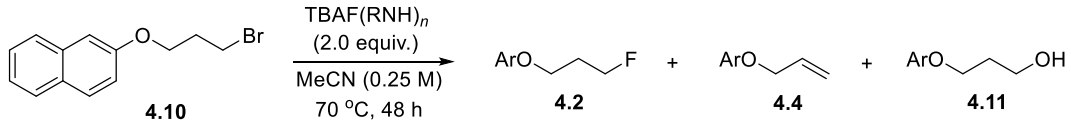

Fluoride Complex	Reaction Composition after 48 h (%, ^{1}H NMR) Fluoride (**4.2**)	Olefin (**4.4**)	Alcohol (**4.11**)	Bromide (**4.10**)
5.7a (3-Me)	75	10	3	11
5.7g (4-OMe)	75	18	7	1
5.7f (4-Me)	79	17	5	0
5.7e (H)	74	11	4	11
5.7j (4-F)	72	10	4	16
5.7h (4-Cl)	75	11	7	7
5.7c (4-NO_2)	78	10	6	6
5.7b (4-CF_3)	51	4	7	39
5.9[a]	49	25	16	10
5.11a	41	9	39	11

[a]Composition after 2 h reaction time.

TBAF(1,3-di-*m*-tolylurea)$_2$ (5.7a)

Table S.5.3. Species distribution over the course of the reaction of TBAF(1,3-di-*m*-tolylurea)$_2$ with alkyl bromide **4.10**.

		Composition (%), Trial 1				*Composition (%), Trial 2*				*Composition (%), Trial 3*			
Entry	t (min)	Fluoride	Olefin	Alcohol	Bromide	Fluoride	Olefin	Alcohol	Bromide	Fluoride	Olefin	Alcohol	Bromide
1	15	6.9	2.2	0.0	90.8	7.7	2.6	0.0	89.7	7.1	2.3	0.0	90.7
2	30	10.0	2.8	0.0	87.2	12.2	2.7	0.0	85.1	11.1	2.9	0.0	86.0
3	60	16.0	3.8	0.0	80.2	18.4	4.4	0.0	77.3	15.8	3.5	0.0	80.7
4	120	24.3	5.0	0.0	70.7	27.1	5.7	0.0	67.2	23.9	5.2	0.0	70.9
5	180	28.7	5.2	1.3	64.8	29.1	5.0	1.6	64.4	28.1	5.3	1.3	65.3
6	240	32.4	5.7	1.5	60.5	33.3	5.7	1.5	59.5	32.1	5.8	1.3	60.8
7	480	42.7	6.7	1.7	49.0	44.9	7.3	1.5	46.2	43.3	7.4	1.5	47.8
8	1440	63.6	9.0	1.9	25.5	65.8	9.4	1.3	23.5	61.8	8.9	2.4	26.9
9	2880	73.4	10.6	2.2	10.6	76.3	10.5	3.0	10.2	75.0	9.9	2.6	12.5

		Concentration (M), Trial 1				*Concentration (M), Trial 2*				*Concentration (M), Trial 3*			
Entry	t (min)	Fluoride	Olefin	Alcohol	Bromide	Fluoride	Olefin	Alcohol	Bromide	Fluoride	Olefin	Alcohol	Bromide
1	15	0.017	0.006	0.000	0.227	0.019	0.006	0.000	0.224	0.018	0.006	0.000	0.227
2	30	0.025	0.007	0.000	0.218	0.030	0.007	0.000	0.213	0.028	0.007	0.000	0.215
3	60	0.040	0.009	0.000	0.201	0.046	0.011	0.000	0.193	0.039	0.009	0.000	0.202
4	120	0.061	0.013	0.000	0.177	0.068	0.014	0.000	0.168	0.060	0.013	0.000	0.177
5	180	0.072	0.013	0.003	0.162	0.073	0.012	0.004	0.161	0.070	0.013	0.003	0.163
6	240	0.081	0.014	0.004	0.151	0.083	0.014	0.004	0.149	0.080	0.014	0.003	0.152
7	480	0.107	0.017	0.004	0.122	0.112	0.018	0.004	0.116	0.108	0.018	0.004	0.119
8	1440	0.159	0.023	0.005	0.064	0.164	0.024	0.003	0.059	0.154	0.022	0.006	0.067
9	2880	0.183	0.026	0.005	0.026	0.191	0.026	0.008	0.025	0.188	0.025	0.006	0.031

Table S.5.4. Summary of kinetic experiments with TBAF(1,3-di-*m*-tolylurea)$_2$.

		Fluoride (%)		Olefin (%)		Alcohol (%)		Bromide (%)	
Entry	t (min)	*Ave.*	*Std. Dev.*	*Ave.*	*Std. Dev.*	*Ave.*	*Std. Dev.*	*Ave.*	*Std. Dev.*
1	15	7.2	0.4	2.4	0.2	0.0	0.0	90.4	0.6
2	30	11.1	1.1	2.8	0.1	0.0	0.0	86.1	1.0
3	60	16.7	1.4	3.9	0.4	0.0	0.0	79.4	1.9
4	120	25.1	1.7	5.3	0.4	0.0	0.0	69.6	2.1
5	180	28.6	0.5	5.2	0.2	1.4	0.2	64.8	0.5
6	240	32.6	0.6	5.7	0.1	1.4	0.1	60.3	0.7
7	480	43.6	1.1	7.1	0.4	1.6	0.1	47.7	1.4
8	1440	63.7	2.0	9.1	0.3	1.9	0.6	25.3	1.7
9	2880	74.9	1.5	10.3	0.4	2.6	0.4	11.1	1.3

		Fluoride (M)		Olefin (M)		Alcohol (M)		Bromide (M)	
Entry	t (min)	*Ave.*	*Std. Dev.*	*Ave.*	*Std. Dev.*	*Ave.*	*Std. Dev.*	*Ave.*	*Std. Dev.*
1	15	0.018	0.001	0.006	0.000	0.000	0.000	0.226	0.002
2	30	0.028	0.003	0.007	0.000	0.000	0.000	0.215	0.003
3	60	0.042	0.004	0.010	0.001	0.000	0.000	0.199	0.005
4	120	0.063	0.004	0.013	0.001	0.000	0.000	0.174	0.005
5	180	0.072	0.001	0.013	0.000	0.003	0.000	0.162	0.001
6	240	0.081	0.002	0.014	0.000	0.003	0.000	0.151	0.002
7	480	0.109	0.003	0.018	0.001	0.004	0.000	0.119	0.003
8	1440	0.159	0.005	0.023	0.001	0.005	0.001	0.063	0.004
9	2880	0.187	0.004	0.026	0.001	0.006	0.001	0.028	0.003

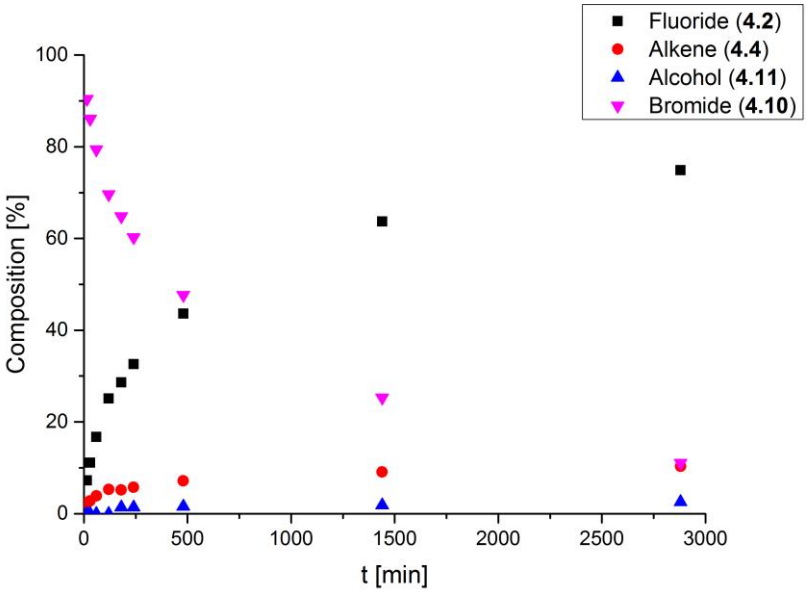

Figure S.5.4. Average species distribution over the course of the reaction of TBAF(1,3-di-*m*-tolylurea)$_2$ with alkyl bromide **4.10**.

TBAF(1,3-bis(4-(trifluoromethylphenyl)urea)$_2$ (5.7b)

Table S.5.5. Species distribution over the course of the reaction of TBAF(1,3-bis(4-(trifluoromethylphenyl)urea)$_2$ with alkyl bromide **4.10**.

		Composition (%), Trial 1				*Composition (%), Trial 2*				*Composition (%), Trial 3*			
Entry	t (min)	Fluoride	Olefin	Alcohol	Bromide	Fluoride	Olefin	Alcohol	Bromide	Fluoride	Olefin	Alcohol	Bromide
1	15	2.2	1.1	0.0	96.7	2.2	1.3	0.0	96.5	1.8	1.1	0.0	97.1
2	30	3.4	1.5	0.0	95.0	4.3	2.0	0.0	93.7	3.2	1.1	0.0	95.6
3	60	6.3	1.6	0.0	92.2	8.6	2.0	0.0	89.4	5.6	1.4	0.0	93.0
4	120	7.8	1.6	0.0	90.5	9.5	1.8	0.0	88.6	8.6	2.0	0.0	89.4
5	180	9.5	1.3	1.8	87.4	11.4	1.6	1.4	85.6	9.6	1.3	1.0	88.0
6	240	11.2	1.6	2.6	84.5	13.9	1.7	1.6	82.8	12.2	1.4	1.3	85.1
7	480	20.4	2.1	1.9	75.5	21.2	2.1	1.4	75.3	19.1	1.7	1.3	77.9
8	1440	37.3	3.3	3.7	55.7	39.1	3.6	3.6	53.8	39.5	3.3	4.1	53.1
9	2880	50.0	3.7	6.7	39.6	52.2	4.2	7.3	36.2	49.6	3.4	7.1	39.8

		Concentration (M), Trial 1				*Concentration (M), Trial 2*				*Concentration (M), Trial 3*			
Entry	t (min)	Fluoride	Olefin	Alcohol	Bromide	Fluoride	Olefin	Alcohol	Bromide	Fluoride	Olefin	Alcohol	Bromide
1	15	0.005	0.0027	0.000	0.242	0.005	0.0033	0.000	0.241	0.004	0.0028	0.000	0.243
2	30	0.009	0.0038	0.000	0.238	0.011	0.0049	0.000	0.234	0.008	0.0028	0.000	0.239
3	60	0.016	0.0039	0.000	0.230	0.022	0.0051	0.000	0.223	0.014	0.0035	0.000	0.233
4	120	0.020	0.0041	0.000	0.226	0.024	0.0046	0.000	0.222	0.021	0.0050	0.000	0.224
5	180	0.024	0.0032	0.005	0.219	0.028	0.0041	0.003	0.214	0.024	0.0033	0.003	0.220
6	240	0.028	0.0041	0.007	0.211	0.035	0.0042	0.004	0.207	0.030	0.0036	0.003	0.213
7	480	0.051	0.0054	0.005	0.189	0.053	0.0053	0.003	0.188	0.048	0.0042	0.003	0.195
8	1440	0.093	0.0083	0.009	0.139	0.098	0.0089	0.009	0.135	0.099	0.0083	0.010	0.133
9	2880	0.125	0.0093	0.017	0.099	0.131	0.0105	0.018	0.091	0.124	0.0086	0.018	0.100

Table S.5.6. Summary of kinetic experiments with TBAF(1,3-bis(4-(trifluoromethylphenyl)urea)$_2$.

		Fluoride (%)		Olefin (%)		Alcohol (%)		Bromide (%)	
Entry	t (min)	*Ave.*	*Std. Dev.*	*Ave.*	*Std. Dev.*	*Ave.*	*Std. Dev.*	*Ave.*	*Std. Dev.*
1	15	2.1	0.2	1.2	0.1	0.0	0.0	96.8	0.3
2	30	3.7	0.6	1.5	0.4	0.0	0.0	94.8	1.0
3	60	6.8	1.6	1.7	0.3	0.0	0.0	91.5	1.9
4	120	8.6	0.9	1.8	0.2	0.0	0.0	89.5	1.0
5	180	10.2	1.1	1.4	0.2	1.4	0.4	87.0	1.2
6	240	12.4	1.4	1.6	0.1	1.9	0.7	84.1	1.2
7	480	20.3	1.1	2.0	0.2	1.5	0.3	76.2	1.4
8	1440	38.6	1.2	3.4	0.1	3.8	0.3	54.2	1.3
9	2880	50.6	1.4	3.8	0.4	7.1	0.3	38.5	2.0

		Fluoride (M)		Olefin (M)		Alcohol (M)		Bromide (M)	
Entry	t (min)	*Ave.*	*Std. Dev.*	*Ave.*	*Std. Dev.*	*Ave.*	*Std. Dev.*	*Ave.*	*Std. Dev.*
1	15	0.005	0.001	0.003	0.000	0.000	0.000	0.242	0.001
2	30	0.009	0.001	0.004	0.001	0.000	0.000	0.237	0.003
3	60	0.017	0.004	0.004	0.001	0.000	0.000	0.229	0.005
4	120	0.022	0.002	0.005	0.000	0.000	0.000	0.224	0.002
5	180	0.025	0.003	0.004	0.000	0.004	0.001	0.218	0.003
6	240	0.031	0.003	0.004	0.000	0.005	0.002	0.210	0.003
7	480	0.051	0.003	0.005	0.001	0.004	0.001	0.191	0.004
8	1440	0.096	0.003	0.008	0.000	0.009	0.001	0.136	0.003
9	2880	0.127	0.004	0.009	0.001	0.018	0.001	0.096	0.005

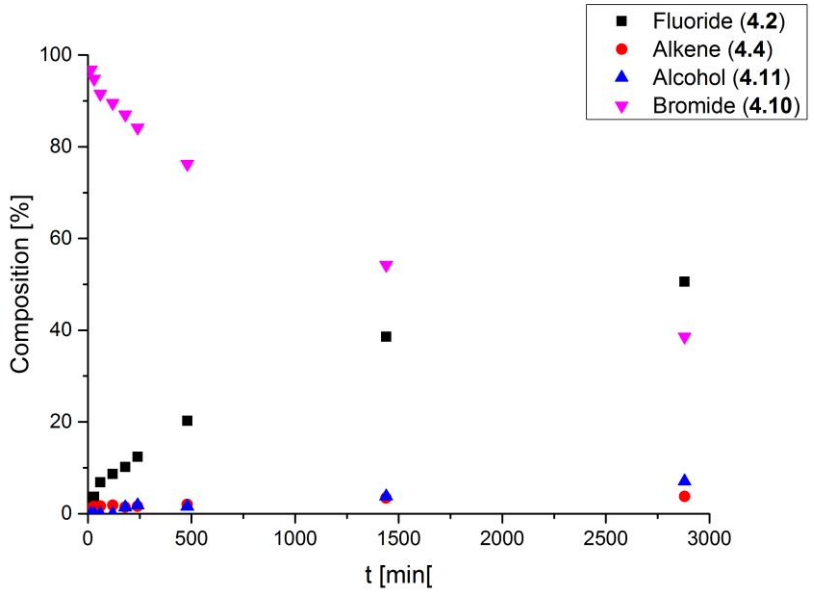

Figure S.5.5. Average species distribution over the course of the reaction of TBAF(1,3-bis(4-(trifluoromethylphenyl)urea)$_2$ with alkyl bromide **4.10**.

TBAF(*N*,2,2-triphenylacetamide)$_2$ (5.9)

Table S.5.7. Species distribution over the course of the reaction of TBAF(*N*,2,2-triphenylacetamide)$_2$ with alkyl bromide **4.10**.

		Composition (%), Trial 1				*Composition (%), Trial 2*				*Composition (%), Trial 3*			
Entry	t (min)	Fluoride	Olefin	Alcohol	Bromide	Fluoride	Olefin	Alcohol	Bromide	Fluoride	Olefin	Alcohol	Bromide
1	0.5	0.0	0.0	0.0	100.0	0.0	0.0	0.0	100.0	0.0	0.0	0.0	100.0
2	1	7.2	3.7	6.4	82.7	7.2	3.9	6.0	83.0	7.1	3.5	6.2	83.2
3	1.5	10.0	5.4	7.9	76.7	9.8	5.6	8.2	76.3	9.7	5.3	8.9	76.0
4	2	11.8	7.2	9.6	71.4	12.0	7.5	10.2	70.3	11.2	7.1	10.1	71.6
5	2.5	13.6	8.0	12.0	66.4	13.7	8.4	11.9	66.0	13.4	8.1	11.9	66.6
6	5	18.9	11.4	12.8	56.9	19.2	11.8	13.4	55.5	18.9	11.5	13.7	55.9
7	10	24.9	14.5	13.9	46.7	25.4	15.4	14.5	44.8	25.1	14.7	14.5	45.7
8	30	36.3	20.2	13.6	30.0	36.5	20.7	14.9	27.8	36.0	19.6	15.5	28.8
9	60	43.5	22.4	15.3	18.8	43.6	22.9	15.7	17.9	42.6	22.5	16.1	18.8
10	120	48.9	24.3	15.7	11.1	48.8	24.6	16.4	10.1	49.4	25.8	14.9	9.9

		Concentration (M), Trial 1				*Concentration (M), Trial 2*				*Concentration (M), Trial 3*			
Entry	t (min)	Fluoride	Olefin	Alcohol	Bromide	Fluoride	Olefin	Alcohol	Bromide	Fluoride	Olefin	Alcohol	Bromide
1	0.5	0.000	0.000	0.000	0.250	0.000	0.000	0.000	0.250	0.000	0.000	0.000	0.250
2	1	0.018	0.009	0.016	0.207	0.018	0.010	0.015	0.207	0.018	0.009	0.016	0.208
3	1.5	0.025	0.013	0.020	0.192	0.025	0.014	0.021	0.191	0.024	0.013	0.022	0.190
4	2	0.029	0.018	0.024	0.178	0.030	0.019	0.026	0.176	0.028	0.018	0.025	0.179
5	2.5	0.034	0.020	0.030	0.166	0.034	0.021	0.030	0.165	0.034	0.020	0.030	0.167
6	5	0.047	0.028	0.032	0.142	0.048	0.030	0.033	0.139	0.047	0.029	0.034	0.140
7	10	0.062	0.036	0.035	0.117	0.063	0.038	0.036	0.112	0.063	0.037	0.036	0.114
8	30	0.091	0.050	0.034	0.075	0.091	0.052	0.037	0.070	0.090	0.049	0.039	0.072
9	60	0.109	0.056	0.038	0.047	0.109	0.057	0.039	0.045	0.106	0.056	0.040	0.047
10	120	0.122	0.061	0.039	0.028	0.122	0.062	0.041	0.025	0.123	0.064	0.037	0.025

Table S.5.8. Summary of kinetic experiments with TBAF(*N*,2,2-triphenylacetamide)$_2$.

		Fluoride (%)		Olefin (%)		Alcohol (%)		Bromide (%)	
Entry	t (min)	*Ave.*	*Std. Dev.*	*Ave.*	*Std. Dev.*	*Ave.*	*Std. Dev.*	*Ave.*	*Std. Dev.*
1	0.5	0.0	0.0	0.0	0.0	0.0	0.0	100.0	0.0
2	1	7.2	0.1	3.7	0.2	6.2	0.2	82.9	0.2
3	1.5	9.8	0.1	5.5	0.2	8.3	0.5	76.4	0.3
4	2	11.7	0.4	7.3	0.2	10.0	0.3	71.1	0.7
5	2.5	13.6	0.1	8.2	0.2	11.9	0.1	66.3	0.3
6	5	19.0	0.2	11.6	0.2	13.3	0.5	56.1	0.7
7	10	25.1	0.2	14.8	0.5	14.3	0.4	45.7	1.0
8	30	36.3	0.3	20.2	0.6	14.7	1.0	28.9	1.1
9	60	43.2	0.6	22.6	0.2	15.7	0.4	18.5	0.5
10	120	49.0	0.3	24.9	0.8	15.7	0.7	10.4	0.6

		Fluoride (M)		Olefin (M)		Alcohol (M)		Bromide (M)	
Entry	t (min)	*Ave.*	*Std. Dev.*	*Ave.*	*Std. Dev.*	*Ave.*	*Std. Dev.*	*Ave.*	*Std. Dev.*
1	0.5	0.000	0.000	0.000	0.000	0.000	0.000	0.250	0.000
2	1	0.018	0.000	0.009	0.000	0.015	0.000	0.207	0.001
3	1.5	0.025	0.000	0.014	0.000	0.021	0.001	0.191	0.001
4	2	0.029	0.001	0.018	0.000	0.025	0.001	0.178	0.002
5	2.5	0.034	0.000	0.020	0.001	0.030	0.000	0.166	0.001
6	5	0.048	0.000	0.029	0.001	0.033	0.001	0.140	0.002
7	10	0.063	0.001	0.037	0.001	0.036	0.001	0.114	0.003
8	30	0.091	0.001	0.050	0.001	0.037	0.003	0.072	0.003
9	60	0.108	0.001	0.057	0.001	0.039	0.001	0.046	0.001
10	120	0.123	0.001	0.062	0.002	0.039	0.002	0.026	0.002

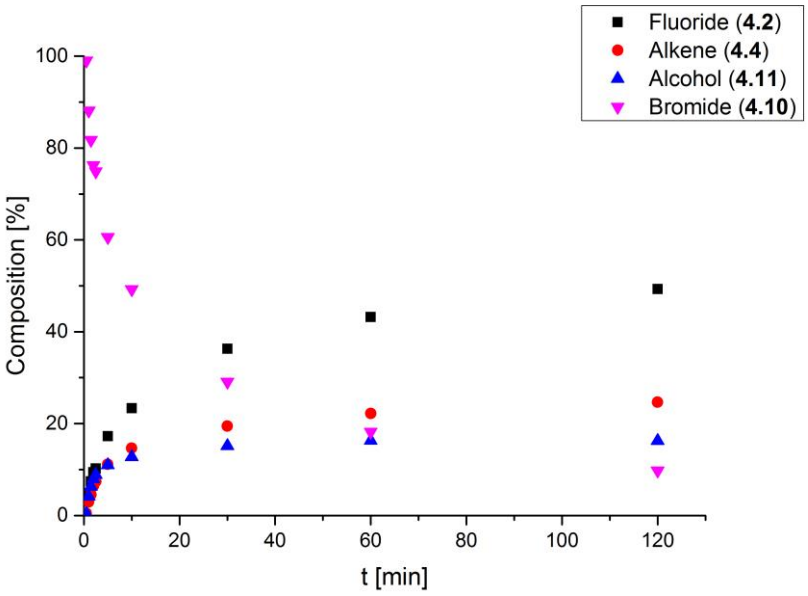

Figure S.5.6. Average species distribution over the course of the reaction of TBAF(*N*,2,2-triphenylacetamide)$_2$ with alkyl bromide **4.10**.

S.5.4. Catalytic Fluorination

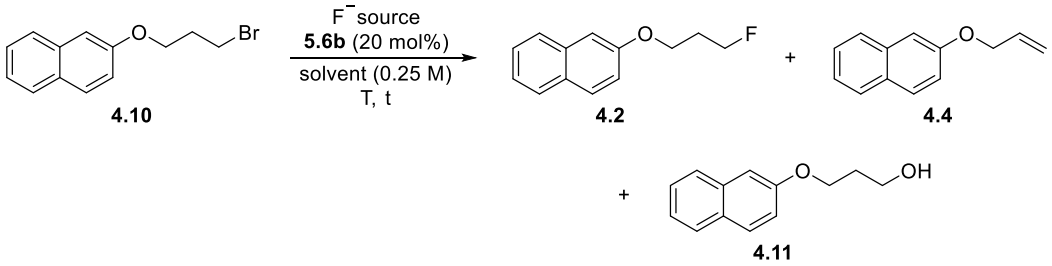

Scheme S.5.6. S_N2 displacement of a primary alkyl bromide (**4.10**) catalysed by 1,3-bis(4-(trifluoromethyl)phenyl)urea (**5.6b**).

A 14-mL screw-top vial was charged with **4.10** (26.5 mg, 0.10 mmol) and the according fluoride source (0.20 mmol; CsF: 30.4 mg, RbF: 20.9 mg, AgF: 25.4 mg) as specified in Table 5.8. **5.6b** (7.0 mg, 0.020 mmol) and solvent (1.0 mL) were added as appropriate (Table 5.8). According to Table 5.8 the mixture was then heated to 40 °C or 70 °C for 23–48 h, after which it was cooled to rt and filtered through a short plug of silica gel, washing the silica gel with EtOAc. The combined rinsings were concentrated *in vacuo*, the remaining crude product was dissolved in $CDCl_3$ and 1-fluoro-3-nitrobenzene (10.6 µL, 0.10 mmol) was added as NMR reference. The mixture was then analysed by ^{1}H and quantitative ^{19}F NMR.

S.5.5. Binding Studies

S.5.5.1. UV-vis Titrations

A stock solution of 1,3-diarylurea (8.0 µM) in MeCN (spectrophotometric grade) was prepared. A TBAF$(H_2O)_3$ solution (2.0 mM) was prepared by weighing out commercial TBAF$(H_2O)_3$ in a vial flushed with Ar and dissolving it in the previously prepared solution

of according 1,3-diarylurea. The exact concentration of fluoride was determined following a published procedure.[389] 2.5 mL of the stock solution of 1,3-diarylurea were subsequently used as sample and a UV-vis spectrum was recorded before 55.2 equiv. of the TBAF$(H_2O)_3$ solution were added in aliquots. After every addition a UV-vis absorption spectrum was recorded. The absorption change at a chosen wavelength was plotted, and the according binding model was fitted using DynaFit 4.[390] Example input files for the determination of association constants for the formation of 1:1 complexes, $K_{a,1:1}$, and in the cases of **5.6b**, **5.6h** and **5.6j**, equilibrium constants for subsequent deprotonation, K_{depr}, are shown below.

Only 1:1 Complex

```
[task]
    task = fit
    data = equilibria
    mechanism = monomer ?
[mechanism]
    SQRAM + F <==> SQRAMF     :     K1     equil
[constants]
    K1 = 1 ?
[responses]
    SQRAM = 0.009625
    SQRAMF = 0.028059 ?
[concentrations]
```

```
        SQRAM = 8
[output]
        directory ./LP-1355/output
[data]
        variable F
        file ./LP-1355/LP-1355-run-3-analysis-ref-TBAF-titr-corrected-eq.txt
        extension txt
[end]
```

1:1 Complex and Deprotonation

Using truncated datasets including only the first 13 (**5.6b**, **5.6h**) or 21 (**5.6j**) data points, an approximate value for $K_{a,1:1}$ (K1 in input file) was calculated using the following input file.

```
[task]
        task = fit
        data = equilibria
        mechanism = monomer ?
[mechanism]
        SQRAM + F <==> SQRAMF      :        K1       equil
[constants]
        K1 = 1 ?
[responses]
        SQRAM = 0.011525
```

```
        SQRAMF = 0.047225 ?
[concentrations]
        SQRAM = 8
[output]
        directory ./LP-1361/output
[data]
        variable F
        file ./LP-1361/LP-1361-run-1-analysis-ref-TBAF-titr-corrected-abs-truncated-3.txt
        extension txt
[end]
```

This value was then used to determine K_{depr} (K2 in input file) using the whole dataset.

```
[task]
        task = fit
        data = equilibria
        mechanism = three species ?
[mechanism]
        SQRAM + F <==> SQRAMF      :          K1       equil
        SQRAMF + F <==> SQRAManion + HF2          : K2      equil
[constants]
        K1 = 0.0930085
        K2 = 1 ?
[responses]
```

SQRAM = 0.011525

SQRAMF = 0.0516889

SQRAManion = 0.047225 ?

[concentrations]

SQRAM = 8

[output]

directory ./LP-1361/output

[data]

variable F

file ./LP-1361/LP-1361-run-1-analysis-ref-TBAF-titr-corrected-abs.txt

extension txt

[end]

Finally, K_{depr} was kept constant to refine $K_{a,1:1}$ using the whole dataset.

[task]

task = fit

data = equilibria

mechanism = three species ?

[mechanism]

SQRAM + F <==> SQRAMF : K1 equil

SQRAMF + F <==> SQRAManion + HF2 : K2 equil

[constants]

K1 = 0.0930085 ?

K2 = 0.0278868

[responses]

SQRAM = 0.011525

SQRAMF = 0.0516889 ?

SQRAManion = 0.0450089

[concentrations]

SQRAM = 8

[output]

directory ./LP-1361/output

[data]

variable F

file ./LP-1361/LP-1361-run-1-analysis-ref-TBAF-titr-corrected-abs.txt

extension txt

[end]

Stacked spectra, plots of absorption changes at certain wavelengths used for fitting the binding model as well as fitted models and residual errors for individual 1,3-diarylureas are shown in Figures S.5.7–S.5.9 and S.5.11–S.5.25

Gaussian deconvolutions of absorption peaks during titrations of **5.6e** and **5.6b** are shown in Figures S.5.10 and S.5.26–S.5.27 respectively.

1,3-Diphenylurea (5.6e)

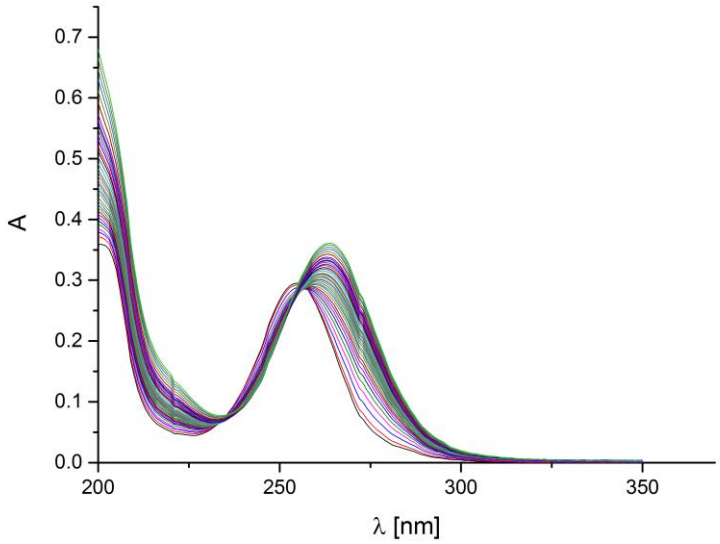

Figure S.5.7. Series of UV-vis spectra recorded over the course of a titration of an 8.0 µM solution of 1,3-diphenylurea in MeCN with 1.58 mM TBAF$(H_2O)_3$ solution.

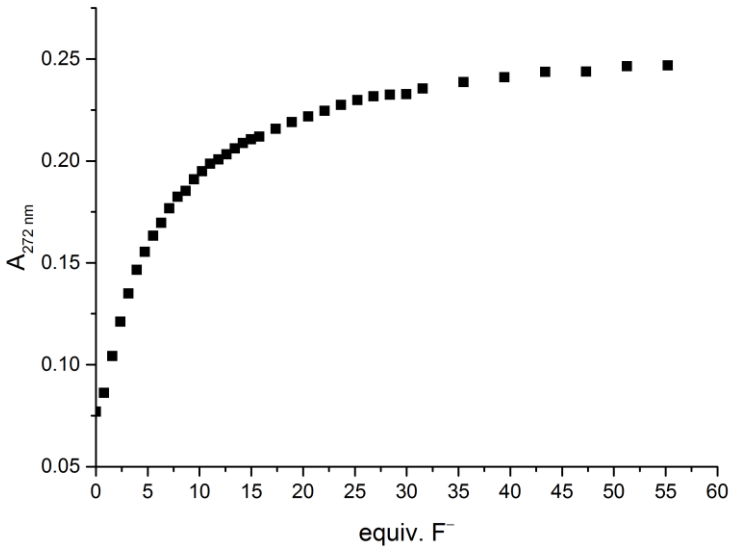

Figure S.5.8. Profile of a UV-vis titration of an 8.0 µM solution of 1,3-diphenylurea in MeCN with 1.58 mM TBAF$(H_2O)_3$ solution at 272 nm.

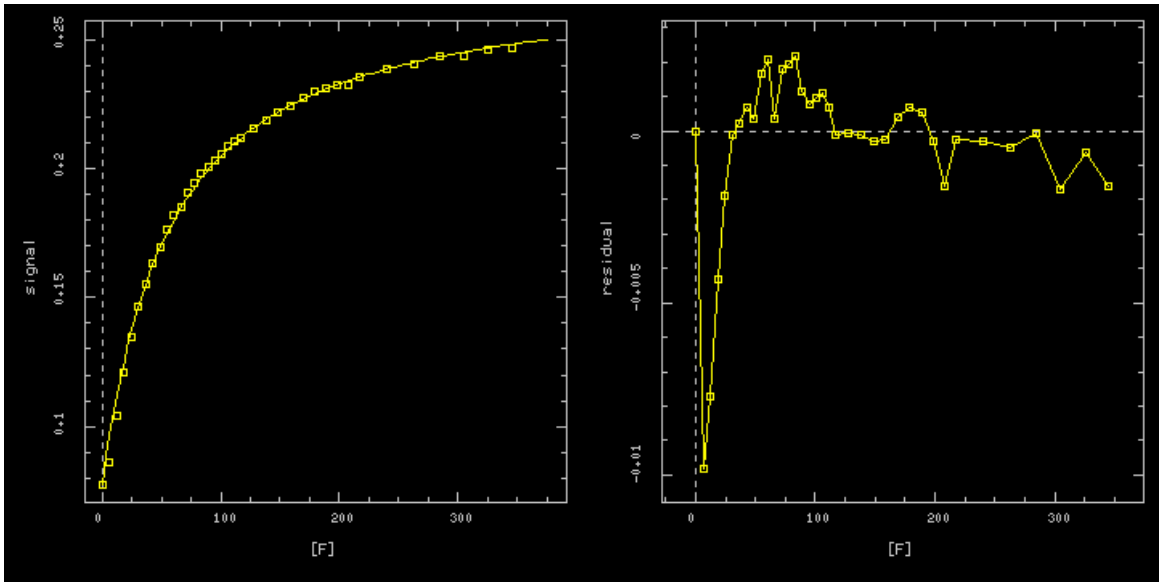

Figure S.5.9. Left: Model for formation of 1:1 complex (line) fitted to measured absorptions at 272 nm (squares) obtained over the course of a titration of a solution of 1,3-diphenylurea (8.0 µM) with $TBAF(H_2O)_3$ (1.58 mM). Right: Residual errors.

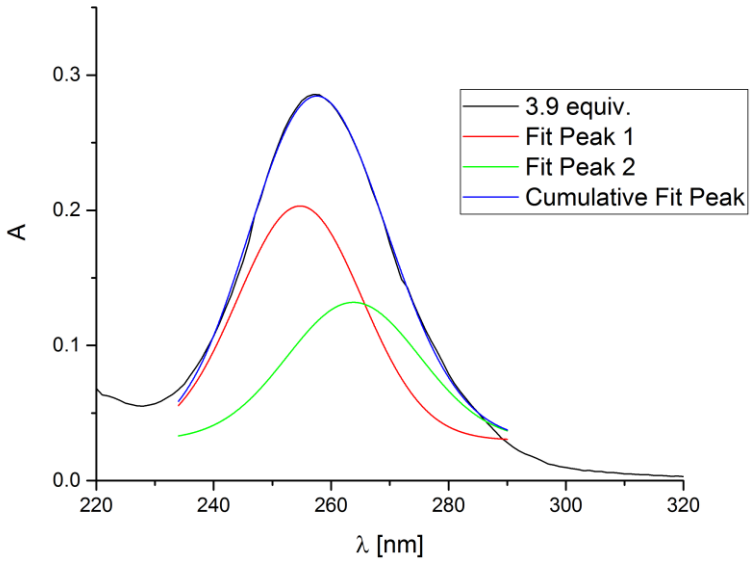

Figure S.5.10. Gaussian deconvolution of absorption peak after addition of 3.9 equiv. $TBAF(H_2O)_3$ (1.58 mM) to 1,3-diphenylurea in MeCN (8.0 µM).

1,3-Bis(4-methylphenyl)urea (5.6f)

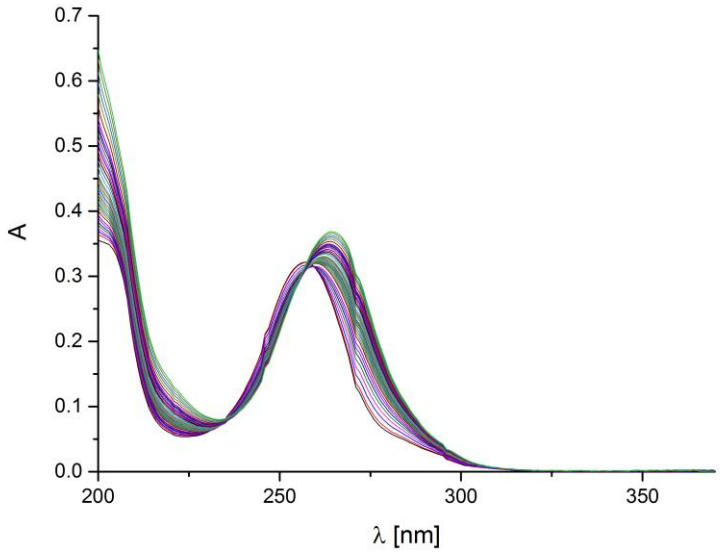

Figure S.5.11. Series of UV-vis spectra recorded over the course of a titration of an 8.0 µM solution of 1,3-bis(4-methylphenyl)urea in MeCN with 1.58 mM TBAF$(H_2O)_3$ solution.

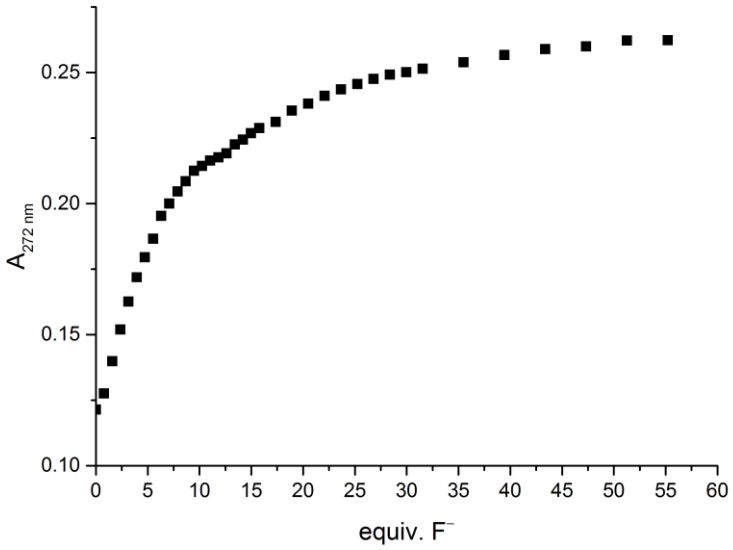

Figure S.5.12. Profile of a UV-vis titration of an 8.0 µM solution of 1,3-bis(4-methylphenyl)urea in MeCN with 1.58 mM TBAF$(H_2O)_3$ solution at 272 nm.

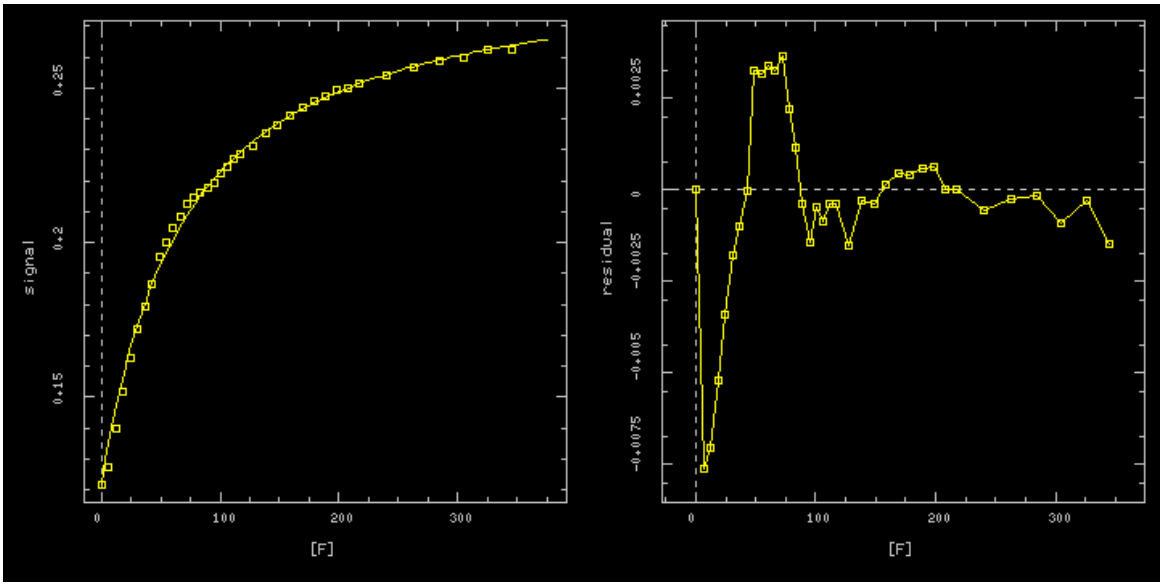

Figure S.5.13. Left: Model for formation of 1:1 complex (line) fitted to measured absorptions at 272 nm (squares) obtained over the course of a titration of a solution of 1,3-bis(4-methylphenyl)urea (8.0 µM) with TBAF$(H_2O)_3$ (1.58 mM). Right: Residual errors.

1,3-Bis(4-methoxyphenyl)urea (5.6g)

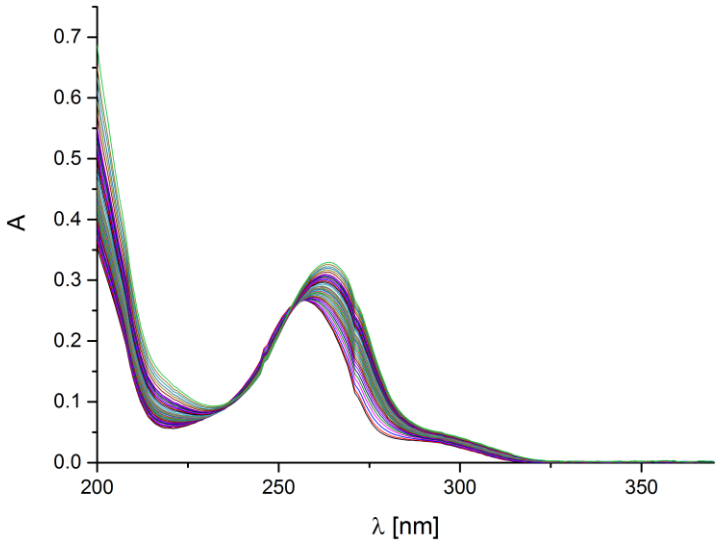

Figure S.5.14. Series of UV-vis spectra recorded over the course of a titration of an 8.0 µM solution of 1,3-bis(4-methoxyphenyl)urea in MeCN with 1.58 mM TBAF$(H_2O)_3$ solution.

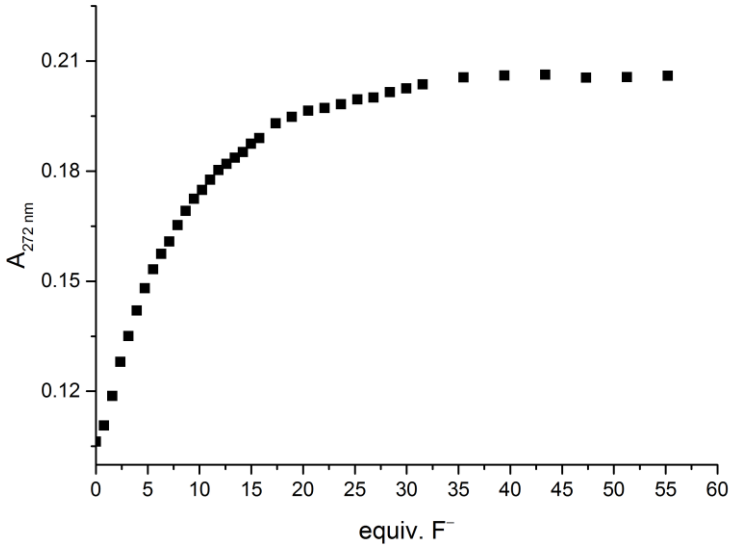

Figure S.5.15. Profile of a UV-vis titration of an 8.0 µM solution of 1,3-bis(4-methoxyphenyl)urea in MeCN with 1.58 mM TBAF$(H_2O)_3$ solution at 272 nm.

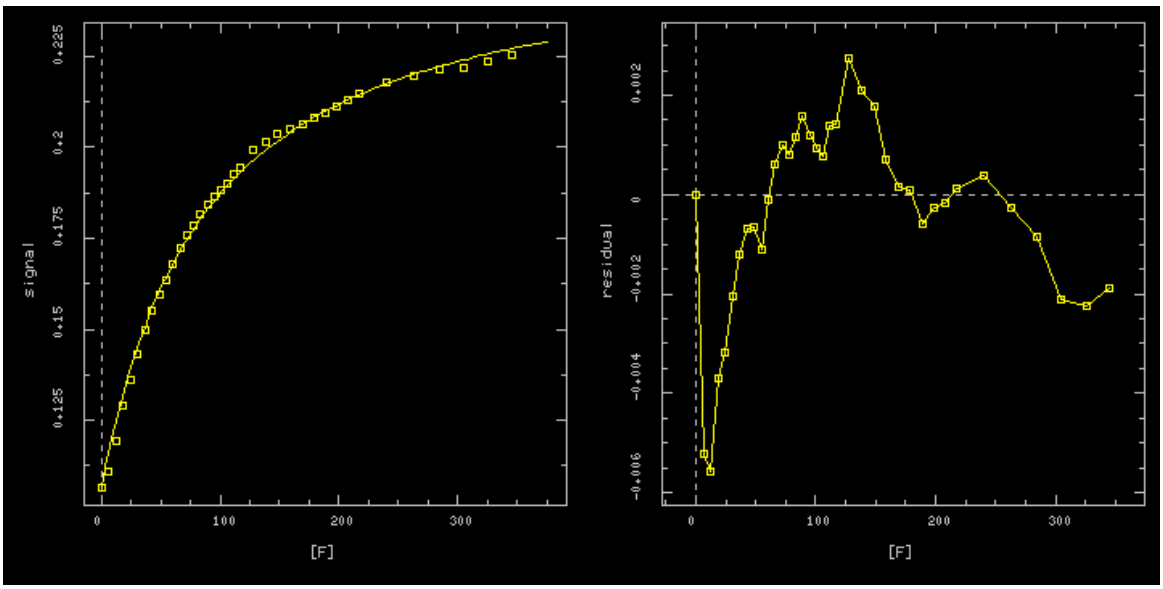

Figure S.5.16. Left: Model for formation of 1:1 complex (line) fitted to measured absorptions at 272 nm (squares) obtained over the course of a titration of a solution of 1,3-bis(4-methoxyphenyl)urea (8.0 µM) with TBAF$(H_2O)_3$ (1.58 mM). Right: Residual errors.

1,3-Bis(4-fluorophenyl)urea (5.6j)

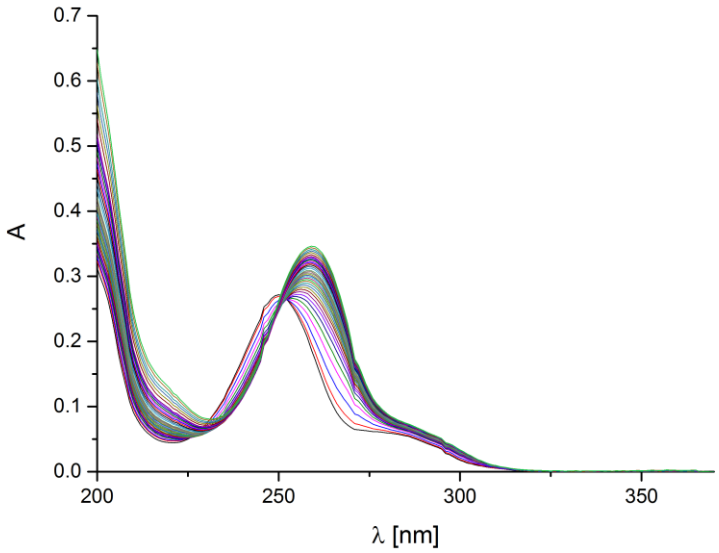

Figure S.5.17. Series of UV-vis spectra recorded over the course of a titration of an 8.0 µM solution of 1,3-bis(4-fluorophenyl)urea in MeCN with 1.58 mM TBAF$(H_2O)_3$ solution.

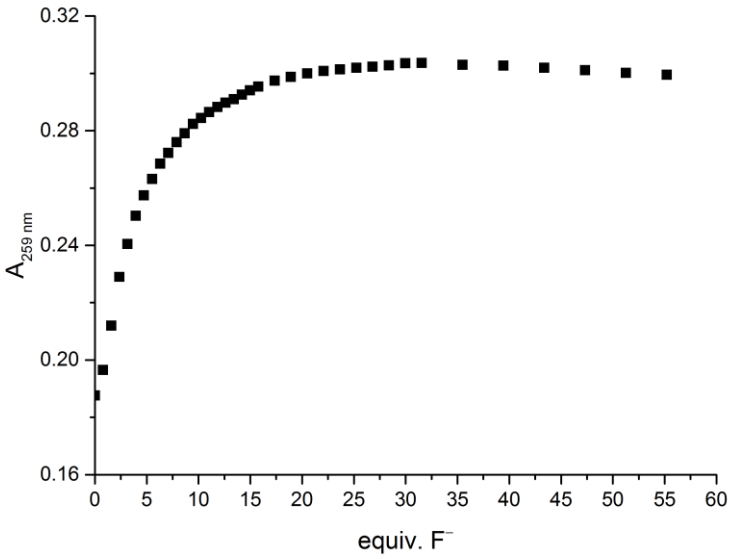

Figure S.5.18. Profile of a UV-vis titration of an 8.0 µM solution of 1,3-bis(4-fluorophenyl)urea in MeCN with 1.58 mM TBAF$(H_2O)_3$ solution at 259 nm.

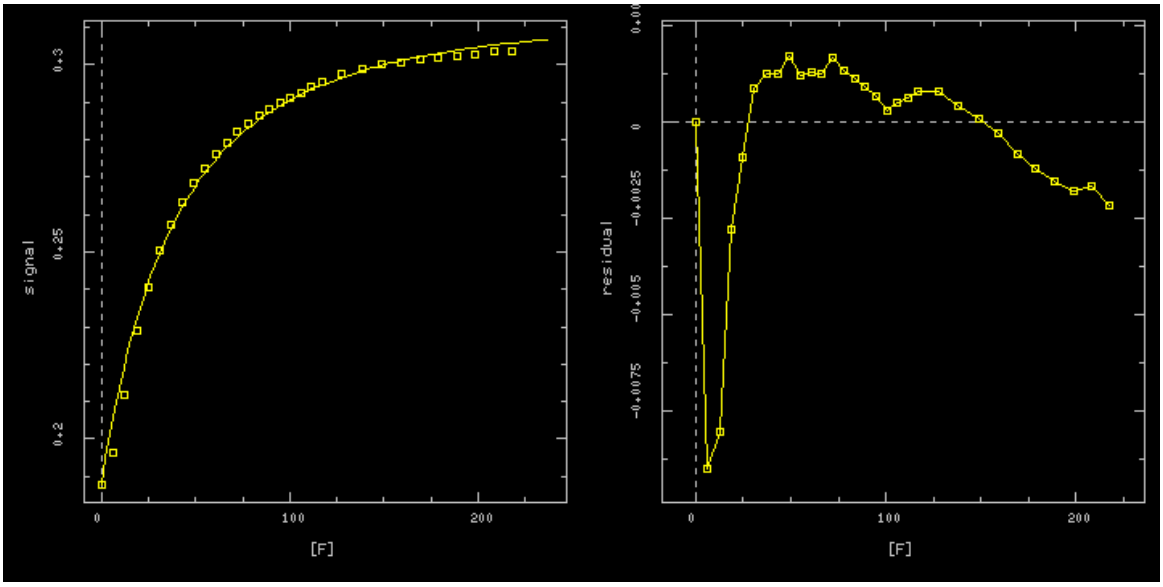

Figure S.5.19. Left: Model for formation of 1:1 complex (line) fitted to measured absorptions at 259 nm (squares) obtained over the course of a titration of a solution of 1,3-bis(4-fluorophenyl)urea (8.0 µM) with TBAF$(H_2O)_3$ (1.58 mM). Right: Residual errors.

1,3-Bis(4-chlorophenyl)urea (5.6h)

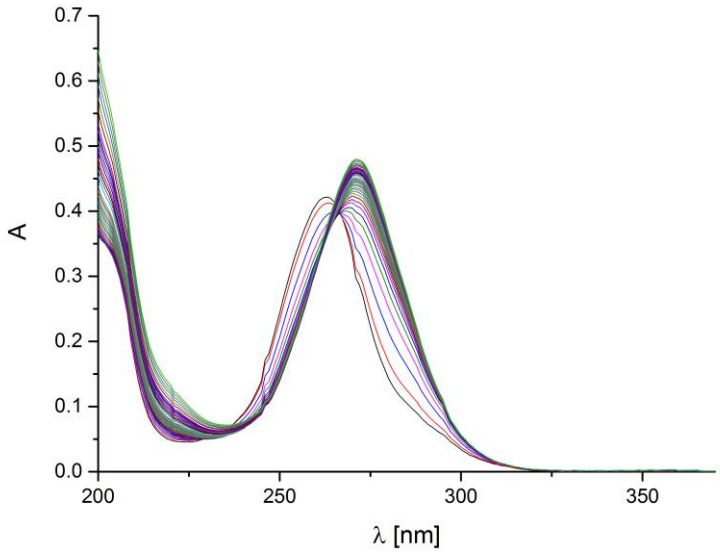

Figure S.5.20. Series of UV-vis spectra recorded over the course of a titration of an 8.0 µM solution of 1,3-bis(4-chlorophenyl)urea in MeCN with 1.58 mM TBAF$(H_2O)_3$ solution.

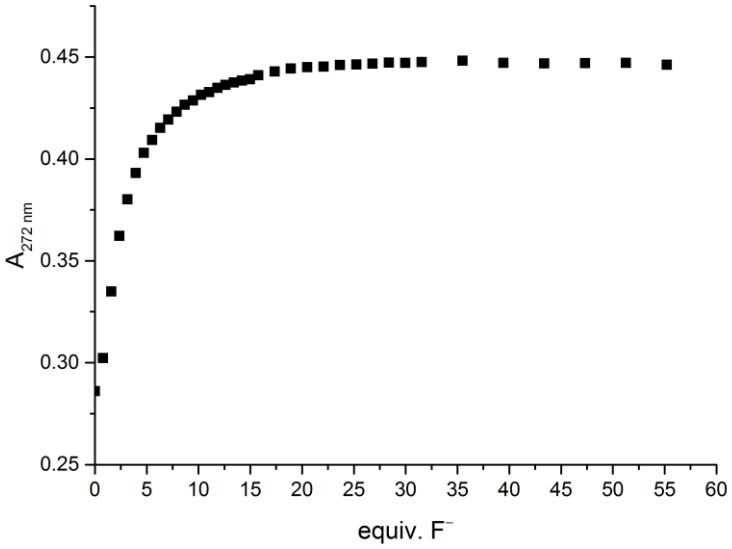

Figure S.5.21. Profile of a UV-vis titration of an 8.0 µM solution of 1,3-bis(4-chlorophenyl)urea in MeCN with 1.58 mM TBAF$(H_2O)_3$ solution at 272 nm.

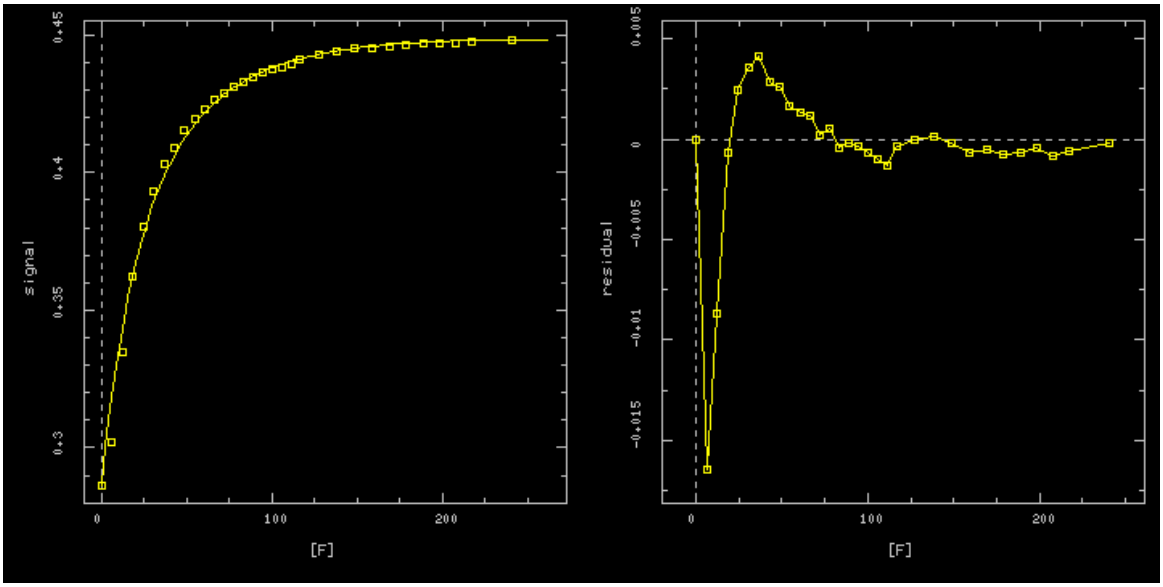

Figure S.5.22. Left: Model for formation of 1:1 complex (line) fitted to measured absorptions at 272 nm (squares) obtained over the course of a titration of a solution of 1,3-bis(4-chlorophenyl)urea (8.0 µM) with TBAF$(H_2O)_3$ (1.58 mM). Right: Residual errors.

1,3-Bis((4-trifluoromethyl)phenyl)urea (5.6b)

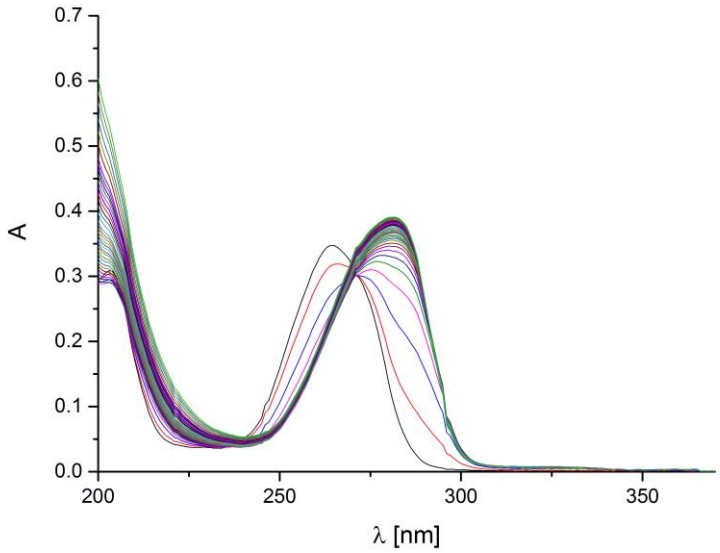

Figure S.5.23. Series of UV-vis spectra recorded over the course of a titration of an 8.0 µM solution of 1,3-bis((4-trifluoromethyl)phenyl)urea in MeCN with 1.58 mM $TBAF(H_2O)_3$ solution.

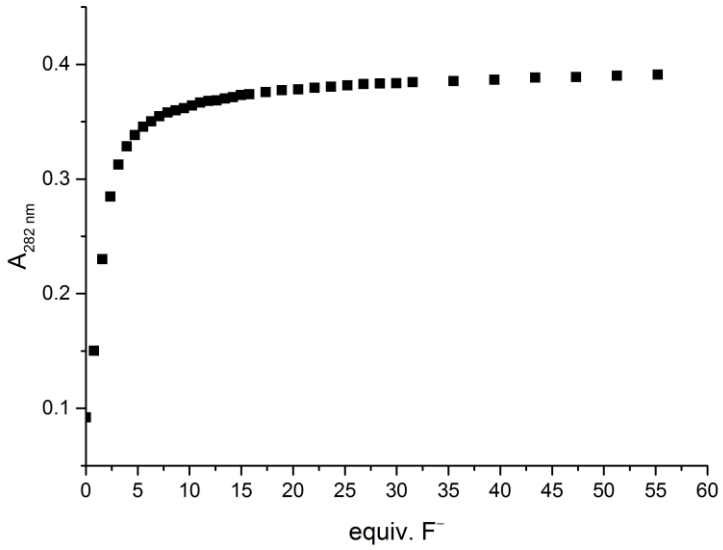

Figure S.5.24. Profile of a UV-vis titration of an 8.0 µM solution of 1,3-bis((4-trifluoromethyl)phenyl)urea in MeCN with 1.58 mM $TBAF(H_2O)_3$ solution at 282 nm.

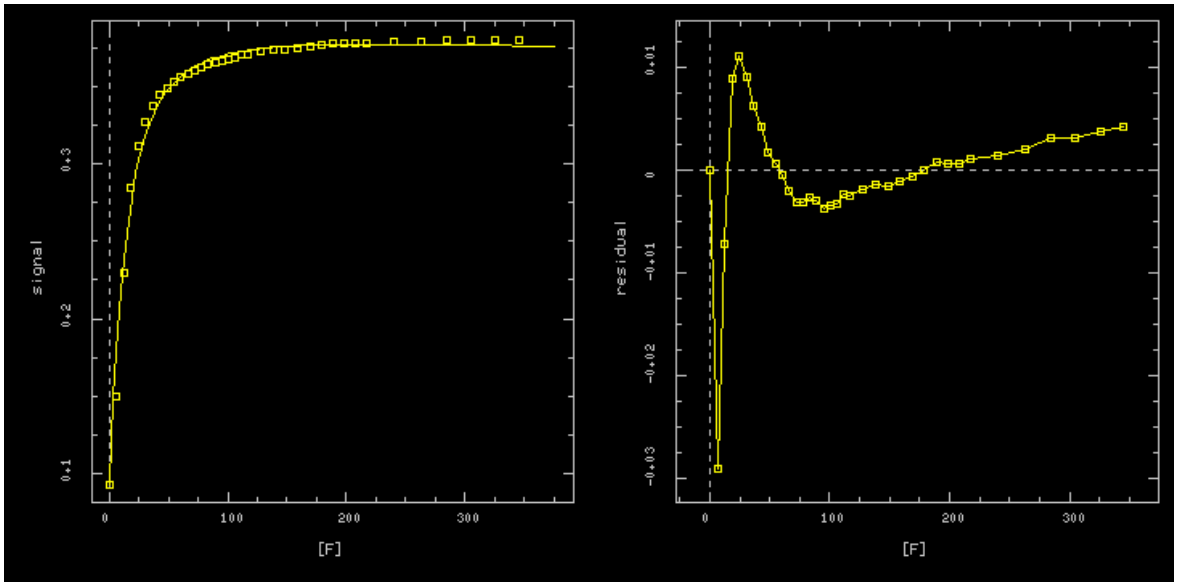

Figure S.5.25. Left: Model for formation of 1:1 complex (line) fitted to measured absorptions at 282 nm (squares) obtained over the course of a titration of a solution of 1,3-bis((4-trifluoromethyl)phenyl)urea (8.0 µM) with TBAF$(H_2O)_3$ (1.58 mM). Right: Residual errors.

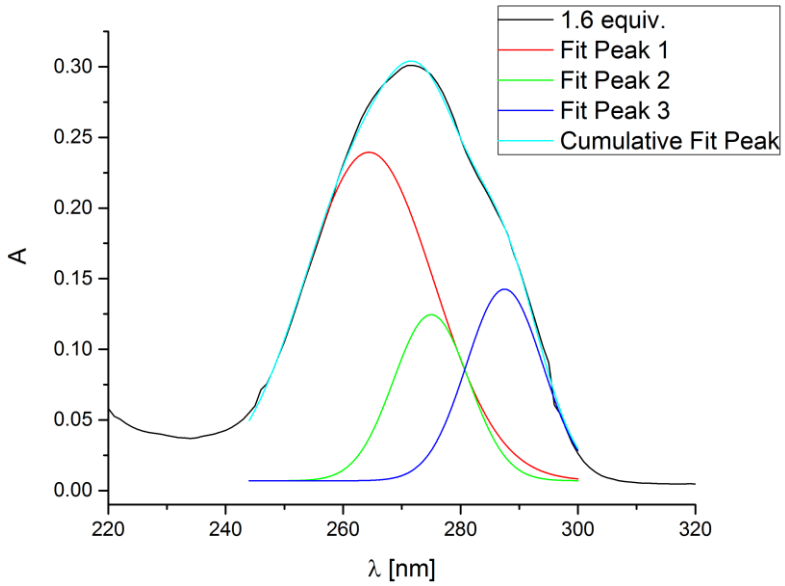

Figure S.5.26. Gaussian deconvolution of absorption peak after addition of 1.6 equiv. TBAF$(H_2O)_3$ (1.58 mM) to 1,3-bis((4-trifluoromethyl)phenyl)urea in MeCN (8.0 µM).

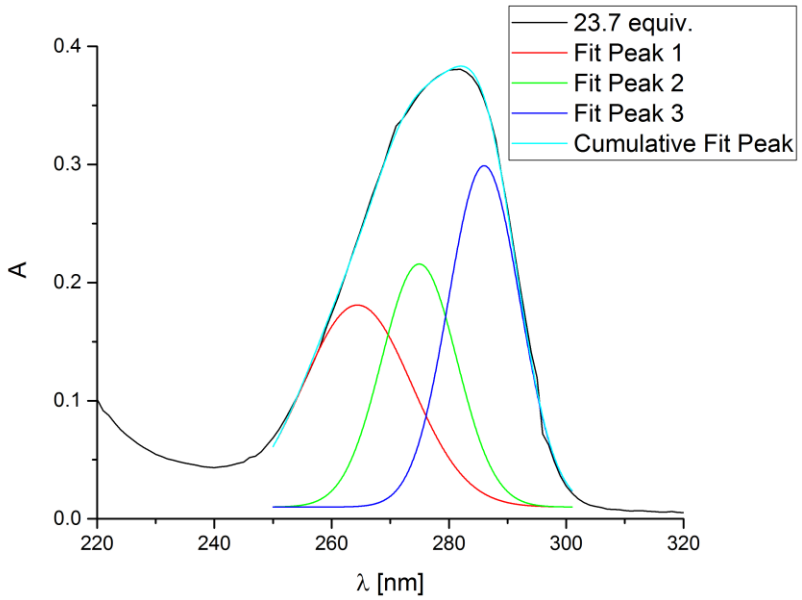

Figure S.5.27. Gaussian deconvolution of absorption peak after addition of 23.7 equiv. TBAF$(H_2O)_3$ (1.58 mM) to 1,3-bis((4-trifluoromethyl)phenyl)urea in MeCN (8.0 µM).

S.5.5.2. NMR Titrations

500 µL of a solution of 1,3-diarylurea (2.0 mM) in 8:2 MeCN/MeCN-d_3 were used as sample. A ^{1}H NMR was recorded on a Bruker AVIIIHD 500 followed by stepwise addition 4.73 eq. of a solution of TBAF$(H_2O)_3$ (78.9 mM)·in 8:2 MeCN/MeCN-d_3. After every addition a ^{1}H NMR was recorded. The chemical shift of the NH as well as aromatic proton signals was plotted against the amount of added TBAF$(H_2O)_3$ and DynaFit4 was used to determine binding constants *via* nonlinear least-squares regression assuming the formation of a 1:1 (urea–fluoride) complex followed by a 2:1 (urea–fluoride) complex.[390] A typical input file is shown below.

Preparation of TBAF$(H_2O)_3$ solution: Commercial TBAF$(H_2O)_3$ was weighed out in a vial, which had been flushed with Ar, and dissolved in 8:2 MeCN/MeCN-d_3. The exact fluoride concentration was determined following a published procedure.[389]

For additional entries in Figure 5.25 the titration with 1,3-Diphenylurea (**5.6e**) was repeated with 10.0 equiv. of H_2O (0.18 µL, 10 µmol) being present over the course of the titration as well as using a 100 mM solution of anhydrous TMAF (9.3 mg, 100 µmol) in anhydrous DMSO (1.0 mL). TMAF was weighed in under an inert atmosphere and DMSO had to be used as solvent as TMAF is insoluble in MeCN at this concentration. For the first control sample a 1.0 mM solution of **5.7e** (1.4 mg, 2.0 µmol) in 8:2 MeCN/MeCN-d_3 (2.0 mL) was prepared, of which 500 µL were used as sample. To 250 µL of the remaining solution of **5.7e** 250 µL of a solution of **5.6e** (2.0 mM) which had been prepared by dissolving **5.6e** (1.7 mg, 8.0 µmol) in 8:2 MeCN/MeCN-d_3 (4.0 mL) was added to give the second control sample.

DynaFit4 Input File

The following shows a typical input file for the determination of $K_{a,2:1}$ (K2 in input file) using the values for $K_{a,1:1}$ (K1 in input file) as obtained from previous UV-vis titrations.

```
[task]
    data = equilibria
    task = fit
    mechanism = three species ?
[mechanism]
```

```
        SQRAM + F <==> SQRAMF      :        K1       equil
        SQRAMF + SQRAM <==> SQRAMFSQRAM    :        K2       equil
 [constants]
        K1 = 15.7
        K2 = 0.25 ?

[responses]
intensive
        SQRAM = 7.288
        SQRAMF = 7.392 ?
        SQRAMFSQRAM = 7.340 ?
[output]
        directory ./LP-1418/output

[data]
        variable F, SQRAM
        plot titration
        file ./LP-1418/LP-1418-analysis-corr-fluoride-TBAF-titr-downf-arom-h-two-vars.txt
        extension txt
[end]
```

Titration profiles as well as fitted models and residual errors for individual 1,3-diarylureas are shown in Figures S.5.29–S.5.34. For labelling of relevant protons, see Figure S.5.28.

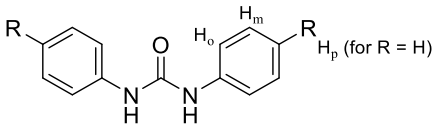

Figure S.5.28. Labelling of protons for NMR titrations.

1,3-Diphenylurea (5.6e)

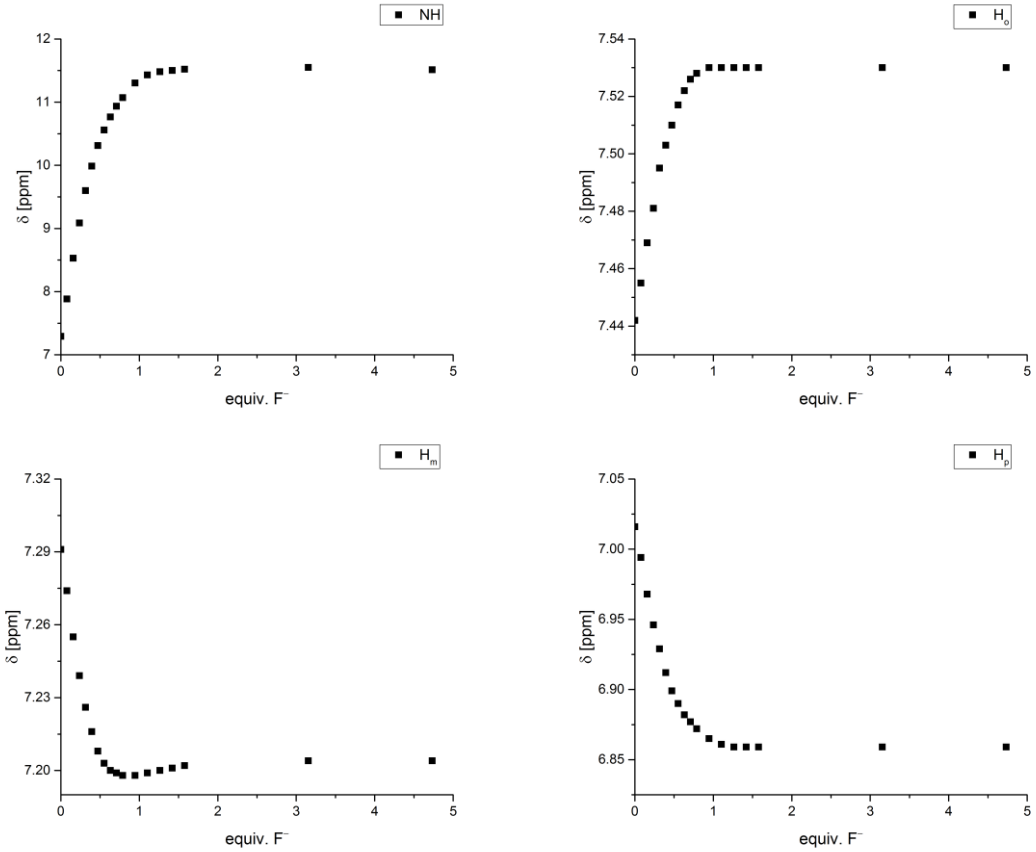

Figure S.5.29. Titration profile of NH, H_o, H_m and H_p protons over the course of a titration of a 2.0 mM solution of 1,3-diphenylurea in 8:2 MeCN/MeCN-d_3 with TBAF$(H_2O)_3$ (78.9 mM).

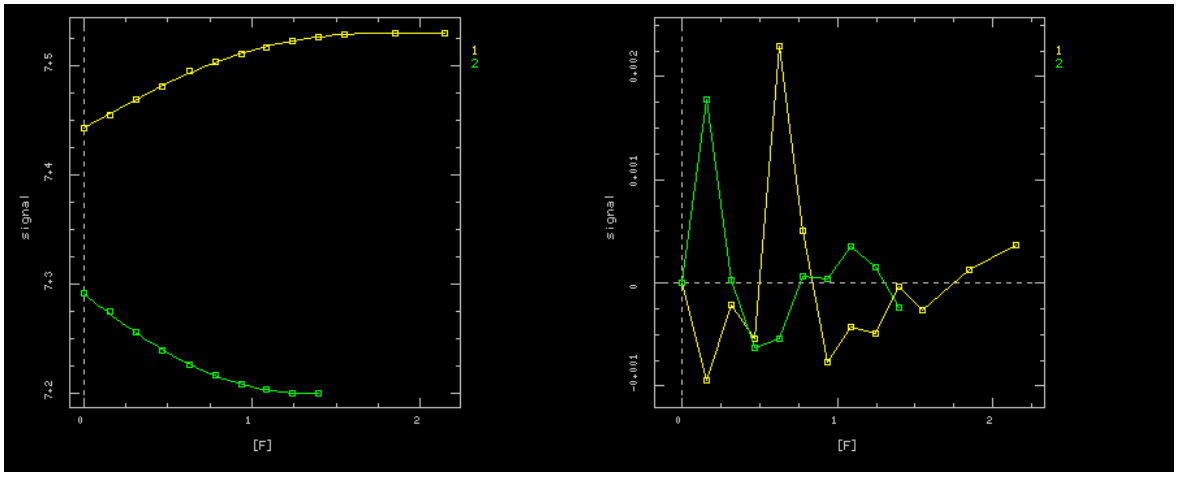

Figure S.5.30. Left: Model for formation of 1:1 and 2:1 complexes (lines) fitted to measured ^{1}H NMR shifts of H_o (yellow squares) and H_m (green squares) obtained over the course of a titration of a 2.0 mM solution of 1,3-diphenylurea in 8:2 MeCN/MeCN-d_3 with TBAF$(H_2O)_3$ (78.9 mM). Right: Residual errors.

1,3-Bis(4-methylphenyl)urea (5.6f)

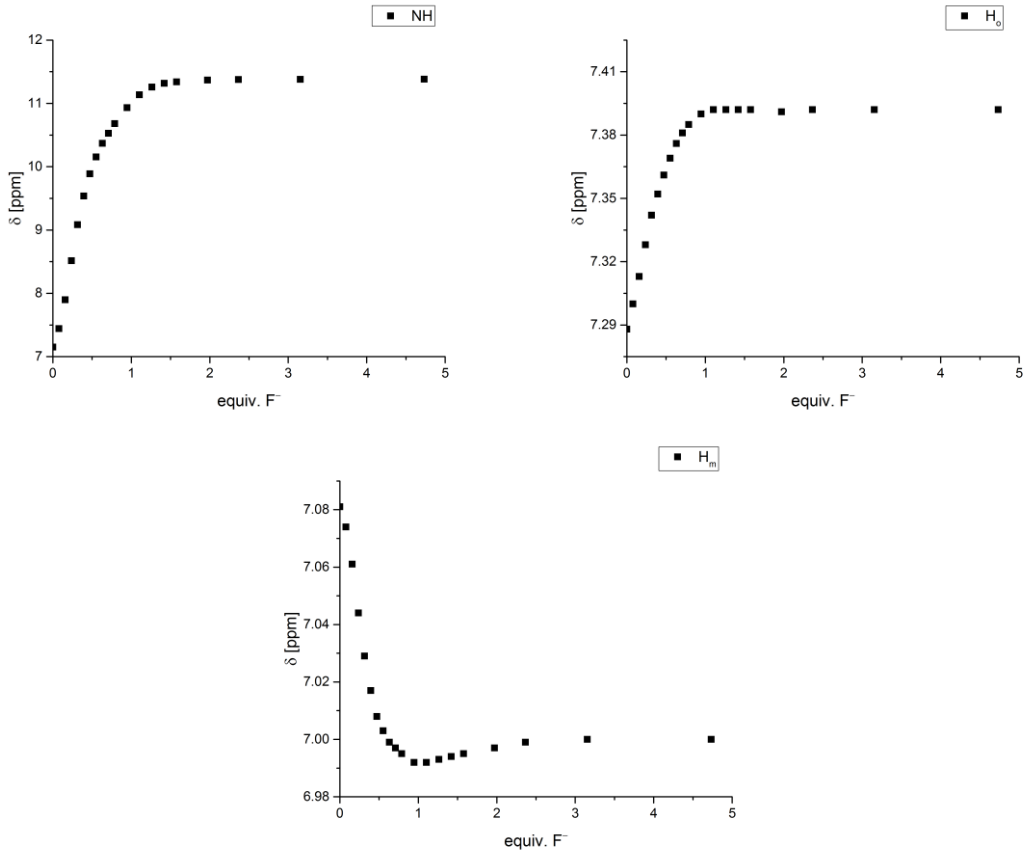

Figure S.5.31. Titration profile of NH, H_o and H_m protons over the course of a titration of a 2.0 mM solution of 1,3-bis(4-methylphenyl)urea in 8:2 MeCN/MeCN-d_3 with TBAF$(H_2O)_3$ (78.9 mM).

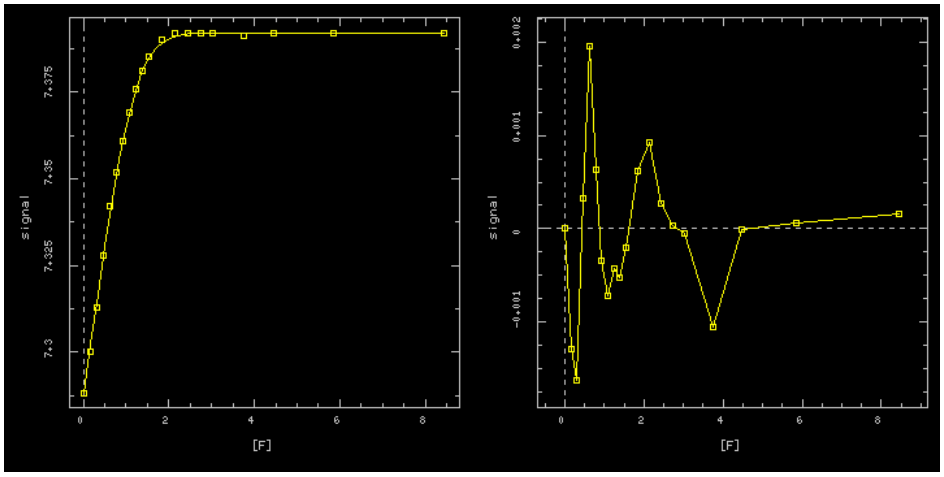

Figure S.5.32. Left: Model for formation of 1:1 and 2:1 complexes (line) fitted to measured ^{1}H NMR shifts of H_o (yellow squares) obtained over the course of a titration of a 2.0 mM solution of 1,3-bis(4-methylphenyl)urea in 8:2 MeCN/MeCN-d_3 with TBAF$(H_2O)_3$ (78.9 mM). Right: Residual errors.

1,3-Bis(4-methoxyphenyl)urea (5.6g)

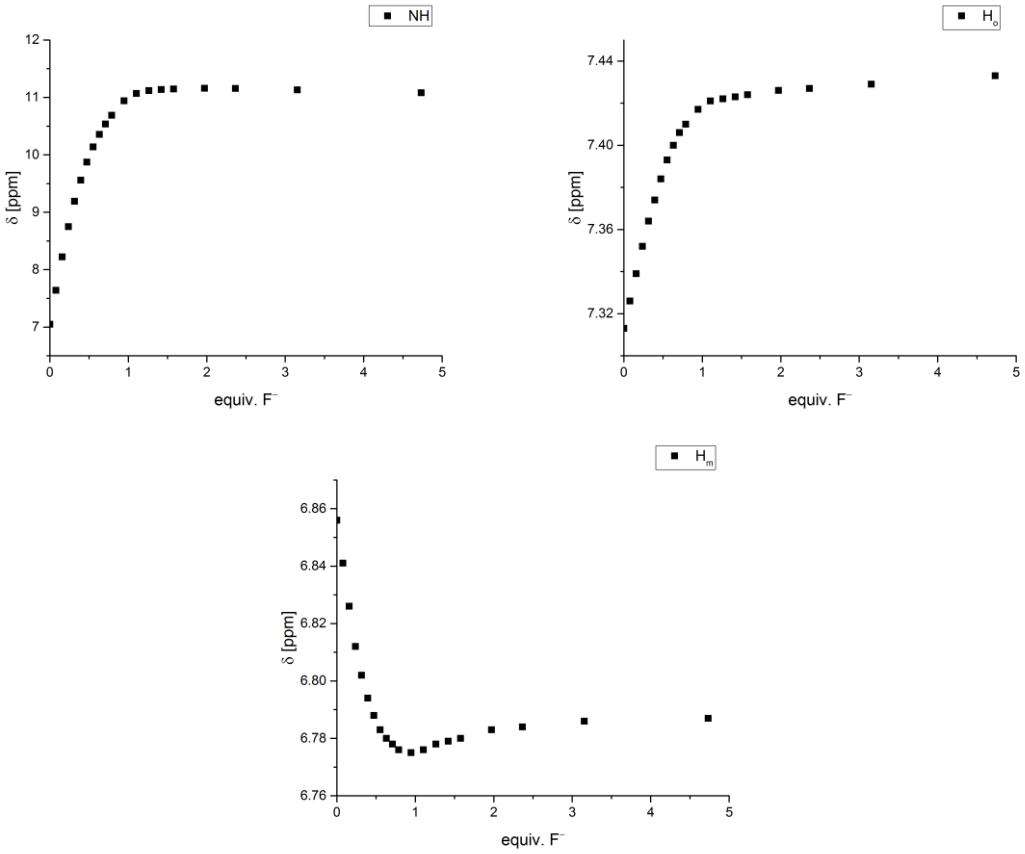

Figure S.5.33. Titration profile of NH, H_o and H_m protons over the course of a titration of a 2.0 mM solution of 1,3-bis(4-methoxyphenyl)urea in 8:2 MeCN/MeCN-d_3 with TBAF$(H_2O)_3$ (78.9 mM).

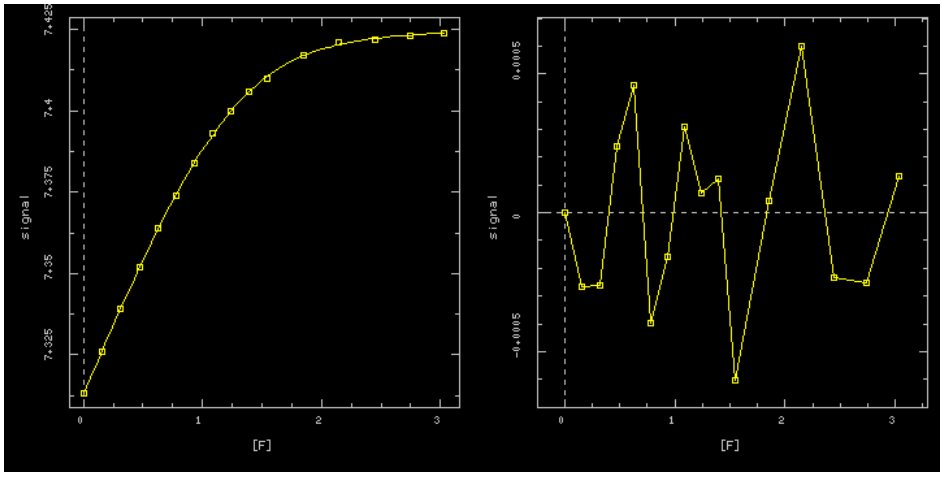

Figure S.5.34. Left: Model for formation of 1:1 and 2:1 complexes (line) fitted to measured ^{1}H NMR shifts of H_o (yellow squares) obtained over the course of a titration of a 2.0 mM solution of 1,3-bis(4-methoxyphenyl)urea in 8:2 MeCN/MeCN-d_3 with TBAF$(H_2O)_3$ (78.9 mM). Right: Residual errors.

S.5.6. Diffusion Ordered NMR Spectroscopy (DOSY)

500 µL of a solution of 1,3-diphenylurea (**5.6e**) (2.0 mM) in MeCN-d_3 containing pentane (1.0 µL) as internal reference were used as sample and the diffusion coefficient, *D*, corresponding to each of the three aromatic ^{1}H signals was determined on a Bruker AVII 500 applying a previously developed pulse sequence (dstebpgp3s).[391] To this sample 2.5 eq. of a stock solution of TBAF$(H_2O)_3$ (81.8 mM) (*vide infra*) in MeCN-d_3 were added stepwise. After the addition of each aliquot the average diffusion coefficient, *D*, of the rapidly interconverting urea species present in the mixture was determined using the same pulse sequence. Data was collected in triplicate, and averages with standard uncertainties (SU) are reported (Table S.5.9). For DOSY parameters refer to Table S.5.9.

Preparation of TBAF$(H_2O)_3$ solution: Commercial TBAF$(H_2O)_3$ was weighed out in a vial, which had been flushed with Ar, and dissolved in MeCN-d_3. The exact concentration was determined following a published procedure.[389]

Table S.5.9. Summary of ^{1}H-DOSY measurements over the course of a titration of a solution of 1,3-diphenylurea in MeCN-d_3 (2.0 mM) with TBAF$(H_2O)_3$ (81.8 mM). Continued on the following page.

	0 eq.			**0.17 eq.**			**0.33 eq.**		
Δ [sec]	0.05			0.05			0.05		
δ [µsec]	700			860			890		
Gradient [%]	2–98			2–98			2–98		
	1	2	3	1	2	3	1	2	3
D(H_o) [$\cdot 10^{-9}$ m^2 s^{-1}]	2.095	2.096	2.108	1.898	1.914	1.926	1.700	1.712	1.705
D(H_m) [$\cdot 10^{-9}$ m^2 s^{-1}]	2.068	2.097	2.090	1.866	1.867	1.885	1.726	1.686	1.694
D(H_p) [$\cdot 10^{-9}$ m^2 s^{-1}]	2.064	2.105	2.121	1.869	1.867	1.901	1.723	1.722	1.700
Average [$\cdot 10^{-9}$ m^2 s^{-1}]	2.094			1.888			1.708		
SU [$\cdot 10^{-9}$ m^2 s^{-1}]	0.017			0.021			0.013		
Pentane (CH_3) [$\cdot 10^{-9}$ m^2 s^{-1}]	4.215	4.223	4.214	4.204	4.225	4.241	4.169	4.248	4.242
Average [$\cdot 10^{-9}$ m^2 s^{-1}]	4.217			4.223			4.220		
SU [$\cdot 10^{-9}$ m^2 s^{-1}]	0.004			0.015			0.036		

	0.5 eq.			**0.67 eq.**			**0.83 eq.**		
Δ [sec]	0.05			0.05			0.05		
δ [µsec]	770			920			920		
Gradient [%]	2–98			2–98			2–98		
	1	2	3	1	2	3	1	2	3
D(H_o) [$\cdot 10^{-9}$ m^2 s^{-1}]	1.633	1.647	1.660	1.663	1.648	1.647	1.688	1.663	1.678
D(H_m) [$\cdot 10^{-9}$ m^2 s^{-1}]	1.646	1.655	1.631	1.649	1.633	1.665	1.678	1.666	1.695
D(H_p) [$\cdot 10^{-9}$ m^2 s^{-1}]	1.631	1.637	1.617	1.658	1.665	1.653	1.679	1.666	1.695
Average [$\cdot 10^{-9}$ m^2 s^{-1}]	1.640			1.653			1.679		
SU [$\cdot 10^{-9}$ m^2 s^{-1}]	0.013			0.010			0.011		
Pentane (CH_3) [$\cdot 10^{-9}$ m^2 s^{-1}]	4.216	4.299	4.196	4.132	4.127	4.179	4.161	4.144	4.222
Average [$\cdot 10^{-9}$ m^2 s^{-1}]	4.237			4.146			4.176		
SU [$\cdot 10^{-9}$ m^2 s^{-1}]	0.045			0.023			0.033		

	1.0 eq.			1.17 eq.			1.33 eq.		
Δ [sec]	0.05			0.05			0.05		
δ [μsec]	770			920			920		
Gradient [%]	2–98			2–98			2–98		
	1	2	3	1	2	3	1	2	3
$D(H_o)$ [$\cdot 10^{-9}$ m^2 s^{-1}]	1.716	1.724	1.714	1.727	1.739	1.724	1.753	1.733	1.731
$D(H_m)$ [$\cdot 10^{-9}$ m^2 s^{-1}]	1.720	1.706	1.687	1.742	1.720	1.734	1.746	1.756	1.726
$D(H_p)$ [$\cdot 10^{-9}$ m^2 s^{-1}]	1.693	1.692	1.680	1.744	1.721	1.718	1.745	1.745	1.748
Average [$\cdot 10^{-9}$ m^2 s^{-1}]	1.704			1.730			1.743		
SU [$\cdot 10^{-9}$ m^2 s^{-1}]	0.015			0.009			0.010		
Pentane (CH_3)	4.221	4.245	4.226	4.098	4.171	4.158	4.120	4.220	4.203
Average [$\cdot 10^{-9}$ m^2 s^{-1}]	4.231			4.142			4.181		
SU [$\cdot 10^{-9}$ m^2 s^{-1}]	0.010			0.032			0.044		

	1.5 eq.			2.0 eq.			2.5 eq.		
Δ [sec]	0.05			0.05			0.05		
δ [μsec]	920			1000			1000		
Gradient [%]	2–98			2–98			2–98		
	1	2	3	1	2	3	1	2	3
$D(H_o)$ [$\cdot 10^{-9}$ m^2 s^{-1}]	1.765	1.733	1.744	1.763	1.763	1.763	1.778	1.758	1.767
$D(H_m)$ [$\cdot 10^{-9}$ m^2 s^{-1}]	1.759	1.728	1.745	1.746	1.755	1.757	1.767	1.748	1.752
$D(H_p)$ [$\cdot 10^{-9}$ m^2 s^{-1}]	1.774	1.763	1.776	1.749	1.742	1.753	1.725	1.741	1.742
Average [$\cdot 10^{-9}$ m^2 s^{-1}]	1.754			1.755			1.753		
SU [$\cdot 10^{-9}$ m^2 s^{-1}]	0.016			0.007			0.015		
Pentane (CH_3) [$\cdot 10^{-9}$ m^2 s^{-1}]	4.193	4.123	4.183	4.128	4.090	4.072	4.099	4.074	4.147
Average [$\cdot 10^{-9}$ m^2 s^{-1}]	4.166			4.097			4.107		
SU	0.031			0.023			0.030		

S.5.7. 1D ^{19}F–^{1}H Heteronuclear nOe NMR Spectroscopy (HOESY)

Fluoride–urea complex **5.7j** (100 mg, 0.13 mmol) was dissolved in 500 µL of the according deuterated solvent. 1D ^{19}F–^{1}H heteronuclear nOe NMR spectroscopy experiments were performed on a Bruker AVII 500 using a previously developed pulse sequence (hoesyfhgppp1d).[489] Build-up curves for nOes to the neighbouring protons of aromatic fluoride as well as fluoride anion (Figure S.5.35) were recorded separately using mixing times varying from 10–400 ms.

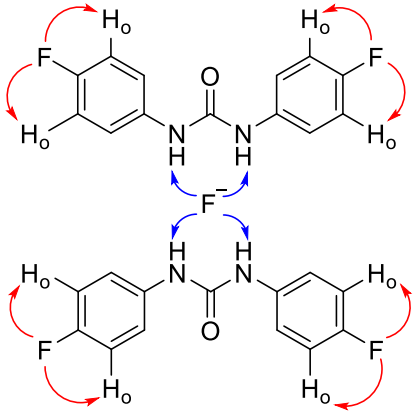

Figure S.5.35. Observed ^{19}F–^{1}H nOe signals.

Figures S.5.36–S.5.43 show the build-up curves for neighbouring protons of aromatic fluoride and fluoride anion in MeCN-d_3 (Figure S.5.36–S.5.37), DCM-d_2 (Figure S.5.38–S.5.39), DMSO-d_6 (Figure S.5.40–S.5.41) and THF-d_8 (Figure S.5.42–S.5.43).

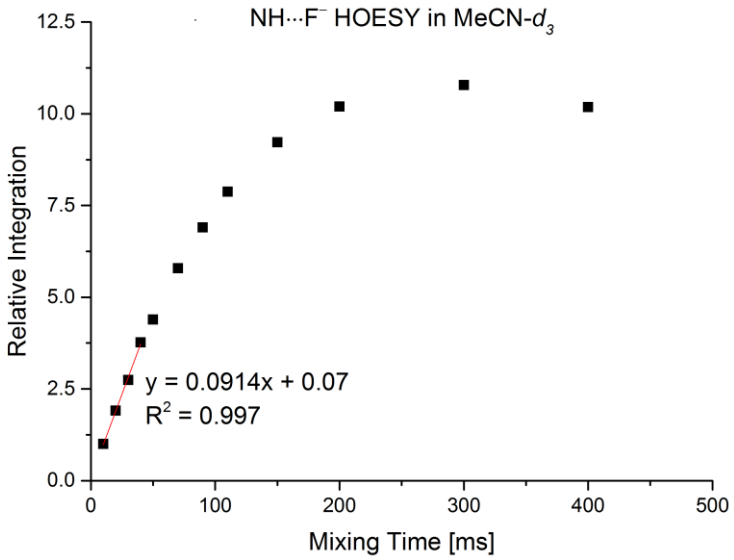

Figure S.5.36. Build-up curve of ^{1}H-nOe signal for fluoride-anion/NH-proton pair in MeCN-d_3.

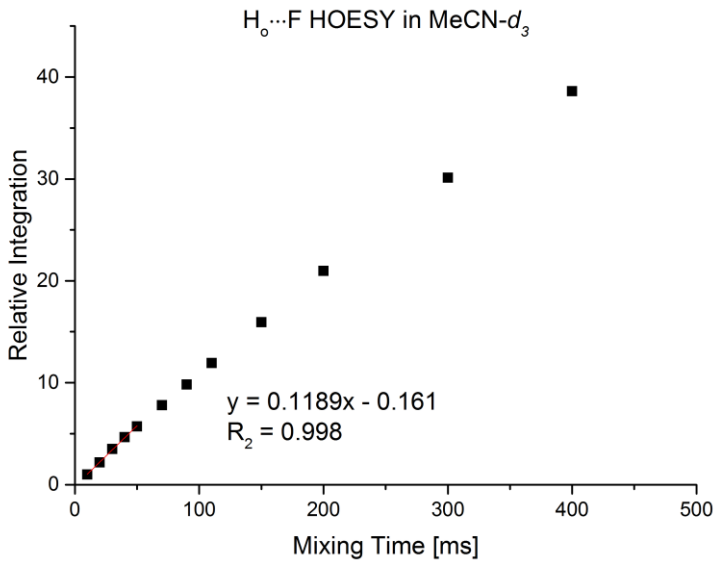

Figure S.5.37. Build-up curve of ^{1}H-nOe signal for aromatic-fluorine/proton pair in MeCN-d_3.

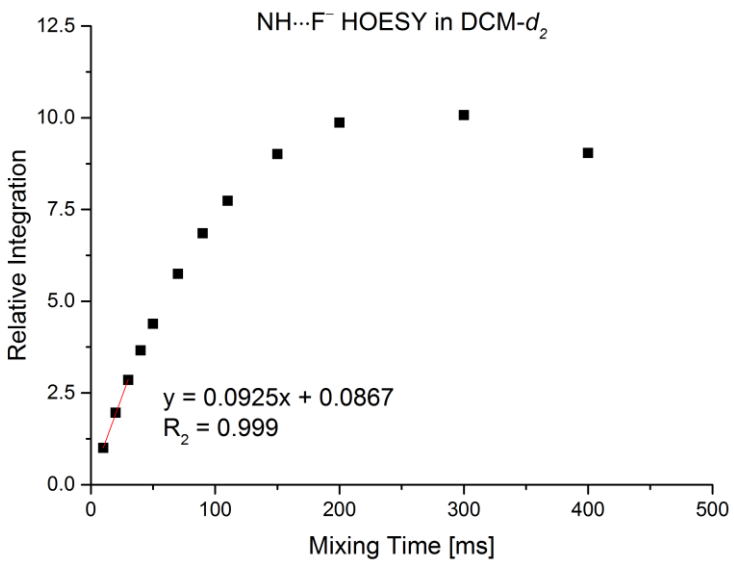

Figure S.5.38. Build-up curve of ^{1}H-nOe signal for fluoride-anion/NH-proton pair in DCM-d_2.

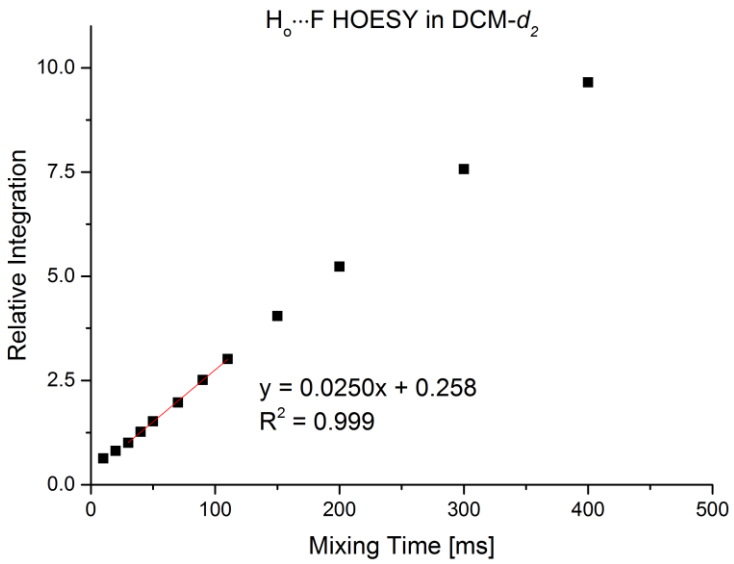

Figure S.5.39. Build-up curve of ^{1}H-nOe signal for aromatic-fluorine/proton pair in DCM-d_2.

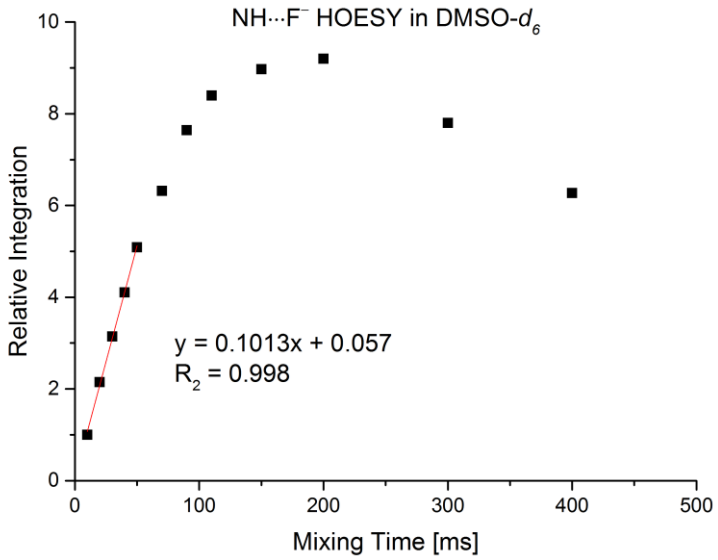

Figure S.5.40. Build-up curve of ^{1}H-nOe signal for fluoride-anion/NH-proton pair in DMSO-d_6.

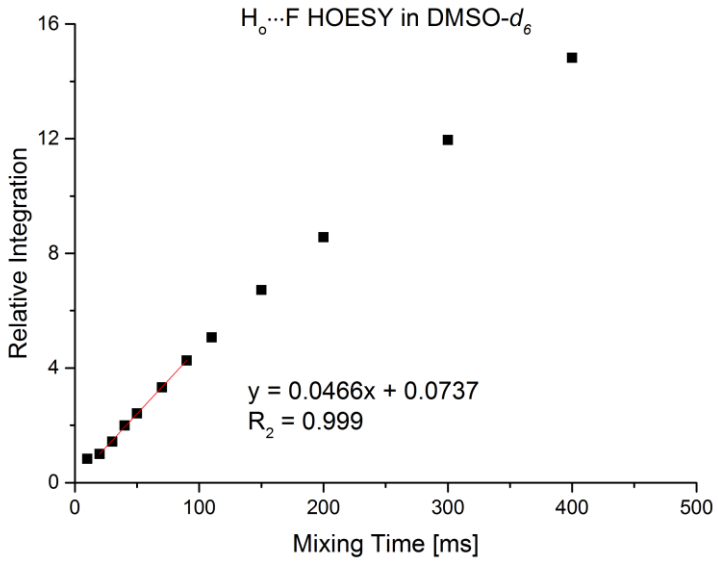

Figure S.5.41. Build-up curve of ^{1}H-nOe signal for aromatic-fluorine/proton pair in DMSO-d_6.

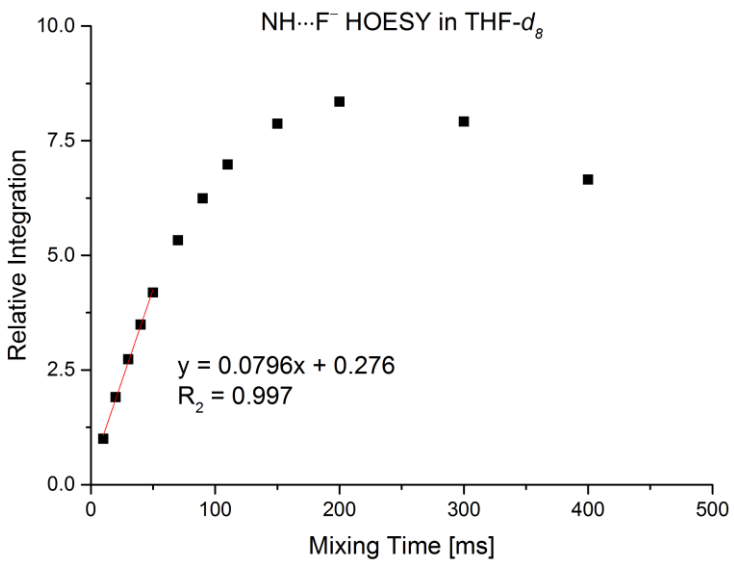

Figure S.5.42. Build-up curve of ^{1}H-nOe signal for fluoride-anion/NH-proton pair in THF-d_8.

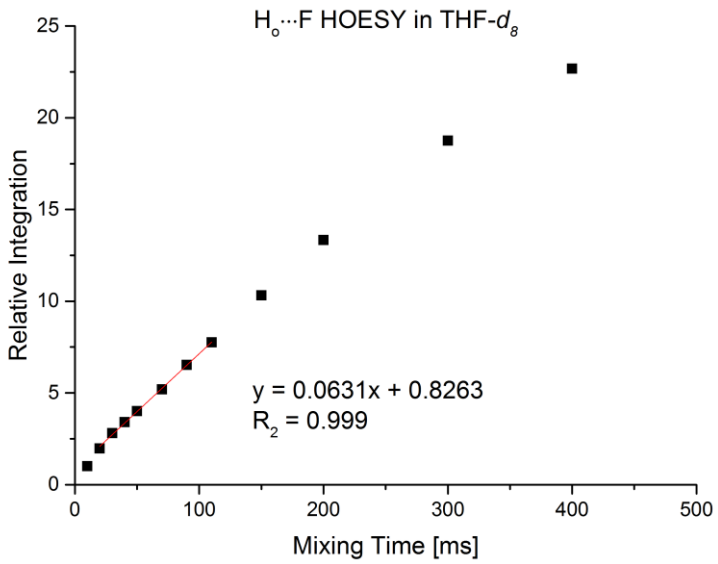

Figure S.5.43. Build-up curve of ^{1}H-nOe signal for aromatic-fluorine/proton pair in THF-d_8.

References

[1] L. Pauling, *The Nature of the Chemical Bond and the Structure of Molecules and Crystals: An Introduction to Modern Structural Chemistry*, Cornell University Press, Ithaca, **1960**.

[2] A. Bondi, *J. Phys. Chem.* **1964**, *68*, 441–451.

[3] T. L. Cottrell, *The Strengths of Chemical Bonds*, Butterworths, London, **1958**.

[4] S. W. Benson, *J. Chem. Educ.* **1965**, *42*, 502.

[5] B. deB. Darwent, *National Standard Reference Data Series*, Washington, DC, **1970**.

[6] D. O'Hagan, *Chem. Soc. Rev.* **2008**, *37*, 308–319.

[7] K. B. Wiberg, *Acc. Chem. Res.* **1996**, *29*, 229–234.

[8] K. B. Wiberg, P. R. Rablen, *J. Am. Chem. Soc.* **1993**, *115*, 614–625.

[9] P.-Y. Lien, R.-M. You, W.-P. Hu, *J. Phys. Chem. A* **2001**, *105*, 2391–2400.

[10] W. R. Dolbier, A. C. Alty, O. Phanstiel, *J. Am. Chem. Soc.* **1987**, *109*, 3046–3050.

[11] G. A. Griffith, I. H. Hillier, A. C. Moralee, J. M. Percy, R. Roig, M. A. Vincent, *J. Am. Chem. Soc.* **2006**, *128*, 13130–13141.

[12] S. N. Pieniazek, K. N. Houk, *Angew. Chem. Int. Ed.* **2006**, *45*, 1442–1445.

[13] L. Dasaradhi, D. O'Hagan, M. C. Petty, C. Pearson, *J. Chem. Soc., Perkin Trans. 2* **1995**, 221–225.

[14] M. L. Trapp, J. K. Watts, N. Weinberg, B. M. Pinto, *Can. J. Chem.* **2006**, *84*, 692–701.

[15] K. B. Wiberg, M. A. Murcko, K. E. Laidig, P. J. MacDougall, *J. Phys. Chem.* **1990**, *94*, 6956–6959.

[16] L. Goodman, H. Gu, V. Pophristic, *J. Phys. Chem. A* **2005**, *109*, 1223–1229.

[17] D. Wu, A. Tian, H. Sun, *J. Phys. Chem. A* **1998**, *102*, 9901–9905.

[18] A. S. Cieplak, *Chem. Rev.* **1999**, *99*, 1265–1336.

[19] L. Hunter, A. M. Z. Slawin, P. Kirsch, D. O'Hagan, *Angew. Chem. Int. Ed.* **2007**, *46*, 7887–7890.

[20] R. J. Abraham, A. D. Jones, M. A. Warne, R. Rittner, C. F. Tormena, *J. Chem. Soc., Perkin Trans. 2* **1996**, 533–539.

[21] H. V Phan, J. R. Durig, *J. Mol. Struct. THEOCHEM* **1990**, *209*, 333–347.

[22] B. J. van der Veken, S. Truyen, W. A. Herrebout, G. Watkins, *J. Mol. Struct.* **1993**, *293*, 55–58.

[23] J. W. Banks, A. S. Batsanov, J. A. K. Howard, D. O'Hagan, H. S. Rzepa, S. Martin-Santamaria, *J. Chem. Soc., Perkin Trans. 2* **1999**, 2409–2411.

[24] R. J. Abraham, S. L. R. Ellison, P. Schonholzer, W. A. Thomas, *Tetrahedron* **1986**, *42*, 2101–2110.

[25] E. T. Kool, H. O. Sintim, *Chem. Commun.* **2006**, 3665–3675.

[26] J. A. Olsen, D. W. Banner, P. Seiler, B. Wagner, T. Tschopp, U. Obst-Sander, M. Kansy, K. Müller, F. Diederich, *ChemBioChem* **2004**, *5*, 666–675.

[27] A. Sun, D. C. Lankin, K. Hardcastle, J. P. Snyder, *Chem. Eur. J.* **2005**, *11*, 1579–1591.

[28] C. R. S. Briggs, M. J. Allen, D. O'Hagan, D. J. Tozer, A. M. Z. Slawin, A. E. Goeta, J. A. K. Howard, *Org. Biomol. Chem.* **2004**, *2*, 732–740.

[29] G. Deniau, A. M. Z. Slawin, T. Lebl, F. Chorki, J. P. Issberner, T. van Mourik, J. M. Heygate, J. J. Lambert, L.-A. Etherington, K. T. Sillar, et al., *ChemBioChem* **2007**, *8*, 2265–2274.

[30] J. A. K. Howard, V. J. Hoy, D. O'Hagan, G. T. Smith, *Tetrahedron* **1996**, *52*, 12613–12622.

[31] J. D. Dunitz, R. Taylor, *Chem. Eur. J.* **1997**, *3*, 89–98.

[32] I. Hyla-Kryspin, G. Haufe, S. Grimme, *Chem. Eur. J.* **2004**, *10*, 3411–3422.

[33] S. A. Harrell, D. H. McDaniel, *J. Am. Chem. Soc.* **1964**, *86*, 4497.

[34] H. D. B. Jenkins, K. F. Pratt, *J. Chem. Soc. Faraday Trans. 2 Mol. Chem. Phys.* **1977**, *73*, 812–821.

[35] J. W. Larson, T. B. McMahon, *J. Am. Chem. Soc.* **1983**, *105*, 2944–2950.

[36] P. N. Noble, R. N. Kortzeborn, *J. Chem. Phys.* **1970**, *52*, 5375–5387.

[37] C.-G. Zhan, D. A. Dixon, *J. Phys. Chem. A* **2004**, *108*, 2020–2029.

[38] R. D. Chambers, *Fluorine in Organic Chemistry*, Blackwell Publishing, Oxford, **2004**.

[39] M. Morgenthaler, E. Schweizer, A. Hoffmann-Röder, F. Benini, R. E. Martin, G. Jaeschke, B. Wagner, H. Fischer, S. Bendels, D. Zimmerli, et al., *ChemMedChem* **2007**, *2*, 1100–1115.

[40] S. Purser, P. R. Moore, S. Swallow, V. Gouverneur, *Chem. Soc. Rev.* **2008**, *37*, 320–330.

[41] D. A. Smith, H. van de Waterbeemd, D. K. Walker, *Methods and Principles in Medicinal Chemistry*, Wiley-VCH, Weinheim, **2006**.

[42] M. Rowley, D. J. Hallett, S. Goodacre, C. Moyes, J. Crawforth, T. J. Sparey, S. Patel, R. Marwood, S. Patel, S. Thomas, et al., *J. Med. Chem.* **2001**, *44*, 1603–1614.

[43] B. E. Smart, *J. Fluor. Chem.* **2001**, *109*, 3–11.

[44] R. T. Jacobs, P. R. Bernstein, L. A. Cronk, E. P. Vacek, L. F. Newcomb, D. Aharony, C. K. Buckner, E. J. Kusner, *J. Med. Chem.* **1994**, *37*, 1282–1297.

[45] S. B. Rosenblum, T. Huynh, A. Afonso, H. R. Davis, N. Yumibe, J. W. Clader, D. A. Burnett, *J. Med. Chem.* **1998**, *41*, 973–980.

[46] M. Van Heek, C. F. France, D. S. Compton, R. L. Mcleod, N. P. Yumibe, K. B. Alton, E. J. Sybertz, H. R. Davis, *J. Pharmacol. Exp. Ther.* **1997**, *283*, 157–163.

[47] B. K. Park, N. R. Kitteringham, P. M. O'Neill, *Annu. Rev. Pharmacol. Toxicol.* **2001**, *41*, 443–470.

[48] N. H. P. Cnubben, S. Peelen, J.-W. Borst, J. Vervoort, C. Veeger, I. M. C. M. Rietjens, *Chem. Res. Toxicol.* **1994**, *7*, 590–598.

[49] R. Franz, *J. Fluor. Chem.* **1980**, *15*, 423–434.

[50] G. Haufe, *J. Prakt. Chem.* **1996**, *338*, 99–113.

[51] G. A. Olah, J. T. Welch, Y. D. Vankar, M. Nojima, I. Kerekes, J. A. Olah, *J. Org. Chem.* **1979**, *44*, 3872–3881.

[52] J. Barluenga, J. M. González, P. J. Campos, G. Asensio, *Angew. Chem. Int. Ed. Engl.* **1985**, *24*, 319–320.

[53] W. Carpenter, *J. Org. Chem.* **1966**, *31*, 2688–2689.

[54] A. S. Pilcher, H. L. Ammon, P. DeShong, *J. Am. Chem. Soc.* **1995**, *117*, 5166–5167.

[55] W. J. Middleton, *J. Org. Chem.* **1975**, *40*, 574–578.

[56] G. S. Lal, G. P. Pez, R. J. Pesaresi, F. M. Prozonic, H. Cheng, *J. Org. Chem.* **1999**, 215–216.

[57] G. S. Lal, G. P. Pez, R. J. Pesaresi, Pro, *Chem. Commun* **1999**, 215–216.

[58] J. Leroy, E. Hebert, C. Wakselman, *J. Org. Chem.* **1979**, *44*, 3406–3408.

[59] F. Beaulieu, L.-P. Beauregard, G. Courchesne, M. Couturier, F. LaFlamme, A. L'Heureux, *Org. Lett.* **2009**, *11*, 5050–5053.

[60] A. L'Heureux, F. Beaulieu, C. Bennett, D. R. Bill, S. Clayton, F. LaFlamme, M. Mirmehrabi, S. Tadayon, D. Tovell, M. Couturier, *J. Org. Chem.* **2010**, *75*, 3401–3411.

[61] O. Mahé, A. L'Heureux, M. Couturier, C. Bennett, S. Clayton, D. Tovell, F. Beaulieu, J.-F. Paquin, *J. Fluor. Chem.* **2013**, *153*, 57–60.

[62] P. Tang, W. Wang, T. Ritter, *J. Am. Chem. Soc.* **2011**, *133*, 11482–11484.

[63] M. K. Nielsen, C. R. Ugaz, W. Li, A. G. Doyle, *J. Am. Chem. Soc.* **2015**, *137*, 9571–

9574.

[64] D. H. R. Barton, A. K. Ganguly, R. H. Hesse, S. N. Loo, M. M. Pechet, *Chem. Commun.* **1968**, 806–808.

[65] D. H. R. Barton, L. S. Godinho, R. H. Hesse, M. M. Pechet, *Chem. Commun.* **1968**, 804–806.

[66] D. H. R. Barton, R. H. Hesse, M. M. Pechet, G. Tarzia, H. T. Toh, N. D. Westcott, *J. Chem. Soc., Chem. Commun.* **1972**, 122–123.

[67] M. A. Tius, *Tetrahedron* **1995**, *51*, 6605–6634.

[68] G. Villalba, R. U. Ayres, H. Schroder, *J. Ind. Ecol.* **2007**, *11*, 85–101.

[69] T. Umemoto, K. Tomita, *Tetrahedron Lett.* **1986**, *27*, 3271–3274.

[70] E. Differding, H. Ofner, *Synlett* **1991**, 187–189.

[71] R. E. Banks, S. N. Mohialdin-Khaffaf, G. S. Lal, I. Sharif, R. G. Syvret, *J. Chem. Soc., Chem. Commun.* **1992**, 595–596.

[72] J. R. Wolstenhulme, J. Rosenqvist, O. Lozano, J. Ilupeju, N. Wurz, K. M. Engle, G. W. Pidgeon, P. R. Moore, G. Sandford, V. Gouverneur, *Angew. Chem. Int. Ed.* **2013**, *52*, 9796–9800.

[73] C.-L. Zhu, M. Maeno, F.-G. Zhang, T. Shigehiro, T. Kagawa, K. Kawada, N. Shibata, J.-A. Ma, D. Cahard, *Eur. J. Org. Chem.* **2013**, 6501–6505.

[74] G. C. Geary, E. G. Hope, K. Singh, A. M. Stuart, *Chem. Commun.* **2013**, *49*, 9263–9265.

[75] F. Yin, Z. Wang, Z. Li, C. Li, C. Liu, X. Wang, Z. Li, L. Cui, C. Li, *J. Am. Chem. Soc.* **2015**, 1–106.

[76] J. C. T. Leung, C. Chatalova-Sazepin, J. G. West, M. Rueda-Becerril, J. F. Paquin, G. M. Sammis, *Angew. Chem. Int. Ed.* **2012**, *51*, 10804–10807.

[77] M. Rueda-Becerril, C. Chatalova Sazepin, J. C. T. Leung, T. Okbinoglu, P. Kennepohl, J.-F. Paquin, G. M. Sammis, *J. Am. Chem. Soc.* **2012**, *134*, 4026–4029.

[78] W. Bockemüller, *Organische Fluorverbindungen*, Verlag Von Ferdinand Enke, Stuttgart, **1936**.

[79] V. N. Ipatieff, A. V Grosse, *J. Am. Chem. Soc.* **1935**, *57*, 1616–1621.

[80] G. A. Olah, S. J. Kuhn, *J. Am. Chem. Soc.* **1960**, *82*, 2380–2382.

[81] G. A. Olah, M. Nojima, I. Kerekes, *Synthesis* **1973**, 779–780.

[82] G. A. Olah, X.-Y. Li, Q. Wang, G. K. Surya Prakash, *Synthesis* **1993**, 693–699.

[83] T. J. Barker, D. L. Boger, *J. Am. Chem. Soc.* **2012**, *134*, 13588–13591.

[84] H. Shigehisa, E. Nishi, M. Fujisawa, K. Hiroya, *Org. Lett.* **2013**, *15*, 5158–5161.

[85] J. A. Akana, K. X. Bhattacharyya, P. Müller, J. P. Sadighi, *J. Am. Chem. Soc.* **2007**, *129*, 7736–7737.

[86] B. C. Gorske, C. T. Mbofana, S. J. Miller, *J. Org. Chem.* **2009**, *11*, 4318–4321.

[87] E. Negishi, in *Handbook of Organopalladium Chemistry for Organic Synthesis* (Ed.: A. de Meijere), John Wiley & Sons, Inc., Weinheim, **2003**, pp. 2783–2788.

[88] S. L. Fraser, M. Y. Antipin, V. N. Khroustalyov, V. V Grushin, *J. Am. Chem. Soc.* **1997**, *119*, 4769–4770.

[89] M. C. Pilon, V. V Grushin, *Organometallics* **1998**, *17*, 1774–1781.

[90] W. J. Marshall, D. L. Thorn, V. V Grushin, *Organometallics* **1998**, *17*, 5427–5430.

[91] A. Yahav, I. Goldberg, A. Vigalok, *J. Am. Chem. Soc.* **2003**, *125*, 13634–13635.

[92] V. V Grushin, *Chem. Eur. J.* **2002**, *8*, 1006–1014.

[93] K. L. Hull, W. Q. Anani, M. S. Sanford, *J. Am. Chem. Soc.* **2006**, *128*, 7134–7135.

[94] X. Wang, T.-S. Mei, J.-Q. Yu, *J. Am. Chem. Soc.* **2009**, *131*, 7520–7521.

[95] K. S. L. Chan, M. Wasa, X. Wang, J.-Q. Yu, *Angew. Chem. Int. Ed.* **2011**, *50*, 9081–9084.

[96] T. Wu, G. Yin, G. Liu, *J. Am. Chem. Soc.* **2009**, *131*, 16354–16355.

[97] T. Furuya, H. M. Kaiser, T. Ritter, *Angew. Chem. Int. Ed.* **2008**, *47*, 5993–5996.

[98] S.-B. Zhao, J. J. Becker, M. R. Gagné, *Organometallics* **2011**, *30*, 3926–3929.

[99] J. M. Racowski, J. B. Gary, M. S. Sanford, *Angew. Chem. Int. Ed.* **2012**, *51*, 3414–3417.

[100] E. Emer, L. Pfeifer, J. M. Brown, V. Gouverneur, *Angew. Chem. Int. Ed.* **2014**, *53*, 4181–4185.

[101] W. Liu, J. T. Groves, *Angew. Chem. Int. Ed.* **2013**, *52*, 6024–6027.

[102] S. Ventre, F. R. Petronijevic, D. W. C. MacMillan, *J. Am. Chem. Soc.* **2015**, *137*, 5654–5657.

[103] V. Varga, M. Lamac, M. Horacek, R. Gyepes, J. Pinkas, *Dalt. Trans.* **2016**, *45*, 10146–10150.

[104] K. Bowden, A. C. Drysdale, G. A. Mogey, *Nature* **1965**, *206*, 1359.

[105] P. M. Maitlis, in *The Organic Chemistry of Palladium*, Academic Press, New York, **1971**, pp. 145–174.

[106] D. A. White, J. R. Doyle, H. Lewis, in *Inorganic Syntheses* (Ed.: F.A. Cotton), John

Wiley & Sons, Inc., Hoboken, NJ, USA, **1972**, pp. 55–65.

[107] M. Tada, Y. Kuroda, T. Sato, *Tetrahedron Lett.* **1969**, 2871–2874.

[108] J. A. Davies, in *Comprehensive Organometallic Chemistry II* (Eds.: E.W. Abel, G.A. Stone, G. Wilkinson), Elsevier, Oxford, **1995**, pp. 291–390.

[109] J. Tsuji, in *Palladium Reagents and Catalysts*, John Wiley & Sons, Inc., **2005**, pp. 519–542.

[110] C. E. Houlden, C. D. Bailey, J. G. Ford, M. R. Gagné, G. C. Lloyd-Jones, K. I. Booker-Milburn, *J. Am. Chem. Soc.* **2008**, *130*, 10066–10067.

[111] B. Zheng, M. A. Schmidt, M. D. Eastgate, *J. Org. Chem.* **2016**, *81*, 3112–3118.

[112] D. D. Bender, F. G. Stakem, R. F. Heck, *J. Org. Chem.* **1982**, *47*, 1278–1284.

[113] S. M. Podhajsky, Y. Iwai, A. Cook-Sneathen, M. S. Sigman, *Tetrahedron* **2011**, *67*, 4435–4441.

[114] L. Liao, M. S. Sigman, *J. Am. Chem. Soc.* **2010**, *132*, 10209–10211.

[115] X. Wu, H.-C. Lin, M.-L. Li, L.-L. Li, Z.-Y. Han, L.-Z. Gong, *J. Am. Chem. Soc.* **2015**, *137*, 13476–13479.

[116] A. Perrier, M. Ferreira, J. N. H. Reek, J. I. van der Vlugt, *Catal. Sci. Technol.* **2013**, *3*, 1375–1379.

[117] A. Behr, L. Johnen, N. Rentmeister, *Adv. Synth. Catal.* **2010**, *352*, 2062–2072.

[118] L. K. Vo, D. A. Singleton, *Org. Lett.* **2004**, *6*, 2469–2472.

[119] A. I. Ayi, M. Remli, R. Guedj, R. Pastor, *J. Fluor. Chem.* **1981**, *17*, 127–143.

[120] U. Nettekoven, J. F. Hartwig, *J. Am. Chem. Soc.* **2002**, *124*, 1166–1167.

[121] J. B. Lambert, L. G. Greifenstein, *J. Am. Chem. Soc.* **1974**, *96*, 5120–5124.

[122] C. Thibaudeau, J. Plavec, J. Chattopadhyaya, *J. Org. Chem.* **1998**, *63*, 4967–4984.

[123] N. A. Cochrane, H. Nguyen, M. R. Gagne, *J. Am. Chem. Soc.* **2013**, *135*, 628–631.

[124] J. F. Hartwig, *Pure Appl. Chem.* **2004**, *76*, 507–516.

[125] A. G. Gilicinski, G. P. Pez, R. G. Syvret, G. S. Lal, *J. Fluor. Chem.* **1992**, *59*, 157–162.

[126] E. W. Oliver, D. H. Evans, *J. Electroanal. Chem.* **1999**, *474*, 1–8.

[127] W. Adcock, G. T. Binmore, A. R. Krstic, J. C. Walton, J. Wilkie, *J. Am. Chem. Soc.* **1995**, *117*, 2758–2766.

[128] P. A. McLaughlin, J. G. Verkade, *Organometallics* **1998**, *17*, 5937–5940.

[129] C. B. Caputo, D. Winkelhaus, R. Dobrovetsky, L. J. Hounjet, D. W. Stephan, *Dalt.*

Trans. **2015**, *44*, 12256–12264.

[130] R. N. Haszeldine, K. Leedham, *J. Chem. Soc.* **1954**, 1261–1264.

[131] G. Rong, R. Keese, *Tetrahedron Lett.* **1990**, *31*, 5615–5616.

[132] X.-Q. Tang, C.-M. Hu, *J. Fluor. Chem.* **1995**, *73*, 133–135.

[133] C. Amato, C. Naud, P. Calas, A. Commeyras, *J. Fluor. Chem.* **2002**, *113*, 55–63.

[134] J.-C. Xiao, Q.-Y. Chen, *Chin. J. Chem.* **2003**, *21*, 1349–1355.

[135] Z. Xiao, H. Hu, J. Ma, Q. Chen, Y. Guo, *Chin. J. Chem.* **2013**, *31*, 939–944.

[136] A.-R. Li, Q.-Y. Chen, *Synthesis* **1997**, 333–336.

[137] H.-P. Guan, X.-Q. Tang, B.-H. Luo, C.-M. Hu, *Synthesis* **1997**, 1489–1494.

[138] X. Yang, Z. Wang, X. Fang, X. Yang, F. Wu, Y. Shen, *Synthesis* **2007**, 1768–1778.

[139] A.-R. Li, Q.-Y. Chen, *Synthesis* **1996**, 606–608.

[140] X.-Q. Tang, C.-M. Hu, *J. Chem. Soc., Chem. Commun.* **1994**, 631–632.

[141] P. Cao, J.-X. Duan, Q.-Y. Chen, *J. Chem. Soc., Chem. Commun.* **1994**, 737–738.

[142] W.-Y. Huang, J.-L. Zhuang, *Chin. J. Chem.* **1991**, *9*, 373–376.

[143] W.-Y. Huang, Y. Xie, *Chin. J. Chem.* **1990**, *8*, 259–264.

[144] X.-C. Guo, Q.-Y. Chen, *J. Fluor. Chem.* **1998**, *88*, 63–70.

[145] S. Ma, X. Lu, *Tetrahedron* **1990**, *46*, 357–364.

[146] J. Chen, C.-M. Hu, *Chin. J. Chem.* **1994**, *12*, 468–476.

[147] Q.-Y. Chen, Y.-B. He, Z.-Y. Yang, *J. Fluor. Chem.* **1986**, *34*, 255–258.

[148] Q.-Y. Chen, Z.-M. Qiu, Z.-Y. Yang, *J. Fluor. Chem.* **1987**, *36*, 149–161.

[149] T. Takagi, T. Kanamori, *J. Fluor. Chem.* **2011**, *132*, 427–429.

[150] C. R. Davis, D. J. Burton, Z.-Y. Yang, *J. Fluor. Chem.* **1995**, *70*, 135–140.

[151] T. Ishihara, M. Kuroboshi, Y. Okada, *Chem. Lett.* **1986**, *15*, 1895–1896.

[152] T. Fuchikami, Y. Shibata, H. Urata, *Chem. Lett.* **1987**, *16*, 521–524.

[153] S. Saito, T. Kawasaki, N. Tsuboya, Y. Yamamoto, *J. Org. Chem.* **2001**, *66*, 796–802.

[154] K. Von Werner, *J. Fluor. Chem.* **1985**, *28*, 229–233.

[155] M. P. Jennings, E. A. Cork, P. V. Ramachandran, *J. Org. Chem.* **2000**, *65*, 8763–8766.

[156] V. V Bardin, N. Y. Adonin, H.-J. Frohn, *Organometallics* **2005**, *24*, 5311–5317.

[157] J. F. Chesa, D. Velasco, F. López-Calahorra, *Synth. Commun.* **2010**, *40*, 1822–1829.

[158] T. Konno, J. Chae, M. Kanda, G. Nagai, K. Tamura, T. Ishihara, H. Yamanaka, *Tetrahedron* **2003**, *59*, 7571–7580.

[159] T. Fuchikami, I. Ojima, *Tetrahedron Lett.* **1984**, *25*, 303–306.

[160] W.-Y. Huang, H.-Z. Zhang, *Chin. J. Chem.* **1992**, *10*, 274–277.

[161] W.-Y. Huang, L. Lü, *Chin. J. Chem.* **1992**, *10*, 268–273.

[162] W.-Y. Huang, L. Lü, Y.-F. Zhang, *Chin. J. Chem.* **1990**, *8*, 68–74.

[163] T. Wada, Y. Sumida, A. Kondoh, H. Yorimitsu, K. Oshima, *Bull. Chem. Soc. Jpn.* **2009**, *82*, 1433–1435.

[164] Y. Li, H. Li, J. Hu, *Tetrahedron* **2009**, *65*, 478–483.

[165] Y. Takeyama, Y. Ichinose, K. Oshima, K. Utimoto, *Tetrahedron Lett.* **1989**, *30*, 3159–3162.

[166] N. O. Brace, *J. Org. Chem.* **1967**, *32*, 2711–2718.

[167] N. O. Brace, J. E. Van Elswyk, *J. Org. Chem.* **1976**, *41*, 766–771.

[168] K. Baum, C. D. Bedford, R. J. Hunad, *J. Org. Chem.* **1982**, *47*, 2251–2257.

[169] S. Q. Liu, S. W. Wang, F.-L. Qing, *J. Fluor. Chem.* **2005**, *126*, 771–778.

[170] X. Fang, X. Yang, X. Yang, S. Mao, Z. Wang, G. Chen, F. Wu, *Tetrahedron* **2007**, *63*, 10684–10692.

[171] A. Tewari, M. Hein, A. Zapf, M. Beller, *Tetrahedron Lett.* **2004**, *45*, 7703–7707.

[172] J. D. Park, F. E. Rogers, J. R. Lacher, *J. Org. Chem.* **1961**, *26*, 2089–2095.

[173] K. Tsuchii, M. Imura, N. Kamada, T. Hirao, A. Ogawa, *J. Org. Chem.* **2004**, *69*, 6658–6665.

[174] E. Soueni, J. M. Tedder, J. C. Walton, *J. Fluor. Chem.* **1981**, *17*, 51–63.

[175] M. H. Habib, T. E. Mallouk, *J. Fluor. Chem.* **1991**, *53*, 53–60.

[176] M. Slodowicz, S. Barata-Vallejo, A. Vázquez, N. S. Nudelman, A. Postigo, *J. Fluor. Chem.* **2012**, *135*, 137–143.

[177] F. Lhermitte, B. Carboni, *Synlett* **1996**, 377–379.

[178] D. Cantacuzene, C. Wakselman, R. Dorme, *J. Chem. Soc., Perkin Trans. 1* **1977**, 1365–1371.

[179] P. Calas, P. Moreau, A. Commeyras, *J. Chem. Soc., Chem. Commun.* **1982**, 433–434.

[180] P. Calas, C. Amatore, L. Gomez, A. Commeyras, *J. Fluor. Chem.* **1990**, *49*, 247–261.

[181] C. Dapremont, P. Calas, A. Commeyras, C. Amatore, *J. Fluor. Chem.* **1992**, *56*, 249–258.

[182] S. Kobayashi, M. Sawaguchi, S. Ayuba, T. Fukuhara, S. Hara, *Synlett* **2001**, 1938–1940.

[183] R. Fields, R. N. Haszeldine, I. Kumadaki, *J. Chem. Soc., Perkin Trans. 1* **1982**, 2211–2217.

[184] M. Hudlicky, *J. Fluor. Chem.* **1981**, *18*, 383–405.

[185] F. Jeanneaux, G. Santini, M. Le Blanc, A. Cambo, J. G. Riess, *Tetrahedron* **1974**, *30*, 4197–4200.

[186] V. Sanchez, J. Greiner, *Tetrahedron Lett.* **1993**, *34*, 2931–2932.

[187] V. Sanchez, A. Manfredi, J. Greiner, J. G. Riess, *Bull. Soc. Chim. Fr.* **1994**, *131*, 648–657.

[188] K. J. MacNeil, D. J. Burton, *J. Org. Chem.* **1993**, *58*, 4411–4417.

[189] D. J. Burton, V. Jairaj, *J. Fluor. Chem.* **2005**, *126*, 797–801.

[190] C.-J. Wallentin, J. D. Nguyen, P. Finkbeiner, C. R. J. Stephenson, *J. Am. Chem. Soc.* **2012**, *134*, 8875–8884.

[191] T. Xu, C. W. Cheung, X. Hu, *Angew. Chem. Int. Ed.* **2014**, *53*, 4910–4914.

[192] Z. Hang, Z. Li, Z.-Q. Liu, *Org. Lett.* **2014**, *16*, 3648–3651.

[193] M.-C. Belhomme, D. Dru, H.-Y. Xiong, D. Cahard, T. Besset, T. Poisson, X. Pannecoucke, *Synthesis* **2014**, *46*, 1859–1870.

[194] G. A. Olah, M. Nojima, L. Kerekes, *Synthesis* **1973**, 780–783.

[195] A. Gregorcic, M. Zupan, *Bull. Chem. Soc. Jpn.* **1987**, *60*, 3083–3085.

[196] S. Eddarir, C. Francesch, H. Mestdagh, C. Rolando, *Bull. Soc. Chim. Fr.* **1997**, *134*, 741–755.

[197] M. Zupan, *Synthesis* **1976**, 473–474.

[198] P. Conte, B. Panunzi, M. Tingoli, *Tetrahedron Lett.* **2006**, *47*, 273–276.

[199] S. Hara, M. Yoshida, T. Fukuhara, N. Yoneda, *Chem. Commun.* **1998**, 965–966.

[200] M. Yoshida, D. Nagahara, T. Fukuhara, N. Yoneda, S. Hara, *J. Chem. Soc., Perkin Trans. 1* **2001**, 2283–2288.

[201] M. Yoshida, K. Kawakami, S. Hara, *Synthesis* **2004**, 2821–2824.

[202] M. Ochiai, Y. Nishi, T. Mori, N. Tada, T. Suefuji, H. J. Frohn, *J. Am. Chem. Soc.* **2005**, *127*, 10460–10461.

[203] R. E. A. Dear, *J. Org. Chem.* **1970**, *35*, 1703–1705.

[204] J. Barluenga, M. A. Rodríguez, J. M. González, P. J. Campos, G. Asensio, *Tetrahedron Lett.* **1986**, *27*, 3303–3306.

[205] S. Rozen, M. Brand, *J. Org. Chem.* **1986**, *51*, 222–225.

[206] D. Dolenc, B. Šket, *Synlett* **1995**, 327–328.

[207] D. F. Shellhamer, B. C. Jones, B. J. Pettus, T. L. Pettus, J. M. Stringer, V. L. Heasley, *J. Fluor. Chem.* **1998**, *88*, 37–39.

[208] Y. Li, X. Liu, D. Ma, B. Liu, H. Jiang, *Adv. Synth. Catal.* **2012**, *354*, 2683–2688.

[209] H. Ukigai, S. Hara, *Tetrahedron Lett.* **2016**, *57*, 1379–1381.

[210] P. Cieplak, P. A. Kollman, J. P. Radomski, in *Biomedical Frontiers of Fluorine Chemistry* (Eds.: I. Ojima, J.R. McCarthy, J.T. Welch), American Chemical Society, Washington DC, **1996**, pp. 11–143.

[211] P. Wipf, T. C. Henninger, S. J. Geib, *J. Org. Chem.* **1998**, *63*, 6088–6089.

[212] P. A. Bartlett, A. Otake, *J. Org. Chem.* **1995**, *60*, 3107–3111.

[213] T. Allmendinger, P. Furet, E. Hungerbühler, *Tetrahedron Lett.* **1990**, *31*, 7297–7300.

[214] T. Allmendinger, E. Felder, E. Hungerbühler, *Tetrahedron Lett.* **1990**, *31*, 7301–7304.

[215] L. G. Boros, B. De Corte, R. H. Gimi, J. T. Welch, Y. Wu, R. E. Handschumacher, *Tetrahedron Lett.* **1994**, *35*, 6033–6036.

[216] J. T. Welch, J. Lin, *Tetrahedron* **1996**, *52*, 291–304.

[217] J.-P. Bégué, D. Bonnet-Delpon, *Bioorganic and Medicinal Chemistry of Fluorine*, John Wiley & Sons, Inc., Hoboken, **2008**.

[218] J. J. Urban, B. G. Tillman, W. A. Cronin, *J. Phys. Chem. A* **2006**, *110*, 11120–11129.

[219] J. Gante, *Angew. Chem. Int. Ed. Engl.* **1994**, *33*, 1699–1720.

[220] A. Niida, K. Tomita, M. Mizumoto, H. Tanigaki, T. Terada, S. Oishi, A. Otaka, K. Inui, N. Fujii, *Org. Lett.* **2006**, *8*, 613–616.

[221] T. Ernet, A. H. Maulitz, E.-U. Wurthwein, G. Haufe, *J. Chem. Soc., Perkin Trans. 1* **2001**, 1929–1938.

[222] G. Haufe, T. C. Rosen, O. G. J. Meyer, R. Fröhlich, K. Rissanen, *J. Fluor. Chem.* **2002**, *114*, 189–198.

[223] T. C. Rosen, S. Yoshida, K. L. Kirk, G. Haufe, *ChemBioChem* **2004**, *5*, 1033–1043.

[224] R. Souzy, B. Ameduri, B. Boutevin, *Prog. Polym. Sci.* **2004**, *29*, 75–106.

[225] J. F. Lontz, W. B. Happoldt, *Ind. Eng. Chem.* **1952**, *44*, 1800–1805.

[226] K. L. Berry, J. H. Peterson, *J. Am. Chem. Soc.* **1951**, *73*, 5195–5197.

[227] A. S. K. Hashmi, T. D. Ramamurthi, F. Rominger, *J. Organomet. Chem.* **2009**, *694*, 592–597.

[228] A. Fürstner, P. W. Davies, *Angew. Chem. Int. Ed.* **2007**, *46*, 3410–3449.

[229] E. Jimenez-Nunez, A. M. Echavarren, *Chem. Commun.* **2007**, 333–346.

[230] A. S. K. Hashmi, *Gold Bull.* **2003**, *36*, 3–9.

[231] C. Chassaing, A. Haudrechy, Y. Langlois, *Tetrahedron Lett.* **1997**, *38*, 4415–4416.

[232] L. G. Voskressensky, N. E. Golantsov, A. M. Maharramov, *Synthesis* **2016**, *48*, 615–643.

[233] M. Sasikumar, Y. V. Suseela, T. Govindaraju, *Asian J. Org. Chem.* **2013**, *2*, 779–785.

[234] C. K. Tan, Y.-Y. Yeung, *Chem. Commun.* **2013**, *49*, 7985–7996.

[235] G. Hernández-Torres, B. Tan, C. F. Barbas, *Org. Lett.* **2012**, *14*, 1858–1861.

[236] H. Eguchi, H. Kawaguchi, S. Yoshinaga, A. Nishida, T. Nishiguchi, S. Fujisaki, *Bull. Chem. Soc. Jpn.* **1994**, *67*, 1918–1921.

[237] S. M. Ahmad, D. C. Braddock, G. Cansell, S. A. Hermitage, *Tetrahedron Lett.* **2007**, *48*, 915–918.

[238] S. E. Denmark, M. T. Burk, *Proc. Natl. Acad. Sci.* **2010**, *107*, 20655–20660.

[239] A. Sakakura, A. Ukai, K. Ishihara, *Nature* **2007**, *445*, 900–903.

[240] C. K. Tan, L. Zhou, Y.-Y. Yeung, *Synlett* **2011**, 1335–1339.

[241] J. A. Kalow, A. G. Doyle, *J. Am. Chem. Soc.* **2010**, *132*, 3268–3269.

[242] D. H. Miles, M. Veguillas, F. D. Toste, *Chem. Sci.* **2013**, *4*, 3427–3431.

[243] Y. M. Wang, J. Wu, C. Hoong, V. Rauniyar, F. D. Toste, *J. Am. Chem. Soc.* **2012**, *134*, 12928–12931.

[244] T. P. Hamilton, H. F. Schaefer, *J. Am. Chem. Soc.* **1991**, *113*, 7147–7151.

[245] P. Kirsch, *Modern Fluoroorganic Chemistry: Synthesis, Reactivity, Applications*, John Wiley & Sons, Inc., Weinheim, **2013**.

[246] C. Hansch, A. Leo, R. W. Taft, *Chem. Rev.* **1991**, *91*, 165–195.

[247] J. A. Bull, A. B. Charette, *J. Am. Chem. Soc.* **2010**, *132*, 1895–1902.

[248] A. Abramovitch, J. P. Varghese, I. Marek, *Org. Lett.* **2004**, *6*, 621–623.

[249] A. Abramovitch, I. Marek, *Eur. J. Org. Chem.* **2008**, 4924–4931.

[250] C. Laurence, K. A. Brameld, J. Graton, J.-Y. Le Questel, E. Renault, *J. Med. Chem.* **2009**, *52*, 4073–4086.

[251] S. Kotha, K. Lahiri, D. Kashinath, *Tetrahedron* **2002**, *58*, 9633–9695.

[252] K. C. Nicolaou, P. G. Bulger, D. Sarlah, *Angew. Chem. Int. Ed.* **2005**, *44*, 4442–4489.

[253] F.-S. Han, *Chem. Soc. Rev.* **2013**, *42*, 5270–5298.

[254] N. Miyaura, A. Suzuki, *Chem. Rev.* **1995**, *95*, 2457–2483.

[255] A. Fürstner, C. Nevado, M. Waser, M. Tremblay, C. Chevrier, F. Teplý, C. Aïssa, E. Moulin, O. Müller, *J. Am. Chem. Soc.* **2007**, *129*, 9150–9161.

[256] I. P. Beletskaya, A. V Cheprakov, *Chem. Rev.* **2000**, *100*, 3009–3066.

[257] A. B. Dounay, L. E. Overman, *Chem. Rev.* **2003**, *103*, 2945–2964.

[258] D. Mc Cartney, P. J. Guiry, *Chem. Soc. Rev.* **2011**, *40*, 5122–5150.

[259] B. C. Ranu, K. Chattopadhyay, *Org. Lett.* **2007**, *9*, 2409–2412.

[260] D. Haas, J. M. Hammann, R. Greiner, P. Knochel, *ACS Catal.* **2016**, *6*, 1540–1552.

[261] A. Krasovskiy, C. Duplais, B. H. Lipshutz, *Org. Lett.* **2010**, *12*, 4742–4744.

[262] A. Krasovskiy, B. H. Lipshutz, *Org. Lett.* **2011**, *13*, 3818–3821.

[263] A. Krasovskiy, B. H. Lipshutz, *Org. Lett.* **2011**, *13*, 3822–3825.

[264] C. G. Bates, P. Saejueng, D. Venkataraman, *Org. Lett.* **2004**, *6*, 1441–1444.

[265] P. Saejueng, C. G. Bates, D. Venkataraman, *Synthesis* **2005**, 1706–1712.

[266] R. Chinchilla, C. Najera, *Chem. Soc. Rev.* **2011**, *40*, 5084–5121.

[267] A. B. Lemay, K. S. Vulic, W. W. Ogilvie, *J. Org. Chem.* **2006**, *71*, 3615–3618.

[268] E. Métay, Q. Hu, E. Negishi, *Org. Lett.* **2006**, *8*, 5773–5776.

[269] E. Negishi, A. Alimardanov, C. Xu, *Org. Lett.* **2000**, *2*, 65–67.

[270] R. Takeuchi, K. Tanabe, S. Tanaka, *J. Org. Chem.* **2000**, *65*, 1558–1561.

[271] D. E. Chavez, E. N. Jacobsen, *Angew. Chem. Int. Ed.* **2001**, *40*, 3667–3670.

[272] D. A. Evans, W. C. Black, *J. Am. Chem. Soc.* **1993**, *115*, 4497–4513.

[273] I. Kadota, H. Takamura, K. Sato, A. Ohno, K. Matsuda, Y. Yamamoto, *J. Am. Chem. Soc.* **2003**, *125*, 46–47.

[274] S.-K. Kang, J.-S. Kim, S.-C. Choi, *J. Org. Chem.* **1997**, *62*, 4208–4209.

[275] S. J. Lee, T. M. Anderson, M. D. Burke, *Angew. Chem. Int. Ed.* **2010**, *49*, 8860–8863.

[276] R. S. Paley, A. de Dios, R. F. de la Pradilla, *Tetrahedron Lett.* **1993**, *34*, 2429–2432.

[277] L. A. Paquette, L. Barriault, D. Pissarnitski, *J. Am. Chem. Soc.* **1999**, *121*, 4542–4543.

[278] J. K. Stille, B. L. Groh, *J. Am. Chem. Soc.* **1987**, *109*, 813–817.

[279] S. E. Denmark, J. Y. Choi, *J. Am. Chem. Soc.* **1999**, *121*, 5821–5822.

[280] J. Montenegro, J. Bergueiro, C. Saá, S. López, *Org. Lett.* **2009**, *11*, 141–144.

[281] S. E. Denmark, D. Wehrli, *Org. Lett.* **2000**, *2*, 565–568.

[282] S. E. Denmark, S.-M. Yang, *J. Am. Chem. Soc.* **2002**, *124*, 2102–2103.

[283] S. E. Denmark, S.-M. Yang, *J. Am. Chem. Soc.* **2002**, *124*, 15196–15197.

[284] Y. Hatanaka, T. Hiyama, *J. Org. Chem.* **1989**, *54*, 268–270.

[285] K. Tamao, K. Kobayashi, Y. Ito, *Tetrahedron Lett.* **1989**, *30*, 6051–6054.

[286] H. Lin, D. Sun, *Org. Prep. Proc. Int.* **2013**, *45*, 341–394.

[287] H. Lu, C. Li, *Org. Lett.* **2006**, *8*, 5365–5367.

[288] M. S. Kabir, M. Lorenz, O. A. Namjoshi, J. M. Cook, *Org. Lett.* **2010**, *12*, 464–467.

[289] B. Malo-Forest, G. Landelle, J. A. Roy, J. Lacroix, R. C. Gaudreault, J. F. Paquin, *Bioorg. Med. Chem. Lett.* **2013**, *23*, 1712–1715.

[290] C. Sambiagio, S. P. Marsden, A. J. Blacker, P. C. McGowan, *Chem. Soc. Rev.* **2014**, *43*, 3525–3550.

[291] K. Jouvin, A. Bayle, F. Legrand, G. Evano, *Org. Lett.* **2012**, *14*, 1652–1655.

[292] K. Jouvin, A. Coste, A. Bayle, F. Legrand, G. Karthikeyan, K. Tadiparthi, G. Evano, *Organometallics* **2012**, *31*, 7933–7947.

[293] M. Taillefer, A. Ouali, B. Renard, J.-F. Spindler, *Chem. Eur. J.* **2006**, *12*, 5301–5313.

[294] C. Hollingworth, V. Gouverneur, *Chem. Commun.* **2012**, *48*, 2929–2942.

[295] K. K. J. Chan, D. O'Hagan, in *Methods in Enzymology: Natural Product Synthesis by Microorganisms and Plants, Part B* (Ed.: D.A. Hopwood), Academic Press, New York, **2012**, pp. 219–235.

[296] C. L. Liotta, H. P. Harris, *J. Am. Chem. Soc.* **1974**, *96*, 2250–2252.

[297] C. L. Liotta, H. P. Harris, M. McDermott, T. Gonzalez, K. Smith, *Tetrahedron Lett.* **1974**, *15*, 2417–2420.

[298] C. L. Liotta, E. E. Grisdale, H. P. Hopkins, *Tetrahedron Lett.* **1975**, *16*, 4205–4208.

[299] C. L. Liotta, in *Synthetic Multidentate Macrocyclic Compounds* (Eds.: R.M. Izatt, J.J. Christensen), Academic Press, New York, **1978**, pp. 111–205.

[300] J. H. Clark, *Chem. Rev.* **1980**, *80*, 429–452.

[301] J. M. Miller, J. H. Clark, *J. Chem. Soc., Chem. Commun.* **1982**, 1318–1319.

[302] J. W. Lee, H. Yan, H. B. Jang, H. K. Kim, S.-W. Park, S. Lee, D. Y. Chi, C. E. Song, *Angew. Chem. Int. Ed.* **2009**, *48*, 7683–7686.

[303] V. H. Jadhav, S. H. Jang, H.-J. Jeong, S. T. Lim, M.-H. Sohn, J.-Y. Kim, S. Lee, J. W. Lee, C. E. Song, D. W. Kim, *Chem. Eur. J.* **2012**, *18*, 3918–3924.

[304] V. H. Jadhav, S. H. Jang, H.-J. Jeong, S. T. Lim, M.-H. Sohn, D. Y. Chi, D. W. Kim, *Org. Lett.* **2010**, *12*, 3740–3743.

[305] H. Yan, H. Bin Jang, J.-W. Lee, H. K. Kim, S. W. Lee, J. W. Yang, C. E. Song, *Angew. Chem. Int. Ed.* **2010**, *49*, 8915–8917.

[306] V. H. Jadhav, W. Choi, S.-S. Lee, S. Lee, D. W. Kim, *Chem. Eur. J.* **2016**, *22*, 4515–4520.

[307] G. Cainelli, F. Manescalchi, M. Panunzio, *Synthesis* **1976**, 472–473.

[308] S. Colonna, A. Re, G. Gelbard, E. Cesarotti, *J. Chem. Soc., Perkin Trans. 1* **1979**, 2248–2252.

[309] J. Aerts, S. Voccia, C. Lemaire, F. Giacomelli, D. Goblet, D. Thonon, A. Plenevaux, G. Warnock, A. Luxen, *Tetrahedron Lett.* **2010**, *51*, 64–66.

[310] N. Ishikawa, T. Kitazume, T. Yamazaki, Y. Mochida, T. Tatsuno, *Chem. Lett.* **1981**, *10*, 761–764.

[311] D. W. Kim, C. E. Song, D. Y. Chi, *J. Am. Chem. Soc.* **2002**, *124*, 10278–10279.

[312] Y.-H. Oh, H. Bin Jang, S. Im, M. J. Song, S.-Y. Kim, S.-W. Park, D. Y. Chi, C. E. Song, S. Lee, *Org. Biomol. Chem.* **2011**, *9*, 418–422.

[313] D. W. Kim, D. Y. Chi, *Angew. Chem. Int. Ed.* **2004**, *43*, 483–485.

[314] J. H. Clark, S. J. Tavener, S. J. Barlow, *Chem. Commun.* **1996**, 2429–2430.

[315] C. B. Murray, G. Sandford, S. R. Korn, *J. Fluor. Chem.* **2003**, *123*, 81–84.

[316] O. Nashiru, D. L. Zechel, D. Stoll, T. Mohammadzadeh, R. A. J. Warren, S. G. Withers, *Angew. Chem. Int. Ed.* **2001**, *40*, 417–420.

[317] D. L. Zechel, S. P. Reid, O. Nashiru, C. Mayer, D. Stoll, D. L. Jakeman, R. A. J. Warren, S. G. Withers, *J. Am. Chem. Soc.* **2001**, *123*, 4350–4351.

[318] D. O'Hagan, C. Schaffrath, S. L. Cobb, J. T. G. Hamilton, C. D. Murphy, *Nature* **2002**, *416*, 279.

[319] C. Schaffrath, H. Deng, D. O'Hagan, *FEBS Lett.* **2003**, *547*, 111–114.

[320] C. Dong, F. Huang, H. Deng, C. Schaffrath, J. B. Spencer, D. O'Hagan, J. H. Naismith,

Nature **2004**, *427*, 561–565.

[321] D. O'Hagan, *J. Fluor. Chem.* **2006**, *127*, 1479–1483.

[322] H. Deng, D. O'Hagan, *Curr. Opin. Chem. Biol.* **2008**, *12*, 582–592.

[323] H. M. Senn, D. O'Hagan, W. Thiel, *J. Am. Chem. Soc.* **2005**, *127*, 13643–13655.

[324] T. Yonezawa, Y. Sakamoto, K. Nogawa, *Preparation of Tetrabutylammonium Fluoride-Alcohol Adducts as Fluorination Agents.*, **1994**, JP06316551 A.

[325] D. W. Kim, D.-S. Ahn, Y.-H. Oh, S. Lee, H. S. Kil, S. J. Oh, S. J. Lee, J. S. Kim, J. S. Ryu, D. H. Moon, et al., *J. Am. Chem. Soc.* **2006**, *128*, 16394–16397.

[326] D. W. Kim, Jeong, S. T. Lim, M.-H. Sohn, J. A. Katzenellenbogen, D. Y. Chi, *J. Org. Chem.* **2008**, *73*, 957–962.

[327] D. W. Kim, H.-J. Jeong, S. T. Lim, M.-H. Sohn, *Angew. Chem. Int. Ed.* **2008**, *47*, 8404–8406.

[328] S. S. Shinde, B. S. Lee, D. Y. Chi, *Org. Lett.* **2008**, *10*, 733–735.

[329] C. Hollingworth, A. Hazari, M. N. Hopkinson, M. Tredwell, E. Benedetto, M. Huiban, A. D. Gee, J. M. Brown, V. Gouverneur, *Angew. Chem. Int. Ed.* **2011**, *50*, 2613–2617.

[330] E. Benedetto, M. Tredwell, C. Hollingworth, T. Khotavivattana, J. M. Brown, V. Gouverneur, *Chem. Sci.* **2013**, *4*, 89–96.

[331] A. E. Mattson, A. M. Zuhl, T. E. Reynolds, K. A. Scheidt, *J. Am. Chem. Soc.* **2006**, *128*, 4932–4933.

[332] J. A. Birrell, J.-N. Desrosiers, E. N. Jacobsen, *J. Am. Chem. Soc.* **2011**, *133*, 13872–13875.

[333] K. M. Engle, L. Pfeifer, G. Pidgeon, G. Giuffredi, A. L. Thompson, R. Paton, J. M. Brown, V. Gouverneur, *Chem. Sci.* **2015**, 5293–5302.

[334] O. Adalsteinsson, A. Lamotte, R. F. Baddour, C. K. Colton, A. Pollak, G. M. Whitesides, *J. Mol. Catal.* **1979**, *6*, 199–225.

[335] R. E. Notari, *J. Pharm. Sci.* **1969**, *58*, 1064–1068.

[336] D. E. Ames, T. F. Grey, *J. Chem. Soc.* **1955**, 631–636.

[337] R. I. Gelb, *Anal. Chem.* **1971**, *43*, 1110–1113.

[338] S. Alvarez, P. Alemany, D. Casanova, J. Cirera, M. Llunell, D. Avnir, *Coord. Chem. Rev.* **2005**, *249*, 1693–1708.

[339] S. Alvarez, B. Menjón, A. Falceto, D. Casanova, P. Alemany, *Inorg. Chem.* **2014**, *53*, 12151–12163.

[340] J. Cirera, P. Alemany, S. Alvarez, *Chem. Eur. J.* **2004**, *10*, 190–207.

[341] N. Schweigert, R. W. Hunziker, B. I. Escher, R. I. L. Eggen, *Environ. Toxicol. Chem.* **2001**, *20*, 239–247.

[342] G. R. Desiraju, T. Steiner, in *The Weak Hydrogen Bond: In Structural Chemistry and Biology*, Oxford University Press, Oxford and New York, **1999**, pp. 1–28.

[343] W. J. McLean, G. A. Jeffrey, *J. Chem. Phys.* **1967**, *47*, 414–417.

[344] S. J. Brooks, P. A. Gale, M. E. Light, *Chem. Commun.* **2006**, 4344–4346.

[345] Q.-Q. Wang, V. W. Day, K. Bowman-James, *Angew. Chem. Int. Ed.* **2012**, *51*, 2119–2123.

[346] M. Arunachalam, P. Ghosh, *Chem. Commun.* **2009**, 5389–5391.

[347] A. Kornath, F. Neumann, H. Oberhammer, *Inorg. Chem.* **2003**, *42*, 2894–2901.

[348] T. Steiner, G. R. Desiraju, *Chem. Commun.* **1998**, 891–892.

[349] E. Arunan, G. R. Desiraju, R. a. Klein, J. Sadlej, S. Scheiner, I. Alkorta, D. C. Clary, R. H. Crabtree, J. J. Dannenberg, P. Hobza, et al., *Pure Appl. Chem.* **2011**, *83*, 1637–1641.

[350] F. C. Gozzo, S. A. Fernandes, D. C. Rodrigues, M. N. Eberlin, A. J. Marsaioli, *J. Org. Chem.* **2003**, *68*, 5493–5499.

[351] A. P. Bento, M. Solà, F. M. Bickelhaupt, *J. Comput. Chem.* **2005**, *26*, 1497–1504.

[352] J. E. Leffler, *Science* **1953**, *117*, 340–341.

[353] G. S. Hammond, *J. Am. Chem. Soc.* **1955**, *77*, 334–338.

[354] T. A. Manz, D. S. Sholl, *J. Comput. Chem.* **2010**, *31*, 1528–1541.

[355] D. E. Gomez, L. Fabbrizzi, M. Licchelli, E. Monzani, *Org. Biomol. Chem.* **2005**, *3*, 1495–1500.

[356] V. Amendola, M. Boiocchi, B. Colasson, L. Fabbrizzi, *Inorg. Chem.* **2006**, *45*, 6138–6147.

[357] V. Blažek Bregović, N. Basarić, K. Mlinarić-Majerski, *Coord. Chem. Rev.* **2015**, *295*, 80–124.

[358] D. Jiménez, R. Martínez-Máñez, F. Sancenón, J. Soto, *Tetrahedron Lett.* **2002**, *43*, 2823–2825.

[359] R. M. Duke, T. Gunnlaugsson, *Tetrahedron Lett.* **2011**, *52*, 1503–1505.

[360] V. Amendola, G. Bergamaschi, M. Boiocchi, L. Fabbrizzi, L. Mosca, *J. Am. Chem. Soc.* **2013**, *135*, 6345–6355.

[361] J. Schiller, R. Pérez-Ruiz, D. Sampedro, E. Marqués-López, R. P. Herrera, D. Díaz Díaz, *Sensors* **2016**, *16*, 658.

[362] R. Mikláš, P. Kasák, F. Devínsky, M. Putala, *Chem. Pap.* **2009**, *63*, 709–715.

[363] M. Boiocchi, L. Del Boca, D. E. Gmez, L. Fabbrizzi, M. Licchelli, E. Monzani, D. E. Go, *J. Am. Chem. Soc.* **2004**, *126*, 16507–16514.

[364] Q. Li, T. C. W. Mak, *Acta Crystallogr. Sect. B* **1998**, *54*, 180–192.

[365] I. Ravikumar, P. S. Lakshminarayanan, M. Arunachalam, E. Suresh, P. Ghosh, *Dalt. Trans.* **2009**, 4160–4168.

[366] M. Li, B. Wu, C. Jia, X. Huang, Q. Zhao, S. Shao, X.-J. Yang, *Chem. Eur. J.* **2011**, *17*, 2272–2280.

[367] R. Zhang, Y. Zhao, J. Wang, L. Ji, X.-J. Yang, B. Wu, *Cryst. Growth Des.* **2014**, *14*, 544–551.

[368] M. Paul, N. N. Adarsh, P. Dastidar, *Cryst. Growth Des.* **2012**, *12*, 4135–4143.

[369] F. H. Herbstein, *Crystalline Molecular Complexes and Compounds, Volume I*, Oxford University Press, Oxford, **2005**.

[370] A. Kormos, I. Móczár, D. Pál, P. Baranyai, T. Holczbauer, A. Palló, K. Tóth, P. Huszthy, *Tetrahedron* **2013**, *69*, 8142–8146.

[371] I. L. Kirby, M. B. Pitak, M. Wenzel, C. Wilson, H. A. Sparkes, S. J. Coles, P. A. Gale, *CrystEngComm* **2013**, *15*, 9003–9010.

[372] L. Pfeifer, K. M. Engle, G. W. Pidgeon, H. A. Sparkes, A. L. Thompson, J. M. Brown, V. E. Gouverneur, *J. Am. Chem. Soc.* **2016**, *138*, 13314–13325.

[373] G. R. Desiraju, J. A. R. P. Sarma, *J. Chem. Sci.* **1986**, *96*, 599–605.

[374] F. H. Allen, *Acta Crystallogr. Sect. B* **2002**, *58*, 380–388.

[375] P. Metrangolo, F. Meyer, T. Pilati, G. Resnati, G. Terraneo, *Angew. Chem. Int. Ed.* **2008**, *47*, 6114–6127.

[376] P. Politzer, J. S. Murray, T. Clark, *Phys. Chem. Chem. Phys.* **2013**, *15*, 11178–11189.

[377] This structure is believed to be modulated (see Experimental Part); the average structure is included for completeness, but work on the full modulated description is ongoing.

[378] J. Emsley, M. Arif, P. A. Bates, M. B. Hursthouse, *J. Chem. Soc., Chem. Commun.* **1989**, 738–739.

[379] S. Dalapati, M. Akhtarul Alam, R. Saha, S. Jana, N. Guchhait, *CrystEngComm* **2012**, *14*, 1527–1530.

[380] D. Trzybinski, A. Sikorski, *CrystEngComm* **2013**, *15*, 6808–6818.

[381] W. Vreugdenhil, P. J. M. W. L. Birker, R. W. M. ten Hoedt, G. C. Verschoor, J. Reedijk, *J. Chem. Soc., Dalt. Trans.* **1984**, 429–432.

[382] C. R. Jones, P. K. Baruah, A. L. Thompson, S. Scheiner, M. D. Smith, *J. Am. Chem. Soc.* **2012**, *134*, 12064–12071.

[383] C. Garau, A. Frontera, P. Ballester, D. Quiñonero, A. Costa, P. M. Deyà, *Eur. J. Org. Chem.* **2005**, 179–183.

[384] V. Amendola, G. Bergamaschi, M. Boiocchi, L. Fabbrizzi, M. Milani, *Chem. Eur. J.* **2010**, *16*, 4368–4380.

[385] J. Alemán, A. Parra, H. Jiang, K. A. Jørgensen, *Chem. Eur. J.* **2011**, *17*, 6890–6899.

[386] C. Gaeta, C. Talotta, P. Della Sala, L. Margarucci, A. Casapullo, P. Neri, *J. Org. Chem.* **2014**, *79*, 3704–3708.

[387] N. Busschaert, I. L. Kirby, S. Young, S. J. Coles, P. N. Horton, M. E. Light, P. A. Gale, *Angew. Chem. Int. Ed.* **2012**, *51*, 4426–4430.

[388] R. B. P. Elmes, P. Turner, K. A. Jolliffe, *Org. Lett.* **2013**, *15*, 5638–5641.

[389] P. Sokkalingam, C.-H. Lee, *J. Org. Chem.* **2011**, *76*, 3820–3828.

[390] P. Kuzmič, *Anal. Biochem.* **1996**, *237*, 260–273.

[391] A. Jerschow, N. Müller, *J. Magn. Reson.* **1997**, *125*, 372–375.

[392] T. D. W. Claridge, *High-Resolution NMR Techniques in Organic Chemistry*, Elsevier, Amsterdam, **2016**.

[393] P. Gans, A. Sabatini, A. Vacca, *Talanta* **1996**, *43*, 1739–1753.

[394] D. A. Wynn, M. M. Roth, B. D. Pollard, *Talanta* **1984**, *31*, 1036–1040.

[395] N. Kornblum, R. A. Smiley, R. K. Blackwood, D. C. Iffland, *J. Am. Chem. Soc.* **1955**, *77*, 6269–6280.

[396] A. B. Pangborn, M. A. Giardello, R. H. Grubbs, R. K. Rosen, F. J. Timmers, *Organometallics* **1996**, *15*, 1518–1520.

[397] J. Cosier, A. M. Glazer, *J. Appl. Crystallogr.* **1986**, *19*, 105–107.

[398] Z. Otwinowski, W. Minor, in *Methods in Enzymology: Macromolecular Crystallography Part A* (Ed.: B.T.-M. in Enzymology), Academic Press, **1997**, pp. 307–326.

[399] CrysAlisPro (Agilent Technologies, Oxford, 2011)

[400] A. Altomare, G. Cascarano, C. Giacovazzo, A. Guagliardi, M. C. Burla, G. Polidori, M. Camalli, *J. Appl. Crystallogr.* **1994**, *27*, 435–436.

[401] L. Palatinus, G. Chapuis, *J. Appl. Crystallogr.* **2007**, *40*, 786–790.

[402] P. Parois, R. I. Cooper, A. L. Thompson, *Chem. Cent. J.* **2015**, *9*, 30.

[403] P. W. Betteridge, J. R. Carruthers, R. I. Cooper, K. Prout, D. J. Watkin, *J. Appl.*

Crystallogr. **2003**, *36*, 1487.

[404] A. L. Thompson, D. J. Watkin, *J. Appl. Crystallogr.* **2011**, *44*, 1017–1022.

[405] R. I. Cooper, A. L. Thompson, D. J. Watkin, *J Appl Crystallogr* **2010**, *43*, 1100–1107.

[406] L. Schröder, D. J. Watkin, A. Cousson, R. I. Cooper, W. Paulus, *J. Appl. Crystallogr.* **2004**, *37*, 545–550.

[407] A. Spek, *J Appl Crystallogr* **2003**, *36*, 7–13.

[408] P. van der Sluis, A. L. Spek, *Acta Crystallogr* **1990**, *A46*, 194–201.

[409] R. I. Cooper, R. O. Gould, S. Parsons, D. J. Watkin, *J. Appl. Crystallogr.* **2002**, *35*, 168–174.

[410] D. A. Keen, M. J. Gutmann, C. C. Wilson, *J. Appl. Crystallogr.* **2006**, *39*, 714–722.

[411] M. Gutmann, *Acta Crystallogr. Sect. A* **2005**, *61*, C164.

[412] G. M. Sheldrick, *Acta Crystallogr Sect. A* **2008**, *A64*, 112–122.

[413] A. L. Spek, *Platon, A Multipurpose Crystallographic Tool*, Utrecht University, Utrecht, **1998**.

[414] C. F. Macrae, I. J. Bruno, J. A. Chisholm, P. R. Edgington, P. McCabe, E. Pidcock, L. Rodriguez-Monge, R. Taylor, J. van de Streek, P. A. Wood, *J. Appl. Crystallogr.* **2008**, *41*, 466–470.

[415] G. A. Molander, A. R. Brown, *J. Org. Chem.* **2006**, *71*, 9681–9686.

[416] A. Falk, A.-L. Göderz, H.-G. Schmalz, *Angew. Chem. Int. Ed.* **2013**, *52*, 1576–1580.

[417] B. Schmidt, R. Berger, *Adv. Synth. Catal.* **2013**, *355*, 463–476.

[418] L. T. Ball, G. C. Lloyd-Jones, C. A. Russell, *Chem. Eur. J.* **2012**, *18*, 2931–2937.

[419] W. Ren, M. Yamane, *J. Org. Chem.* **2009**, *74*, 8332–8335.

[420] M. D. Greenhalgh, S. P. Thomas, *J. Am. Chem. Soc.* **2012**, *134*, 11900–11903.

[421] S.-H. Cho, B. Ma, S. T. Nguyen, J. T. Hupp, T. E. Albrecht-Schmitt, *Chem. Commun.* **2006**, 2563–2565.

[422] E. Alacid, C. Nájera, *J. Org. Chem.* **2009**, *74*, 2321–2327.

[423] P. Dydio, J. N. H. Reek, *Angew. Chem. Int. Ed.* **2013**, *52*, 3878–3882.

[424] S. E. Denmark, C. R. Butler, *J. Am. Chem. Soc.* **2008**, *130*, 3690–3704.

[425] J. G. Duboudin, B. Jousseaume, A. Saux, *J. Organomet. Chem.* **1979**, *168*, 1–11.

[426] T. Olpp, R. Brückner, *Synthesis* **2004**, 2135–2152.

[427] K. Ando, *J. Org. Chem.* **1998**, *63*, 8411–8416.

[428] S. Radomkit, P. Sarnpitak, J. Tummatorn, P. Batsomboon, S. Ruchirawat, P. Ploypradith, *Tetrahedron* **2011**, *67*, 3904–3914.

[429] S. K. Taylor, D. S. Bischoff, C. L. Blankespoor, P. A. Deck, S. M. Harvey, P. L. Johnson, A. E. Marolewski, S. W. Mork, D. H. Motry, R. Van Eenenaam, *J. Org. Chem.* **1990**, *55*, 4202–4207.

[430] T. Azemi, M. Kitamura, K. Narasaka, *Tetrahedron* **2004**, *60*, 1339–1344.

[431] G. W. Kabalka, M. Al-Masum, *Org. Lett.* **2006**, *8*, 11–13.

[432] A. Lishchynskyi, K. Muñiz, *Chem. Eur. J.* **2012**, *18*, 2212–2216.

[433] A. L. Krasovskiy, S. Haley, K. Voigtritter, B. H. Lipshutz, *Org. Lett.* **2014**, *16*, 4066–4069.

[434] W. Liu, J. T. Groves, *Angew. Chem. Int. Ed.* **2013**, *52*, 6024–6027.

[435] A. Volkov, K. P. J. Gustafson, C.-W. Tai, O. Verho, J.-E. Bäckvall, H. Adolfsson, *Angew. Chem. Int. Ed.* **2015**, *54*, 5122–5126.

[436] A. K. Yadav, V. P. Srivastava, L. D. S. Yadav, *Chem. Commun.* **2013**, *49*, 2154–2156.

[437] C. York, G. K. Surya Prakash, G. A. Olah, *Tetrahedron* **1996**, *52*, 9–14.

[438] K.-Y. Kim, B. C. Kim, H. B. Lee, H. Shin, *J. Org. Chem.* **2008**, *73*, 8106–8108.

[439] E. Fritz-Langhals, *Tetrahedron Lett.* **1994**, *35*, 1851–1854.

[440] J.-B. Xia, C. Zhu, C. Chen, *J. Am. Chem. Soc.* **2013**, *135*, 17494–17500.

[441] M.-H. Yang, S. S. Matikonda, R. A. Altman, *Org. Lett.* **2013**, *15*, 3894–3897.

[442] F. D. Greene, W. A. Remers, J. W. Wilson, *J. Am. Chem. Soc.* **1957**, *79*, 1416–1420.

[443] T. Sagae, S. Ogawa, N. Furukawa, *Tetrahedron Lett.* **1993**, *34*, 4043–4046.

[444] S. Bresciani, D. O'Hagan, *Tetrahedron Lett.* **2010**, *51*, 5795–5797.

[445] T. Umemoto, R. P. Singh, Y. Xu, N. Saito, *J. Am. Chem. Soc.* **2010**, *132*, 18199–18205.

[446] A. Collado, A. Gomez-Suarez, A. R. Martin, A. M. Z. Slawin, S. P. Nolan, *Chem. Commun.* **2013**, *49*, 5541–5543.

[447] P. de Frémont, N. M. Scott, E. D. Stevens, S. P. Nolan, *Organometallics* **2005**, *24*, 2411–2418.

[448] O. S. Morozov, A. V Lunchev, A. A. Bush, A. A. Tukov, A. F. Asachenko, V. N. Khrustalev, S. S. Zalesskiy, V. P. Ananikov, M. S. Nechaev, *Chem. Eur. J.* **2014**, *20*, 6162–6170.

[449] C. M. Wyss, B. K. Tate, J. Bacsa, M. Wieliczko, J. P. Sadighi, *Polyhedron* **2014**, *84*, 87–95.

[450] E. Y. Tsui, P. Müller, J. P. Sadighi, *Angew. Chem. Int. Ed.* **2008**, *47*, 8937–8940.

[451] D. S. Laitar, P. Müller, T. G. Gray, J. P. Sadighi, *Organometallics* **2005**, *24*, 4503–4505.

[452] M. Spraul, K. Griesbaum, *Chem. Ber.* **1983**, *116*, 2641–2652.

[453] G. Boche, U. Fährmann, *Chem. Ber.* **1981**, *114*, 4005–4009.

[454] C.-H. Chien, S. Fujita, S. Yamoto, T. Hara, T. Yamagata, M. Watanabe, K. Mashima, *Dalt. Trans.* **2008**, 916–923.

[455] Y.-S. Lee, Y.-H. Cho, S. Lee, J.-K. Bin, J. Yang, G. Chae, C.-H. Cheon, *Tetrahedron* **2015**, *71*, 532–538.

[456] R. Tomita, T. Koike, M. Akita, *Angew. Chem. Int. Ed.* **2015**, *54*, 12923–12927.

[457] C. A. Witham, P. Mauleón, N. D. Shapiro, B. D. Sherry, F. D. Toste, *J. Am. Chem. Soc.* **2007**, *129*, 5838–5839.

[458] R. Cai, M. Lu, E. Y. Aguilera, Y. Xi, N. G. Akhmedov, J. L. Petersen, H. Chen, X. Shi, *Angew. Chem. Int. Ed.* **2015**, *54*, 8772–8776.

[459] X. Li, X. Liu, H. Chen, W. Wu, C. Qi, H. Jiang, *Angew. Chem. Int. Ed.* **2014**, *53*, 14485–14489.

[460] Y. Okuno, M. Yamashita, K. Nozaki, *Eur. J. Org. Chem.* **2011**, 3951–3958.

[461] Y.-Y. Liu, X.-H. Yang, X.-C. Huang, W.-T. Wei, R.-J. Song, J.-H. Li, *J. Org. Chem.* **2013**, *78*, 10421–10426.

[462] N. G. Pschirer, U. H. F. Bunz, *Tetrahedron Lett.* **1999**, *40*, 2481–2484.

[463] N. Shibakawa, K. Yoneda, T. Katsube, T. Kanda, K. Ito, K. Yamamoto, N. Iwase, S. Ushiyama, *Substituted Biaryl Compound*, **2016**, EP2980075 A4.

[464] K. Semba, T. Fujihara, J. Terao, Y. Tsuji, *Chem. Eur. J.* **2012**, *18*, 4179–4184.

[465] B. Lu, C. Li, L. Zhang, *J. Am. Chem. Soc.* **2010**, *132*, 14070–14072.

[466] E. C. McLaughlin, M. P. Doyle, *J. Org. Chem.* **2008**, *73*, 4317–4319.

[467] J. Xiang, R. Yuan, R. Wang, N. Yi, L. Lu, H. Zou, W. He, *J. Org. Chem.* **2014**, *79*, 11378–11382.

[468] M. Yoshida, S. Yoshikawa, T. Fukuhara, N. Yoneda, S. Hara, *Tetrahedron* **2001**, *57*, 7143–7148.

[469] O. A. Wong, Y. Shi, *J. Org. Chem.* **2009**, *74*, 8377–8380.

[470] D. G. Lloyd, R. B. Hughes, D. M. Zisterer, D. C. Williams, C. Fattorusso, B. Catalanotti, G. Campiani, M. J. Meegan, *J. Med. Chem.* **2004**, *47*, 5612–5615.

[471] G. Fraenkel, J. H. Duncan, J. Wang, *J. Am. Chem. Soc.* **1999**, *121*, 432–443.

[472] V. K. Aggarwal, F. Sandrinelli, J. P. H. Charmant, *Tetrahedron: Asymmetry* **2002**, *13*, 87–93.

[473] W. S. Jeon, E. Kim, Y. H. Ko, I. Hwang, J. W. Lee, S.-Y. Kim, H.-J. Kim, K. Kim, *Angew. Chem. Int. Ed.* **2005**, *44*, 87–91.

[474] V. H. Jadhav, H.-J. Jeong, S. T. Lim, M.-H. Sohn, C. E. Song, D. W. Kim, *Tetrahedron* **2013**, *69*, 3577–3583.

[475] M. Ohkubo, S. Mochizuki, T. Sano, Y. Kawaguchi, S. Okamoto, *Org. Lett.* **2007**, *9*, 773–776.

[476] V. Barone, M. Cossi, *J. Phys. Chem. A* **1998**, *102*, 1995–2001.

[477] J.-D. Chai, M. Head-Gordon, *Phys. Chem. Chem. Phys.* **2008**, *10*, 6615–6620.

[478] L. E. Roy, P. J. Hay, R. L. Martin, *J. Chem. Theory Comput.* **2008**, *4*, 1029–1031.

[479] M. Cossi, N. Rega, G. Scalmani, V. Barone, *J. Comput. Chem.* **2003**, *24*, 669–681.

[480] R. F. Ribeiro, A. V Marenich, C. J. Cramer, D. G. Truhlar, *J. Phys. Chem. B* **2011**, *115*, 14556–14562.

[481] M. O. Anderson, H. Yu, C. Penaranda, B. A. Maddux, I. D. Goldfine, J. F. Youngren, R. K. Guy, *J. Comb. Chem.* **2006**, *8*, 784–790.

[482] W. C. Drewe, S. Neidle, *Chem. Commun.* **2008**, 5295–5297.

[483] X.-Q. Li, W.-K. Wang, Y.-X. Han, C. Zhang, *Adv. Synth. Catal.* **2010**, *352*, 2588–2598.

[484] Z. Shuguang, Y. Ting, Y. Jicheng, L. Dahuai, X. Jing, *J. Chem. Res.* **2013**, *37*, 315–319.

[485] J. W. Lim, K. H. Kim, H. R. Moon, J. N. Kim, *Tetrahedron Lett.* **2016**, *57*, 784–787.

[486] W. Ye, J. Mo, T. Zhao, B. Xu, *Chem. Commun.* **2009**, 3246–3248.

[487] A. Rostami, A. Colin, X. Y. Li, M. G. Chudzinski, A. J. Lough, M. S. Taylor, *J. Org. Chem.* **2010**, *75*, 3983–3992.

[488] V. Mlynárik, *Org. Magn. Reson.* **1981**, *17*, 178–179.

[489] L. E. Combettes, P. Clausen-Thue, M. A. King, B. Odell, A. L. Thompson, V. Gouverneur, T. D. W. Claridge, *Chem. Eur. J.* **2012**, *18*, 13133–13141.